National Library
of Canada

Bibliothèque nationale
du Canada

Canadian Theses Service

Service des thèses canadiennes

Ottawa, Canada
K1A 0N4

NOTICE

The quality of this microform is heavily dependent upon the quality of the original thesis submitted for microfilming. Every effort has been made to ensure the highest quality of reproduction possible.

If pages are missing, contact the university which granted the degree.

Some pages may have indistinct print especially if the original pages were typed with a poor typewriter ribbon or if the university sent us an inferior photocopy.

Previously copyrighted materials (journal articles, published tests, etc.) are not filmed.

Reproduction in full or in part of this microform is governed by the Canadian Copyright Act, R.S.C. 1970, c. C-30.

AVIS

La qualité de cette microforme dépend grandement de la qualité de la thèse soumise au microfilmage. Nous avons tout fait pour assurer une qualité supérieure de reproduction.

S'il manque des pages, veuillez communiquer avec l'université qui a conféré le grade.

La qualité d'impression de certaines pages peut laisser à désirer, surtout si les pages originales ont été dactylographiées à l'aide d'un ruban usé ou si l'université nous a fait parvenir une photocopie de qualité inférieure.

Les documents qui font déjà l'objet d'un droit d'auteur (articles de revue, tests publiés, etc.) ne sont pas microfilmés.

La reproduction, même partielle, de cette microforme est soumise à la Loi canadienne sur le droit d'auteur, SRC 1970, c. C-30.

NL-339 (r. 88/04)

Canada

THE UNIVERSITY OF ALBERTA

FOAM FLOW IN POROUS MEDIA

BY

TERRI ANN MACDONALD

A THESIS
SUBMITTED TO THE FACULTY OF GRADUATE STUDIES AND RESEARCH
IN PARTIAL FULFILLMENT OF THE REQUIREMENTS FOR THE DEGREE
OF MASTER OF SCIENCE
IN
PETROLEUM ENGINEERING

DEPARTMENT OF MINING, METALLURGICAL AND PETROLEUM
ENGINEERING

EDMONTON, ALBERTA
FALL, 1988

Permission has been granted to the National Library of Canada to microfilm this thesis and to lend or sell copies of the film.

The author (copyright owner) has reserved other publication rights, and neither the thesis nor extensive extracts from it may be printed or otherwise reproduced without his/her written permission.

L'autorisation a été accordée à la Bibliothèque nationale du Canada de microfilmer cette thèse et de prêter ou de vendre des exemplaires du film.

L'auteur (titulaire du droit d'auteur) se réserve les autres droits de publication; ni la thèse ni de longs extraits de celle-ci ne doivent être imprimés ou autrement reproduits sans son autorisation écrite.

ISBN 0-315-45625-6

THE UNIVERSITY OF ALBERTA
RELEASE FORM

NAME OF AUTHOR:	Terri Ann MacDonald
TITLE OF THESIS:	Foam Flow In Porous Media
DEGREE:	Master Of Science, Petroleum Engineering
YEAR THIS DEGREE GRANTED:	Fall, 1988

Permission is hereby granted to **THE UNIVERSITY OF ALBERTA LIBRARY** to reproduce single copies of this thesis and to lend or sell such copies for private, scholarly, or scientific research purposes only.

The author reserves other publication rights, and neither the thesis nor extensive extracts from it may be printed or otherwise reproduced without the author's written permission.

Terri MacDonald

P.O. Box 66
Rochester, Alberta.
T0G 1Z0

Date: August 30, 1988

THE UNIVERSITY OF ALBERTA
FACULTY OF GRADUATE STUDIES AND RESEARCH

The undersigned certify that they have read and recommend to the Faculty of Graduate Studies and Research, for acceptance, a thesis entitled FOAM FLOW IN POROUS MEDIA submitted by TERRI ANN MACDONALD in partial fulfillment of the requirements for the degree of MASTER OF SCIENCE in PETROLEUM ENGINEERING.

....
Dr. S.M. Farouq Ali
(Supervisor)

DL Flock
....
Dr. D.L. Flock

JM Whiting
....
Dr. J.M. Whiting

M. N. Oguztoreli
....
Dr. M.N. Oguztoreli
(External Examiner)

DATED : August 30, 1988

To My Husband, Derek Morrison
For His Love and Support,

And To My Loving Parents,
Roderick and Ina MacDonald

Abstract

This research was directed toward the study of foam flow in porous media and consisted of a series of experiments, under a variety of conditions.

A large portion of the work carried out in this study involved the design and construction of the apparatus. This apparatus was designed to examine foam flow at elevated temperatures (up to 250°C) and high pressures (up to 500 psi), while allowing visual observation of the foam at the core inlet and outlet.

Several sets of experiments were carried out to analyze the effect of surfactant concentration, gas/liquid rates, temperature, pressure, and permeability. It was observed that the presence of an oil saturation had an adverse effect on the formation of foam. It was found that there was an optimal surfactant concentration for foam formation however, this optimum varied with the absolute permeability.

For the experimental conditions, the mobility of the gas phase in the presence of foam was found to increase with increasing absolute permeability. This observation is in contrast to some of the previous research where it was suggested that foam would preferentially block highly permeable channels.

As this was this first study of its kind at this university, one of the objectives was to analyze a broad range of parameters while keeping the type of surfactant constant. Future work on this project should involve the use of other surfactants.

In the light of this research "foam flooding" with SD1000 does not seem to be a viable secondary recovery method. If a surfactant, that is not adversely affected by an oil saturation, were utilized, the results may have been different.

Acknowledgements

I would like to express my deep gratitude to Dr. S.M. Farouq Ali for his guidance and support during the course of this study.

Helpful suggestions provided by Dr. D.L. Flock and Dr. R. Islam are gratefully acknowledged.

Special thanks are extended to Mr. R. Smith, for his help with the design and construction of the apparatus, and also to Mr. J. Czuroski for his assistance in the laboratory.

Ms. L. Detwiler is acknowledged, for her help in typing the manuscript, as is Mr. D.J. Morrison for his assistance in the preparation of the graphs.

The financial support provided by NSERC was greatly appreciated.

Table of Contents

Abstract v
Acknowledgements vii
List of Tables xi
List of Figures xiii
List of Plates xxii
Nomenclature xxiii

I Introduction 1

II Statement of the Problem 2

III Literature Review 4
  3.1 Foam Characterization 4
  3.2 The Mechanism of Foam Flow 10
  3.3 Mobility 13
  3.4 Gas Permeability 15
  3.5 Rheology 15
  3.6 Foam Flow Analysis 20
  3.7 Factors Influencing Foam Flow in Porous Media 22
    3.7.1 Quality 22
    3.7.2 Absolute Permeability 23
    3.7.3 Surfactant Type and Concentration 23
    3.7.4 Pressure 26
    3.7.5 Temperature 27
    3.7.6 Oil Saturation 29
    3.7.7 Salinity 30
    3.7.8 Gas Velocity 31
    3.7.9 Surface Viscosity and Interfacial Tension 32

IV Experimental Apparatus and Procedure 34
  4.1 Preliminary Experiments 34
  4.2 Coreholder Packing and Saturation 39
    4.2.1 Packing Procedure 39
    4.2.2 Packing Materials 40
    4.2.3 Wet Packing 41
    4.2.4 Dry Packing 42
    4.2.5 Alternate Pore Volume Determination 43
    4.2.6 Consolidated Core Preparation 45
    4.2.7 Oil Saturation of the Sandpacks 46
  4.3 Pre-Foamed Temperature-Controlled Co-Injection Runs 47

4.3.1 Experimental Equipment 53
4.3.1.1 Injection System 53
4.3.1.2 Oven Interior 54
4.3.1.2 Foam Generator 54
4.3.1.3 Sightglasses 58
4.3.1.4 Dual Core Runs 59
4.3.1.5 Outlet System 59
4.3.1.6 Sample Analysis 62
4.3.2 Experimental Procedure for the Pre-Foamed Temperature-Controlled Co-injection Runs 64
4.3.3 Operational Difficulties 68

V Discussion 71
5.1 Introduction 71
5.1.2 Experimental Results 75
5.2 Preliminary Runs 78
5.2.1 Water Base Case 79
5.2.2 Surfactant SD 1000 83
5.2.3 Surfactant XP100 88
5.2.4 Dow Surfactant 96
5.2.5 Dow Surfactant - Coreholder Oriented Vertically 102
5.2.6 Comparison of Gas Displacement Tests for Surfactant Saturated and Water Saturated Cores 106
5.2.7 Preliminary Water-Nitrogen Co-Injection Test 115
5.2.8 Overall Evaluation 115
5.3 Nitrogen-Surfactant Co-Injection Runs 118
5.3.1 Typical Nitrogen-Surfactant Co-Injection Run 118
5.3.2 Effect of Surfactant Concentration 129
5.3.2.1 Core Absolute Permeability 3.5 to 8.1 darcies 134
5.3.2.2 Absolute Permeability Range 12.2 darcies to 17.5 darcies 149
5.3.2.3 Absolute Permeability Range 28.7 to 30 darcies 167
5.3.2.4 Absolute Permeability 0.65 darcies 176
5.3.2.5 Overall Evaluation of the Interrelationship of Surfactant Concentration and Absolute Permeability 181
5.3.3 Effect of Temperature 186
5.3.3.1 Surfactant SD1000 186

5.3.3.2 Dow Surfactant..........207
5.3.4 Effect of Oil Saturation..........218
5.3.5 Effect of Surfactant Type..........234
5.3.6 Effect of Residual Gas Saturation..........239
5.3.7 Effect of the Foam Generator..........245
5.3.8 Effect of Surfactant-Nitrogen Ratio..........251
5.3.9 Effect of Nitrogen Injection Without Surfactant Co-Injection..........256
5.4 Dual Core Runs..........260
5.5 Mathematical Model of Foam Flow in a Porous Medium..........282
5.5.1 Mathematical Foundations..........285
5.5.2 Solution Technique..........288
5.6 Discussion of Numerical Simulator Results..........291
5.6.1 Adsorption..........291
5.6.2 Relative Permeability..........293
5.6.3 Effect of Absolute Permeability..........293
5.6.4 Comparison of Experimental and Numerical Simulator Results..........294
VI Conclusions..........305

List of Tables

Table Page

5.1 List of Preliminary Runs 72
5.2 List of Co-Injection Runs 73
5.3 Comparison of Packing Methods 80
5.4 Experimental Data for Run 1P Water Base Case 81
5.5 Experimental Data for Run 2P: 1% SD1000 84
5.6 Experimental Data for Run 3P: 5% SD1000 86
5.7 Experimental Data for Run 4P: 1% XP100 90
5.8 Experimental Data for Run 5P: 5% XP100 93
5.9 Experimental Data for Run 6P: 1% Dow surfactant 97
5.10 Experimental Data for Run 7P: 5% Dow surfactant 99
5.11 Experimental Data for Run 8P: 1% Dow surfactant Vertically Oriented Core 103
5.12 Experimental Data for Run 9P: 5% Dow surfactant Vertically Oriented Core 105
5.13 Experimental Data for Run 11: 1% SD1000 119
5.14 Experimental Data for Run 21: NoSurfactant 130
5.15 Experimental Data for Run 1: 1% SD1000 135
5.16 Experimental Data for Run 19: 2.5% SD1000 138
5.17 Experimental Data for Run 3: 5% SD1000 143
5.18 Experimental Data for Run 7: 1% SD1000 150
5.19 Experimental Data for Run 18: 2.5% SD1000 156
5.20 Experimental Data for Run 5: 5% SD1000 160
5.21 Experimental Data for Run 17: 1% SD1000 169
5.22 Experimental Data for Run 6: 5% SD1000 174
5.23 Experimental Data for Run 14: 1% SD1000 179
5.24 Experimental Data for Run 13: 1% SD1000 54°C 188
5.25 Experimental Data for Run 16: 1% SD1000 90°C 193
5.26 Experimental Data for Run 9: 1% SD1000 90°C 198
5.27 Experimental Data for Run 15: 1% SD1000 125°C 203
5.28 Experimental Data for Run 23: 1% Dow surfactant 209
5.29 Experimental Data for Run 27: 1% Dow surfactant 125°C 214

Table Page

5.30 Experimental Data for Run 8:
No Surfactant Residual Oil Saturation 219
5.31 Experimental Data for Run 2: 1% SD1000
Residual Oil Saturation 223
5.32 Experimental Data for Run 4: 5% SD1000
Residual Oil Saturation 226
5.33 Experimental Data for Run 22: 5% SD1000
Residual Oil Saturation 125° C 231
5.34 Experimental Data for Run 10: 1% SD1000
Residual Gas Saturation 240
5.35 Experimental Data for Run 12: 1% SD1000
No Foam Generator 247
5.36 Experimental Data for Run 20: 1% SD1000
Quality = 72% 254
5.37 Experimental Data for Run 24: 1% Dow surfactant
No Continuous Surfactant Injection 261
5.38 Experimental Data for Run 25 Core A:
1% SD1000 Dual Core Run 267
5.39 Experimental Data for Run 25 Core C:
1% SD1000 Dual Core Run 269
5.40 Experimental Data for Run 26 Core A:
1% SD1000 125°C Dual Core Run 273
5.41 Experimental Data for Run 26 Core B:
1% SD1000 125°C Dual Core Run 274
5.42 Experimental Data for Run 27 Core A:
1% SD1000 125°C Dual Core Run 278
5.43 Experimental Data for Run 27 Core B:
1% SD1000 125°C Dual Core Run 280

List of Figures

Figure Page

4.1 Preliminary Run Equipment Configuration.......35
4.2 Refractive Index vs. Brine Concentration (By Weight).......44
4.3 Nitrogen-Surfactant Co-Injection Equipment.......49
4.4 Single Core Outlet System.......50
4.5 Nitrogen-Surfactant Co-Injection for Dual Core Run.......51
4.6 Dual Core Outlet System.......52
4.6A Foam Generator Schematic.......57
4.7 Refractive Index vs. Surfactant Concentration.......63
4.8 Crossplot of Concentration Determined by Spectrophotomoter and Refractive Index vs. Concentration.......65
4.9 Concentration Determined By Spectrophotometric Analysis vs. Concentration.......66
5.1 Flow Chart of Nitrogen-Surfactant Co-Injection Run.......77
5.2 Run 1P: Cumulative Volume Produced vs. Time.......82
5.3 Run 2P: Cumulative Water Produced vs. Time.......85
5.4 Run 3P: Cumulative Water Produced vs. Time.......87
5.5 Cumulative Volume Produced and Time to Gas Breakthrough vs. SD1000 Surfactant Concentration.......89
5.6 Run 4P: Cumulative Water Produced vs. Time.......91
5.7 Run 5P: Cumulative Water Produced vs. Time.......94
5.8 Cumulative Volume Produced and Time to Gas Breakthrough vs. XP100 Surfactant Concentration.......95
5.9 Run 6P: Cumulative Water Produced vs. Time.......98
5.10 Run 7P: Cumulative Water Produced vs. Time.......100
5.11 Cumulative Volume Produced and Time to Gas Breakthrough vs. Dow Surfactant Concentration.......101
5.12 Run 8P: Cumulative Water Produced vs. Time.......104
5.13 Run9P: Cumulative Water Produced vs. Time.......107
5.14 Cumulative Volume Produced and Time to Gas Breakthrough vs. Dow Surfactant Concentration With Core Oriented Vertically.......108

Figure Page

5.15 Comparison of Run 10P and Run 11P Volume Water Produced vs. Volume Injected 110
5.16 Comparison of Run 10P and Run 11P Fraction of Instantaneous Volume of Fluid Produced To Volume Injected vs. Cumulative Volume Injected 111
5.17 Comparison of Run 10P and Run 11P Pressure Drop Across the Core vs. Cumulative Nitrogen Injected 113
5.18 Run 11P: Pressure Drop Across the Core vs. Injection Time 114
5.19 Run 12P: Pressure Drop Across the Core vs. Nitrogen Co-Injection With Water 116
5.20 Run 11: Pressure Drop vs. Time, Nitrogen-Surfactant Co-Injection, 1% SD1000 122
5.21 Run 11: Cumulative Volume Produced vs. Time, Nitrogen-Surfactant Co-Injection, 1% SD1000 125
5.22 Concentration Determined by UV Spectrophotometer Analysis vs. Corrected Cumulative Volume Produced, Nitrogen-Surfactant Co-Injection, 1% SD1000 128
5.23 Run 21: Cumulative Volume Produced vs. Time, No Surfactant 131
5.24 Run 21: Pressure Drop vs. Time, No Surfactant 133
5.25 Run 1: Cumulative Volume Produced vs. Time, Nitrogen-Surfactant Co-Injection, 1% SD1000 136
5.26 Run 1: Pressure Drop vs. Time, Nitrogen-Surfactant Co-Injection, 1% SD1000 137
5.27 Run 19: Cumulative Volume Produced vs. Time, Nitrogen-Surfactant Co-Injection, 1% SD1000 139
5.28 Run 19: Pressure Drop vs. Time, Nitrogen-Surfactant Co-Injection, 1% SD1000 141
5.29 Run 19: Concentration Determined by UV Spectrophotometer Analysis vs. Corrected Cumulative Volume Produced, Nitrogen-Surfactant Co-Injection, 5% SD1000 142

Figure Page

5.30 Run 3: Cumulative Volume Produced vs. Time, Nitrogen-Surfactant Co-Injection, 5% SD1000....144
5.31 Run 3: Pressure Drop vs. Time, Nitrogen-Surfactant Co-Injection, 5% SD1000....146
5.32 Comparison of Runs: 1, 19, 3, and 12P Crossplot of Total Mobility and Relative Mobility vs. Concentration of SD1000....147
5.33 Comparison of Runs: 1, 19, 3, and 12P Mobility Reduction Factor vs. Concentration of SD1000....148
5.34 Run 7: Cumulative Volume Produced vs. Time, Nitrogen-Surfactant Co-Injection, 1% SD1000....151
5.35 Run 7: Pressure Drop vs. Time, Nitrogen-Surfactant Co-Injection, 1% SD1000....153
5.36 Run 7: Concentration Determined by UV Spectrophotometer Analysis vs. Corrected Cumulative Volume Produced, Nitrogen-Surfactant Co-Injection, 1% SD1000....154
5.37 Run 18: Cumulative Volume Produced vs. Time, Nitrogen-Surfactant Co-Injection, 2.5% SD1000....157
5.38 Run 18: Pressure Drop vs. Time, Nitrogen-Surfactant Co-Injection, 2.5% SD1000....158
5.39 Run 18: Concentration Determined by UV Spectrophotometer Analysis vs. Corrected Cumulative Volume Produced, Nitrogen-Surfactant Co-Injection, 2.5% SD1000....159
5.40 Comparison of Runs: 21, 11, 7, 18 and 5 Crossplot of Gas Breakthrough Times and Volumes vs. Concentration of SD1000....161
5.41 Run 5: Cumulative Volume Produced vs. Time, Nitrogen-Surfactant Co-Injection, 5% SD1000....163
5.42 Run 5 Pressure Drop vs. Time, Nitrogen-Surfactant Co-Injection, 5% SD1000....164
5.43 Run 5: Concentration Determined by UV Spectrophotometer Analysis vs. Corrected Cumulative Volume Produced, Nitrogen-Surfactant Co-Injection, 5% SD1000....165

Figure Page

5.44 Comparison of Runs: 11, 7, 18, 5 and 21 Crossplot of Total Mobility and Relative Mobility vs. Concentration of SD1000 166

5.45 Comparison of Runs: 11, 7, 18, 5 and 21 Mobility Reduction Factor vs. Concentration of SD1000 168

5.46 Run 17: Cumulative Volume Produced vs. Time, Nitrogen-Surfactant Co-Injection, 1% SD1000 170

5.47 Run 17: Pressure Drop vs. Time, Nitrogen-Surfactant Co-Injection, 1% SD1000 172

5.48 Run 17: Concentration Determined by UV Spectrophotometer Analysis vs. Corrected Cumulative Volume Produced, Nitrogen-Surfactant Co-Injection, 1% SD1000 173

5.49 Run 6: Cumulative Volume Produced vs. Time, Nitrogen-Surfactant Co-Injection, 5% SD1000 175

5.50 Run 6 Pressure Drop vs. Time, Nitrogen-Surfactant Co-Injection, 5% SD1000 177

5.51 Run 6: Concentration Determined by UV Spectrophotometer Analysis vs. Corrected Cumulative Volume Produced, Nitrogen-Surfactant Co-Injection, 5% SD1000 178

5.52 Run 14: Cumulative Volume Produced vs. Time, Nitrogen-Surfactant Co-Injection, 1% SD1000 Consolidated Core 180

5.53 Run 14: Pressure Drop vs. Time, Nitrogen-Surfactant Co-Injection, 1% SD1000 Consolidated Core 182

5.54 Run 14: Concentration Determined by UV Spectrophotometer Analysis vs. Corrected Cumulative Volume Produced, Nitrogen-Surfactant Co-Injection, 1% SD1000 Consolidated Core 183

5.55 Comparison of Runs: Crossplot of Relative Mobility vs. Concentration of SD1000 185

5.56 Comparison of Runs: Crossplot of Total Mobility vs. Concentration of SD1000 187

5.57 Run 13: Cumulative Volume Produced vs. Time, Nitrogen-Surfactant Co-Injection, 1% SD1000 54°C 189

Figure Page

5.58 Run 13: Pressure Drop vs. Time, Nitrogen-Surfactant Co-Injection, 1% SD1000 54°C 191
5.59 Run 13: Concentration Determined by UV Spectrophotometer Analysis vs. Corrected Cumulative Volume Produced, Nitrogen-Surfactant Co-Injection, 1% SD1000 54°C 192
5.60 Run 16 Cumulative Volume Produced vs. Time, Nitrogen-Surfactant Co-Injection, 1% SD1000 90°C 194
5.61 Run 16: Pressure Drop vs. Time, Nitrogen-Surfactant Co-Injection, 1% SD1000 90°C 195
5.62 Run 16: Concentration Determined by UV Spectrophotometer Analysis vs. Corrected Cumulative Volume Produced, Nitrogen-Surfactant Co-Injection, 1% SD1000 90°C 197
5.63 Run 9 Cumulative Volume Produced vs. Time, Nitrogen-Surfactant Co-Injection, 1% SD1000 90°C 199
5.64 Run 9: Pressure Drop vs. Time, Nitrogen-Surfactant Co-Injection, 1% SD1000 90°C 200
5.65 Run 9: Concentration Determined by UV Spectrophotometer Analysis vs. Corrected Cumulative Volume Produced, Nitrogen-Surfactant Co-Injection, 1% SD1000 90°C 201
5.66 Run 15 Cumulative Volume Produced vs. Time, Nitrogen-Surfactant Co-Injection, 1% SD1000 125°C 204
5.67 Run 15: Pressure Drop vs. Time, Nitrogen-Surfactant Co-Injection, 1% SD1000 125°C 205
5.68 Comparison of the Differential Pressure for Runs Conducted at Elevated Temperatures 206
5.69 Run 15: Concentration Determined by UV Spectrophotometer Analysis vs. Corrected Cumulative Volume Produced, Nitrogen-Surfactant Co-Injection, 1% SD1000 125°C 208
5.70 Run 23 Cumulative Volume Produced vs. Time, Nitrogen-Surfactant Co-Injection, 1% Dow Surfactant 210

Figure Page

5.71 Run 23: Pressure Drop vs. Time, Nitrogen-Surfactant Co-Injection, 1% Dow Surfactant 211

5.72 Run 23: Concentration Determined by UV Spectrophotometer Analysis vs. Corrected Cumulative Volume Produced, Nitrogen-Surfactant Co-Injection, 1% Dow Surfactant 213

5.73 Run 27 Cumulative Volume Produced vs. Time, Nitrogen-Surfactant Co-Injection, 1% Dow Surfactant 125°C........215

5.74 Run 27: Pressure Drop vs. Time, Nitrogen-Surfactant Co-Injection, 1% Dow Surfactant 125°C........216

5.75 Run 27: Concentration Determined by UV Spectrophotometer Analysis vs. Corrected Cumulative Volume Produced, Nitrogen-Surfactant Co-Injection, 1% Dow Surfactant 125°C........217

5.76 Run 8: Cumulative Volume Produced vs. Time, Nitrogen-Surfactant Co-Injection, Residual Oil Saturation No Surfactant........220

5.77 Run 8: Pressure Drop vs. Time, Nitrogen-Surfactant Co-Injection, Residual Oil Saturation No Surfactant........221

5.78 Run 2 Cumulative Volume Produced vs. Time, Nitrogen-Surfactant Co-Injection, Residual Oil Saturation1% SD1000........224

5.79 Run 2: Pressure Drop vs. Time, Nitrogen-Surfactant Co-Injection, Residual Oil Saturation 1% SD1000 225

5.80 Run 4 Cumulative Volume Produced vs. Time, Nitrogen-Surfactant Co-Injection, Residual Oil Saturation 5% SD1000........227

5.81 Run 4: Pressure Drop vs. Time, Nitrogen-Surfactant Co-Injection, Residual Oil Saturation 5% SD1000........229

5.82 Run 4: Concentration Determined by UV Spectrophotometer Analysis vs. Corrected Cumulative Volume Produced, Nitrogen-Surfactant Co-Injection, Residual Oil Saturation 5% SD1000 230

Figure Page

5.83 Run 22 Cumulative Volume Produced vs. Time, Nitrogen-Surfactant Co-Injection, Residual Oil Saturation 1% SD1000 125°C 232

5.84 Run 22: Pressure Drop vs. Time, Nitrogen-Surfactant Co-Injection, Residual Oil Saturation 1% SD1000 125°C 233

5.85 Comparison of the Relative Mobility for Runs 2, 4, 8, and 22 235

5.86 Comparison of the Differential Pressure for Run 11 and Run 23, SD1000 and Dow Surfactants, Respectively 237

5.87 Comparison of the Differential Pressure for Run 15 and Run 27, SD1000 and Dow Surfactants Respectively 125°C 238

5.88 Run 10 Cumulative Volume Produced vs. Time, Nitrogen-Surfactant Co-Injection, Residual Gas Saturation 1% SD1000 241

5.89 Comparison of the Cumulative Volumes Produced for Run 10 (Residual Gas Saturation) and Run 11, 1% SD1000 242

5.90 Run 10: Pressure Drop vs. Time, Nitrogen-Surfactant Co-Injection, Residual Gas Saturation 1% SD1000 243

5.91 Comparison of the Differential Pressure for Run 10 (Residual Gas Saturation) and Run 11, 1% SD1000 244

5.92 Run 10: Concentration Determined by UV Spectrophotometer Analysis vs. Corrected Cumulative Volume Produced, Nitrogen-Surfactant Co-Injection, Residual Gas Saturation 1% SD1000 246

5.93 Run 12: Cumulative Volume Produced vs. Time, Nitrogen-Surfactant Co-Injection, No Foam Generator 1% SD1000 248

5.94 Comparison of the Cumulative Volumes Produced for Run 12 (No Foam Generator) and Run 11, 1% SD1000 249

5.95 Run 12: Pressure Drop vs. Time, Nitrogen-Surfactant Co-Injection, No Foam Generator 1% SD1000 250

Figure Page

5.96 Comparison of the Differential Pressure for Run 12 (No Foam Generator) and Run 11, 1% SD1000 252
5.97 Run 12: Concentration Determined by UV Spectrophotometer Analysis vs. Corrected Cumulative Volume Produced, Nitrogen-Surfactant Co-Injection, No Foam Generator 1% SD1000 253
5.98 Run 20 Cumulative Volume Produced vs. Time, Nitrogen-Surfactant Co-Injection, Quality=72.0 % 1% SD1000 255
5.99 Run 20: Pressure Drop vs. Time, Nitrogen-Surfactant Co-Injection, 1% SD1000 Quality=72.0 %....................257
5.100 Comparison of the Differential Pressure for Run 20 (No Foam Generator) and Run 11, 1% SD1000 Quality=72.0 % 258
5.101 Run 20: Concentration Determined by UV Spectrophotometer Analysis vs. Corrected Cumulative Volume Produced, Nitrogen-Surfactant Co-Injection, 1% SD1000 Quality=72.0 % 259
5.102 Run 24: Cumulative Volume Produced vs. Time, Nitrogen Injection, 1% Dow Surfactant 125°C....................262
5.103 Comparison of the Cumulative Volumes Produced vs. Time for Run 27 and Run 24 (No Surfactant Injection), 1% Dow Surfactant 263
5.104 Run 24 Pressure Drop vs. Time, Nitrogen Injection, 1% Dow Surfactant 125°C....................264
5.105 Comparison of the Differential Pressure for Run 24 (No Surfactant Co-Injection) and Run 27 1% Dow Surfactant 125°C....................265
5.106 Run 25A: Concentration Determined by UV Spectrophotometer Analysis vs. Corrected Cumulative Volume Produced, Nitrogen-Surfactant Co-Injection, 1% SD1000 Dual Core Experiments 268

Figure Page

5.107 Comparison of the Cumulative Volumes Produced vs. Time for Run 25: Core A and Core C, 1% SD1000 Dual Core Experiments....270

5.108 Run 25: Pressure Drop vs. Time, Nitrogen-Surfactant Co-Injection, 1% SD1000 Dual Core Experiments....271

5.109 Run 26B: Cumulative Volume Produced vs. Time, Nitrogen Injection, 1% SD1000 125°C Dual Core Experiments....275

5.110 Comparison of the Cumulative Volumes Produced vs. Time for Run 26: Core A and Core B, 1% SD1000 125°C Dual Core Experiments....276

5.111 Run 26: Pressure Drop vs. Time, Nitrogen-Surfactant Co-Injection, 1% SD1000 125°C Dual Core Experiments....277

5.112 Comparison of the Cumulative Volumes Produced vs. Time for Run 28: Core A and Core B, 1% SD1000 125°C Dual Core Experiments....281

5.112A Flow Diagram for Numerical Simulator....292

5.113 Comparison of Experimental and Simulated Results of Differential Pressure for Run 11....295

5.114 Comparison of Experimental and Simulated Results of Differential Pressure for Run 18....297

5.115 Comparison of Experimental and Simulated Results of Differential Pressure for Run 5....298

5.116 Comparison of Experimental and Simulated Results of Differential Pressure for Run 14....299

5.117 Comparison of Experimental and Simulated Results of Differential Pressure for Run 17....300

5.118 Comparison of Experimental and Simulated Results of Differential Pressure for Run 13....302

5.119 Comparison of Experimental and Simulated Results of Differential Pressure for Run 15....303

5.120 Comparison of Experimental and Simulated Results of Differential Pressure for Run 16....304

List of Plates

Page

Plate 1: Co-injection Equipment 48

Plate 2: Oven Interior 55

Plate 3: Outlet System 60

Nomenclature

A	Cross-sectional area, m^2
A	Constant
B	Constant
B_g	Formation volume factor for gas, m^3/sm^3
B_w	Formation volume factor for water, m^3/sm^3
C_{ws}	Surfactant concentration, mass fraction
D	Constant
k	Absolute permeability, m^2
k_{rw}	Relative permeability to water, fraction
k_{rg}	Relative permeability to gas, fraction
K_1, K_2	Constants
p	Pressure, Pa
p_1, p_2	Constants
p_g	Gas phase pressure, Pa
p_{cgw}	Gas-water capillary pressure, Pa
p_w	Water phase pressure, Pa
q_g^*	Gas injection rate per unit volume of rock, sm^3/m^3-s
q_w^*	Water injection rate per unit volume of rock, sm^3/m^3-s
S_g	Gas saturation, fraction
S_o	Oil saturation, fraction
S_w	Water saturation, fraction
S_{wr}	Irreducible water saturation, fraction
t	Time, s
V_b	Block volume, m^3
Z	Depth below a reference point, m

Δx	Block length, m
μ_{fm}	Effective viscosity of foam, Pa·s
μ_g	Gas phase viscosity, Pa·s
μ_w	Water phase viscosity, Pa·s
ρ_r	Rock density, kg/m^3
ρ_w	Water phase density, kg/sm^3
ϕ	Porostiy, fraction
Φ_w	$= p_w - \rho_w gZ$, Pa

I Introduction

Foam, in the petroleum industry, has been used successfully in a number of areas, which include drilling, cementing and well workovers. The possibility of using foam as a secondary recovery method to lower gas phase mobility, and consequently improve the mobility ratio, is examined in this study.

Foam tested outside the porous medium exhibits non-Newtonian behaviour, with a high apparent viscosity. This has made researchers investigate the possibility of injecting a foam, or creating one in-situ, as a secondary recovery process. There have been a few field tests, with very limited success.

Another use of foam, rather than to use it to improve mobility ratio, is the possibility of using foam to preferentially block highly permeable channels.

The emphasis of this work was on the foam flooding conducted with co-injected surfactant solution and nitrogen. The purpose of this research was two-fold: to analyze to effect of surfactant, added in different ways to a gas flood, and to analyze the effect on foam formation, of surfactant concentration, oil saturation, and absolute permeability. In this way it was possible to analyze the assumptions upon which foam simulators are based.

II Statement of the Problem

The main objectives of this research project were as follows:

1. To design and build experimental apparatus developed to analyze foam flow at elevated temperatures (up to 250° C) and pressure (500 psi). The design criteria for this experimental equipment were:
    - i) to develop a system whereby gas and surfactant injection rates can be controlled independently.
    - ii) to develop experimental apparatus whereby sightglasses are used to view foam at different points along the system, at experimental conditions.
    - iii) to develop a sampling method for the effluent that would not significantly change the outlet conditions.

2. To conduct a series of experimental runs to examine the effect of changing variables. These variables include:
    - i) temperature
    - ii) absolute permeability
    - iii) surfactant concentration
    - iv) surfactant type
    - v) oil saturation
    - vi) use of a foam generator.

3. To examine the results of the mathematical foam simulator that was developed in this research and consequently used to examine the assumptions utilized in developing the simulator.

III Literature Review

Foam is a gas-liquid dispersion formed by mixing a gas and a liquid. This liquid must contain a surface-active agent. The surface energy of gas-liquid foams naturally tends to decrease, hence, these foams are thermodynamically unstable.

The uses of foam in the petroleum industry include drilling (and completion), cementing, workovers, and secondary recovery. There has been a suggestion that foams could be used to prevent gas leakage from underground storage reservoirs.[1,2,3] As a drilling fluid, foams have the advantage of low water content, and therefore are suitable in underpressured or water sensitive reservoirs.[1,3,4] For cementing work, foams offer the advantage of reduced cement utilization and decreased cement weight. Foams are used in secondary recovery because of their low mobility, and/or due to their ability to act as temporary blocking agents.

3.1 Foam Characterization

There are a number of criteria which must be looked at when attempting to characterize a foam: quality, texture, stability, and resiliency.

Quality (Γ) is the ratio of gas volume to the total volume (the volume of gas plus the liquid volume). Terms used to define quality are: high, low, wet, and dry.

$$\Gamma = \frac{\text{gas volume}}{\text{total foam volume}} \tag{1}$$

According to Minssieux[3], foam quality can range from 50 to 99 per cent. Below a quality of 50 percent the foam mixture resembles suspended bubbles in a liquid and cannot be considered as a single phase. Friedmann and Jensen[5] found that at a quality below 50 per cent the "loose" foam broke down quickly.

Fried[6] identified foams by their expansion factor:

$$F_x = \frac{\text{total foam volume}}{\text{liquid volume}} \tag{2}$$

so,

$$\Gamma = 1 - \frac{1}{F_x}\,. \tag{3}$$

Due to the fact that the gas phase within a foam is compressible, foam quality depends on pressure. The relation has been shown[3,7,8] as:

$$\Gamma = \frac{1}{1 + \frac{p}{p_a}\left[\frac{1}{\Gamma_a} - 1\right]}\,. \tag{4}$$

Where Γ_a is quality at atmospheric conditions, p_a is atmospheric pressure, and Γ and p refer to test conditions. It is assumed that Boyle's Law applies, and that gas solubility is negligible.

For this to be true we must also assume the liquid volume is incompressible and $V_l = V_{la}$. Therefore, $PV_g = P_aV_{ga}$ where:

$$V_g = \frac{V_l}{\left[\frac{1}{\Gamma} - 1\right]} \tag{5}$$

and

$$V_{ga} = \frac{V_{la}}{\left[\frac{1}{\Gamma_a} - 1\right]} \tag{6}$$

hence,

$$\frac{P}{P_a} = \frac{\left[\frac{1}{\Gamma} - 1\right]}{\left[\frac{1}{\Gamma_a} - 1\right]} . \tag{7}$$

David and Marsden[14] determined, assuming that the compressibility of the liquid phase is negligible, that:

$$c_f = -\left[\frac{1}{V_f}\frac{\partial V_f}{\partial P}\right]_T \tag{8}$$

which is equivalent to

$$c_f = \frac{V_g}{V_g + V_l}\left[-\frac{1}{V_g}\frac{\partial V_g}{\partial p}\right]_T . \tag{9}$$

Therefore,

$$c_f = \Gamma\, c_g , \tag{10}$$

where c_f is the conpressiblity of the foam, c_g is the compressibilty of the gas, V_f is the total volume of the foam, and V_g is the volume of the gas phase.

Clark[9,10] described quality in terms of specific surface area per unit volume (cm^2/cc). An optical transmission method was also developed to determine texture based on the fact that light is reflected and scattered by randomly oriented interfaces.

Texture refers to the uniformity and size of bubbles. Texture can be defined in terms of: fine, coarse, homogeneous and nonhomogeneous. Intuitively, it would seem that finer textured foams have more gas-liquid interfaces per unit volume, hence a lower quality. Minssieux[3] found that the foam formed a structure that becomes more and more orderly as the proportion of gas becomes higher. In other words, the texture became more uniform as the quality increased.

Stability and resiliency both refer to the longevity and resistance to breakage of the foam. Minssieux[3] described two mechanisms by which foams decay. The first mechanism is the drainage of liquid and statistical rupture of films. When this is the dominant mechanism stability increases as quality increases. The second mechanism is the diffusion of gas between adjacent bubbles of different sizes. This is the dominant mechanism in the case where the liquid phase is very viscous. In this case, stability increases as quality decreases. Ross[11] also discussed the importance of gelatinous surface layers to reduce gravity drainage. It is important to stress that increasing quality does not, by definition, necessarily imply increasing stability or more favourable mobility.

Minssieux[3] found, with respect to resiliency, that foams can undergo a number of compressions and decompressions due to the elasticity of liquid films stabilized by surfactant molecules. It was also noted that this was contingent upon the amount of foam degradation.

Ross[11] described the thermodynamic instability of foam by the use of Gibb's function, for a one component system where surface energy is significant.

$$dG = VdP - SdT + \gamma dA \qquad (11)$$

where γ is interfacial tension and, A is surface area per mole.

At constant p and T:

$$\gamma = \left[\frac{\partial G}{\partial A} \right]_{p,T} . \tag{12}$$

Therefore,

$$\Delta G = \left[\gamma \Delta A \right]_{p,T} . \tag{13}$$

The decrease in bubble area is caused by a decrease in Gibb's free energy, therefore a foam composed of a pure liquid is thermodynamically unstable. To ensure thermodynamic stability, the equation requires additional terms of opposite sign, such that the sign for the whole ΔG expression is changed. This can be brought about by a solute that is surface-active. The foam will continue to be mechanically fragile unless the continuous phase is a solid as in the case of foam insulation.

Considering the stability of a single vertical soap film, Lord Rayleigh[12] found that the surface tension above and below the film cannot be the same. The surface tension at the top of the film must be greater than at the lower portions, otherwise the central portion of the film would collapse. Ross[11] found that the persistence of a liquid film also depends on the presence of a coherent surface layer on each side of the film. Between these layers the excess liquid can flow downward.

Another important factor concerning stability as described by Ross[11,13], is the Marangoni effect. This describes the effect, whereby the movement of a surface layer from areas of low to areas of high surface tension is accompanied by the motion of relatively thick layers of underlying fluid. This can amount to several microns in depth. This allows for the renewal of lost liquid.

3.2 The Mechanism of Foam Flow

There has been much written about the mechanism of foam flow. The simplest mechanism, which has been accepted by several investigators[3,6,8,14], is that the foam components flow simultaneously through pore channels. Khan[9] agreed, stating that the flow regime was an intimate gas-liquid mixture. This approach allowed the application of Darcy's law as it pertains to foam as a homogeneous body, with gas and liquid flowing at the same rate, with a high apparent viscosity. Albrecht and Marsden[2] felt that gas and liquid flow with the same average velocity. The utility of Darcy's law for foam as a single phase will be discussed in a subsequent section.

The ability of foam to flow as a single homogeneous unit was discussed by Dietz, Bruining, and Heijna[15]. They analyzed the minimum bubble size that can be formed within a foam, based upon a minimum film thickness of 50 Å. After an analysis of the pore size distribution within sandpacks they ascertained that the foam bubbles are generally too large to flow within the pore structure. For a foam of 95 per cent quality the absolute permeability necessary was 18 darcies. Therefore they postulated that foam would not flow as a homogeneous body under normal reservoir conditions, so the term "foam-drive" is meaningless.

The exact mechanism of foam flow has not been identified, however, there has been a progression of ideas toward a common theory. One early reference to flow mechanism was made by Bernard, Holm, and Jacobs[16]. They reported that gas was the discontinuous phase and liquid was continuous. Since the liquid films contact each other the liquid is conducted between the films. In this way the liquid flows relatively uninhibited by the gas. The velocity of the gas and liquid are not the same. Holm[1] later reported that gas moved through the system by breaking and reforming bubbles and the liquid moved through the film network. Other investigators[1,17] suggested that a large portion of the gas was trapped in the system and a small fraction flowed according to Darcy's law.

Mast[18] reported that some liquid and gas were transported as foam, the amount, however, was dependent upon foam stability. He felt that a stable foam would be transported primarily as a foam, although some breakage and foam regeneration would occur.

Owete and Brigham[19] described the behaviour of foam, as observed in micromodels of differing pore structure and dimensions. They observed that the liquid flow was continuous through the lamellae. The orientation of the films separating air bubbles was either diagonal to the direction of the flow between matrix grains or horizontal, that is, perpendicular to the direction of flow. The horizontal films tend to collapse as the pressure in the system builds up. The diagonal films, which form early, tend to retain the positions and orientation. The diagonal films continually thin, draining liquid through the film network. The air moves through the system as long bubbles, whose shapes are defined by the matrix grains and diagonal films.

The pore structure was found to influence greatly the flow mechanism. In the homogeneous model the displacement of lamellae was the dominant mechanism. It was observed that, on occasion, local pore pressure caused the air to displace liquid in a direction opposite to the general flow. These reverse flows can cause liquid or gas to be trapped in some pore spaces.

For the heterogeneous model the dominant mechanism was "break and reform". This mechanism is described as "snap off". In this instance the "parent-bubble" recedes while the dislodged portion propagates through the pore system.

From the previous discussion, it is unlikely that foam flows through the pore structure as a homogeneous unit. It appears that the gas component flows by "breaking and reforming" and the liquid propagates through the film network, as a free phase for heterogeneous models, and that flow occurs by the displacement of lamellae for homogeneous models.

3.3 Mobility

One of the main problems encountered in secondary recovery is the problem of channelling as a result of gravity override. In an attempt to divert displacing fluid to unswept zones the use of foam has been proposed. Foam, as the displacing fluid, is also used to obtain a more favourable mobility ratio with the displaced fluid. Fried[6] generated foam externally and injected it into a porous medium, which had previously been subjected to a conventional gas or water drive, and found that additional oil could be recovered. He attributed the incremental recovery to an increased apparent viscosity and decreased effective gas permeability. While injecting the foam, the pressure drop across the core increased significantly. In some cases, for very stable foams, the flow was effectively "plugged off". Raza[20] found the pressure drop occurs mainly across foam-filled portions of the medium.

Bernard[21] reported increased displacement efficiency by foams generated in-situ. He accomplished this in two ways. In the first case, the core was completely saturated with fluids, oil or water, containing the foaming agent and followed this with a gas drive. In the second case, the core was saturated with surfactant-free fluids; a surfactant-containing slug was injected, followed by a gas drive. Albrecht and Marsden[2] and Owete, Al-Khafaji, Wang, Castanier, Sanyal, and Brigham[22] were some of the investigators who generated foam in-situ. Owete et al.[22] noted that in-situ foaming was operationally and economically more attractive than surface foaming. With in-situ foaming, Duerksen[23] and Isaacs, McCarthy, and Maunder[24] found constant regeneration is required for foam to be effective.

Bernard and Holm[25] found that gas permeability was much lower in the presence of foam, at the same gas saturation, than in its absence. The ability of foam to impede gas flow in a core saturated with water is generally agreed upon by all investigators. There is some controversy, as discussed in the previous section, about the mechanism and the virtue of labeling the process as "foam-flow".

Investigators have attempted to use Darcy's law to analyze the flow of foam ever since Bond and Holbrook[26] patented the idea of foam flow as a recovery method in 1958.

$$q = -\frac{kA}{\mu}\frac{dp}{dx} \tag{14}$$

The linear flow rate, the pressure gradient, and the cross sectional area can easily be measured. The effective permeability and apparent viscosity, however, are difficult to determine. This prompted Marsden and Khan[9] to look at how mobility, which is the effective permeability divided by apparent viscosity, changed with quality. They found that the mobility decreased almost linearly with increasing quality. All of the data did not fall on a single line, rather several straight lines, depending upon the permeability.

3.4 Gas Permeability

Foam is very effective in reducing the effective gas permeability in porous media. The permeability to water, though, according to Bernard, Holm, and Jacob[16], did not change whether foam was present or not. Therefore, relative permeabilitv to a liquid is a single-valued function of liquid saturation regardless of foam presence. They felt that the decreasing permeability to water was a function of an increased trapped gas saturation. Raza[20] found that the relative permeability to water at constant water saturation was dependent upon the flow rate. He concluded that the relative gas permeability-saturation relationship was not applicable for foam flow.

3.5 Rheology

In order to determine the apparent viscosity of foam it is important to understand foam rheology. Sibree[27] reported that foam has an apparent viscosity greater than its constituent phases. He also found that the apparent viscosity decreased with increasing shear to a certain point at which it becomes constant. Viscosity was measured by a concentric cylinder viscometer.

Raza and Marsden[14] studied the apparent viscosity of foam by the use of capillary tubes of different diameters. They found that at low shear rates foam flowed as a Newtonian fluid; at higher shear rates foam flowed as a pseudoplastic fluid. At even higher shear rates, corresponding to turbulent flow they suggested that foam might pass into a third regime and flow as a Newtonian fluid. Grove, Wise, Marsh, and Gray[28] found that the apparent viscosity of foam was constant, with increasing shear rate. Grove et al.[28] analyzed foam under conditions of turbulent flow.

Raza and Marsden[14] characterized the type of behaviour the foam exhibited by the analytical method developed by Mooney[29].

$$S = K\left(\frac{d\bar{u}}{dr}\right)^n \qquad (15)$$

where S is the shear stress,

$$\frac{d\bar{u}}{dr} = \text{shear rate},$$

K is the consistency index, $\bar{u}$ is the average or bulk velocity, and n is the flow behaviour index.

From this it follows that

$$\frac{r_i \Delta P}{2L} = K\left(\frac{4\,\bar{u}}{r_i}\right)^n = K\left(\frac{4\,q}{\pi\, r_i^3}\right)^n, \tag{16}$$

where ΔP is the pressure drop, L is the length, q is the volumetric flow rate, and r_i is the internal radius.

Raza and Marsden[14] describe that a logarithmic plot of

$$\frac{r_i \Delta P}{2L} \text{ vs. } \frac{4\bar{u}}{r_i} \tag{17}$$

provided values for K and n. For a Newtonian fluid n is unity and exhibits a parabolic velocity distribution across the diameter of the capillary tube. When the flow enters the second regime, where foam behaves as a pseudoplastic, the value of n is less than unity. This value of the behaviour index indicates a more piston-like flow. Within the capillary tube most of the shear takes place at the tube wall. The majority of the fluid flows as a slightly-sheared plug in the centre of the tube.

The data was further analyzed to calculate the effect of surface slip. A plot of

$$\frac{4\bar{u}}{r_i} \text{ vs. } \frac{1}{r_i} \qquad (18)$$

at selected shear rates did not produce a straight line. The nonlinearity suggested that there were other factors influencing the measurements that completely overshadowed the effect of surface slip.

Patton, Holbrook, and Hsu[30] also attempted to use Mooney's method to calculate the effect of surface slip. They determined that a fixed-slip velocity could not be calculated, which shows that bubbles both slip and flow simultaneously. This indicated that foam does not behave as rigid particles.

Blauer, Mitchell, and Kohlhaas[31] concluded that foam behaved as a Bingham plastic fluid. Reidenbach, Harris, Lee, and Lord[32] described foam as a yield pseudoplastic fluid when the flow was laminar.

Apparent viscosity, as measured in capillary tubes, has been studied by several investigators. Fried[6] found that apparent viscosity was proportional to the capillary radius. Raza and Marsden[14] found apparent viscosity increased proportionally with the fourth power of the capillary radius. Hirasaki and Lawson[33] found that apparent viscosity increased proportionally with the square of the capillary radius for a large tube radius compared to bubble size and increased to the power of 2.5 for a small radius compared to bubble size. After performing their capillary tube studies, they felt that texture was a key parameter in foam analysis. The flow mechanism, lamellae per unit length, and the radius of curvature at the gas liquid interface were all greatly effected by the foam texture. It should be noted here that Best, Tam, and Isaacs[34] felt that unless apparent viscosity of foam was studied in a vessel several orders of magnitude larger than the foam bubbles, wall effects dominated its rheology.

Another conclusion drawn by these investigators[6,13,30,33] was that the apparent viscosity increased with increasing quality. Marsden and Khan[9] found that apparent viscosity increased almost linearly with increasing quality at a constant shear rate. Their experiments were conducted in a viscometer which was modified by the addition of fins. It was felt that this would immobilize a layer of foam, and allow the shear within the foam itself to be obtained. They also found that apparent viscosity decreased with increasing shear. David and Marsden[8] analyzed apparent viscosity data and found, after correcting for slip, that apparent viscosity was independent of quality.

There is a problem associated with apparent viscosity determined externally and utilizing it for foam flow within porous media. The apparent viscosity must be determined at the same shear rate, due to the fact that foams behave as non-Newtonian fluids. The significance of externally generated apparent viscosity data is in the trends that are observed as shear rate or quality are increased.

3.6 Foam Flow Analysis

To analyze foam, but avoid the problem of finding effective permeability and apparent viscosity, Maini[37] studied the mobility reduction factor. He compared the mobility of a foam with a standard, either steam or water. This enabled him to compare different types of foam.

Best et al.[34] felt the mechanism of foam flow was best modelled by changes in gas phase permeability, which was best represented by changes in effective permeability, not absolute viscosity, of the gas phase. They obtained effective permeability for each phase by achieving steady state flow and applying Darcy's law to each phase. The saturation was obtained by a careful material balance. Minssieux[3] analyzed foam, by Darcy's law, as a single fluid. He analyzed foams by

$$\frac{dp}{dx} = \frac{q\mu_{foam}}{kA}, \qquad (19)$$

in terms of mass,

$$w = q \cdot \gamma_f , \tag{20}$$

with

$$\gamma_f = 1 + \Gamma(\gamma_g - 1) \tag{21}$$

where γ_f is the specific gravity of foam, γ_g is the specific gravity of gas, w is the foam flow rate, and

$$\mu_f = \frac{dp}{dx}\frac{kA}{w}\left(1 + \Gamma\left(\gamma_g - 1\right)\right). \tag{22}$$

Neglecting the weight of the gas phase,

$$\mu_f = \frac{dp}{dx}\frac{kA}{w}\left(1 - \Gamma\right). \tag{23}$$

By this relationship he determined that apparent viscosity decreased with increasing quality. This contradicted the apparent viscosity relationship obtained in a viscometer.

Heller, Lien, and Kuntamukkula[36] report that Minssieux calculated apparent foam viscosity from a standard viscometer and used these numbers to calculate a relative permeability using Darcy's law. As can be seen from the previous discussion this was not the procedure he used. Minssieux calculated the apparent viscosity by the use of Darcy's law as outlined previously. This accounts for

Minssieux's presentation of two very different apparent viscosity-quality graphical correlations.

3.7 Factors Influencing Foam Flow in Porous Media

3.7.1 Quality

Minssieux[3] found that the drive efficiency, which corresponds to the most favourable mobility ratio, was higher at lower foam quality. The lower quality foams showed more resistance to flow, hence the mobility ratio became more favourable with decreasing quality. This is also consistent with his calculated apparent viscosity versus quality relationship mentioned previously. Minssieux created foam in-situ and displaced a residual oil saturatation. He calculated the quality based on the injection conditions. Holm[1] found a decrease in mobility with decreasing quality; this is in agreement with Minssieux. Minssieux's quality-stability relationship, presented earlier, was that foam stability decreased as quality increased for a viscous liquid phase; foam stability increased with quality otherwise.

Marsden and Khan[8] found a decrease in mobility with increasing quality. Heller et al.[36] agreed, finding a slight decrease in mobility with increasing quality. These results are consistent with the investigators[6,13,30,33] who found an increase in apparent viscosity with increasing quality. When quality becomes very high, viscosity decreases rapidly. This was identified by Grove et al.[28], and later by Patton et al.[30].

3.7.2 Absolute Permeability

Bernard and Holm[25] reported that the foam was very effective in reducing the permeability to gas. They also report that the greater the specific permeability of the porous media, the greater was the effectiveness of foam in reducing gas permeability. In fact, they suggested that this effect would cause the selective plugging of highly permeable channels. This is explained in two ways by Best et al.[34]: the lower flux in a less permeable core causes a reduced shear rate, hence an increased apparent viscosity, and capillary resistance becomes more important once the viscous pressure drops.

Owete and Brigham[19] found that mobility reduction factors decreased to a constant value with absolute permeability but were quick to point out the differences in the experimental procedure.

3.7.3 Surfactant Type and Concentration

The type of foaming agent is important because of the adsorption on rock surfaces of some surfactants. Minssieux found that the anionic surfactants generated a low quality, but relatively stable, foam; nonionic surfactants generated a high quality, but unstable foam, while the cationic surfactants exhibited very high adsorption on the rock surfaces.

The effect of surfactant concentration on foam stability and quality was investigated by Raza[20]. He found that the foam quality increased with increasing concentration, up to a point at which further addition of surfactant had no effect on the quality. He found that the time to gas breakthrough increased with increased concentration initially but the addition of surfactant beyond this was detrimental and the breakthrough time actually decreased. Raza concluded that the addition of surfactant was beneficial up to the critical micelle concentration (CMC). Above this concentration the surfactant molecules grouped together and caused the foam films to lose stability and resiliency.

Maini and Ma[37] also observed the appearance of an optimum surfactant concentration, for stability and mobility reduction factor. They explained this phenomenon by looking at the surface tension gradient. When an interface is stretched, the surfactant concentration is locally reduced. This reduction in surfactant causes a surface tension gradient to be set up, which acts to eliminate surface deformation. When surface concentration is high, surface-active molecules are readily available in the immediate vicinity of the locally reduced concentration and will eliminate the surface tension gradient. Therefore a concentration which is too high (above CMC) will reduce the ability of the system to resist surface deformations (which are believed to be the precursor of film rupture). They also said that the optimum concentration for stability provided the most favourable mobility reduction factor. This evidence is disputed by a number of other researchers who suggest that there is no maximum.

Chiang, Sanyal, Castanier, Brigham, and Sufi[38] found that the average saturation behind the front was at the "optimum" surfactant concentration (CMC). They performed stability experiments and claim that the most stable foam occurred at the CMC. Interestingly, they justify this by explaining that the most stable foams have the shortest foam height. This implies that lower quality foams must be the most stable. As has been noted in previous sections, this is not an accepted fact. Beyond this, analysis of their relative foam height versus concentration graph, which demonstrates a number of time-line curves, shows that the largest decrease in relative foam height with time, occurred at the critical micelle concentration. It should also be noted that there is no definition stated in the article for relative foam height. Chiang et al.[38] also found that in-situ foaming increased in their model up to a certain point; after that an increase in surfactant had little effect on the performance of the process.

A similar effect has been found by many other researchers[19,24,39] where addition of surfactant beyond the optimum had no detrimental effect. Huh and Handy[39] found that the concentration for maximum stability of foams was higher than the critical micelle concentration. They also stated that micelle formation enhanced lamellae stability. Huh, Cochrane, and Kovarik[40] increased surfactant concentration far above the CMC. They found improved foam generation and reduced mobility with increased surfactant concentration up to 5%, which was the highest concentration that they tested. This was confirmed by Lee and Heller[41] who found decreasing mobility well above the CMC. Huh et al.[40] found that there was no significant change in bubble size with increasing surfactant concentration. They noted that the formation of micelles above the CMC accelerated the movement of surface active molecules to the interface, when the lamellae were stretched or experienced thinning. Owete and Brigham[19] also found that surfactant concentration did not change the basic flow mechanism for the homogeneous model. In the heterogeneous model the generation of more bubbles caused gas to flow through more pore channels, and decreased gas mobility up to a peak concentration, where the beneficial effects of increased saturation leveled off. He said that surfactant concentration probably influenced air mobility only to the extent that it affected the rate of thinning of the liquid films.

3.7.4 Pressure

Grove et al.[28] found that an increase in pressure caused a decrease in viscosity. He reasoned that increased pressure reduced the volume of air relative to the volume of liquid. This is equivalent to a foam of lower expansion factor, or one of lower quality. This is consistent with his finding that viscosity decreased with increasing foam density, stated in consistent terms, viscosity increased with increasing quality.

The effect of pressure on foam quality was also examined by Wang[42]. He found an increase in quality with increasing pressure. He also stated that increasing pressure promoted foam stability. This implies that increasing quality yields increasing stability. Friedmann and Jensen[5] found that low pressures were detrimental to foam stability within porous media.

3.7.5 Temperature

Wang[42] found that an increase in temperature decreased both the quality and stability of foam. Maini and Ma[37] found that foam decayed faster and liquid drained more rapidly as temperature increased. Robin[43] found that the efficiency of foams decreased considerably with temperature. This is probably due to the fact that the surfactant used decomposed or was unable to cause foam at high temperatures. Some surfactants are biodegradable; the chemical bond can be oxygenated or hydrolyzed. These effects can be catalyzed by reservoir rock components and all are accelerated by increased temperature according to Elson and Marsden[44]. Novosad, Maini, and Huang[45] found that adsorption decreased with an increase in temperature.

In an attempt to determine the thermal stability of surfactants several investigators[22,23,37,46,47] have developed screening tests. These screening tests generally include generating a foam at elevated temperatures and analyzing its stability.

Elson and Marsden[44] used screening techniques, and injected foaming solution followed by gas to test surfactants. They found that anionic surfactant generally had the greatest stability, while the nonionic ones were generally the least stable. Some foaming solutions known to foam well at room temperature did not foam at all at elevated temperatures. These were generally nonionic. They were, however, able to generate foam at 100°C, within a porous medium with the more thermally resistant foaming solutions. Owete et al.[22] was also able to generate foams in-situ under steam injection conditions. Isaacs et al.[24] found that for steam foams it was very important to have a non-condensable gas phase co-injected with steam.

Dilgren et al.[48] studied thermal resistivity of foaming agents and obtained good results with commercially available dodecylbenzene sodium sulphates. They also found that alpha olefin sodium sulphonates yielded stronger foams than the alkylbenzene sulphonates. Maini and Ma[37] ranked the sulphonate surfactants in terms of thermal stability, in order of descending stability as follows: alkylbenzene sulphonate, alpha olefin sulphonate, petroleum sulphonate. The results of the screening tests are difficult to relate to each other except to note that the sulphonates are widely used, and show the best thermal stability.

3.7.6 Oil Saturation

Many investigators[1,3,16] have noted the detrimental effect of oil saturation, on the ability of surfactants to form foam. Minssieux[3] equated this effect to a lack of stability. He noted that the use of a stabilizing agent, particularly one capable of increasing the viscosity of the aqueous phase, could alleviate this problem. Kuhlman[49] noted that the foamability of a surfactant was lowered by hydrocarbons which have the same size as the hydrophobe of the surfactant. Holm[1] concluded the flow mechanism remained the same; the oil saturation lowered the capability of foam to trap gas.

Isaacs et al.[24] found that there was an optimum surfactant concentration beyond which the mobility could not be reduced. In the presence of oil this optimum shifted to a higher concentration. In a later study by Isaacs, Jian, Green, McCarthy, and Maunder[50] experiments were performed within a porous medium up to 180°C. They found that foams could not be formed at oil saturations above 0.15 pv (pore volume). This is consistent with Fried's[6] findings. He attempted to displace fluids in a core with 100 per cent liquid saturation, of which over 80 per cent was a high viscosity state oil. This proved unsuccessful. He reasoned that the application of foam drives would probably be restricted to secondary recovery.

Friedmann and Jensen[5] found that a residual oil saturation greater than 20 per cent was detrimental to foam generation. McPhee, Tehrani, and Jolly[51] found foam stability was lost at residual oil saturations as low as nine per cent.

Maini[35] conducted experiments in which combinations of oil types and different surfactants were tested. He found that the presence of oil could sharply improve the mobility reduction capabilities of foam, for the correct combination of oil and surfactant. For incompatible samples, the presence of oil could prove detrimental. Robin[43] found some surfactants that were not affected by contact with a hydrocarbon phase.

3.7.7 Salinity

The effect of salt on foam formation is, not surprisingly, another point of contention for foam researchers. Bernard and Holm[25] found that brine had little effect on foam effectiveness. Brine was very detrimental to the performance of the surfactants tested by Duerksen[23]. They tested the surfactants in a brine containing 500 ppm calcium chloride and one per cent sodium chloride. Al-Khafaji, Wang, Castanier, and Brigham[46] found that calcium chloride caused surfactant degradation at concentrations greater than 0.5 per cent by weight, while sodium chloride caused surfactant degradation and surfactant precipitation at concentrations greater than two per cent by weight.

Kanda and Schechter[52] report that the addition of electrolyte would cause the CMC to be reduced. They tested surfactants at two per cent by weight sodium chloride. It was found that the breakthrough time increased but the permeability reduction was less.

In Isaacs et al.[24] stability experiments, concentrations of 4 per cent by weight were used. At the temperature used (160° C) the concentration of brine may actually be much higher. The foam stability was unaffected by the brine. Even a surfactant, known to be intolerant to brine at ambient conditions, was unaffected by the brine. Dilgren et al.[48] experimented with brine concentration on steam foams. They found the permeability reduction was more favourable with the addition of sodium chloride, up to a concentration of one per cent by weight. The permeability reduction factor was insensitive to sodium chloride solutions of one to five per cent by weight. This led the researchers to claim that certain surfactants required sodium chloride to be effective as a steam foam.

3.7.8 Gas Velocity

Lee and Heller[41] studied the effect of velocity and found it was only important at low surfactant concentrations. Friedmann and Jensen[5], however, conducted experiments where quality and surfactant concentration were held constant. They found that bubble size increased and stability decreased as velocity decreased. If the flow was too slow, no foam would be produced. Flow rate had a direct effect on foam texture. The higher flow rates produced smaller and more uniform foams. Huh et al.[40] determined that an increased flow rate improved sweep efficiency.

Isaacs et al.[24] suggested that for a given permeability there was a minimum critical velocity below which foam would not be formed. He found that lowering the absolute permeability required an increase in steam velocity. Critical velocity was found to be roughly proportional to the inverse of absolute permeability. Best et al.[34] stated that with increasing velocity, the viscous forces appeared to overcome the resistance of foam bubbles to flow. At very high velocities, the effect of surfactant solution on the effective permeability of gas would be small.

Hanssen[53] studied gas blocking ability as a function of foam generation differential pressure. He determined that the gas blocking ability was relatively insensitive to foam generation differential pressure.

3.7.9 Surface Viscosity and Interfacial Tension

Kanda and Schechter[52] found that displacement efficiency and breakthrough time increased with increasing surface viscosity of surfactant solution. They determined that displacement efficiency decreased and breakthrough time increased with increasing surface tension. Slattery[54] found that displacement efficiency increased as surface viscosity and surface tension increased. However, given a specific pressure gradient, there exists a critical value of surface tension above which foam cannot be displaced.

Owete[19] discussed increasing surface viscosity to increase foam stability. High surface viscosity is known to reduce the rate of liquid film thinning, which would increase lamellae stability. Therefore, a high surface viscosity is desirable.

In an earlier experiment, Owete et al.[22] found that the surface tension and surfactant foamability were not strongly related. Kuhlman[49] discussed the importance of the interfacial tension. The interplay between the gas, the surfactant solution, and the oil surface free energy will determine the spontaneous spreading of the oil or surfactant solution. They determined that water spreading was likely when oil saturation was low, and the gas saturation was high. Oil spreading occurs when oil saturation is high and the gas-oil interfacial tension is low. Spreading oil can be detrimental to foam stability near the optimum salinity region. They felt that spreading oil could be beneficial under reservoir conditions.

IV Experimental Apparatus and Procedure

This chapter presents a description of the equipment utilized and the experimental procedure followed in the study. The research was conducted in two stages. The first stage consisted of a series of preliminary exploratory runs. These runs were performed of necessity on a more simplified version of the apparatus. The second stage of experiments employed the more complete and instrumented version of the apparatus. The main components of the apparatus in the final form were: a co-injection system, a foam generator, an oven, and an effluent product collection system. Details of the experimental procedure, such as the packing and saturation of the model, and effluent sample analysis are given below.

4.1 Preliminary Experiments

This research constitutes the first attempt to study and characterize the flow of foam in porous media. As a result, while making use of the published literature, considerable care was exercised in the design of the apparatus, which was effected in response to the results of preliminary experiments. Then runs were performed to identify potential problems in the experimental design and also to provide a comparison of the surfactants available.

The apparatus used is illustrated in Figure 4.1. The equipment consisted of a 2000 psi nitrogen tank with a regulator, a three-way

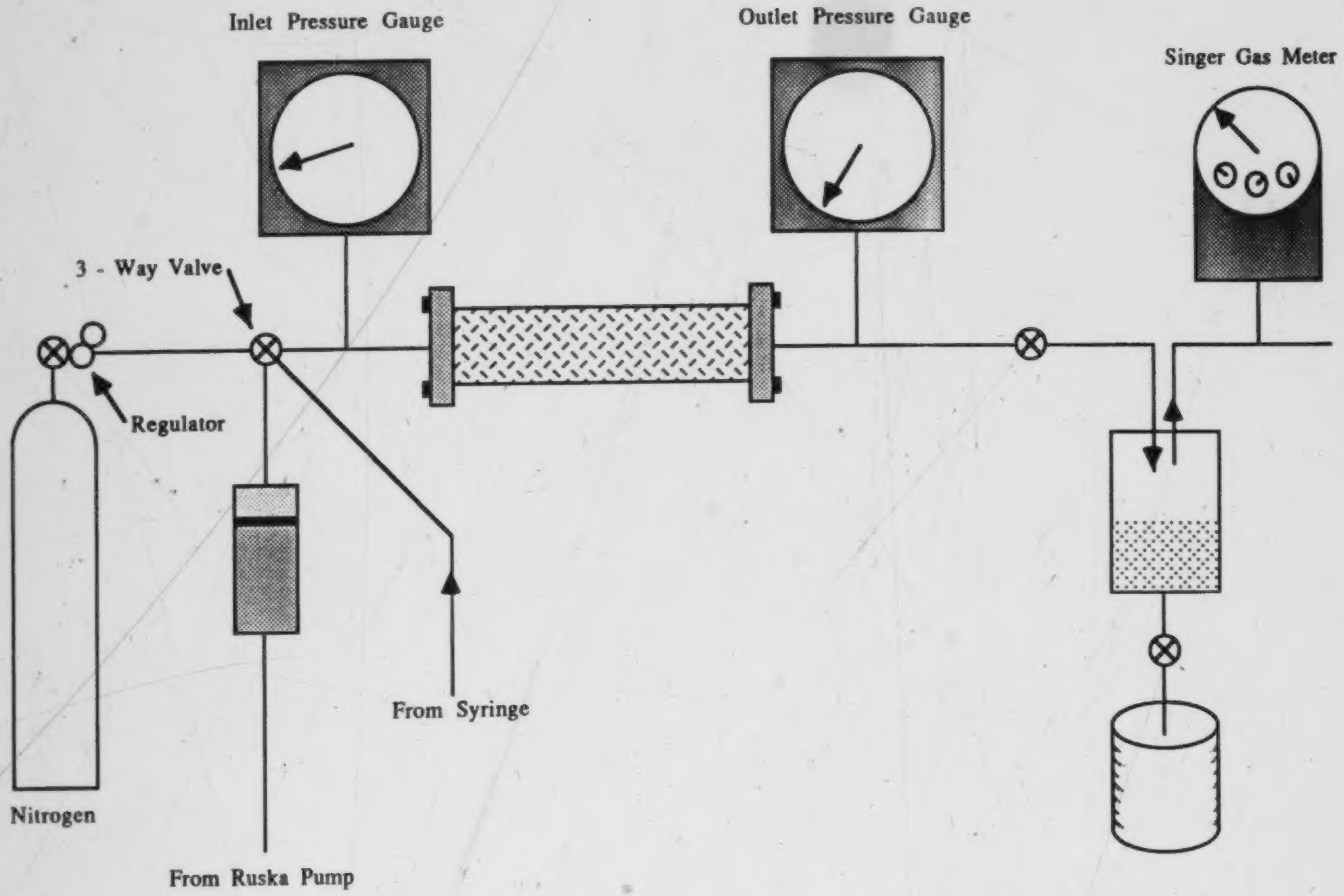
Inlet Pressure Gauge
Outlet Pressure Gauge
Singer Gas Meter
3 - Way Valve
Regulator
Nitrogen
From Ruska Pump
From Syringe

Figure 4.1 Preliminary Run Equipment Configuration

valve, a packed coreholder, inlet and outlet pressure gauges and a Singer* gas meter. The coreholder dimensions and the packing procedure used are described in the next section. The inlet pressure was set as 6.4 psi using the pressure regulator, and was not adjusted between runs for consistency. A the three-way valve was installed at the core inlet, which could be positioned to receive an injected surfactant slug or to flush the coreholder with fluids from the Ruska** pump. The coreholder outlet pressure was atmospheric. As the run progressed, the fluids moved through an enclosed containment flask; the produced gas left the flask and was directed through the gas meter after trial runs at higher pressures.

A pressure of 6.4 psi was chosen after trials run at higher pressures. The flow rate generated by a higher pressure would have been operationally difficult to work with. The initial breakthrough time would have been too short to measure accurately. It was decided that the largest manageable inlet pressure would be chosen to ensure that the gas velocity would be high enough to generate a foam.

Therefore 6.4 psi was chosen. The largest manageable pressure drop was chosen to ensure that there were no problems with too small a gas velocity to generate foam This was done to ensure being above critical foam velocity, as was described in the Literature Review.

---

* Canadian Meter Division of Singer Company of Canada
9919-65 Ave. Edmonton, Alta 434-8705
** Ruska Inc. 6121 Hillcroft, Houston, Texas 77036

It was decided that the most demonstrative way to test the effect of foam was to perform a gas flood with and without the addition of a surfactant slug. This was the purpose of the preliminary runs. The procedure used for these runs is presented below.

The packed coreholder was initially saturated 100 per cent with water. The first step of the run was to assure that the inlet pressure was regulated, which was checked on the inlet pressure gauge. When this pressure was achieved, the coreholder outlet valve was closed and the three-way valve was turned to inject nitrogen from its initially closed position. With the outlet valve closed the system would "pressure up". At this point the exit valve was opened and the timing was started.

When the first bubble of gas was produced from the coreholder, the outlet valve was closed. The time from starting injection until the first bubble of gas appeared and the volume produced from the core were recorded. Following this, the outlet valve was opened and the nitrogen was allowed to flow through the coreholder. The stop-watch was restarted and the flow was allowed to continue until 60 seconds. This was the second stage of the run. In this way each core was flushed for a total of 60 seconds in the initial tests. During this second stage the pressure at the outlet end was examined on the outlet pressure gauge and an outlet pressure was estimated. The outlet gauge reading was subject to large variations during the first stage as slugs of liquid exited the core. During the second stage of the test the outlet pressure was generally more nearly constant.

The coreholder was then flushed vertically with water, from the bottom up. The volume of liquid used to flush through the core was consistent at 500 ml.

The above procedure was then repeated; this was the first resaturation test. The surfactant run was performed on the second resaturation. This was done to allow a direct comparison between the first and second resaturation, both having a residual gas sasturation. The core was injected with nitrogen until gas breakthrough. At this point, the time and the volume produced were recorded. Nitrogen was allowed to flow for the remainder of one minute. The core was then saturated with 500 ml of water, while held in the vertical position.

At this point, the three-way valve was set to inject a surfactant slug. This was accomplished with a syringe fitted to the plastic tubing used. A 40 ml slug of surfactant solution was injected into the core. The excess fluid in the core was allowed to flow from the outlet. The system was then closed at the outlet end, and the three-way valve was set to accept the nitrogen from the regulator to enter the coreholder. The outlet valve was then opened, and timing started. Nitrogen was injected until the first bubble of gas appeared at the outlet. At this point, the outlet valve was closed. The time until gas breakthrough and volume collected at breakthrough were recorded.

Depending on the time required for the initial breakthrough, nitrogen injection was continued for the remainder of a minute, or, if the breakthrough time was greater than one minute the experiment was terminated when gas breakthrough occurred.

4.2 Coreholder Packing and Saturation

4.2.1 Packing Procedure

The coreholder used for these runs was 60.75 cm in length and 4.95 cm in diameter. Three coreholders were built and alternately used for this project. The end-caps for the coreholder were changed from ceramic to sintered screens so that the end-caps would less significantly change the foam properties.

For the preliminary runs the coreholder was packed in various ways with Ottawa sand mesh size 70 to 140. The sandpacks were packed dry and wet, and the packing vibration technique was varied to determine the best packing method, based upon the reproducibility of the pack properties. The pore volume was measured by evacuation and by effluent analysis using the refractometer. The use of the refractomater to determine pore volume is discussed in Section 4.2.5, Alternate Pore Volume Determination. The porosity and absolute permeability were determined for each run.

The inlet end of the coreholder was fitted with an extension and an O-ring. The extension was a transparent model of the coreholder. When attached to the core it acted to extend the core length. This allowed the packing to take place right up into the extension and maintain a more consistent packing throughout the coreholder.

Two vibrators were used in this study. During the preliminary runs the vibrators were alternated and the resulting porosity and permeability were evaluated.

4.2.2 Packing Materials

The primary materials used to pack the coreholders were distilled water, sand and glass beads. The distilled water used had a pH of approximately 7.5. Ottawa sand with a mesh size of 70-140, as opposed to the glass beads, was used in the preliminary runs. For the remaining runs glass beads were used. They were obtained from Sil Silica* and Rotair** Industries. The number associated with the beads identifies the range of bead diameters. The most common bead size used was the #9 with a mesh size of 80 to 120. The #7 had a mesh size of 50 to 70 and #5 was 30 to 50. Sieve analysis of the glass beads revealed that the beads were consistently slightly larger than the specified diameter range.

---

* Sil Silica 8824-53 Ave. Edmonton, Alta 465-1608

** Rotair Industries 7722-9 Ave. Edmonton, Alta 440-2775

The surfactants used in this study were Chevron Chaser^{tm} SD1000, Dow experimental sulphonated surfactant Chevron Chaser^{tm} XP100. The oil used in this study was Brooks Pan Canadian. The viscosity as determined utilizing the Brookfield viscometer with an ultralow adaptor was 52 cp.

4.2.3 Wet Packing

The wet-packed sandpacks were prepared by performing calculations to assure that the water and sand were alternately loaded in a specific manner. The sand was loaded through a funnel that had been modified to a predetermined diameter, and contacted a measured volume of water. This was done to consistently allow the sand to fall into a five to ten cm layer of water. The total amount of sand loaded into the core was 2250 g.

The coreholder was continuously vibrated while the sand and water were loaded. When the coreholder was completely full it was then vibrated for 8 hours. The extension was removed and the upper end of the coreholder was levelled. The sand collected was dried and weighed and the end-cap was placed on the core.

At this point heating tapes were placed around the core and the water was evaporated out. This drying technique was employed for three days. The core was then cooled for approximately 8 hours. In order to determine the pore volume, the coreholder was subjected to a vacuum of 1 psi for 4 hours. Distilled water was then imbibed into the coreholder. The imbibed volume was taken to be the pore volume.

A permeability test was then performed on the core. This was accomplished, while maintaining 100 per cent water saturation. The flow rate was measured and an absolute permeability measurement was obtained.

4.2.4 Dry Packing

The dry packing method consisted of loading 2250 gm of sand (or glass beads) into the coreholder, through the funnel, in the three batches of 750 g. This allowed an excess of approximately four inches, to remain in the top-extension. The coreholder was vibrated while the sand was loaded. When full, the coreholder was vibrated continuously for 8 hours. The advantage of the dry packing method is quicker determination of pore volume, since drying the core was unnecessary.

After vibration, the extension was removed and the excess glass beads were weighed. The coreholder was then evacuated with a vacuum pressure of 1 psi. The imbibed liquid was assumed to be the pore volume.

4.2.5 Alternate Pore Volume Determination

The initial method for determining pore volume was the imbibition of distilled water into a dried and evacuated core. This was compared to the value found by calculating the remaining glass bead weight divided by the experimentally determined glass bead density.

In order to verify this method of determining pore volume, a plot of refractive index, as measured on the Erma New Abbe refractometer*, versus the brine concentration was generated, It showed a straight line of refractive index versus brine concentration. Such a plot is presented in Figure 4.2.

To find the pore volume a 2 per cent (by weight) solution of NaCl in water was injected into a core (the pore volume of a typical core had been determined previously by imbibition). The effluent from the core was collected and weighed. The refractive index was

---

* purchased through Fisher Scientific 10720-178 St.
Edmonton, Alta 483-2123

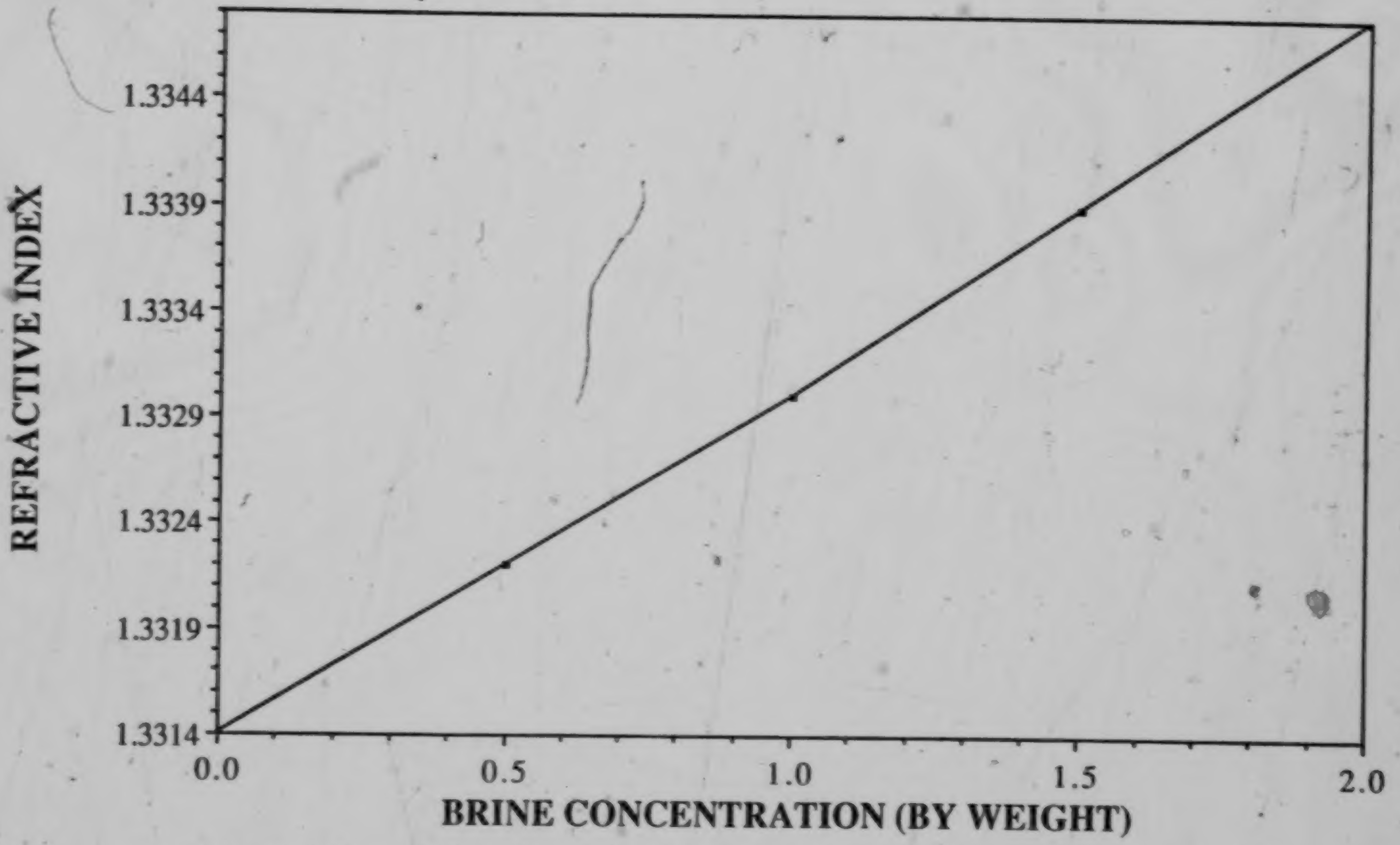

Figure 4.2 Refractive Index Vs. Brine Concentration (By Weight)

measured. This was plotted versus the cumulative volume. The curve produced was analyzed using a digitizer to measure the area on both sides of the curve. The pore volume was chosen such that a vertical line drawn through this point generated equal areas on both sides of the curve.

This method produced results very similar to those obtained by the imbibition method. Because of the relative ease of utilizing the imbibition method and because the introduction of brine, no matter how well the core was flushed, could adversely effect the runs, imbibition was chosen to be the standard pore volume determination method.

4.2.6 Consolidated Core Preparation

The consolidated cores used were 5 cm in diameter and 60 cm in length. These dimensions are very similar to the original coreholder used. Larger diameter coreholders with the original flanges were used.

The consolidated cores used were Berea sandstone cores. These cores were fired at 750 °C to reduce the amount of swelling clays, and increase the permeability. The core ends were covered in aluminium foil for protection. The core surface was then painted with an epoxy to render it impermeable.

The sealed core was then placed in a coreholder. It was centered and stabilized within the coreholder. A lead-nickel alloy, "Cerrobend" (MP 70 °C) was poured around the sides of the core and allowed to cool. The excess alloy was removed, by turning the core face, in the machine shop.

4.2.7 Oil Saturation of the Sandpacks

In order to obtain a core with residual oil saturation, the core was subjected to a series of floods. The core was initially 100 per cent water saturated; the porosity and absolute permeability were determined as outlined in the previous section.

The core was flooded with 1000 cc of oil at a rate of 1 cc per minute. The amount of effluent water was carefully monitored. This flood took place vertically from the top downward. The flood progressed from the core inlet to the outlet. The inlet end of the core had the sight glass attached to it. This orientation, flooding from the top down was chosen because the specific gravity of the oil was less than that of the water.

Once the oil was flushed through the core, the coreholder was flipped upside-down. Water was then injected into the coreholder from the bottom up toward the outlet end of the coreholder. This was done using a continuous-displacement pump at a rate of 3 cc per minute until there was no oil present in the effluent. The amount of water used was often as high as 15,000 cc.

4.3 Pre-Foamed Temperature-Controlled Co-Injection Runs

Plate 1 shows the experimental equipment designed to co-inject nitrogen and surfactant solution in order to generate foam and examine its flow through a porous medium. The equipment was designed for operation at elevated temperatures (max. 250° C) and pressures. Equipment design and trouble-shooting constituted a large portion of this research, since this was the first study of this type at this university. The equipment was designed after careful consideration of the apparatus utilized by other investigators. The design was significantly modified by problems and procedures identified in the preliminary runs.

A diagram of the single core apparatus is presented in Figures 4.3 and 4.4. A diagram of the dual core apparatus is presented in Figures 4.5 and 4.6. A description of the apparatus and the design concerns are presented in the following section. The equipment also allowed experiments to be performed with dual coreholders tested at the same time. The coreholders used for these runs were of the same dimensions as for the preliminary runs.

Plate 1: Co-injection Equipment

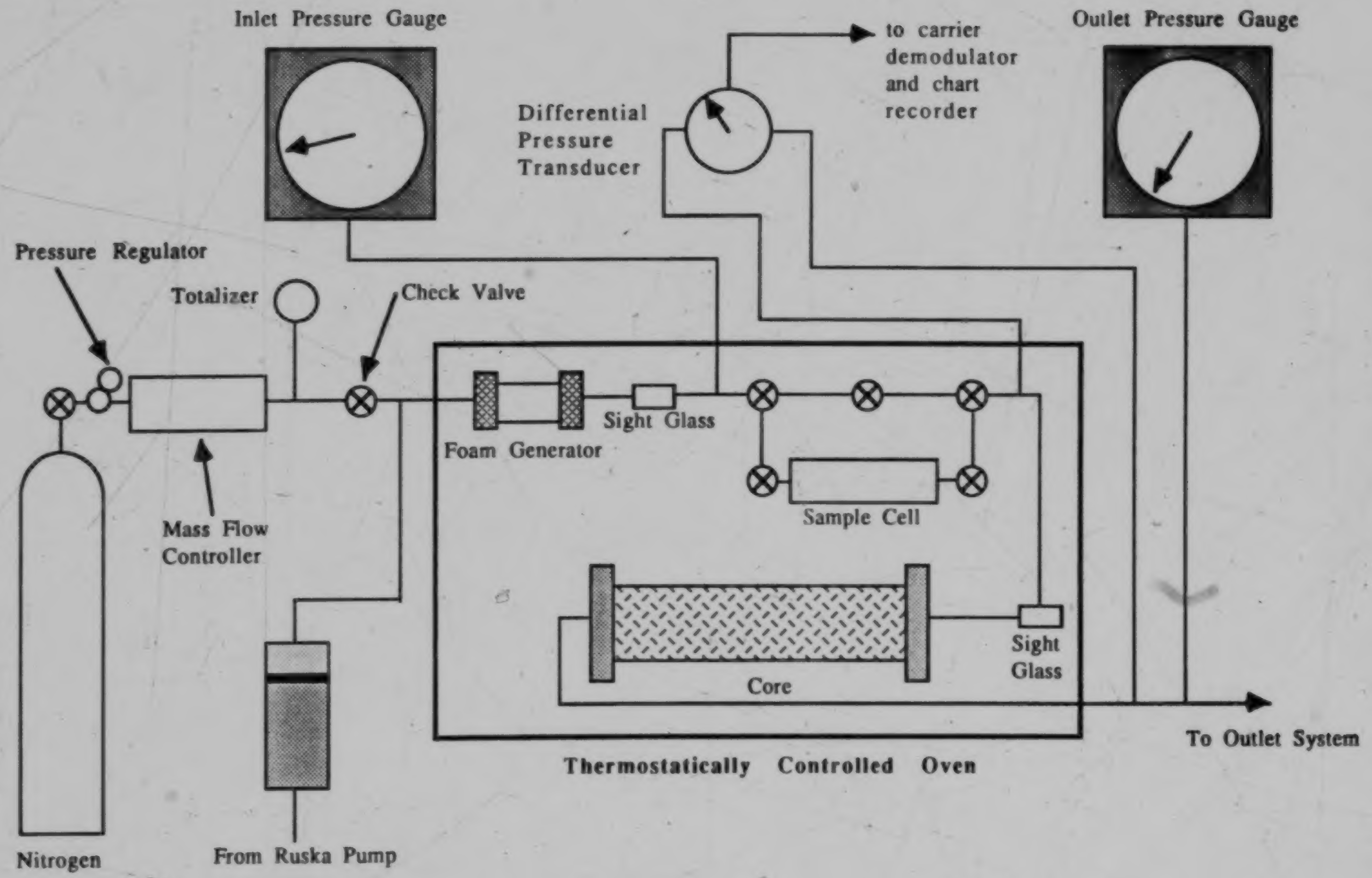
Inlet Pressure Gauge
to carrier demodulator and chart recorder
Outlet Pressure Gauge
Differential Pressure Transducer
Pressure Regulator
Totalizer
Check Valve
Sight Glass
Foam Generator
Sample Cell
Mass Flow Controller
Sight Glass
Core
To Outlet System
Thermostatically Controlled Oven
Nitrogen
From Ruska Pump

Figure 4.3 Nitrogen-Surfactant Co-injection Equipment

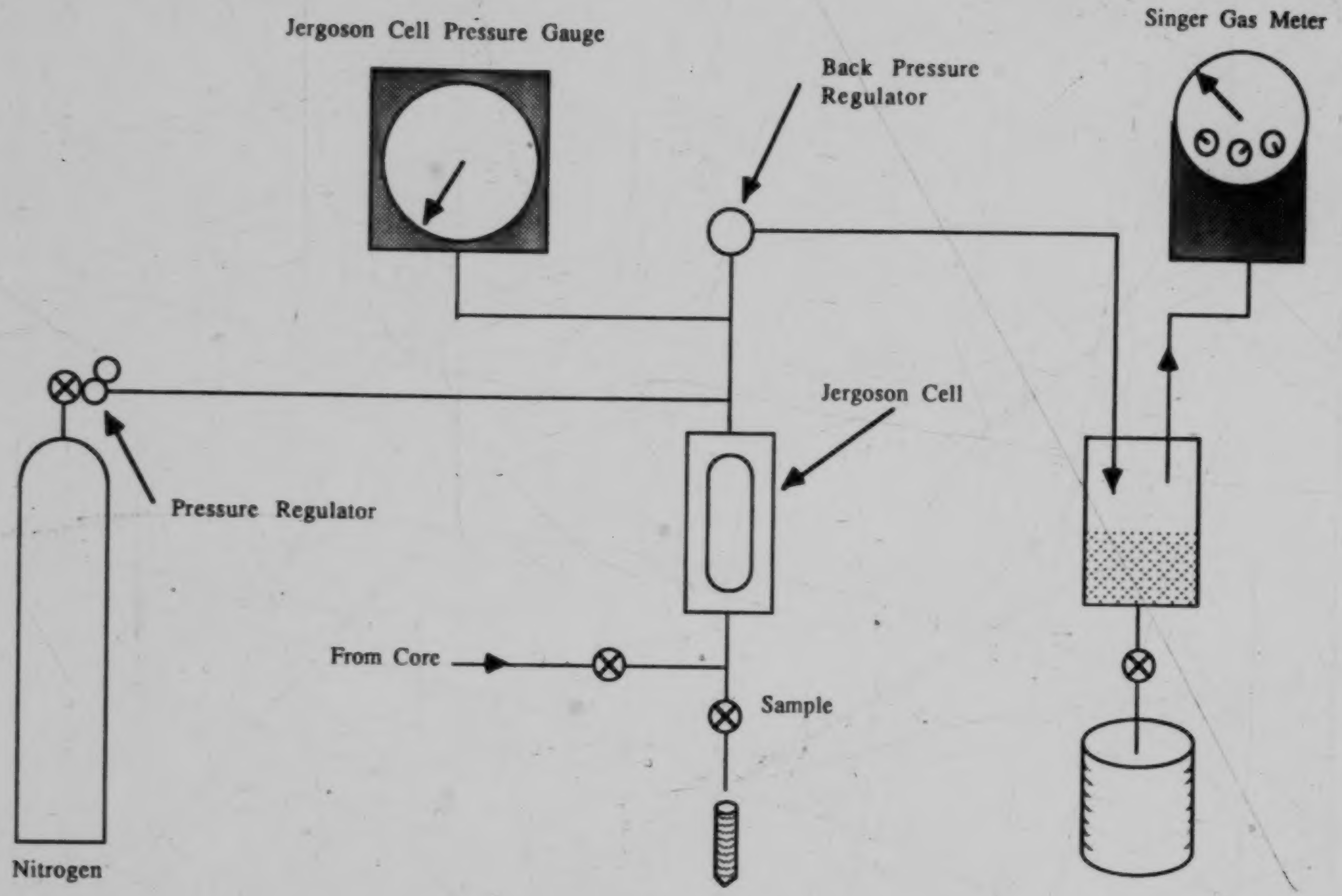
Jergoson Cell Pressure Gauge
Back Pressure Regulator
Singer Gas Meter
Jergoson Cell
Pressure Regulator
From Core
Sample
Nitrogen

Figure 4.4 Single Core Outlet System

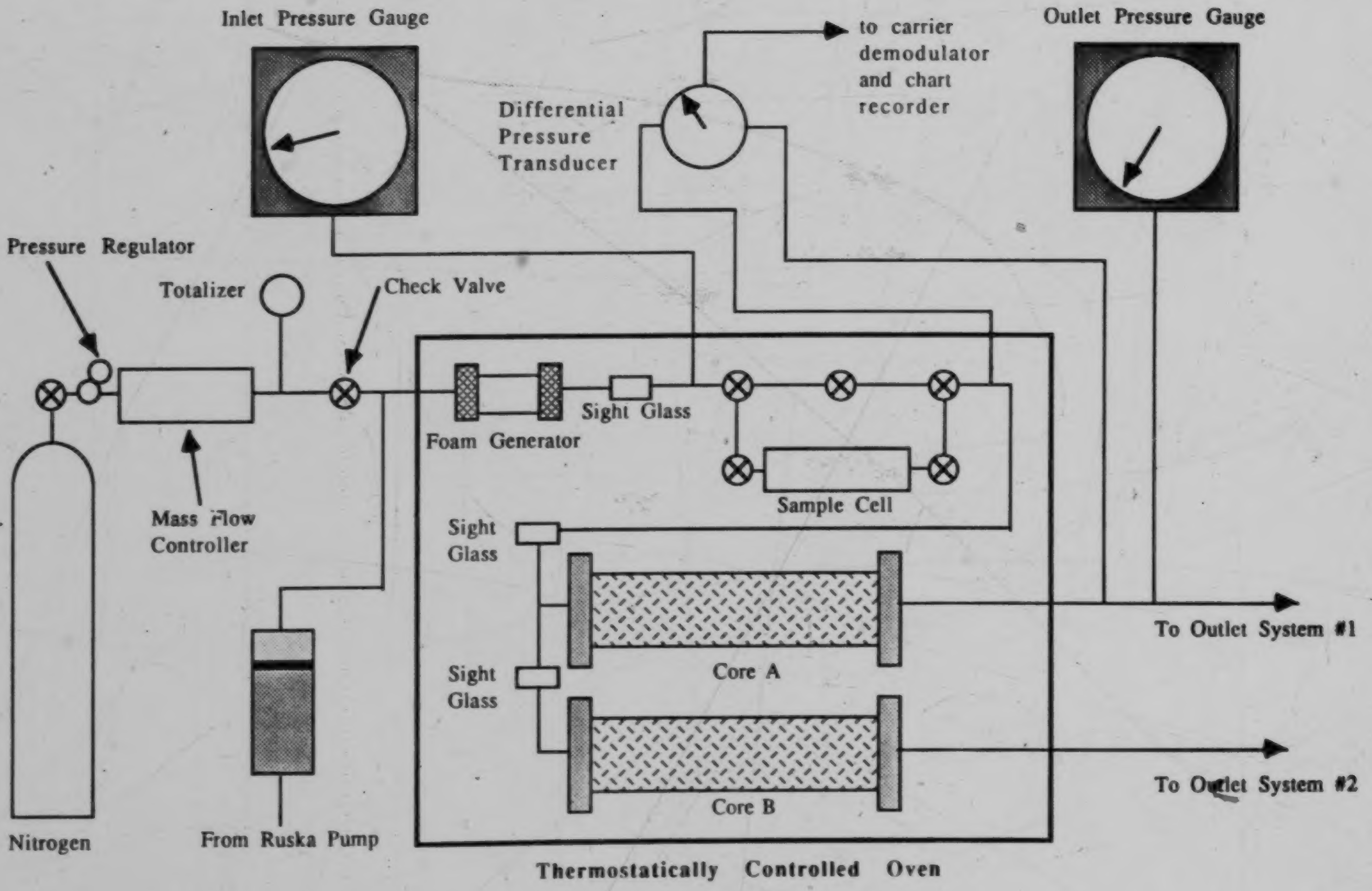
Inlet Pressure Gauge
Differential Pressure Transducer
to carrier demodulator and chart recorder
Outlet Pressure Gauge
Pressure Regulator
Totalizer
Check Valve
Foam Generator
Sight Glass
Sample Cell
Mass Flow Controller
Sight Glass
Sight Glass
Core A
Core B
To Outlet System #1
To Outlet System #2
Nitrogen
From Ruska Pump
Thermostatically Controlled Oven

Figure 4.5 Dual Core Nitrogen-Surfactant Co-injection Equipment

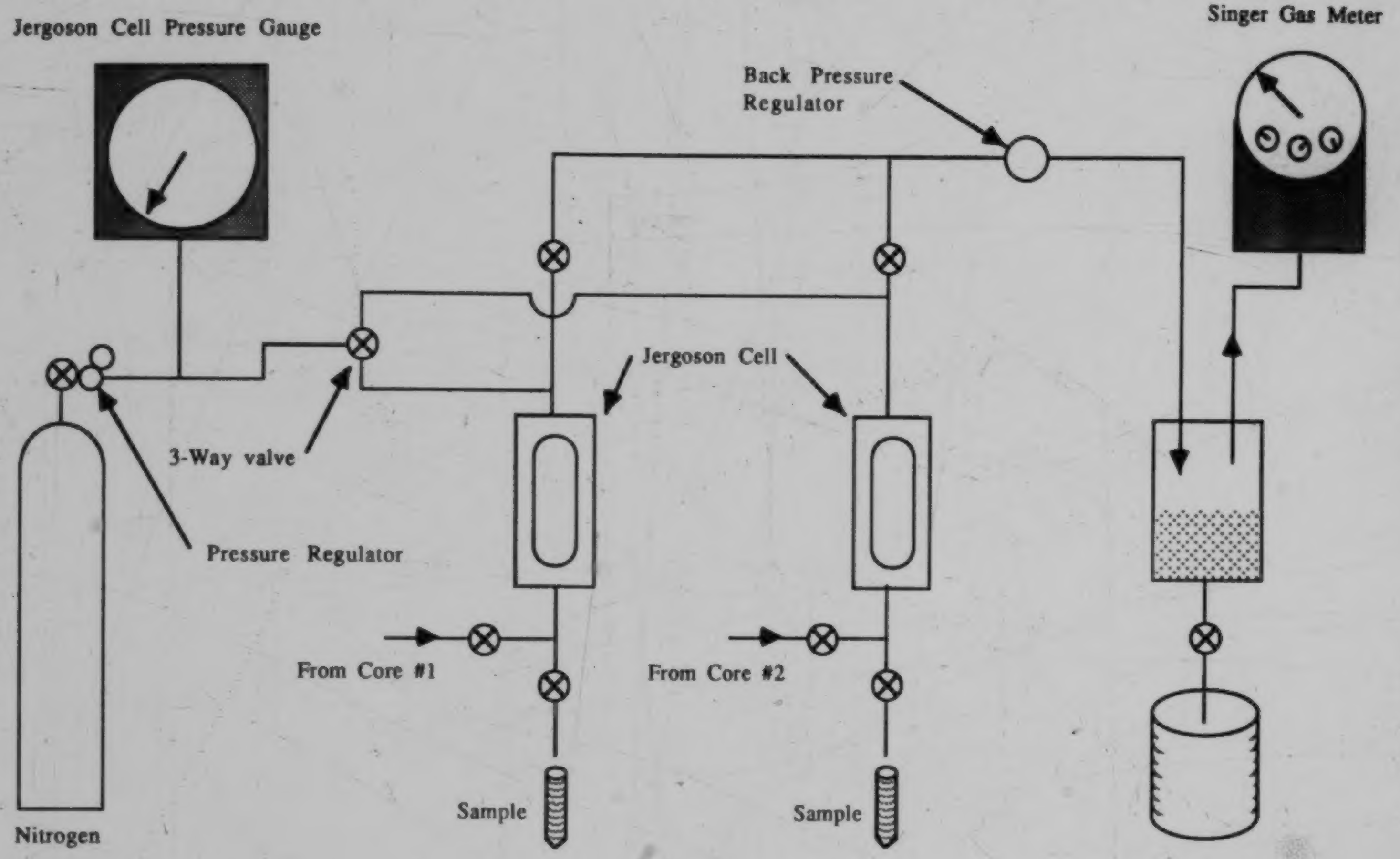
Jergoson Cell Pressure Gauge
Singer Gas Meter
Back Pressure Regulator
3-Way valve
Pressure Regulator
Jergoson Cell
From Core #1
From Core #2
Sample
Sample
Nitrogen

Figure 4.6 Dual Core Outlet System

4.3.1 Experimental Equipment

4.3.1.1 Injection System

The injection of the nitrogen was controlled by a pressure regulator and a mass flow controller. The regulator was set such that the system could not exceed the maximum design pressure. The mass flow controller (MFC) was a Matheson* controller model 8240. This controller was designed specifically for measuring nitrogen. The units of the system were cc per minute. The maximum allowable rate was 1000 cc per minute. A totalizer was attached to the MFC such that the cumulative nitrogen volume injected could be determined instantaneously. The value read on the MFC was at one atmosphere and 60°F. The value read on the totalizer was converted to an appropriate volume when the pressure was higher than atmospheric.

A Ruska pump was employed to inject the liquid phase. The pump had two 1000 cc cylinders attached to the outlet end. This effectively quadrupled the pump volume, from 500 to 2000 cc. By changing the gear ratios the pump rate could be altered. The most common rate used was 1 cc per minute.

The mass flow controller (MFC) and the Ruska pump both fed into the same flex-line which attached to the inlet of the foam generator. In this way the nitrogen and the liquid phase were co-injected. By controlling the pump rate and adjusting the MFC, the injection ratio, and hence the approximate quality were regulated.

---

* Matheson Gas Products Canada Inc. 12143-68St.
Edmonton, Alta 471-4036

4.3.1.2 Oven Interior

At this point the co-injection fluids entered the Napco* thermostatically controlled oven. Plate 2 shows the interior of the oven. The foam generator, the sight-glasses and the coreholder were all located within the oven.

The oven was 23 by 37 inces wide. The maximum temperature allowable within the oven was 250° C. One of the main features of this oven was that it is equipped with a fan to circulate the heat. This oven was modified to include windows. These windows allowed the viewing of foam through the sight-glasses, at elevated temperatures. The oven was also modified to include lights.

4.3.1.2 Foam Generator

The co-injected nitrogen and surfactant solution first passed through a coil which led to the foam generator. The purpose of the

---

* purchased through Sargent Welch Scientific of Canada 459-6246

Plate 2: Oven Interior

coil was to increase the temperature of the nitrogen-surfactant mixture to oven conditions.

The foam generator consisted of a coreholder that was packed dry with #9 glass beads for consistency. To prepare the core 125 g of glass beads were slowly poured into the vibrating coreholder. The small vibrator was used to prepare the foam generator. A schematic of the foam generator is presented in Fig 4.6A.

A small coreholder of the necessary size was conveniently available. The end-caps literally screwed onto the central core tube. This made it very difficult to prevent the glass beads from getting in the end-cap threads. If glass beads became imbedded in the end-cap, or under the o-ring, the foam generator leaked.

The end-caps for this coreholder were fitted with screens to hold the glass beads in place. Two layers of screens were placed on both end-caps. A fine screen was placed behind the more coarse one in order to keep fines from flowing with the foam.

In order to pack the foam generator a top-extension was designed to screw onto the coreholder. When the core was loaded with glass beads and the vibration completed, the extra glass beads used were removed. This was accomplished by removing the rubber stoppers on the sides of the top-extension. The stoppers were removed one at a time. While attached to the core stand the

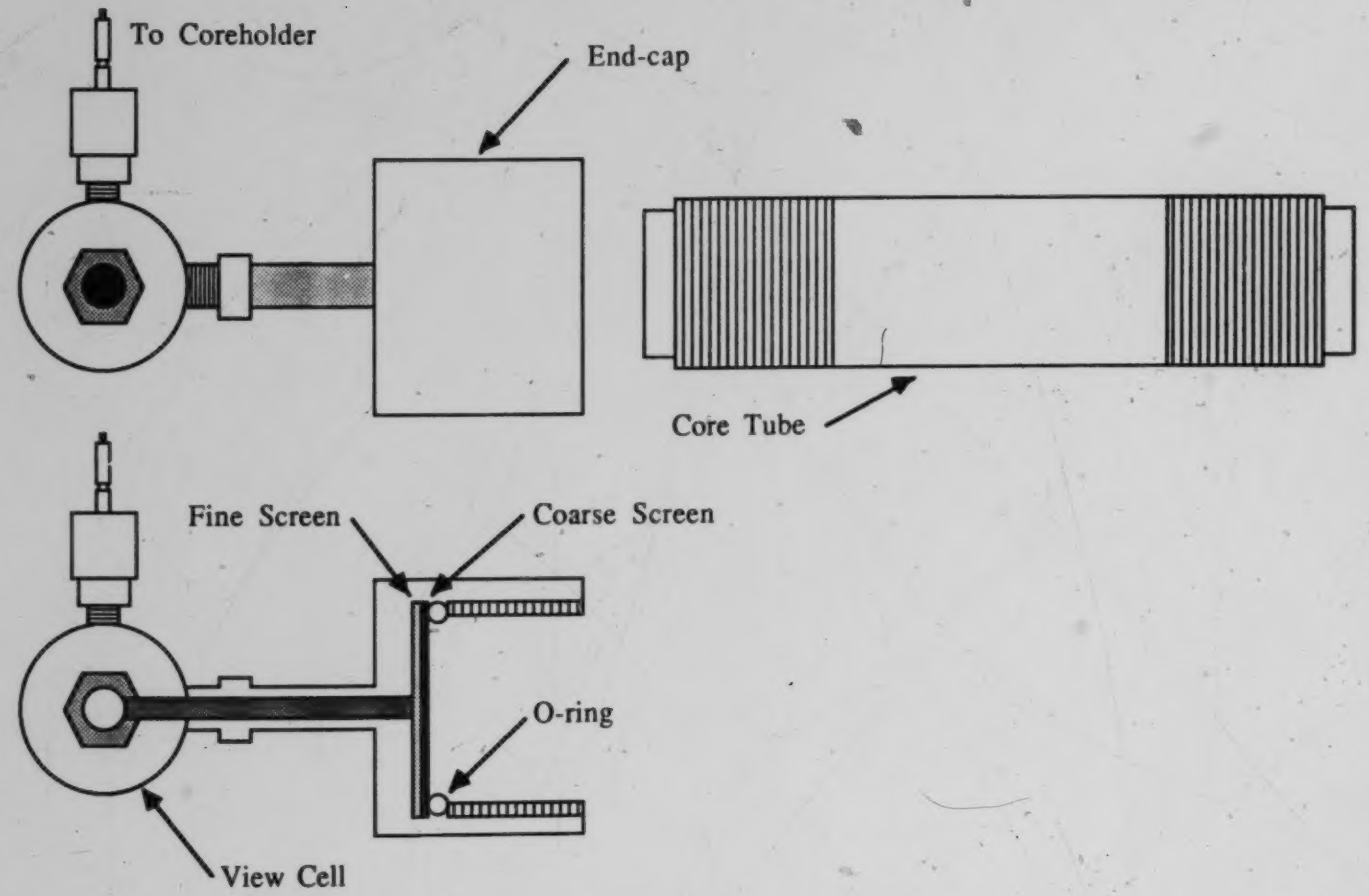
To Coreholder
End-cap
Core Tube
Fine Screen
Coarse Screen
O-ring
View Cell

Figure 4.6A Foam Generator Schematic

coreholder could be tipped to unload the extra sand. This excess was collected and weighed.

The second end-cap was then placed on the coreholder. The air in the coreholder was evacuated by vacuuming for 2 hours. Next, distilled water was imbibed into the coreholder. The permeability of this coreholder was not determined for each run. It was however, determined for three runs and found to be very consistent.

4.3.1.3 Sightglasses

A sightglass was added to the outlet end of the foam generator. This permitted the viewing of the foam immediately after formation. A tube was added to direct the fluids to the transparent portion of the sight-glass immediately after they exited the foam generator. A sightglass was also added to the inlet end of the main coreholder. The sightglass was attached to the coreholder and the foam generator end-caps. This positioning was also useful for pore volume determination. When the sightglass were full of water, the imbibition process was complete. It was also helpful in identifying coreholder end-cap leaks. When a leak occurred, the sightglass did not fill completely.

Between these sightglasses a sample cell was added. The sightglasses were designed to provide visual evidence of the foam formation and to suggest when the sample cell was full.

The sightglasses were positioned such that if an explosion took place they would not blow toward the operator and therefore pointed down. Two small mirrors were attached to the apparatus to enable the operator to observe the foam. Lights were situated in the oven such that they would shine through the sightglasses and make this visual observation easier.

4.3.1.4 Dual Core Runs

For the majority of the runs a single core was employed. For selected runs, the system was modified to incorporate a second coreholder. For this the injection system remained unchanged. The outlet was modified, as discussed in the next section.

4.3.1.5 Outlet System

At the outlet end of the main coreholder a system was developed whereby the effluent could be visualized and sampled. Sampling was problematic because it was important to view the effluent under experimental conditions. Plate 3 shows the outlet system.

A Jergoson gauge allows visual observation along the length of the cell. This cell can handle fluids to 1000 psi at 100° F and 585 psi at 600° F. This cell was positioned vertically such that the effluent

Plate 3: Outlet System

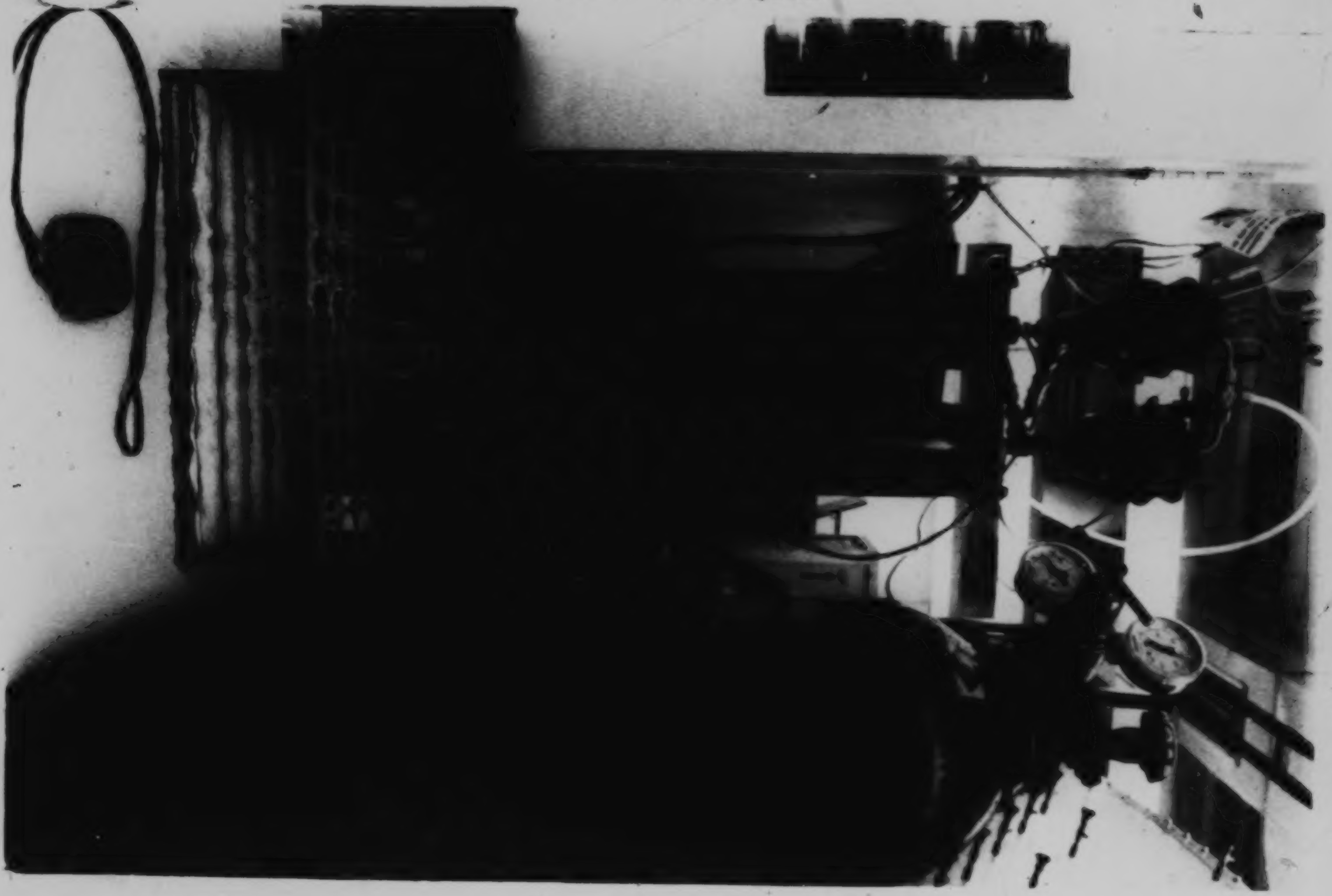

entered the bottom of the cell. At the inlet end of this cell a valve was placed that could isolate the cell from the rest of the system. At the base of the cell a valve allowed the emptying of the cell to atmospheric conditions. A back pressure regulator was placed at the top of the cell so that it would only "see" nitrogen. The accuracy of the back pressure regulator was significantly reduced by the introduction of a second, or third, phase.

Placed at the outlet of the Jergoson cell, but before the back pressure regulator, was a pressure line. This line was attached to a second nitrogen tank.

As the effluent exited the coreholder, it moved vertically up the Jergoson cell. The pressure in the cell regulated the outlet conditions for the main coreholder. When the effluent reached the 50 ml mark, the cell was isolated from the coreholder by closing the aforementioned valve.

The effluent drained out of the cell when the sample valve was open. The samples were collected in 50 ml centrifuge tubes to allow quick volumetric measurements. The sample valve was then closed.

The second nitrogen tank was then used to repressure the cell. The back pressure regulator established the proper pressure. This was verified by the positioning of a pressure gauge that measured the cell pressure. This gauge was visible at the outlet. At this point the valve to the cell entrance was opened and the system again reached equilibrium. The sample procedure generally took less than 15 seconds.

The addition of a second coreholder necessitated a second Jergoson cell. This cell was fitted with the same valves as the first one. The outlet of both cores was regulated to 50 psi, so that there was only one differential pressure profile recorded.

4.3.1.6 Sample Analysis

The effluent was collected continuously throughout the experiment. The volume of the sample was recorded. To determine the surfactant concentration of the effluent, the refractive index was measured. While performing the experiments it was determined that the ultraviolet (UV) spectrophotometer reading was a more accurate method of determining surfactant concentration.

A plot of refractive index versus concentration was generated and found to be a straight line. The plot was used to analyze the effluent and determine concentration. This plot is included as Figure 4.7. The gradations on this scale are very large. Although the refractive index accurately reflected the surfactant breakthrough it did not give an accurate picture of the surfactant adsorption.

The ultraviolet (UV) spectrophotometer was then used to determine concentration. This method was used by Huh and

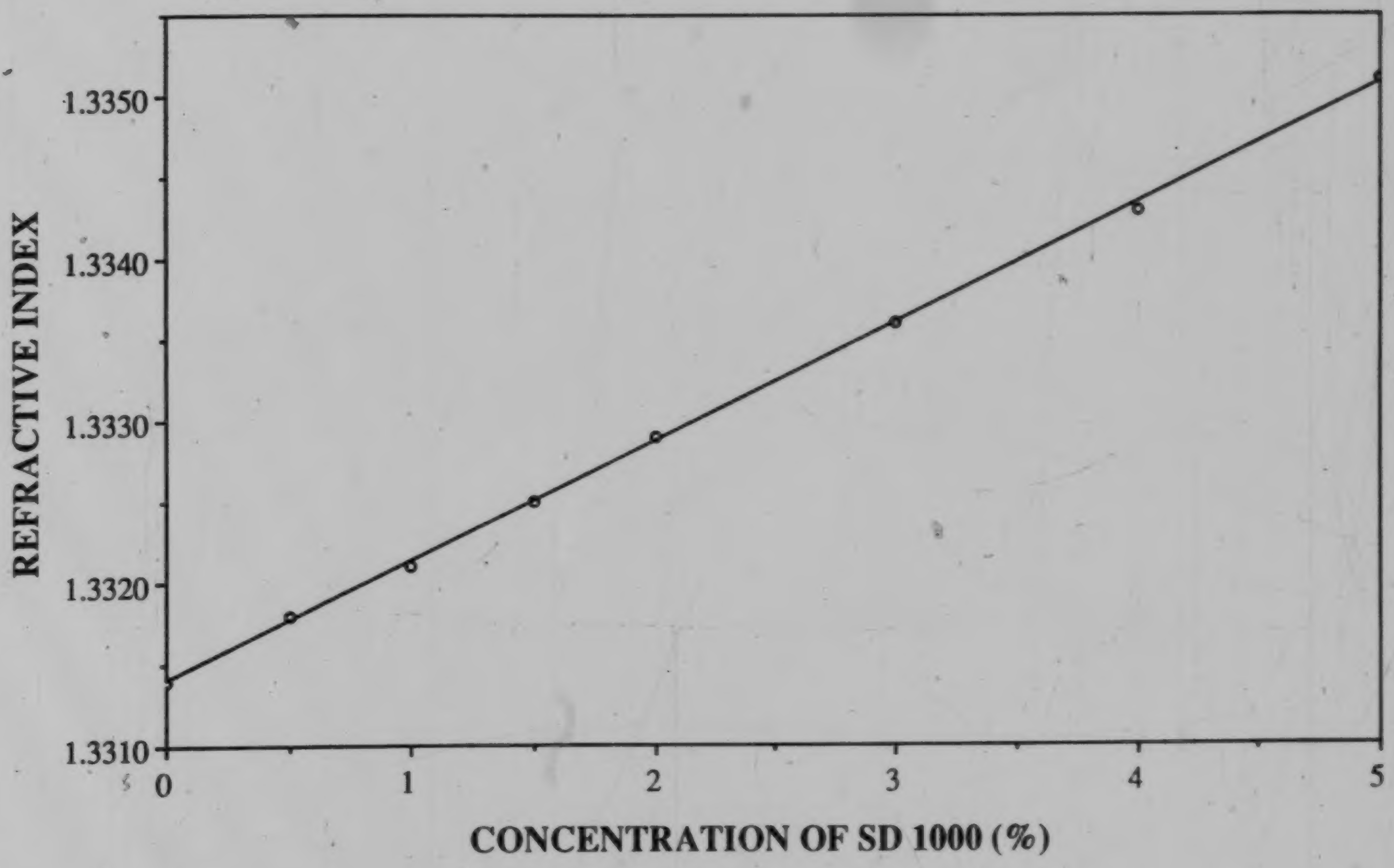

Figure 4.7 Refractive Index Vs. Surfactant Concentration

Handy[39]. A comparison of concentration determined by refractive index and by spectrophotometer analysis is given in Figure 4.8. The ultraviolet spectrophometer determines surfactant concentration based on the fundamental law of absorption which is that the rate of decrease in radiant power with the length of the light path b, or with the concentration of the absorbing material C, will follow an experimental progression:

$$T = 10^{-A} = 10^{-abc}$$

where A is the absorbance and a is the absorbivity. Therefore

$$A = abc,$$

and a plot of A versus C yields a straight line with a slope of ab. This plot will pass through the origin. To use the spectrophotometer various surfactant concentrations were tested over the wavelength range, to determine the location of a characteristic peak. At this point a calibration graph was generated to test the accuracy of the spectrophotometer. This graph is included as Figure 4.9

4.3.2 Experimental Procedure for the Pre-Foamed Temperature-Controlled Co-injection Runs

In order to perform an experiment a surfactant solution of the appropriate concentration was prepared. The surfactant was

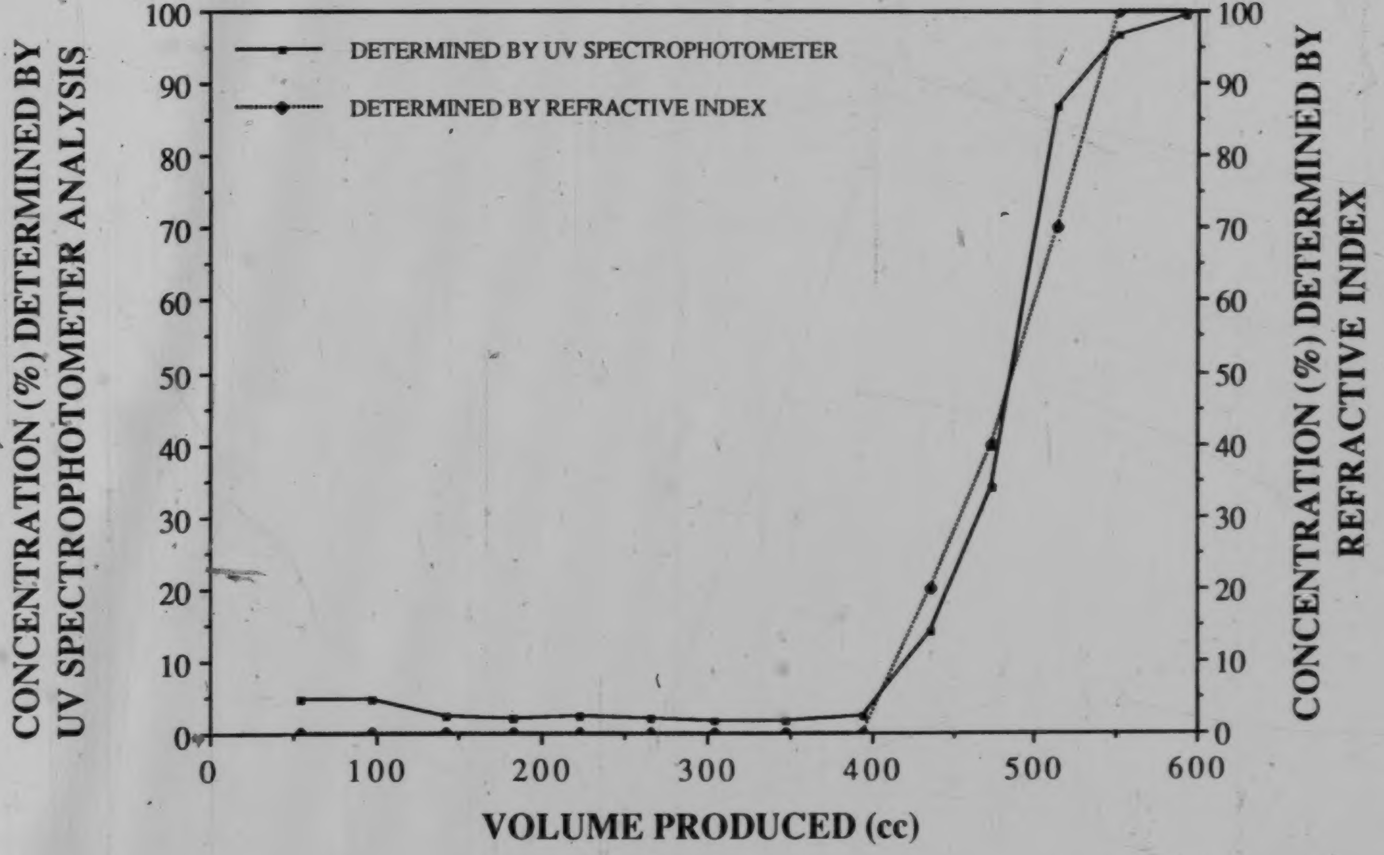

Figure 4.8 Crossplot of Concentration Determined by Spectrophotometer and Refractive Index Vs. Concentration

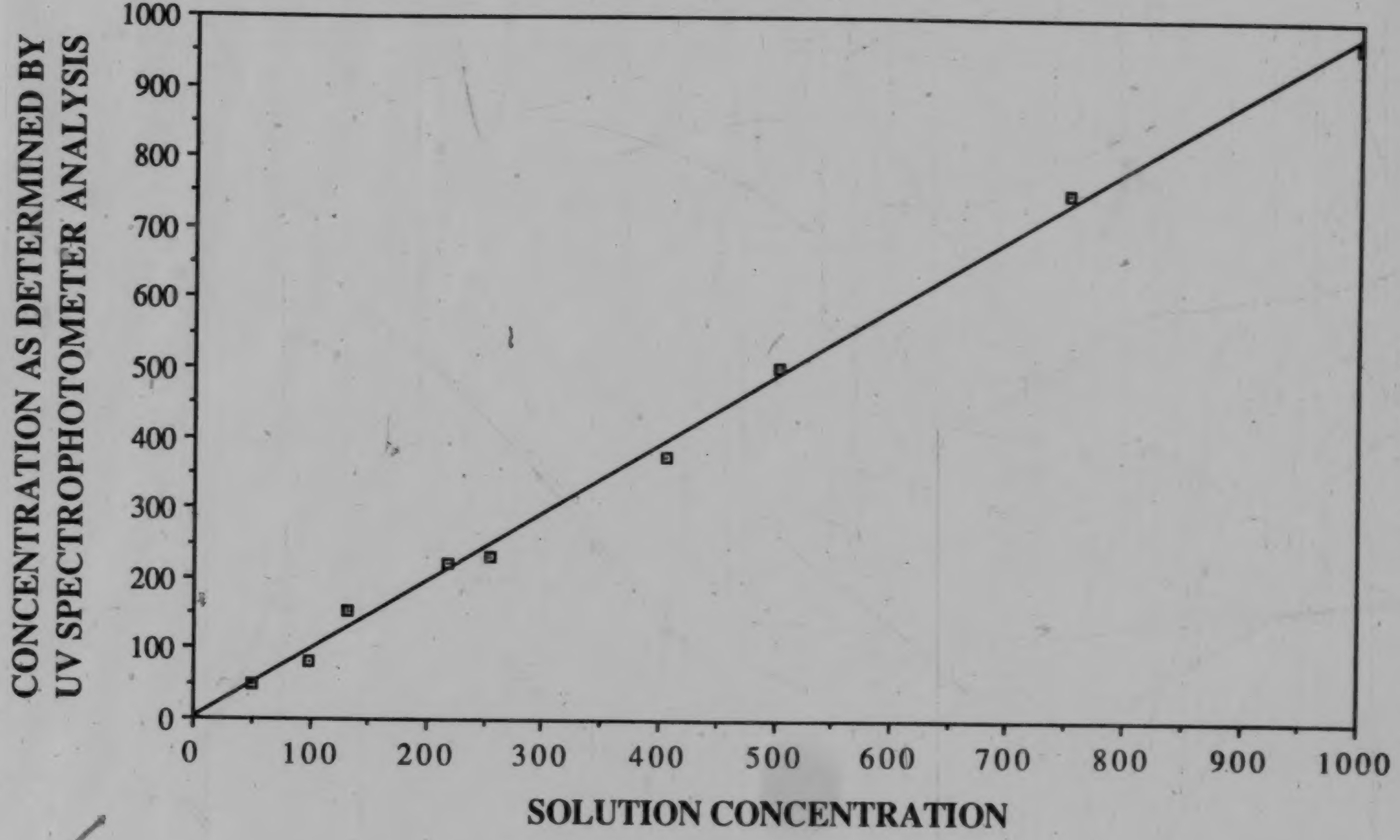

Figure 4.9 Concentration Determined By Spectrophotometric Analysis Vs. Concentration

weighed on a Mettler* balance to four decimal places. The solution was weighed on a digital scale to two decimal places. The solution was stirred and then poured into the Ruska pump cylinder.

The foam generator and coreholder were positioned in the oven and connected to the system with quick-fits. The inlet end of the system was closed and a surfactant slug was injected. The outlet pressure was carefully monitored until it reached the appropriate back pressure. The Jergoson cell was then filled with nitrogen until the back pressure was matched. The outlet valve was then opened and the slug injection continued until the desired slug volume was reached. The back pressure regulator maintained a constant back pressure.

The injection line was then disconnected. The mass flow controller was set to the desired rate. The injection line was constantly depressured until the stabilized rate was achieved. The Ruska pump co-injected the surfactant solution with nitrogen at a preset rate.

The surfactant solution and the nitrogen both flowed into the injection line. The nitrogen line was equipped with a check valve to prevent the surfactant solution from entering the nitrogen line. When the injection line was re-connected, the totalizer was set to zero and the timer started.

---

* purchased through Fisher Scientific 107-178 St.
Edmonton, Alta 483-2123

The Jergoson cell was graduated such that when fifty millimeters of solution had entered the cell it could be sampled. The sampling procedure was outlined previously. When each sample was collected, the time, pressure, and totalizer readings were recorded. The sample volume was also recorded. The refractive index or the spectrophotometer reading of the sample was then determined.

4.3.3 Operational Difficulties

Due to the fact that it was necessary to design and build the equipment, there were several operational difficulties encountered in the initial runs.

The first problem encountered was developing a standard technique in which the maximum information could be determined with the most consistent procedure. The results of the runs first performed were not included in the study due to the fact that the data was collected inconsistently. Developing a consistent run procedure, involved performing the run several times, in which the procedure was varied. This resulted in discarding several initial runs.

Other problems encountered in the initial runs included: leaks in coreholder end-caps and foam generator, valve leaks and problematic or non-existent sampling.

The outlet end of the equipment was re-designed when the initial runs were complete. It was initially designed simply to measure the effluent volume. To sample the effluent in regular intervals and analyze the concentration, a sample valve was added. The sample procedure involved shutting off the exit valve while a sample was taken. It was felt that this did not significantly affect the experimental results. This is evidenced by the fact that the differential pressure was the same before and after the sampling procedure, once the system had reached steady state. Although the sampling method could be improved (refer to Chapter 4) the alternatives were too costly and time consuming to be considered at this time.

During the runs performed at high temperatures (125 - 130° C) there was a problem sampling the effluent at atmospheric pressure. A system was developed whereby flexible plastic tubing was wound around the bolts of the Jergoson cell. A pump circulated cold water around the cell. Due to problems with the circulatory pump, bags of ice were eventually used to cool the flex-lines that led to the Jergoson cell. At the highest temperatures used in this study it was not difficult to cool the effluent to the liquid phase at atmospheric conditions.

If the temperature was to be increased significantly a better cooling system, such as the one described, would be necessary.

The original dual core experimental apparatus used two back pressure regulators. It was determined that it was too difficult to adjust both back pressure regulators to precisely the same pressure. Because of this, the flow could take place in the less permeable coreholder.

The outlet system was therefore re-designed to utilize only one back pressure regulator. To do this a different configuration of valves was developed to maintain the identical back pressure in both Jergoson cells.

V Discussion

5.1 Introduction

This chapter presents the results and discussion of an experimental analysis of foam flow within porous media. Considerable emphasis was placed on the design and construction of the experimental apparatus utilized. The runs conducted, along with initial core and foam properties are listed in Tables 5.1 and 5.2.

This study was conducted to analyze the flow of foam in porous media. Specifically, the research was performed to determine the value of foam as a secondary recovery method. To do this, experimental runs were performed to evaluate foamability with changing variables, such as: absolute permeability, surfactant concentration, surfactant type, temperature, residual oil saturation and quality of foam. Experiments were also performed to examine the ability of foam to act as a blocking agent in porous media.

This chapter contains an introduction to the study, and proceeds to a description of the experimental result presentation. The preliminary runs performed, and the nitrogen-surfactant co-injected runs are examined individually, and in categories, to examine the effect of changing variables. Finally, a discussion and comparison of experimental and simulator results is presented based upon the numerical simulator that was developed and utilized.

Table 5.1 Preliminary Runs

Run	Core Orient.	Surfactant Type	Surfactant Conc. (%)	Porosity (%)	Absolute Perm. (darcies)	Steady-State Pressure Drop Across the Core (psi)
#1P	H	None	0	34.0	28.1	5.1
#2P	H	SD 1000	1	34.1	32.5	6.1
#3P	H	SD 1000	5	32.8	28.1	6.5
#4P	H	XP 100	1	34.2	27.8	5.5
#5P	H	XP 100	5	34.3	30.0	6.3
#6P	H	Dow	1	31.9	26.5	6.3
#7P	H	Dow	5	32.2	26.9	6.5
#8P	V	Dow	1	31.5	25.8	6.5
#9P	V	Dow	5	31.6	26.5	6.5
#10P	H	None	0	?	3.5	1.2
#11P	H	SD 1000	1	32.8	3.1	11.2

P = Preliminary
H = Horizontal Core
V = Vertical Core

Table 5.2 Temperature Controlled Co-injection Nitrogen-Surfactant Runs

Run #	Surf. Type	Surf. Conc. %	Abs. Perm. darcies	Temp. °C	Oil Sat. %	Porosity %	Steady State p. (psi)	Quality	Steady State Sw	Total Mobility	Relative Mobility	Mobility Reduction Factor	Comments
#12P	None	0.0	4.7	20	0.0	33.2	2.00	0.9307	***	5.5800	1.1870	1.000	No Sw Data Available
8	None	0.0	8.1	20	25.1	34.0	1.75	0.9308	0.6069	6.3789	0.7875	1.000	
1	SD 1000	1.0	6.2	20	0.0	33.2	11.00	0.9262	0.3250	0.9526	0.1536	5.500	
2	SD 1000	1.0	6.2	20	20.4	33.2	2.50	0.9304	0.7243	4.4416	0.7164	1.429	
9	SD 1000	1.0	7.8	90	0.0	32.7	13.50	0.9386	0.3162	0.9324	0.1195	6.750	
10	SD 1000	1.0	3.5	20	Sgr	32.9	5.25	0.9290	0.3420	2.0748	0.5928	2.620	
19	SD 1000	2.5	7.1	20	0.0	33.1	11.25	0.9299	0.3204	0.9299	0.1310	5.625	
3	SD 1000	5.0	5.2	20	0.0	33.4	9.00	0.9272	0.3879	1.1799	0.2269	4.500	
4	SD 1000	5.0	7.1	20	21.7	32.8	3.00	0.9301	0.7613	3.6883	0.5195	1.714	
21	None	0.0	13.5	20	0.0	32.3	1.25	0.9310	0.8861	8.9623	0.6639	1.000	
11	SD 1000	1.0	12.2	20	0.0	33.3	5.00	0.9292	0.3882	2.1824	0.1789	4.000	
7	SD 1000	1.0	15.0	20	0.0	33.7	2.50	0.9304	0.5190	4.4416	0.2961	2.000	
12	SD 1000	1.0	12.7	20	0.0	32.7	6.75	0.9283	0.3042	1.5972	0.1258	5.400	No Foam Generator
20	SD 1000	1.0	15.1	20	0.0	32.3	6.25	0.7647	0.5074	2.1019	0.1392		4:50 cc/min. Surf:N2
13	SD 1000	1.0	12.1	54	0.0	32.2	12.75	0.9326	0.3093	0.8997	0.0744	10.200	
16	SD 1000	1.0	11.5	90	0.0	33.2	19.00	0.9364	0.2013	0.6494	0.0556	15.200	
15	SD 1000	1.0	13.0	125	0.0	33.2	>55.00	0.9267	0.2632	0.1758	0.0135	44.000	No Steady State
22	SD 1000	1.0	13.2	125	20.0	32.2	2.25	0.9479	0.5245	6.5924	0.4994	0.000	

Sgr = Residual Gas Saturation

Table 5.2 Temperature Controlled Co-injection Nitrogen-Surfactant Runs

Run #	Surf. Type	Surf. Conc. %	Abs. Perm. darcies	Temp. °C	Oil Sat. %	Porosity %	Steady State p. (psi)	Quality	Steady State Sw	Total Mobility	Relative Mobility	Mobility Reduction Factor	Comments
18	SD 1000	2.5	15.2	20	0.0	32.3	7.50	0.9279	0.3353	1.4302	0.0941	6.000	
5	SD 1000	5.0	17.5	20	0.0	32.0	4.50	0.9294	0.3598	2.4333	0.1390	3.600	
17	SD 1000	1.0	30.0	20	0.0	32.5	2.25	0.9305	0.3157	4.9438	0.1648		
6	SD 1000	5.0	28.7	20	0.0	33.4	0.50	0.9314	0.3623	22.5261	0.7849		
14	SD 1000	1.0	0.7	20	0.0	18.0	27.50	0.9183	0.7149	0.3439	0.5291		Consolidated Core
23	Dow	1.0	10.9	20	0.0	33.4	>100	0.8849	0.2496	0.0671	0.0062		No Steady State
24	Dow	1.0	13.1	125	0.0	33.6	*Error						Problem with run
27	Dow	1.0	11.2	125	0.0	32.4	>200	0.8791	0.0694	0.0320	0.0029		No Steady State
#25A	SD 1000	1.0	16.0	20	0.0	34.0	1.60						Dual core run
#25B	SD 1000	1.0	7.5	20	0.0	34.7	1.60						
#26A	SD 1000	1.0	5.3	125	0.0	33.5	2.10						Dual core run
#26B	SD 1000	1.0	17.1	125	0.0	32.8	2.10						
#28A	SD 1000	1.0	7.5	125	0.0	33.7	3.6						Dual core run
#28B	SD 1000	1.0	18.4	125	0.0	34.4	3.6						

5.1.2 Experimental Results

The data for the preliminary runs is given in Table 5.3 to Table 5.12 and Figure 5.2 to Figure 5.19. The co-injected nitrogen-surfactant run data is available in Table 5.13 to Table 5.112 and Figure 5.20 to Figure 5.112.

Experimental runs of several types were conducted. Preliminary runs were performed to test the ability of foam to reduce gas phase mobility, and to examine foam flow in its simplest form. It was generally determined that the addition of surfactant, prior to gas injection, caused a delay in gas breakthrough time, and an increase in produced volume at breakthrough. Various surfactants were compared during this analysis. These experiments provided valuable insight into potential design problems associated with foam flow experiments that proved helpful for the design of the co-injection apparatus.

The next series of runs involved a comparison of produced volumes and differential pressures for two cores. One of these cores was initially saturated with water, the other one was completely saturated with a surfactant solution. These two runs, and the following runs, were performed on the modified equipment.

The first series of co-injection runs performed was a comparison of Maini's[35] base cases where the water-nitrogen ratio was changed. A water base case with effluent sampling was later performed with which the surfactant runs could be compared.

The variables examined included: absolute permeability, surfactant concentration, temperature, residual oil saturation, foam quality, and to residual trapped gas saturation. Use of a foam generator was carefully studied. Temperature, surfactant concentration, and residual oil saturation were also altered in combination with each other. A flowchart of the runs performed is presented in Figure 5.1.

In several runs, dual cores were used. This was done to test the theory that foam will act as a blocking agent, preferentially blocking the high permeability channels.

Data analysis of the later runs included comparison tables and plots of the cumulative volume and differential pressure versus the elapsed time, and the concentration, versus the number of pore volumes of effluent collected.

The final stage of this research included the development and the use of a two-phase foam simulator. Comparisons of the experimental and simulated results are presented.

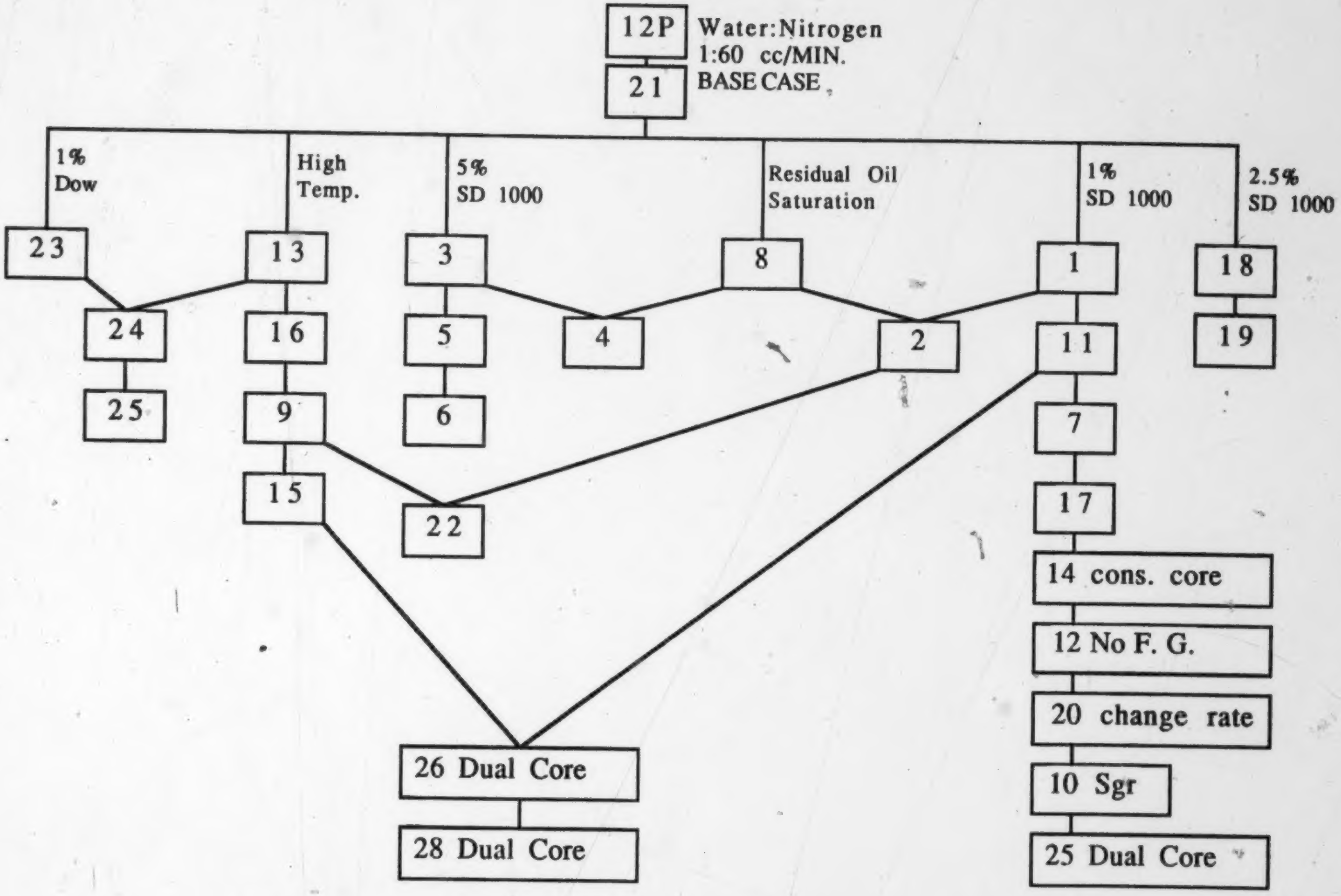
12P
Water:Nitrogen
1:60 cc/MIN.
BASE CASE
21
1%
Dow
High
Temp.
5%
SD 1000
Residual Oil
Saturation
1%
SD 1000
2.5%
SD 1000
23
13
3
8
1
18
24
16
5
4
2
11
19
25
9
6
7
15
22
17
14 cons. core
12 No F. G.
20 change rate
26 Dual Core
10 Sgr
28 Dual Core
25 Dual Core

Figure 5.1 Flow Chart of Co-Injected Runs Performed

5.2 Preliminary Runs

The preliminary runs were performed to test the ability of certain surfactants to form a foam at room temperature, and to determine if there was a reduction in gas phase mobility in the presence of a foam. The equipment used for these runs was presented in Figure 4.1. These runs were conducted without the use of a foam generator. These runs were performed with three surfactants: XP100, SD1000 and Dow surfactant. Two runs were performed, using the Dow surfactant, with the coreholder held vertically. The value of the preliminary run data lies more in the trends that were identified than in the numerical values obtained.

At this point, a brief reiteration of the preliminary run procedure is presented. The water saturated coreholder was initially flooded with nitrogen. Following this, the volume produced at gas breakthrough, the time until gas breakthrough, and the volume produced at 60 seconds were recorded. The coreholder was then oriented vertically, and resaturated with water; this was the first resaturation. The gas flood was repeated, and the same values were recorded. The second gas flood was performed to provide a base case with residual gas saturation. This was done in order to provide a comparison for the second resaturation, performed with an injected slug of surfactant. (The procedure utilized for the preliminary runs was outlined in the previous chapter (Section 4.1 Preliminary Experiments).

For each run, a separate core was packed. The packing method was varied to examine the effect of: dry or wet packing, or changing the vibrator size. As can be seen from Table 5.3, the dry packing method with the large vibrator produced a sandpack with lower absolute permeabilities and porosities.

5.2.1 Water Base Case

The data for the water base case Run 1P, is given in Table 5.4, and plotted in Figure 5.2. From the graph it is evident that the percent pore volume produced at breakthrough, and at sixty seconds, is greater for the initial flood than for either resaturation flood. The percent pore volume produced at breakthrough is 22.6 for the initial flood compared to 18.3 for the first resaturation, and 17.3 for the second. This difference is due to the residual gas saturation present in the coreholder following the initial gas flood, which acts to reduce liquid pore volume.

It is noteworthy that the first and second resaturations yield similar results. This suggests that the residual gas saturation is unchanged by the second resaturation. This assumption was utilized to determine the preliminary run core flooding sequence. In each case, the surfactant run was the second resaturation, and the numerical values were compared with the first resaturation data. This was done because the packing method was not consistent, and

Table 5.3 Comparison of Packing Methods

Run	Pack Type	Vibrator Size	Porosity %	Absolute Perm. darcies
#1P	Wet	Small	34.0	28.1
#2P	Wet	Large	34.1	32.5
#3P	Dry	Small	32.8	28.1
#4P	Wet	Small	34.2	27.8
#5P	Wet	Small	34.3	30.0
#6P	Dry	Small	31.9	26.5
#7P	Dry	Small	32.2	26.9
#8P	Dry	Large	31.5	25.8
#9P	Dry	Large	31.6	26.5

P = Preliminary

Experimental Data For Run #1P
Water Base Case

Sandpack
Surfactant: None
Absolute Permeability: 28.1 darcies
Porosity: 34.0%
Pore Volume: 399 cc
Inlet Pressure: 6.5 psi
Back Pressure: Atmospheric

Procedure	**Volume (cc)**	**Pore Volume (%)**	**Time (s)**		**Outlet Pressure (psi) (est.)**
Initial Flood	90	22.6	14.3	breakthrough	
	235	58.9	60		1.6
Resaturated	73	18.3	12.5	breakthrough	
	218	54.6	60		1.6
Resaturated	69	17.3	11.8	breakthrough	
	214	53.6	60		1.5

Table 5.4 Experimental Data for Run 1P Water Base Case

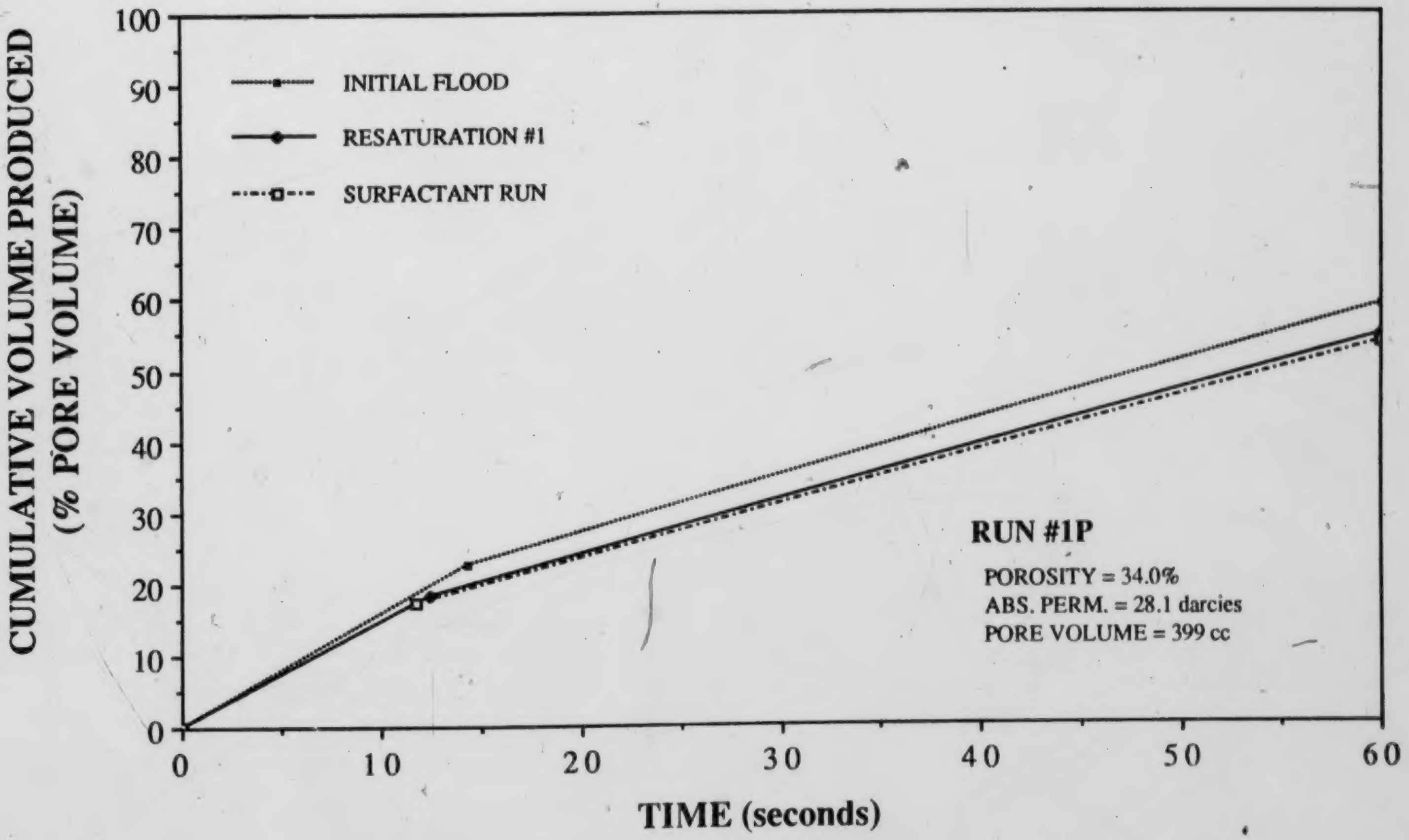

Figure 5.2 Run 1P: Cumulative Volume Produced Vs. Time

the porosity and absolute permeability varied for each packed coreholder.

5.2.2 Surfactant SD 1000

Runs 2P and 3P were performed using surfactant SD1000. The data for Run 2P, in which a 40 ml slug of 1 percent SD 1000 was used, is given in Table 5.5. This slug size was approximately 10 percent of the coreholder pore volume. The time to gas breakthrough increased from 14.2 seconds in the first resaturation to 33.7 seconds, once the surfactant slug was added. The percent pore volume produced increased from 21.3 to 36.3 at breakthrough. From Figure 5.3 it can be seen that the percent pore volume produced at 60 seconds is only slightly higher for the surfactant run than it is for the first resaturation, 53.9 compared to 49.6. The outlet pressure was lower in the surfactant run, than in the water runs, 6.1 psi compared to 1.43 psi, due to the blocking action by the foam. The small surfactant slug of 1 percent solution was probably too diluted and too small to show a large effect on fluid production, however the gas breakthrough time was significantly delayed.

Run 3P utilized a 40 ml slug of 5 percent SD1000. The data is presented in Table 5.6. The gas breakthrough time was extended from 10.2 seconds for the first resaturation to 180 seconds for the surfactant run. The percent pore volume produced at breakthrough increased from 18.5 to 50.9. This is depicted in Figure 5.4. There

Experimental Data For Run #2P
1% Surfactant SD 1000

Sandpack

Surfactant:	SD 1000	**Porosity:**	34.1%
Concentration:	1%	**Pore Volume:**	399 cc
Surfactant Slug Size:	40 cc	**Inlet Pressure:**	6.5 psi
Absolute Permeability:	32.5 darcies	**Back Pressure:**	Atmospheric

Procedure	Volume (cc)	Pore Volume (%)	Time (s)		Outlet Pressure (psi) (est.)
Initial Flood	100	25.1	18.1	breakthrough	
	205	51.4	60		1.6
Resaturated	85	21.3	14.2	breakthrough	
	198	49.6	60		1.6
Surfactant Run	145	36.3	33.7	breakthrough	
	215	53.9	60		0.4

Table 5.5 Experimental Data for Run 2P: 1% SD1000

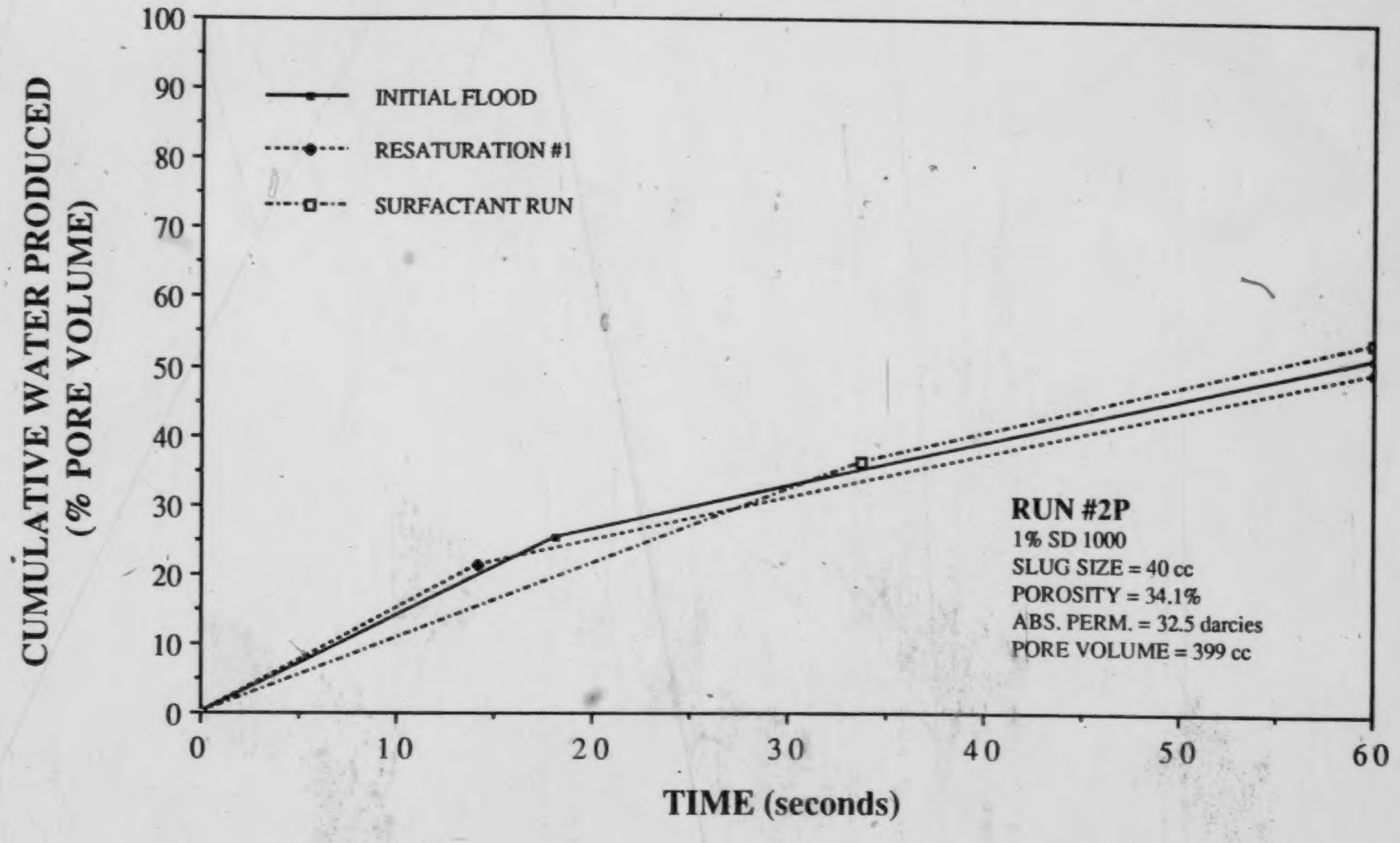

Figure 5.3 Run 2P Cumulative Water Produced Vs. Time

Experimental Data For Run #3P
5% Surfactant SD 1000

Sandpack

Surfactant:	SD 1000	**Porosity:**	32.8%
Concentration:	5%	**Pore Volume:**	383 cc
Surfactant Slug Size:	40 cc	**Inlet Pressure:**	6.5 psi
Absolute Permeability:	28.1 darcies	**Back Pressure:**	atmospheric

Procedure	**Volume (cc)**	**Pore Volume (%)**	**Time (s)**		**Outlet Pressure (psi) (cst.)**
Initial Flood	129	33.7	19.4	breakthrough	
	252	65.8	60		1.6
Resaturated	71	18.5	10.2	breakthrough	
	199	52.0	60		1.8
Surfactant Run	195	50.9	180	breakthrough	
	232	60.6	225		0.0
	247	64.5	300		
	257	67.1	450		

Table 5.6 Experimental Data for Run 3P: 5% SD1000

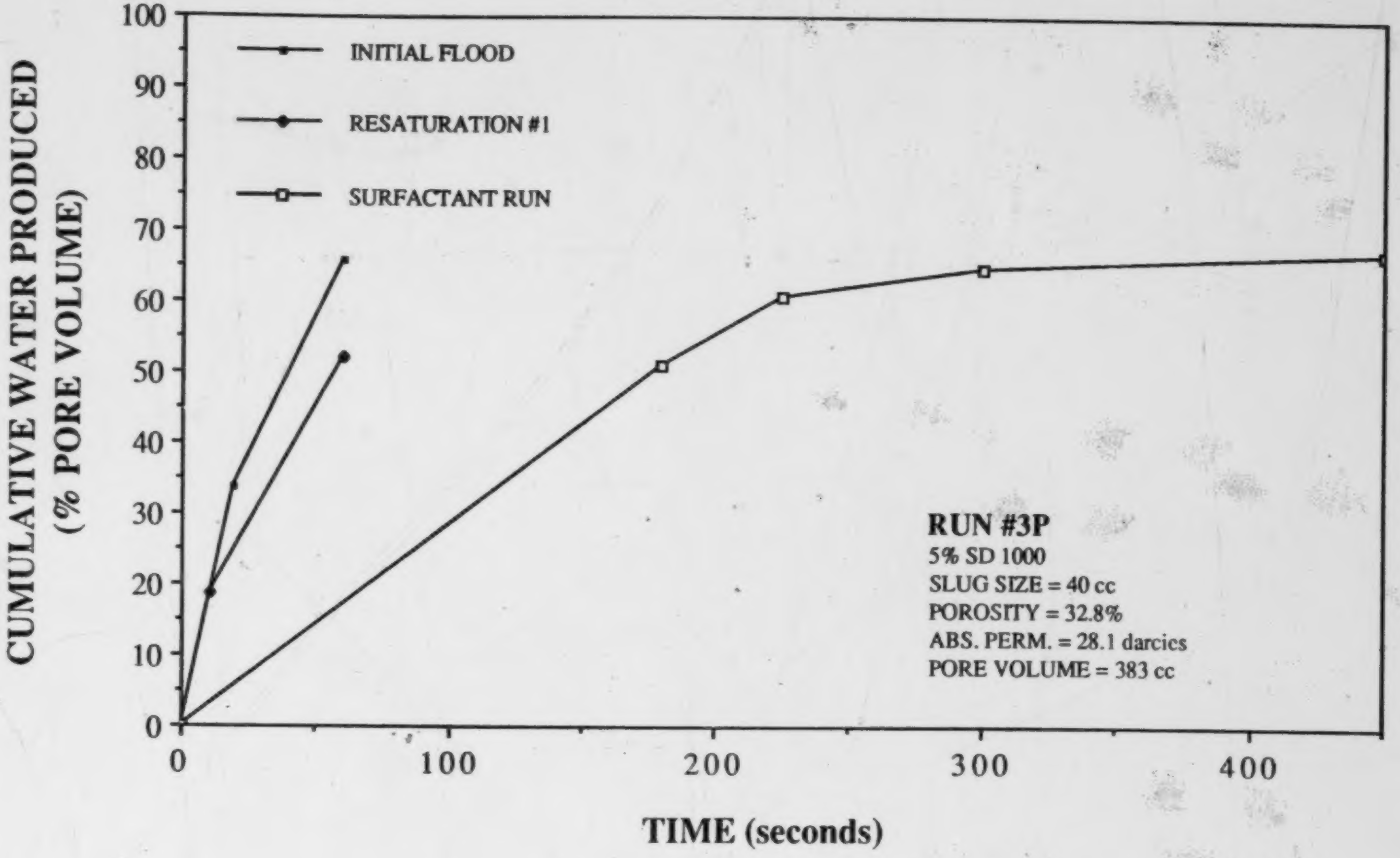

Figure 5.4 Run 3P: Cumulative Water Produced Vs. Time

was no increase in outlet pressure established, therefore the differential pressure across the core was increased by the foam.

Figure 5.5 is a graphical representation of the results obtained for surfactant SD1000 at breakthrough conditions. It is evident that breakthrough times and volumes are increased by the use of the surfactant. From this graph, it would also seem that a 5 percent solution is superior to a 1 percent SD1000 solution, as far as flow resistance is concerned. Although this is possible, due to the nature of the preliminary runs, this result is not conclusive. When the 5 percent solution was injected into the porous medium it likely became diluted. This injected solution would be equivalent to a 1 percent solution of the five times the slug volume. To determine the value of increased surfactant concentration a continuous surfactant injection, as was used for the co-injected runs, would be more meaningful.

5.2.3 Surfactant XP100

Runs 4P and 5P utilized the next surfactant tested, XP100. Table 5.7 provides the data for Run 4P, the 1 percent surfactant case. The differential pressure established across the coreholder during the surfactant flood was 5.43 psi. This is slightly larger than the 4.86 psi established with water. The gas breakthrough time increased from 10.7 seconds for the first resaturation to 25 seconds with the addition of surfactant. Figure 5.6 shows that the percent pore

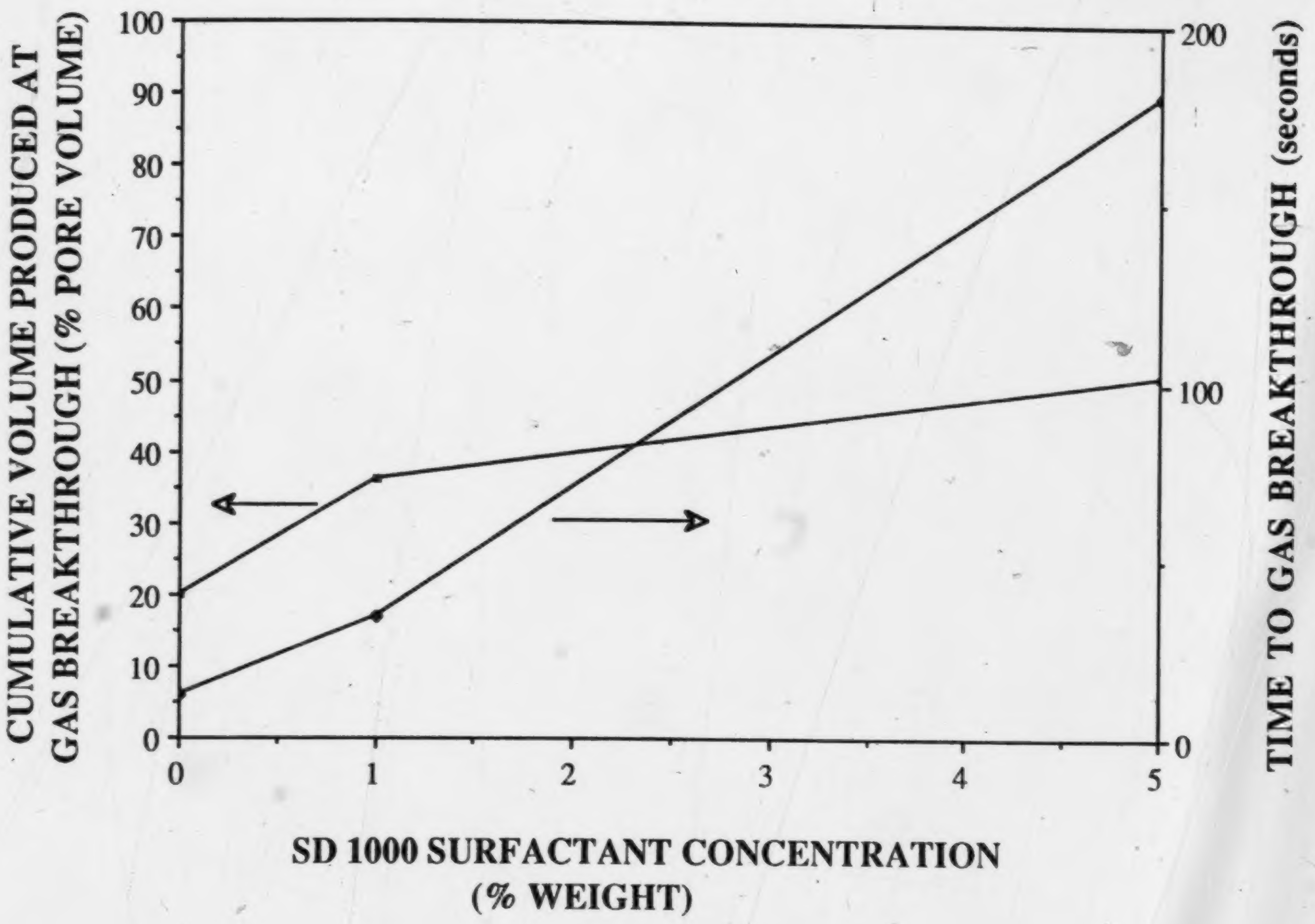

Figure 5.5 Cumulative Volume Produced at Gas Breakthrough and Time to Gas Breakthrough Vs. SD1000 Surfactant Concentration

Experimental Data For Run #4P
1% Surfactant XP 100

Sandpack

Surfactant:	XP 100	**Porosity:**	34.2%
Concentration:	1%	**Pore Volume:**	400 cc
Surfactant Slug Size:	40 cc	**Inlet Pressure:**	6.5 psi
Absolute Permeability:	27.8 darcies	**Back Pressure:**	Atmospheric

Procedure	**Volume (cc)**	**Pore Volume (%)**	**Time (s)**		**Outlet Pressure (psi) (est.)**
Initial Flood	80	20.0	12.9	breakthrough	
	229	57.3	60		1.6
Resaturated	63	15.8	10.7	breakthrough	
	208	52.0	60		1.6
Surfactant Run	90	22.5	25	breakthrough	
	202	50.5	60		1.0

Table 5.7 Experimental Data for Run 4P: 1% XP100

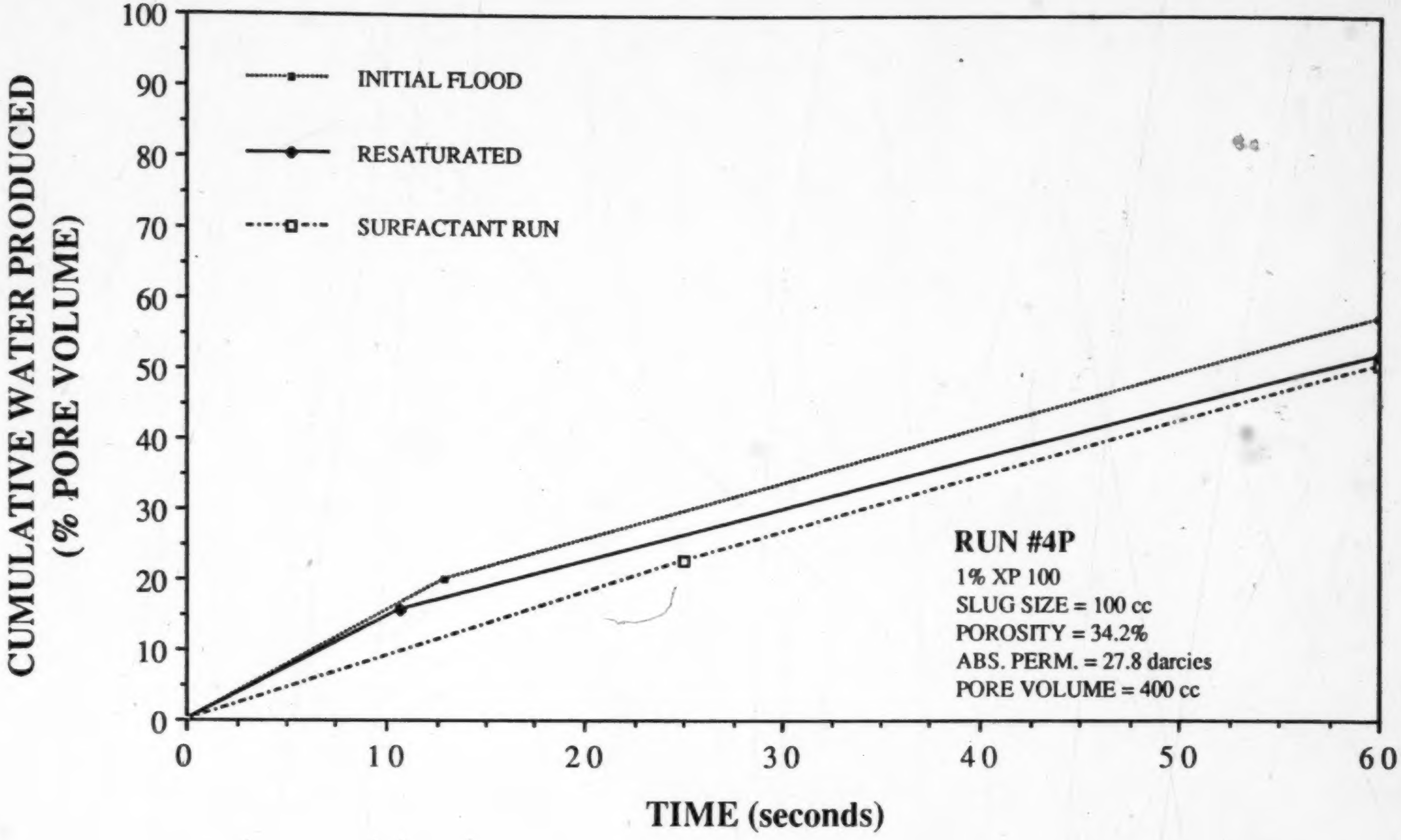

Figure 5.6 Run 4P: Cumulative Water Produced Vs. Time

volume produced is greater, 22.5 at gas breakthrough for the surfactant case, than for the first resaturation, 15.8.

The graph also shows that at 60 seconds the volume of produced fluids is slightly less for the surfactant case than for the first resaturation. This is an important result because it shows that, although the surfactant delayed gas breakthrough it did not result in increased fluid production. This is possibly because a small amount of foam was generated, following gas breakthrough. The effect of this was to lower the gas mobility after gas breakthrough.

The data for Run 5P is presented in Table 5.8. This run utilized a 5 percent XP100 solution. The results of this run are interesting, as can be seen in Figure 5.7, because the surfactant run had a shorter gas breakthrough time and produced less fluid at gas breakthrough. It is interesting that, rather than having no effect, the 5 percent surfactant solution was detrimental to increased fluid production. Once gas breakthrough occurred, it is interesting to note that the fluid production increased by only 22 cc at 60 seconds. For the first resaturation this amount was 130 cc. The pressure drop established across the coreholder was 6.14 psi; for the 1 percent XP100 run the pressure drop was 5.43 psi. This surfactant was very difficult to dissolve in water at room temperature, having been designed for use at elevated temperatures. It is possible that large surfactant particles became plugged in the pore spaces. This would account for the low volume of produced fluids and the high differential pressure. Figure 5.8 shows a comparison of 1 and 5 percent solutions of XP100

Experimental Data For Run #5P
5% Surfactant XP 100

Sandpack

Surfactant:	XP 100	**Porosity:**	34.3%
Concentration:	5%	**Pore Volume:**	395 cc
Surfactant Slug Size:	40 cc	**Inlet Pressure:**	6.5 psi
Absolute Permeability:	30.0 darcies	**Back Pressure:**	Atmospheric

Procedure	Volume (cc)	Pore Volume (%)	Time (s)		Outlet Pressure (psi) (est.)
Initial Flood	110	27.8	16	breakthrough	
	245	62.0	60		1.6
Resaturated	65	16.5	11.8	breakthrough	
	195	49.4	60		1.6
Surfactant Run	50	12.7	9.7	breakthrough	
	87	22.0	60		0.3

Table 5.8 Experimental Data for Run 5P: 5% XP100

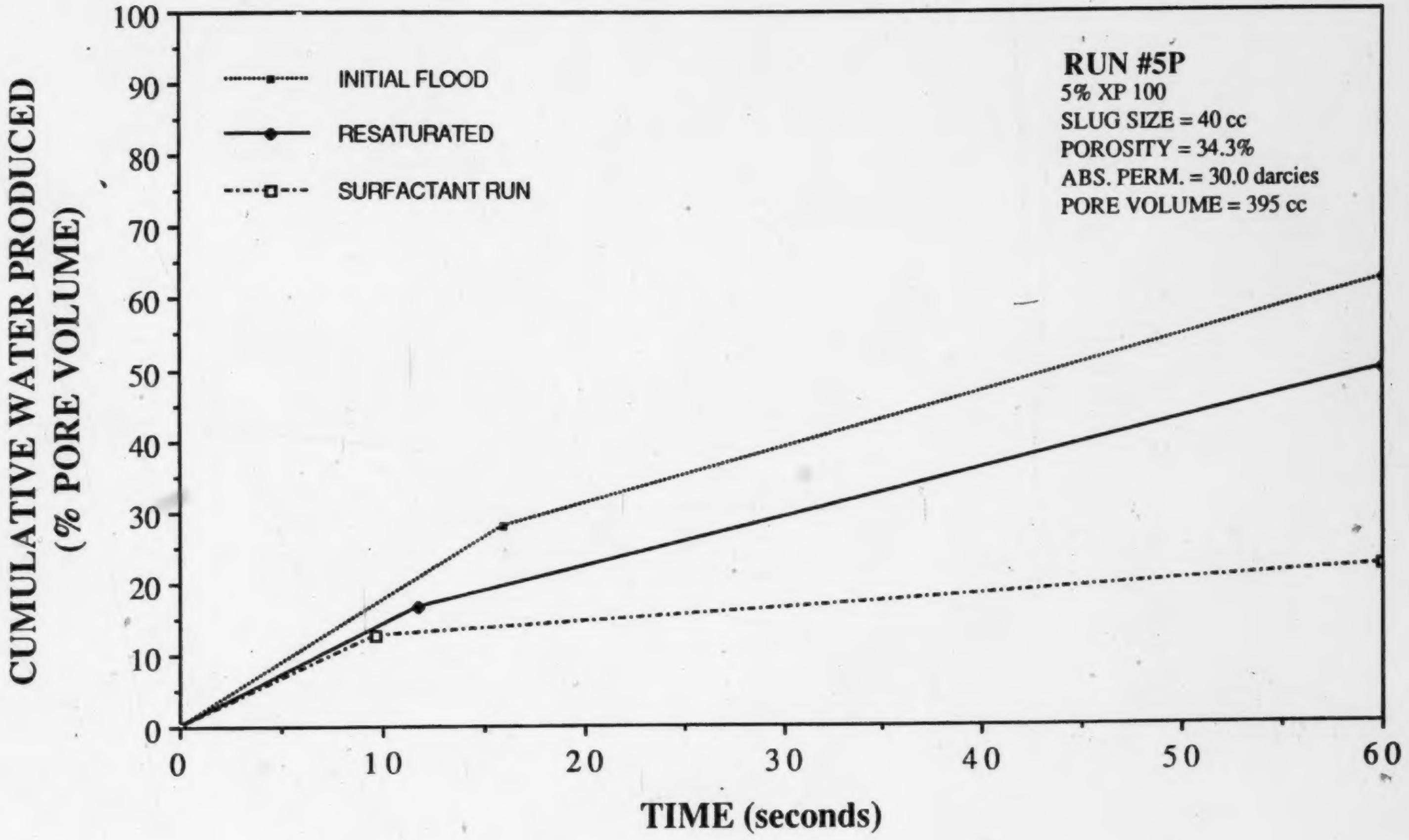

Figure 5.7 Run 5P: Cumulative Water Produced Vs. Time

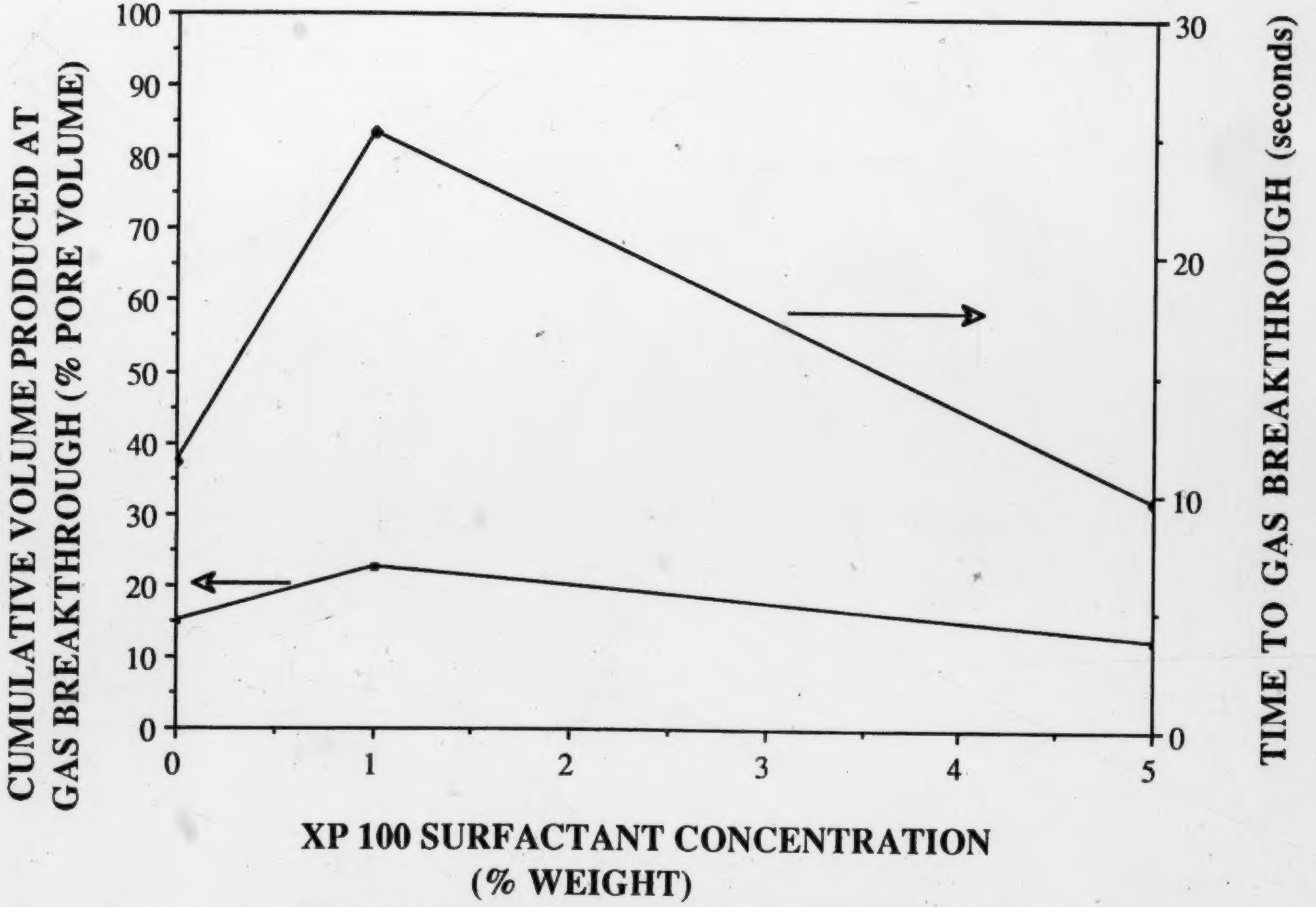

Figure 5.8 Cumulative Volume Produced at Gas Breakthrough and Time to Gas Breakthrough Vs. XP100 Surfactant Concentration

at gas breakthrough conditions. If this displacement were repeated at an elevated temperature the performance of this surfactant would be better, according to the specifications.

5.2.4 Dow Surfactant

Runs 6P-9P were conducted using the Dow surfactant. The data for Run 6P is given in Table 5.9. This run was conducted using a 1 percent surfactant solution. The gas breakthrough time was significantly delayed from 12.9 seconds for the first resaturation to 128.5 seconds for the surfactant run. As can be seen in Figure 5.9, the percent pore volume produced at breakthrough was 62.5 for the surfactant case compared to 12.9 for the first resaturation. The differential pressure increased to 6.14 psi from 4.71 psi, due to the presence of the surfactant, which led to foam generation.

For Run 7P, a 5 percent Dow surfactant solution was used. The run data is given in Table 5.10. The gas breakthrough was again delayed by the surfactant, from 10.2 seconds to 180 seconds. The percent pore volume increased to 75.3 at gas breakthrough from 10.6 for the first resaturation. This is graphically depicted in Figure 5.10. The foam decreased gas mobility such that the pressure at the outlet end of the core was atmospheric. The pressure differential established across the coreholder was, therefore, the maximum possible based upon the design criteria. The results for the 1 and 5 percent data at gas breakthrough are presented in Figure 5.11. The

Experimental Data For Run #6P
1% Dow Surfactant Horizontal

Sandpack

Surfactant:	Dow	**Porosity:**	31.9%
Concentration:	1%	**Pore Volume:**	373 cc
Surfactant Slug Size:	40 cc	**Inlet Pressure:**	6.5 psi
Absolute Permeability:	26.5 darcies	**Back Pressure:**	Atmospheric

Procedure	Volume (cc)	Pore Volume (%)	Time (s)		Outlet Pressure (psi) (est.)
Initial Flood	77	20.6	13.5	breakthrough	
	245	65.7	60		1.6
Resaturated	48	12.9	7.6	breakthrough	
	211	56.6	60		1.7
Surfactant Run	233	62.5	128.5	breakthrough	
	298	79.9	300		0.3

Table 5.9 Experimental Data for Run 6P: 1% Dow Surfactant

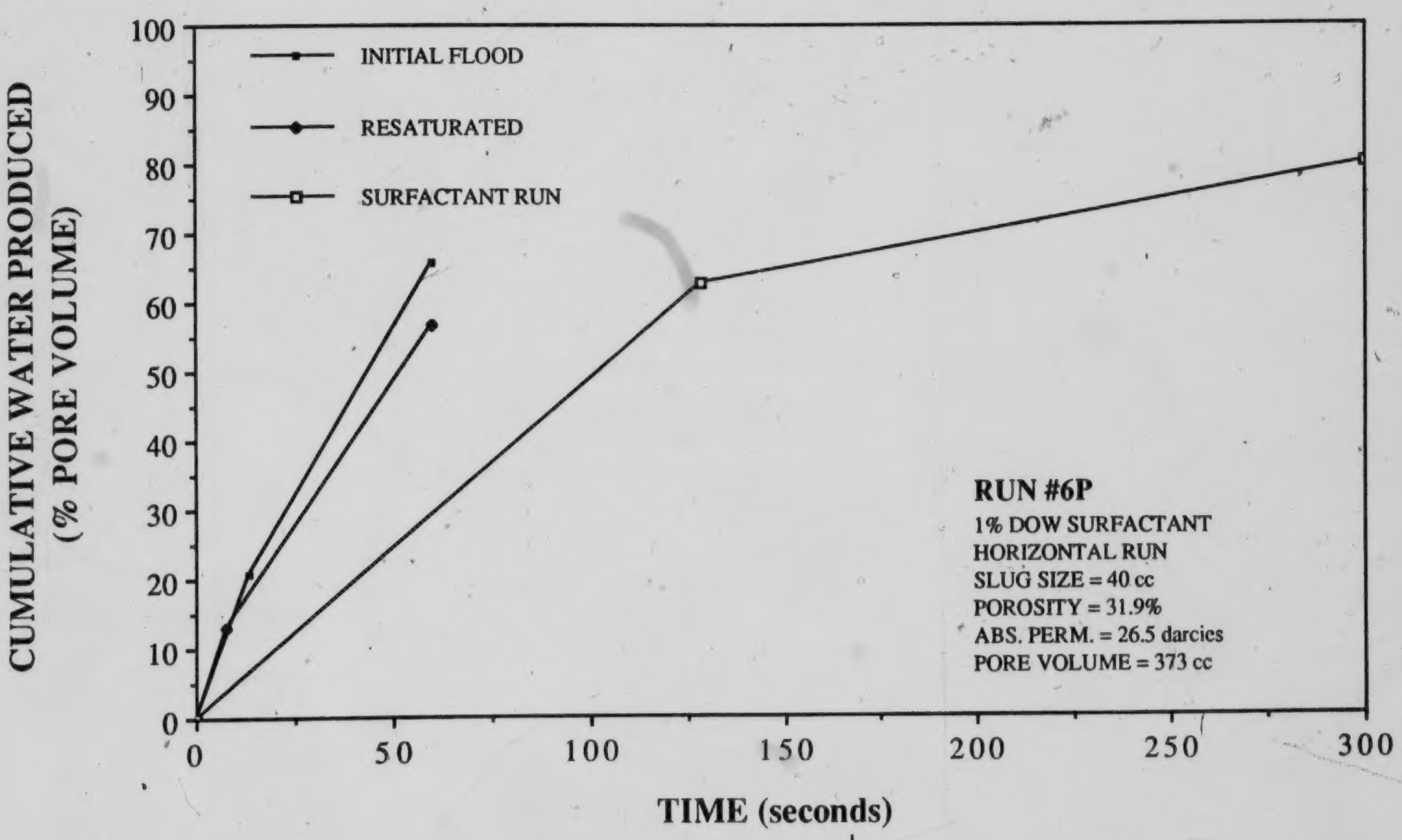

Figure 5.9 Run 6P: Cumulative Water Produced Vs. Time

Experimental Data For Run #7P
5% Dow Surfactant Horizontal

Sandpack

Surfactant:	Dow	**Porosity:**	32.2%
Concentration:	5%	**Pore Volume:**	376 cc
Surfactant · Slug Size:	40 cc	**Inlet Pressure:**	6.5 psi
Absolute Permeability:	26.9 darcies	**Back Pressure:**	Atmospheric

Procedure	**Volume (cc)**	**Pore Volume (%)**	**Time (s)**		**Outlet Pressure (psi) (est.)**
Initial Flood	95	25.3	19.4	breakthrough	
	249	66.2	60		1.6
Resaturated	40	10.6	10.2	breakthrough	
	215	57.2	60		1.8
Surfactant Run	283	75.3	180	breakthrough	
					0.0

Table 5.10 Experimental Data for Run 7P: 5% Dow Surfactant

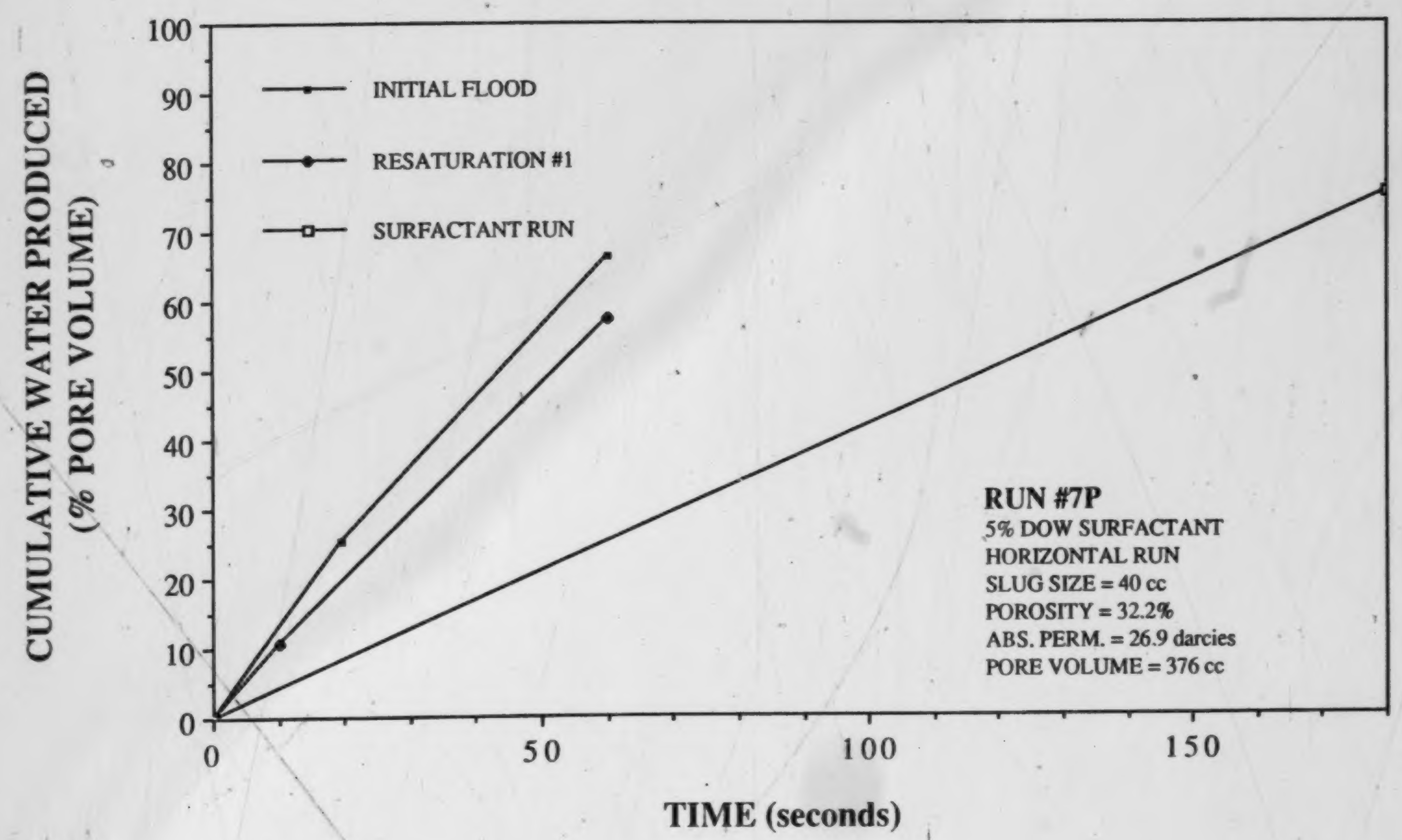

Figure 5.10 Run 7P: Cumulative Water Produced Vs. Time

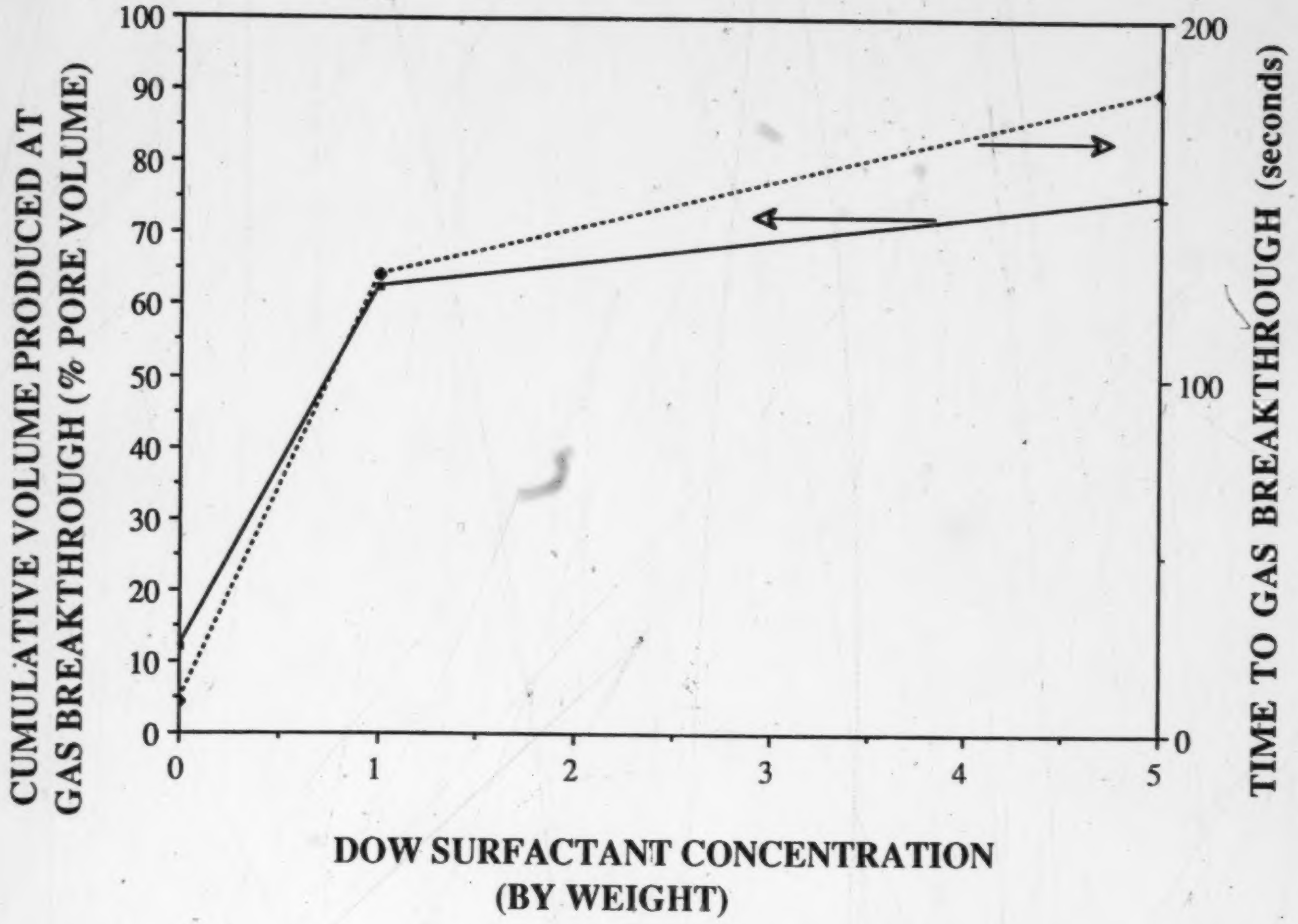

Figure 5.11 Cumulative Volume Produced at Gas Breakthrough and Time to Gas Breakthrough Vs. Dow Surfactant Concentration

system shows a definite response to the addition of a surfactant slug prior to a gas flood.

5.2.5 Dow Surfactant - Coreholder Oriented Vertically

The next several runs were also performed using the Dow surfactant, with core in the vertical position. The gas was injected from the bottom of the system, upward. It was found that the gas breakthrough time for the first resaturation was only 2 seconds for the vertical pack. For this reason the surfactant flood was performed on the first resaturation, rather than the second, as was normally done.

The data for Run 8P is given in Table 5.11. The surfactant caused the gas breakthrough time to increase to 313 seconds. The percent pore volume produced was 65.5 at gas breakthrough. Figure 5.12 provides a graphical illustration of the data. The time to gas breakthrough was longer, and the percent pore volume produced at gas breakthrough was considerably larger, than was determined for the initial gas flood values for this run.

The data for the vertical 5 percent Dow surfactant case, Run 9P, is given in Table 5.12. The time to gas breakthrough was 1056 seconds. This is a remarkable increase, considering that the initial flood breakthrough time was 11.5 seconds. The percent pore volume

Experimental Data For Run #8P
1% Dow Surfactant Vertical

Sandpack			
Surfactant:	Dow	**Porosity:**	31.5%
Concentration:	1%	**Pore Volume:**	368 cc
Surfactant Slug Size:	40 cc	**Inlet Pressure:**	6.5 psi
Absolute Permeability:	25.8 darcies	**Back Pressure:**	Atmospheric

Procedure	**Volume (ml)**	**Pore Volume (%)**	**Time (s)**		**Outlet Pressure (psi) (est.)**
Initial Flood	82	22.3	11.8	breakthrough	
	230	62.5	60		1.6
					0.0
Surfactant Run	241	65.5	313	breakthrough	
	320	87.0	420		0.0

Table 5.11 Experimental Data for Run 8P: 1% Dow Surfactant Vertically Oriented Core

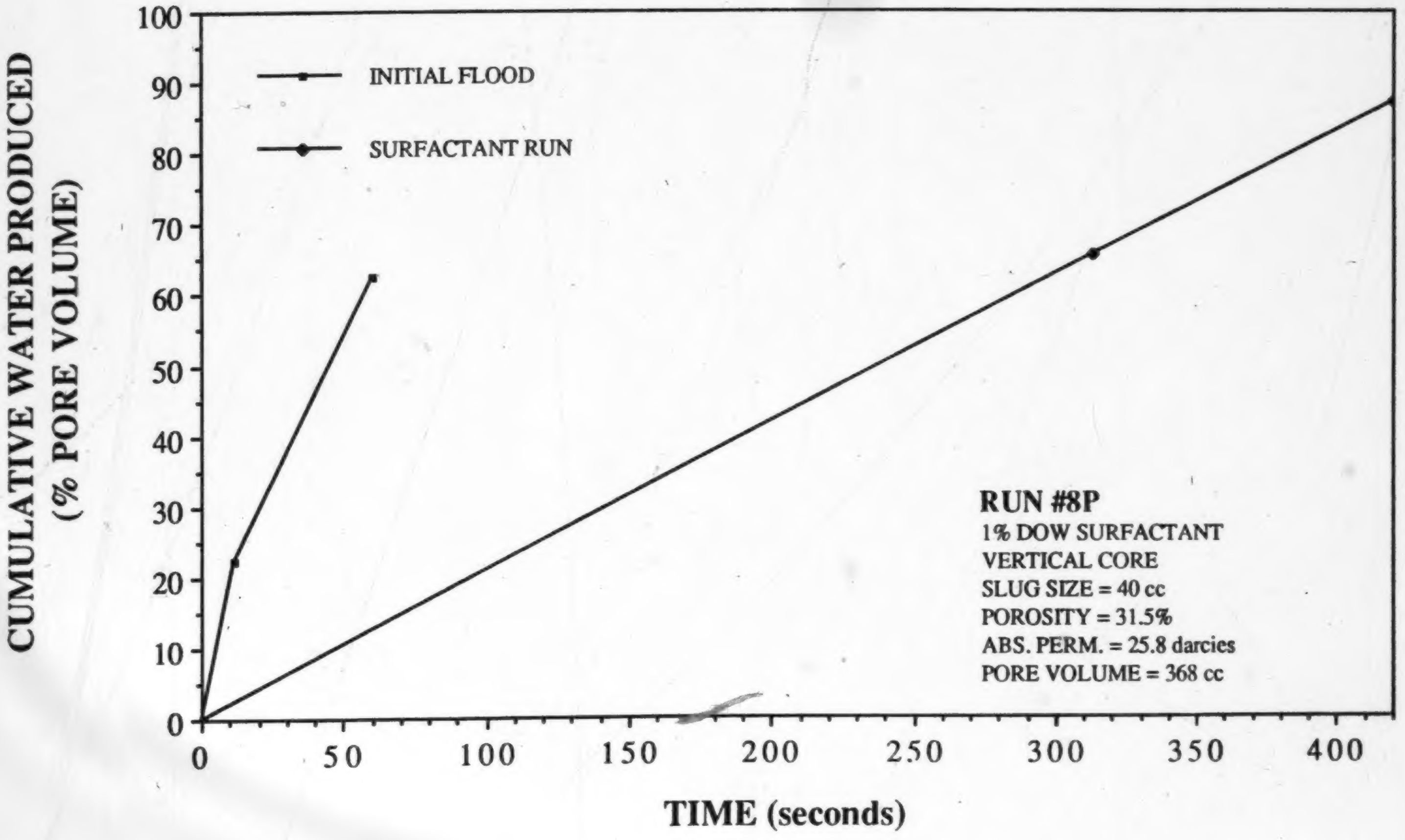

Figure 5.12 Run 8P: Cumulative Water Produced Vs. Time

Experimental Data For Run #9P
5% Dow Surfactant Vertical

Sandpack

Surfactant:	Dow	**Porosity:**	31.6%
Concentration:	5%	**Pore Volume:**	370 cc
Surfactant Slug Size:	40 cc	**Inlet Pressure:**	6.5 psi
Absolute Permeability:	26.5 darcies	**Back Pressure:**	Atmospheric

Procedure	**Volume (cc)**	**Pore Volume (%)**	**Time (s)**		**Outlet Pressure (psi)** (est.)
Initial Flood	68	18.4	11.5	breakthrough	
	234	63.2	60		1.6
Surfactant Run	290	78.4	1056	breakthrough	0.0

Table 5.12 Experimental Data for Run 9P: 5% Dow Surfactant Vertically Oriented Core

produced at gas breakthrough was 78.4 for the surfactant case. This data is graphically presented in Figure 5.13.

Figure 5.14 presents a comparison of the gas breakthrough conditions for varying Dow surfactant concentrations, with a vertically oriented core. It should be reiterated at this point that due to the small slug size used, the improved results found for the increased concentration are not necessarily an indication that the 5 percent surfactant concentration was superior to the 1 percent solution at reducing gas mobility.

The value of the preliminary runs lies more in the trends identified than in the numerical values obtained. With this in mind there are a few conclusions that can be derived from these experiments. The addition of a surfactant slug prior to a nitrogen flood delays gas breakthrough and increases the volume produced at breakthrough. At room temperature the Dow surfactant appears to be superior to SD1000, which is superior to XP100, as a foam producer. The more effective the surfactant is as a foam forming agent the higher the pressure drop across the core.

5.2.6 Comparison of Gas Displacement Tests for Surfactant Saturated and Water Saturated Cores

The next runs, 10P and 11P, were performed to compare a water-saturated and surfactant-saturated cores. Both cores were

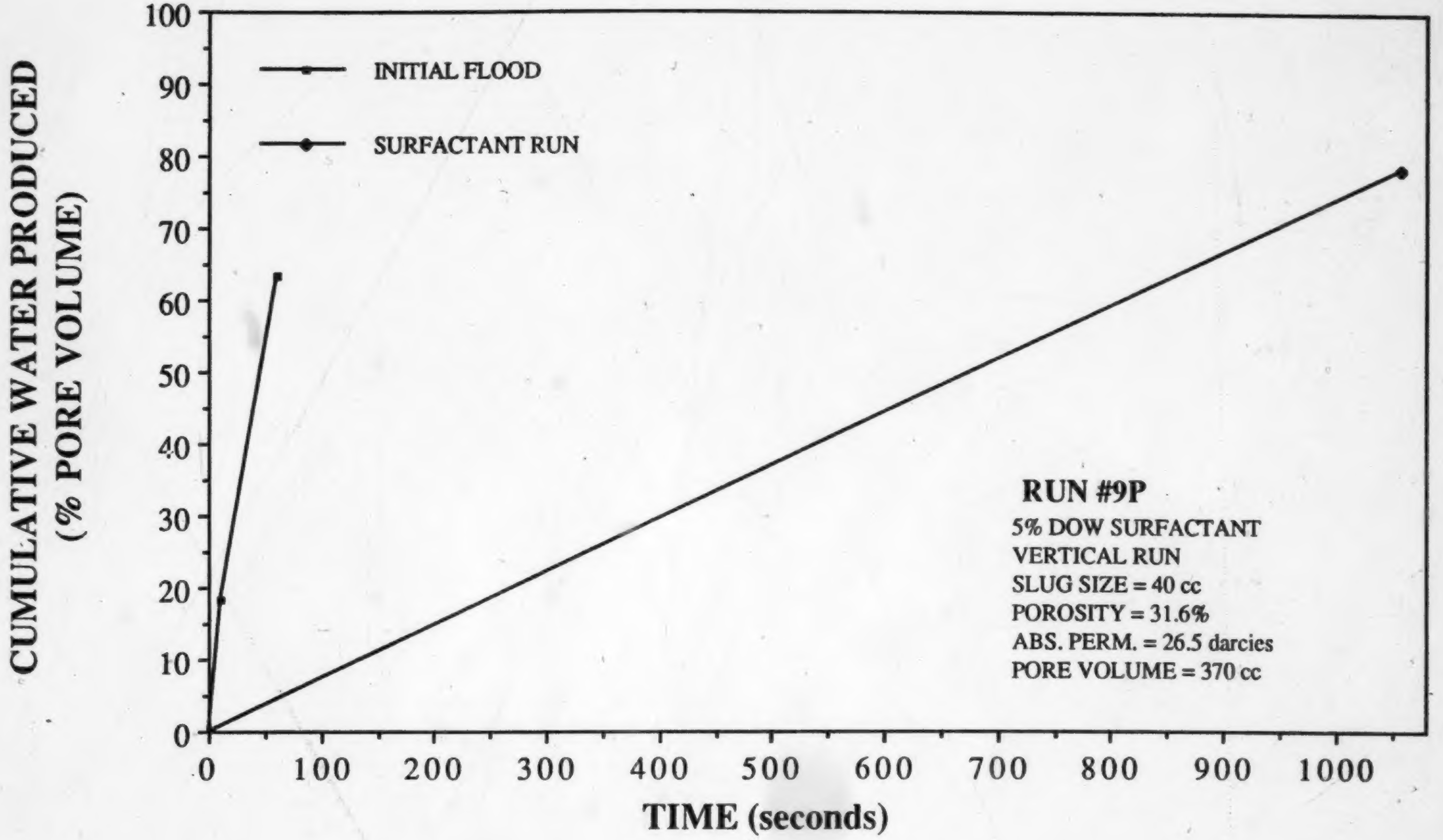

Figure 5.13 Run 9P: Cumulative Water Produced Vs. Time

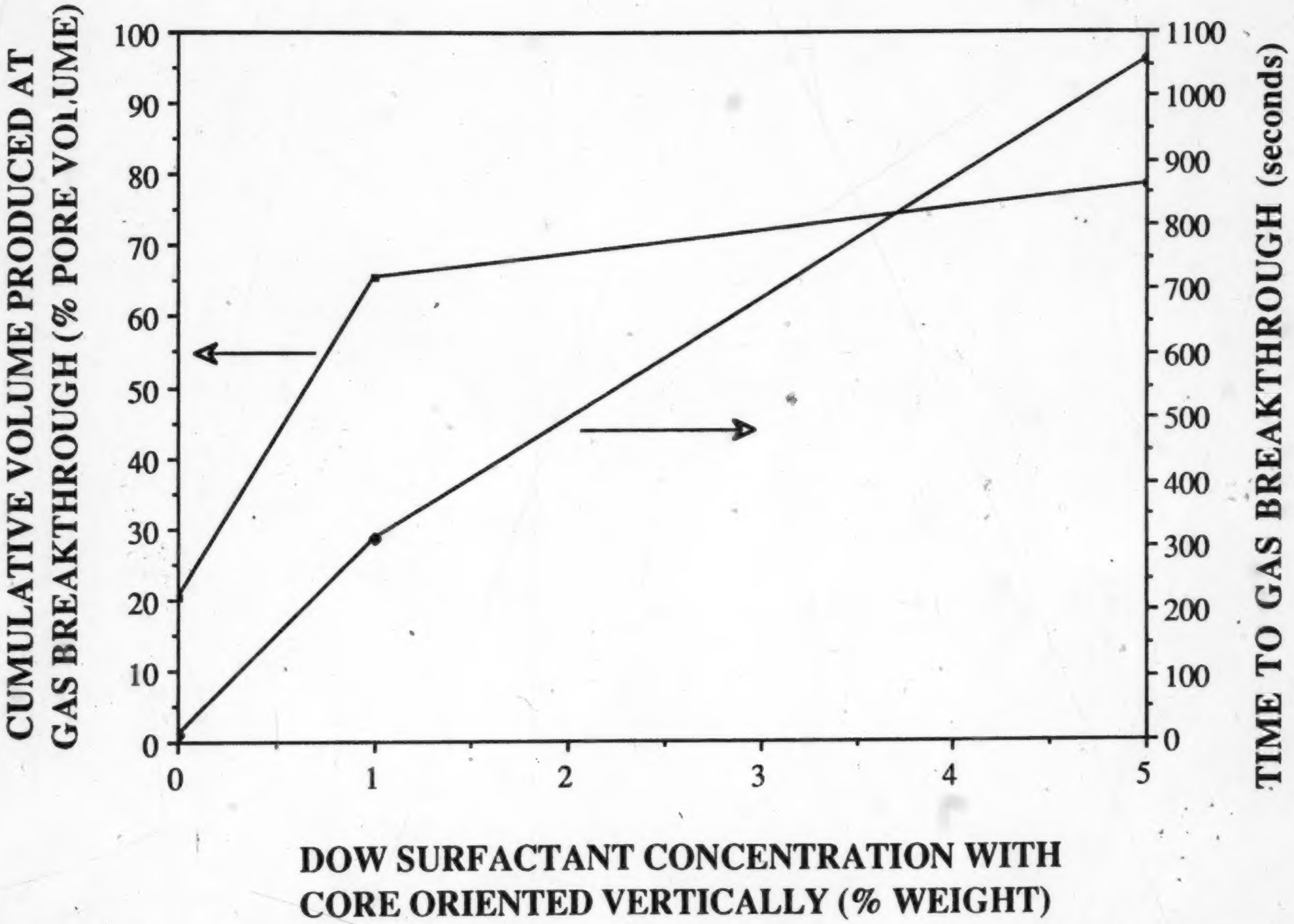

Figure 5.14 Cumulative Volume Produced at Gas Breakthrough and Time to Gas Breakthrough Vs. Dow Surfactant Concentration With Core Oriented Vertically

packed with glass beads. The water saturated core had an absolute permeability of 3.5 darcies; the surfactant saturated core had a permeability of 3.1 darcies.

The surfactant-saturated core was originally saturated with water, and then flooded with 3000 cc of 1 percent SD1000. The effluent was analyzed with the spectrophotometer until it matched the displacing fluid.

Both runs involved nitrogen injection only, using the mass flow controller. These runs were performed on the modified equipment, by-passing the foam generator. The nitrogen flow rate was 20 cc/minute at one atmosphere and 60° F. The results are presented in Figure 5.15. The cumulative volume of displaced (produced) fluid is plotted versus the cumulative volume of nitrogen injected.

The fluid production was much higher for the surfactant case, Run 11P, than the water case, Run 10P. Comparing the volume produced at 70 minutes for both cores, it was observed that 92 percent of the surfactant saturated core was produced, and 50 percent of the water saturated core.

Figure 5.16 is a plot of the volume of water produced per minute divided by the volume of nitrogen injected per minute, versus the cumulative volume of nitrogen injected. It clearly shows the difference between the surfactant and the water run, with respect to the gas breakthrough. For the surfactant case Run 11P, 82

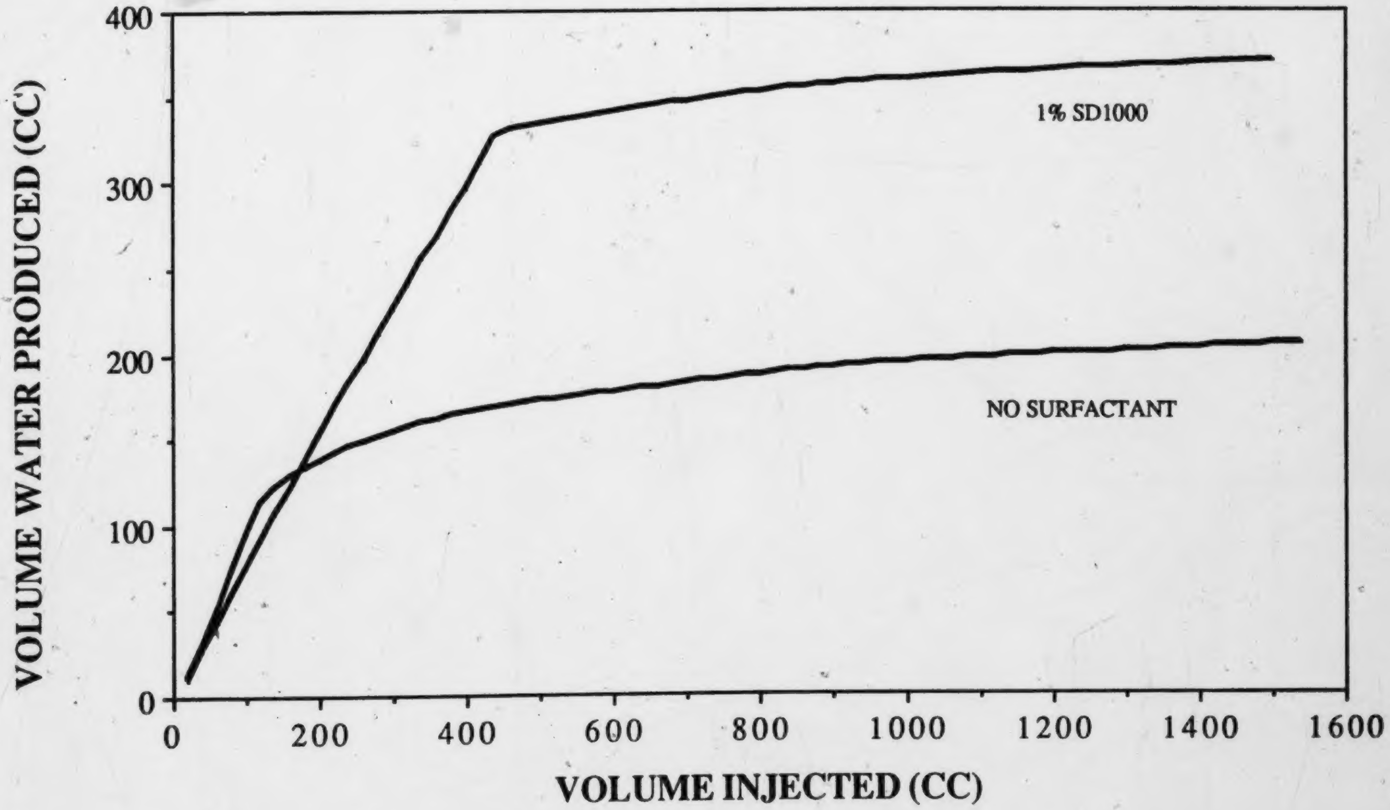

Figure 5.15 Comparison of Run 10P and Run 11P Volume Water Produced Vs. Volume Injected

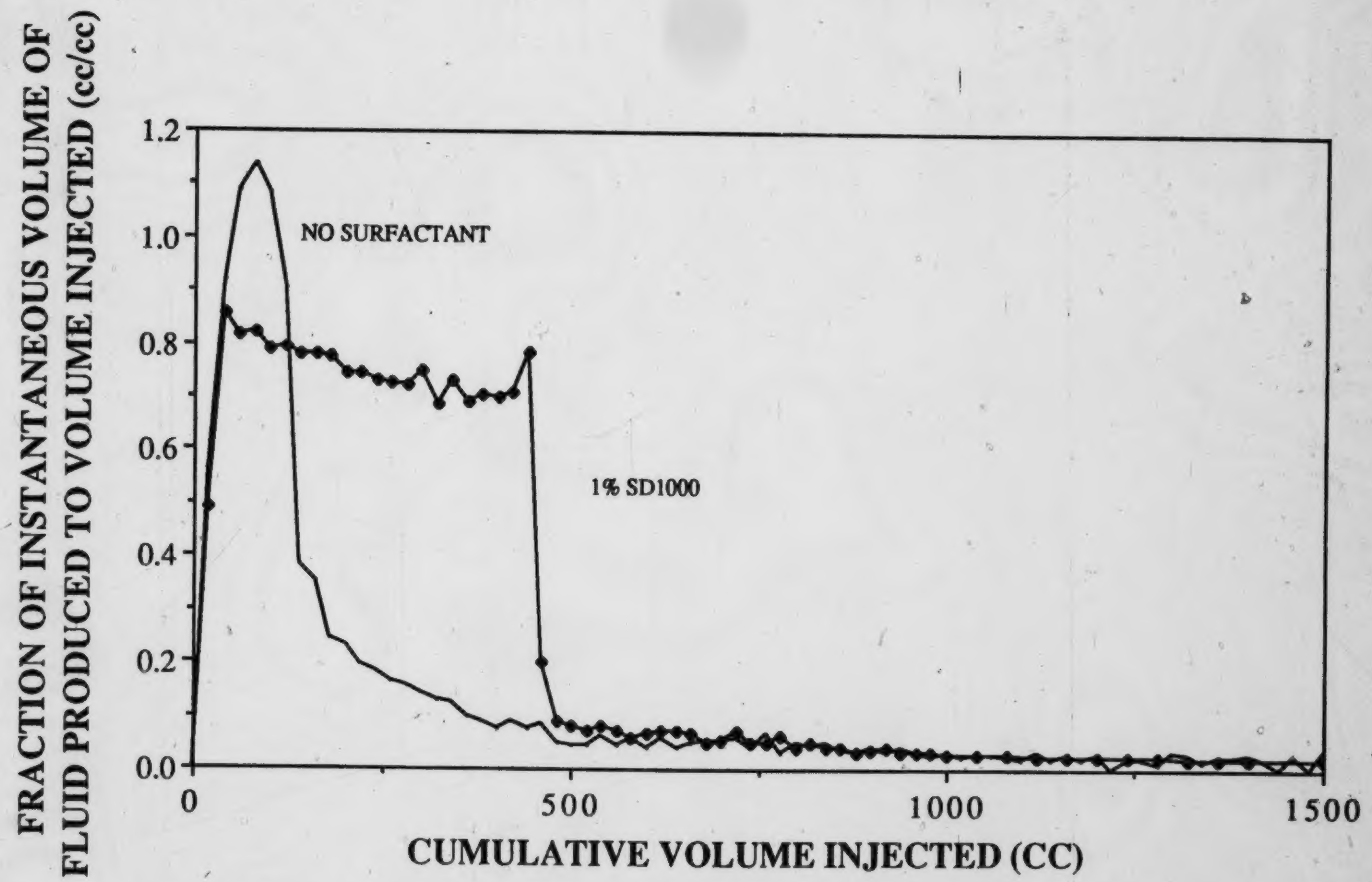

Figure 5.16 · Comparison of Run 10P and Run 11P Fraction of Instantaneous Volume of Fluid Produced to Volume Injected Vs. Cumulative Volume Injected

percent of the pore volume was displaced at gas breakthrough, and 28 percent for Run 10P. From this plot the movement of the gas front can be analyzed. The surfactant causes a more piston-like flow regime as described by Raza and Marsden[14]. This is discussed in Section 5 of the Literature Review. The gas front moved as a narrow finger through the water saturated core.

The differential pressure established across the two cores is plotted in Figure 5.17. The pressure across the core for Run 10P, the water case is 1.0 psi. For the surfactant case, Run 11P, a pressure differential with a maximum at 12.9 psi, during the fluid production, was established. The increase in the pressure drop caused by the surfactant is large.

The surfactant-filled core, following the initial experiment, was subjected to gas injection, and connected to the differential pressure recorder, for 46 hours. The results are presented in Figure 5.18. The pressure continued to increase to a maximum of 14 psi. The pressure was relatively stable around 11.2 psi, for 24 hours. This suggests that the effect of the surfactant is not short term. It must be remembered that this core was completely saturated with surfactant.

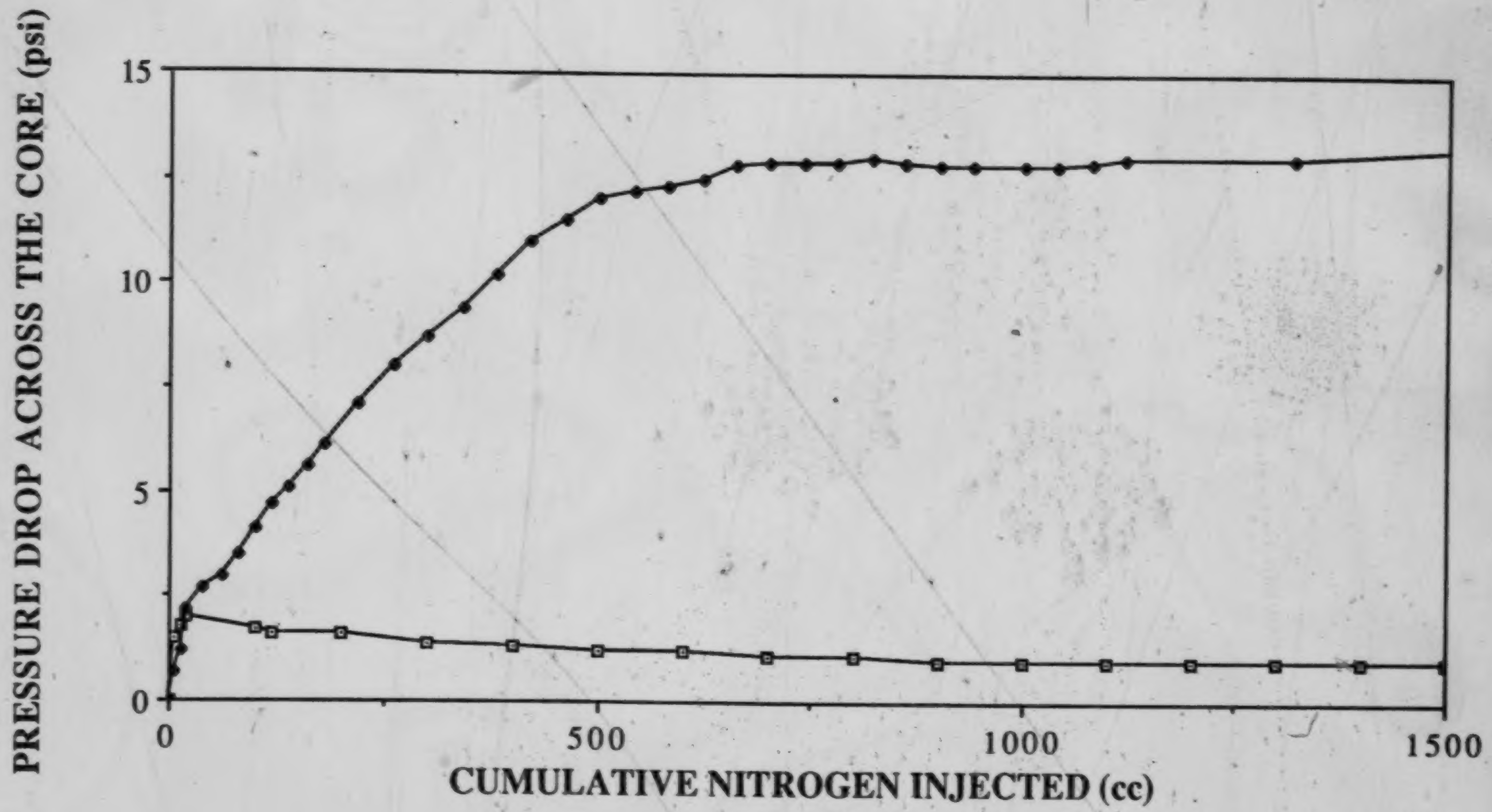

Figure 5.17 Comparison of Run 10P and Run 11P Pressure Drop Across the Core Vs. Cumulative Nitrogen Injected

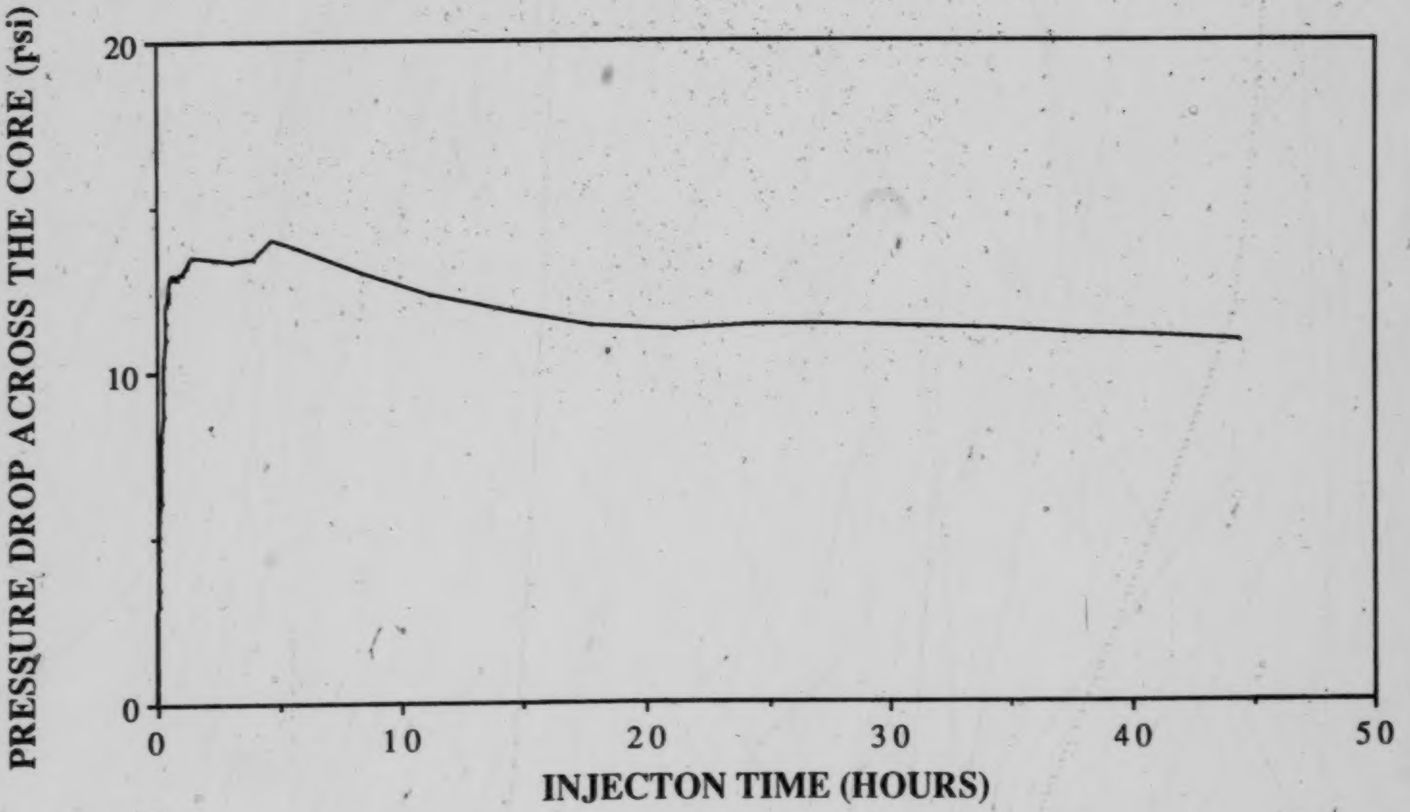

Figure 5.18 Run 11P: Pressure Drop Across the Core Vs. Injection Time

5.2.7 Preliminary Water-Nitrogen Co-Injection Test

The last of the preliminary runs, Run 12P, was performed in an attempt to repeat Maini's[35] base water cases. Maini's runs were performed on a 3.7 darcy unconsolidated sandpack. The coreholder used for this study was packed with glass beads and had an absolute permeability of 4.8 darcies. The main difference between the two sets of runs are the back pressures used. Maini's back pressure was 2000 psi, while for this study 50 psi was used. The results are presented in Figure 5.19 In both sets of runs the pressure drop increased as the ratio of gas injected was increased.

5.2.8 Overall Evaluation

For the initial nitrogen displacement tests (Runs 1P-9P), there are a number of conclusions that can be reached. The Dow surfactant caused the lowest gas mobility, which was manifested in the longest time until breakthrough. The surfactants rank Dow, SD1000 then XP100 in descending order in terms of ability to reduce gas mobility.

In slug injection, the 5 percent solutions of Dow surfactant and SD1000 delayed gas breakthrough more than the 1 percent solution. For Dow surfactant, the runs performed in the vertical position show very similar results to those performed horizontally.

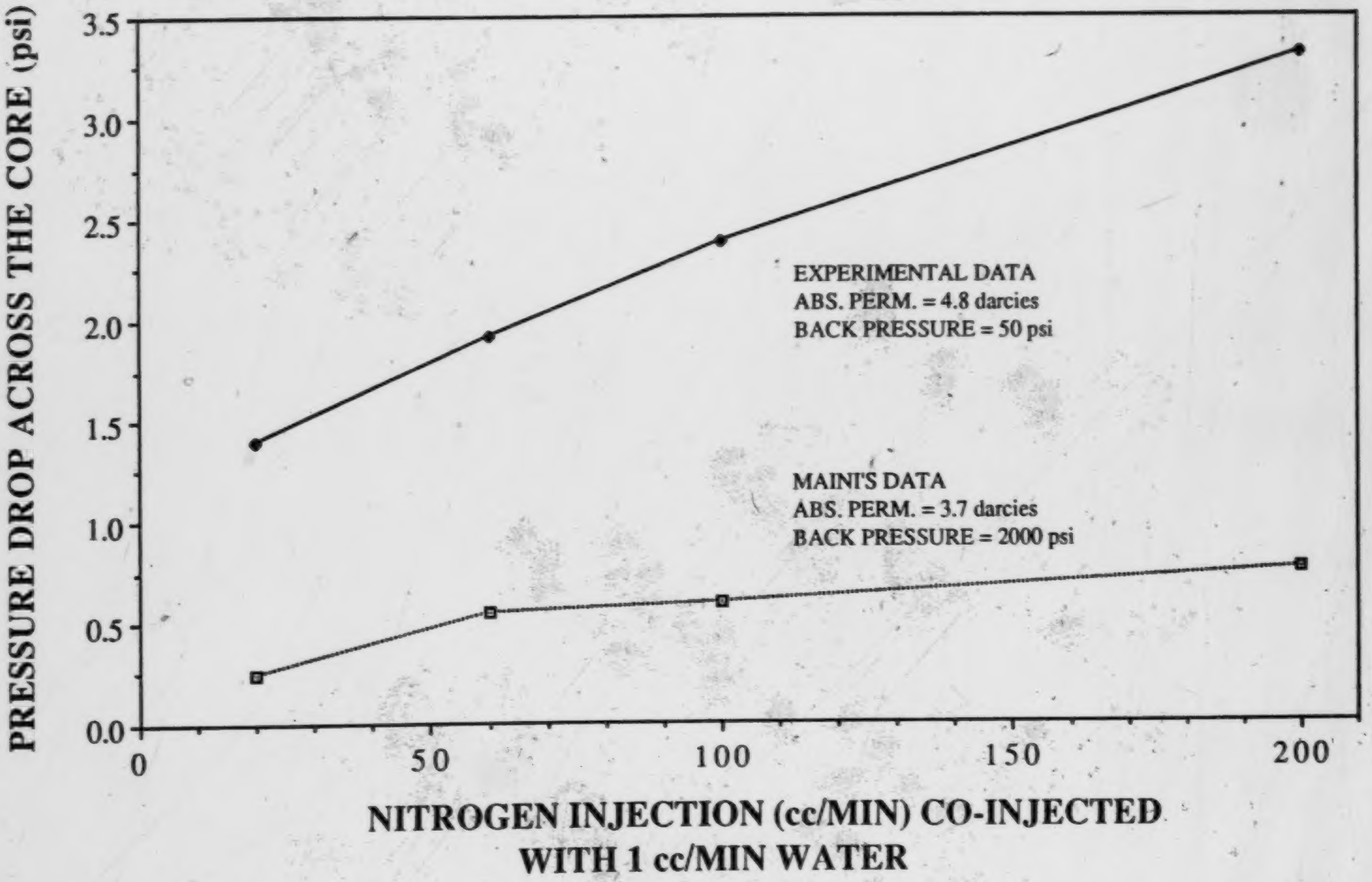

Figure 5.19 Run 12P: Pressure Drop Across the Core Vs. Nitrogen Co-Injection With Water

The preliminary runs established the need for an outlet system in which the effluent could be observed. The outlet system was designed such that sampling took place from the bottom of the view cell so that the liquid effluent would not destroy the foam exiting the core.

5.3 Nitrogen-Surfactant Co-Injection Runs

These runs were performed to examine the effect of several variables on the total mobility, and therefore the gas phase mobility, in the presence of a pre-generated foam. These variables include: absolute permeability of the porous medium, surfactant concentration, surfactant type, temperature, residual oil saturation, residual gas saturation and quality.

For these runs, nitrogen and a surfactant solution were co-injected into a foam generator. The effluent from the foam generator entered the coreholder, to which a back pressure had been applied. The effluent from the coreholder entered a visual sample cell, and was tested for surfactant concentration using a refractometer and an ultraviolet spectrophotometer.

5.3.1 Typical Nitrogen-Surfactant Co-Injection Run

In order to provide a clear understanding of the experimental results, and the pertinent calculations, Run 11 will be examined as an example, and described in detail. The data for this run is given in Table 5.13.

Within the table, the glass bead pack characteristics such as: porosity, absolute permeability and glass bead size are given, along with surfactant type and concentration, residual oil saturation,

Experimental Data For Run #11
1% SD 1000 Glass Bead Size #9

Surfactant:	SD 1000	**Glass Bead Size:**	#9 * New Supplier
Concentration:	1%	**Residual Oil Saturation:**	no
Absolute Permeability:	12.2 darcies	**Temperature:**	Ambient
Porosity:	33.3%	**Gas Breakthrough:**	32:40 (min.)
Back Pressure:	50 psi	**Totalizer Reading @ BT.:**	200.0

Time (s)	Volume (cc)	Cum. Vol. (cc)	Spectro. Conc. ppm	Pressure Drop (psi)	Simulated Pressure Drop (psi)	Totalizer Reading
150	51	51.0	48.5	1.00	2.4	15
390	50	101.0	26.6	1.25	3.4	40
600	45	146.0	14.4	2.25	5.4	62
825	48	194.0	52.7	3.00	6.4	84
1080	56	250.0	90.6	4.00	6.4	111
1290	44	294.0	3.9	4.50	6.4	132
1530	54	348.0	1.8	5.00	6.4	157
1740	46	394.0	550.0	5.00	6.4	180
1980	46	440.0	3418.0	5.00	6.4	202
5685	57	497.0	5321.0	5.00	6.4	585
8355	44	541.0	7801.0	5.00	6.4	852
11295	48	589.0	8368.4	5.00	6.4	1155
14810	56	645.0	8533.0	5.00	6.4	1514
17460	45	690.0	8552.0	5.00	6.4	1785
20100	42	732.0	8529.0	5.00	6.4	2053
23040	48	780.0	8538.0	5.00	6.4	2351

Table 5.13 Experimental Data for Run 11: 1% SD1000

temperature, and gas breakthrough time determined for the run. The first column in the table represents the time, from commencement of co-injection, until the sample was collected. The sample volume and cumulative sample volume are presented in the next two columns.

The concentration of surfactant in the effluent is given in the next column. The concentration is given in parts per million (ppm) when sampled by the UV spectrophotometer, or in percent of injection fluid concentration, when sampled by the refractometer.

The next column gives the pressure drop across the core recorded at the sample times. For certain runs the next column gives the simulated pressure drop. The last column gives the totalizer reading. This is the cumulative volume of nitrogen injected into the core at each sample time. To determine the cumulative gas injected, at atmospheric conditions and 60° F, the totalizer reading must be multiplied by 10.

The surfactant concentration was 1 percent SD1000 for run 11. The glass bead pack had an absolute permeability of 12.2 darcies. This run was performed with a nitrogen-surfactant solution injection ratio of 60:1 cc/min. The amount of nitrogen was regulated by the mass flow controller and read at one atmosphere and 60° F. Therefore, to determine the quality of the foam we must correct the nitrogen volume for pressure and in some runs also for temperature. The nitrogen volume was corrected using the ideal gas law.

$$\frac{P_1V_1}{T_1} = \frac{P_2V_2}{T_2}$$

The pressure used in the calculation was:

$$P_{\text{system ave.}} = \frac{\Delta P_{ss}}{2} + P_{BP}$$

where ΔP_{ss} is the differential pressure developed at steady state conditions and P_{BP} is the back pressure.

The foam quality,

$$\Gamma = \frac{V_g}{V_g + V_l}$$

where V_g = volume of gas phase, V_l = volume of liquid phase, was therefore 94.4 percent for this run. To determine this value it was assumed that the liquid phase was incompressible and that the surfactant solution and the nitrogen mixed completely to form a foam.

The steady state differential pressure was determined by the pressure history. For Run 11 this is presented in Figure 5.20. For this run, it is clear that the differential pressure stabilized at 5 psi. The differential pressure stabilized shortly before gas breakthrough.

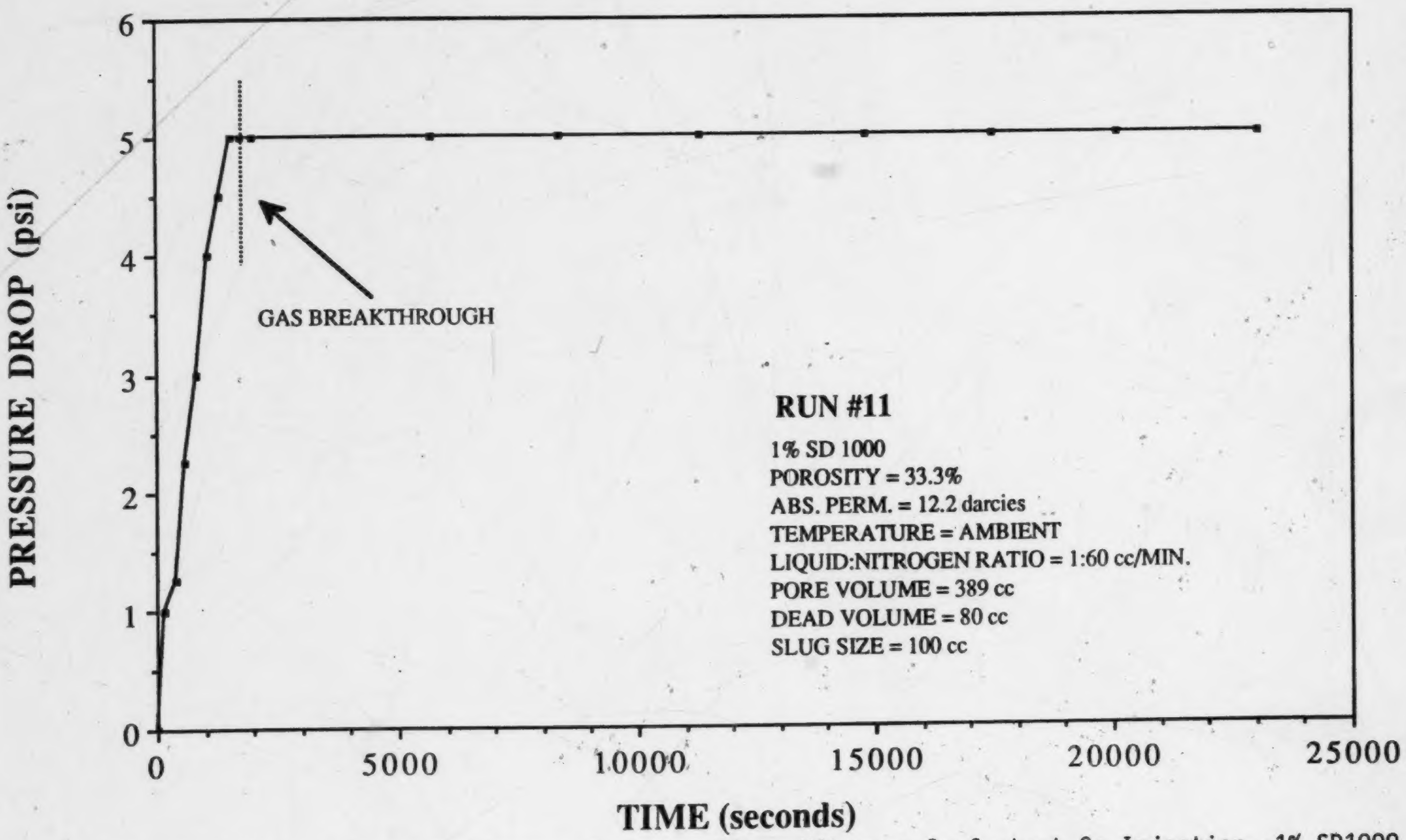

Figure 5.20 Run 11: Pressure Drop Vs. Time, Nitrogen Surfactant Co-Injection, 1% SD1000

From the stabilized differential pressure the total foam mobility can be calculated. Using the equation,

$$\left(\frac{k_w}{\mu_w} + \frac{k_g}{\mu_g}\right) = \frac{q_T L}{A \, \Delta P}$$

where q_T is the total flow rate. The total mobility for Run 11 is 2.75 darcies/cp. To determine total relative mobility, total mobility is divided by the absolute permeability. For Run 11 this value would be 0.225 cp^{-1}.

Relative mobility allows us to look at foam mobility with dependence on one less variable. This is useful for a comparison of foam runs with water base runs. To compare the foam runs with one another and to determine the effectiveness of the foam as a selective blocking agent, total foam mobility provides a better understanding of where the flow would take place.

Maini[35] compared runs by considering the mobility reduction factor. To determine this, he divided the total mobility for a given test by the mobility for a single phase water base case, performed with co-injected gas and liquid phases, at the same ratio as the test case. No other variables in the equation changed for the test case, so he was effectively dividing the pressure drop across the test core by the pressure drop across the base case. For the present research, two steady state water base pressure drops were determined, one at 4.8 darcies and the other one at 13.5 darcies. The runs were compared with the base case, employing the nearest absolute permeability. For Run 11 the mobility reduction factor was 4.

The constant differential pressure suggests that steady state conditions were reached. This is supported by Figure 5.21, the cumulative volume produced versus time graph. Gas breakthrough occurred at 32.7 minutes. The cumulative volume produced at breakthrough was 440 cc.

The slope of the cumulative volume produced curve changes drastically following gas breakthrough. The liquid production rate becomes identically the same as the liquid injection rate. When the injection rate is subtracted from the cumulative volume produced, the result, 399 cc, is found to be a constant.

The fact that this number is a constant suggests that the surfactant solution volume injected helps to maintain lamellae thickness. As discussed by Owete[35], in the absence of continuous surfactant injection the lamallae are thin, losing their stability and resiliency. The constant liquid volume supports the suggestion that steady state conditions were reached for this run, which also enables the determination of residual liquid saturation within the core. The residual liquid saturation was determined by performing a liquid volumetric balance on the system.

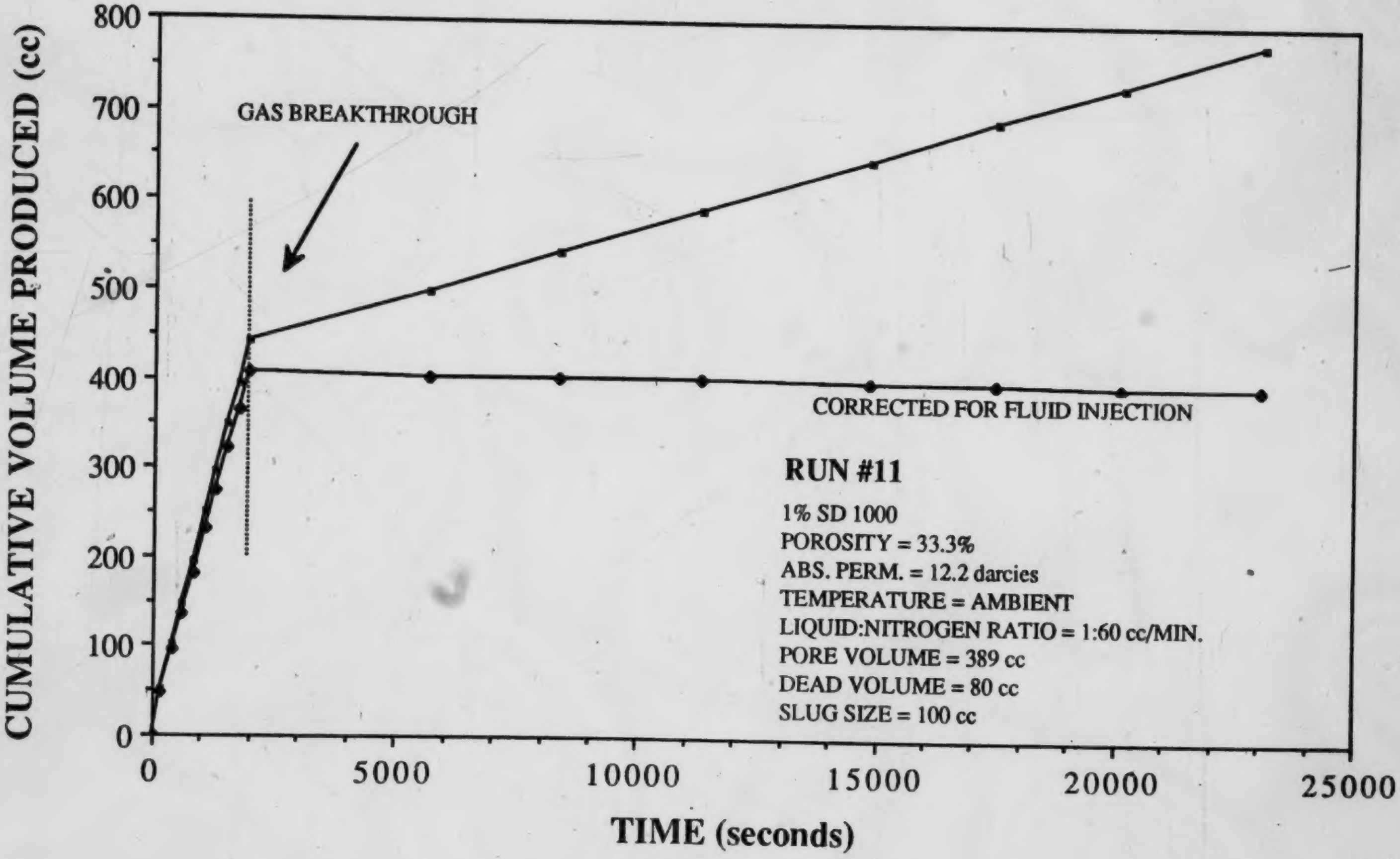

Figure 5.21 Run 11: Cumulative Volume Produced Vs. Time, Nitrogen Surfactant Co-injection, 1% SD1000

The total fluids present in the core at any time are:

$$T_F = T_R + T_P$$

$$T_F = V_{fg} + V_l + V_{ch} + V_{is} + r_i\,(t)$$

where: V_{fg} is the volume in the foam generator, V_l is the volume in the lines and sight glasses, V_{ch} is the volume in the coreholder, V_{is} is the volume of injected slug, r_i is the injection rate, t is the time elapsed from the beginning of the experiment, T_F is the total fluid in the system, T_P is the total fluid produced, T_R is the total fluid remaining in system.

T_P is the cumulative volume produced. The remaining volume in the system is not all located in the coreholder;

$$T_R = V_{rfg} + V_{rl} + V_{rch},$$

where V_{rfg} is the volume remaining in the foam generator, V_{rl} is the volume remaining in the lines and sightglasses, and V_{rch} is the volume remaining in the coreholder.

If,

$$S_w = \frac{V_{rch}}{\phi A},$$

then

$$S_w \, fnc(t) = \frac{T_f \, fnc(t) - T_p \, fnc(t) - V_{rfg} - V_{rl}}{\phi A}$$

When we have reached steady state conditions, S_w, is no longer a function of time and becomes constant. The residual liquid saturation was 38.6 percent for Run 11.

During each experiment, the following were determined: V_{fg}, V_{ch}, V_{is}, f, T_F, r_i and T_P. The liquid volume of the foam generator, V_{fg}, was determined by evacuating the dry coreholder with a vacuum pump, and was followed by imbibition of liquid into the foam generator. The value of the liquid volume remaining in the foam generator, V_{rfg}, was determined by weighing the foam generator glass beads following an experiment. The glass beads were dried and then weighed again.

The volume of the liquid in the lines was determined by filling the empty lines, with liquid from the Ruska pump, and recording the liquid volume. The volume of the remaining liquid in the lines and sightglasses, V_{rl}, was estimated following visual observation of the sightglasses and by draining the lines.

Figure 5.22 shows a UV spectrophotometric analysis of Run 11. The surfactant concentration measured is plotted versus the corrected cumulative volume in pore volumes. The cumulative volume was corrected for 60 cc of movable dead volume, which was

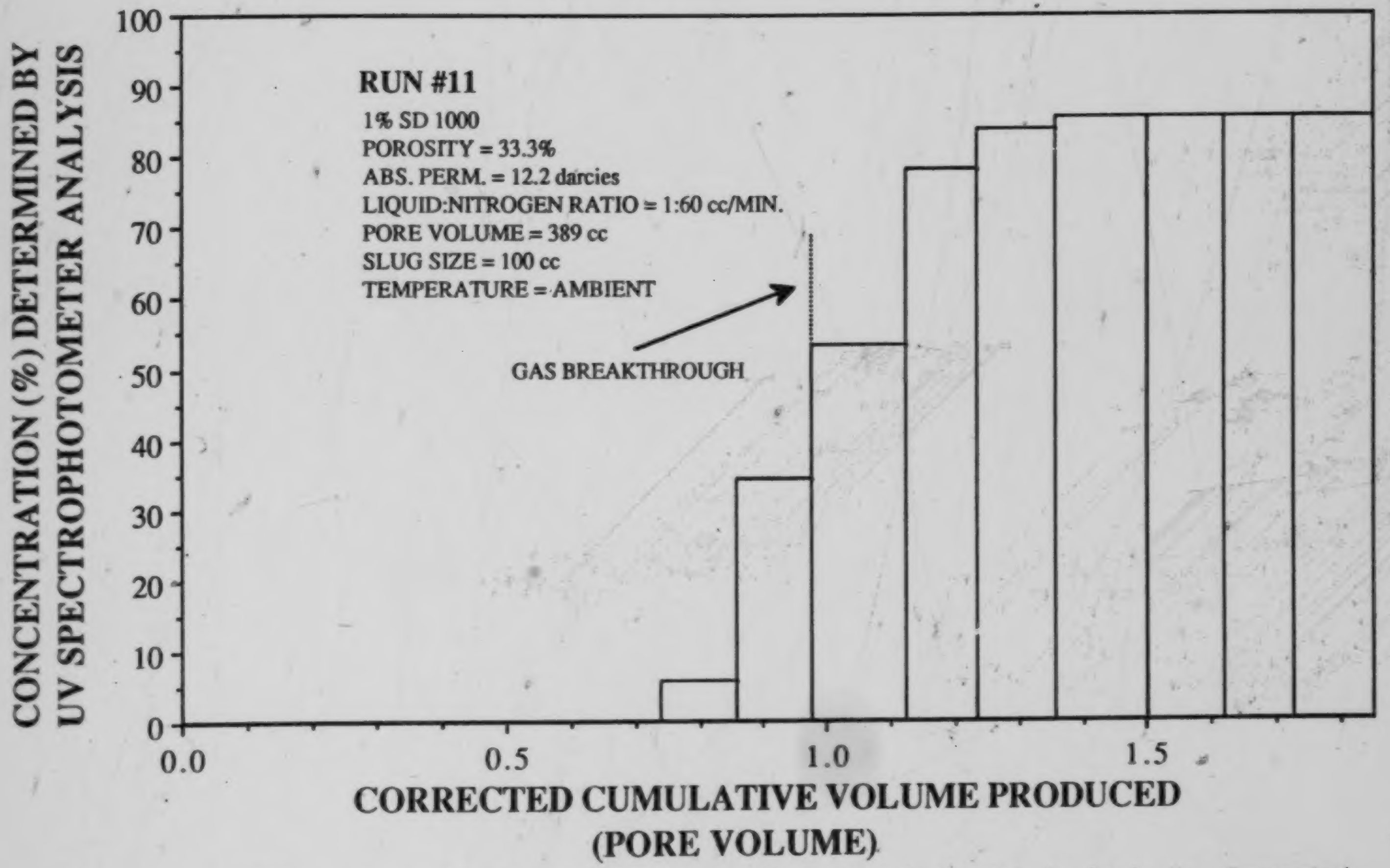

Figure 5.22 Concentration Determined by UV Spectrophotometer Analysis Vs. Corrected Cumulative Volume Produced, Nitrogen Surfactant Co-injection, 1% SD1000

occupied by water. The mixing zone for this run was 0.5 pore volume. The maximum concentration obtained was 85 percent of the surfactant injection.

5.3.2 Effect of Surfactant Concentration

Surfactant SD1000

In order to examine the effect of surfactant concentration it is logical to first analyze a water-nitrogen run for comparison. Run 21 was performed on a 13.5 darcy glass bead pack.

Table 5.14 gives the experimental data. This run was performed at room temperature without the use of the surfactant. Nitrogen and water were co-injected into the glass bead pack in the same manner as for the surfactant runs. A 100 cc water slug was also used to increase the pressure (back pressure of 50 psi) and to maintain consistency. The gas breakthrough occurred at 12.17 minutes and the volume produced at breakthrough was 185 cc. From Figure 5.23, the corrected cumulative volume produced curve shows a rounded curvature after gas breakthrough; this is unlike the trend observed for Run 11, in which the corrected cumulative volume produced plot became a horizontal line, after changing slope sharply at gas breakthrough. The sharply changing slope is due to the fact that foam caused a more piston-like displacement pattern in the core. The mobility of the gas for the water case, Run 21, was

Experimental Data For Run 21
Water Base Case Glass Bead Size #9

Surfactant:	None	**Glass Bead Size:**	#9
Concentration:	0.0%	**Residual Oil Sat.:**	no
Absolute Permeability:	13.5 darcies	**Temperature:**	Ambient
Porosity:	32.3%	**Gas Breakthrough:**	12:10 (min.)
Back Pressure:	50 psi	**Totalizer Reading @ BT.:**	74

Time (s)	Volume (cc)	Cum. Vol. (cc)	Pressure Drop (psi)	Totalizer Reading
30	51	51.0	0.25	3
330	46	97.0	1.00	33
540	45	142.0	1.75	54
750	43	185.0	1.50	76
1620	33	218.0	1.25	165
3480	31	249.0	1.25	355
5040	38	287.0	1.25	510
7020	32	319.0	1.25	713
7920	15	334.0	1.25	805
9000	18	352.0	1.25	915
10050	17	369.0	1.25	1015
13020	51	420.0	1.25	1319
15300	38	458.0	1.25	1550
18180	48	506.0	1.25	1845
21480	55	561.0	1.25	2184

Table 5.14 Experimental Data for Run 21: No Surfactant

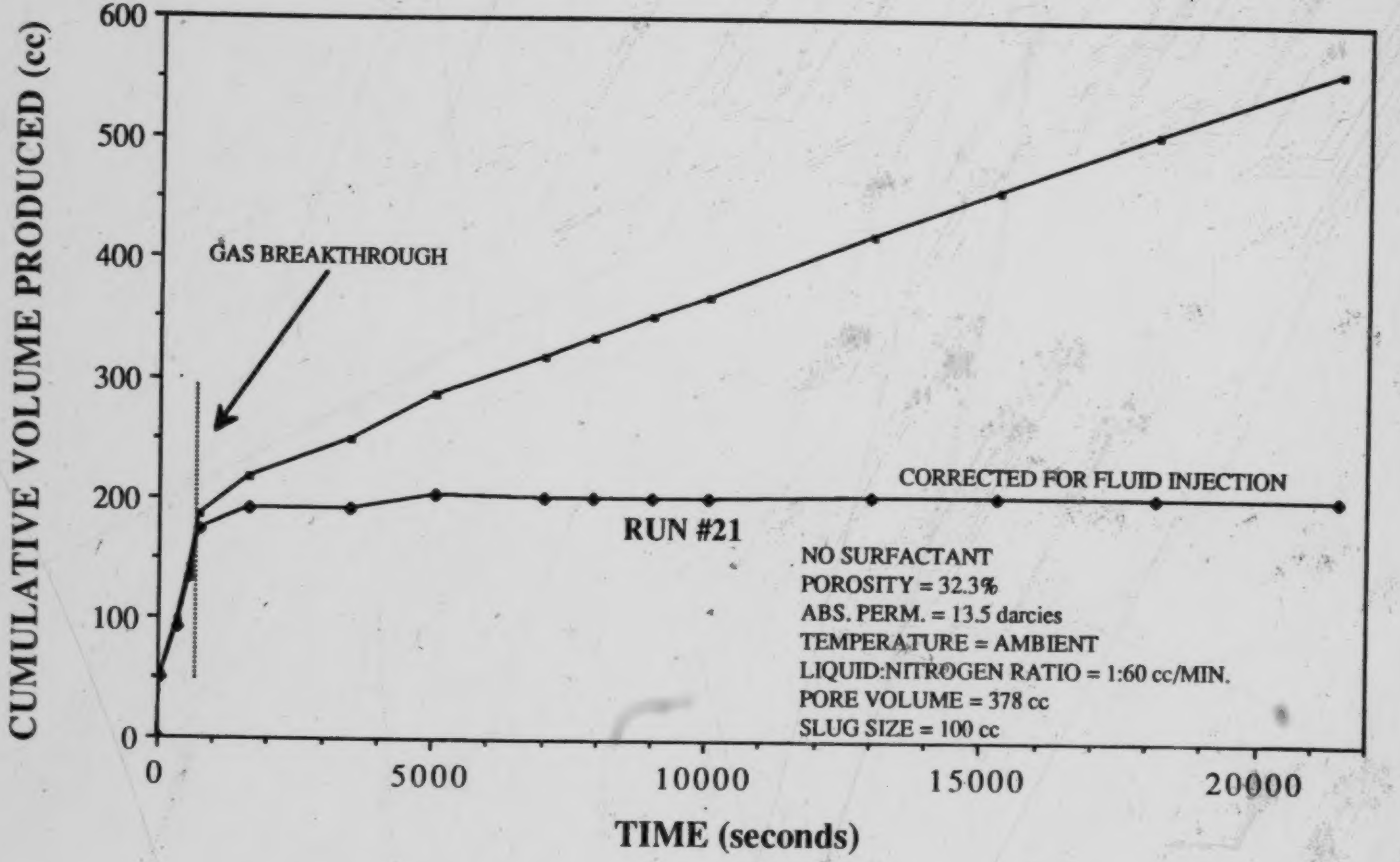

Figure 5.23 Run 21: Cumulative Volume Produced Vs. Time, No Surfactant

much higher than the mobility of water, which caused an inefficient displacement.

The steady state residual water saturation in the glass bead pack was 88.6 percent. The steady state residual water saturation for Run 11 was 38.6 percent, clearly indicating the superiority of foam as a displacing agent.

Figure 5.24 shows the differential pressure profile for Run 21. The pressure dropped sharply near the point of gas breakthrough, when the resistance to gas flow was decreased. The steady state differential pressure across the core was 1.25 psi. The total mobility was 8.9623 darcies/cp for this run; the total relative mobility was 0.6639 cp^{-1}.

Run 12P was also a water-nitrogen base case. This run was performed before the volumetric sampling procedure was established. From the data collected, the pressure drop across the core was 2.0 psi. This is slightly higher than the pressure drop of 1.25 psi found for Run 21. This is not an unexpected result as the absolute permeability was 4.7 darcies for Run 12P and 13.5 darcies for Run 21. The total mobility was 5.6 darcies/cp for Run 12P; the relative mobility was 1.187 cp^{-1}.

The runs performed can be grouped into distinct categories with respect to absolute permeability. This grouping is evident in Table 5.2. The effect of surfactant concentration will be described in

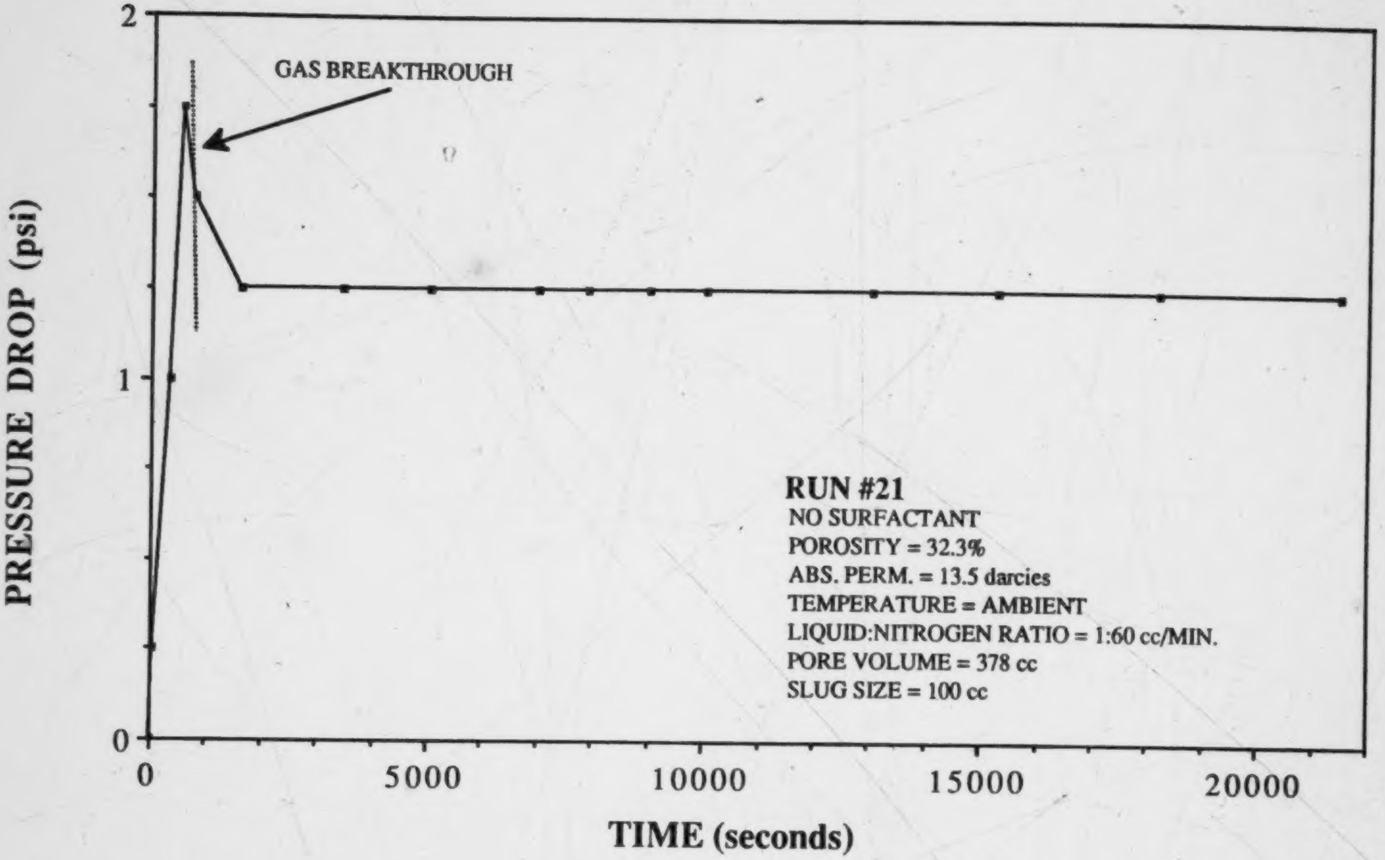

Figure 5.24 Run 21: Pressure Drop Vs. Time, No Surfactant

absolute permeability categories initially and then correlated with each other.

5.3.2.1 Core Absolute Permeability 3.5 to 8.1 darcies

To determine the effect of surfactant concentration for this permeability range, Runs 1, 19 and 3 will be examined and compared with the base case 12P, with an absolute permeability of 4.7 darcies. Run 1 was performed with a 1 percent concentration of SD1000 on a 6.2 darcy glass bead pack. Table 5.15 gives the data for Run 1. The plot of cumulative volume produced versus time is presented as Figure 5.25. From this plot we see that the corrected cumulative volume produced became a constant, 422 cc, after gas breakthrough which occurred at 40 minutes.

The cumulative volume produced at gas breakthrough was 462 cc. The differential pressure profile, Figure 5.26, shows the pressure becoming constant, at 11 psi, after gas breakthrough.

The residual liquid saturation within the core was 32.5 percent. The total mobility was reduced to 0.9526 darcies/cp from the water base case, Run 12P, with a total mobility of 5.580 darcies/cp.

Run 19 was performed on a 7.1 darcy glass bead pack with 2.5 percent SD1000. Table 5.16 presents the data for Run 19. The corrected cumulative volume produced, shown in Figure 5.27 became

Experimental Data For Run #1
1% SD 1000 Glass Bead Size #9

Surfactant:	SD 1000	**Glass Bead Size:**	#9
Concentration:	1%	**Residual Oil Saturation:**	no
Absolute Permeability:	6.2 darcies	**Temperature:**	Ambient
Porosity:	33.2%	**Gas Breakthrough**	40:00 (min.)
Back Pressure:	50 psi	**Totalizer Reading @ BT.:**	241

Time (s)	Volume (cc)	Cum. Vol. (cc)	Pressure Drop (psi)	Totalizer Reading
0	0	0.0	0	0
600	145	145.0	4.50	60
1000	140	260.0	6.00	100
1560	56	341.0	9.50	156
2400	121	462.0	11.00	240
3660	21	483.0	11.00	366
5190	25	508.0	11.00	516
6150	16	524.0	11.00	615
6420	5	529.0	11.00	643
9400	50	579	11.00	939
12000	43	622	11.00	1199
14400	40	662	11.00	1438

Table 5.15 Experimental Data for Run 1: 1% SD1000

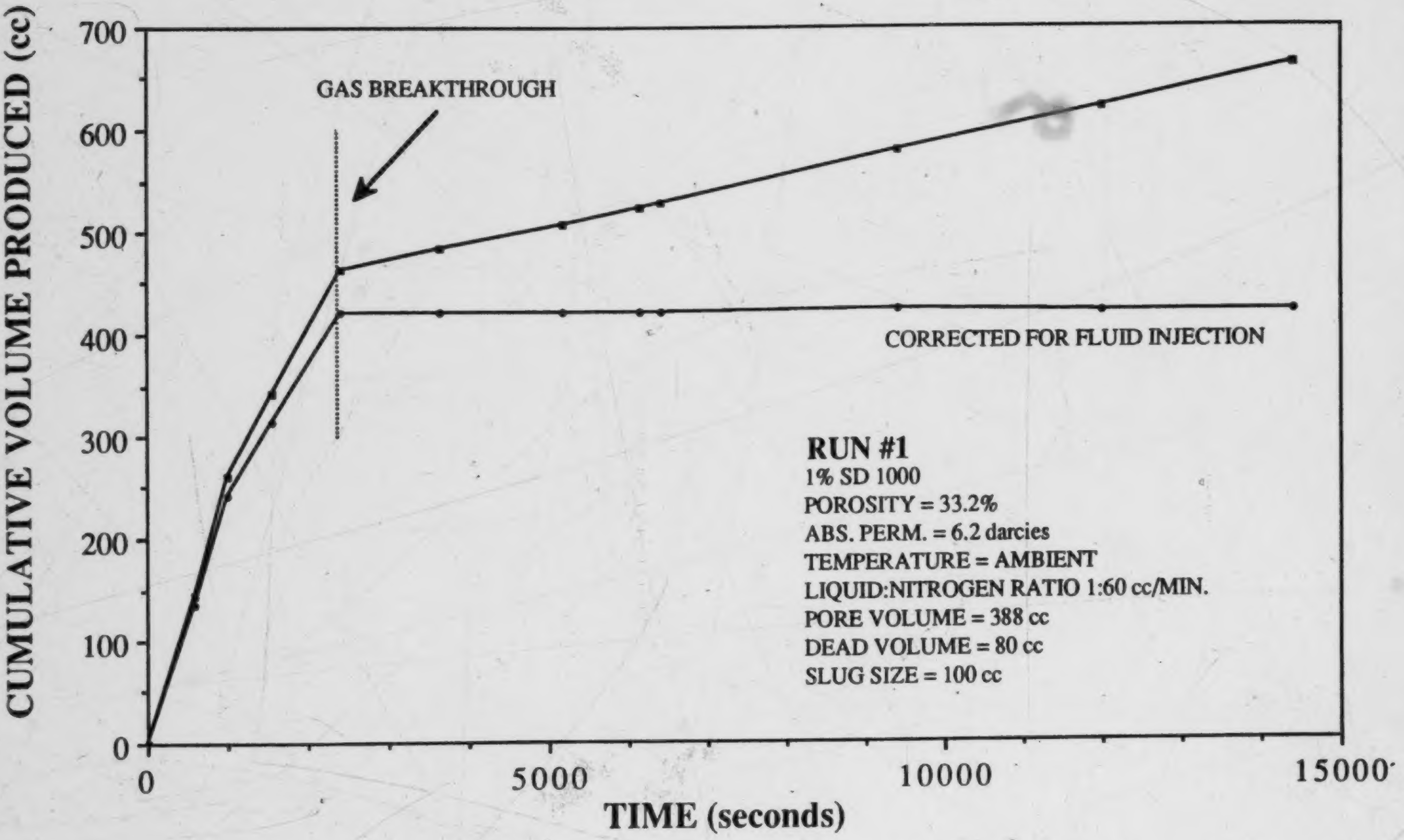

Figure 5.25 Run 1: Cumulative Volume Produced Vs. Time, Nitrogen Surfactant Co-injection, 1% SD1000

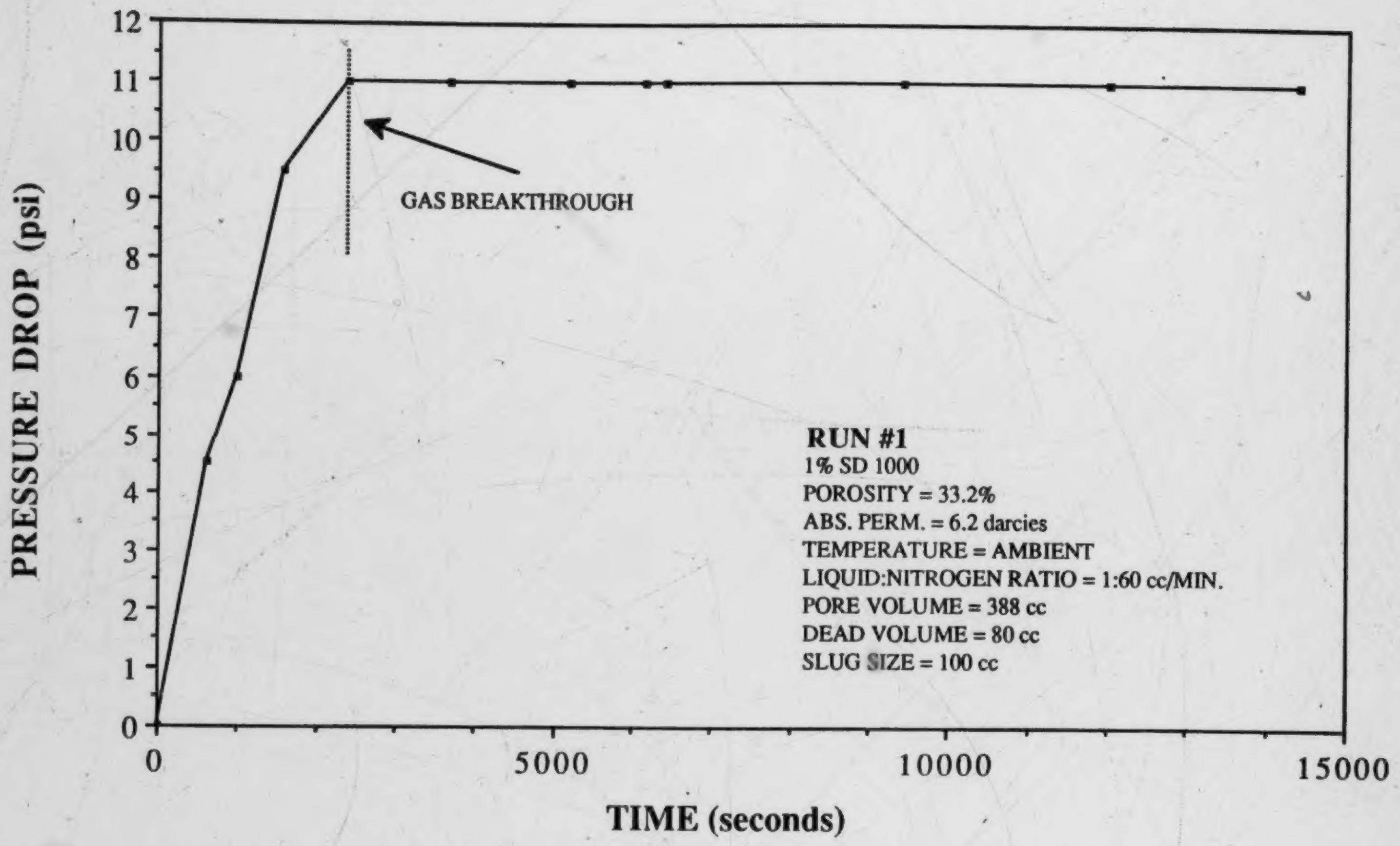

Figure 5.26 Run 1: Pressure Drop Vs. Time, Nitrogen Surfactant Co-injection, 1% SD1000

Experimental Data For Run 19
2.5% SD 1000 Glass Bead Size #10

Surfactant:	SD 1000	**Glass Bead Size:**	#10
Concentration:	2.50%	**Residual Oil Sat.:**	no
Absolute Permeability:	7.1 darcies	**Temperature:**	Ambient
Porosity:	33.1%	**Gas Breakthrough:**	39:00 (min.)
Back Pressure:	50 psi	**Totalizer Reading @ BT.:**	237

Time (s)	Volume (cc)	Cum. Vol. (cc)	Spectro. Conc. ppm	Pressure Drop (psi)	Totalizer Reading
180	53	51.0	113	2.00	18
450	53	104.0	22	2.00	45
690	50	154.0	19	3.75	70
960	54	208.0	69	5.50	98
1230	50	258.0	73	6.50	124
1470	44	302.0	8	7.25	148
1740	53	355.0	55	8.50	175
2010	52	407.0	151	9.75	204
2280	53	460.0	6357	10.75	231
6240	75	535.0	18575	11.75	632
9150	52	587.0	22976	11.75	922
12300	50	637.0	24355	11.25	1241
15840	58	695.0	23246	11.25	1601
19080	46	741.0	23566	11.25	1933
21660	43	784.0	24382	11.25	2183

Table 5.16 Experimental Data for Run 19: 2.5% SD1000

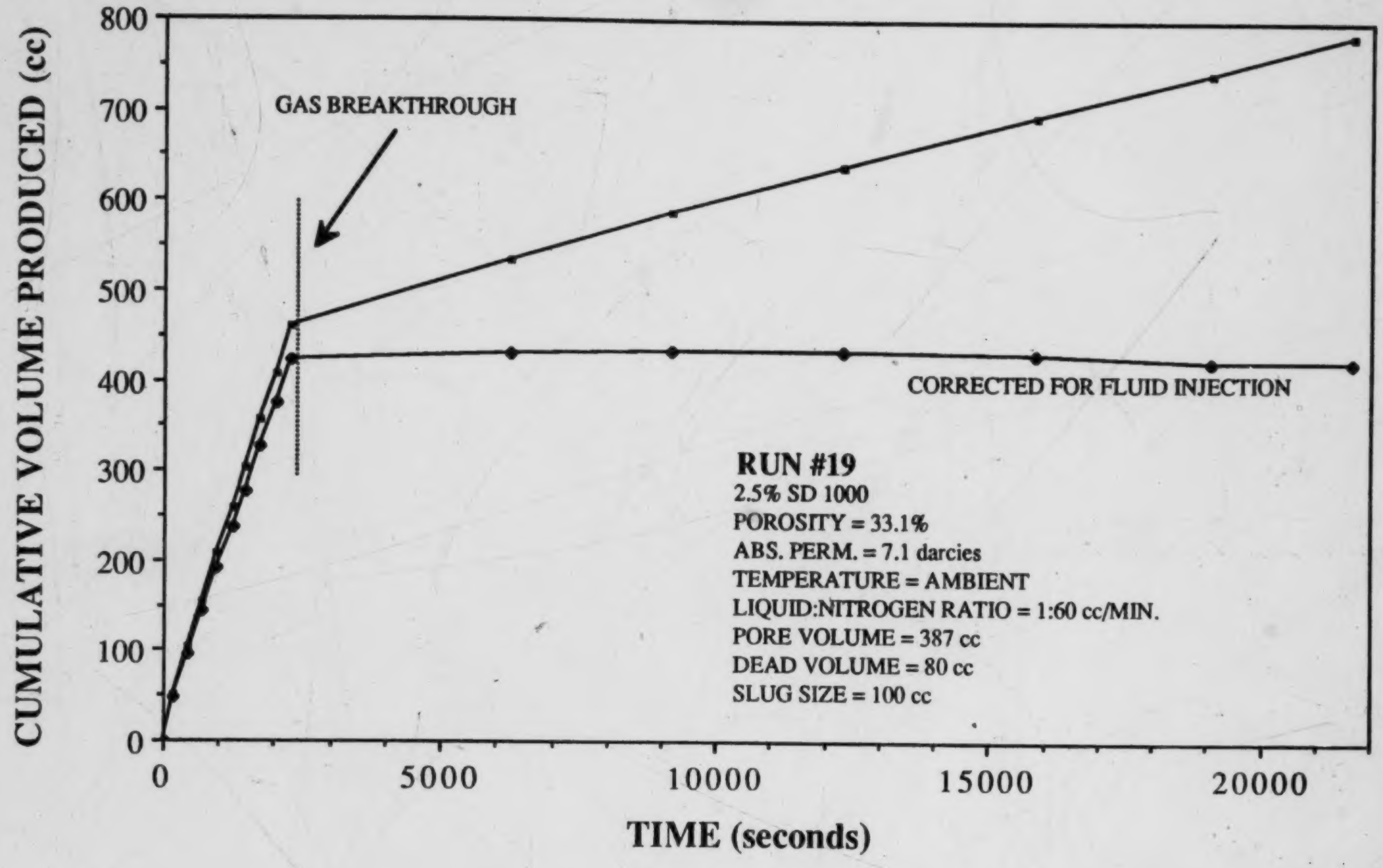

Figure 5.27 Run 19: Cumulative Volume Produced Vs. Time, Nitrogen Surfactant Co-injection, 2.5% SD1000

a constant at 423 cc. The residual liquid saturation becomes 31.90 percent, compared to Run 1, the 1 percent case, which had a residual liquid saturation of 32.50 percent.

The gas breakthrough time was 39 minutes; the cumulative volume produced at this point was 460 cc. These values are very similar to those for Run 1. From Figure 5.28, it is evident that the pressure drop across the coreholder did not stabilize at gas breakthrough. It took longer for steady state conditions to be achieved. This was also observed for the corrected cumulative volume produced; steady state was achieved later in the run.

The total mobility for this run was 0.9299 darcies/cp; the value for Run 1 was 0.9526 darcies/cp. The total relative mobility for this run was 0.1310 darcies/cp; for Run 1 the value was 0.1536 cp^{-1}.

Figure 5.29 shows the effluent surfactant concentration determined by ultraviolet spectrophotometer analysis. The concentration values seen in Table 5.16, in ppm, were converted into percentage of the injected fluid concentration, viz. 25,000 ppm. The concentration never reached 100 percent for this run.

The last run analyzed in this series is Run 3. This run was performed with 5 percent SD1000 on a 5.2 darcy glass bead pack. The data is given in Table 5.17. The corrected cumulative volume produced was steady at 400 cc as can be seen from Figure 5.30.

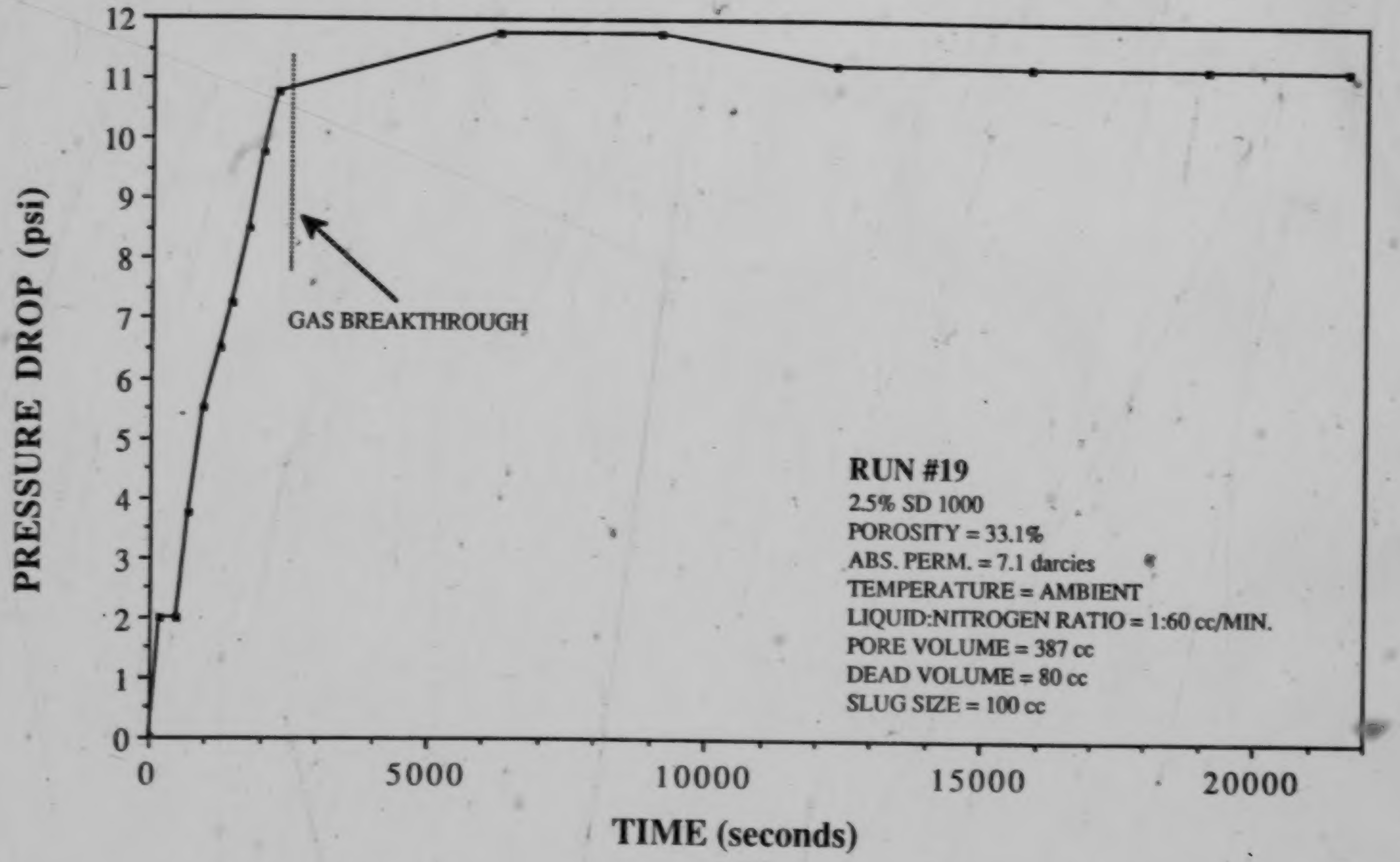

Figure 5.28 Run 19: Pressure Drop Vs. Time, Nitrogen Surfactant Co-injection, 2.5% SD1000

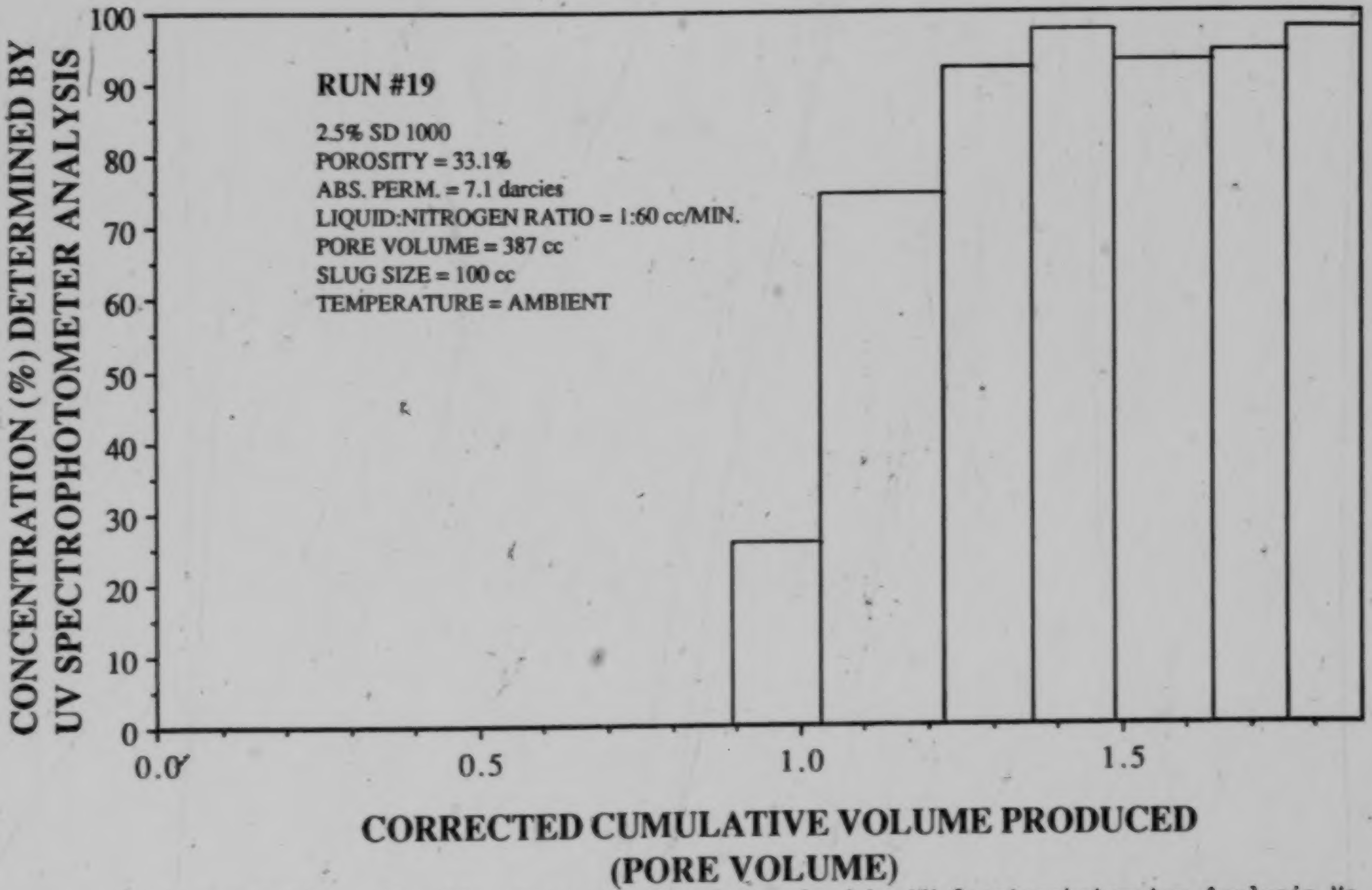

Figure 5.29 Run 19: Concentration Determined by UV Spectrophotometer Analysis Vs. Corrected Cumulative Volume Produced, Nitrogen Surfactant Co-injection, 2.5% SD1000

Experimental Data For Run 3
5% SD 1000 Glass Bead Size #9

Surfactant:	SD 1000	**Glass Bead Size:**	#9
Concentration:	5%	**Residual Oil Saturation:**	no
Absolute Permeability:	5.2 darcies	**Temperature:**	Ambient
Porosity:	33.4%	**Gas Breakthrough:**	36:50 (min.)
Back Pressure:	50 psi	**Totalizer Reading @ BT.:**	224

Time (s)	Volume (cc)	Cum. Vol. (cc)	Refrac. Index Conc. (%)	Pressure Drop (psi)	Totalizer Reading
285	66.0	51.0	0	1.25	27
585	51.5	102.5	0	2.25	57
870	67.0	169.5	0	4.00	87
1125	49.0	218.5	0	5.25	112
1470	63.0	281.5	0	7.00	145
1770	67.5	349.0	0	8.00	178
2100	65.0	414.0	10	8.75	211
3450	39.0	453.0	55	9.25	344
4980	27.0	480.0	80	9.00	501
7080	37.0	517.0	95	9.00	709
9900	47.0	564.0	100	9.00	991
12600	45.0	609.0	100	9.00	1261

Table 5.17 Experimental Data for Run 3: 5% SD1000

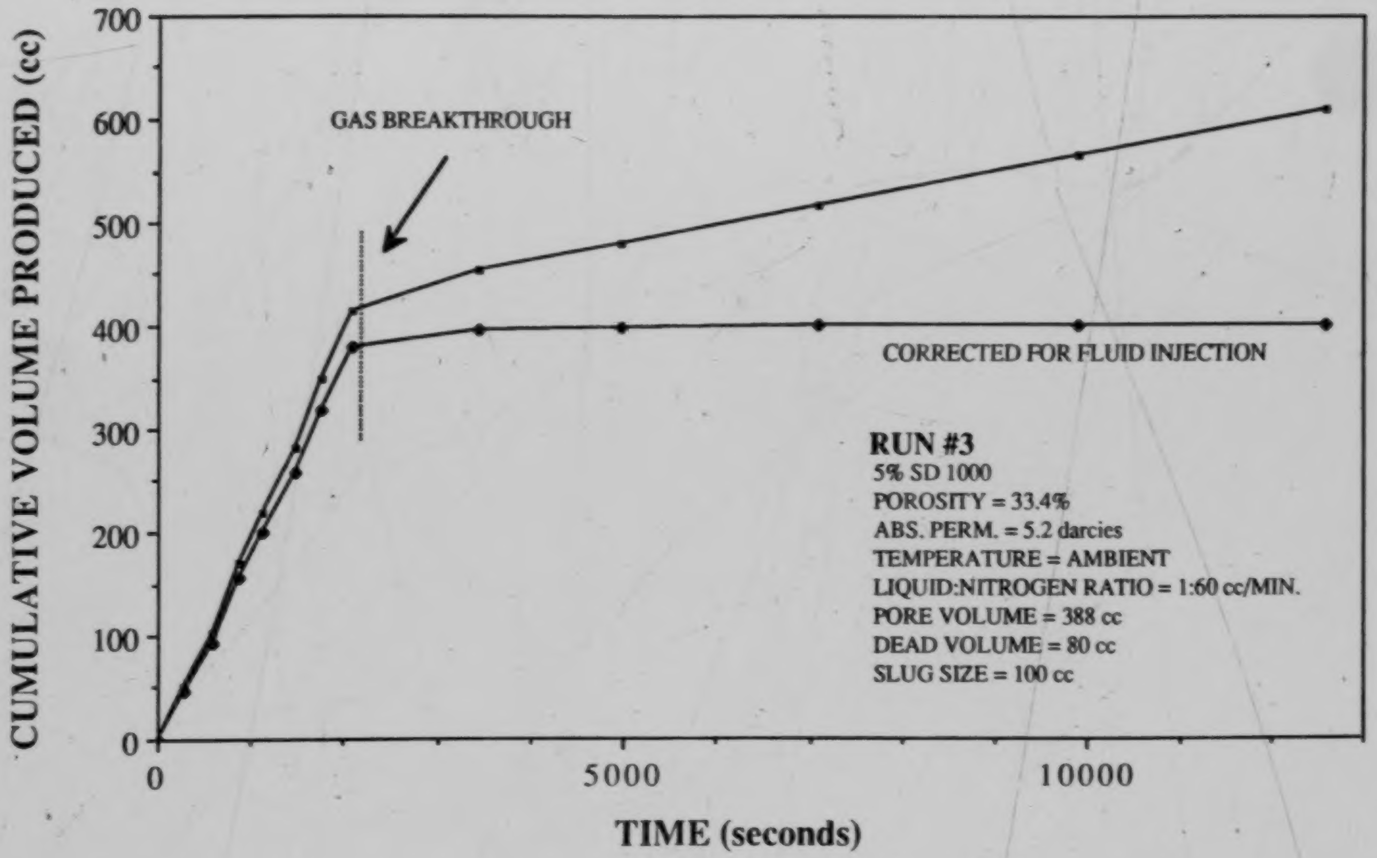

Figure 5.30 Run 3: Cumulative Volume Produced Vs. Time, Nitrogen Surfactant Co-injection, 5% SD1000

The residual liquid saturation was 0.3879, which is higher than that for either Run 1 (0.3250) or Run 19 (0.3197). Gas breakthrough occurred at 36.8 minutes for this run. The gas breakthrough time was longer for both the Run 1, the 1 percent run, (39 minutes) and Run 19, the 2.5 percent run, (40 minutes). The cumulative volumes produced at gas breakthrough were 414 cc for this run, and 462 cc and 460 cc for Runs 1 and 19, respectively. The steady state pressure drop across the core was 9.0 psi. The pressure drop graph is presented in Figure 5.31.

The total mobility for Run 3 was 1.180 darcies/cp. A comparison of the total mobilities for Run 12P and Runs 1, 19 and 3 is presented in Figure 5.32. This plot shows that the total mobility was much lower for the surfactant runs than for the base water run. This plot also shows that the 1 percent and 2.5 percent runs performed slightly better than the 5 percent run. There was some degradation in foam performance at a concentration of 5 percent. Also presented on this plot is the total relative mobility versus concentration. This plot shows that the relative mobility was lowest at 2.5 percent. The relative mobility at 1 percent was also very low.

Figure 5.33 shows the mobility reduction factor as a function of the concentration of SD1000. From this plot it is seen that the 1 and 2.5 percent cases exhibited virtually the same results. From the previous discussion it would seem that the addition of surfactant reduces the total mobility and therefore the gas mobility.

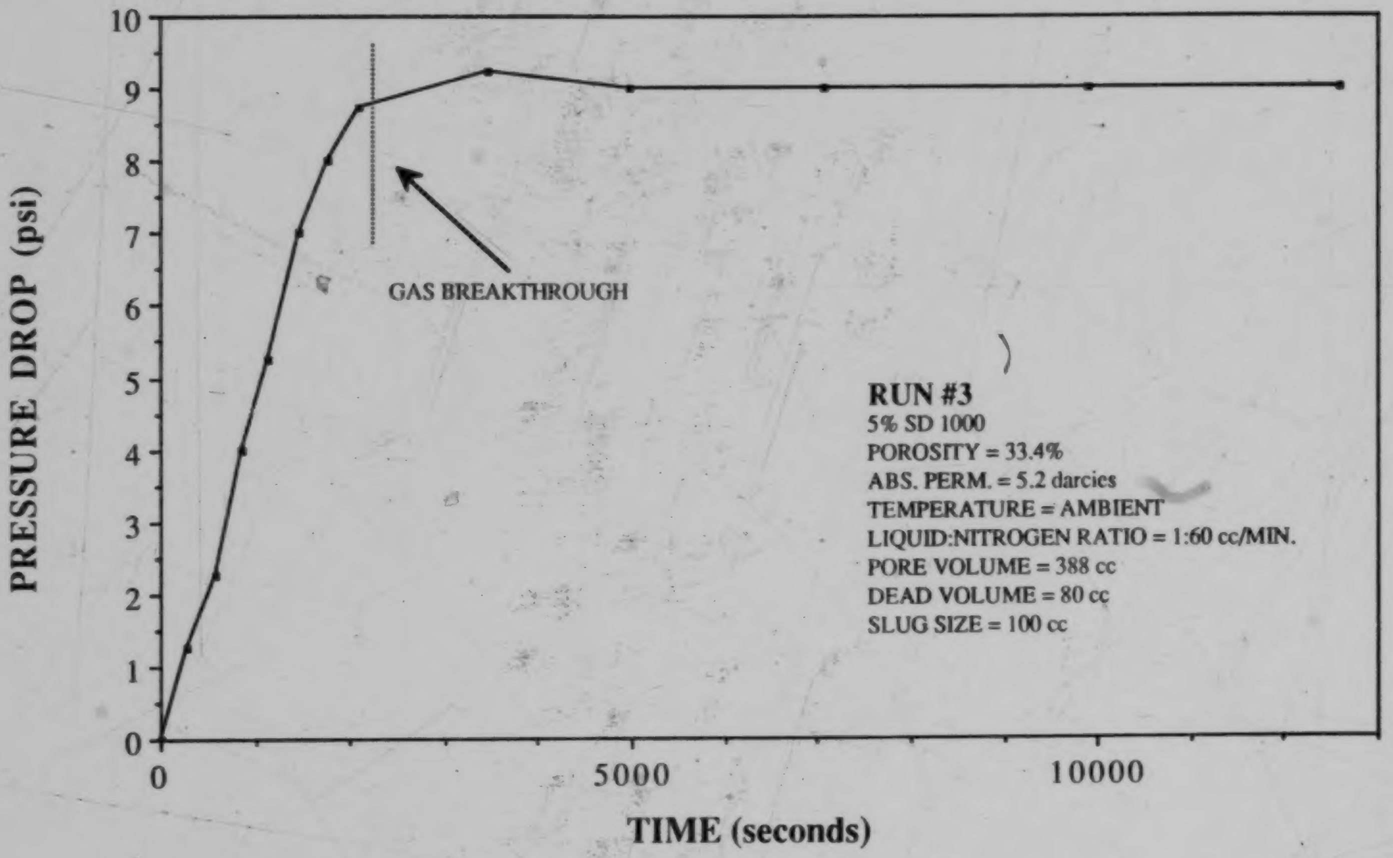

Figure 5.31 Run 3: Pressure Drop Vs. Time, Nitrogen Surfactant Co-injection, 5% SD1000

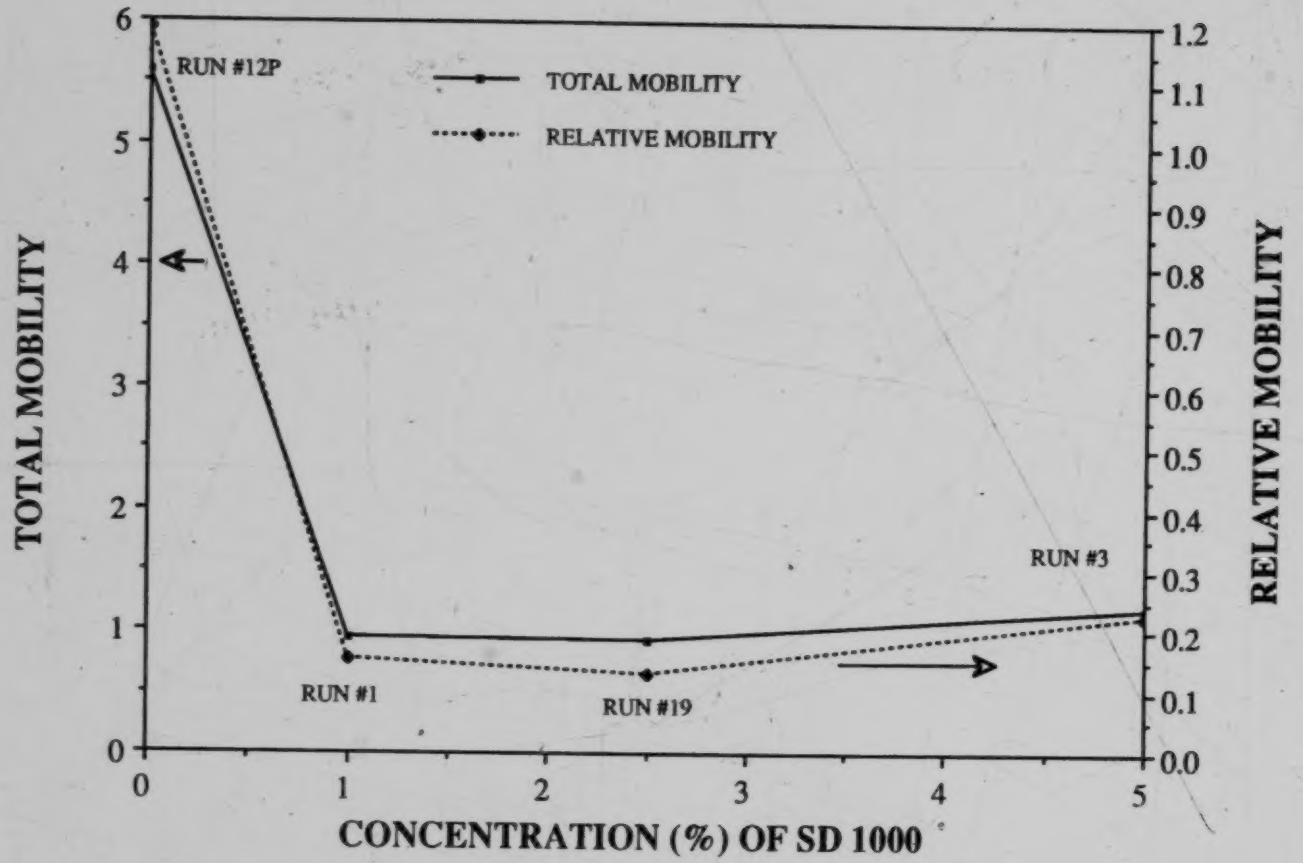

Figure 5.32 Comparison of Runs: 1, 19, 3, and 12P Crossplot of Total Mobility and Relative Mobility Vs. Concentration of SD1000

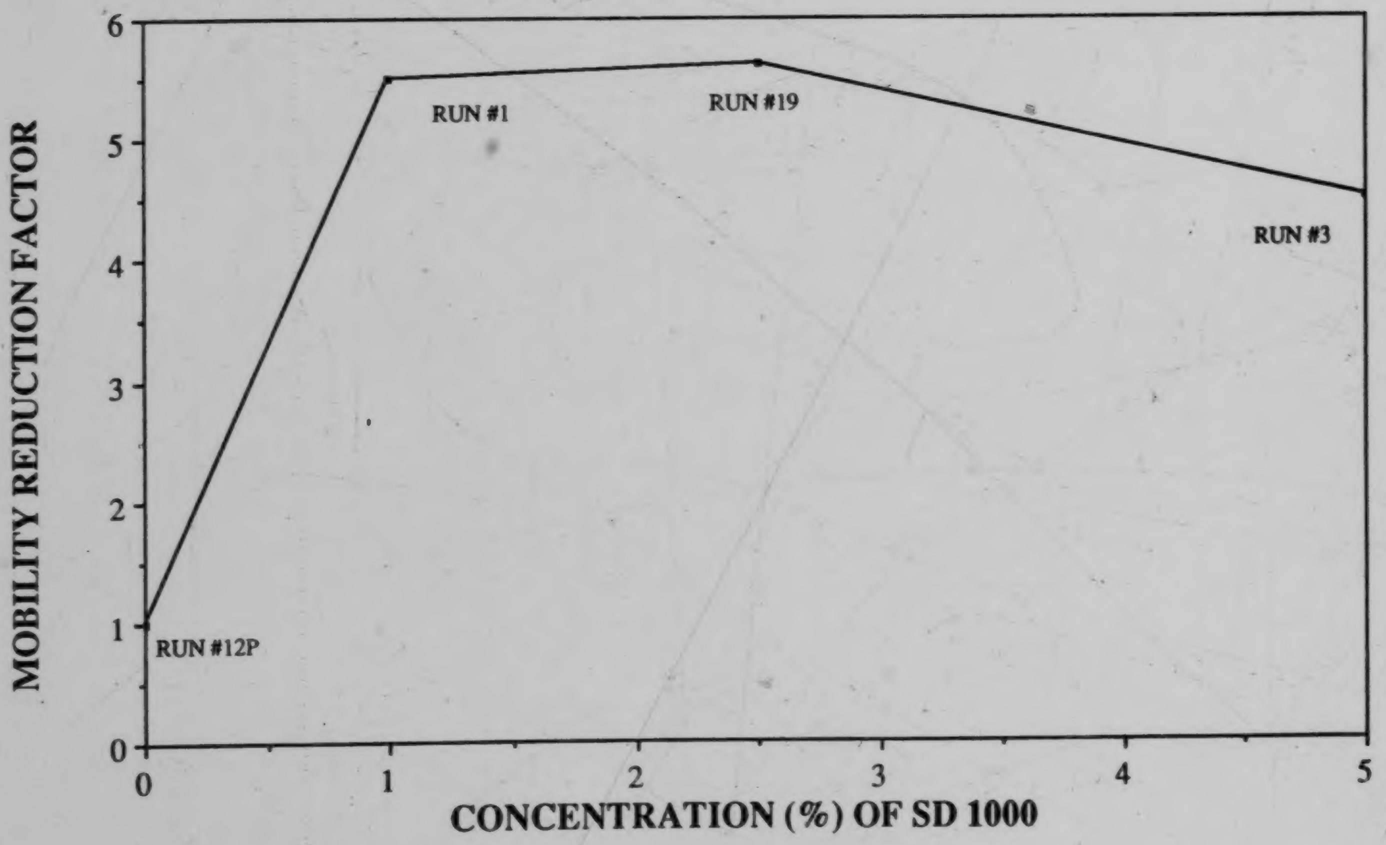

Figure 5.33 Comparison of Runs: 1, 19, 3, and 12P Mobility Reduction Factor Vs. Concentration of SD1000

There is a slight increase in gas phase mobility at 5 percent concentration. The 2.5 percent SD1000 run seems incrementally better at reducing gas phase mobility than the 1 percent run; this increase is however, within the range of experimental error, hence no clear conclusion as to which concentration is superior, can be drawn, but it is clear that the ability to cause gas phase mobility reduction is not directly proportional to increased surfactant concentration.

5.3.2.2 Absolute Permeability Range 12.2 darcies to 17.5 darcies

To examine the effect of surfactant concentration on glass bead packs in this permeability range, Runs 11, 7, 18 and 5 will be compared with the base case, Run 21. Run 11 was examined in Section 5.3.1, (Typical Run History). The total mobility for this run was 2.18 darcies/cp.

Run 7 is basically a repeat of this run. Table 5.18 provides the run data. The gas breakthrough for this run occurred at 25.3 minutes with 323 cc of liquid produced. Figure 5.34 shows that the corrected cumulative volume produced curve has a pronounced curvature. This curvature occurs after the gas breakthrough, which suggests that gas by-passed the surfactant slug, causing low displacement efficiency. The residual water saturation for this core

Experimental Data For Run #7
1% SD 1000 Glass Bead Size #7

Surfactant:	SD 1000	**Glass Bead Size:**	#7
Concentration:	1%	**Residual Oil Saturation:**	no
Absolute Permeability:	15.0 darcies	**Temperature:**	Ambient
Porosity:	33.7%	**Gas Breakthrough:**	25:19 (min.)
Back Pressure:	50 psi	**Totalizer Reading @ BT.:**	155

Time (s)	Volume (cc)	Cum. Vol. (cc)	Refractive Index Conc. (%)	Pressure Drop (psi)	Totalizer Reading
195	54.5	54.5	0	0.75	20
440	48.0	102.5	0	0.75	45
690	52.0	154.5	0	1.75	69
915	46.0	200.5	0	2.00	93
1155	50.0	250.5	0	2.25	117
1385	48.0	298.5	0	2.75	140
1575	25.0	323.5	0	2.75	160
2250	48.0	371.5	0	2.50	228
3420	33.5	405.0	35	2.50	346
6270	49.0	454.0	70	2.50	633
8880	42.0	496.0	100	2.50	924

Table 5.18 Experimental Data for Run 7: 1% SD1000

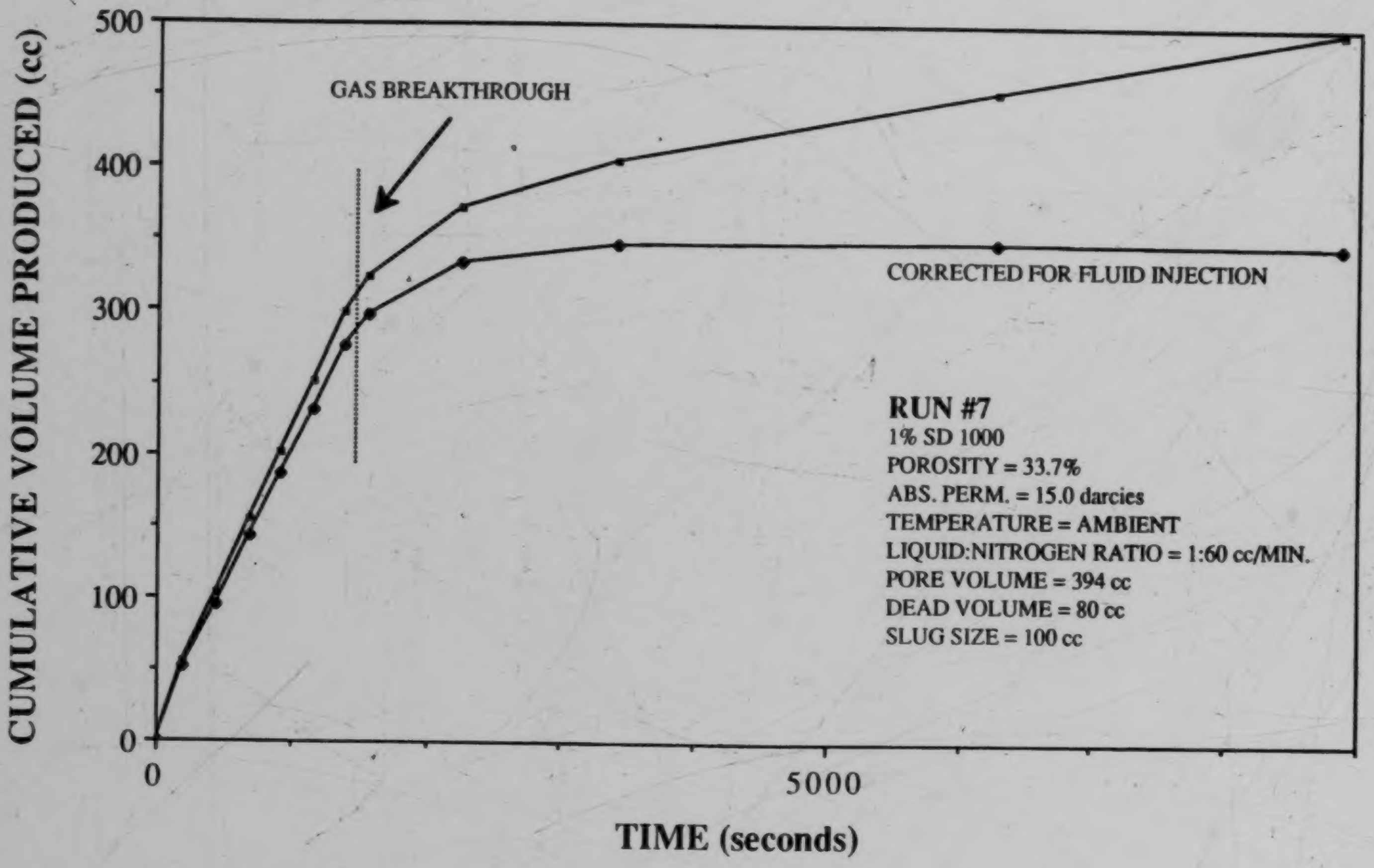

Figure 5.34 Run 7: Cumulative Volume Produced Vs. Time, Nitrogen Surfactant Co-injection, 1% SD1000

was 51.9 percent; this can be compared to 38.8 percent for Run 11, which also utilized 1 percent SD1000.

The differential pressure profile for Run 7 is presented in Figure 5.35. The pressure drop across the core stabilized at 2.5 psi. The differential pressure established for Run 11 was 5 psi.

The concentration graph for Run 7 is presented in Figure 5.36. It shows that the first increase in surfactant concentration, to 35 percent, occurred at 0.79 corrected pore volumes. Gas breakthrough occurred at 0.67 corrected pore volume. The gas bypassed the surfactant solution and maintained an increased mobility. For Run 11, the 46 cc sample collected at gas breakthrough had a surfactant concentration of 34 percent of the original concentration of the displacing fluid. For this run, the nitrogen did not entirely bypass the surfactant solution as it did in Run 7.

By analyzing the cumulative volume produced graph and the surfactant concentration graph it appears that Run 7 did not behave as a typical surfactant run. The cumulative volume profile and the gas breakthrough point are not indicative of the surfactant runs. The mobility for this run was 4.44 darcies/cp. It would seem that something interfered with the displacement efficiency. It is possible that there was some residual oil or rust in the sightglass that contaminated the system. Rust was noticed in the sightglasses when the water saturated coreholder was packed a few days before use. Following this run, the run procedure was altered to include back

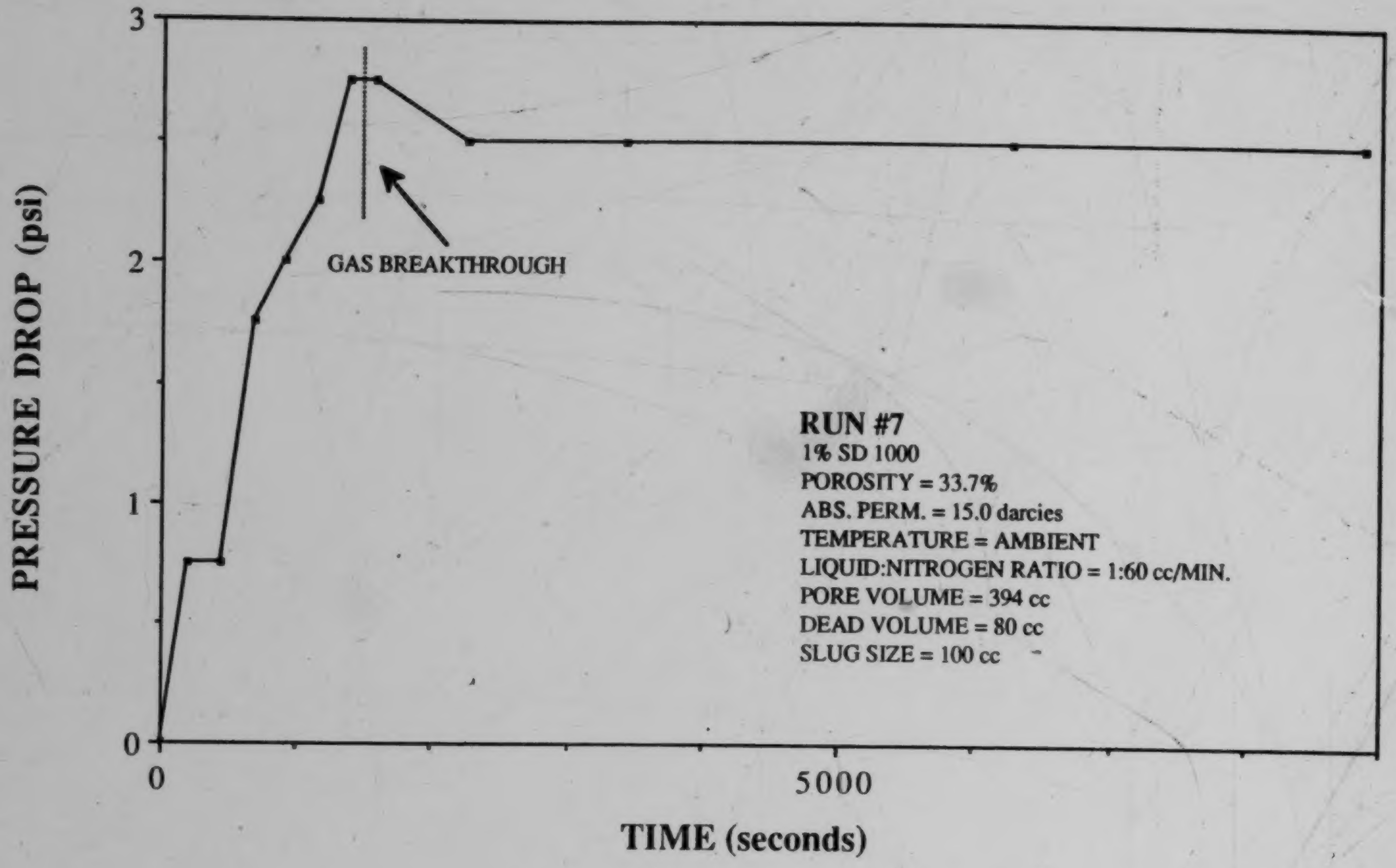

Figure 5.35 Run 7: Pressure Drop Vs. Time, Nitrogen Surfactant Co-injection, 1% SD1000

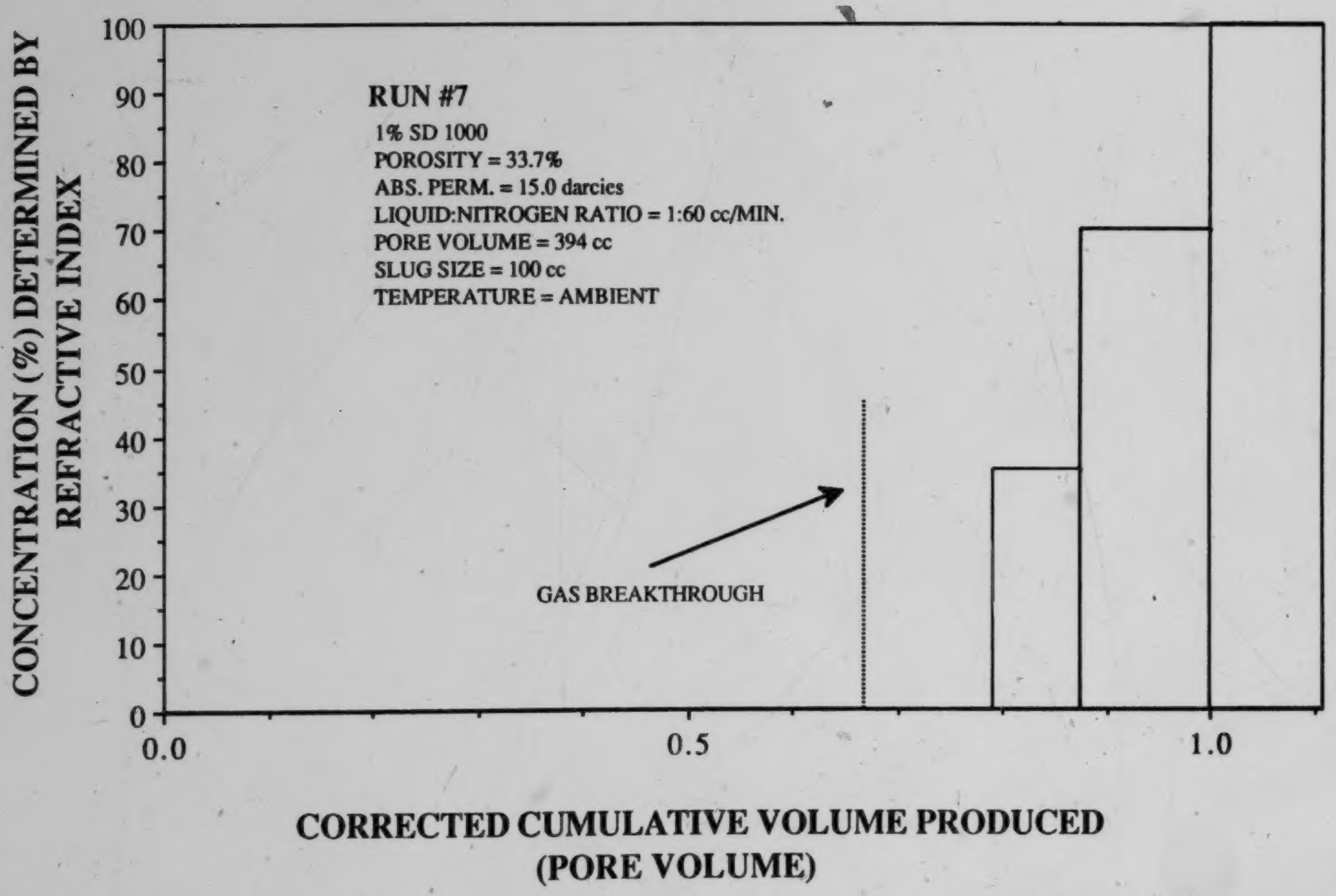

Figure 5.36 Run 7: Concentration Determined by UV Spectrophotometer Analysis Vs. Corrected Cumulative Volume Produced, Nitrogen Surfactant Co-injection, 1% SD1000

flushing the coreholder with 1 pore volume of distilled water prior to the experiment.

Run 18 was performed with 2.5 percent SD1000, on a 15.2 darcy glass bead pack. Table 5.19 gives the run data. The time until gas breakthrough was 37 minutes, and the volume produced at this point was 451 cc. The residual liquid saturation within the core was 0.335. The cumulative volume produced versus time is graphically presented in Figure 5.37. This graph shows the expected surfactant run production profile. The corrected volume produced shows a sharp change in slope at gas breakthrough.

The differential pressure profile is presented in Figure 5.38, which shows an increase in differential pressure following gas breakthrough. This represents a longer stabilization period. From the concentration graph, Figure 5.39, we see that there was a wide surfactant mixing range within the core. The total mobility for Run 18 was 1.43 darcies/cp. The relative mobility was 0.0941 cp^{-1}.

Run 5 was performed using a 5 percent solution of SD1000 on a 17.5 darcy glass bead pack. The data for this run is given in Table 5.20. The time until gas breakthrough was 34 minutes for this run with a cumulative produced volume of 437.5 cc. A comparison of gas breakthrough times and volumes for Runs 21, 11, 7, 18 and 5 is presented in Figure 5.40.

Experimental Data For Run 18
2.5% SD 1000 Glass Bead Size #7

Surfactant:	SD 1000	**Glass Bead Size:**	#7
Concentration:	2.50%	**Residual Oil Sat.:**	no
Absolute Permeability:	15.2 darcies	**Temperature:**	Ambient
Porosity:	32.3%	**Gas Breakthrough:**	37:00 (min.)
Back Pressure:	50 psi	**Totalizer Reading @ BT.:**	226

Time (s)	Volume (cc)	Cum. Vol. (cc)	Spectro. Conc. ppm	Pressure Drop (psi)	Simulated Pressure Drop (psi)	Totalizer Reading
195	55	51.0	87	1.00	2.1	19
420	47	98.0	28	1.25	3.5	43
690	54	152.0	25	2.50	4.3	70
945	50	202.0	69	3.00	5.2	95
1170	47	249.0	74	3.50	7.0	120
1440	55	304.0	26	4.00	8.0	147
1710	50	354.0	631	5.00	8.0	173
1980	53	407.0	7580	5.00	8.0	200
2235	44	451.0	9477	5.25	8.0	230
5100	48	499.0	20579	6.50	8.0	520
8100	49	548.0	22936	7.00	8.0	826
11700	59	607.0	24154	7.00	8.0	1188
16200	74	681.0	24169	7.25	8.0	1640
19020	45	726.0	25196	7.50	8.0	1938
21600	42	768.0	25740	7.50	8.0	2200

Table 5.19 Experimental Data for Run 18: 2.5% SD1000

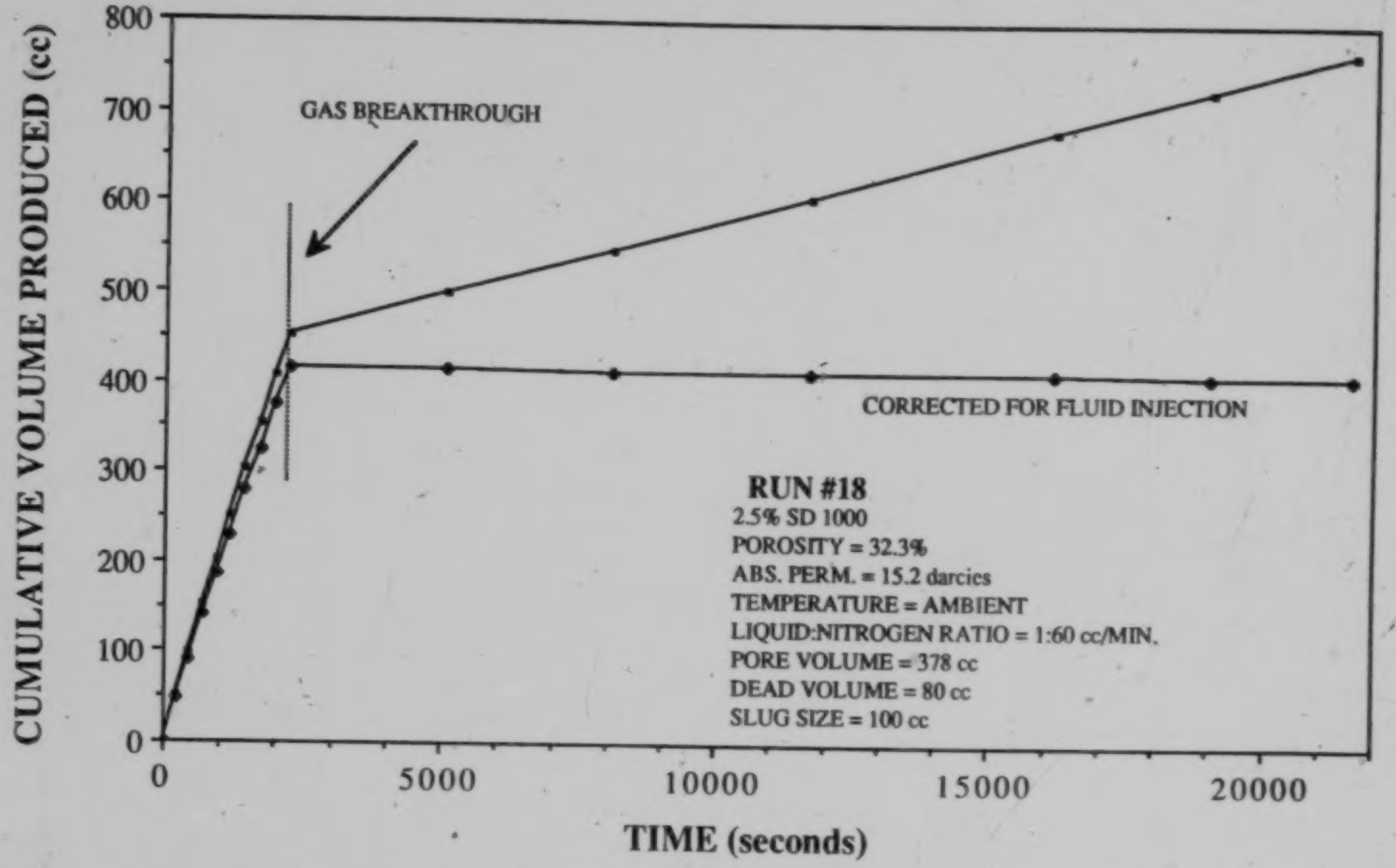

Figure 5.37 Run 18: Cumulative Volume Produced Vs. Time, Nitrogen Surfactant Co-injection, 2.5% SD1000

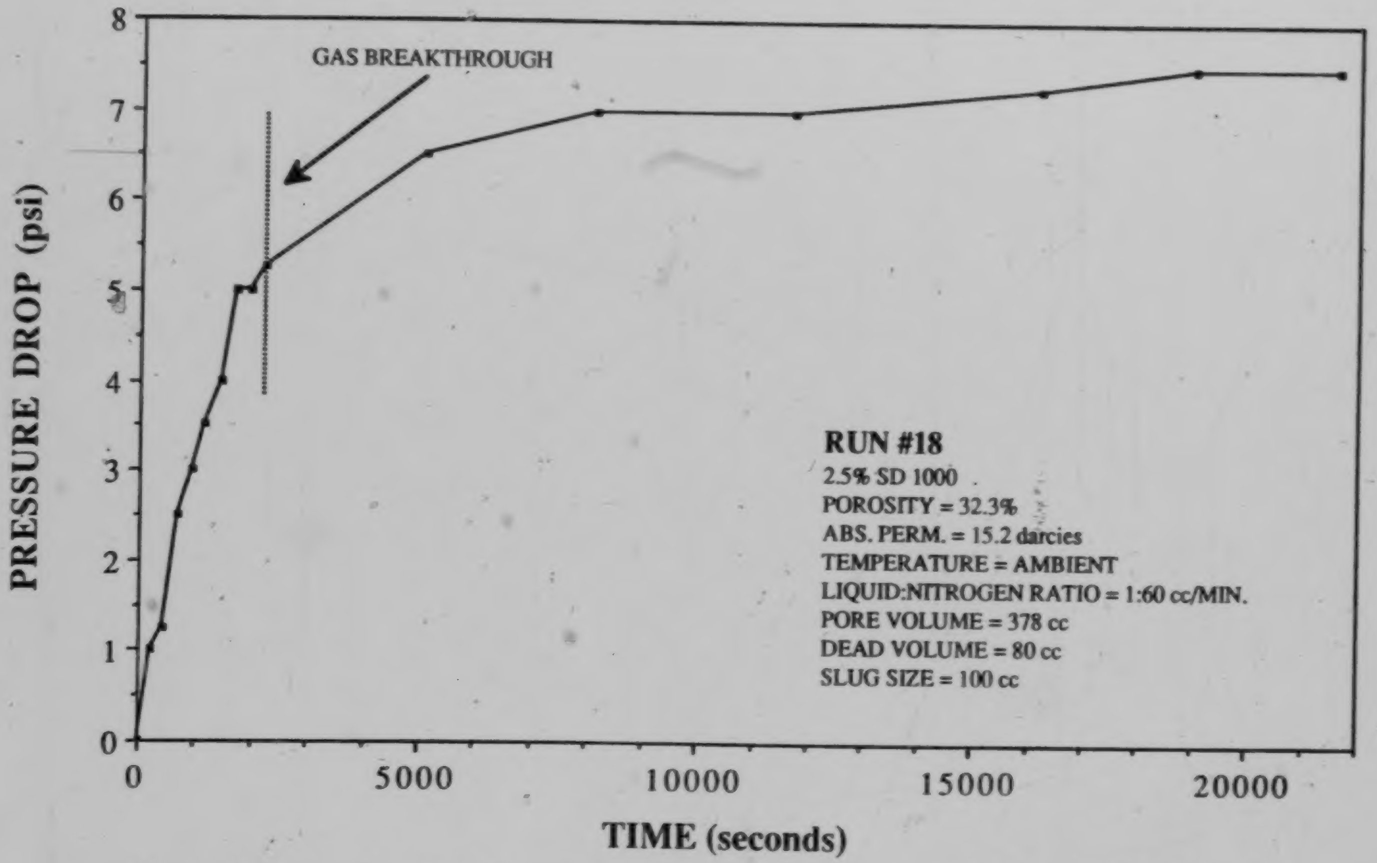

Figure 5.38 Run 18: Pressure Drop Vs. Time, Nitrogen Surfactant Co-injection, 2.5% SD1000

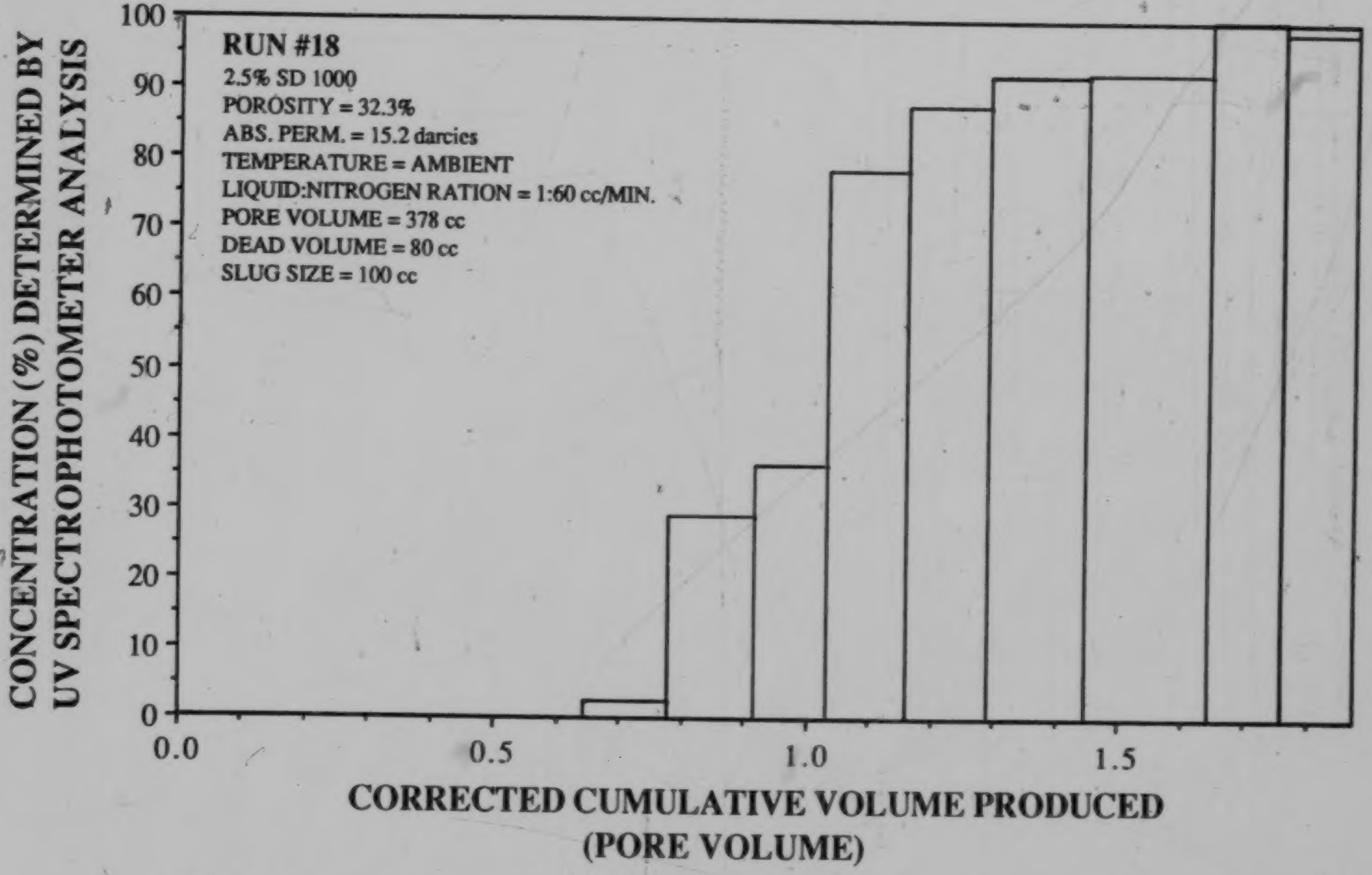

Figure 5.39 Run 18: Concentration Determined by UV Spectrophotometer Analysis Vs. Corrected Cumulative Volume Produced, Nitrogen Surfactant Co-injection, 2.5% SD1000

5

Experimental Data For Run #5
5% SD 1000 Glass Bead Size #9

Surfactant:	SD 1000	**Glass Bead Size:**	#9
Concentration:	5%	**Residual Oil Saturation:**	no
Absolute Permeability:	17.5 darcies	**Temperature:**	Ambient
Porosity:	32.0%	**Gas Breakthrough:**	34:00 (min.)
Back Pressure:	50 psi	**Totalizer Reading @ BT.:**	206

Time (s)	Volume (cc)	Cum. Vol. (cc)	Refrac. Index Conc. (%)	Pressure Drop (psi)	Simulated Pressure Drop (psi)	Totalizer Reading
180	58.0	51.0	0	0.50	1.90	18
395	42.0	93.0	0	0.75	3.10	39
635	50.0	143.0	0	1.50	4.50	63
855	47.0	190.0	0	2.00	7.00	85
1080	50.0	240.0	0	2.75	7.00	109
1320	51.5	291.5	0	3.50	7.00	133
1590	52.0	343.5	0	4.00	7.00	155
1830	52.0	395.5	15	4.50	7.00	185
2040	42.0	437.5	50	4.75	7.00	206
4740	43.0	480.5	65	4.50	7.00	478
8340	58.0	538.5	95	4.50	7.00	848
10980	41.0	579.5	100	4.50	7.00	1108

Table 5.20 Experimental Data for Run 5: 5% SD1000

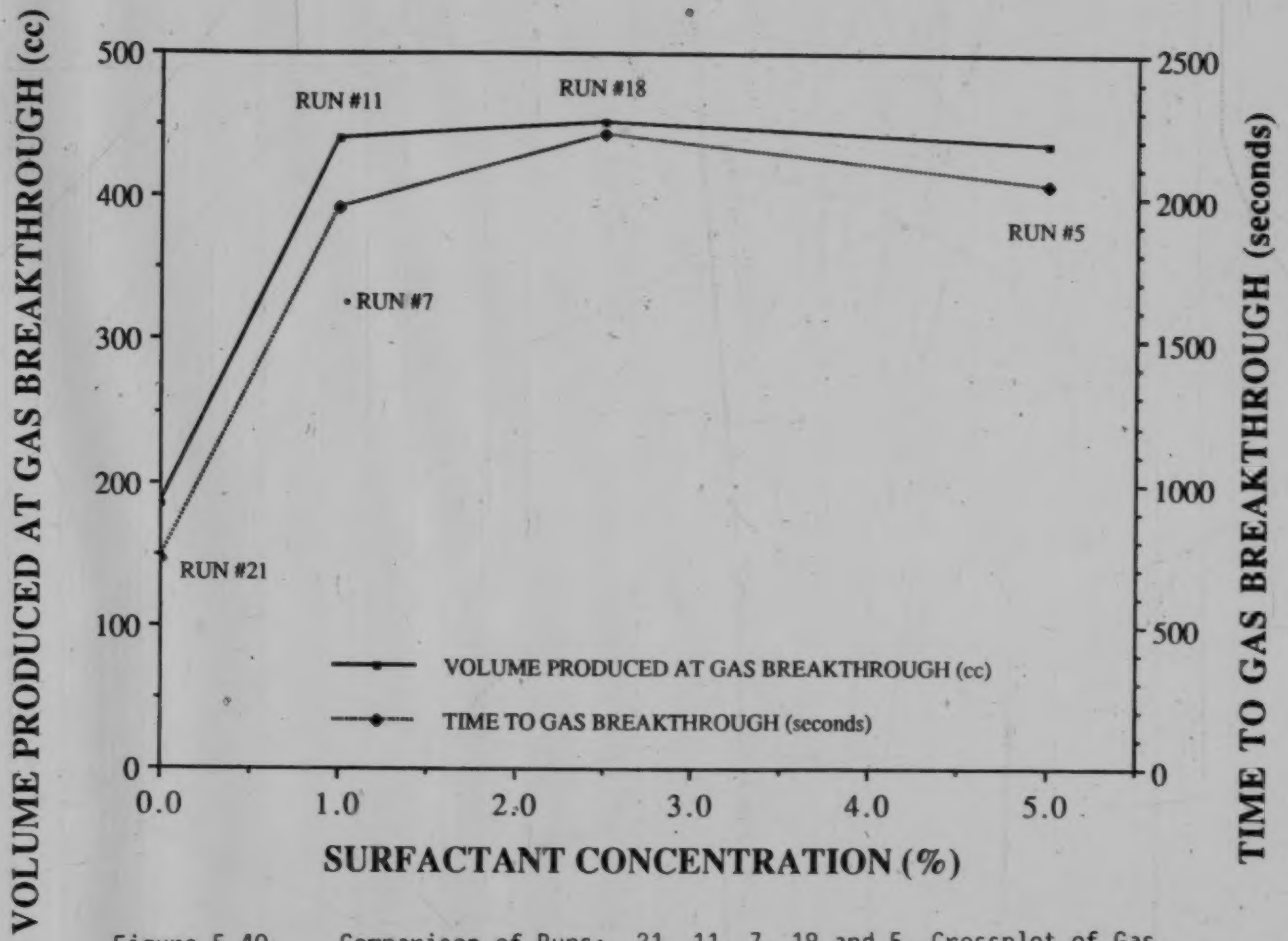

Figure 5.40 Comparison of Runs: 21, 11, 7, 18 and 5 Crossplot of Gas Breakthrough Times and Volumes Vs. Concentration of SD1000

The longest breakthrough time is associated with the 2.5 percent concentration, as is the largest volume produced at gas breakthrough. From Figure 5.41, the plot of cumulative volume produced, the corrected volume produced is 400 cc. This curve exhibits the characteristics typically associated with the SD1000 surfactant runs. The residual water saturation for this run was 36.0 percent. The residual values were 33.5 percent for Run 18, the 2.5 percent run, 38.8 percent for Run 11, the 1 percent run, and 51.9 percent for Run 7, the second 1 percent run. The inconsistency of the value for Run 7 with the other runs, in the grouping, is further proof that a contaminating substance inhibited the formation of foam in this run. The residual water saturation was 88.2 percent for Run 21, the base case.

Figure 5.42 is the differential pressure plot for Run 5. The pressure dropped slightly after gas breakthrough but stabilized at 4.5 psi. From Figure 5.43, the effluent concentration graph, it is evident that there was a large mixing zone because there was a delay before the effluent refractive index matched the injection fluid. At gas breakthrough, the effluent sample contained 50 percent surfactant.

The mobility comparison for this permeability range is presented in Figure 5.44. The total mobility for the 5 percent run was 2.43 darcies/cp and the relative mobility was 0.139 cp^{-1}. From Figure 5.44 it can be seen that the greatest total mobility decrease occurred at 2.5 percent SD1000. This concentration also produced

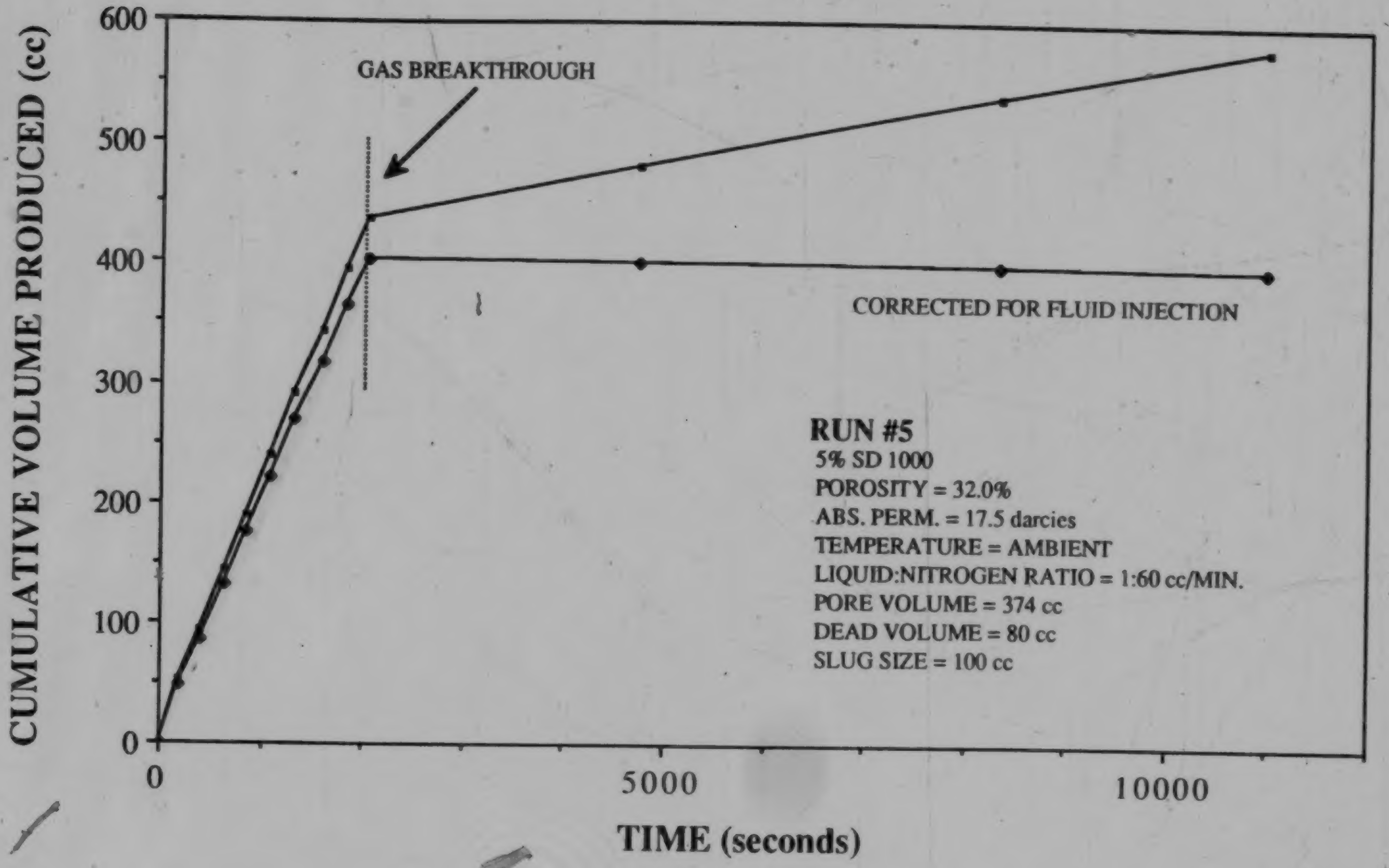

Figure 5.41 Run 5: Cumulative Volume Produced Vs. Time, Nitrogen Surfactant Co-injection, 5% SD1000

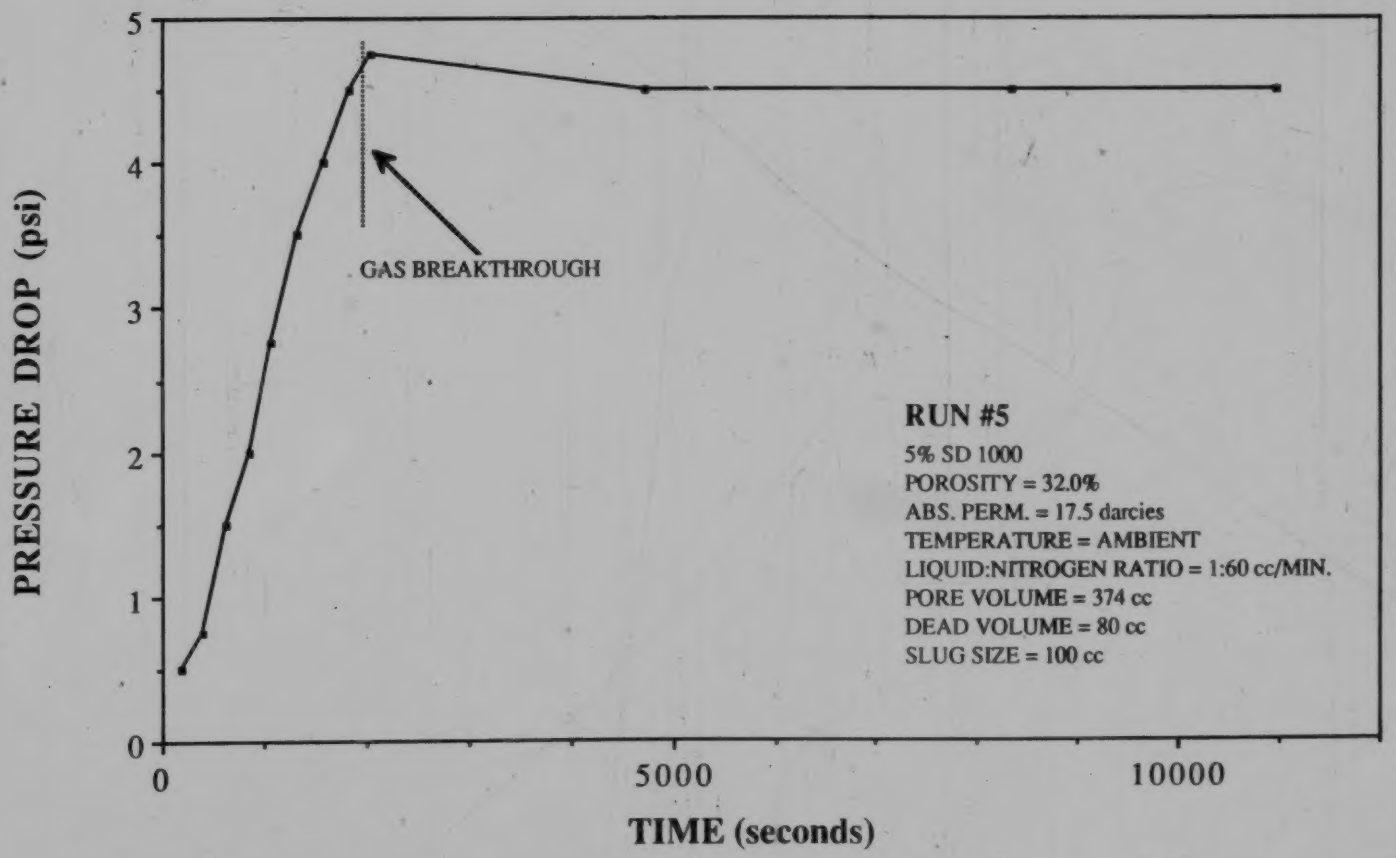

Figure 5.42 Run 5: Pressure Drop Vs. Time, Nitrogen Surfactant Co-injection, 5% SD1000

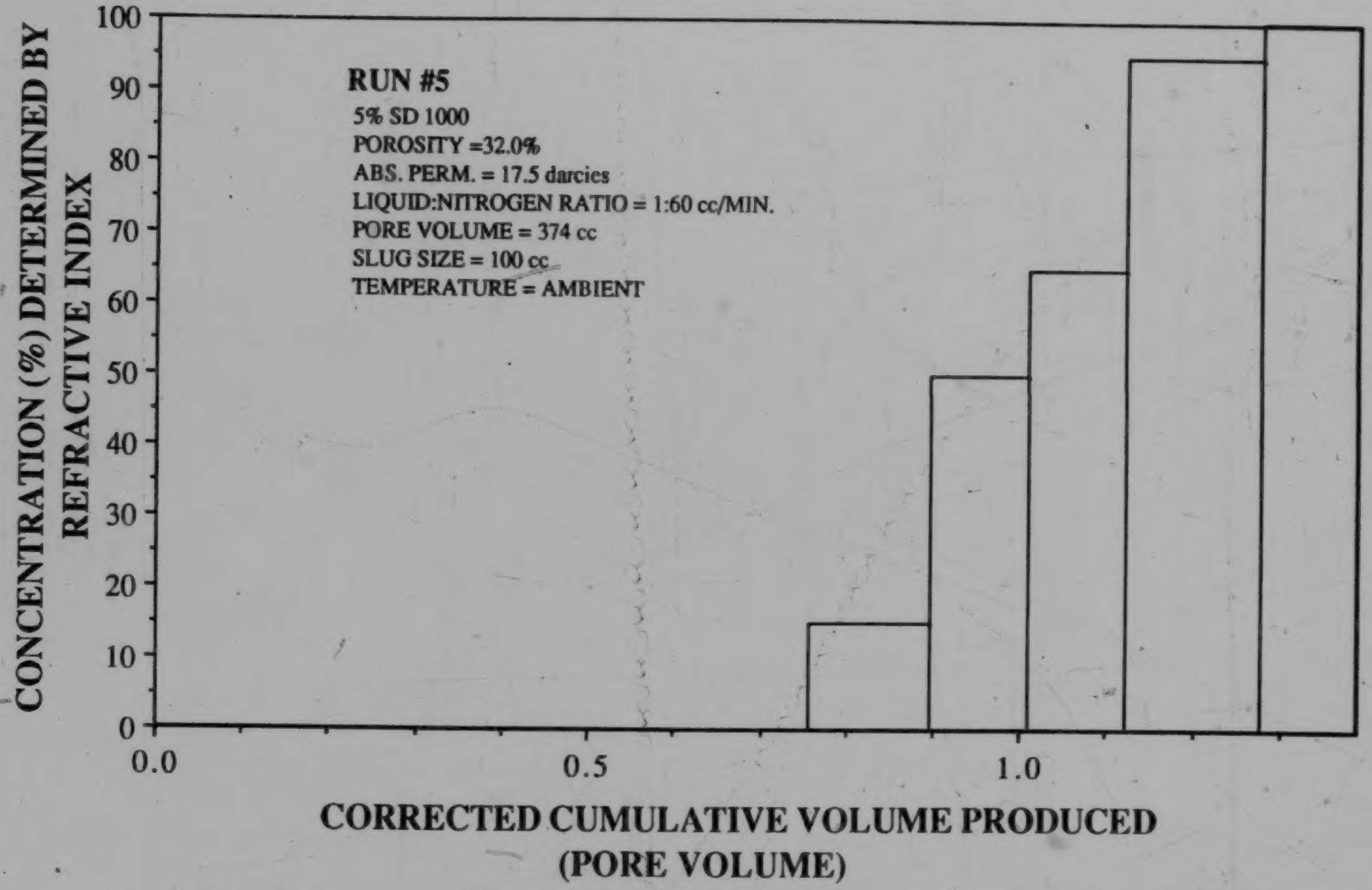

Figure 5.43 Run 5: Concentration Determined by UV Spectrophotometer Analysis Vs. Corrected Cumulative Volume Produced, Nitrogen Surfactant Co-injection, 5% SD1000

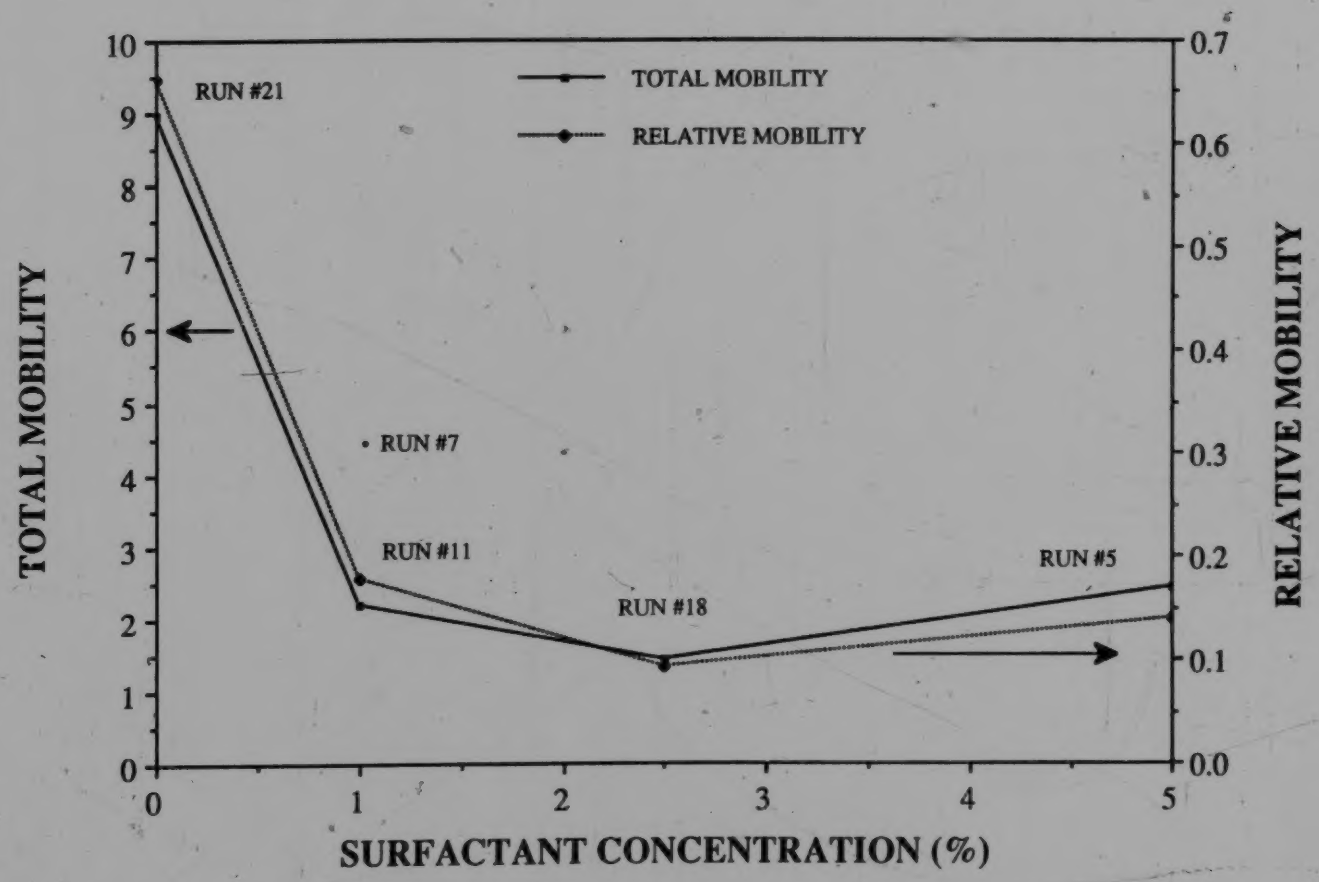

Figure 5.44 Comparison of Runs: 11, 7, 18, 5 and 21 Crossplot of Total Mobility and Relative Mobility Vs. Concentration of SD1000

the lowest relative mobility. For this permeability range the 5 percent concentration produced a lower relative mobility than the 1 percent concentration. For the last permeability range examined, this was not the case. It is possible that the total relative mobility versus concentration profile changes its shape for different absolute permeability ranges.

The mobility reduction factor versus surfactant concentration graph, Figure 5.45, confirms that this concentration reduced gas mobility to the greatest extent. The mobility reduction factor was also greater for Run 5, the 5 percent case (3.6), than for Run 11, the 1 percent case (2).

5.3.2.3 Absolute Permeability Range 28.7 to 30 darcies

Only two runs were performed in this permeability range, because the surfactant did not seem to reduce the mobility significantly. Run 17 was performed with 1 percent SD1000 on a 30 darcy core. The data for this run is given in Table 5.21. The gas breakthrough time for this run was 34.1 minutes and the volume produced at gas breakthrough was 450 cc.

Figure 5.46 shows that this run exhibits the typical cumulative volume produced versus time trend. The steady state corrected cumulative volume was 411 cc, while the residual liquid saturation

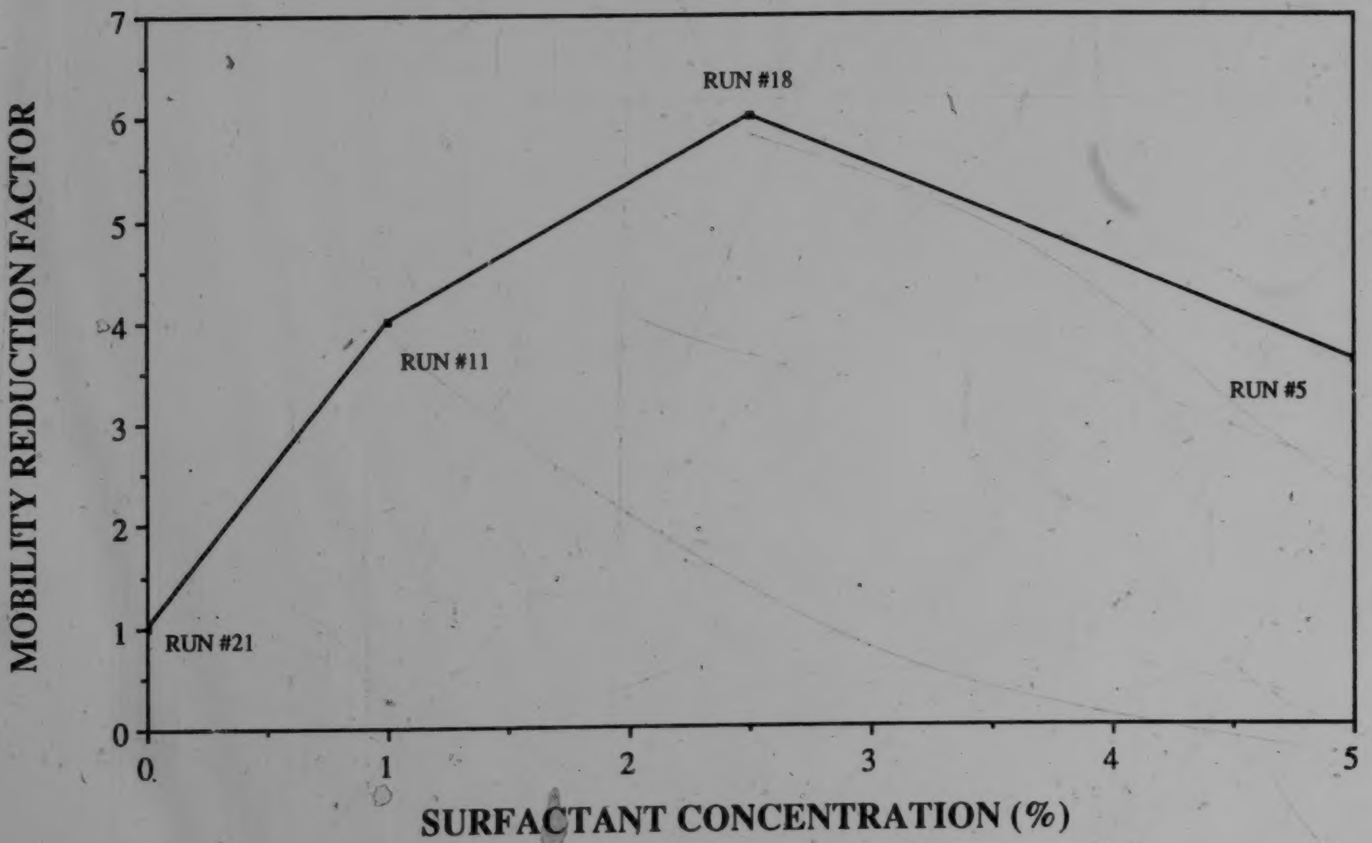

Figure 5.45 Comparison of Runs: 11, 7, 18, 5 and 21 Mobility Reduction Factor Vs. Concentration of SD1000

Experimental Data For Run #17
1% SD 1000 Glass Bead Size #3

Surfactant: SD 1000
Concentration: 1%
Absolute Permeability: 30 darcies
Porosity: 32.5%
Back Pressure: 50 psi

Glass Bead Size: #3
Residual Oil Saturation: no
Temperature: Ambient
Gas Breakthrough: 34:10 (min.)
Totalizer Reading @ BT.: 209

Time (s)	Volume (cc)	Cum. Vol. (cc)	Spectro. Conc. ppm	Pressure Drop (psi)	Simulated Pressure Drop (psi)	Totalizer Reading
150	53	51.0	63	0.75	2.1	15
300	43	94.0	80	0.75	3.2	36
570	46	140.0	26	0.75	3.5	58
780	46	186.0	13	1.00	4.3	78
1020	50	236.0	57	1.25	5.2	103
1230	44	280.0	58	1.50	6.4	125
1440	44	324.0	16	1.50	6.4	148
1650	45	369.0	10	1.50	6.4	168
1890	48	417.0	161	1.75	6.4	192
2100	33	450.0	2425	1.75	6.4	214
4740	50	500.0	6281	2.00	6.4	488
7650	47	547.0	7527	2.00	6.4	780
11930	67	614.0	8296	2.00	6.4	1205
16080	65	679.0	8541	2.25	6.4	1638
18060	42	721.0	8764	2.25	6.4	1837
20160	35	756.0	8308	2.25	6.4	2050
23460	55	811.0	8737	2.25	6.4	2394

Table 5.21 Experimental Data for Run 17: 1% SD1000

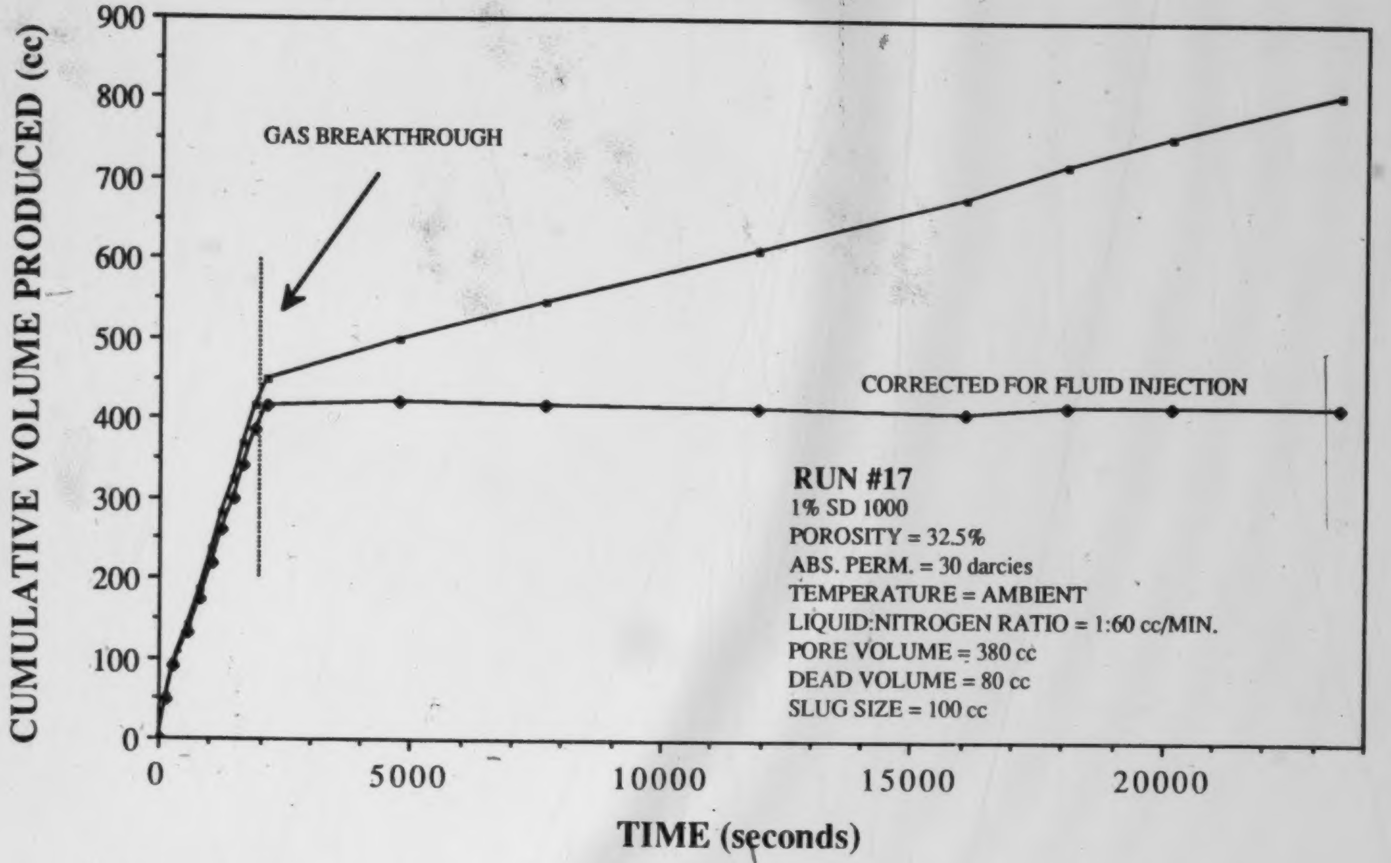

Figure 5.46 Run 17: Cumulative Volume Produced Vs. Time, Nitrogen Surfactant Co-injection, 1% SD1000

was 31.6 percent. The residual liquid saturation for the Section 5.31, Typical Run History (Run 11), was 38.8 percent.

The differential pressure established across the core is presented in Figure 5.47. The stabilized pressure drop was 2.25 psi. The total mobility for Run 17 was 4.94 darcies/cp. The relative mobility was 0.165 cp^{-1}.

The effluent surfactant concentration versus corrected pore volume on the graph is presented in Figure 5.48. The surfactant concentration of the sample collected at gas breakthrough suggests that the gas did not bypass the surfactant slug.

The large volume of effluent produced at gas breakthrough and the surfactant concentration at gas breakthrough suggests that the surfactant had a positive effect on liquid displacement. However, the high total mobility associated with this run suggests that the foam was less effective in the 30 darcy core.

Run 6 was performed with a 5 percent solution of SD1000 on a 28.7 darcy core. Table 5.22 gives the run data. Gas breakthrough occurred at 33 minutes with 441 cc of effluent produced. These values are very similar to those determined for Run 17 (34.2 minutes, 450 cc). The cumulative volume produced and corrected volumes found in Figure 5.49 show the typical surfactant run trend. The residual liquid saturation for this run was 36.2 percent compared with 31.6 percent for Run 17, the 1 percent case.

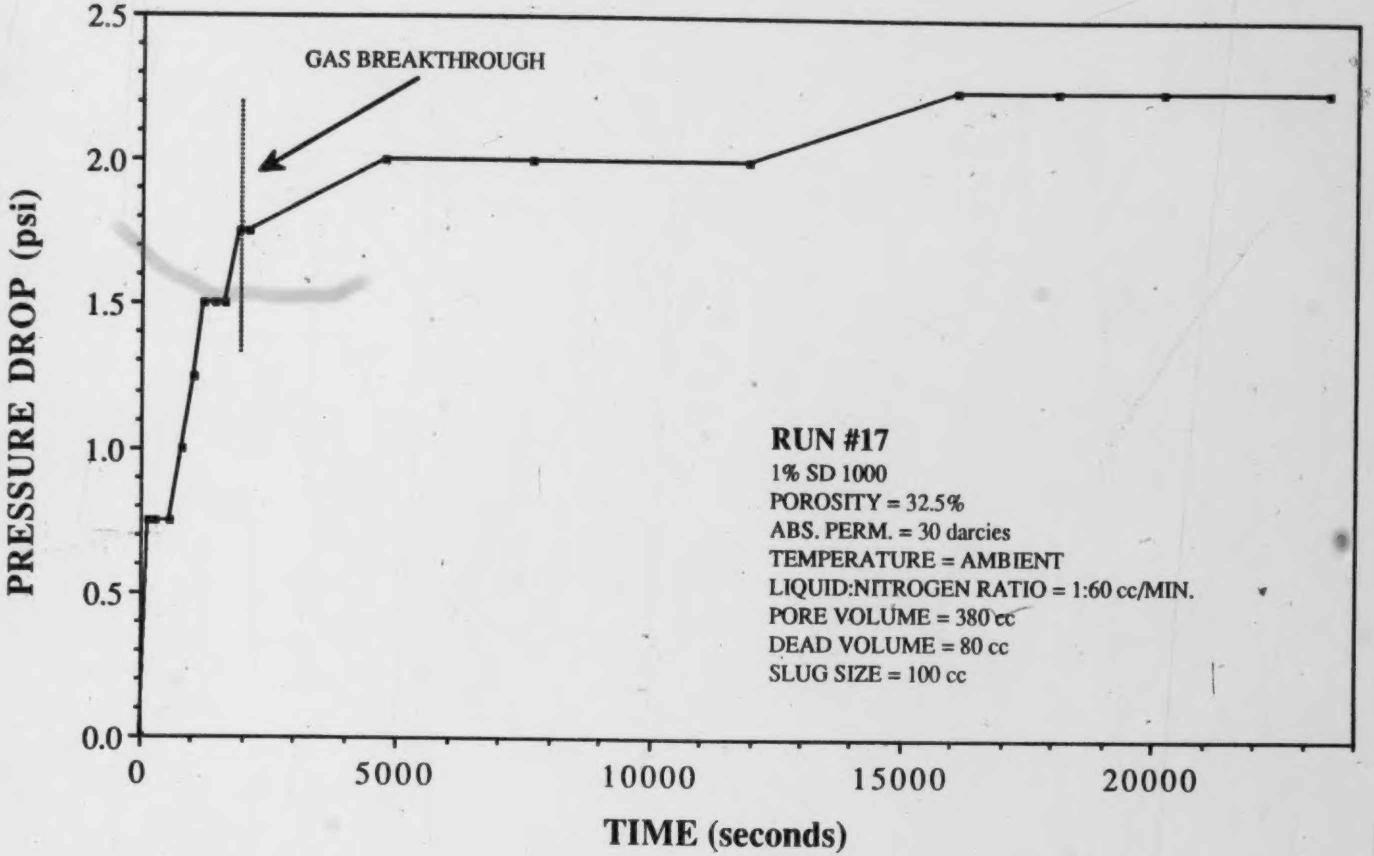

Figure 5.47 Run 17: Pressure Drop Vs. Time, Nitrogen Surfactant Co-injection, 1%SD1000

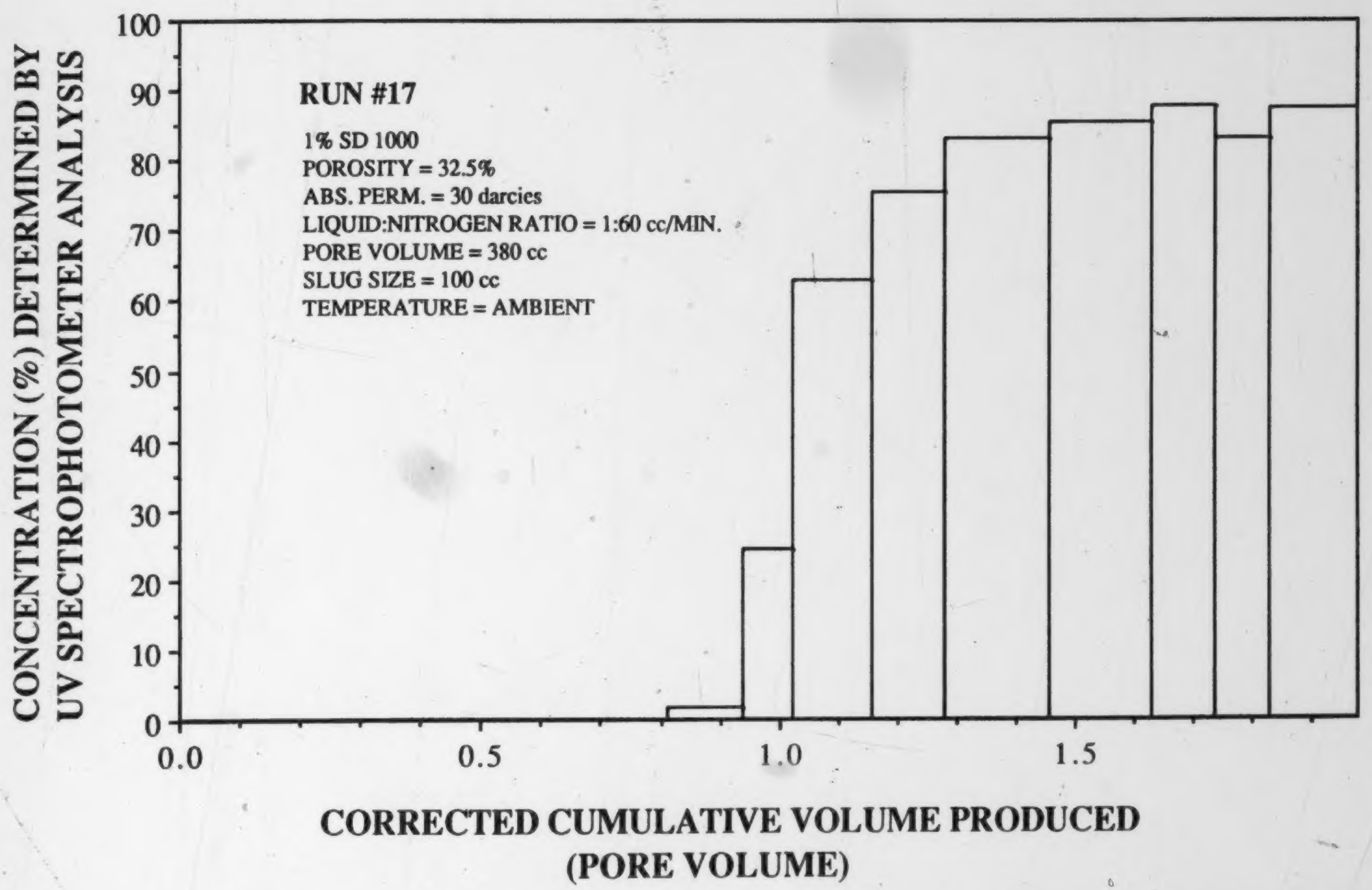

Figure 5.48 Run 17: Concentration Determined by UV Spectrophotometer Analysis Vs. Corrected Cumulative Volume Produced, Nitrogen Surfactant So-injection, 1% SD1000

Experimental Data For Run #6
5% SD 1000 Glass Bead Size #5

Surfactant: SD 1000
Concentration: 5%
Absolute Permeability: 28.7 darcies
Porosity: 33.4%
Back Pressure: 50 psi
Glass Bead Size: #5
Residual Oil Saturation: no
Temperature: Ambient
Gas Breakthrough: 33:00 (min.)
Totalizer Reading @ BT.: 200

Time (s)	Volume (cc)	Cum. Vol. (cc)	Refrac. Index Conc. (%)	Pressure Drop (psi)	Totalizer Reading
165	50	51.0	0	0.25	17
400	47	98.0	0	0.25	40
615	47	145.0	0	0.50	61
840	48	193.0	0	0.50	85
1050	45	238.0	0	0.50	106
1305	57	295.0	0	0.50	132
1530	49	344.0	0	0.50	155
1760.	50	394.0	5	0.50	176
1990	47	441.0	20	0.50	201
3600	28	469.0	50	0.50	362
6600	50	519.0	75	0.50	664
9540	49	568.0	100	0.50	954
12600	51	619.0	100	0.50	1267

Table 5.22 Experimental Data for Run 6: 5% SD1000

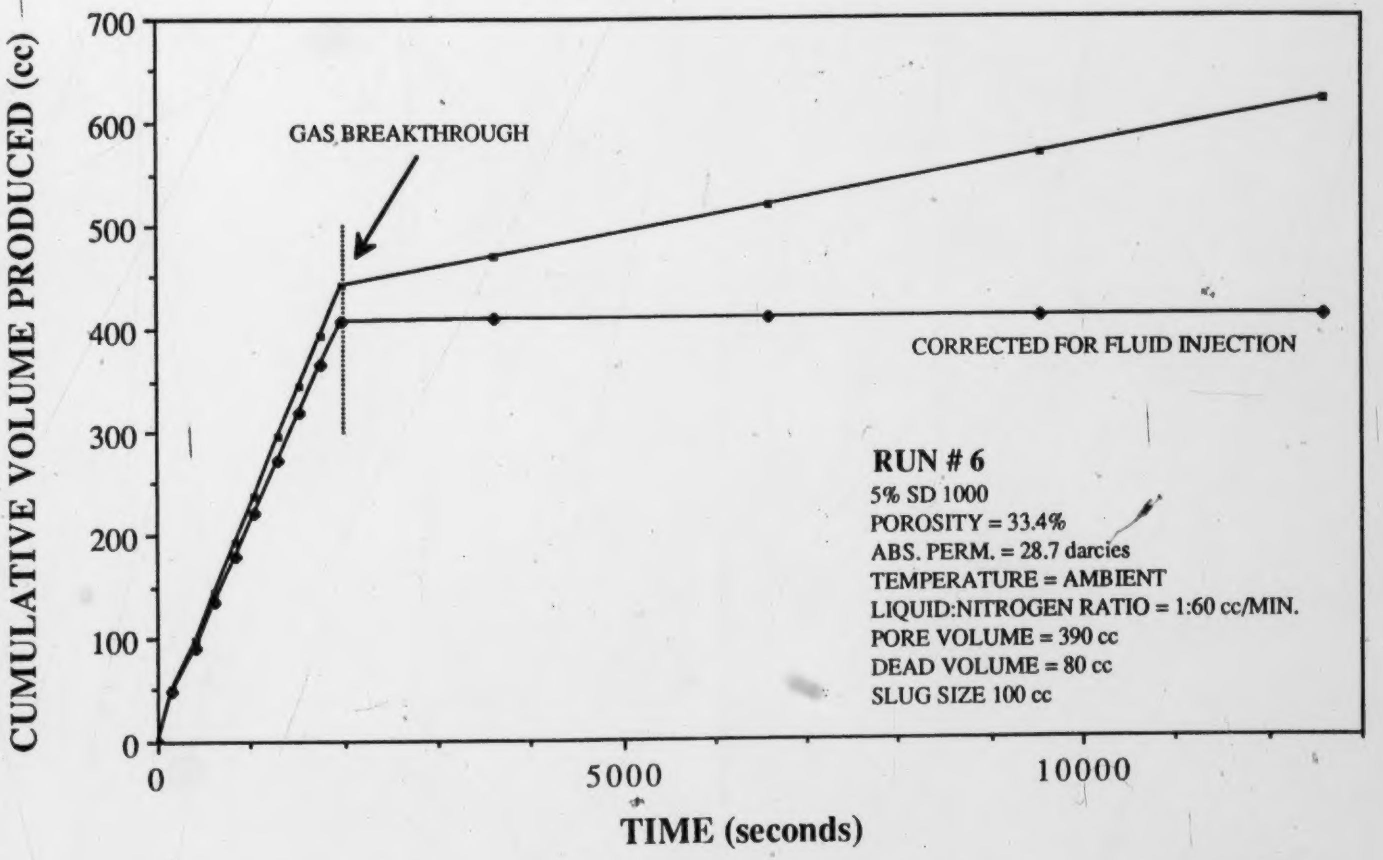

Figure 5.49 Run 6: Cumulative Volume Produced Vs. Time, Nitrogen Surfactant Co-injection, 5% SD1000

The differential pressure across the core, depicted in Figure 5.50, was 0.5 psi. This is significantly lower than that for Run 17 (2.25 psi). The total mobility for this run was 22.5 darcies/cp compared with 4.94 darcies/cp for Run 17. The relative mobility was 0.785 cp^{-1}. The 1 percent SD1000 solution seems to be remarkably better than 5 percent at reducing the gas phase mobility.

The concentration versus corrected volume produced is graphically presented in Figure 5.51. It shows a normal mixing zone in which the concentration was 20 percent at gas breakthrough.

5.3.2.4 Absolute Permeability 0.65 darcies

Consolidated Core

The last run to be examined in this section is Run 14, which was performed using a 1 percent solution of SD1000 in a 0.65 darcy consolidated core. The data for this run is given in Table 5.23.

Gas breakthrough occurred at 22.1 minutes with 238 cc of fluid produced. The corrected cumulative volume, which can be seen in Figure 5.52, was 220 cc. The residual liquid in this core was 71.5 percent.

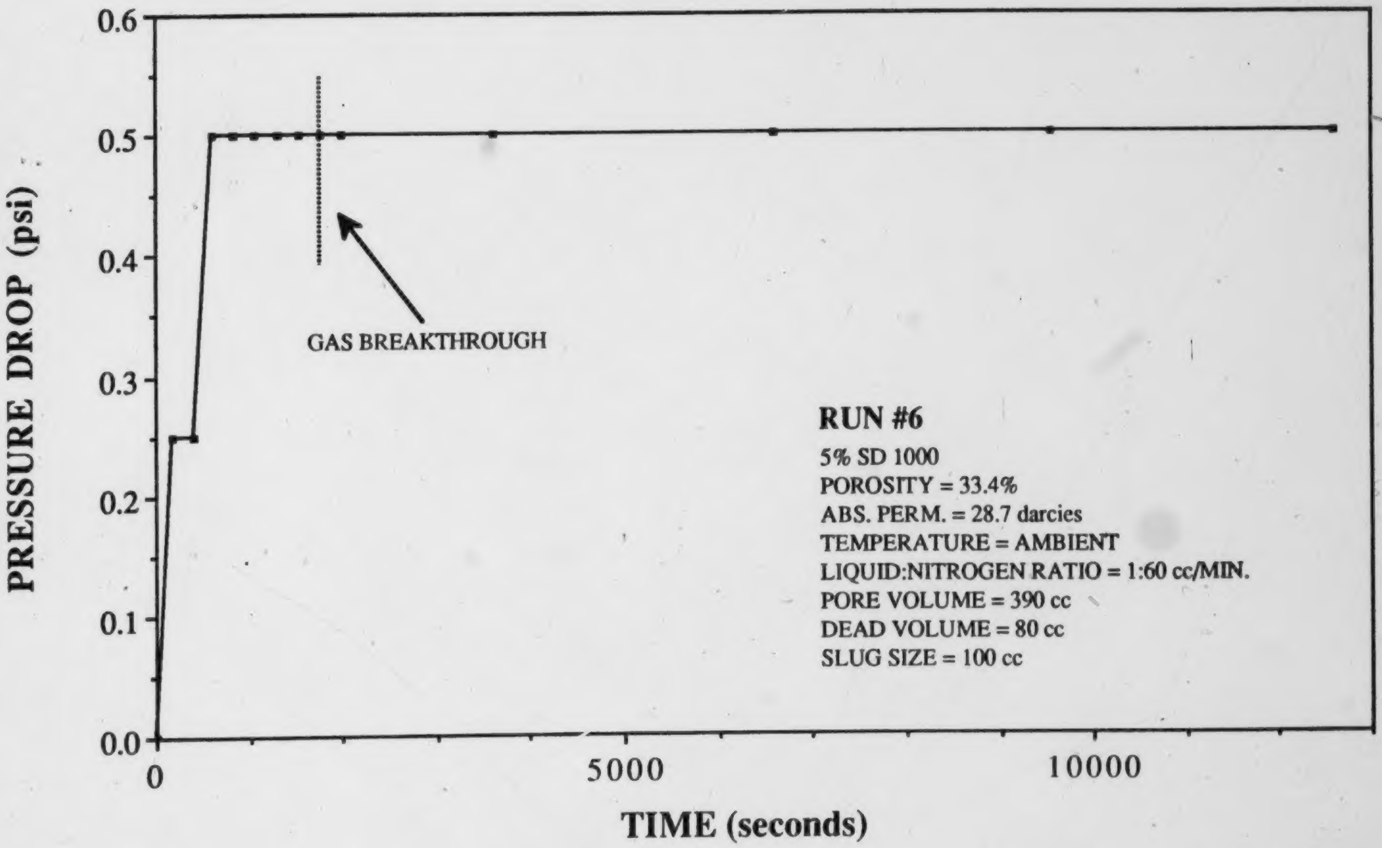

Figure 5.50 Run 6: Pressure Drop Vs. Time, Nitrogen Surfactant Co-injection, 5% SD1000

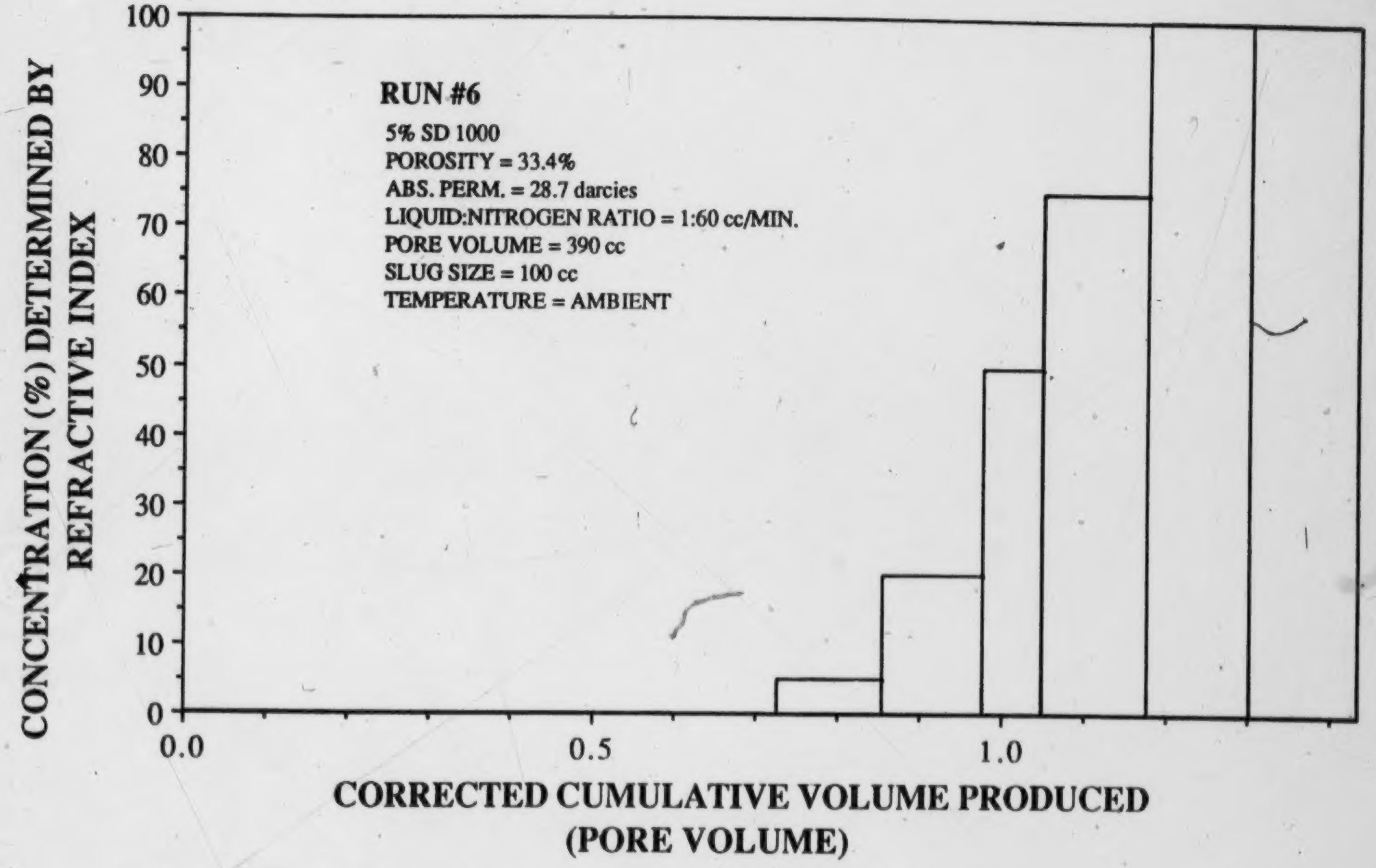

Figure 5.51 Run 6: Concentration Determined by UV Spectrophotometer Analysis Vs. Corrected Cumulative Volume Produced, Nitrogen Surfactant Co-injection, 5% SD1000

Experimental Data For Run #14
1% SD 1000 Consolidated Core

Surfactant: SD 1000
Concentration: 1%
Absolute Permeability: 0.65 darcies
Porosity: 18.0%
Back Pressure: 50 psi

Residual Oil Saturation: no
Temperature: Ambient
Gas Breakthrough: 22:05 (min.)
Totalizer Reading @ BT.: 134

Time (s)	Volume (cc)	Cum. Vol. (cc)	Spectro. Conc. ppm	Pressure Drop (psi)	Simulated Pressure Drop (psi)	Totalizer Reading
30	50	51.0	174	1.00	7.20	3
420	48	99.0	198	13.00	8.30	43
690	48	147.0	120	15.50	9.60	70
975	45	192.0	114	20.75	10.50	99
1230	46	238.0	179	23.50	10.50	125
3180	42	280.0	229	24.50	10.50	322
5820	45	325.0	178	24.50	10.50	589
9045	54	379.0	1201	25.25	10.50	916
12600	53	432.0	8545	26.75	10.50	1277
15600	49	481.0	9953	27.25	10.50	1585
18780	52	533.0	9997	27.50	10.50	1905
21180	40	573.0	9813	27.50	10.50	2153

Table 5.23 Experimental Data for Run 14: 1% SD1000

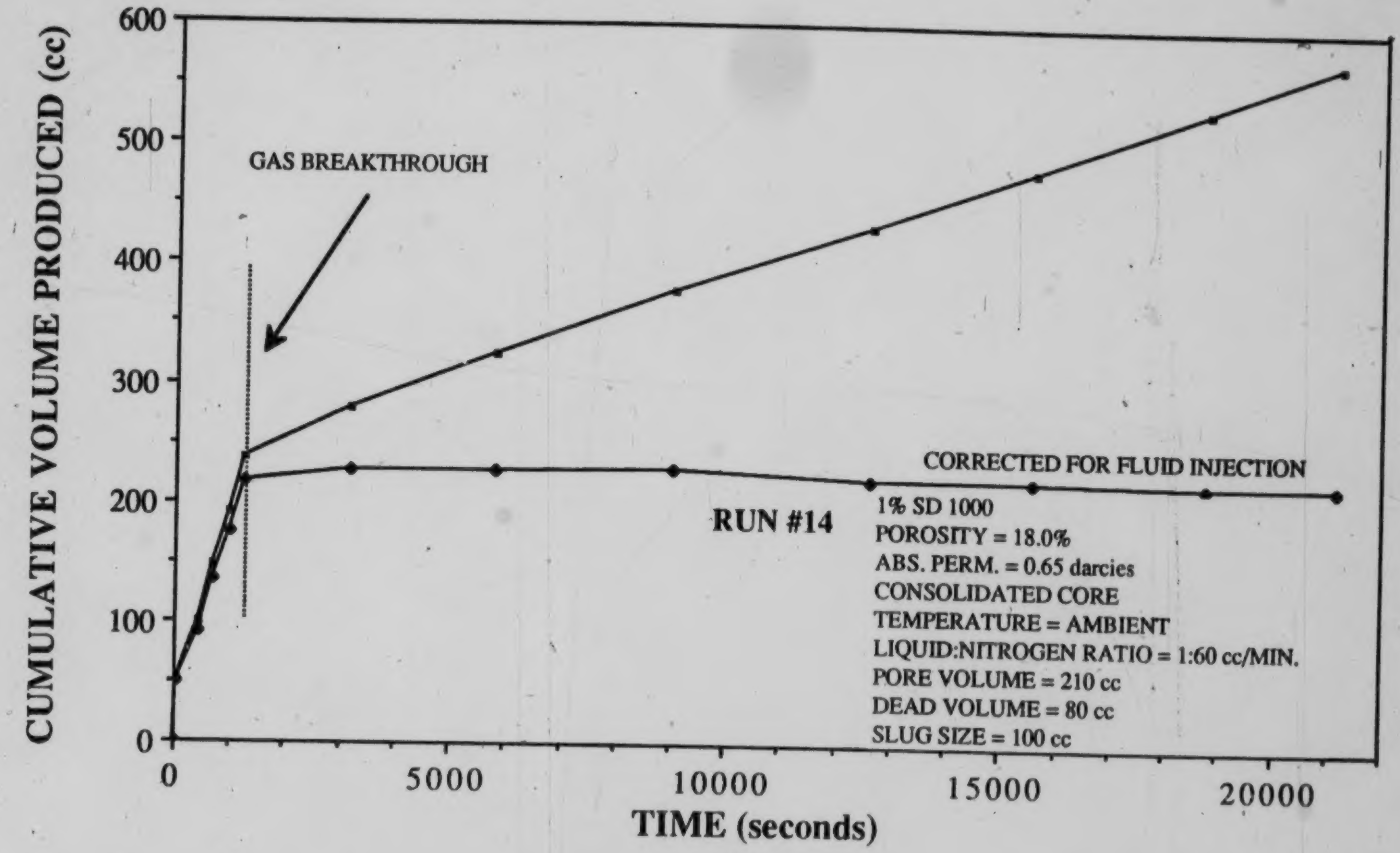

Figure 5.52 Run 14: Cumulative Volume Produced Vs. Time, Nitrogen Surfactant Co-injection, 1% SD1000 Consolidated Core

From Figure 5.53, the concentration versus corrected effluent produced plot, it is observed that the concentration did not increase until 1.25 pore volumes were produced. This may be indicative of high surfactant adsorption in the consolidated core. This was not observed in the unconsolidated packs.

The differential pressure across the core is graphically presented in Figure 5.54. The pressure drop was stabilized at 27.5 psi. The mobility associated with the run was 0.344 darcies/cp. The relative mobility was 0.529 cp^{-1}.

5.3.2.5 Overall Evaluation of the Interrelationship of Surfactant Concentration and Absolute Permeability

From the discussion for the lowest permeability range, (4.7 to 7.1 darcies), it was observed that the 1 percent and 2.5 percent SD1000 solutions, Run 1 and Run 19 respectively, exhibited very similar total and relative mobilities and mobility reduction factors. These concentrations were superior to the water base case Run 12P, and slightly better than the 5 percent surfactant case Run 3, at reducing gas mobility.

From the discussion of the 12.2 to 17.1 darcy permeability range, the 2.5 percent SD1000 solution was determined to reduce total and relative mobility and increase the mobility reduction factor to the greatest extent. For this permeability range the 5 percent

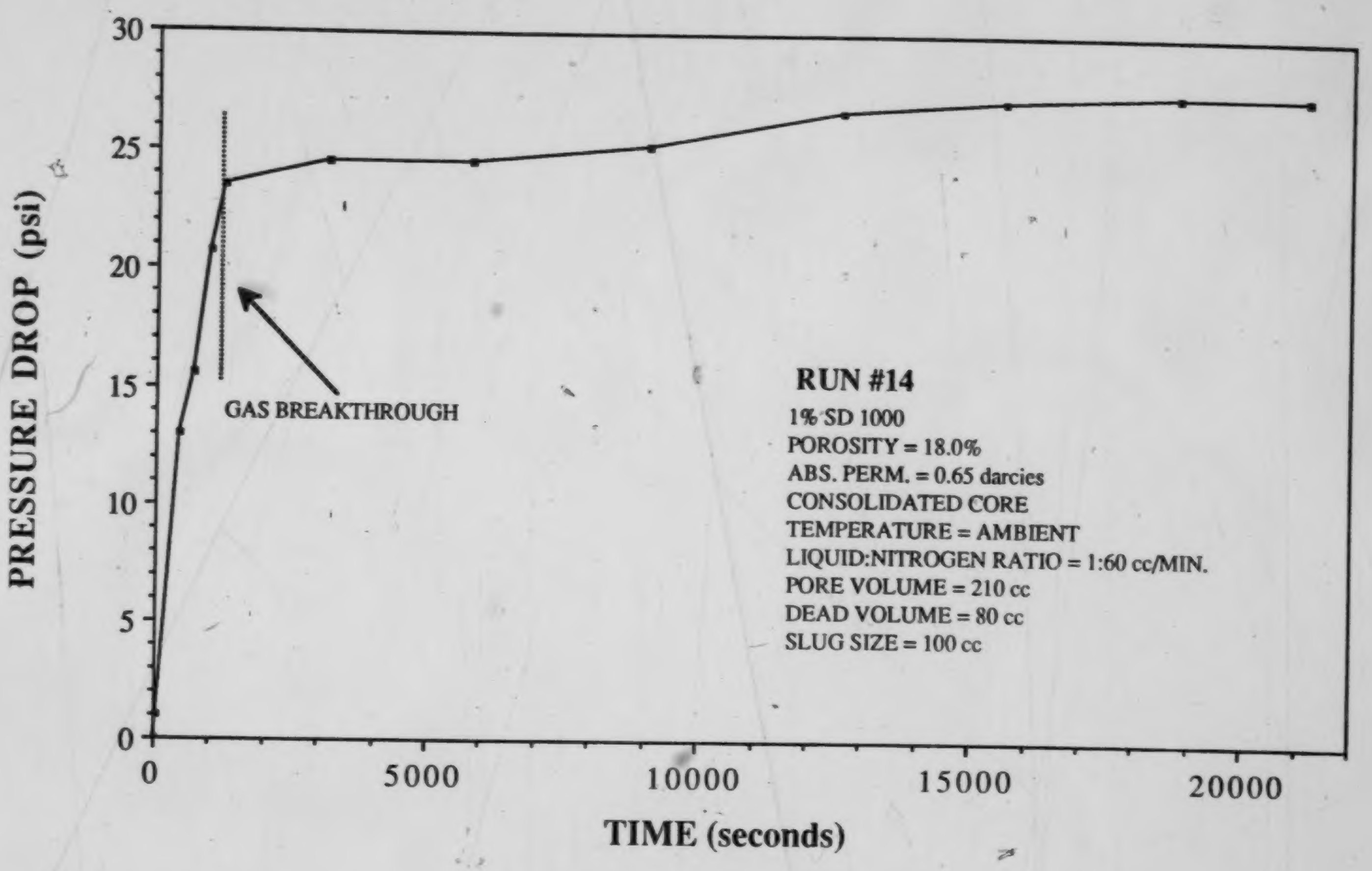

Figure 5.53 Run 14: Pressure Drop Vs. Time, Nitrogen Surfactant Co-injection, 1% SD1000 Consolidated Core

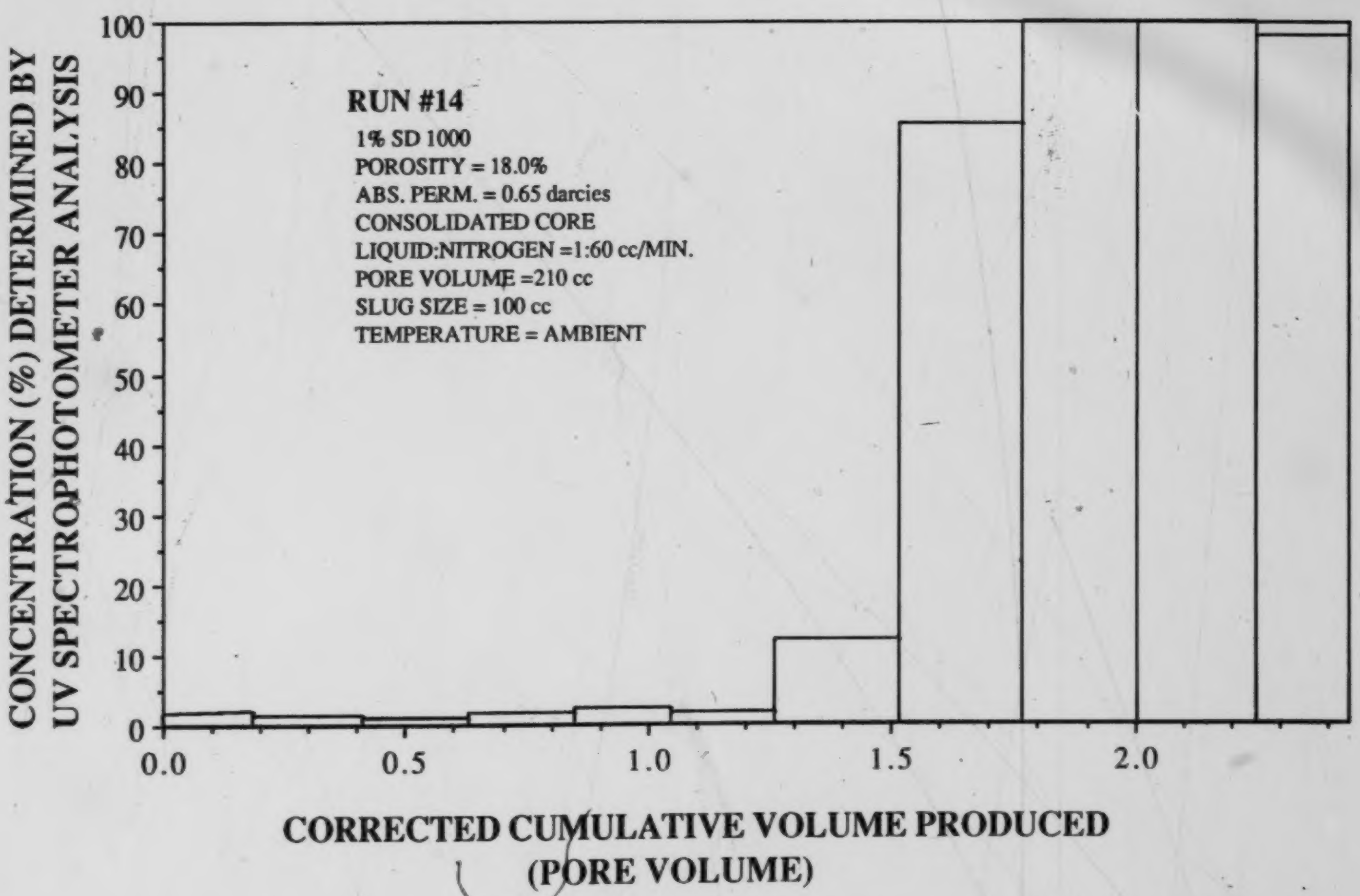

Figure 5.54 Run 14: Concentration Determined by UV Spectrophotometer Analysis Vs. Corrected Cumulative Volume Produced, Nitrogen Surfactant Co-injection, 1% SD1000 Consolidated Core

concentration does not seem to have a detrimental effect on gas mobility. For the highest permeability range (28.7 to 30 darcies) the relative mobility for the 5 percent SD1000 case was 0.785 cp^{-1}; the relative mobility was 0.165 cp^{-1} for the 1 percent case. The higher surfactant concentration proved very detrimental to gas mobility.

Analysis of these permeability ranges suggests that there is an optimum concentration for mobility reduction. This optimum may vary with absolute permeability.

Figure 5.55 shows the relative mobility versus concentration graph. The points associated with 1 and 2.5 percent SD1000 are very similar to one another for the unconsolidated packs. This suggests that the foam was equally effective at reducing gas mobility in these cores. The relative mobility for Run 17, the 30 darcy, 1 percent SD1000 run, is very similar to the relative mobilities found for the less permeable cores. This suggests that the foam flow mechanism was the same as it was for the less permeable cores.

Recall that Dietz et al.[15] calculated that an 18 darcy core was required to host bubbles for a 95 quality foam. The foam quality was 93 percent for Run 17 (permeability 30 darcies). Therefore even when the pore spaces are large enough to host a foam, it does not flow as a homogeneous body. Although relative mobility gives an indication of how the foam was affecting flow, total mobility reflects the actual flow capacity. Figure 5.56 presents the total mobility for the runs discussed.

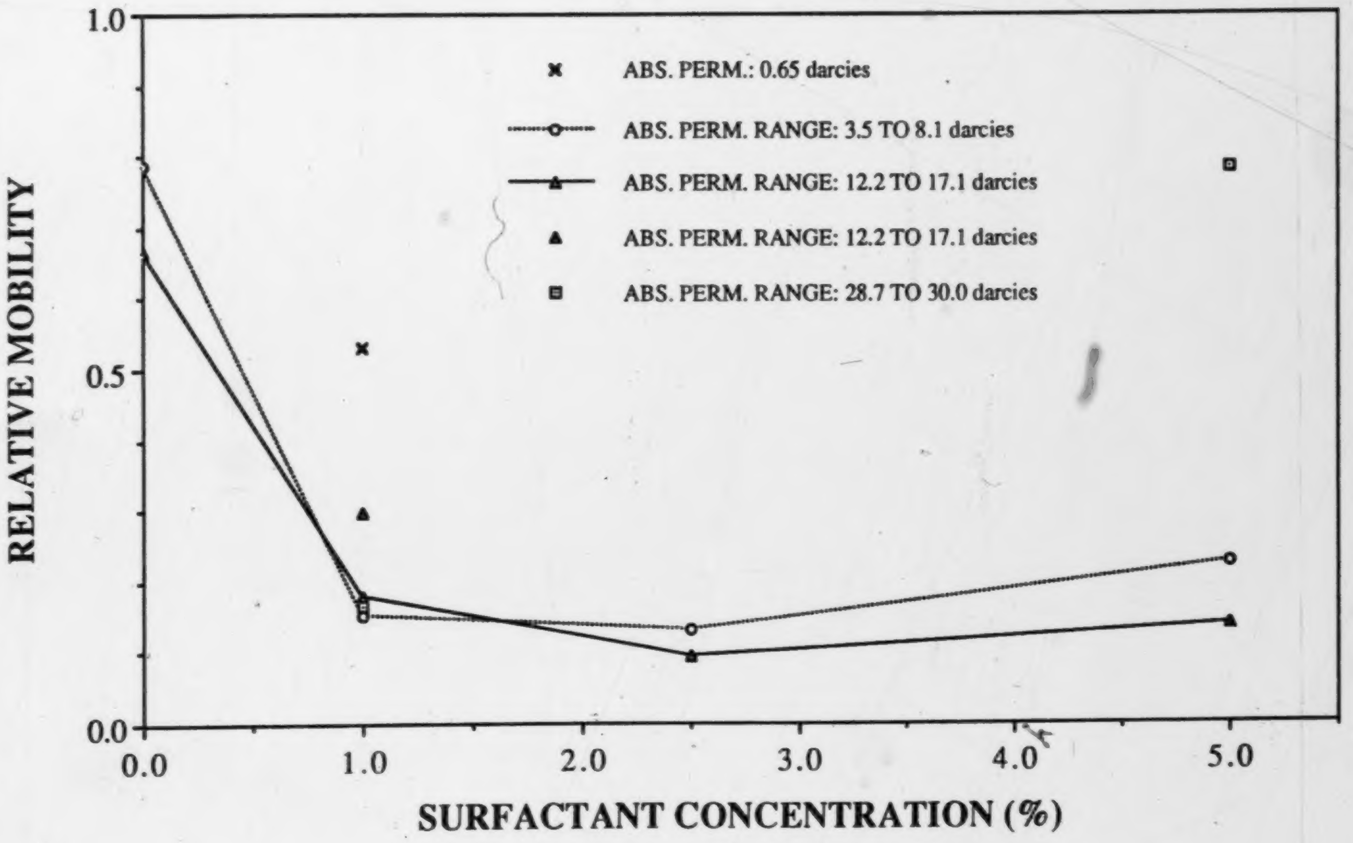

Figure 5.55 Comparison of Runs: Crossplot of Relative Mobility Vs. Concentration of SD1000 for runs in which Abs. Perm. and Surfactant Conc. changed only

The total mobility is higher for the more permeable runs. For Run 6 (the 5 percent, 28.6 darcy case), the total mobility was 22.5 darcies/cp and was not plotted on Figure 5.56. This indicates that foam would not cause selective blocking in the more permeable channels. This finding is contradictory to the findings of Bernard and Holm[25]. This result will be further analyzed in the analysis of dual core runs.

5.3.3 Effect of Temperature

Runs 13, 9, 16 and 15 were performed at elevated temperatures with 1 percent SD1000. These runs will be examined in this section along with Run 23 and Run 27 which were performed with Dow surfactant.

5.3.3.1 Surfactant SD1000

Run 13 was performed at 54° C on a 12.1 darcy glass bead pack. The data for Run 13 is given in Table 5.23. The time until gas breakthrough was 33.75 minutes and the volume produced at gas breakthrough was 447 cc. From Figure 5.57, the stabilized corrected volume produced was 420 cc. The residual liquid saturation was 30.9 percent.

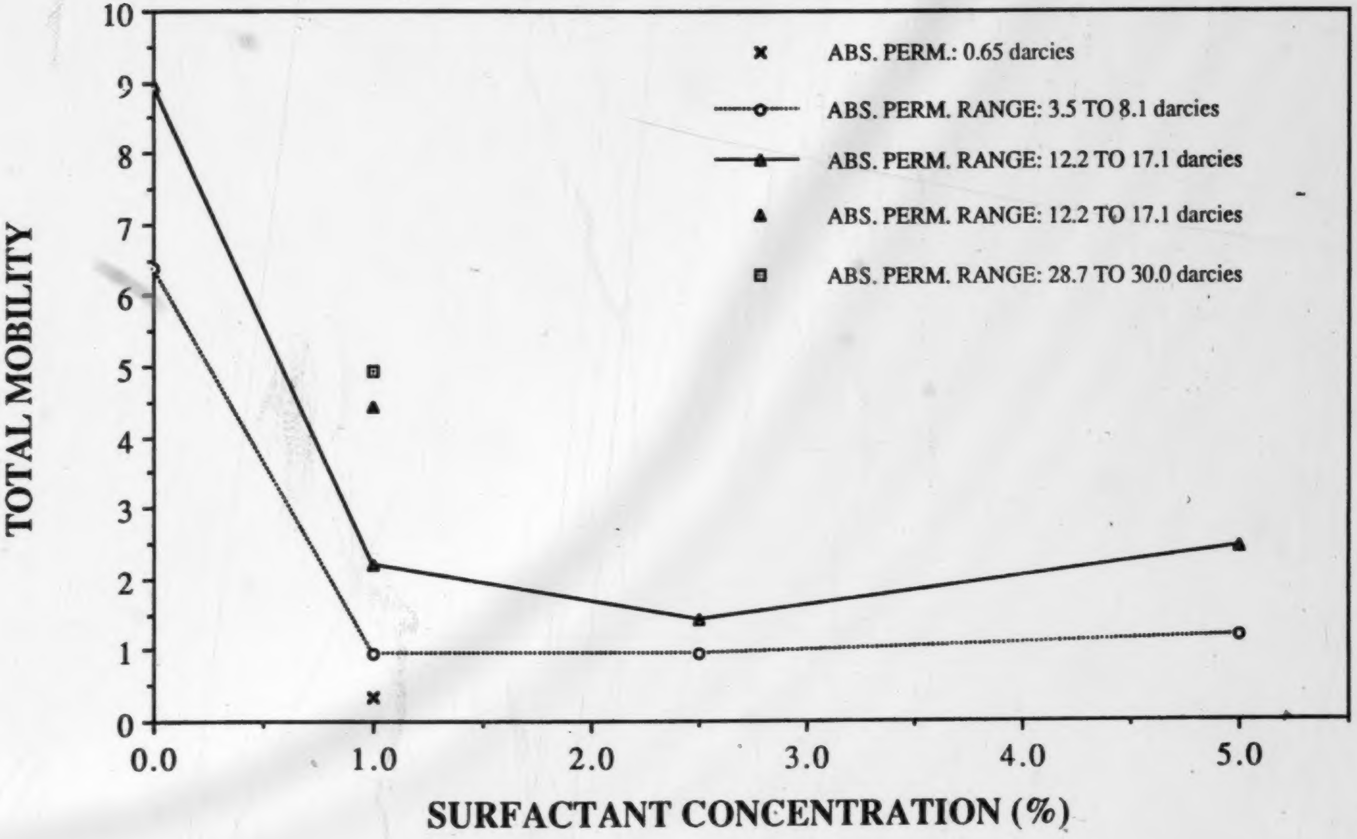

Figure 5.56 Comparison of Runs: Crossplot of Total Mobility Vs. Concentration of SD1000 for runs in which Abs. Perm. and Surfactant Conc. changed only

Experimental Data For Run #13
1% SD 1000 Glass Bead Size #9

Surfactant:	SD 1000	**Glass Bead Size:**	#9 * New Supplier
Concentration:	1%	**Residual Oil Saturation:**	no
Absolute Permeability:	12.1 darcies	**Temperature:**	54° C
Porosity:	32.2%	**Gas Breakthrough:**	33:45 (min.)
Back Pressure:	50 psi	**Totalizer Reading @ BT.:**	206

Time (s)	Volume (cc)	Cum. Vol. (cc)	Spectro. Conc. ppm	Pressure Drop (psi)	Simulated Pressure Drop (psi)	Totalizer Reading
150	48	51.0	62.6	1.00	2.4	15
345	42	93.0	80.4	1.00	3.4	36
540	44	137.0	6.6	2.00	5.4	55
750	44	181.0	2.8	3.00	6.4	76
960	49	230.0	55.8	3.75	6.4	98
1170	46	276.0	75	4.25	6.4	118
1350	40	316.0	71.5	5.25	6.4	137
1590	49	365.0	126.3	6.00	6.4	160
1770	41	406.0	2233	6.50	6.4	180
2055	41	447.0	5862	7.75	6.4	209
4230	46	493.0	7369	9.75	6.4	431
7500	55	548.0	8403	11.25	6.4	764
10410	46	594.0	8501	12.50	6.4	1053
12660	39	633.0	8993	12.75	6.4	1281
15720	49	682.0	9126	12.75	6.4	1588
18720	50	732.0	9075	12.75	6.4	1894
21780	48	780	8942	12.75	6.4	2203

Table 5.24 Experimental Data for Run 13: 1% SD1000 54°C

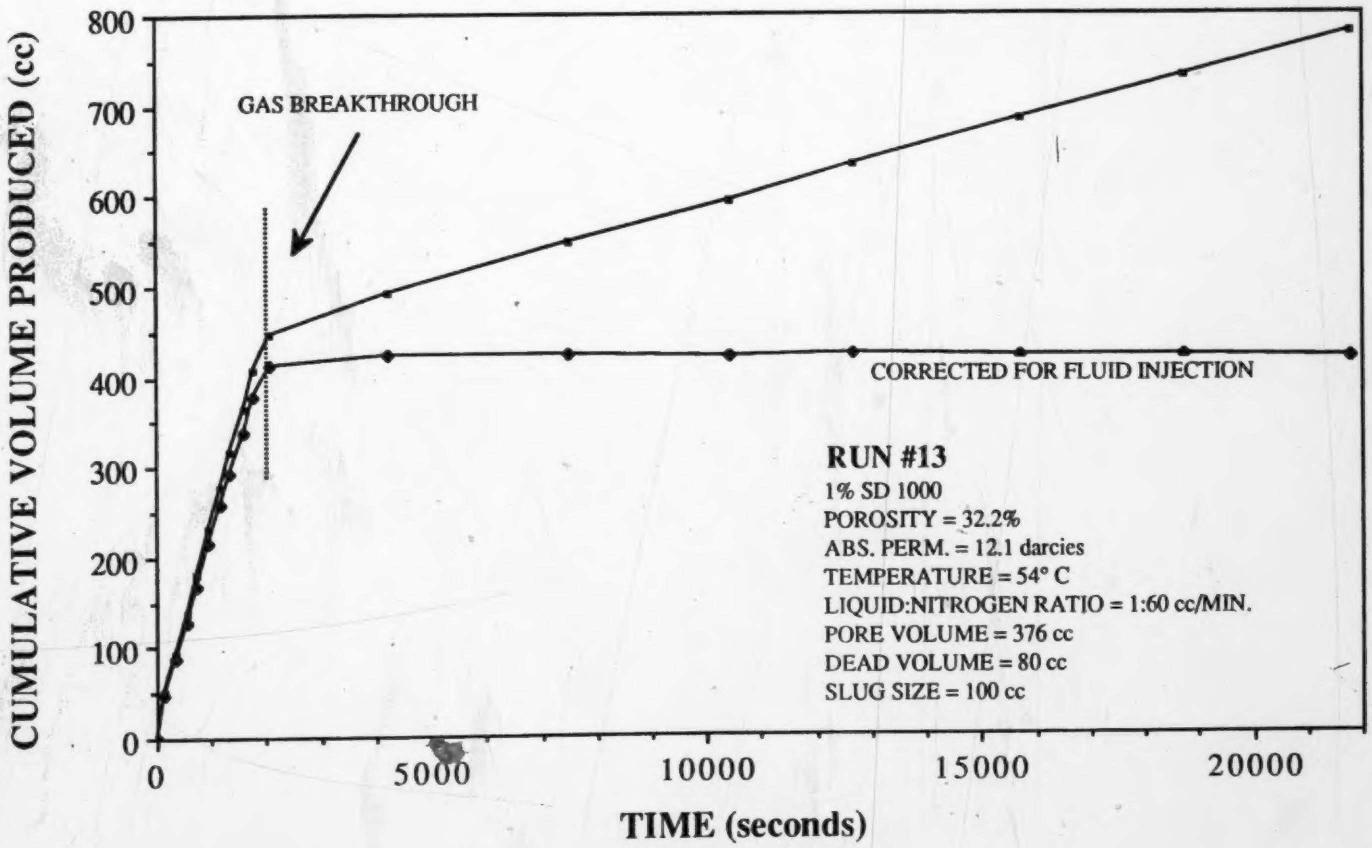

Figure 5.57 Run 13: Cumulative Volume Produced Vs. Time, Nitrogen Surfactant Co-injection, 1% SD1000 54°C

The differential pressure profile is presented in Figure 5.58. The pressure drop across the core continued to rise following gas breakthrough, until it reached 12.75 psi. Run 11, was a 1 percent run in the same permeability range. The steady state pressure drop for this run was 5.0 psi. The total mobility for Run 13 was 0.900 darcies/cp; the relative mobility was 0.0744 cp^{-1}. The mobility was 2.18darcies/cp for Run 11, and the relative mobility was 0.179 cp^{-1}.

The concentration graph is presented in Figure 5.59. The sample taken at gas breakthrough had a concentration of 58.6 percent, which suggests a very efficient displacement.

Run 16 was performed at 90° C on a 11.5 darcy core. The data for this run is given in Table 5.25. The gas breakthrough time was 33.5 minutes; this is very similar to the 54° C case, Run 13, (33.7 minutes). The volume produced at gas breakthrough was 478 cc. From Figure 5.60, the stabilized corrected volume produced was 470 cc. The residual liquid saturation was 20.1 percent.

The differential pressure profile is presented in Figure 5.61. The pressure drop continued to increase following gas breakthrough, as it did in Run 13. The pressure levelled off at 19.0 psi. The mobility for this run was 0.649 darcies/cp; the relative mobility was 0.0556 cp^{-1}.

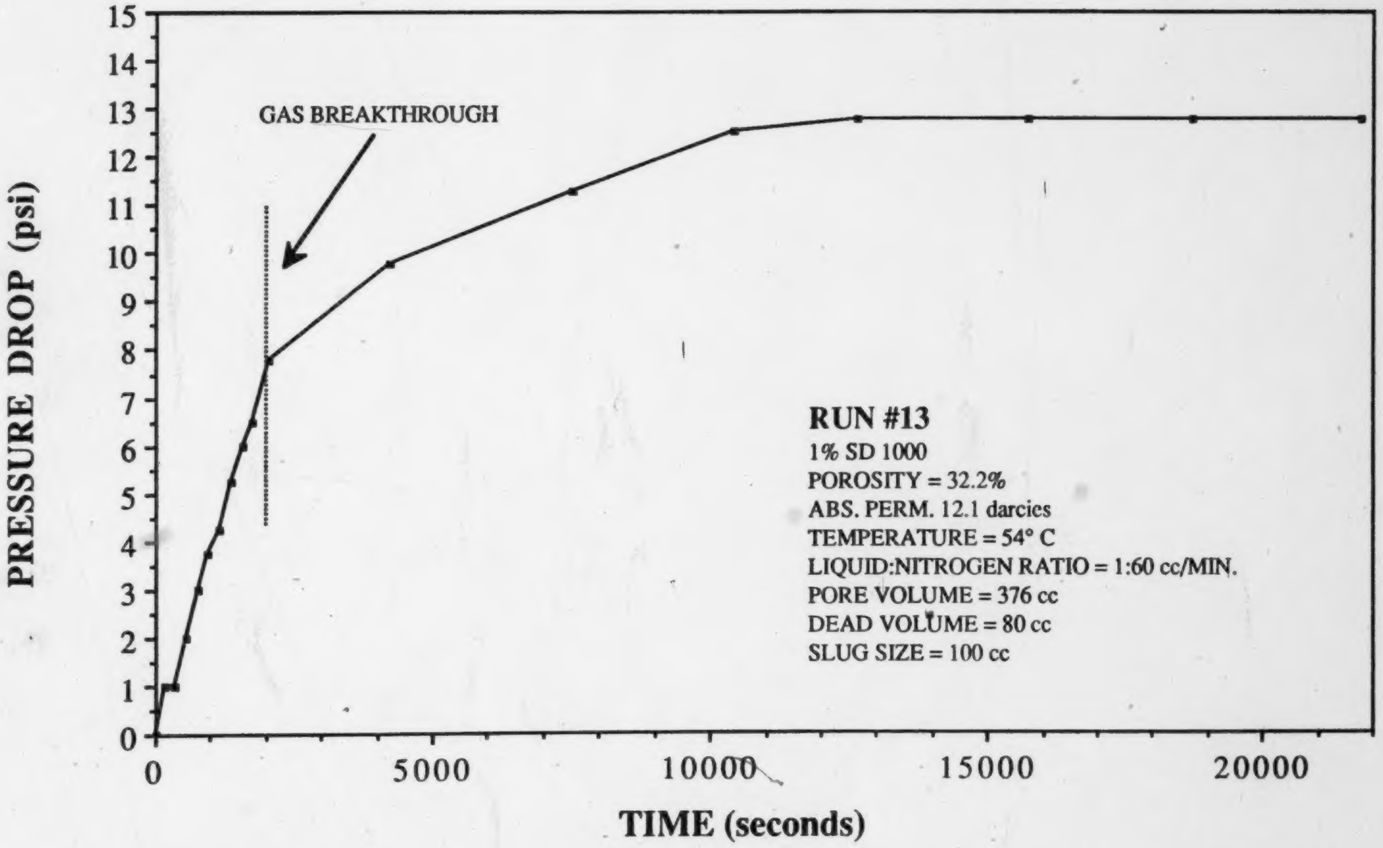

Figure 5.58 Run 13: Pressure Drop Vs. Time, Nitrogen Surfactant Co-injection, 1% SD1000 54°C

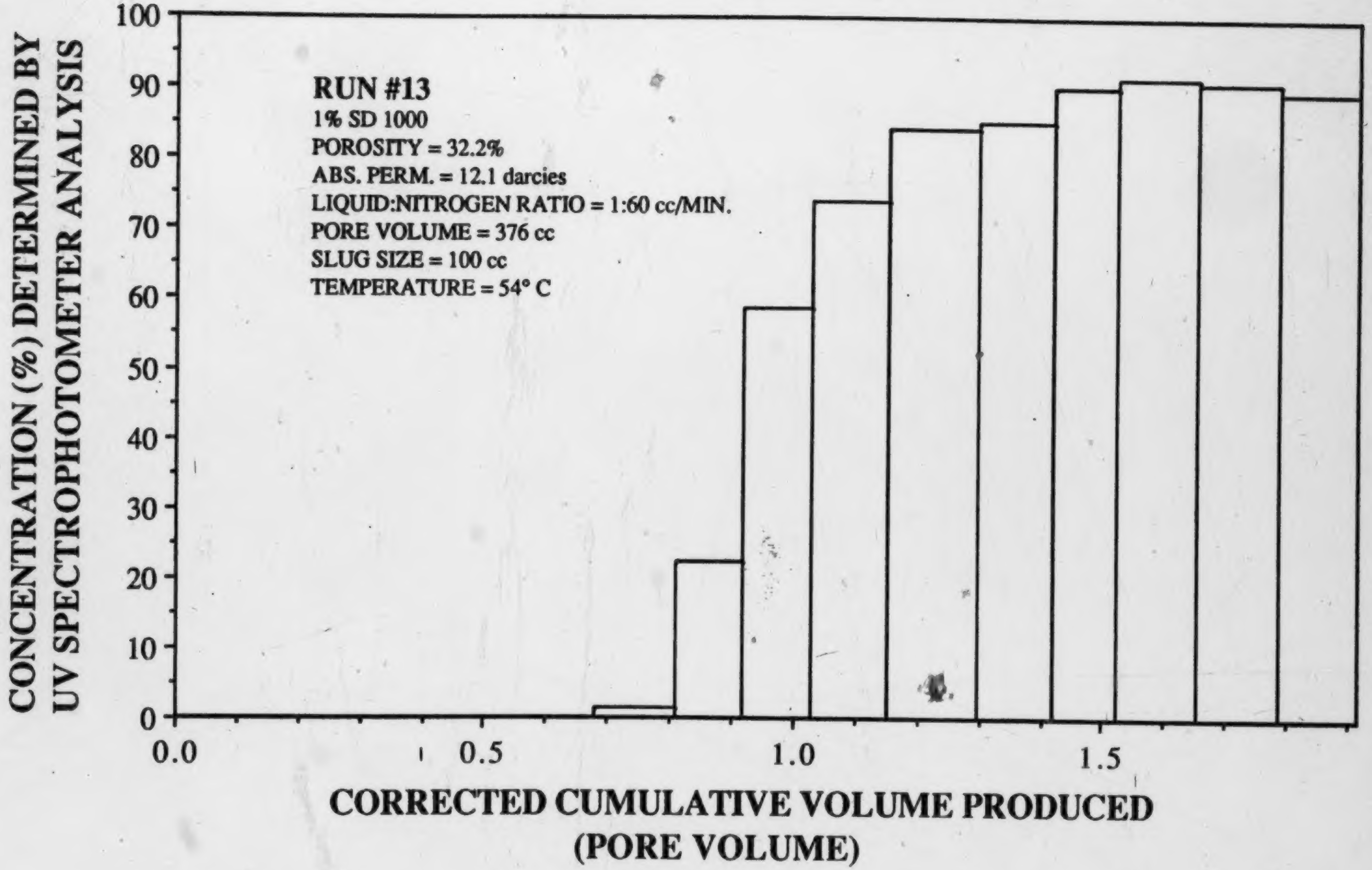

Figure 5.59 Run 13: Concentration Determined by UV Spectrophotometer Analysis Vs. Corrected Cumulative Volume Produced, Nitrogen Surfactant Co-injection, 1% SD1000 54°C

Experimental Data For Run #16
1% SD 1000 Glass Bead Size #9

Surfactant:	SD 1000	**Glass Bead Size:**	#9 * New Supplier
Concentration:	1%	**Residual Oil Saturation:**	no
Absolute Permeability:	11.5 darcies	**Temperature:**	90° C
Porosity:	33.2%	**Gas Breakthrough:**	33:30 (min.)
Back Pressure:	50 psi	**Totalizer Reading @ BT.:**	204.0

Time (s)	Volume (cc)	Cum. Vol. (cc)	Spectro. Conc. ppm	Pressure Drop (psi)	Simulated Pressure Drop (psi)	Totalizer Reading
195	49	51.0	222	1.25	2.5	20
315	44	95.0	28	1.25	3.5	38
570	48	143.0	65	2.25	6.0	58
780	48	191.0	86	3.00	6.6	78
1005	52	243.0	6	4.00	6.6	101
1170	51	294.0	8	5.00	6.6	124
1440	52	346.0	60	7.50	6.6	145
1680	53	399.0	478	9.25	6.6	171
1890	48	447.0	3982	11.00	6.6	192
2040	31	478.0	6057	12.25	6.6	206
3900	50	528.0	10076	17.25	6.6	394
6600	50	578.0	9640	19.50	6.6	664
9480	50	628.0	9632	20.25	6.6	954
12180	45	673.0	9950	20.50	6.6	1229
15360	53	726.0	9873	19.75	6.6	1548
19620	71	797.0	9627	18.75	6.6	1974
23460	61	858.0	9669	18.75	6.6	2367

Table 5.25 Experimental Data for Run 16: 1% SD1000 90°C

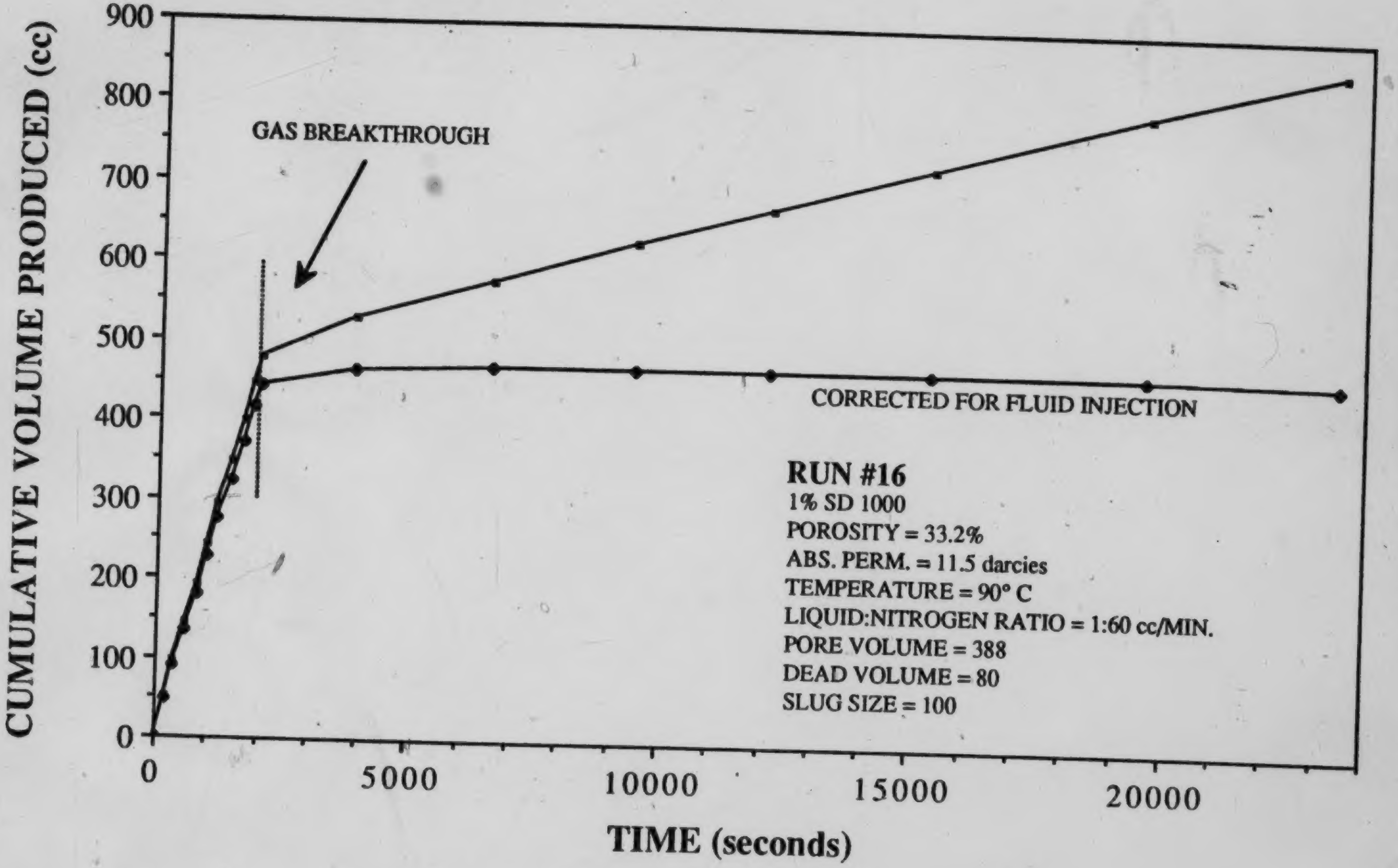

Figure 5.60 Run 16: Cumulative Volume Produced Vs. Time, Nitrogen Surfactant Co-injection, 1% SD1000 90°C

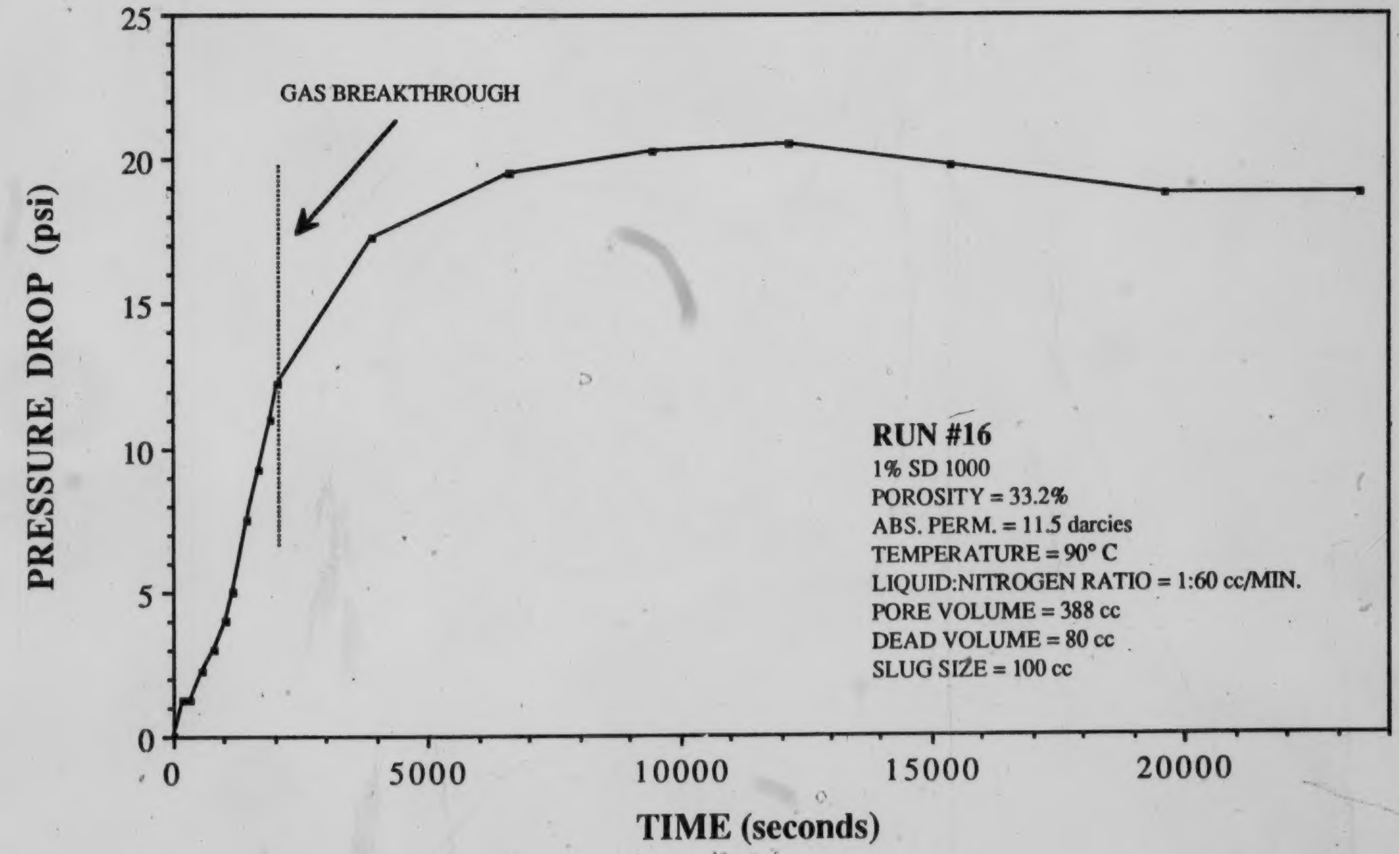

Figure 5.61 Run 16: Pressure Drop Vs. Time, Nitrogen Surfactant Co-injection, 1% SD1000 90°C

The concentration graph presented in Figure 5.62 shows a small mixing zone. The concentration of the sample collected at gas breakthrough was 60.6 percent.

Run 9 was also performed at 90°C, but with a 7.8 darcy glass bead pack. The data for this run is given in Table 5.26. The gas breakthrough time was 28.9 minutes. The volume produced was 436 cc. From Figure 5.63, the cumulative volume produced versus time, the curves exhibit the normal surfactant run trend. The stabilized corrected volume produced was 321 cc. The residual liquid saturation was 31.6 percent. The residual liquid saturation for Run 16 was 20.1 percent

From Figure 5.64, it was observed that the differential pressure profile stabilizes just prior to gas breakthrough. This is not the same trend that was observed for the other elevated temperature runs. The pressure drop was 13.5 psi for this run. The total mobility was calculated to be 0.932 darcies/cp; the relative mobility was 0.120 cp^{-1}

The concentration graph is presented in Figure 5.65. The concentration of the sample collected at gas breakthrough was 34.0 percent. Two methods of calculating concentration were utilized for this run. Table 5.26 shows that the two methods provide similar results.

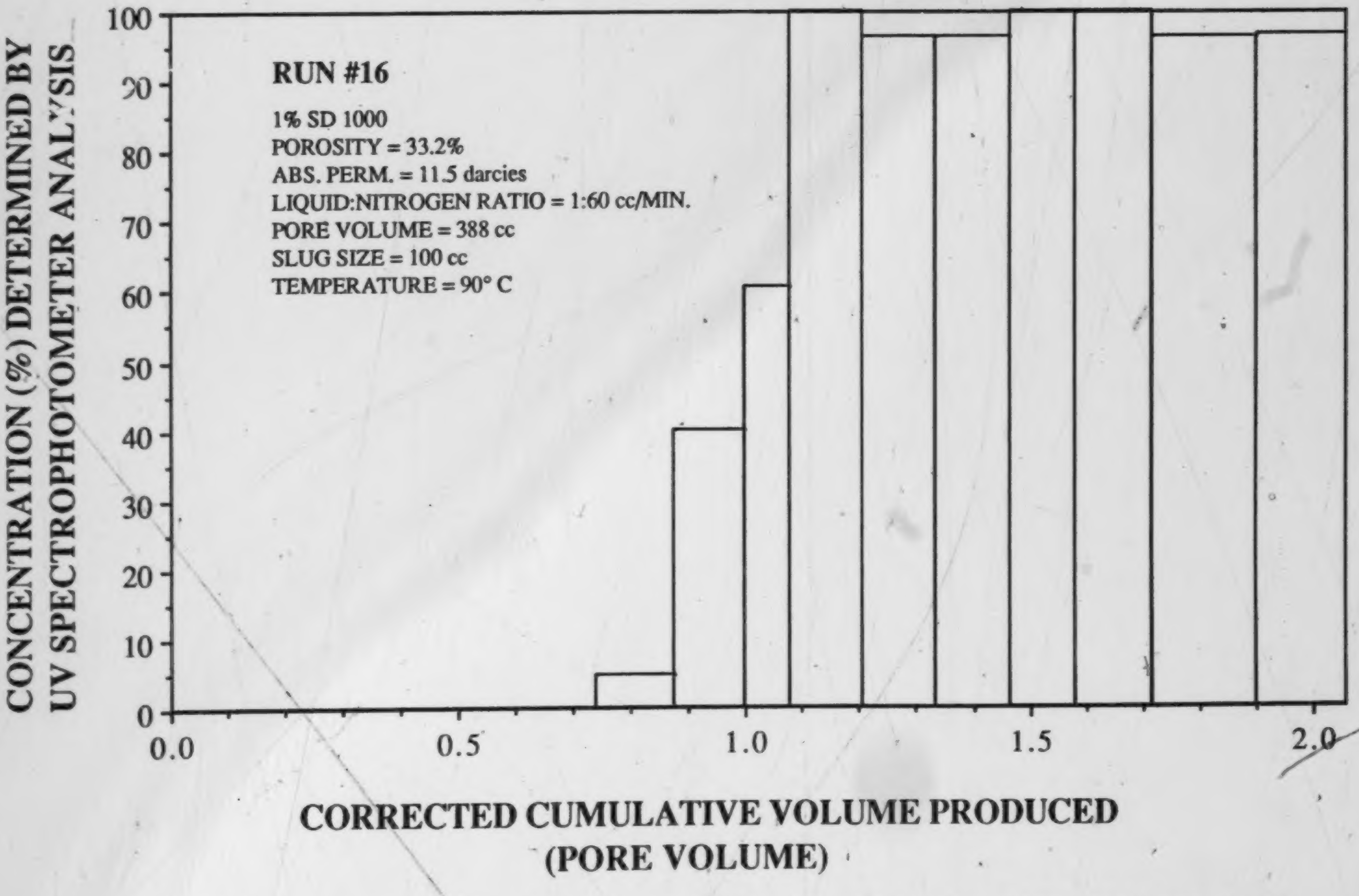

Figure 5.62 Run 16: Concentration Determined by UV Spectrophotometer Analysis Vs. Corrected Cumulative Volume Produced, Nitrogen Surfactant Co-injection, 1% SD1000 90°C

Experimental Data For Run #9
1% SD 1000 Glass Bead Size #9

Surfactant: SD 1000
Concentration: 1%
Absolute Permeability: 7.8 darcies
Porosity: 32.7%
Back Pressure: 50 psi

Glass Bead Size: #9
Residual Oil Saturation: no
Temperature: 90° C
Gas Breakthrough: 28:50 (min.)
Totalizer Reading @ BT.: 175

Time (s)	Volume (cc)	Cum. Vol. (cc)	Refractive Index Conc. (%)	Spectro. Conc. ppm	Pressure Drop (psi)	Totalizer Reading
15	55	55.0	0	468	0.25	2
300	43	98.0	0	454	1.75	31
465	44	142.0	0	226	3.75	47
645	41	183.0	0	185.3	5.25	65
795	40	223.0	0	246.2	7.00	80
960	43	266.0	0	200.6	8.50	91
1155	38	304.0	0	160.2	10.50	116
1320	43	347.0	0	166.7	12.50	134
1500	48	395.0	0	238.4	13.75	153
1665	41	436.0	35	3404	13.75	169
3200	37	473.0	70	8510	13.50	324
5610	41	514.0	100	8670	13.50	566
7775	37	551.0	100	9660	13.50	787
10320	42	593.0	100	9920	13.50	1042

Table 5.26 Experimental Data for Run 9: 1% SD1000 90°C

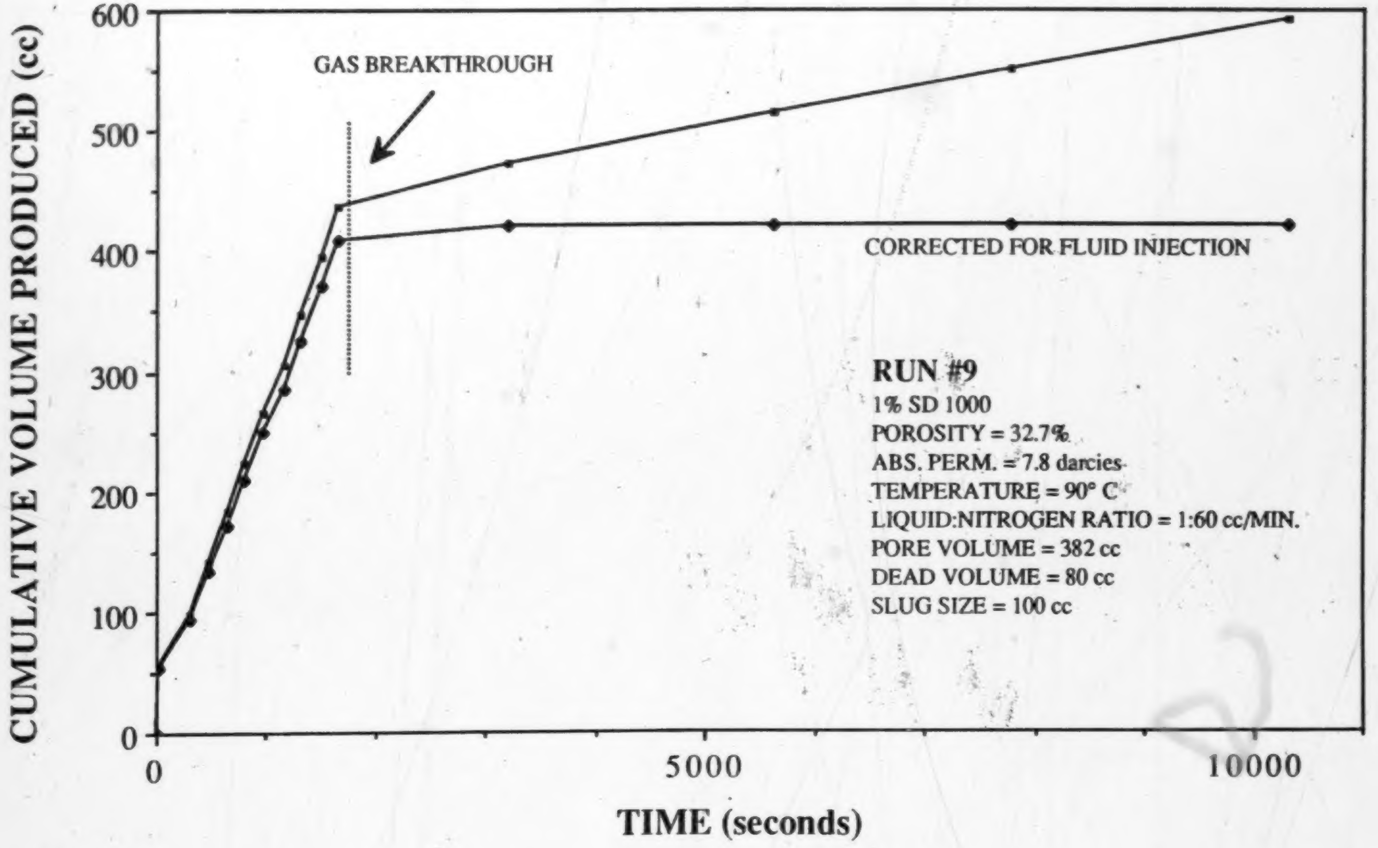

Figure 5.63 Run 9: Cumulative Volume Produced Vs. Time, Nitrogen Surfactant Co-injection, 1% SD1000 90°C

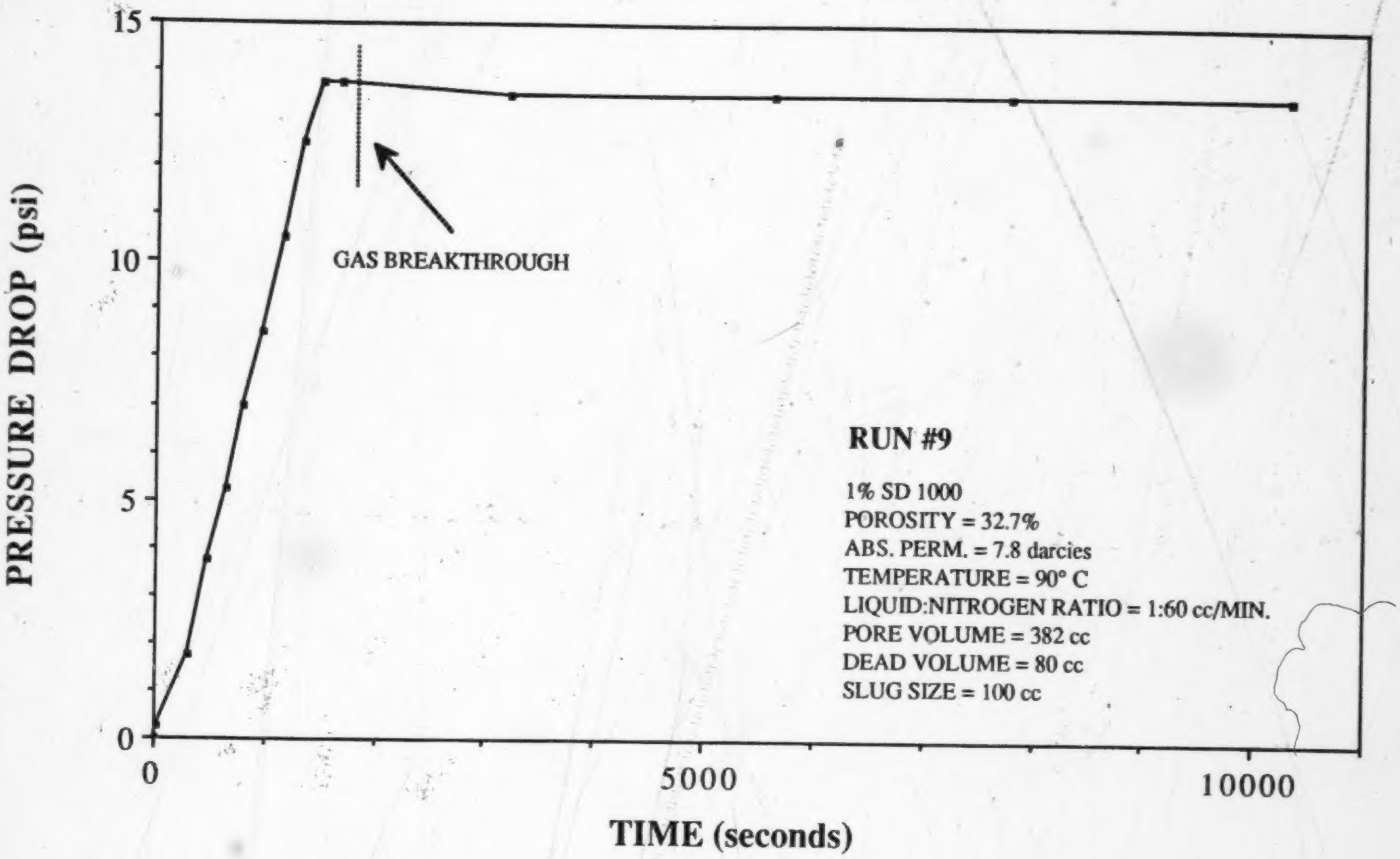

Figure 5.64 Run 9: Pressure Drop Vs. Time, Nitrogen Surfactant Co-injection, 1% SD1000 90°C

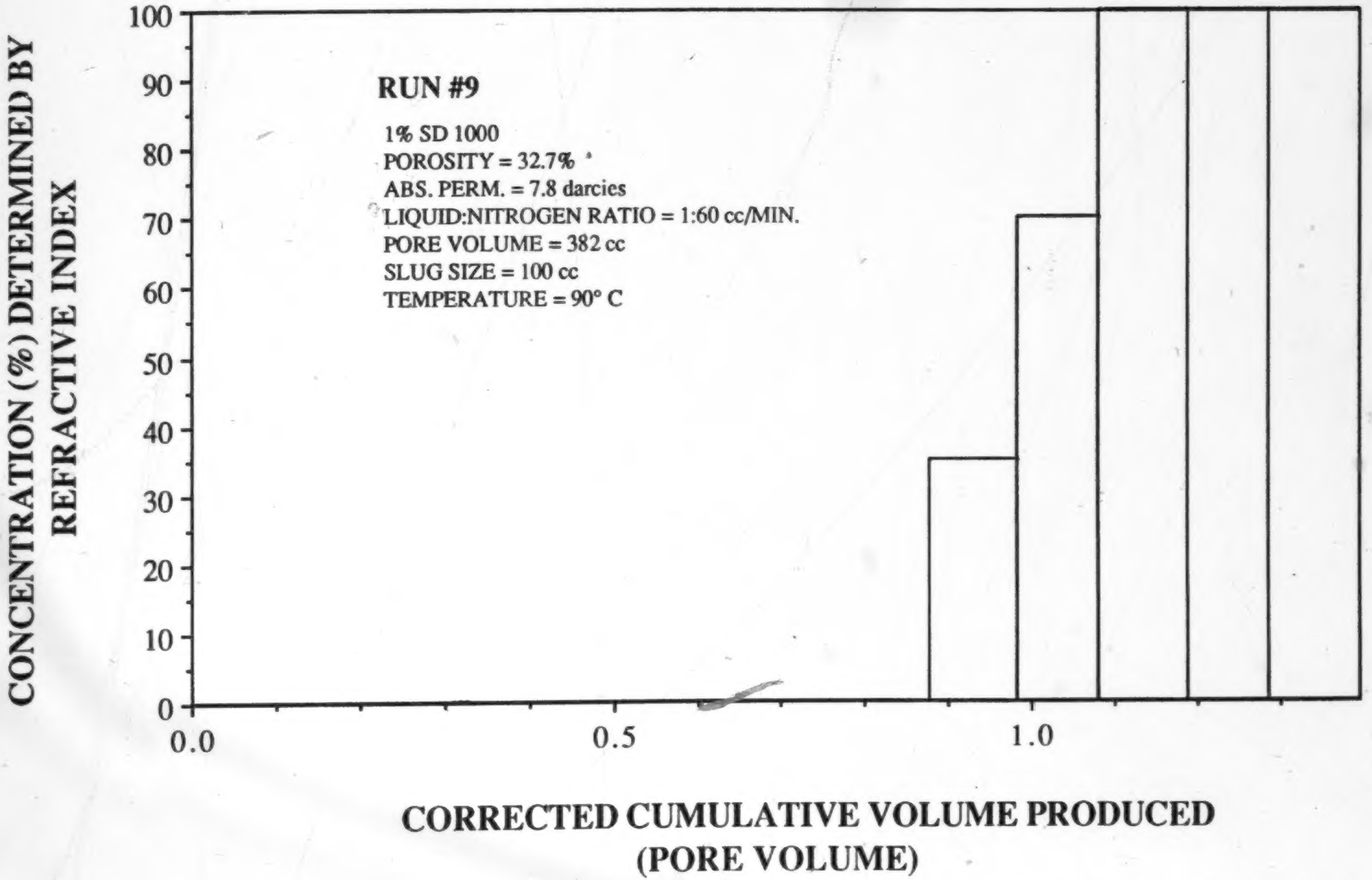

Figure 5.65 Run 9: Concentration Determined by UV Spectrophotometer Analysis Vs. Corrected Cumulative Volume Produced, Nitrogen Surfactant Co-injection, 1% SD1000 90°C

The last 1 percent SD1000, elevated temperature run examined was Run 15. This run was performed at 125° C, on a 13 darcy glass bead pack. The data for this run is given in Table 5.27. The time until gas breakthrough was 28.5 minutes. The gas breakthrough times became shorter as the temperature increased. This is due to the expansion of nitrogen at elevated temperatures. The volume of liquid produced at gas breakthrough was 482 cc. This volume increased with increasing temperature, with the exception of Run 9.

The cumulative volume produced versus time, for Run 15, is presented as Figure 5.66. The residual liquid saturation is 26.3 percent. The corrected volume curve shows some instability at later times; the last data point suggests that the system was returning to equilibrium. The decrease in corrected volume corresponds to the time at which the Ruska pump was turned off and the surfactant cylinder was refilled. The refilling also accounts for the dip in the pressure differential profile seen in Figure 5.67.

The differential pressure profile shows that steady state was not reached. The run was concluded when the differential pressure reached 58 psi. The pressure transducer plate used was designed for a maximum of 50 psi. The pressure profile for the elevated temperature runs is presented in Figure 5.68.

There was a steady increase in surfactant performance with increased temperature. The total mobility for Run 15 was less than 0.174 darcies/cp. The exact value is not known because steady state

Experimental Data For Run #15
1% SD 1000 Glass Bead Size #9

Surfactant: SD 1000
Concentration: 1%
Absolute Permeability: 13.0 darcies
Porosity: 33.2%
Back Pressure: 50 psi
Glass Bead Size: #9 * New Supplier
Residual Oil Saturation: no
Temperature: 125°C
Gas Breakthrough: 28:30 (min.)
Totalizer Reading @ BT.: 172

Time (s)	Volume (cc)	Cum. Vol. (cc)	Spectro. Conc. ppm	Pressure Drop (psi)	Simulated Pressure Drop (psi)	Totalizer Reading
135	49	51.0	140	0.75	7.20	15
300	45	96.0	134	0.75	8.30	29
465	55	151.0	80	1.75	9.60	44
630	47	198.0	75	2.75	10.50	63
780	43	241.0	142	4.00	10.50	78
960	45	286.0	170	5.25	10.50	96
1125	47	333.0	115	7.25	10.50	113
1320	52	385.0	229	9.00	10.50	133
1500	48	433.0	3968	11.25	10.50	152
1680	49	482.0	5989	12.25	10.50	169
3120	49	531.0	6722	23.25	10.50	318
6060	46	577.0	8164	30.50	10.50	611
8640	32	609.0	8143	30.75	10.50	867
12480	60	669.0	8543	34.00	10.50	1222
16260	55	724.0	8847	38.00	10.50	1635
18900	43	767.0	7815	42.00	10.50	1902
21900	44	811.0	7665	43.25	10.50	2201
24900	23	834.0	7105	39.50	10.50	2502
29100	60	894.0	8276	51.50	10.50	2922
32280	49	943.0	6983	56.00	10.50	3250
33840	22	1003.0	7200	58.25	10.50	3404

Table 5.27 Experimental Data for Run 15: 1% SD1000 125°C

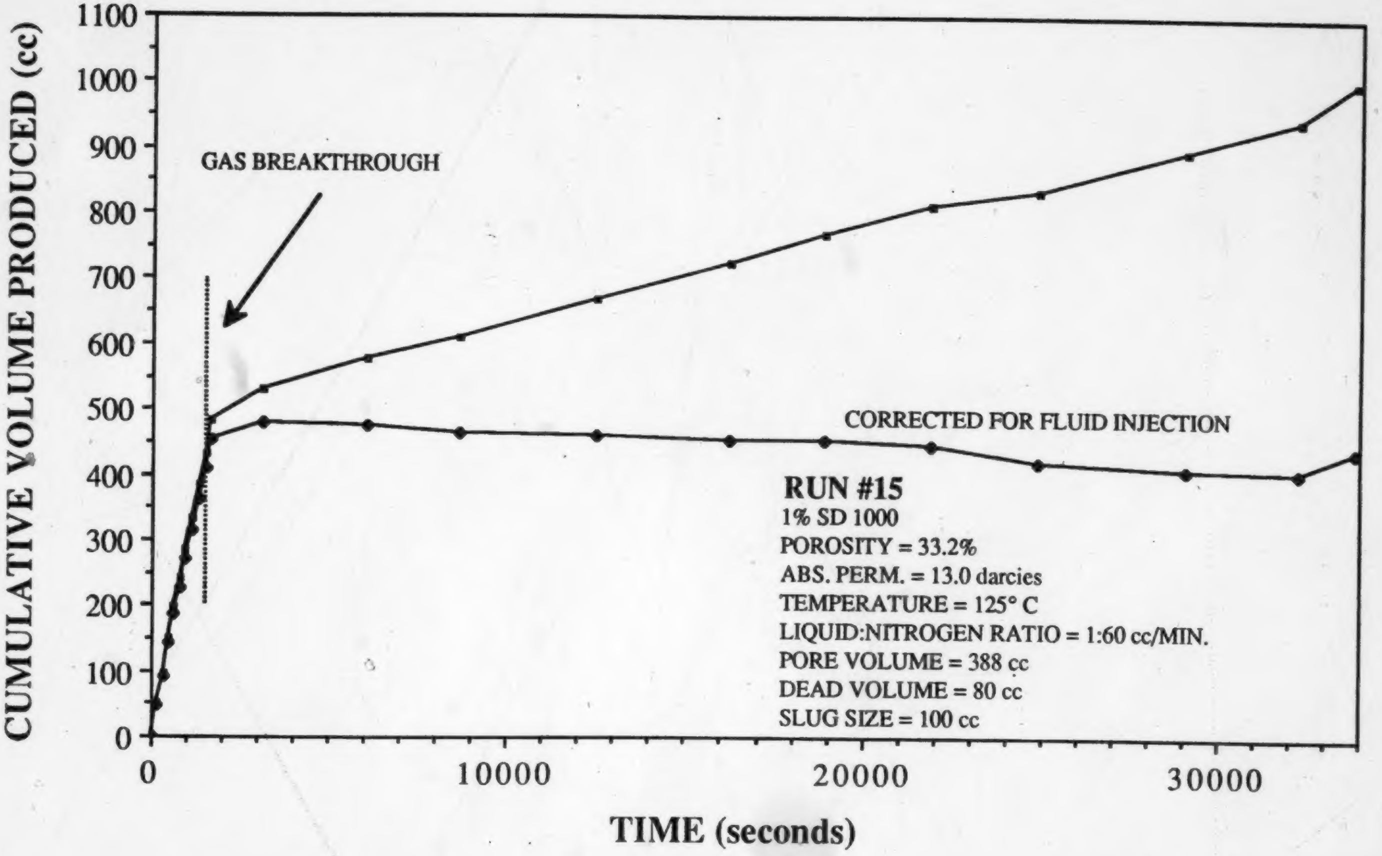

Figure 5.66 Run 15: Cumulative Volume Produced Vs. Time, Nitrogen Surfactant Co-injection, 1% SD1000 125°C

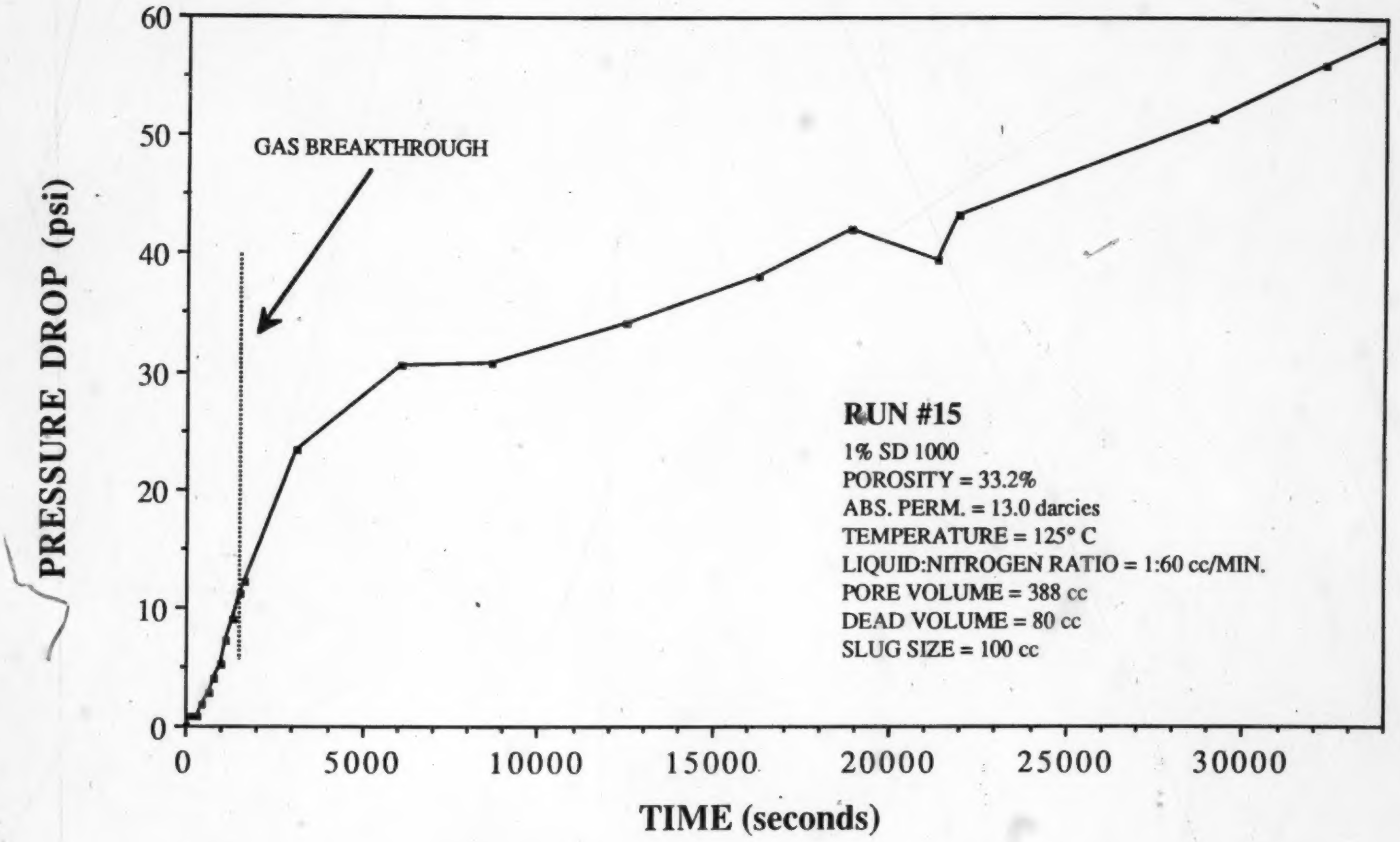

RUN #15
1% SD 1000
POROSITY = 33.2%
ABS. PERM. = 13.0 darcies
TEMPERATURE = 125° C
LIQUID:NITROGEN RATIO = 1:60 cc/MIN.
PORE VOLUME = 388 cc
DEAD VOLUME = 80 cc
SLUG SIZE = 100 cc

Figure 5.67 Run 15: Pressure Drop Vs. Time, Nitrogen Surfactant Co-injection, 1% SD1000 125°C

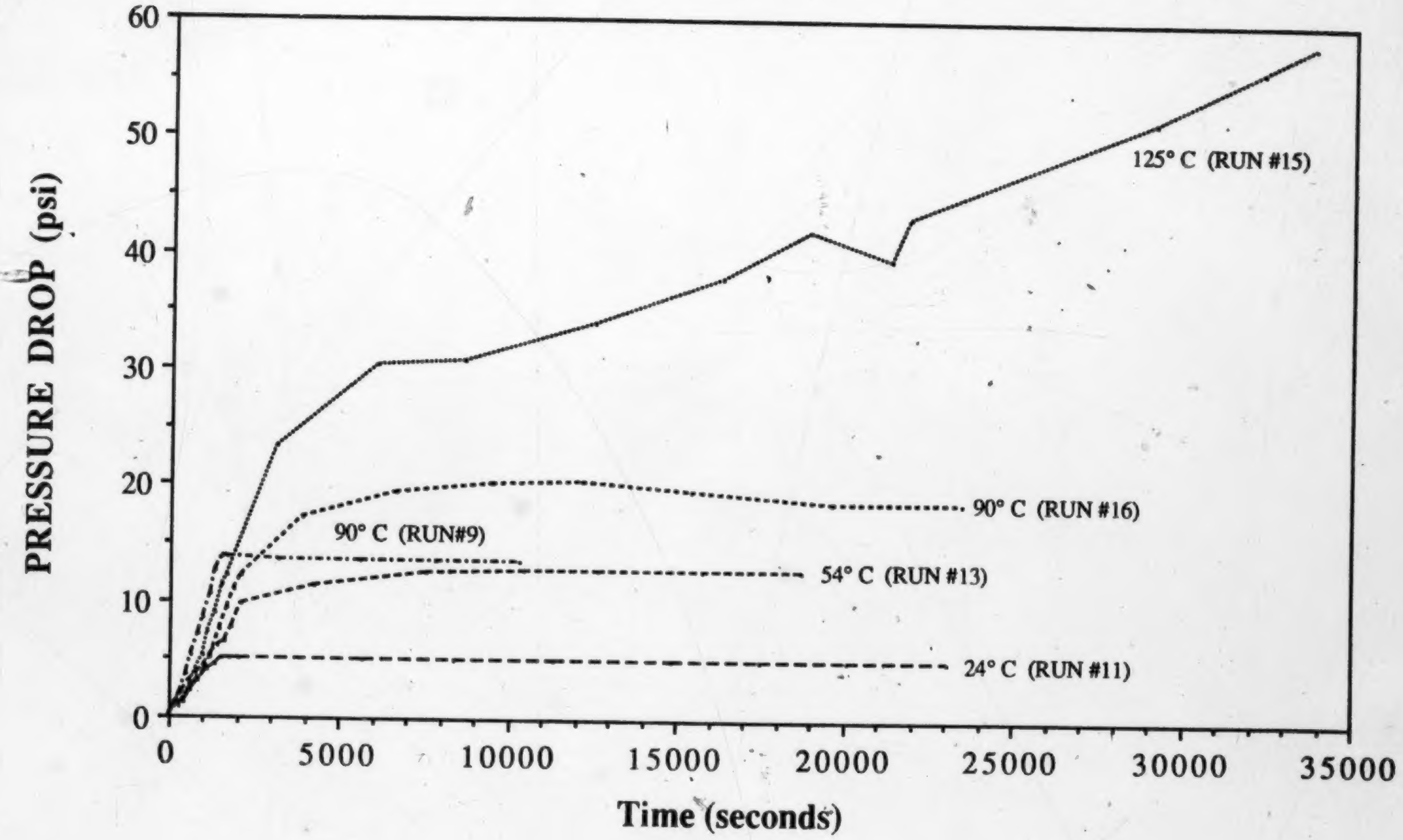

Figure 5.68 Comparison of the differential pressure for runs conducted at elevated temperatures

was not achieved. This experiment was allowed to run 50 percent longer than the typical run, in an attempt to achieve steady state.

The concentration graph is presented in Figure 5.69. The concentration at gas breakthrough was 59.9 percent. The concentration never exceeded 85 percent, which suggests that increased temperature, caused an increased adsorption.

5.3.3.2 Dow Surfactant

Two runs will be compared in this section, both utilizing 1 percent Dow surfactant. Run 23 was performed at ambient conditions and Run 27 at 125° C.

The data for Run 23 is given in Table 5.27. This run was performed on a 10.9 darcy glass bead pack. The gas breakthrough time was 109.5 minutes. The volume produced at gas breakthrough was 558 cc. The cumulative volume produced versus time is presented in Figure 5.70. The corrected cumulative volume produced shows an uncharacteristic curvature prior to gas breakthrough for a surfactant run. This is due to the constantly increasing system pressure. The residual liquid saturation was 25.0 percent.

The differential pressure profile is presented in Figure 5.71. Although the pressure did not reach steady state, the pressure did

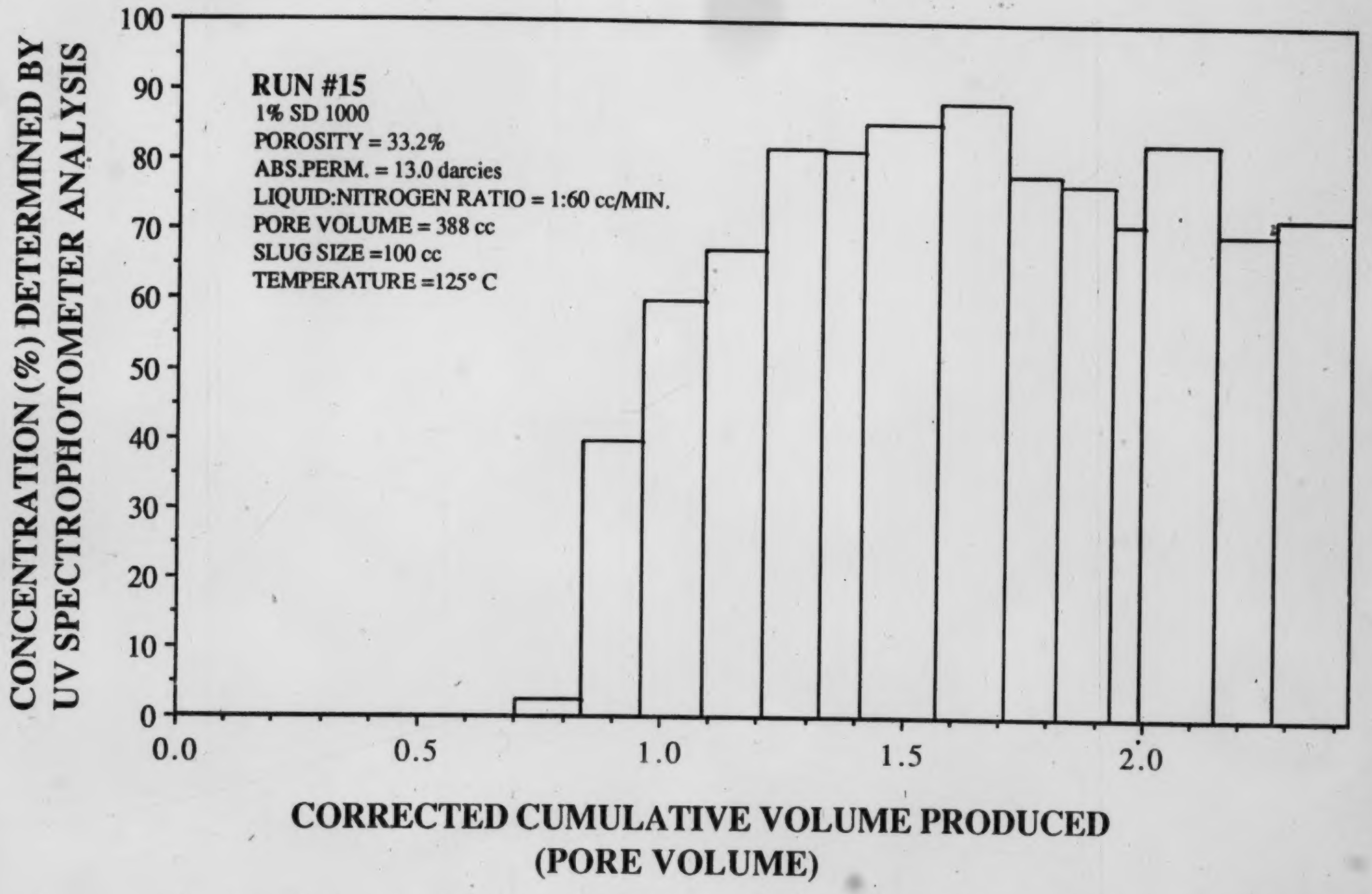

Figure 5.69 Run 15: Concentration Determined by UV Spectrophotometer Analysis Vs. Corrected Cumulative Volume Produced, Nitrogen Surfactant Co-injection, 1% SD1000 125°C

Experimental Data For Run 23
1% Dow Surfactant Glass Bead Size #9

Surfactant:	Dow	**Glass Bead Size:**	#9
Concentration:	1.0%	**Residual Oil Sat.:**	no
Absolute Permeability:	10.9 darcies	**Temperature:**	Ambient
Porosity:	33.4%	**Gas Breakthrough:**	1:49:30
Back Pressure:	50 psi	**Totalizer Reading @ BT.:**	672

Time (s)	Volume (cc)	Cum. Vol. (cc)	Spectro. Conc. ppm	Pressure Drop (psi)	Totalizer Reading
210	54	51.0	59.0	0.50	22
480	53	104.0	43.0	0.75	50
750	44	148.0	13.0	1.50	74
1050	47	195.0	24.0	3.25	107
1410	48	243.0	24.0	7.50	143
1800	44	287.0	28.0	10.00	184
2250	50	337.0	8.0	14.50	229
2700	48	385.0	16.0	16.25	274
3270	49	434.0	1835.0	18.00	333
3960	46	480.0	5570.0	21.25	403
5280	45	525.0	7401.0	29.75	538
6600	33	558.0	9600.0	52.50	674
8880	47	605.0	10599.0	108.00	904
12540	62	667.0	9772.0	97.75	1159
16560	61	728.0	9804.0	100.75	1298
18600	35	763.0	9700.0	103.50	1366
22200	55	818.0	10440.0	115.25	1483
24600	39	857.0	10701.0	105.50	1563

Table 5.28 Experimental Data for Run 23: 1% Dow Surfactant

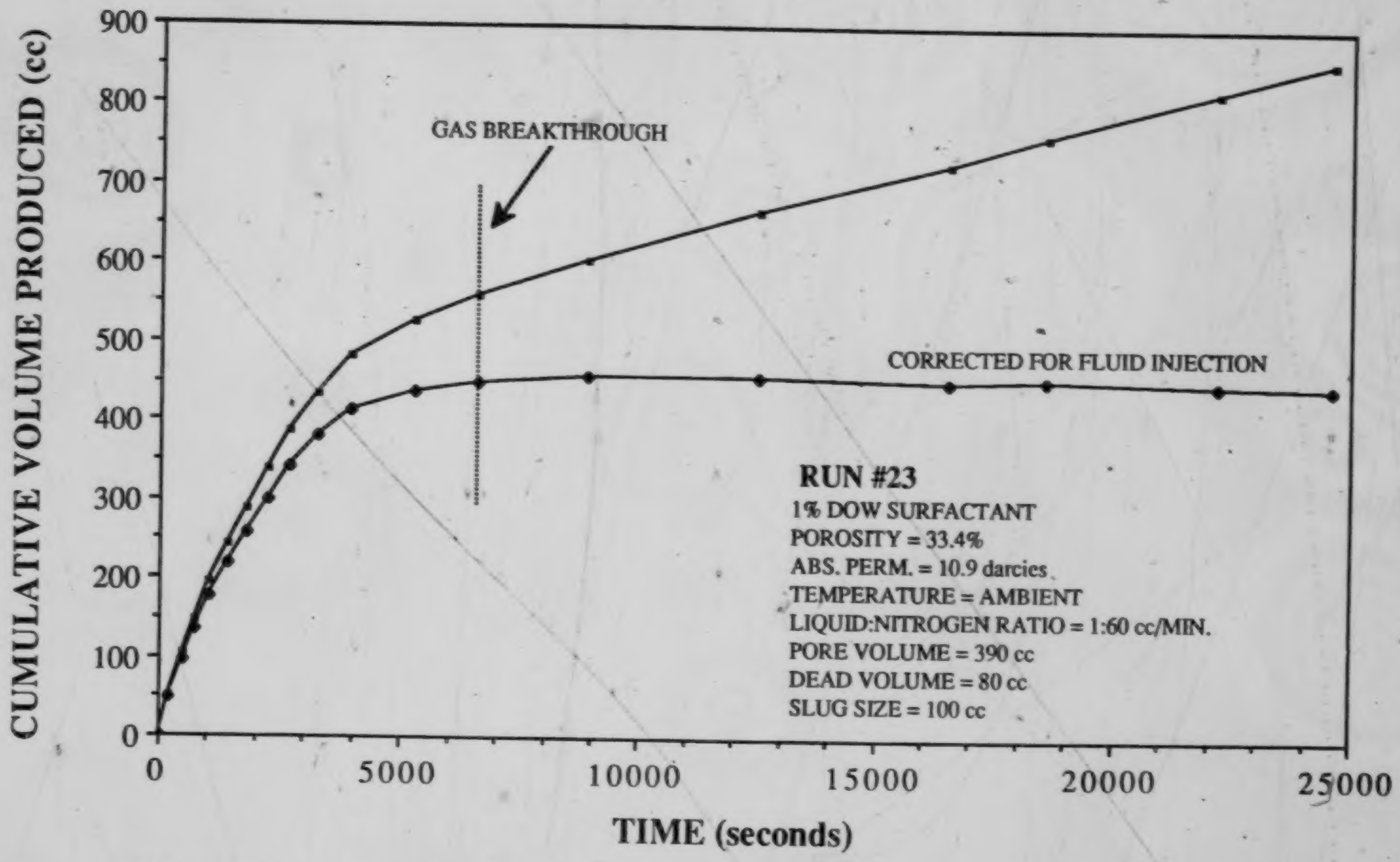

Figure 5.70 Run 23: Cumulative Volume Produced Vs. Time, Nitrogen Surfactant Co-injection, 1% Dow Surfactant

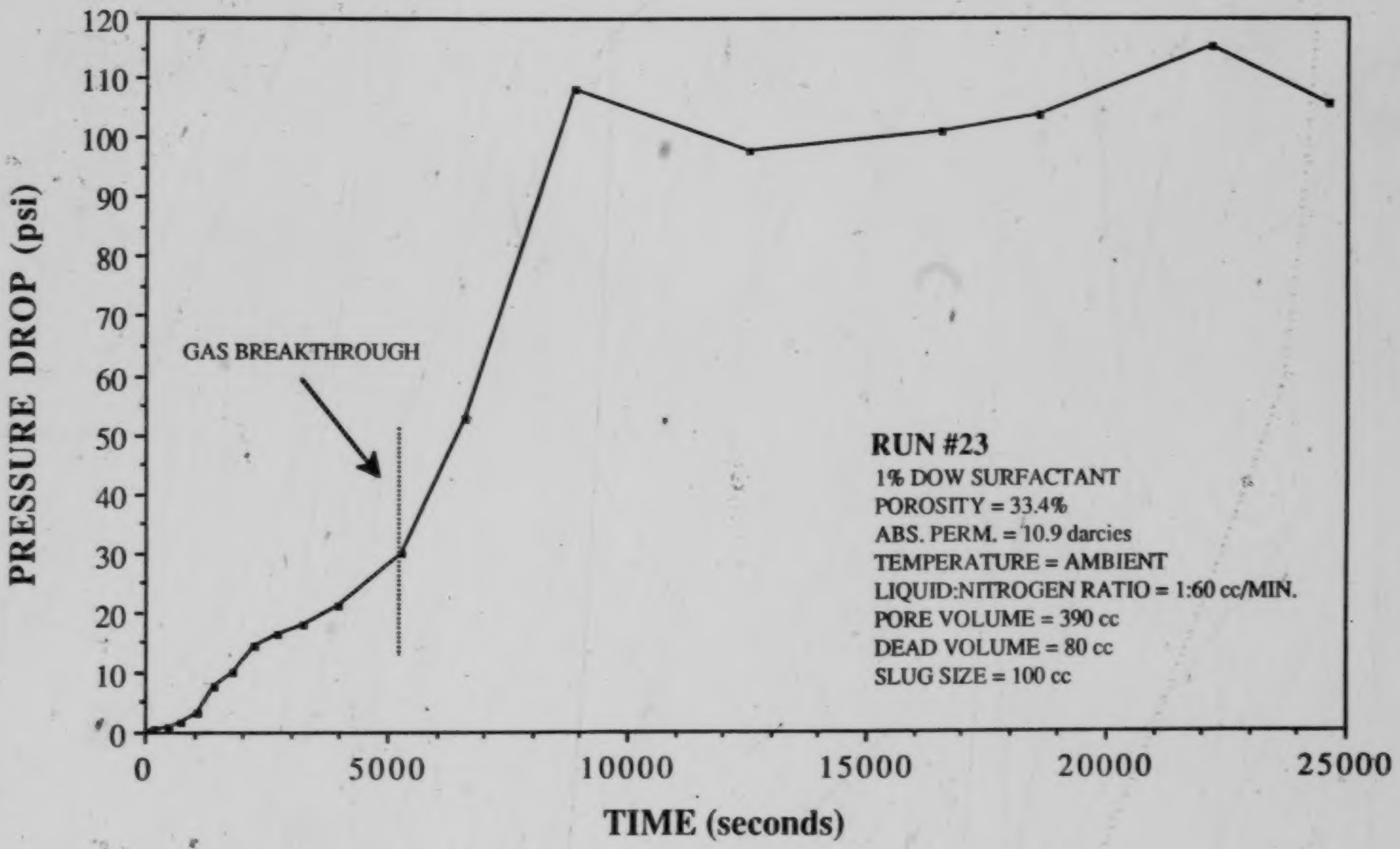

Figure 5.71 Run 23: Pressure Drop Vs. Time, Nitrogen Surfactant Co-injection, 1% Dow Surfactant

level off around 105 psi. The total mobility was less than 0.0671 darcies/cp; the relative mobility was 0.0062 cp^{-1}.

The concentration graph is presented in Figure 5.72. The concentration of the sample collected at gas breakthrough was 96.0 percent. This indicates a very high displacement efficiency. The effluent concentration reached 100 percent during the run.

Run 27 was performed, at 125° C, on a 11.2 darcy glass bead pack. The data for this run is given in Table 5.29. The gas breakthrough time for this run was 71 minutes. The volume produced at this point was 581 cc. The cumulative volume produced versus time graph is presented in Figure 5.73. The stabilized corrected volume produced was 554 cc. The residual liquid saturation was 6.9 percent.

The differential pressure profile is presented in Figure 5.74. The pressure drop rose continuously throughout the run. There were no signs that the run was approaching steady state. The run was discontinued because the system was approaching the design pressure. The total mobility was less than 0.032 darcies/cp for this run; this is even lower than that found for Run 23. The increased temperature caused a mobility reduction; this was also observed for SD1000.

The concentration graph is presented in Figure 5.75. The concentration at gas breakthrough was 70.3 percent. The effluent

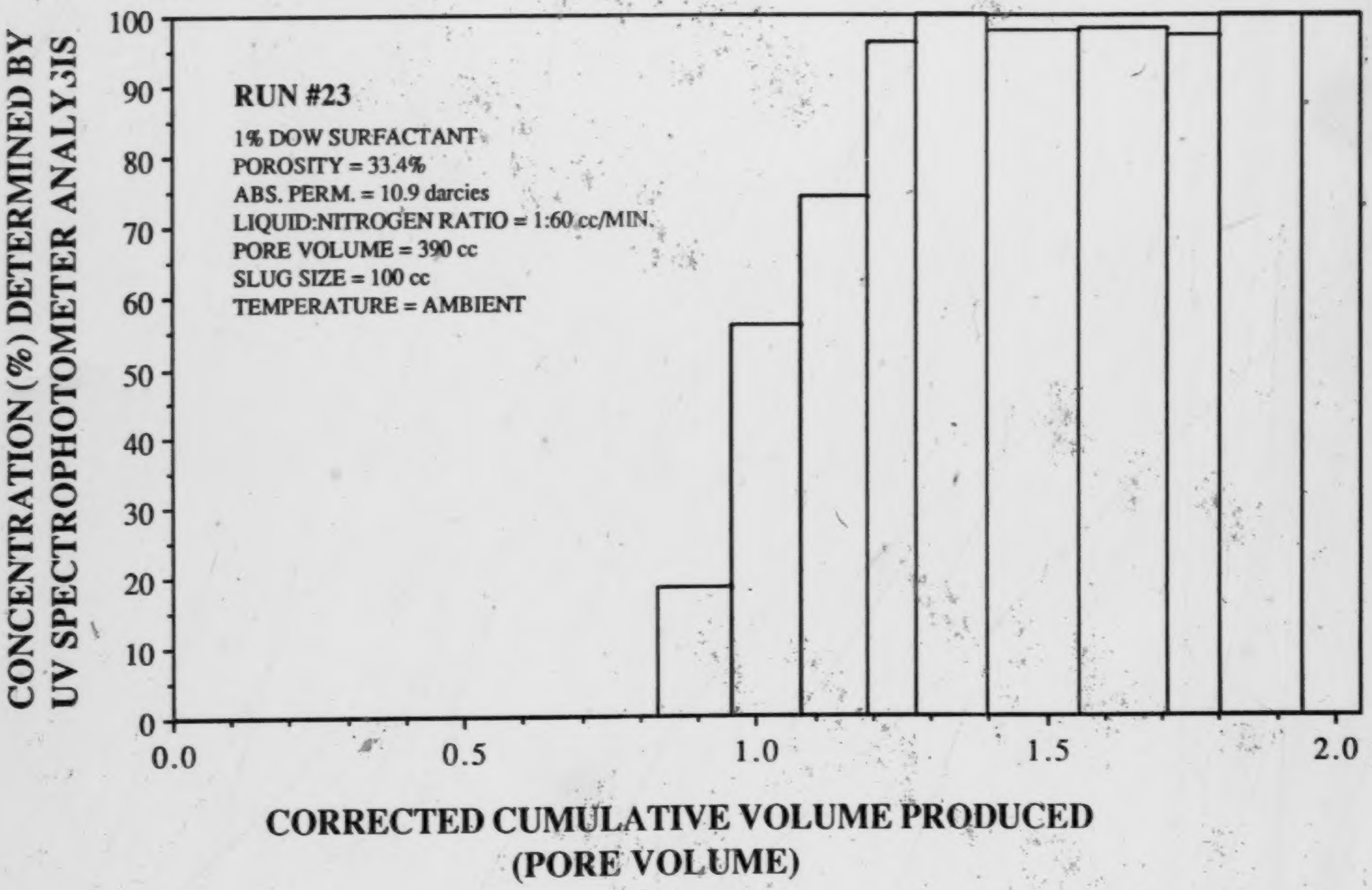

Figure 5.72 Run 23: Concentration Determined by UV Spectrophotometer Analysis Vs. Corrected Cumulative Volume Produced, Nitrogen Surfactant Co-injection, 1% Dow Surfactant

Experimental Data For Run 27
1% Dow Surfactant Glass Bead Size #9

Surfactant:	Dow	**Glass Bead Size:**	#9
Concentration:	1.0%	**Residual Oil Sat.:**	no
Absolute Permeability:	11.2 darcies	**Temperature:**	125° C
Porosity:	32.4%	**Gas Breakthrough:**	1:11:00
Back Pressure:	50 psi	**Totalizer Reading @ BT.:**	420

Time (s)	Volume (cc)	Cum. Vol. (cc)	Spectro. Conc. ppm	Pressure Drop (psi)	Totalizer Reading
90	46	46.0	35.4	0.7	9
300	45	91.0	32.5	1.1	34
480	48	139.0	21.0	1.6	51
720	48	187.0	14.0	4.4	75
1020	47	234.0	24.0	9.6	106
1290	49	283.0	22.0	16.3	133
1530	50	333.0	17.0	21.8	158
1770	49	382.0	15.0	29.4	182
2160	51	433.0	615.0	41.0	222
3060	52	485.0	3647.0	72.6	312
3810	53	538.0	6685.0	101.0	390
4290	43	581.0	7032.0	104.5	422
6930	47	628.0	8558.0	137.6	641
9390	41	669.0	7821.0	206.3	794

Table 5.29 Experimental Data for Run 27: 1% Dow Surfactant 125°C

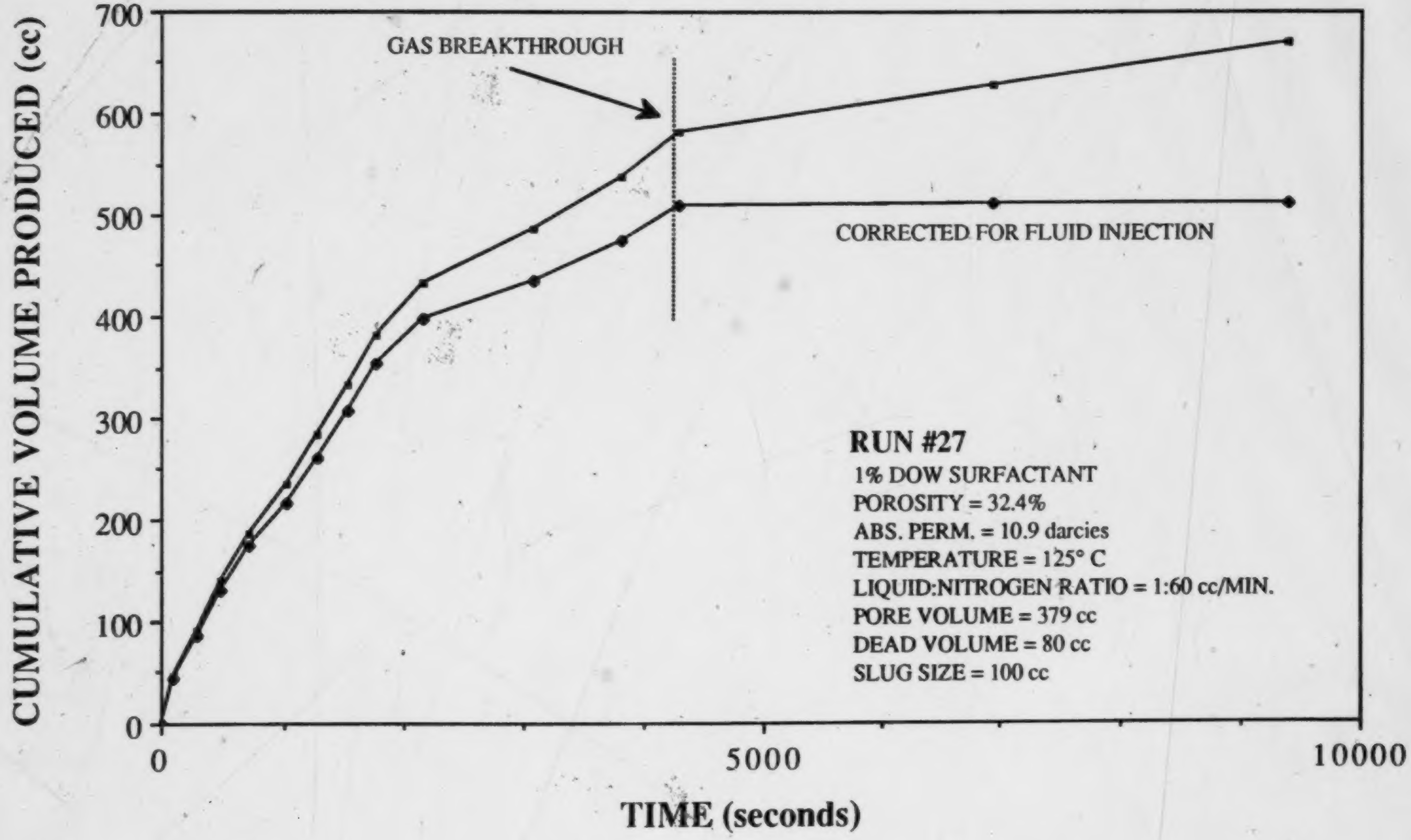

Figure 5.73 Run 27: Cumulative Volume Produced Vs. Time, Nitrogen Surfactant Co-injection, 1% Dow Surfactant 125°C

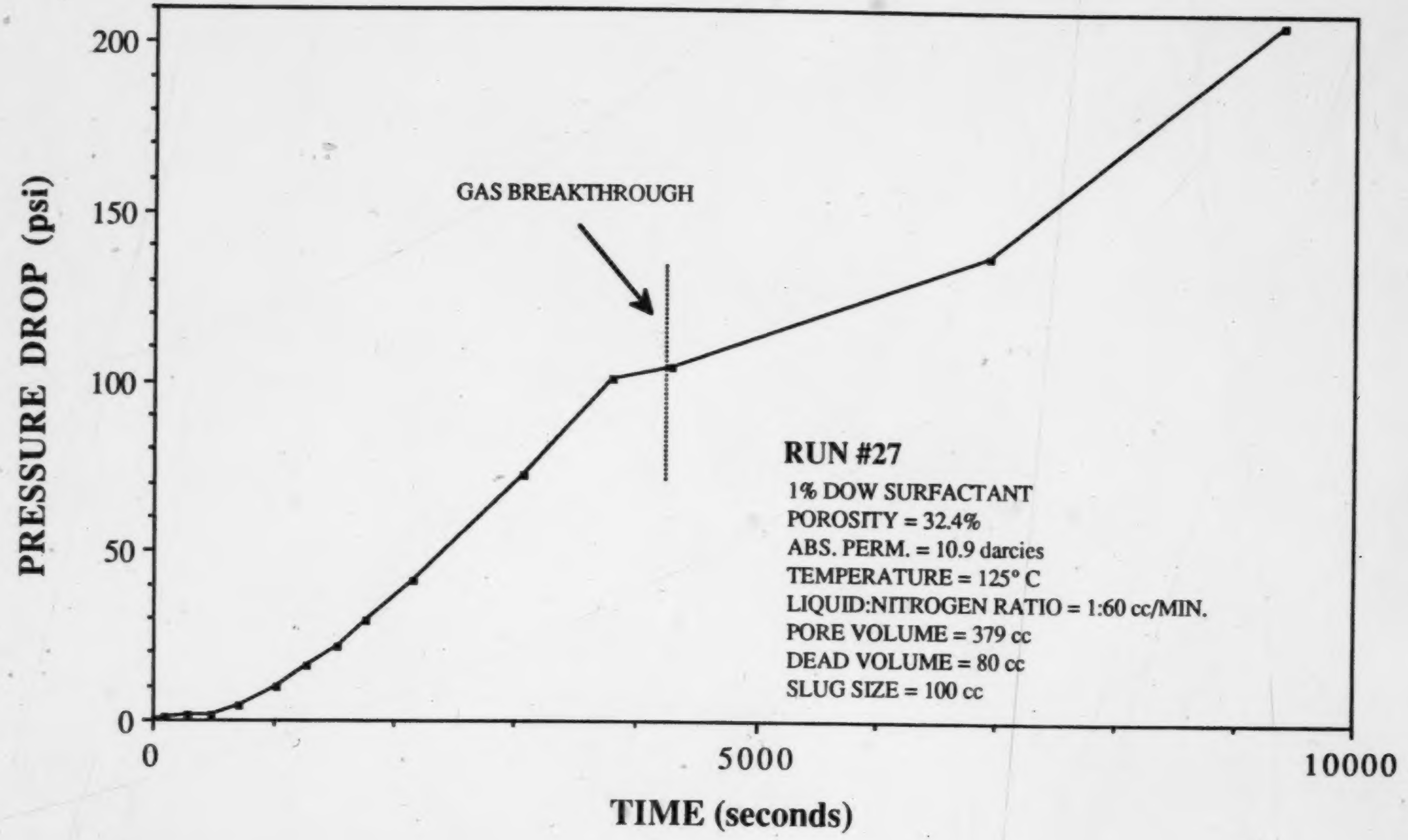

Figure 5.74 Run 27: Pressure Drop Vs. Time, Nitrogen Surfactant Co-injection, 1% Dow Surfactant 125°C

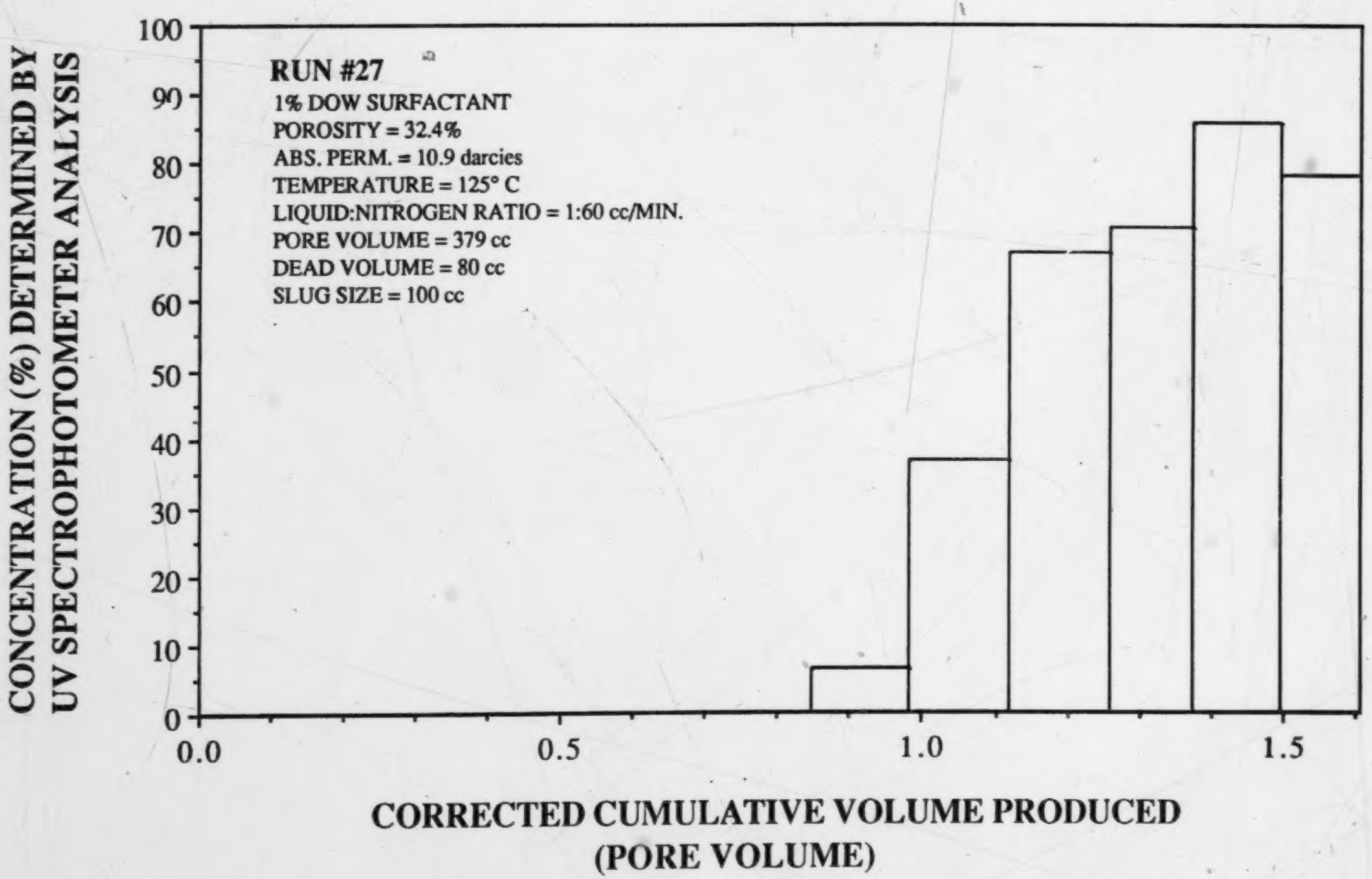

Figure 5.75 Run 27: Concentration Determined by UV Spectrophotometer Analysis Vs. Corrected Cumulative Volume Produced, Nitrogen Surfactant Co-injection, 1% Dow Surfactant 125°C

concentration determined for this run did not exceed 85.5 percent. This also suggests that surfactant adsorption increases with increased temperature.

5.3.4 Effect of Oil Saturation

There were four runs performed to examine the effect of residual oil saturation within the glass bead pack. These were Runs 2, 4, 8 and 22.

Run 8 was performed with no surfactant on a 8.1 darcy glass bead pack, with a residual oil saturation of 25.1 percent. The data for this run is given in Table 5.30. The gas breakthrough time for this run was 17 minutes with 203 cc of liquid produced at that point. The cumulative volume is presented in Figure 5.76. The stabilized corrected cumulative volume produced is 217 cc. There was no residual oil produced during this run. The residual water saturation was 60.7 percent.

The differential pressure profile is presented in Figure 5.77. The pressure rose prior to gas breakthrough, to a maximum of 3.75 psi, but fell off to 1.75 psi at steady state. The total mobility for this run was 6.378 darcies/cp; the relative mobility was 0.7875 cp^{-1}.

Run 2 was performed with 1 percent SD1000, on a 6.2 darcy glass bead pack with a residual oil saturation of 20.4 percent. The

Experimental Data For Run #8
Glass Bead Size #9

Surfactant:	none	**Glass Bead Size:**	#9
Concentration:	0%	**Residual Oil Saturation:**	25.10%
Absolute Permeability:	8.05 darcies	**Temperature:**	Ambient
Porosity:	34.0%	**Gas Breakthrough:**	17:00 (min.)
Back Pressure:	50 psi	**Totalizer Reading @ BT.:**	102

Time (s)	**Volume (cc)**	**Cum. Vol. (cc)**	**Pressure Drop (psi)**	**Totalizer Reading**
210	49	49.0	3.25	22
465	52	101.0	3.75	47
705	52	153.0	2.75	72
930	50	203.0	1.75	94
1710	26	229.0	1.75	173
2940	20.5	249.5	1.75	298
5565	43	292.5	1.75	562
6465	15	307.5	1.75	652
7710	21	328.5	1.75	860
8820	19	347.5	1.75	1046

Table 5.30 Experimental Data for Run 8: No Surfactant Res Oil Sat

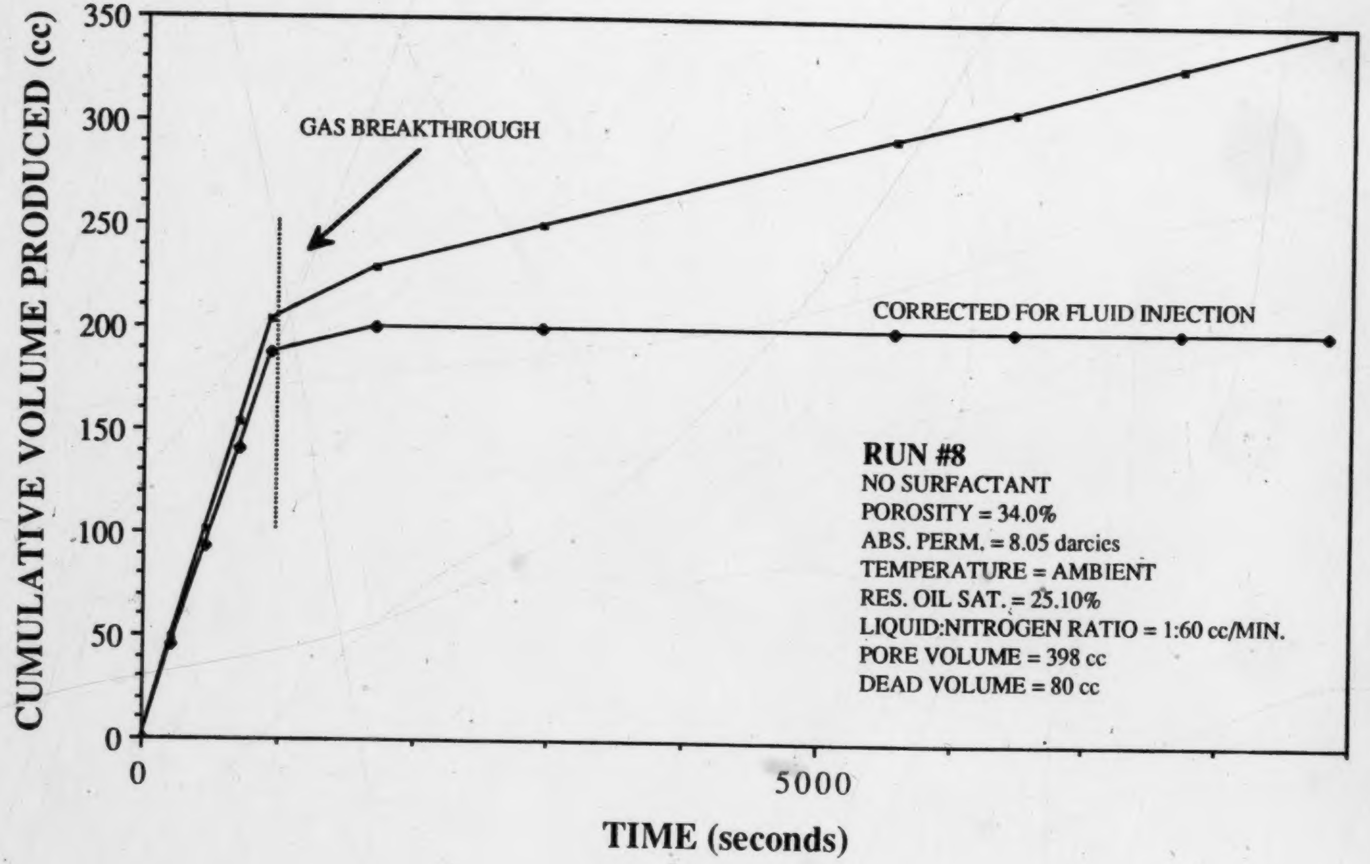

Figure 5.76 Run 8: Cumulative Volume Produced Vs. Time, Nitrogen Surfactant Co-injection, Residual Oil Saturation No Surfactant

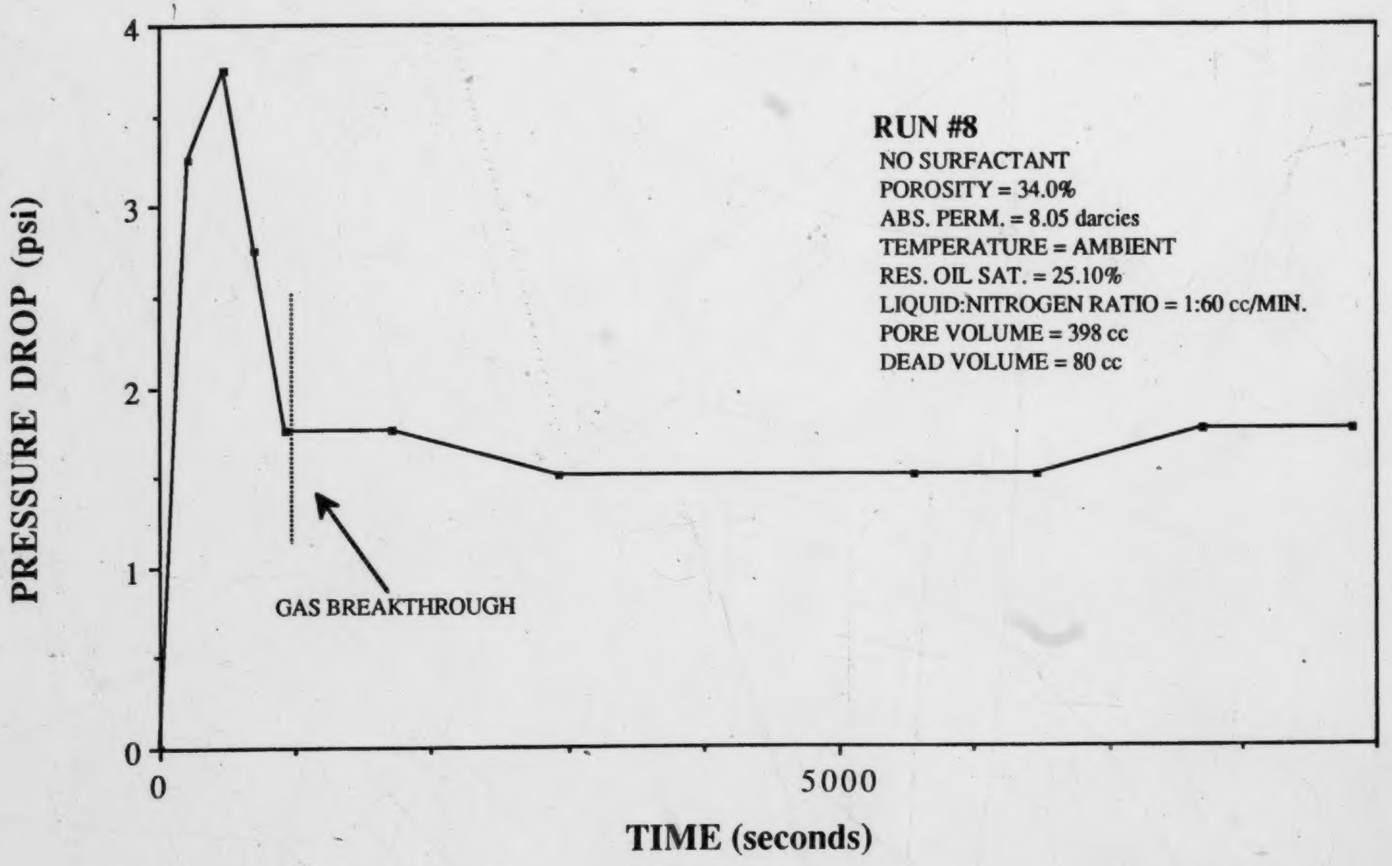

Figure 5.77 Run 8: Pressure Drop Vs. Time, Nitrogen Surfactant Co-injection, Residual Oil Saturation No Surfactant

data for this run is located in Table 5.31. The gas breakthrough time for this run was 11.3 minutes; the volume produced at this point was 250.5 cc, with no oil production. Table 5.31 shows the oil produced for this run took place following gas breakthrough. The cumulative volume produced versus time is presented in Figure 5.78. The stabilized corrected cumulative volume is 260 cc. The total oil volume produced was 5.5 cc, or 6.9 percent of the residual oil saturation. The residual water saturation for this core was 72.4 percent.

The differential pressure profile is presented in Figure 5.79. The pressure drop increased until gas breakthrough at which point it became steady at 2.5 psi. The total mobility for this run was 4.44 darcies/cp. The relative mobility was 0.7164 cp^{-1}.

Run 4 was performed with a 5 percent SD1000 solution, on a 7.1 darcy glass bead pack with a residual oil saturation of 21.7 percent. The data for this run is given in Table 5.32. The gas breakthrough time for this run was 22.8 minutes; the volume of water produced at this point was 258 cc. There was no oil produced at this point. The cumulative water plus oil volume produced is presented in Figure 5.80. The total oil volume produced was 7 cc, or 8.4 percent of the residual oil saturation corrected cumulative volume produced stabilized at 244 cc. Therefore the residual water saturation was 76.1 percent.

Experimental Data For Run #2
1% SD 1000 Glass Bead Size #9

Surfactant:	SD 1000	**Glass Bead Size:**	#9
Concentration:	1%	**Residual Oil Saturation:**	20.4%
Absolute Permeability:	6.2 darcies	**Temperature:**	Ambient
Porosity:	33.2%	**Gas Breakthrough:**	11:20 (min.)
Back Pressure:	50 psi	**Totalizer Reading @ BT.:**	68

Time (s)	Volume (cc)	Volume Of Oil Produced (cc)	Cumulative Volume (cc)	Pressure Drop (psi)	Totalizer Reading
0	100.0	0.0	100.0	0	0
147	49.0	0.0	151.0	0.25	15
345	50.0	0.0	201.0	0.50	35
570	49.5	0.0	250.5	2.50	58
2010	46.0	2.0	298.5	2.50	203
5250	47.0	2.0	347.5	2.50	527
7740	42.0	1.0	390.5	2.50	778
10000	38.0	0.5	429.0	2.50	1020

Table 5.31 Experimental Data for Run 2: 1% SD1000 Res Oil Sat

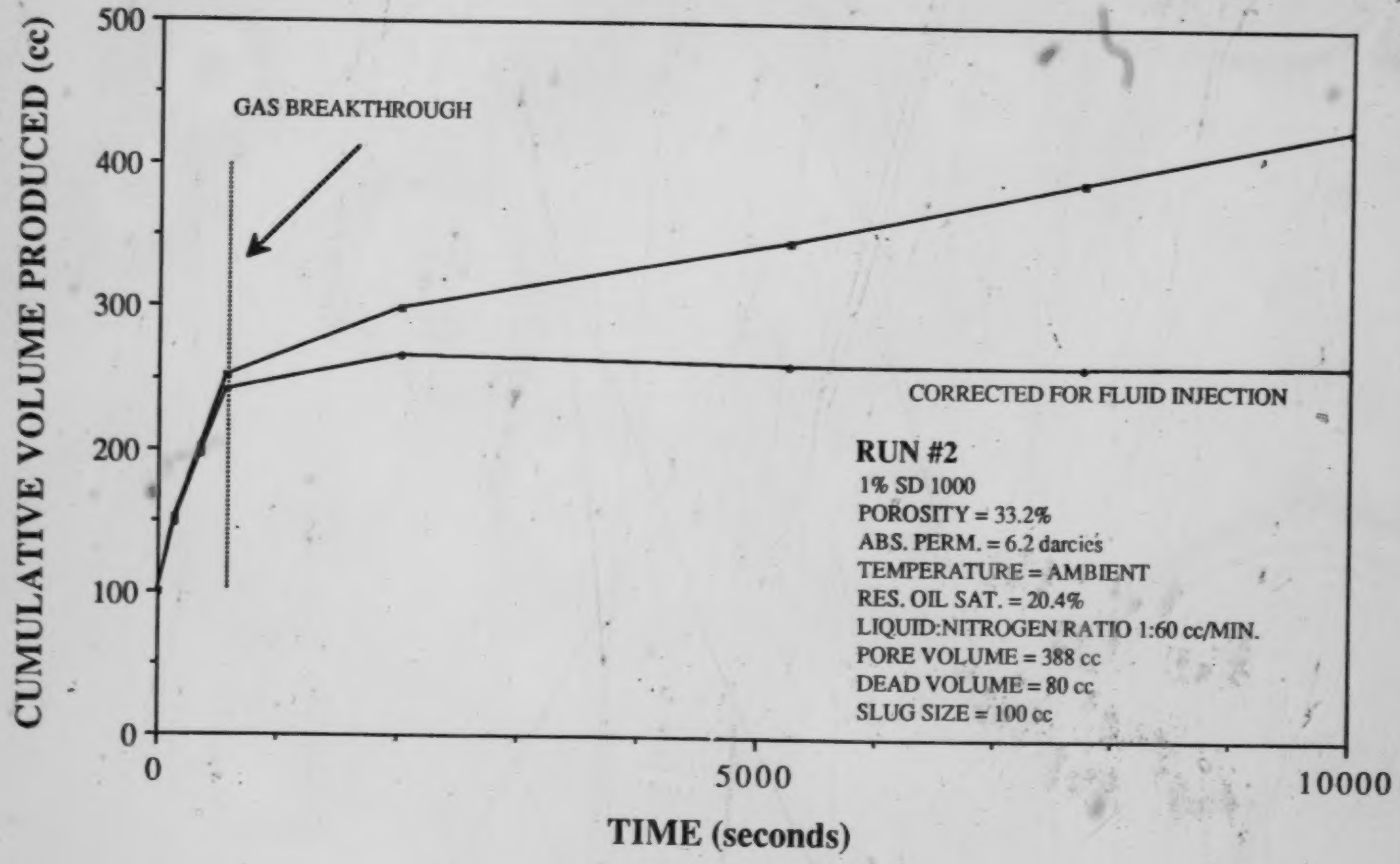

Figure 5.78 Run 2: Cumulative Volume Produced Vs. Time, Nitrogen Surfactant Co-injection, Residual Oil Saturation 1% SD1000

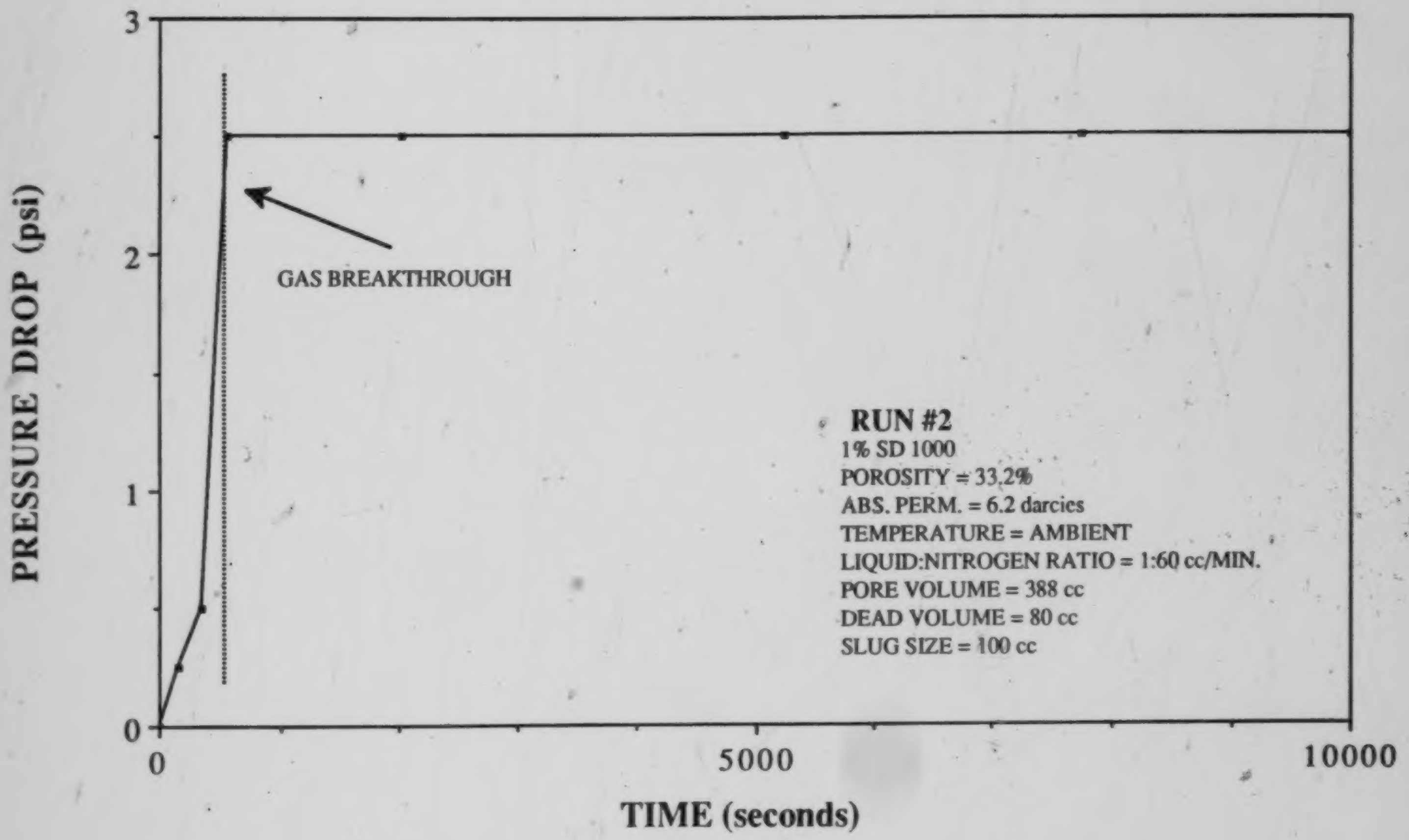

Figure 5.79 Run 2: Pressure Drop Vs. Time, Nitrogen Surfactant Co-injection, Residual Oil Saturation 1% SD1000

Experimental Data For Run #4
5% SD 1000 Glass Bead Size #9

Surfactant: SD 1000
Concentration: 5%
Absolute Permeability: 7.1 darcies
Porosity: 32.8%
Back Pressure: 50 psi

Glass Bead Size: #9
Residual Oil Saturation: 21.7%
Temperature: Ambient
Gas Breakthrough: 22:50 (min.)
Totalizer Reading @ BT.: 139

Time (s)	Volume (cc)	Volume Of Oil Produced (cc)	Cumulative Volume (cc)	Refrac. Index Conc. (%)	Pressure Drop (psi)	Totalizer Reading
300	53.5	0.0	51.0	0	2.75	30
555	51.0	0.0	102.0	0	3.50	55
780	48.0	0.0	150.0	0	3.75	78
1020	51.0	0.0	201.0	0	3.75	102
1290	57.0	0.0	258.0	0	3.50	129
2640	31.0	0.5	289.5	15	3.00	265
4365	29.5	0.5	319.5	50	3.00	439
5940	26.0	1.0	346.5	70	3.00	599
8340	37.0	2.0	385.5	95	3.00	845
11220	44.0	2.0	431.5	100	3.00	1132
14160	45.0	1.0	477.5	100	3.00	1430

Table 5.32 Experimental Data for Run 4: 5% SD1000 Residual Oil Saturation

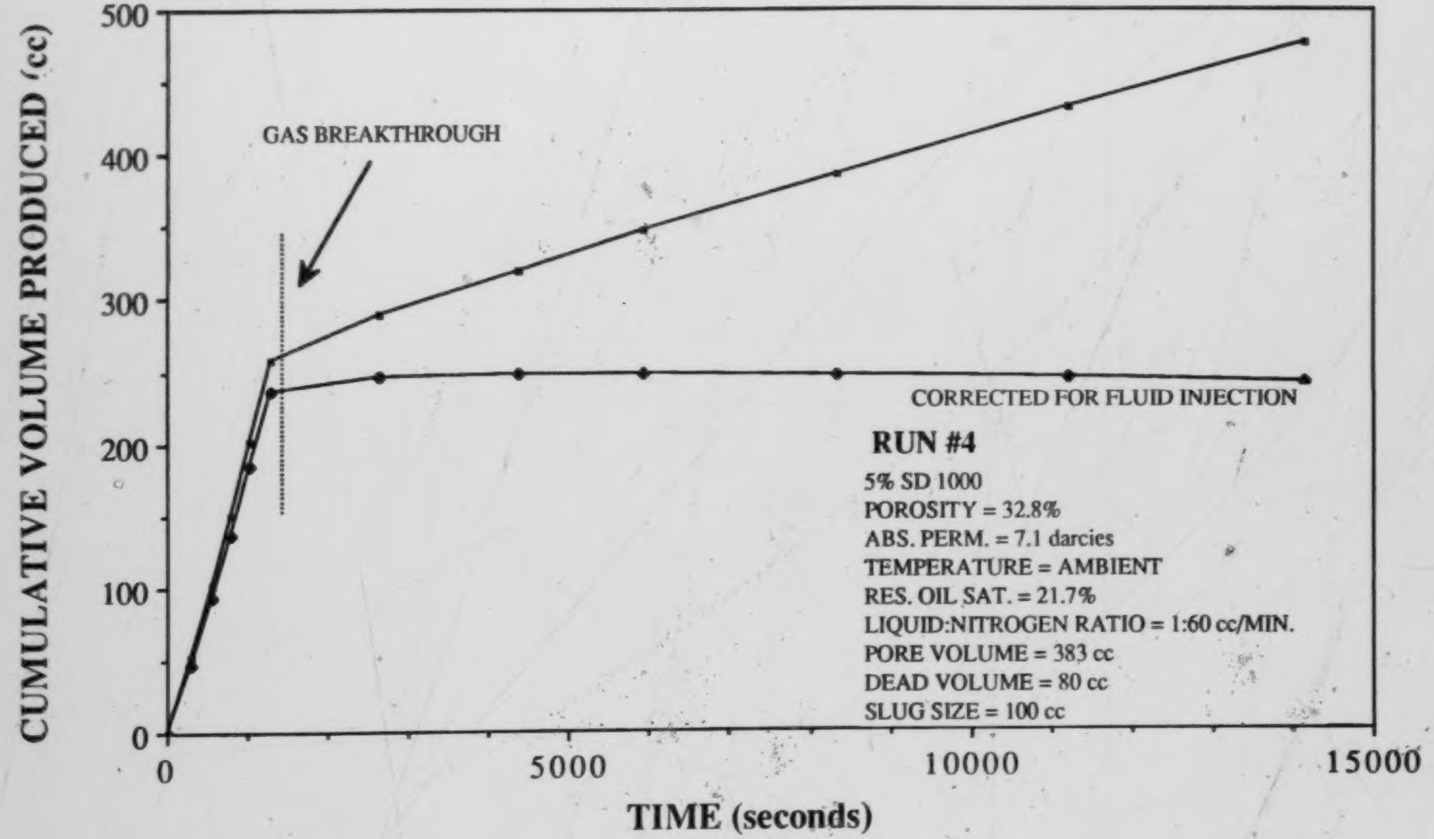

Figure 5.80 Run 4: Cumulative Volume Produced Vs. Time, Nitrogen Surfactant Co-injection, Residual Oil Saturation 5% SD1000

The differential pressure profile is presented in Figure 5.81. The pressure drop increased prior to gas breakthrough, to 3.75. Following gas breakthrough the pressure stabilized at 3.0 psi. The total mobility for this run was 3.68 darcies/cp. The relative mobility was 0.5195 cp^{-1}

The concentration graph for this run is presented in Figure 5.82. The effluent concentration at gas breakthrough was zero. This suggests that the gas bypassed the surfactant and was produced ahead of the surfactant slug.

Due to the decreased gas mobility found at elevated temperatures, Run 22 was performed at 125° C, with 1 percent SD1000 on a 13.2 darcy glass bead pack with a residual oil saturation of 25.6 percent. The data for this run are given in Table 5.33. The gas breakthrough occurred at 13.6 minutes, the volume produced at this point was 250 cc. The cumulative volume of fluids produced versus time is presented in Figure 5.83. The corrected cumulative volume produced continued to increase following gas breakthrough. The stabilized corrected volume produced was 322 cc. The total oil volume produced was 17 cc, or 17.6 percent of the residual oil saturation. The residual water saturation was 52.4 percent.

The differential pressure versus time is presented in Figure 5.84. The pressure drop across the core decreased following gas breakthrough, and then increased and stabilized at 2.25 psi. The total mobility for this run was 6.59 darcies/cp.

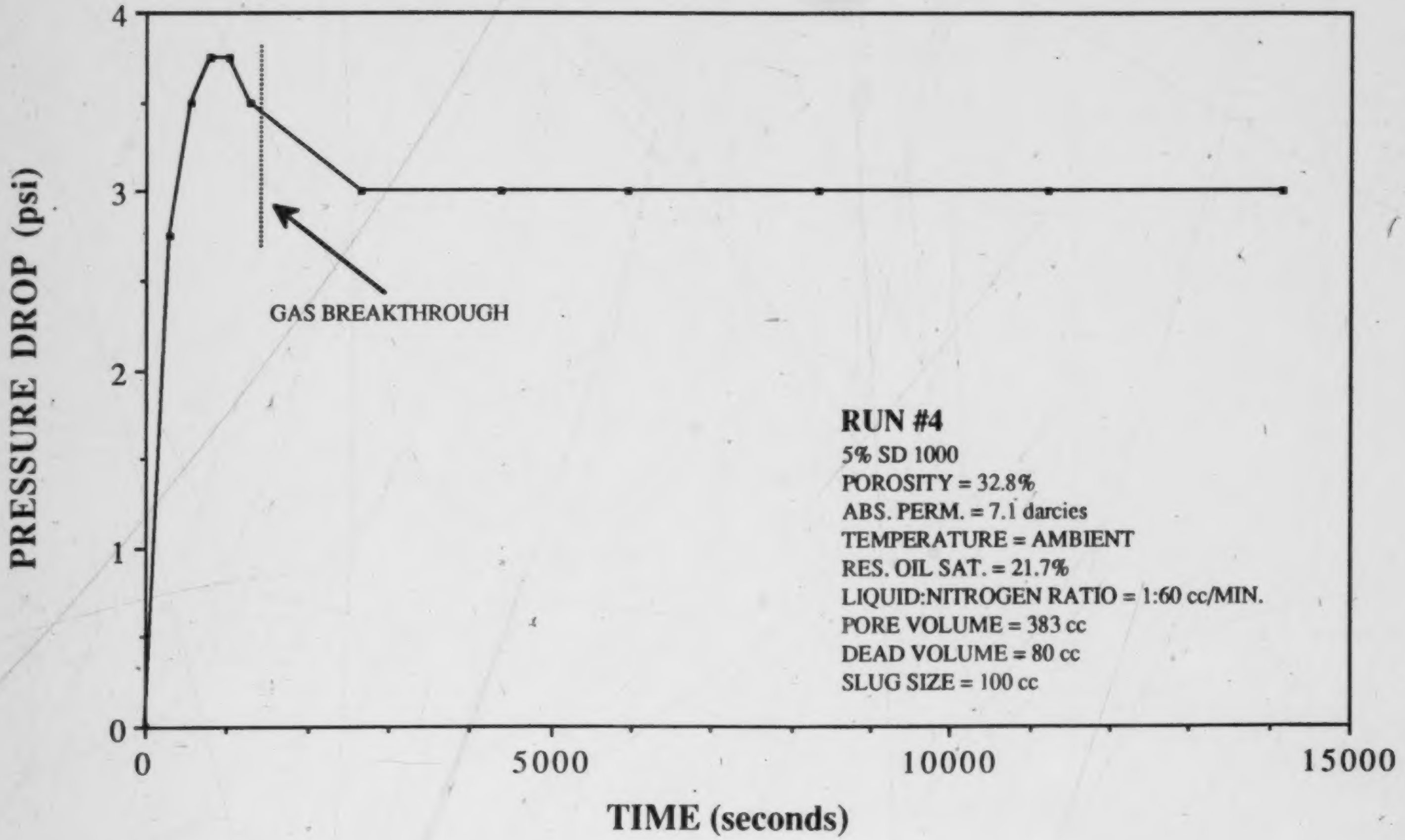

Figure 5.81 Run 4: Pressure Drop Vs. Time, Nitrogen Surfactant Co-injection, Residual Oil Saturation 5% SD1000

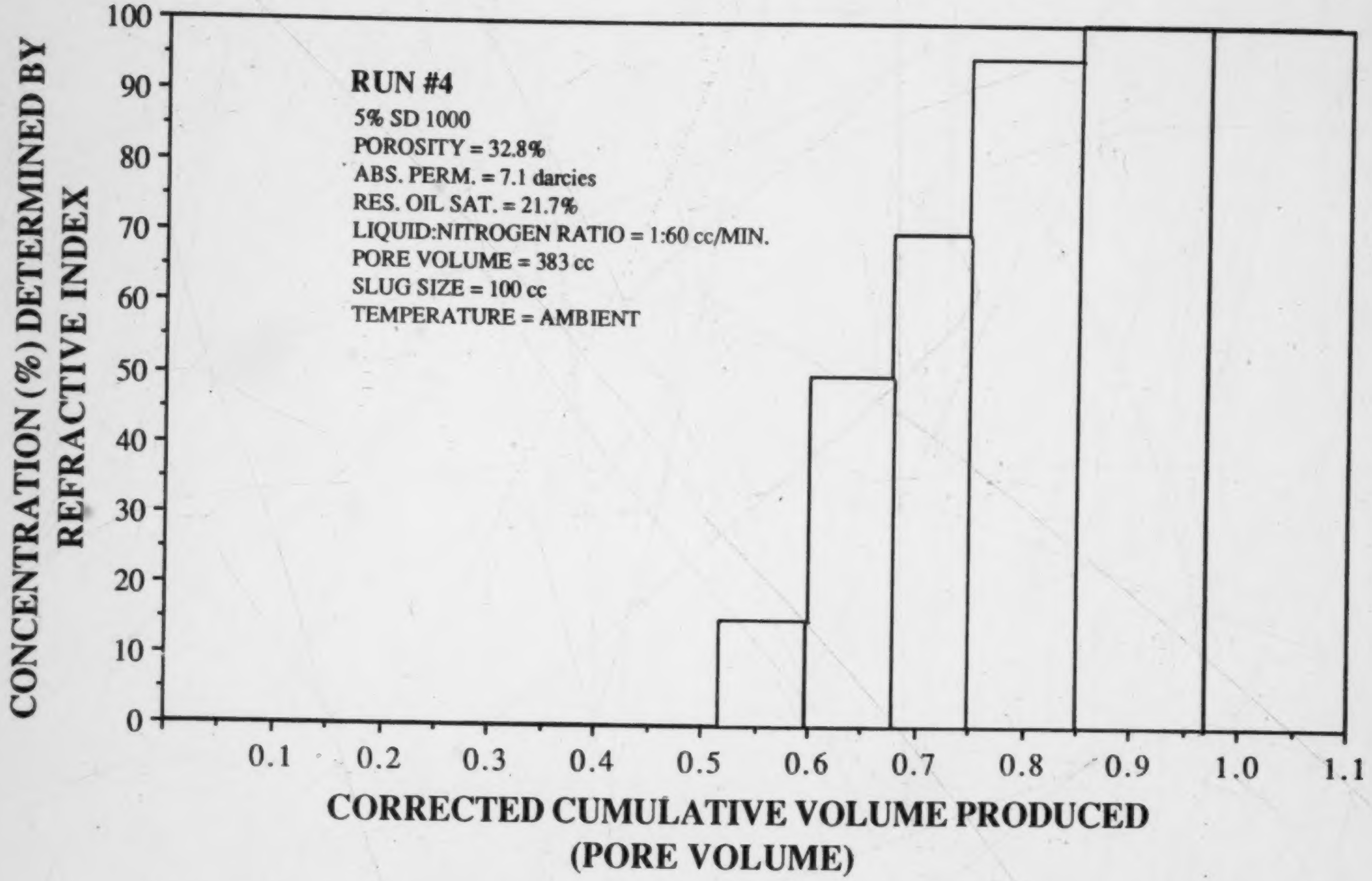

Figure 5.82 Run 4: Concentration Determined by UV Spectrophotometer Analysis Vs. Corrected Cumulative Volume Produced, Nitrogen Surfactant Co-injection, Residual Oil Saturation 5% SD1000

Experimental Data For Run 22
1% SD 1000 Glass Bead Size #9

Surfactant:	SD 1000	**Glass Bead Size:**	#9
Concentration:	1.0%	**Residual Oil Sat.:**	25.6%
Absolute Permeability:	13.2 darcies	**Temperature:**	125° C
Porosity:	32.2%	**Gas Breakthrough:**	13:35 (min.)
Back Pressure:	50 psi	**Totalizer Reading @ BT.:**	84

Time (s)	Volume (cc)	Volume Of Oil Produced (cc)	Cumulative Volume (cc)	Spectro. Conc. ppm	Pressure Drop (psi)	Totalizer Reading
180	51.0	0.0	51.0	57.0	1.50	18
330	53.0	0.0	104.0	89.0	2.50	33
480	49.0	0.0	153.0	59.0	2.50	48
630	49.0	0.0	202.0	53.0	2.50	64
765	48.0	0.0	250.0	81.0	2.50	78
840	18.0	0.0	268.0	130.0	2.50	87
1560	32.0	1.0	301.0	801.0	2.25	159
4140	64.5	3.5	369.0	1724.0	2.00	422
6390	50.0	3.0	422.0	5689.0	2.00	650
8640	44.0	4.0	470.0	7314.0	2.25	880
11280	44.0	2.0	516.0	7986.0	2.25	1147
13680	36.0	1.0	553.0	8687.0	2.25	1395
16380	42.0	1.0	596.0	8796.0	2.25	1667
18840	39.5	0.5	636.0	8656.0	2.25	1917
21960	47.5	0.5	684.0	8721.0	2.25	2237
23400	22.5	0.5	707.0	8860.0	2.25	2393

Table 5.33 Experimental Data for Run 22: 5% SD1000 Residual Oil Saturation 125°C

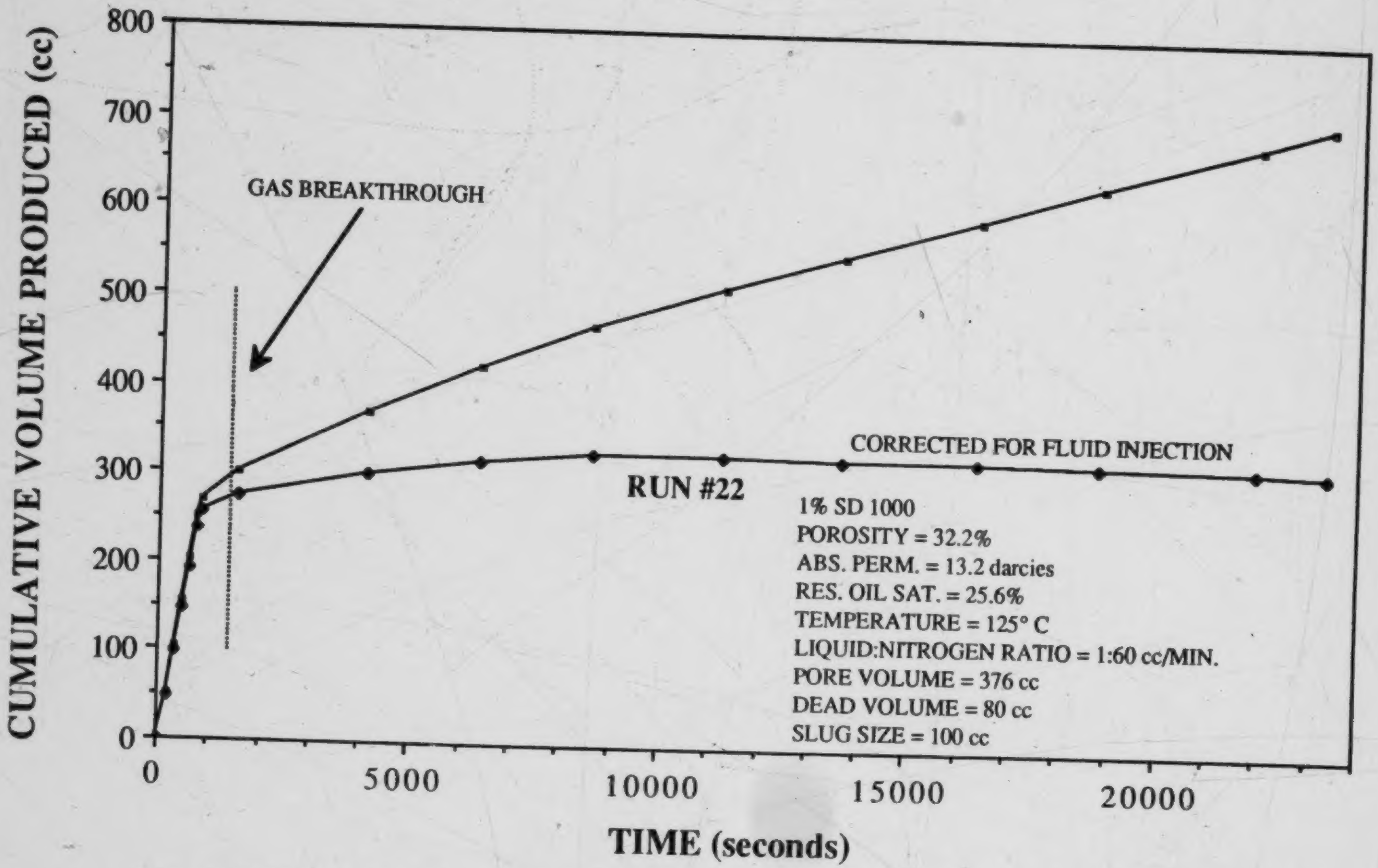

Figure 5.83 Run 22: Cumulative Volume Produced Vs. Time, Nitrogen Surfactant Co-injection, Residual Oil Saturation 1% SD1000 125°C

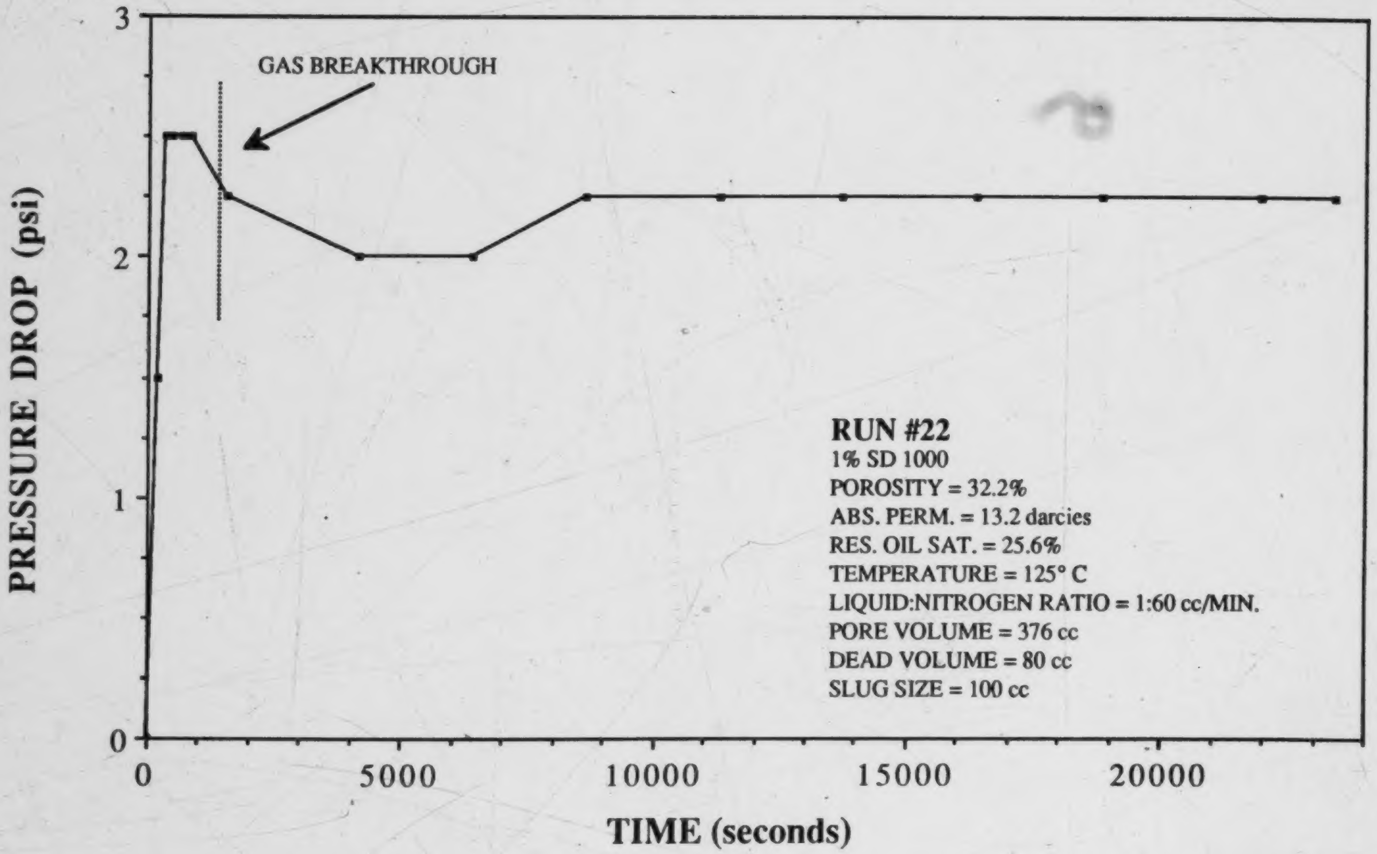

Figure 5.84 Run 22: Pressure Drop Vs. Time, Nitrogen Surfactant Co-injection, Residual Oil Saturation 1% SD1000 125°C

Relative mobility was used to determine the effectiveness of the surfactant at reducing gas mobility. This was done to analyze the effect of surfactant and temperature independent of the glass bead pack permeability. Run 22, which was conducted at an elevated temperature of 125° C, with a 1 percent surfactant solution, exhibited the lowest relative mobility. A relative mobility comparison is presented in Figure 5.85 for Runs 2, 4, 8 and 22.

The relative mobility in Run 11, the 1 percent surfactant run in which no residual oil was present was 0.154 cp^{-1}. With the addition of oil, the relative mobility in the 1 percent SD1000 run, Run 2, was 0.716 cp^{-1}. This value is very similar to the relative mobility of the oil-saturated core run where no surfactant was used (Run 8) viz. 0.787 cp^{-1}. The relative mobility in Run 4, the 5 percent run, was 0.5195 cp^{-1}. This suggests that additional surfactant is needed when oil is present. Isaacs et al.[24] found that the optimum surfactant concentration was shifted to a higher concentration in the presence of oil.

5.3.5 Effect of Surfactant Type

Two surfactants were used during the co-injection series of runs, viz. Chevron Chaser SD1000 and Dow surfactant. The runs examined to compare these surfactants are: Run 11, Run 15, (performed with 1% SD1000), Run 23 and Run 27, (performed with

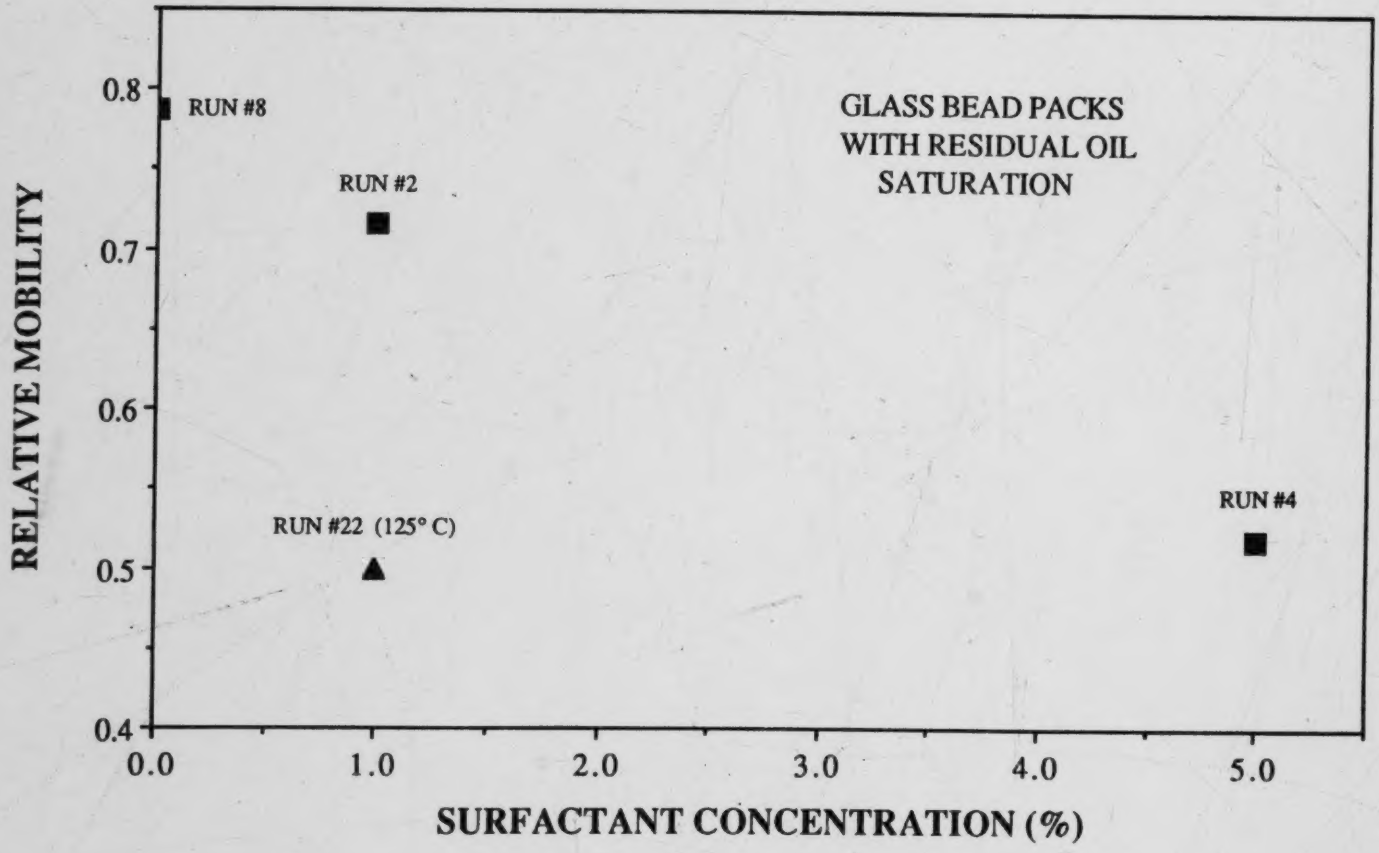

Figure 5.85 Comparison of the Relative Mobility for Runs 2, 4, 8 and 22

1% Dow Surfactant). All of these runs have been examined in detail in the previous sections.

For both runs performed at room temperature, Run 11 and Run 23, a 1 percent surfactant solution was used. A comparison of pressure profiles for these runs is presented in Figure 5.86. It is apparent that the Dow surfactant caused a much greater pressure drop across the core. Run 23 never reached a stabilization point. The experiment was terminated when the differential pressure exceeded the transducer limit. The gas phase mobility was much less for the Dow surfactant; 0.250 darcies/cp compared with 2.18 darcies/cp for the SD1000 case.

The differential pressures for the two runs performed at 125° C are compared in Figure 5.87. The differential pressure for Run 27 reached 200 psi. The total mobility was less than 0.0694 darcies/cp for the Dow surfactant. The total mobility was 0.176 darcies/cp for Run 15, the SD1000 run. The Dow surfactant produced a lower total mobility both at ambient conditions and at 125° C.

In order to visually examine the reaction of the foams formed by these surfactants a bench test was performed. One percent solutions of two surfactants were agitated in closed containers; a small amount of oil was introduced into each system. In the Dow surfactant solution the oil mixed with the foam and caused very small oil droplets to be mixed with the foam. In the SD1000 solution, the foam immediately dissipated, leaving a small amount of oil

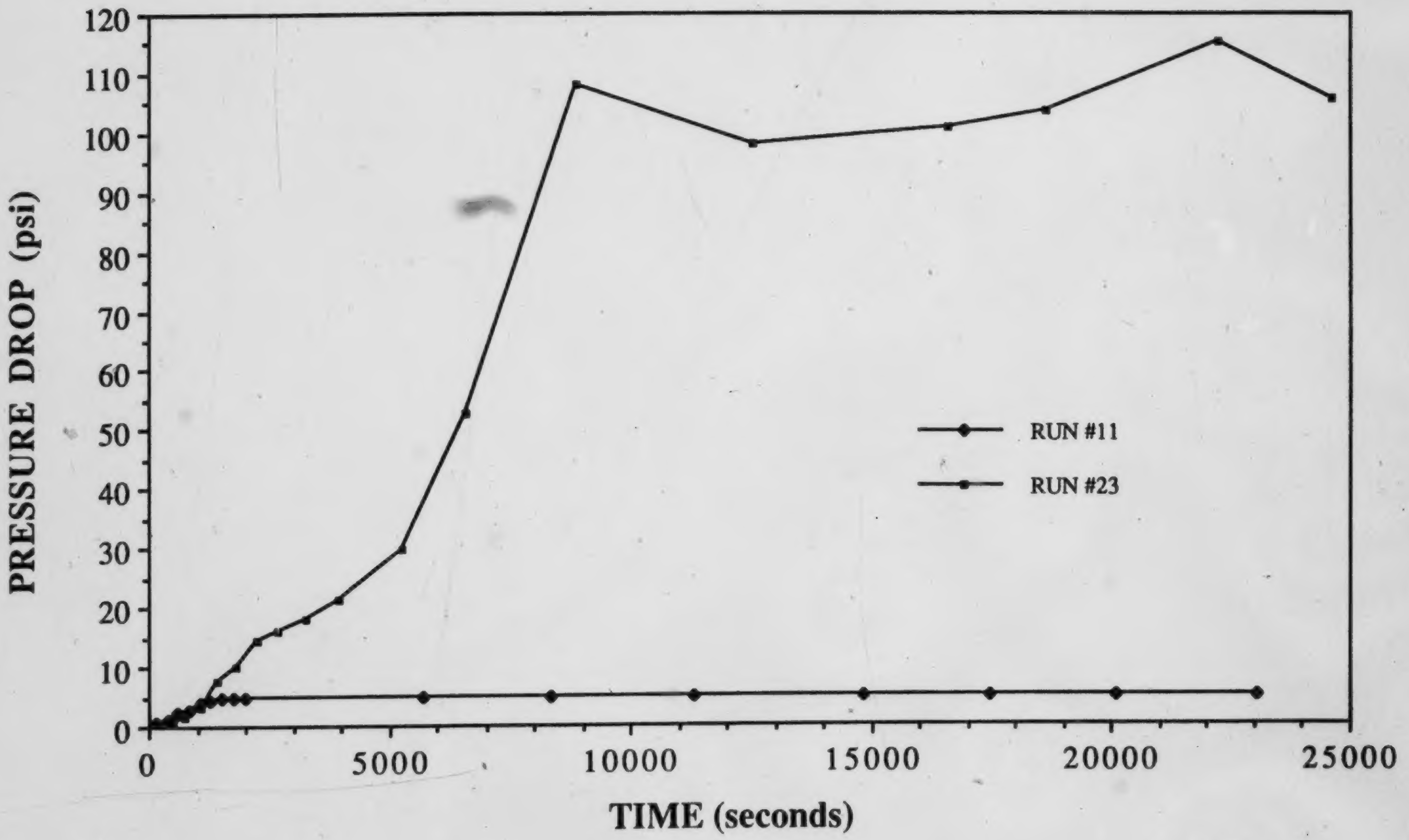

Figure 5.86 Comparison of the differential pressure for Run 11 and Run 23, SD1000 and Dow surfactants respectively

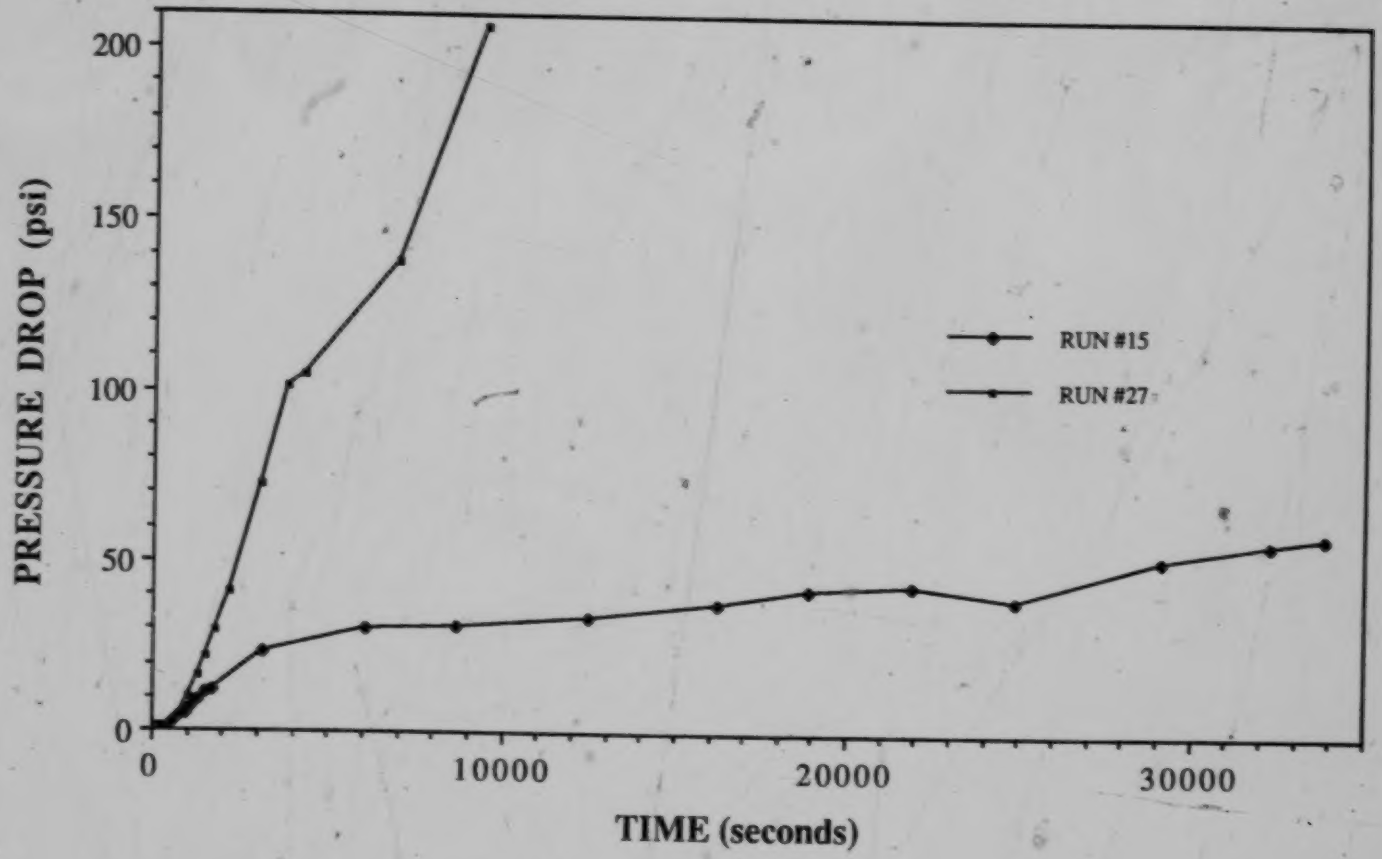

Figure 5.87 Comparison of the differential pressure for Run 15 and Run 27, SD1000 and Dow surfactants respectively 125°C

floating on the surface. Therefore it would seem that the Dow surfactant is more resistant to oil contamination than SD1000.

5.3.6 Effect of Residual Gas Saturation

Run 10 was performed with a residual gas saturation of 19 percent in the core. This run was performed with 1 percent SD1000 on a 3.5 darcy glass bead pack. The data for this run is given in Table 5.34. The gas breakthrough time was 31.5 minutes. The volume produced at this point was 383 cc. The cumulative volume produced versus time is presented in Figure 5.88. The stabilized corrected cumulative volume was 340 cc. A comparison of the cumulative volumes for this run and Run 1, performed with SD1000, is presented in Figure 5.89. This plot shows the similarity of the runs. The residual gas saturation decreased the amount of liquid available for production. The residual liquid saturation in the core was calculated to be 34.2 percent.

The differential profile, presented in Figure 5.90 shows that the pressure increased until gas breakthrough at which point it dropped slightly and stabilized at 5.25 psi. A comparison of this pressure drop with that in Run 1, is presented in Figure 5.91. This graph shows that the increased trapped gas saturation did not promote foam development. The relative mobility in this Run was 0.593 cp^{-1} compared with 0.154 cp^{-1} for Run 1.

Experimental Data For Run #10
1% SD 1000 Glass Bead Size #9

Surfactant: SD 1000
Concentration: 1%
Absolute Permeability: 3.5 darcies
Porosity: 32.9%
Back Pressure: 50 psi

Glass Bead Size: #9
Residual Gas Saturation: 19.0%
Temperature: Ambient
Gas Breakthrough: 31:30 (min.)
Totalizer Reading @ BT.: 192

Time (s)	Volume (cc)	Cumulative Volume (cc)	Refractive Index Conc. (%)	Spectro. Conc. ppm	Pressure Drop (psi)	Totalizer Reading
300	47	47.0	0	89.2	1.00	31
450	44	91.0	0	60.3	1.75	55
750	37	128.0	0	63.5	3.00	78
930	38	166.0	0	48.7	3.00	93
1110	43	209.0	0	64.4	3.75	112
1350	49	258.0	0	80.4	4.25	136
1560	47	305.0	0	89.1	5.25	158
1770	47	352.0	0	2002	5.75	180
2055	31	383.0	35	3597	5.75	209
5040	42	425.0	70	7284.1	5.25	512
7470	39	464.0	100	10002	5.25	758
10020	43	507.0	100	9987	5.25	1019
12960	49	556.0	100	9978	5.25	1318
15840	47	603.0	100	9892	5.25	1617

Table 5.34 Experimental Data for Run 10: 1% SD1000 Residual Gas Saturation

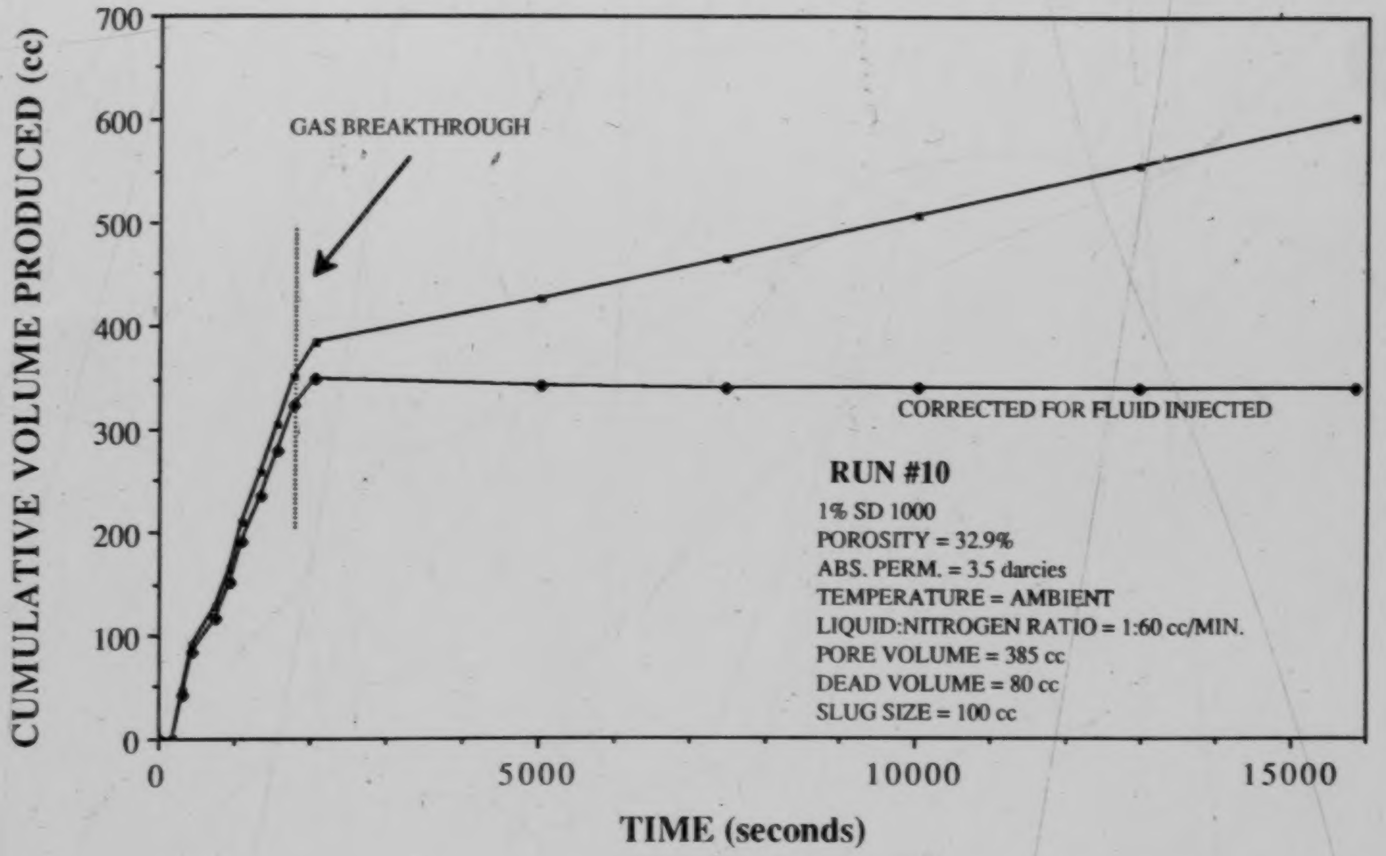

Figure 5.88 Run 10: Cumulative Volume Produced Vs. Time, Nitrogen Surfactant Co-injection, Residual Gas Saturation 1% SD1000

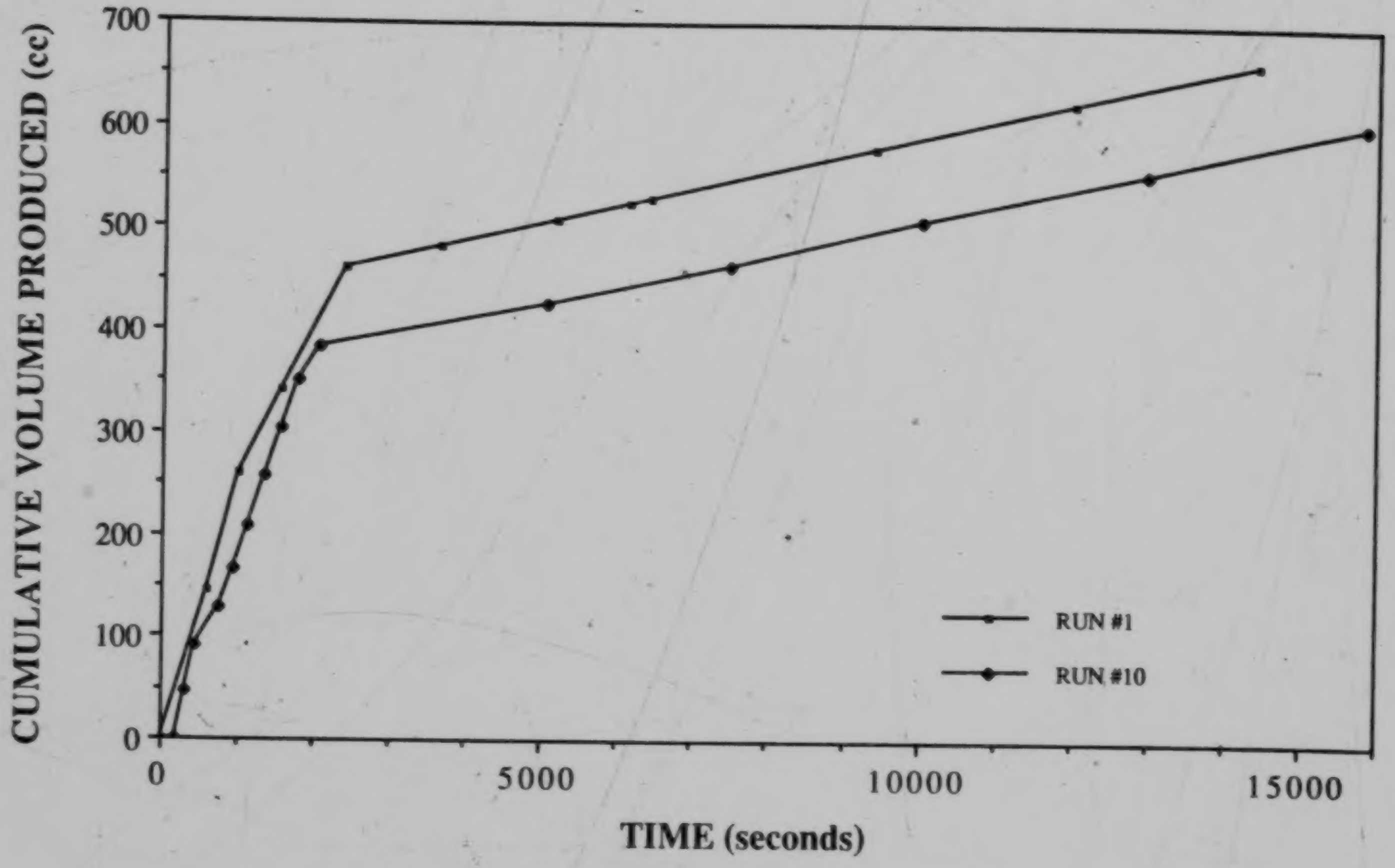

Figure 5.89 Comparison of the Cumulative Volumes Produced for Run 10 (Residual Gas Saturation) and Run 11, 1% SD1000

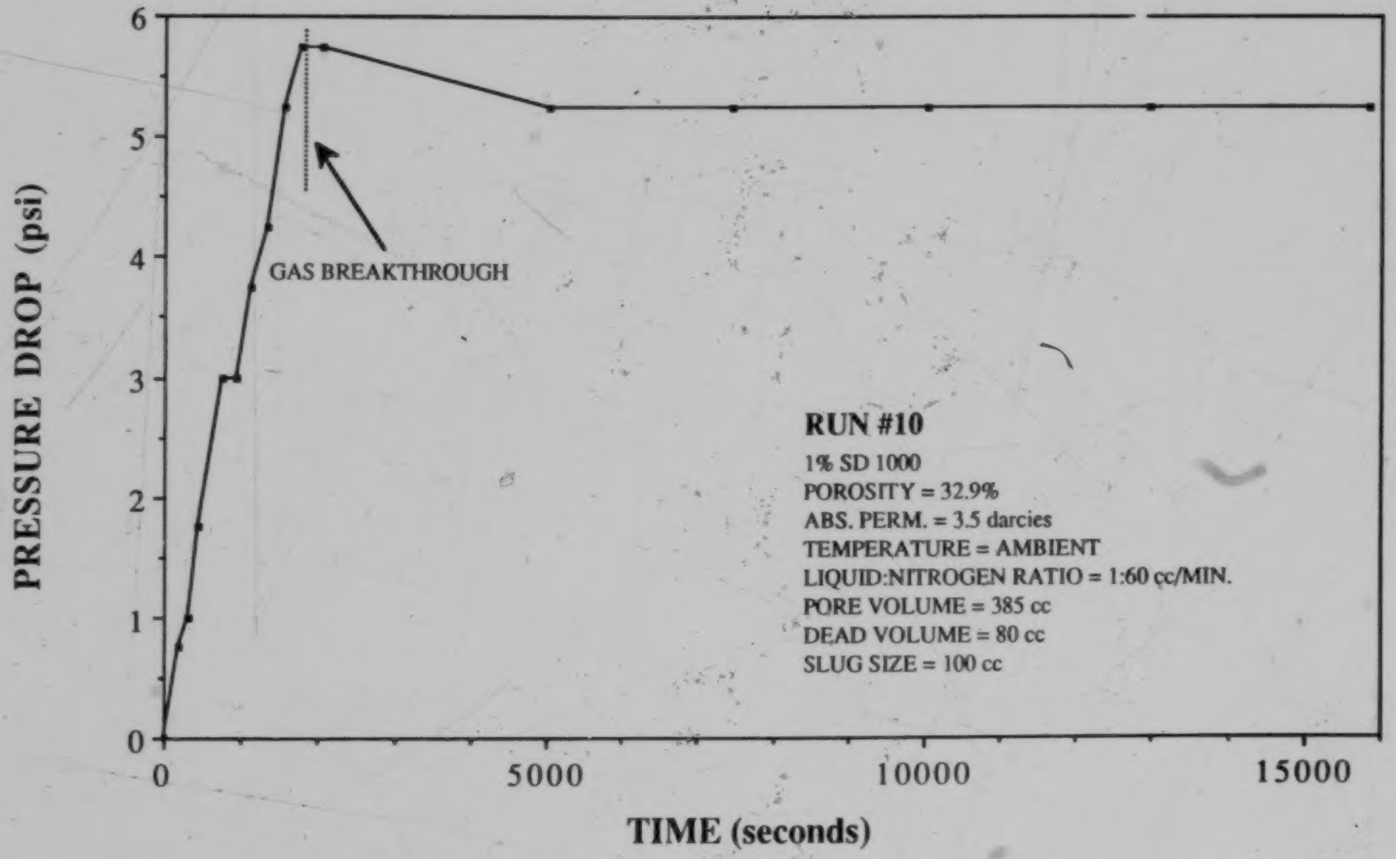

Figure 5.90 Run 10: Pressure Drop Vs. Time, Nitrogen Surfactant Co-injection, Residual Gas Saturation 1% SD1000

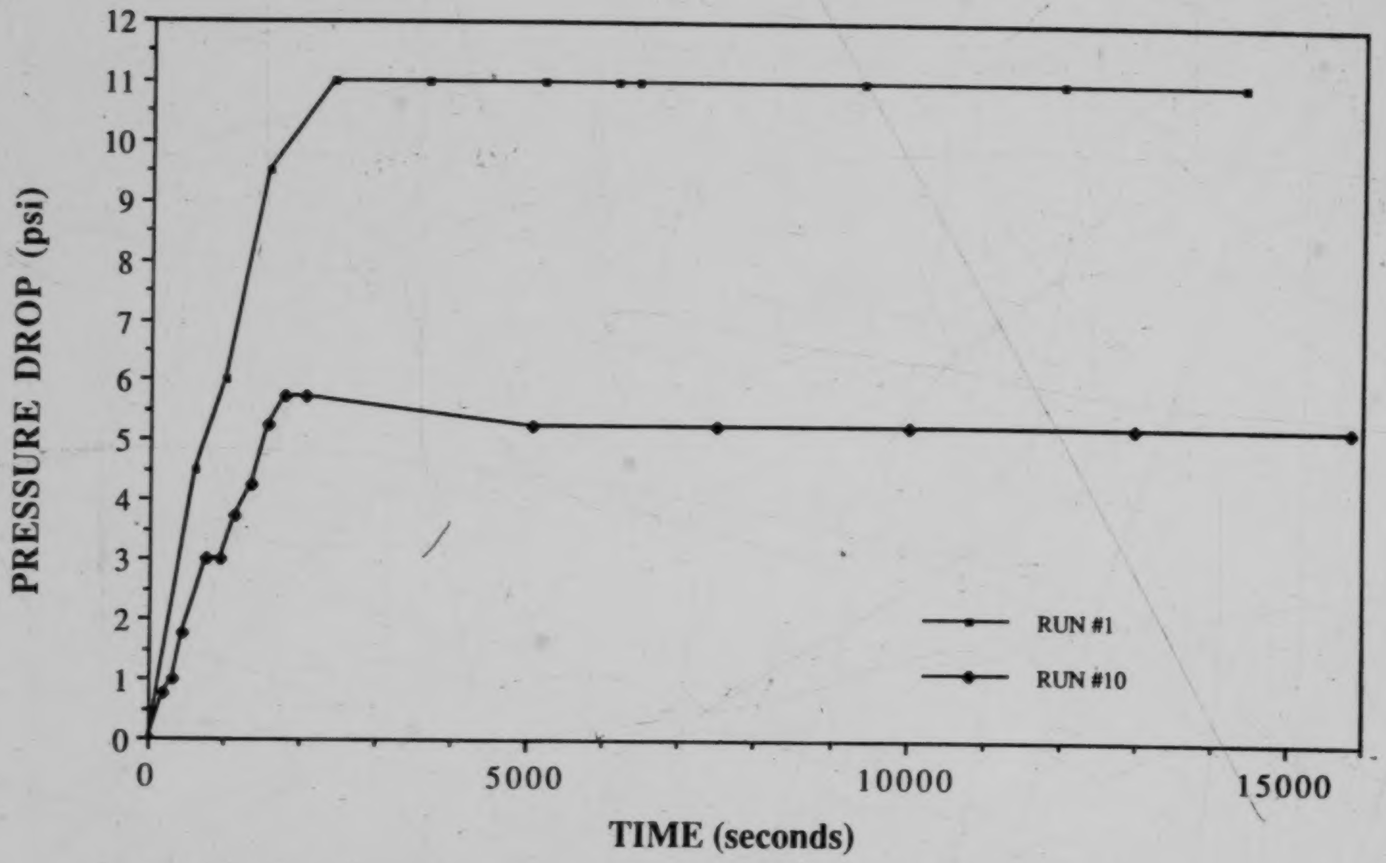

Figure 5.91 Comparison of the Differential Pressure for Run 10 (Residual Gas Saturation) and Run 11, 1% SD1000

The concentration graph is presented in Figure 5.92. The surfactant concentration of the sample collected at gas breakthrough was 36.0 percent. Therefore the run showed a typical surfactant run displacement.

5.3.7 Effect of the Foam Generator

In all runs, except Run 12, a foam generator was used prior to the inlet of the test core. Runs 11 and 12 are discussed here to examine the effect of the foam generator on the displacement behaviour. Run 12 was performed without the use of a foam generator. Instead, an equivalent volume of tubing was used. The data for this run is given in Table 5.35. The time until gas breakthrough was 33.75 minutes; the volume produced at gas breakthrough was 459.5 cc. Figure 5.93 is a graphical representation of the cumulative volume produced versus time. The stabilized corrected produced volume was 425 cc. The residual water saturation was 30.4 percent.

Figure 5.94 is a comparison of the cumulative volume produced versus time for Run 12 and Run 11, which utilized a foam generator. The produced volumes for these runs are very similar.

The differential pressure profile is presented in Figure 5.95. The stabilized pressure drop was 6.75 psi. A comparison of the differential pressures for Run 11 and Run 12 is presented in Figure

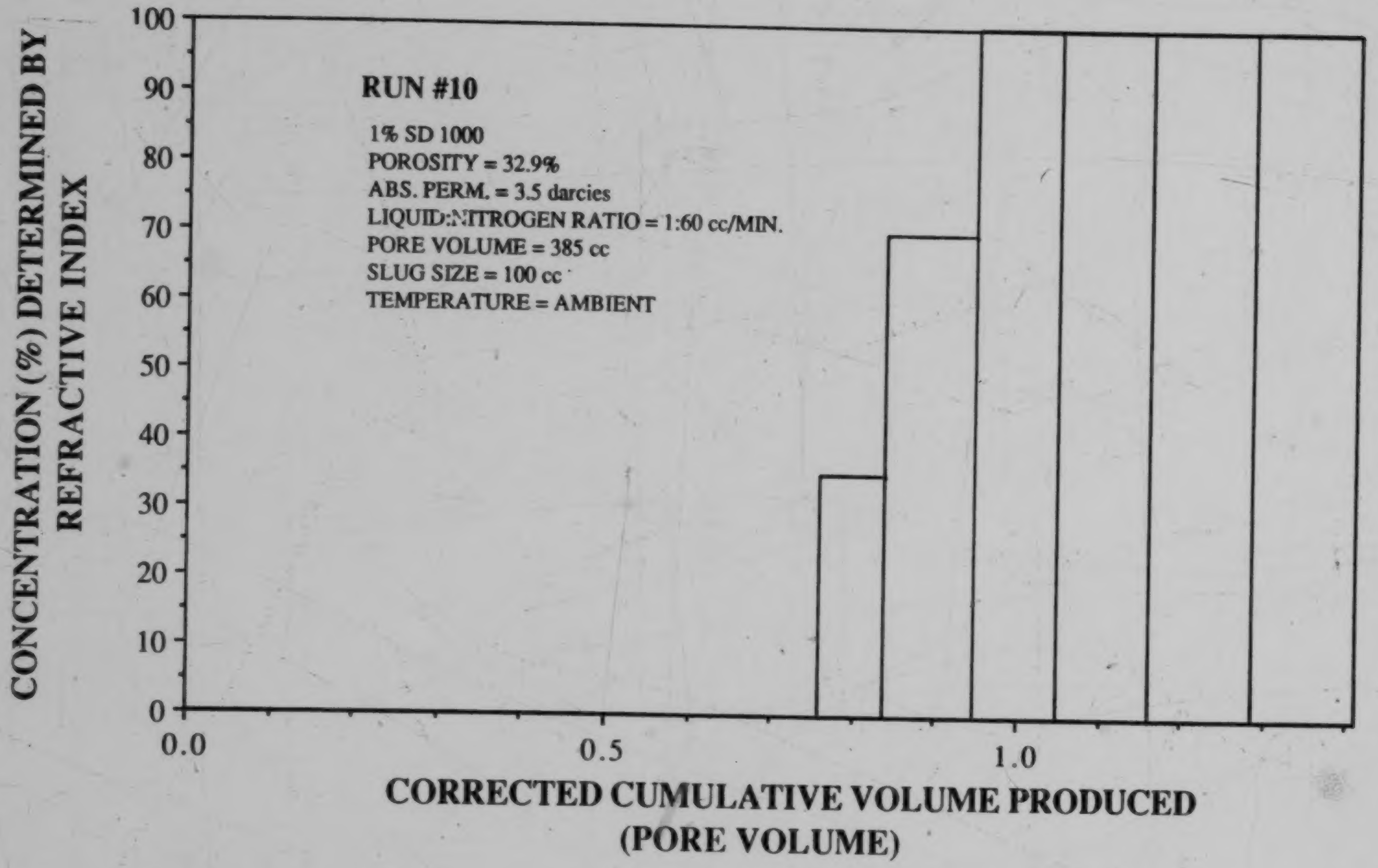

Figure 5.92 Run 10: Concentration Determined by UV Spectrophotometer Analysis Vs. Corrected Cumulative Volume Produced, Nitrogen Surfactant Co-injection, Residual Gas Saturation 1% SD1000

Experimental Data For Run #12
1% SD 1000 Glass Bead Size #9

Surfactant:	SD 1000	**Glass Bead Size:**	#9 * New Supplier
Concentration:	1%	**Residual Oil Saturation:**	no
Absolute Permeability:	12.7 darcies	**Temperature:**	Ambient
Porosity:	32.7%	**Gas Breakthrough:**	33:45 (min.)
Back Pressure:	50 psi	**Totalizer Reading @ BT.:**	199
		No Foam Generator	

Time (s)	Volume (cc)	Cum. Vol. (cc)	Spectro. Conc. ppm	Pressure Drop (psi)	Totalizer Reading
150	50	51.0	63.1	1.25	14
345	45	96.0	85.3	1.50	34
555	48	144.0	2.1	2.00	56
780	48	192.0	4.3	2.75	78
1020	53	245.0	48.9	3.50	102
1230	49	294.0	84.6	4.25	125
1470	48.5	342.5	10.2	5.00	147
1695	50	392.5	60.1	5.75	171
1920	47	439.5	2956	6.25	194
2070	20	459.5	5971	6.50	201
4485	42	501.5	7897	6.75	452
7140	46	547.5	8320	6.75	720
10380	53.5	601.0	9529	6.75	1048
13020	42.5	643.5	9904	6.75	1310
15960	48	691.5	9506	6.75	1610
18930	50	741.5	9266	6.75	1890
21840	45	786.5	9210	6.75	2201

Table 5.35 Experimental Data for Run 12: 1% SD1000 No Foam Generator

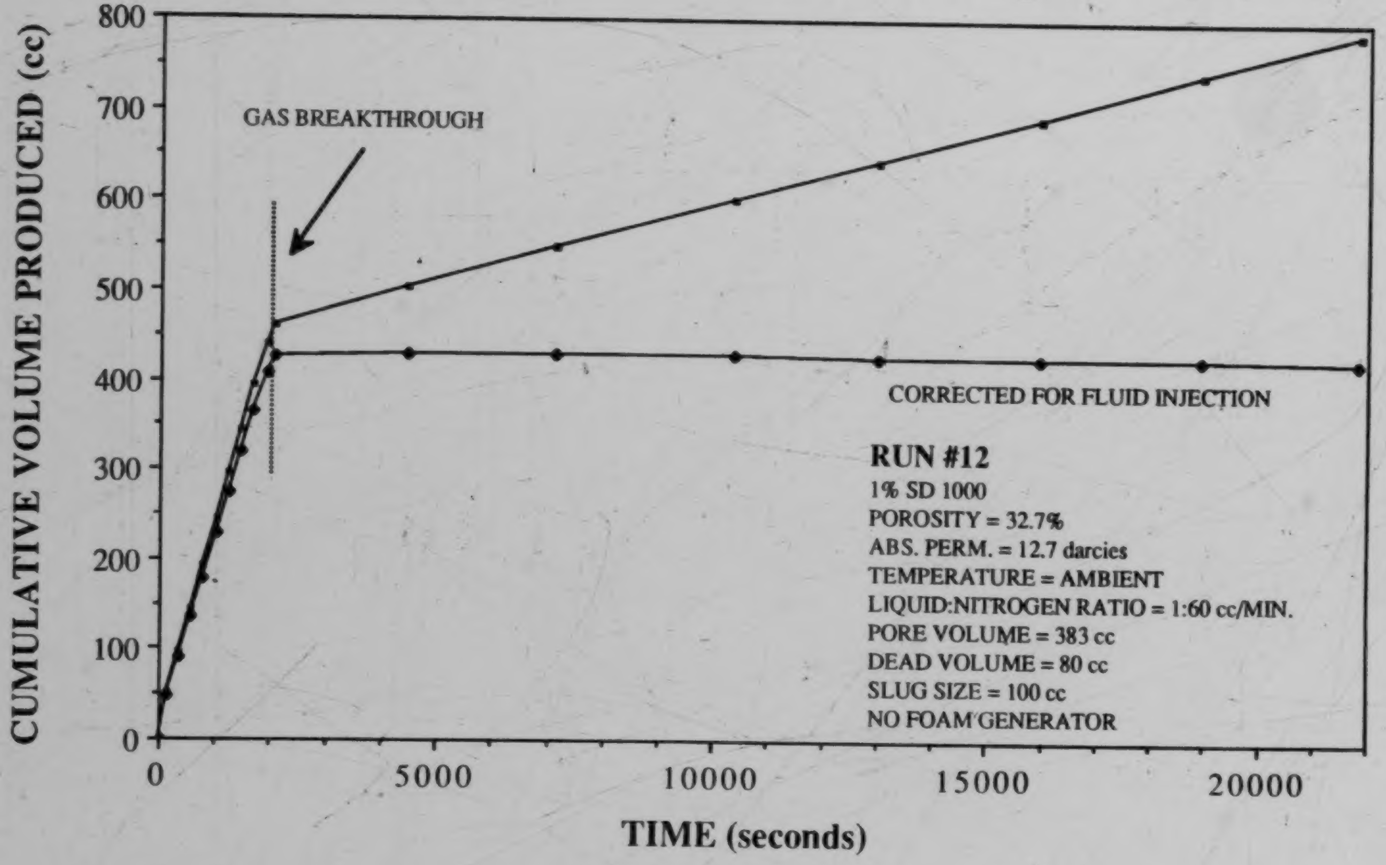

Figure 5.93 Run 12: Cumulative Volume Produced Vs. Time, Nitrogen Surfactant Co-injection, No Foam Generator 1% SD1000

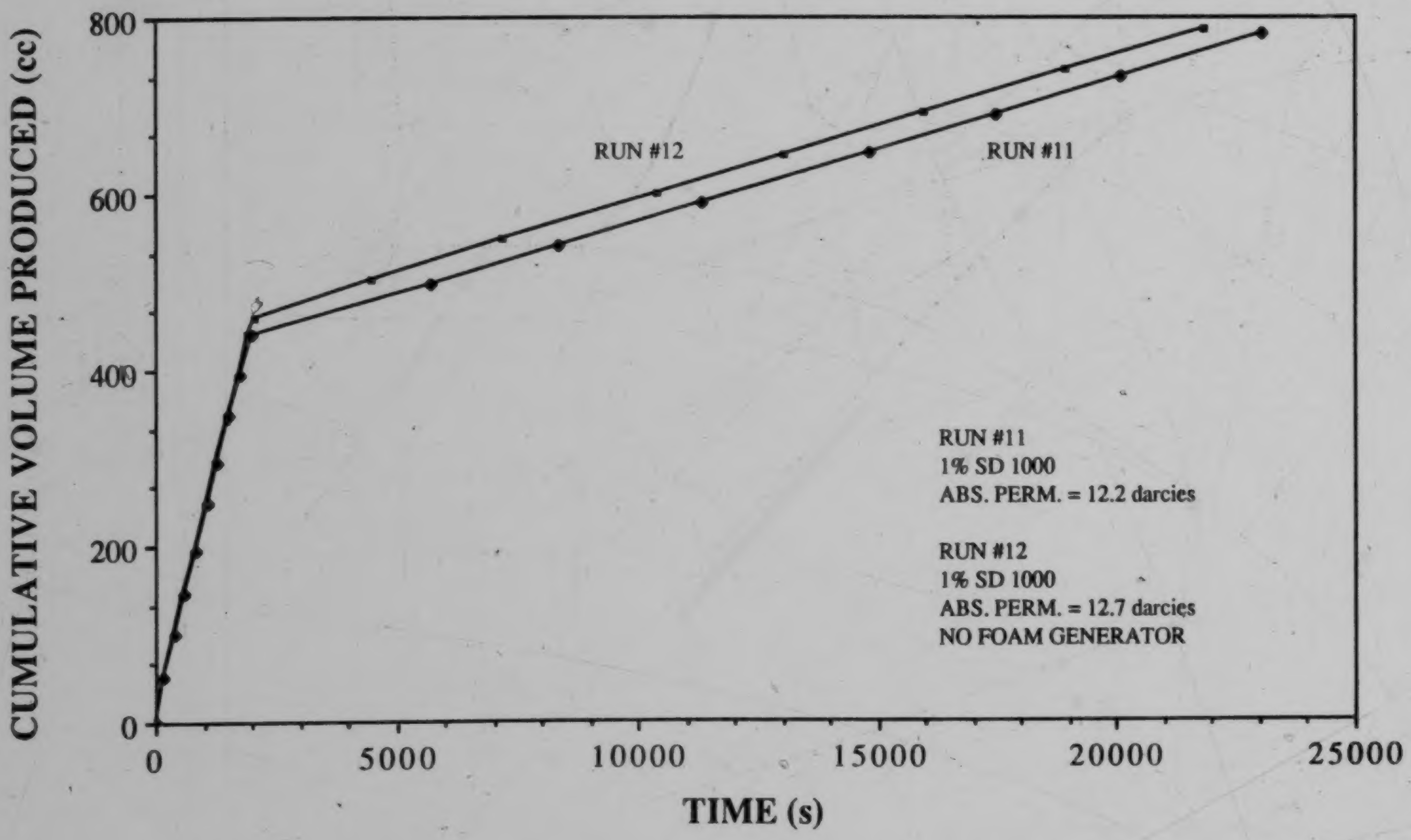

Figure 5.94 Comparison of the Cumulative Volumes Produced for Run 12 (No Foam Generator) and Run 11, 1% SD1000

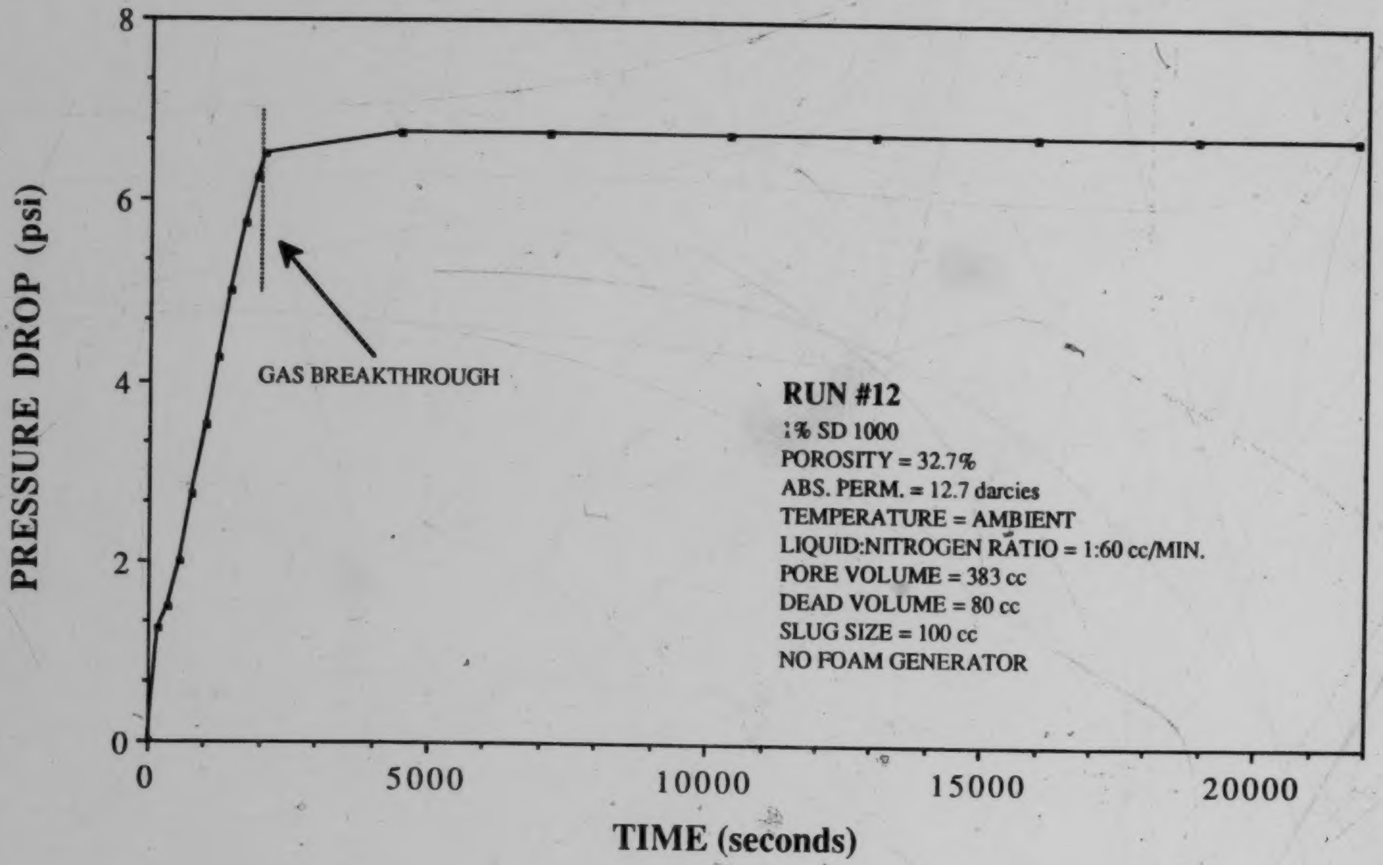

Figure 5.95 Run 12: Pressure Drop Vs. Time, Nitrogen Surfactant Co-injection, No Foam Generator 1% SD1000

5.96. From the graph the difference between these runs seems significant, however the difference is possibly within the range of experimental error. Therefore it can be concluded that the lack of a foam generator had no significant effect on the foam mobility. In fact, a foam generator may have disturbed the system and lowered the ability of the foam to reduce gas phase mobility.

The concentration graph, Figure 5.97, shows a typical mixing zone for an SD1000 surfactant run. The surfactant concentration of the sample collected at gas breakthrough was 59.7 percent. For Run 11 the concentration of this sample was 34.2 percent. (Refer to Figure 5.22)

5.3.8 Effect of Surfactant-Nitrogen Ratio

If the surfactant solution and nitrogen injection rates determine foam quality, then the quality for this run was 76.1 percent. The data for this run is given in Table 5.36. Run 20 was performed with a 1 percent solution of SD1000 on a 15.1 darcy glass bead pack. The surfactant solution, nitrogen ratio was 4:50 cc per minute. The lower gas rate was used to keep the total injected flow similar to that used, in the other runs. The gas breakthrough time was 34.5 minutes, and the volume produced at breakthrough was 495.0 cc. The cumulative volume produced versus time is presented in Figure 5.98. The stabilized corrected cumulative volume produced was 352 cc. The residual liquid saturation was 50.7 percent.

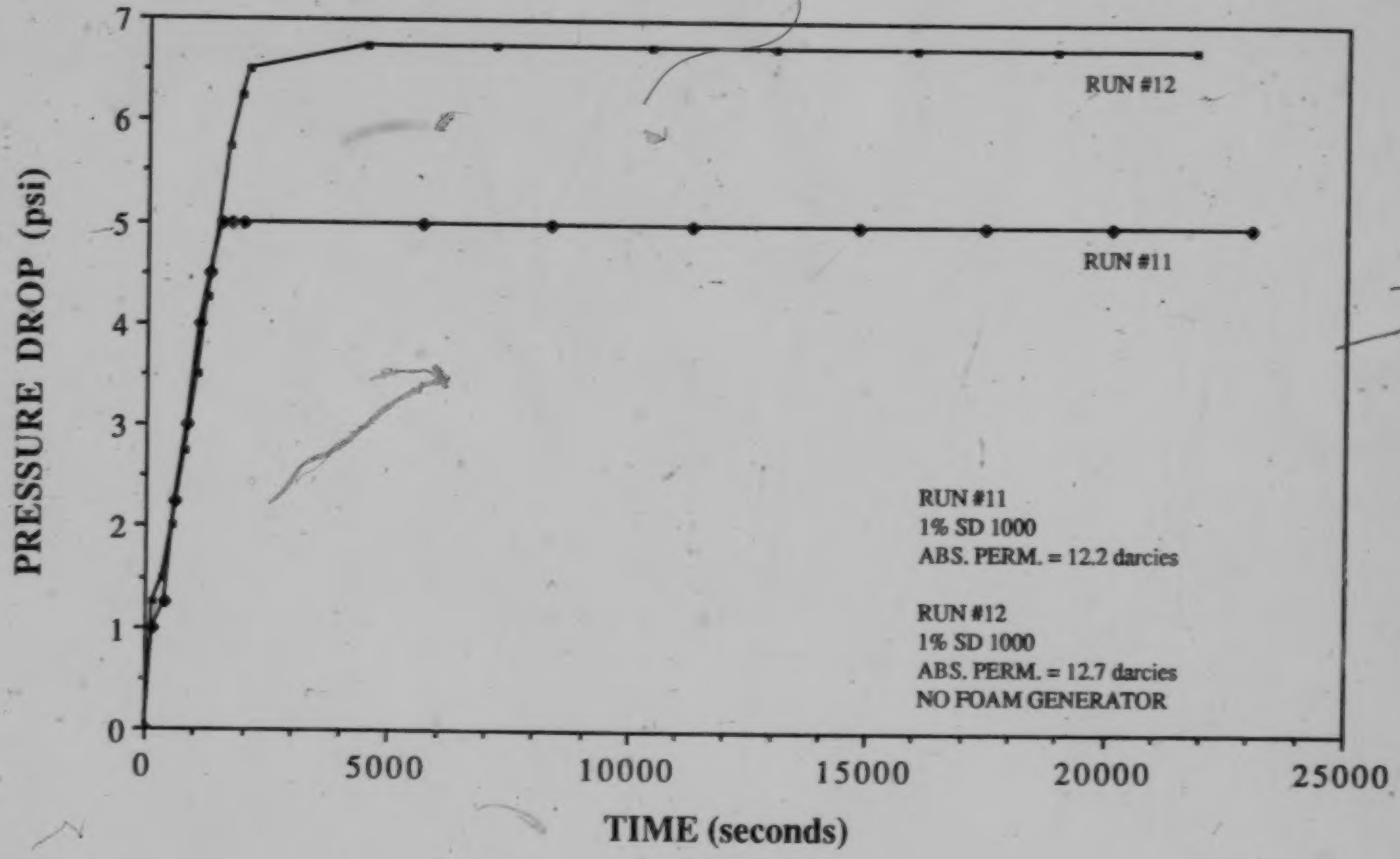

Figure 5.96 Comparison of the Differntial Pressure for Run 12 (No Foam Generator) and Run 11, 1% SD1000

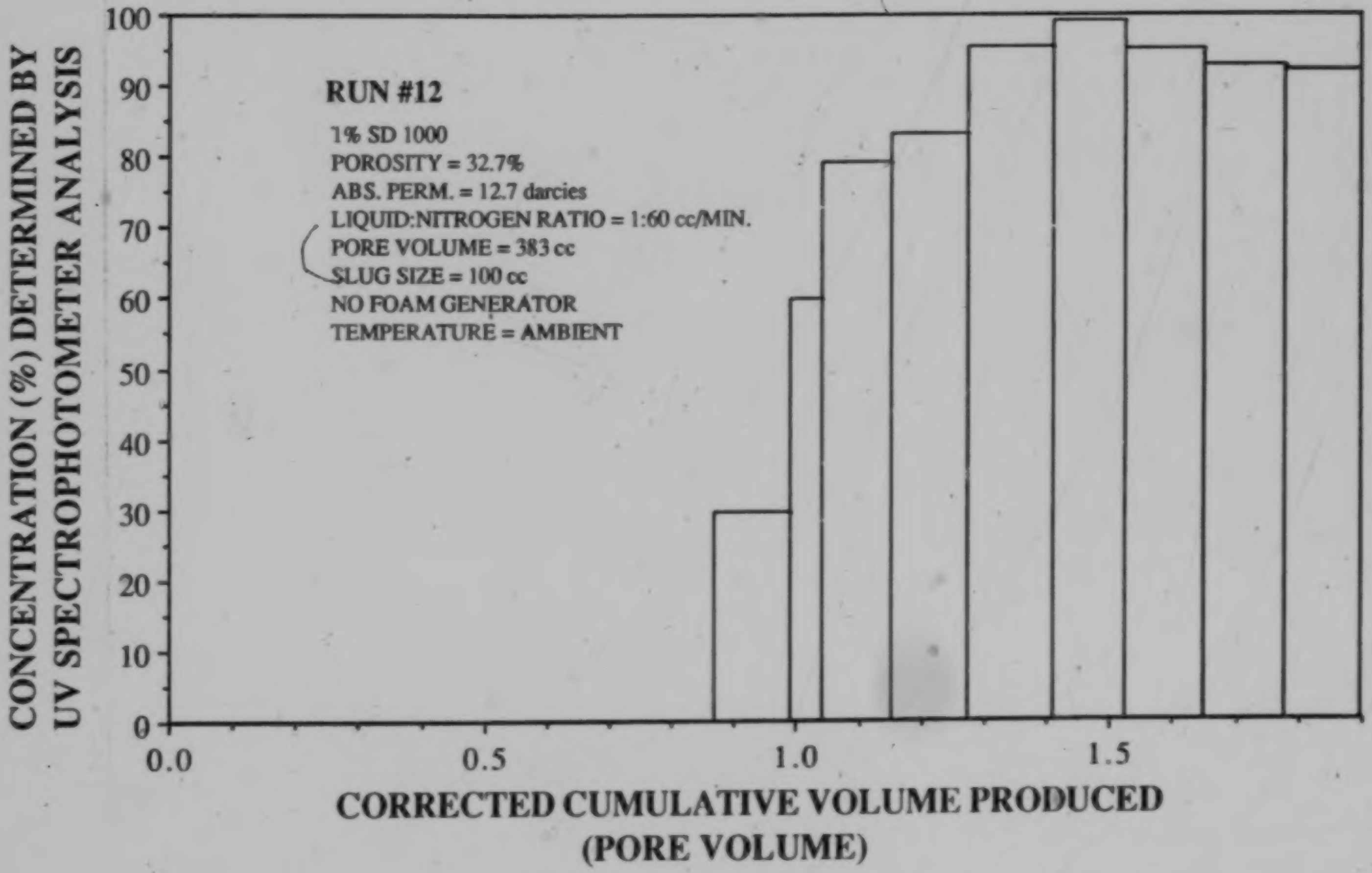

Figure 5.97 Run 12: Concentration Determined by UV Spectrophotometer Analysis Vs. Corrected Cumulative Volume Produced, Nitrogen Surfactant Co-injection, No Foam Generator, 1% SD1000

Experimental Data For Run 20
1% SD 1000 Glass Bead Size #9

Surfactant: SD 1000
Concentration: 1.00%
Absolute Permeability: 15.1 darcies
Porosity: 32.3%
Back Pressure: 50 psi
Glass Bead Size: #9
Residual Oil Sat.: no
Temperature: Ambient
Gas Breakthrough: 34:30 (min.)
Totalizer Reading @ BT.: 178

Time (s)	Volume (cc)	Cum. Vol. (cc)	Spectro. Conc. ppm	Pressure Drop (psi)	Totalizer Reading
120	51	51.0	126.0	0.75	11
300	49	100.0	108.0	1.25	31
570	51	151.0	6.0	2.25	50
780	49	200.0	2.0	3.00	67
1020	55	255.0	82.0	3.50	87
1230	50	305.0	92.0	4.25	105
1440	49	354.0	10.0	4.75	123
1650	48	402.0	196.0	5.50	142
1860	48	450.0	3165.0	6.25	159
2070	45	495.0	6275.0	6.50	178
2790	49	544.0	7407.0	6.25	240
3690	62	606.0	8398.0	6.25	317
4950	82	688.0	10002.0	6.25	429
5760	58	746.0	9996.0	6.25	496
6780	67	813.0	9763.0	6.25	581
8100	82	895.0	9350.0	6.25	696
9540	76	971.0	9986.0	6.25	875
11160	117	1088.0	9846.0	6.25	958
12330	80	1168.0	9645.0	6.25	1055
13740	96	1264.0	9985.0	6.25	1180
14700	68	1332.0	9862.0	6.25	1256
15420	40	1372.0	9756.0	6.25	1308

Table 5.36 Experimental Data for Run 20: 1% SD1000 Quality = 72%

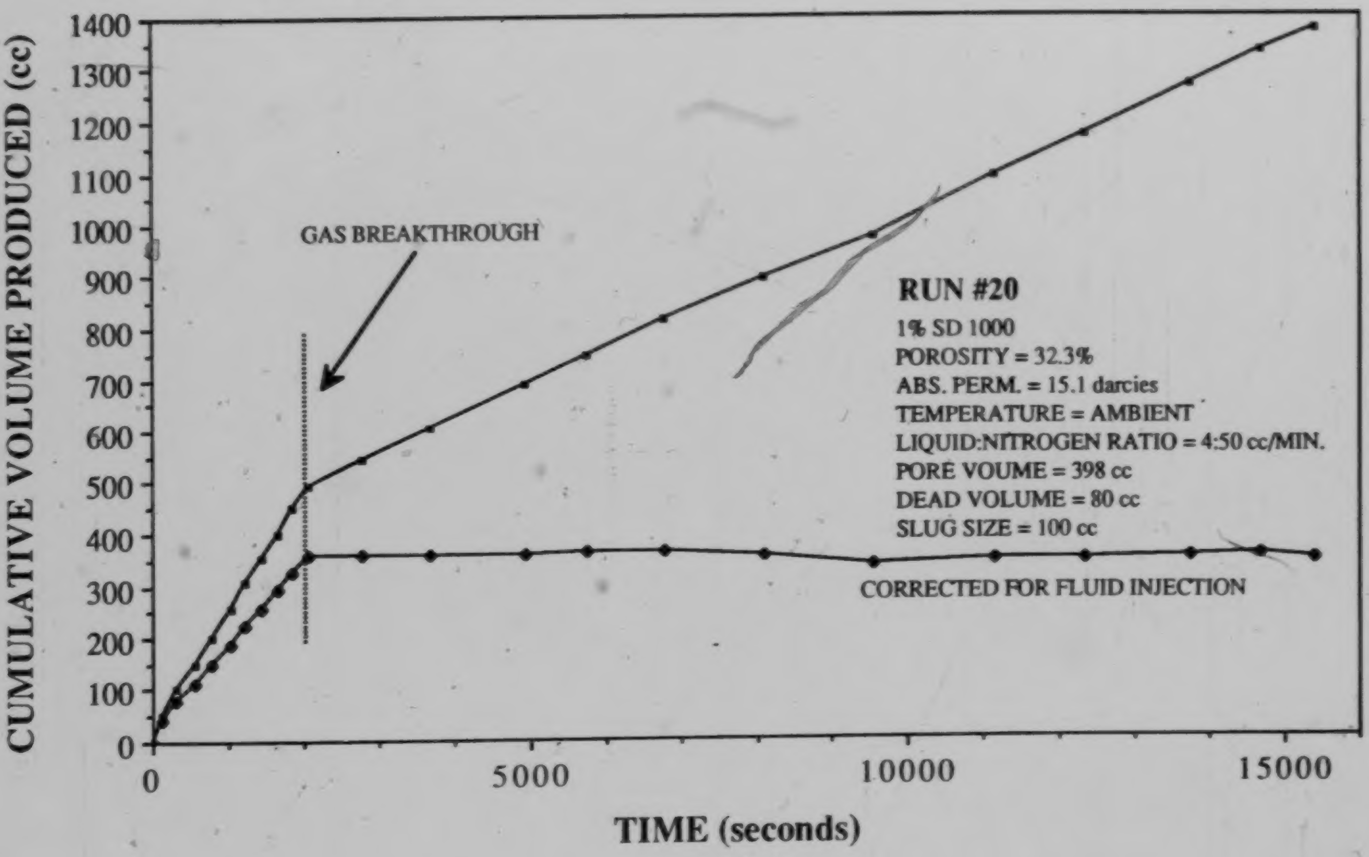

Figure 5.98 Run 20: Cumulative Volume Produced Vs. Time, Nitrogen Surfactant Co-injection, Quality = 72% 1% SD1000

The differential pressure profile is presented in Figure 5.99. The stabilized pressure drop was 6.25 psi. Figure 5.100 is a comparison of the pressure profiles for Run 11 and Run 20.

The stabilized differential pressure for Run 11 was 5.0 psi. The difference in stabilized pressures was very small. The relative mobility for Run 20 was 0.139 cp^{-1} and a 0.179 cp^{-1} for Run 11. Therefore it can be concluded that decreasing foam quality (72.3 percent to 93 percent) has a small effect on reducing gas mobility.

The concentration graph for Run 20 is presented in Figure 5.101. The surfactant concentration of the sample collected at gas breakthrough was 62.7 percent. It can be concluded that the gas did not bypass the surfactant.

5.3.9 Effect of Nitrogen Injection Without Surfactant Co-Injection

This run was performed to determine the effect of injecting nitrogen only, without surfactant co-injection. A slug of 100 cc of surfactant solution was injected into the core prior to nitrogen injection as was done for all co-injection runs.

Run 24 was performed with 1 percent Dow surfactant, at 125° C, on a 13.1 darcy glass bead pack. There was no surfactant co-

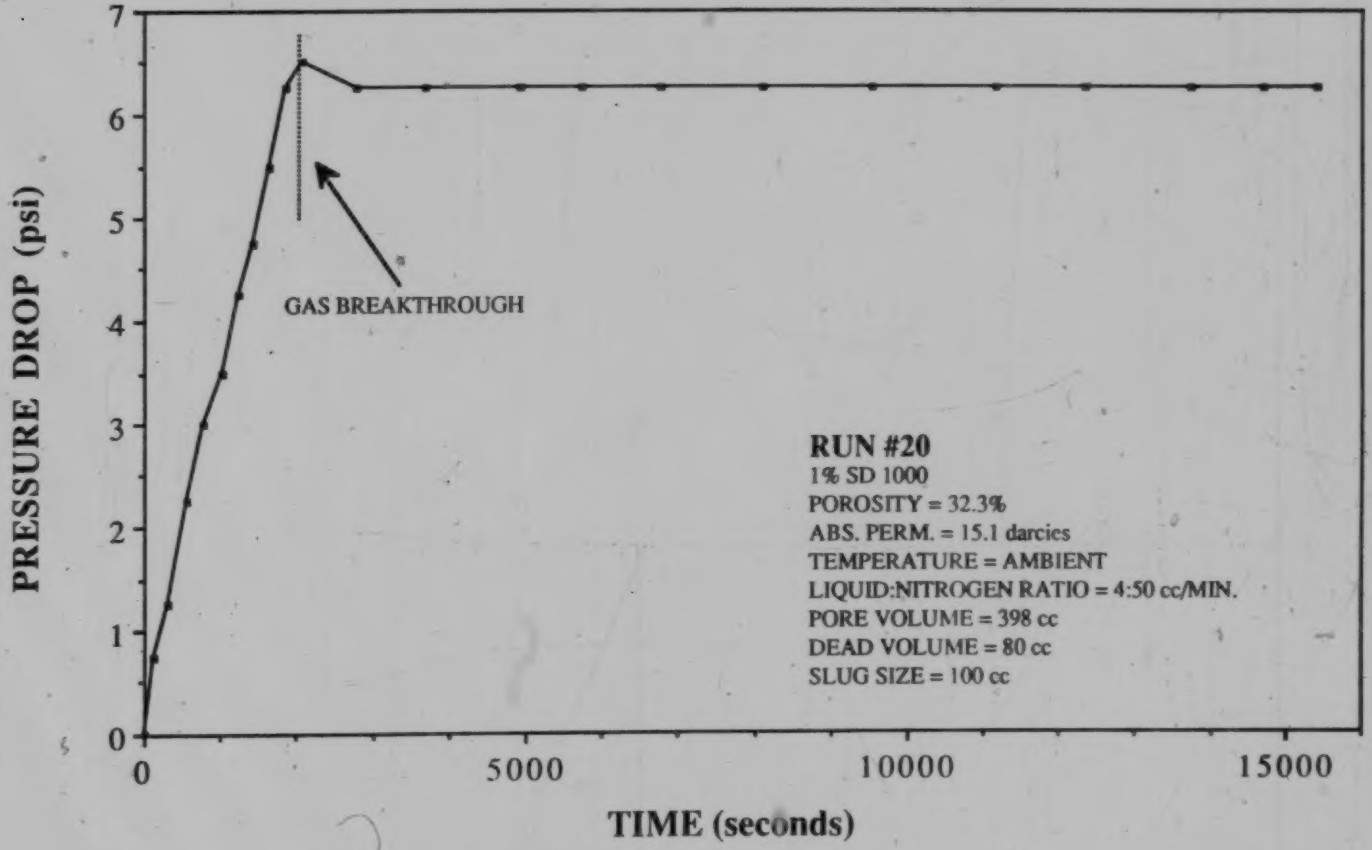

Figure 5.99 Run 20: Pressure Drop Vs. Time, Nitrogen Surfactant Co-injection, 1% SD1000 Quality = 72.0%

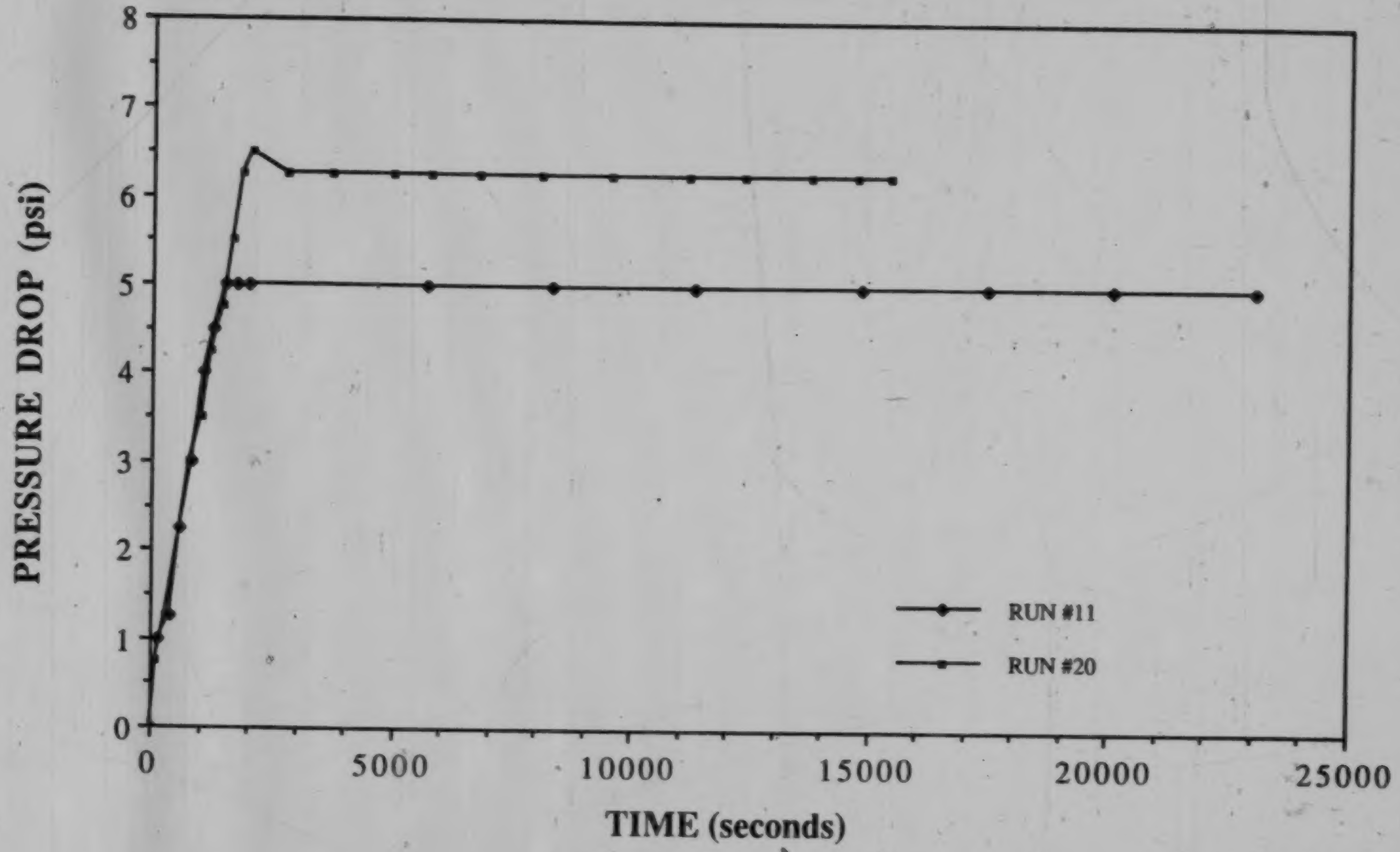

Figure 5.100 Comparison of the Differential Pressure for Run 20 (No Foam Generator) and Run 11, 1% SD1000 Quality = 72.0%

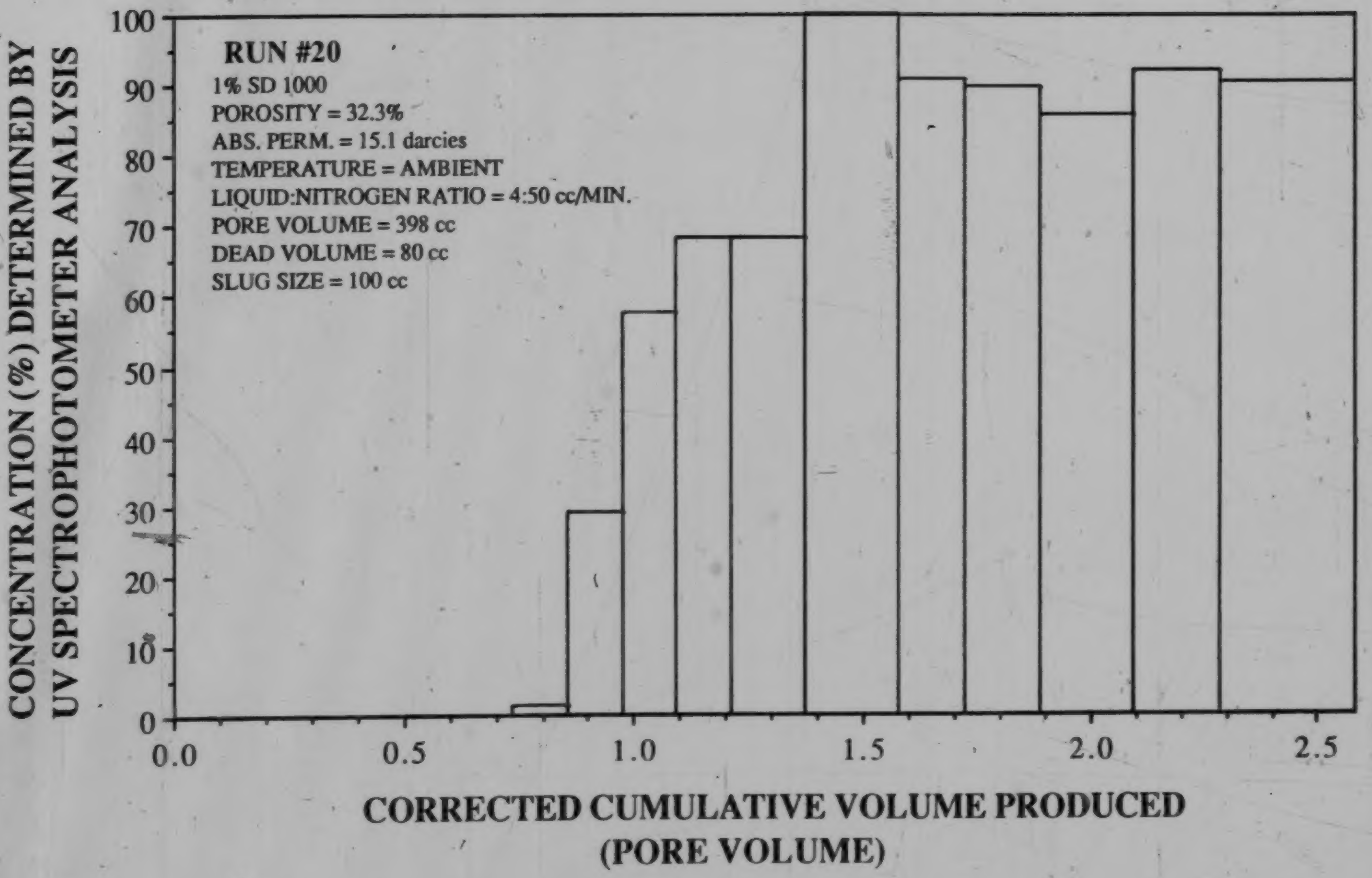

Figure 5.101 Run 20: Concentration Determined by UV Spectrophotometer Analysis Vs. Corrected Cumulative Volume Produced, Nitrogen Surfactant Co-injection, 1% SD1000 Quality = 72.0%

injected during this run. The data for this run is given in Table 5.37. The gas breakthrough time for this run was 32.5 minutes. The volume produced at gas breakthrough was 513 cc. The cumulative volume produced versus time is presented in Figure 5.102. It is interesting to compare this curve with that of Run 27, in which there was co-injection. The curves, as seen in Figure 5.103, show a similar initial trend but diverge at gas breakthrough.

The differential pressure profile is presented in Figure 5.104. The pressure continued to increase following gas breakthrough, but fell off drastically afterward, to 2 psi. Figure 5.105 provides a comparison with Run 27. This comparison indicates that without continuous surfactant injection, foams have little stability, particularly at a high temperature.

Recall that Run 11P maintained a pressure differential for 40 hours. The difference is probably due to two factors: the core for Run 11P was flushed several times with the surfactant solution until the effluent contained 100 percent of the injected surfactant concentration, and this run was performed at 125° C.

5.4 Dual Core Runs

Three runs were performed utilizing the dual core system. These runs were performed to examine the ability ~~of~~ foam to selectively block high permeability channels. For these runs a

Experimental Data For Run 24
1% Dow Surfactant Glass Bead Size #9

Surfactant:	Dow	**Glass Bead Size:**	#9
Concentration:	1.0%	**Residual Oil Sat.:**	no
Absolute Permeability:	13.1 darcies	**Temperature:**	125° C
Porosity:	33.6%	**Gas Breakthrough:**	32:30 (min.)
Back Pressure:	50 psi	**Totalizer Reading @ BT.:**	199

Time (s)	Volume (cc)	Cum. Vol. (cc)	Spectro. Conc. ppm	Pressure Drop (psi)	Totalizer Reading
30	44	51.0	56.0	0.25	3
255	47	98.0	42.0	0.50	26
420	46	144.0	13.0	1.20	43
600	45	189.0	13.0	4.10	62
810	46	235.0	19.0	7.60	82
990	45	280.0	24.0	10.10	101
1200	52	332.0	7.0	13.80	123
1380	42	374.0	14.0	15.70	141
1560	45	419.0	54.0	18.40	159
1740	45	464.0	1425.0	20.50	176
1920	49	513.0	3886.0	22.30	196
4560	15	528.0	5872.0	30.10	461
5340	5	533.0	6702.0	10.00	546
7140	2	535.0	7790.0	2.00	714

Table 5.37 Experimental Data for Run 24: 1% Dow Surfactant
No Continuous Surfactant Injection

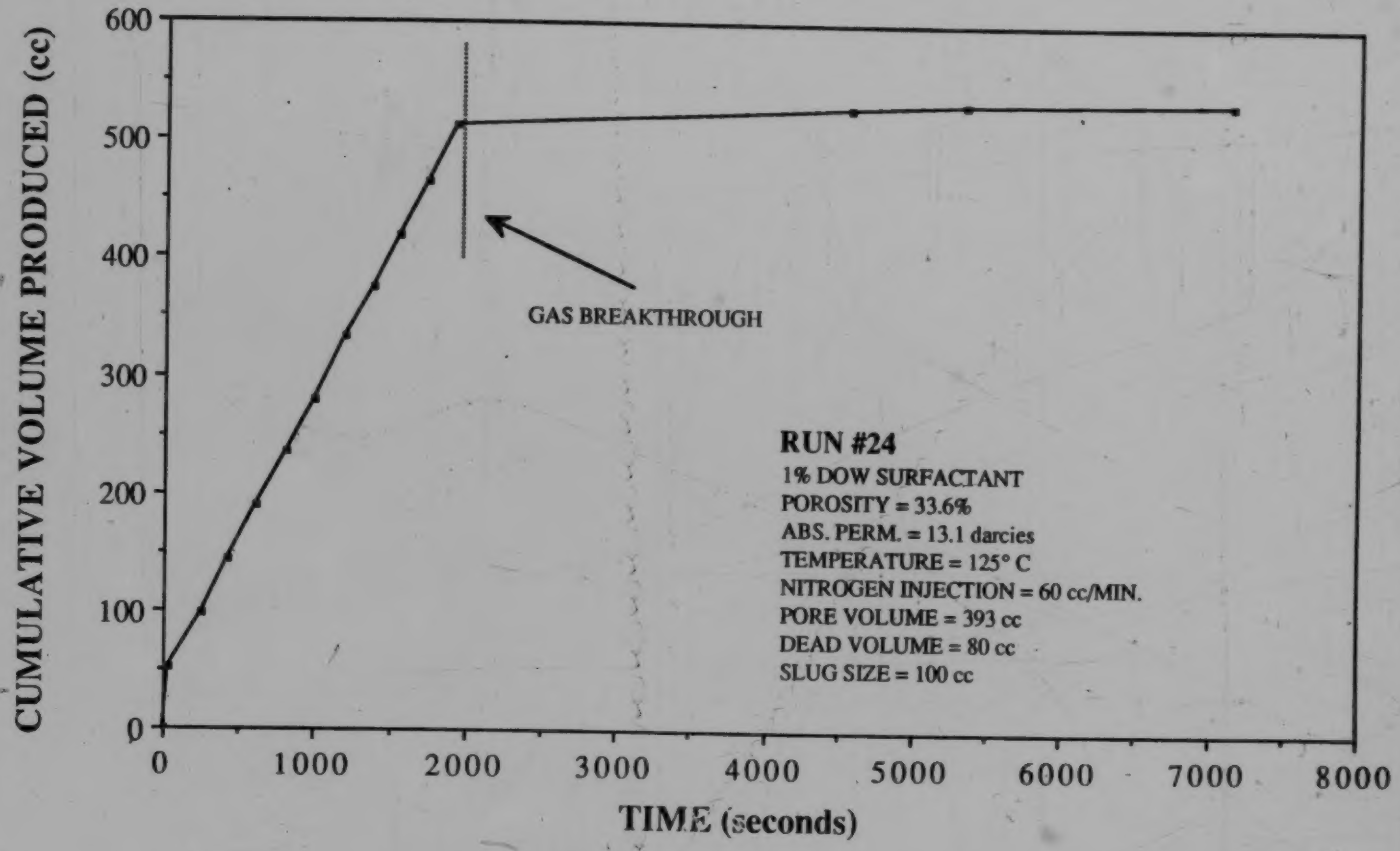

Figure 5.102 Run 24: Cumulative Volume Produced Vs. Time, Nitrogen Injection, 1% Dow Surfactant 125°C

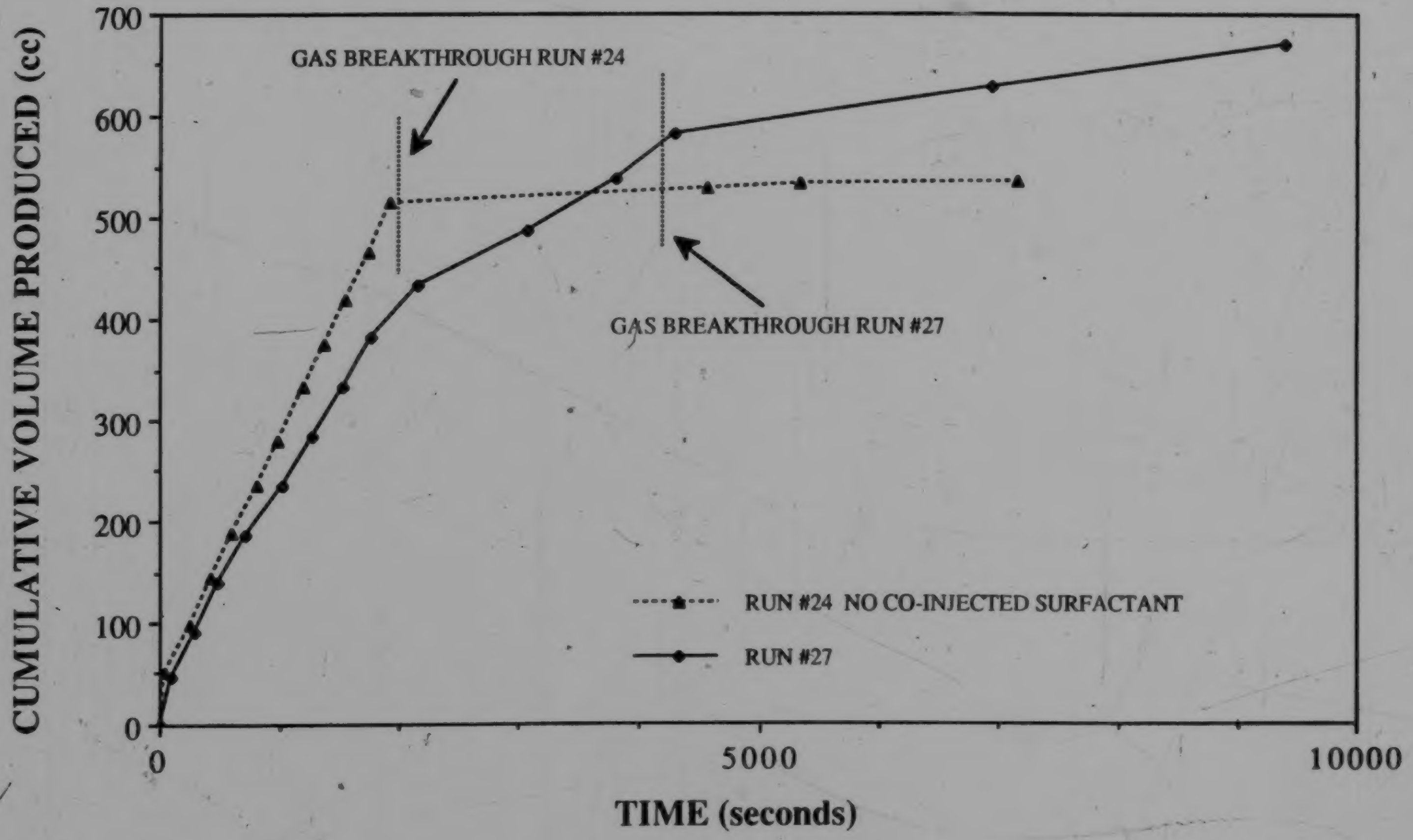

Figure 5.103 Comparison of the Cumulative Volumes Produced Vs. Time for Run 27 and Run 24 (No Surfactant Injection), 1% Dow Surfactant

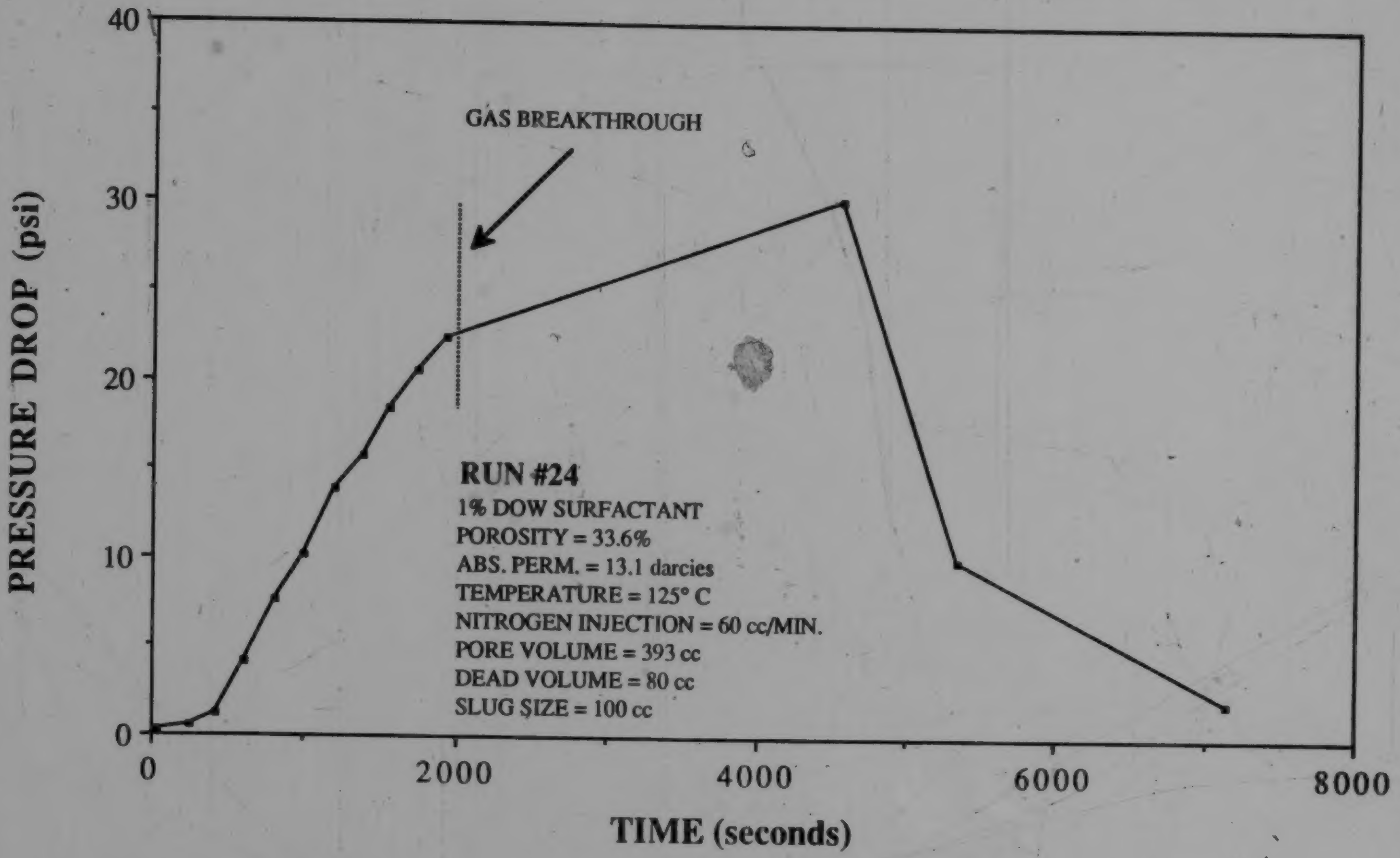

Figure 5.104 Run 24: Pressure Drop Vs. Time, Nitrogen Injection, 1% Dow Surfactant 125°C

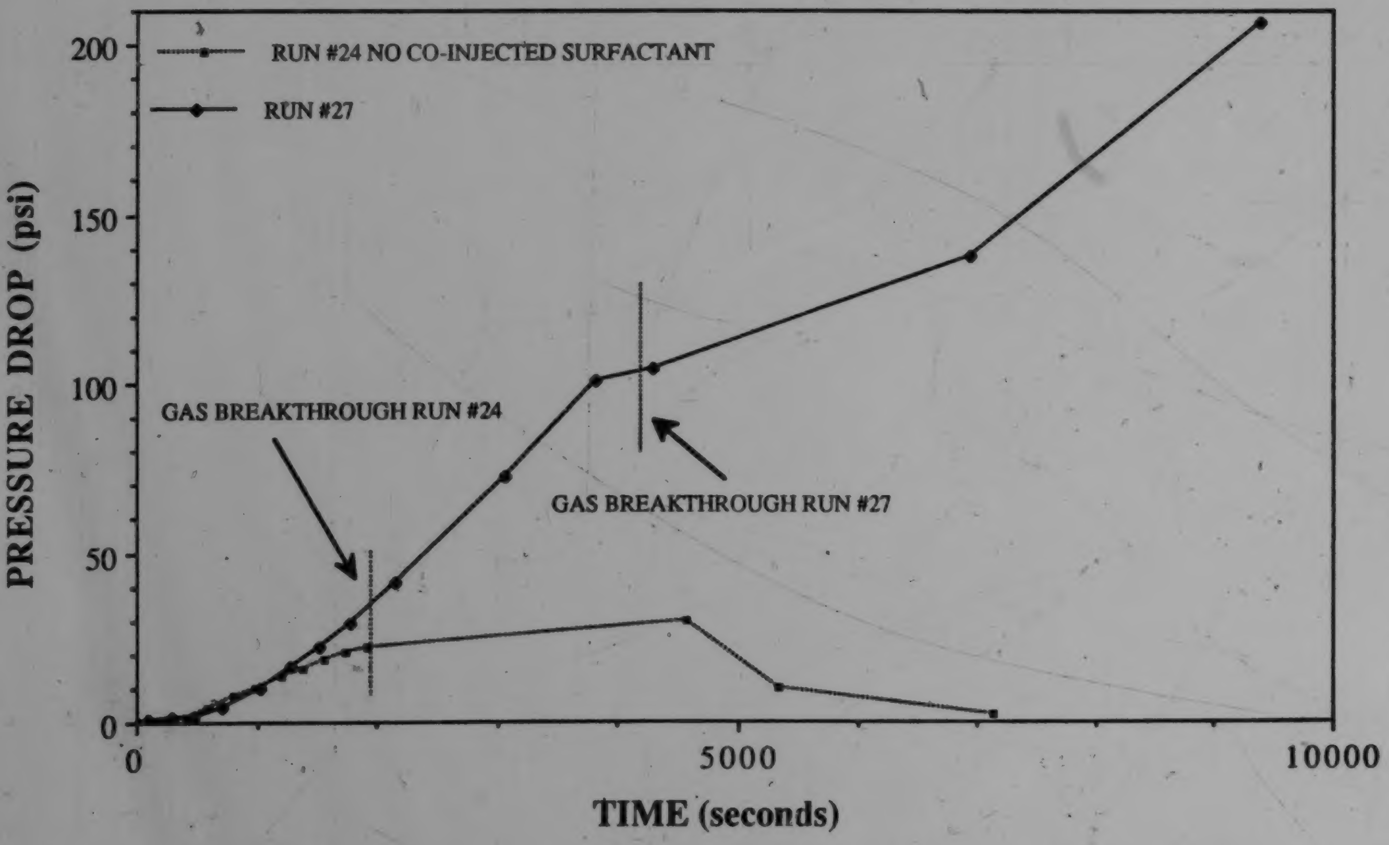

Figure 5.105 Comparison of the Differential Pressure for Run 24 (No Surfactant Co-injection) and Run 27, 1% Dow Surfactant 125°C

surfactant slug size of 150 cc was used. The co-injected fluids exited the foam generator and were allowed to flow through each core. The back pressure was the same for each core. Run 25 was performed with a 1 percent solution of SD1000 on two glassbead packs, with permeabilities of 7.5 and 16 darcies. Table 5.38 gives the data for Run 25, Core A, the 16 darcy core. The corrected liquid volume produced from the core stabilized at 403 cc. The gas breakthrough time for this core was 34 minutes. The volume produced at gas breakthrough was 453 cc. From Figure 5.106, the concentration graph, the mixing zone seems to be very large. This was probably due to the fact that the larger slug size penetrated far into the more permeable core. This caused the surfactant to mix more, with the water saturating the core.

The data for Run 25, Core C, is given in Table 5.39. The gas breakthrough time for this core was 217 minutes. The volume produced at this point was 206 cc. A comparison of the cumulative volumes produced for Core A and Core C is presented in Figure 5.107. It is evident that the majority of the flow took place in the more permeable core. The foam did not cause blocking of the more permeable core. The differential pressure plot is presented in Figure 5.108. The maximum pressure established was 16 psi.

Run 26 was performed at 125° C, with 1 percent SD1000, on two glass bead packs. Core A had an absolute permeability of 5.3 darcies; Core B had an absolute permeability 17.1 darcies. There was a problem with the outlet system for this run, which caused the

Experimental Data For Run 25, Core A
1% SD 1000 Glass Bead Size #3

Surfactant:	SD 1000	**Glass Bead Size:**	#3
Concentration:	1.0%	**Residual Oil Sat.:**	no
Absolute Permeability:	16.0 darcies	**Temperature:**	Ambient
Porosity:	34.0%	**Gas Breakthrough:**	34:00 (min.)
Back Pressure:	50 psi	**Totalizer Reading @ BT.:**	210

Time (s)	Volume (cc)	Cum. Vol. (cc)	Spectro. Conc. ppm	Pressure Drop (psi)	Totalizer Reading
30	77	51.0	96.0	0.60	3
360	47	98.0	88.0	0.70	38
570	44	142.0	28.0	1.00	57
870	55	197.0	28.0	1.10	89
1110	47	244.0	70.0	1.10	115
1320	50	294.0	84.0	1.10	135
1530	46	340.0	28.0	1.10	155
1740	47	387.0	540.0	1.10	180
1950	43	430.0	4476.0	1.40	200
2100	23	453.0	6716.0	1.20	215
4380	30	483.0	7207.0	1.40	445
7080	45	528.0	7245.0	1.40	728
10320	50	578.0	8443.0	1.40	1065
13200	48	626.0	7918.0	1.50	1351
16800	60	686.0	8806.0	1.50	1725
20400	57	743.0	9903.0	1.60	2093
23100	40	783.0	8422.0	1.60	2370

Table 5.38 Experimental Data for Run 25 Core A: 1% SD1000
Dual Core Run

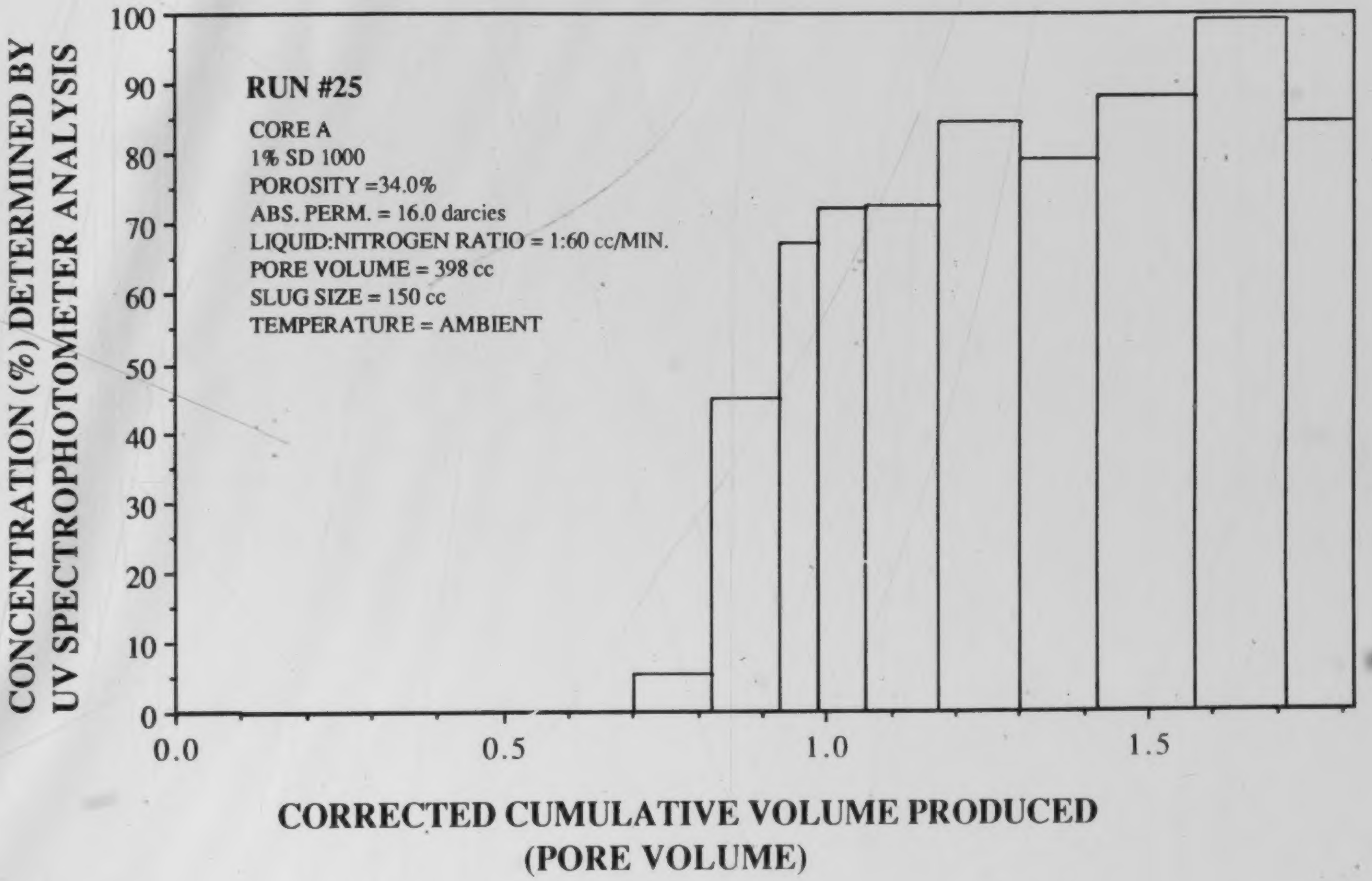

Figure 5.106 Run 25A: Concentration Determined by UV Spectrophotometer Analysis Vs. Corrected Cumulative Volume Produced, Nitrogen Surfactant Co-injection, 1% SD1000 Dual Core Experiments

Experimental Data For Run 25, Core C
1% SD 1000 Glass Bead Size #10

Surfactant:	SD 1000	**Glass Bead Size:**	#10
Concentration:	1.0%	**Residual Oil Sat.:**	no
Absolute Permeability:	7.5 darcies	**Temperature:**	Ambient
Porosity:	34.7%	**Gas Breakthrough:**	3:37:00
Back Pressure:	50 psi	**Totalizer Reading @ BT.:**	1337

Time (s)	Volume (cc)	Cum. Vol. (cc)	Spectro. Conc. ppm	Pressure Drop (psi)	Totalizer Reading
1380	27	51.0	90.0	1.10	142
4440	44	95.0	85.0	1.40	454
7140	55	150.0	65.0	1.40	732
10380	56	206.0	49.0	1.20	1069
16860	11	217.0	508.0	1.50	1726
20460	5	222.0	4111.0	1.60	2096
23160	14	236.0	6356.0	1.60	2371

Table 5.39 Experimental Data for Run 25 Core C: 1% SD1000
Dual Core Run

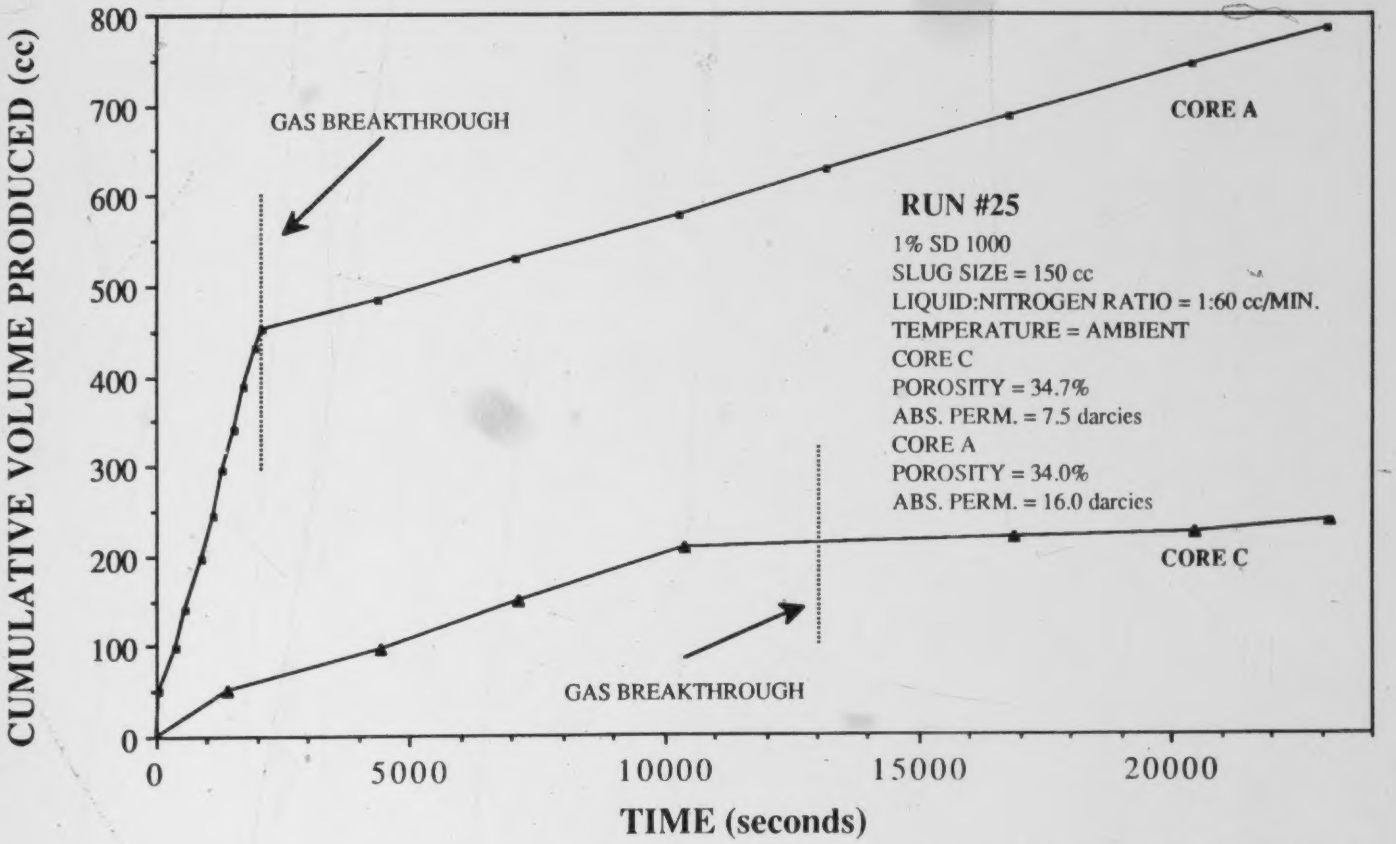

Figure 5.107 Comparison of the Cumulative Volumes Produced Vs. Time for Run 25: Core A and Core C, 1% SD1000 Dual Core Experiments

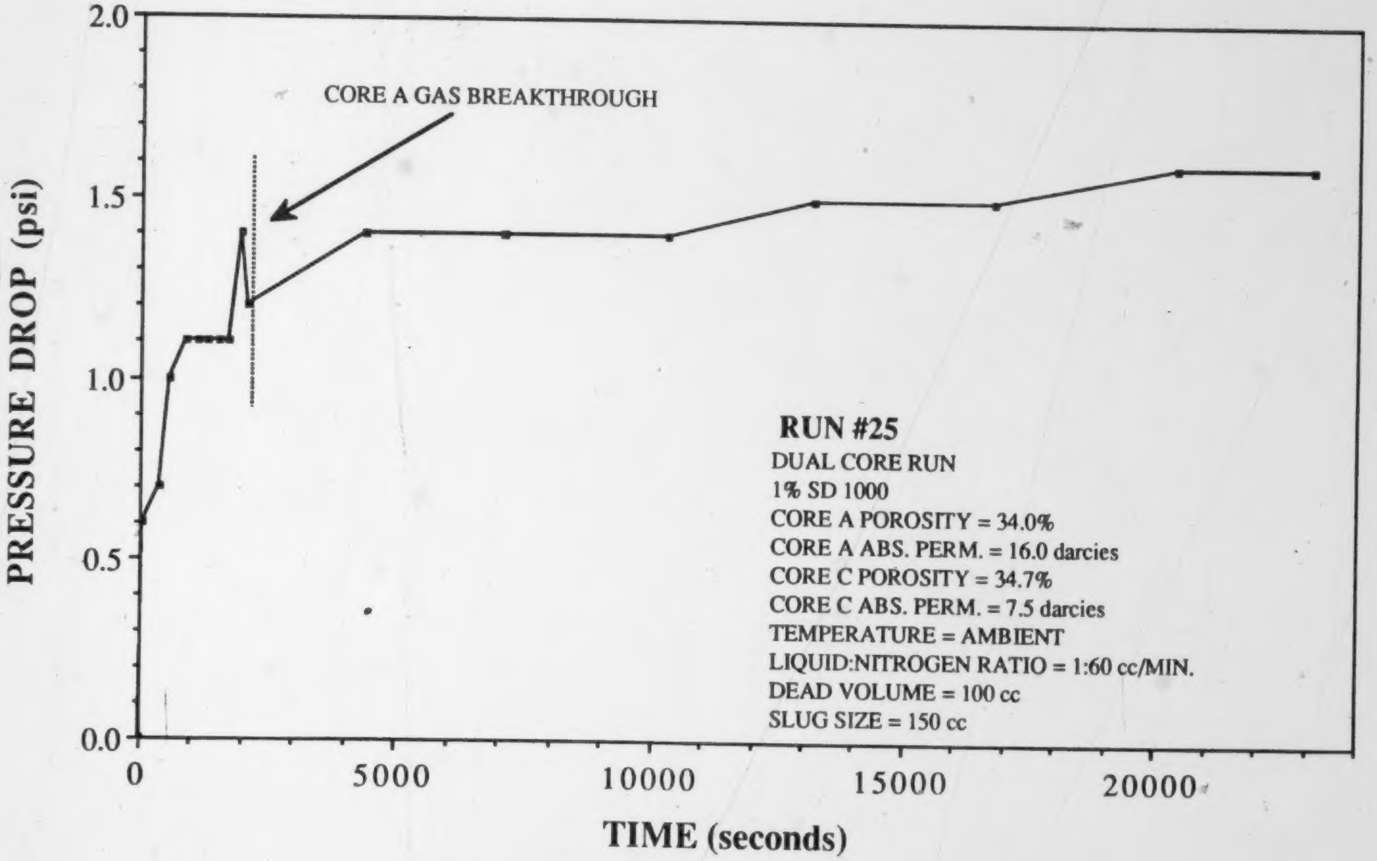

Figure 5.108 Run 25: Pressure Drop Vs. Time, Nitrogen Surfactant Co-injection, 1% SD1000 Dual Core Experiments

surfactant slug to be primarily produced through the less permeable core, Core A.

The data for Core A is given in Table 5.40. The gas breakthrough time for run was 278 minutes. The volume produced at gas breakthrough was 558 cc. The effluent surfactant concentration at gas breakthrough was 88.0 percent of the injected fluid concentration.

Table 5.41 gives the data for Core B. The gas breakthrough time for this run was 22.75 minutes. The volume produced at gas breakthrough was 346 cc. From Figure 5.109, it is evident that corrected cumulative produced is a constant. This suggests that the injected liquid was moving almost exclusively through the more permeable core. Figure 5.110 is a comparison of Core A and Core B. The curve for Core A shows the preferential injection of the slug into this core. It should be noted that the less permeable core with surfactant showed a similar liquid production rate as the more permeable core after the more permeable core experienced gas breakthrough. The differential pressure versus time graph is presented in Figure 5.111.

The last dual core run performed was a repeat of Run 26. Run 28 was performed at 125° C, on two glassbead packs, with permeabilities of 7.5 and 18.2 darcies, for Core A and Core B, respectively. The data for Core A is given in Table 5.42. The gas

Experimental Data For Run 26, Core A
1% SD 1000 Glass Bead Size #10

Surfactant:	SD 1000	**Glass Bead Size:**	#10
Concentration:	1.0%	**Residual Oil Sat.:**	no
Absolute Permeability:	5.3 darcies	**Temperature:**	125° C
Porosity:	33.5%	**Gas Breakthrough:**	4:38:00
Back Pressure:	50 psi	**Totalizer Reading @ BT.:**	141

Time (s)	Volume (cc)	Cum. Vol. (cc)	Spectro. Conc. ppm	Pressure Drop (psi)	Totalizer Reading
0	101	101.0	80.0	0.00	0
240	52	153.0	123.0	0.60	26
360	52	205.0	83.0	0.60	38
2100	43	248.0	77.0	1.10	217
5040	51	299.0	140.0	1.10	516
6720	52	351.0	130.0	1.30	687
8340	29	380.0	201.0	1.50	853
10800	48	428.0	225.0	1.90	996
12600	53	481.0	2234.0	2.10	1103
13620	37	518.0	6371.0	2.10	1385
16740	40	558.0	8797.0	2.10	1700
19200	5	563.0	8478.0	2.10	1950

Table 5.40 Experimental Data for Run 26 Core A: 1% SD1000 Dual Core Run

Experimental Data For Run 26, Core B
1% SD 1000 Glass Bead Size #3

Surfactant:	SD 1000	**Glass Bead Size:**	# 3
Concentration:	1.0%	**Residual Oil Sat.:**	no
Absolute Permeability:	17.1 darcies	**Temperature:**	125° C
Porosity:	32.8%	**Gas Breakthrough:**	22:45 (min.)
Back Pressure:	50 psi	**Totalizer Reading @ BT.:**	16680

Time (s)	Volume (cc)	Cum. Vol. (cc)	Spectro. Conc. ppm	Pressure Drop (psi)	Totalizer Reading
480	41	51.0	111.0	0.80	57
660	50	101.0	75.0	0.90	68
825	49	150.0	46.0	0.90	85
975	55	205.0	60.0	0.90	102
1110	44	249.0	100.0	1.00	113
1260	48	297.0	78.0	1.10	129
1470	49	346.0	54.0	1.10	149
1980	47	393.0	125.0	1.10	204
4980	43	436.0	5468.0	1.20	510
6780	51	487.0	7729.0	1.30	695
8400	32	519.0	10003.0	1.50	858
10740	43	562.0	9860.0	1.90	1099
13740	50	612.0	9993.0	2.10	1397
16380	45	657.0	10000.0	2.10	1663
19260	46	703.0	9998.0	2.10	1954

Table 5.41 Experimental Data for Run 26 Core B: 1% SD1000
125°C Dual Core Run

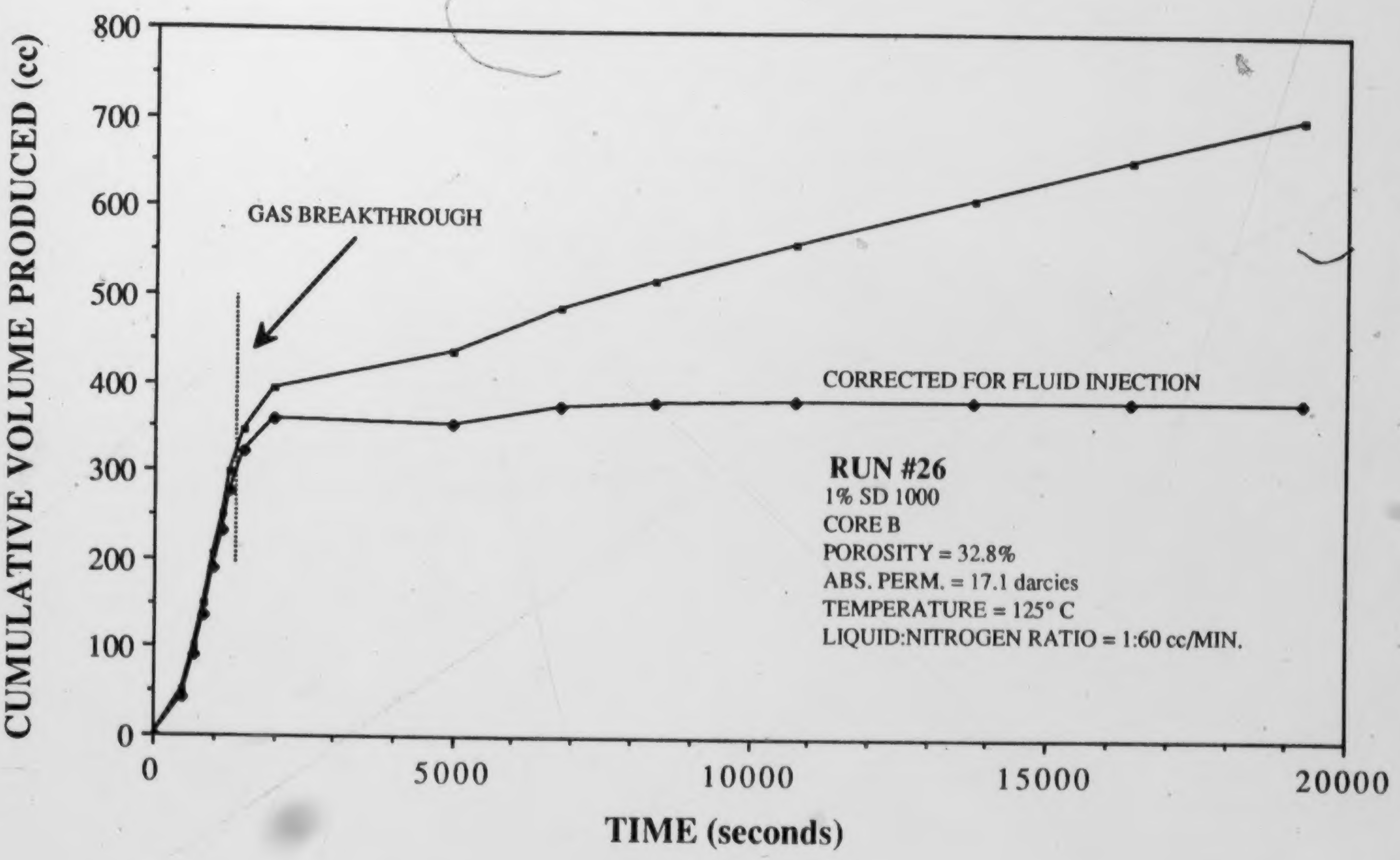

Figure 5.109 Run 26B: Cumulative Volume Produced Vs. Time, Nitrogen Injection, 1% SD1000 125°C Dual Core Experiments

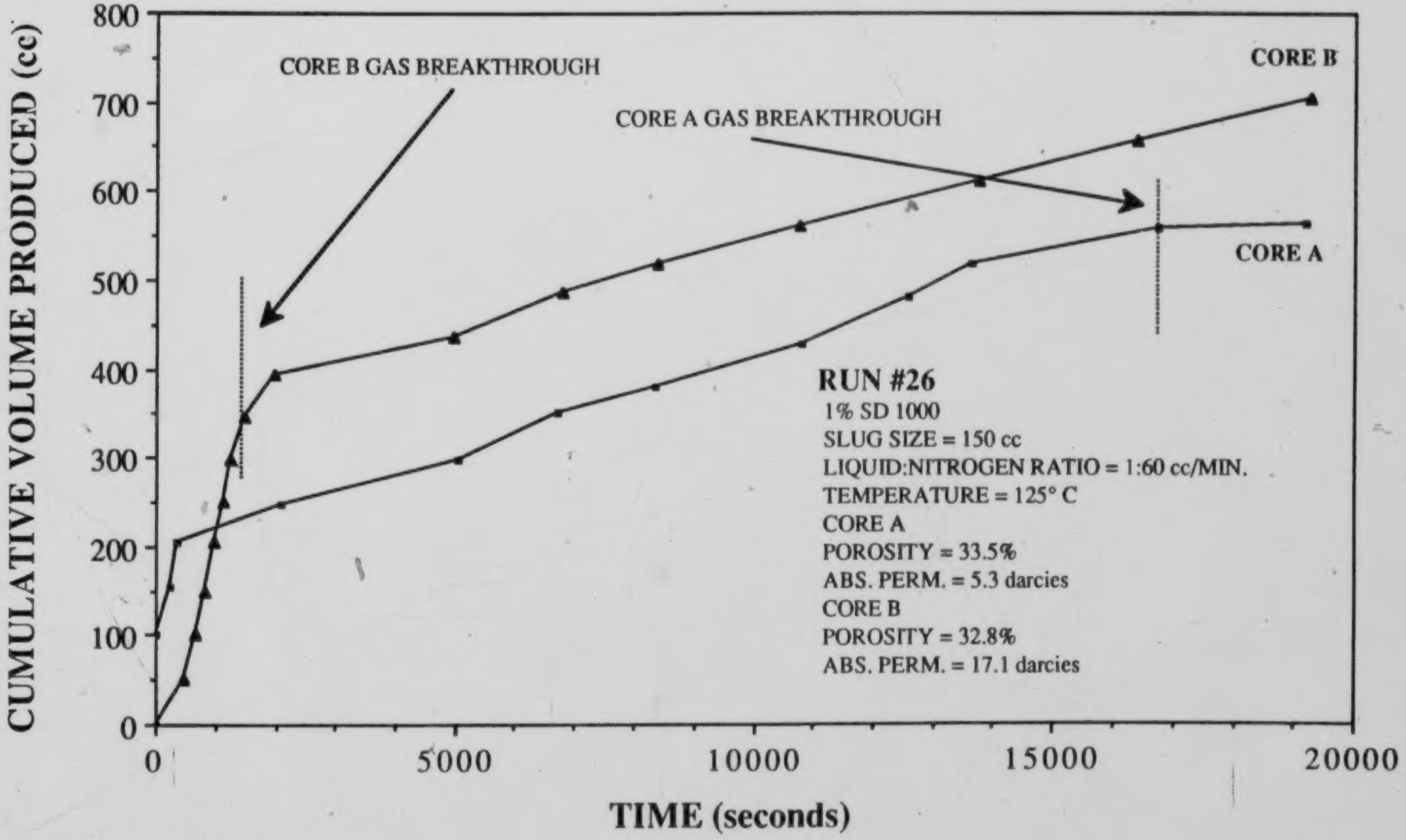

Figure 5.110 Comparison of the Cumulative Volumes Produced Vs. Time for Run 26B: Core A and Core B, 1% SD1000 125°C Dual Core Experiments

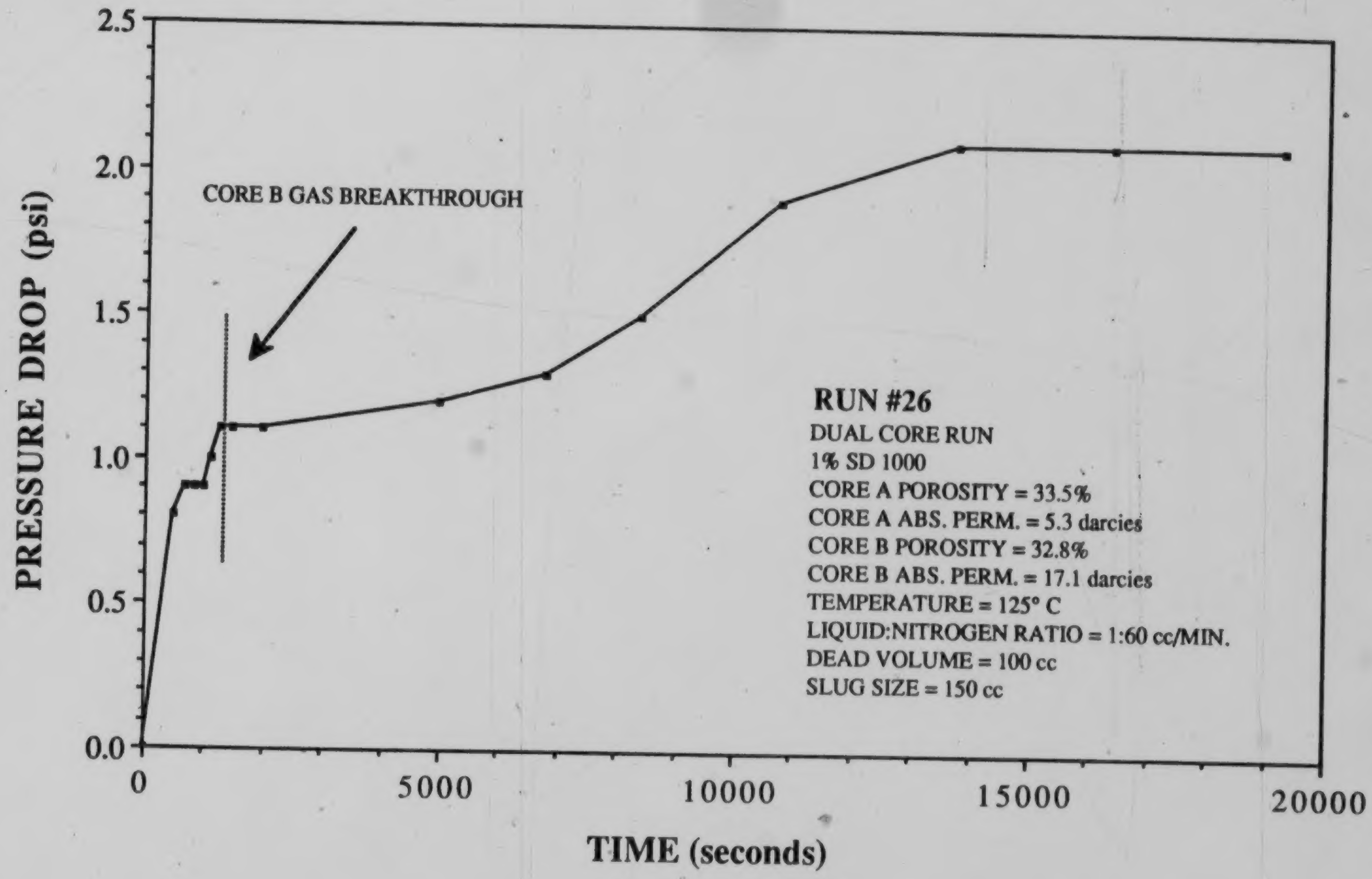

Figure 5.111 Run 26: Pressure Drop Vs. Time, Nitrogen Surfactant Co-injection, 1% SD1000 125°C Dual Core Experiments

Experimental Data For Run 28, Core A
1% SD1000 Glass Bead Size #10

Surfactant:	SD 1000	**Glass Bead Size:**	#10
Concentration:	1.0%	**Residual Oil Sat.:**	no
Absolute Permeability:	7.5 darcies	**Temperature:**	125° C
Porosity:	33.7%	**Gas Breakthrough:**	1:04:00
Back Pressure:	50 psi	**Totalizer Reading @ BT.:**	386

Time (s)	Volume (cc)	Cum. Vol. (cc)	Spectro. Conc. ppm	Pressure Drop (psi)	Totalizer Reading
210	33	33.0	79.0	0.4	21
600	40	73.0	106.0	1.1	61
1080	42	115.0	114.0	1.7	109
1530	47	162.0	94.0	2.4	158
2040	47	209.0	59.0	2.6	207
2760	58	267.0	58.0	2.9	277
3780	78	345.0	113.0	3.6	380
4680	40	385.0	181.0	4.6	472
8760	37	422.0	309.0	5.5	885
15300	43	465.0	502.0	3.9	1547
19560	42	507.0	3350.0	3.6	1981
23760	38	545.0	7650.0	3.6	2402
25710	16	561.0	8960.0	3.6	2600

Table 5.42 Experimental Data for Run 27 Core A: 1% SD1000
125° C Dual Core Run

breakthrough time was 30 minutes. The volume produced at gas breakthrough was 420 cc.

The data for Core B is presented in Table 5.43. The gas breakthrough occurred at 64 minutes. The cumulative volume produced for this core was 345 cc. Figure 5.112 is a comparison of the cumulative volume produced for both cores. The slope of the curve for Core B is slightly less than that for Core A. This suggests that a slight blocking effect took place in the more permeable core, much less however than one would expect.

The pressure drop across the core was 2.4 psi. For Run 22, which was performed on a 13 darcy glass bead pack with 1 percent SD1000 and at 125° C, the steady state pressure drop across the core was 12.25 psi. The injection rate was the same for this system, with two cores, as it was for a single core. It could be expected that the pressure, like the rate could be reduced by a factor of 2, however 6.12 psi was not achieved.

It is possible that the low pressure drop developed across the core is a result of increased gravity segregation due to the low average flow rate.

Experimental Data For Run 28, Core B
1% SD1000 Glass Bead Size #7

Surfactant:	SD 1000	**Glass Bead Size:**	# 7
Concentration:	1.0%	**Residual Oil Sat.:**	no
Absolute Permeability:	18.4 darcies	**Temperature:**	125° C
Porosity:	34.4%	**Gas Breakthrough:**	30:00
Back Pressure:	50 psi	**Totalizer Reading @ BT.:**	183

Time (s)	Volume (cc)	Cum. Vol. (cc)	Spectro. Conc. ppm	Pressure Drop (psi)	Totalizer Reading
30	57	57.0	79.0	0.2	3
300	42	99.0	133.0	0.4	29
510	49	148.0	42.0	0.9	52
750	46	194.0	40.0	1.3	76
990	48	242.0	77.0	1.7	100
1230	52	294.0	70.0	2.0	124
1470	49	343.0	38.0	2.2	148
1710	49	392.0	755.0	2.4	173
1800	28	420.0	3961.0	2.4	189
2280	45	465.0	6275.0	2.7	230
3840	49	514.0	7376.0	3.6	386
6360	52	566.0	9421.0	4.8	643
8850	37	603.0	9775.0	5.4	890
15360	34	637.0	9823.0	3.9	1549
19800	25	662.0	9784.0	3.6	2000
23820	29	691.0	9850.0	3.6	2408
25740	13	704.0	9800.0	3.6	2603

Table 5.43 Experimental Data for Run 27 Core B: 1% SD1000
125°C Dual Core Run

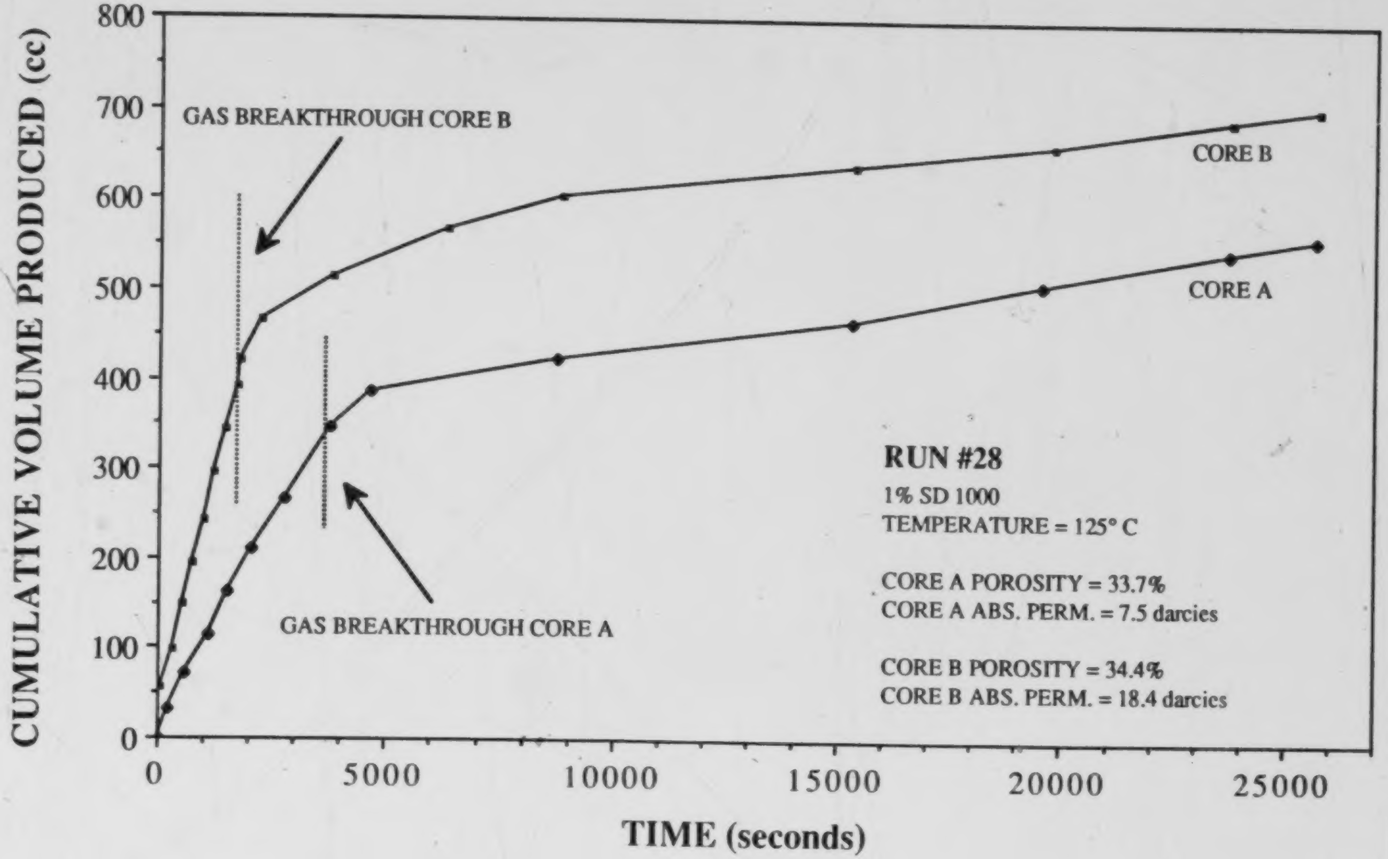

Figure 5.112 Comparison of the Cumulative Volumes Produced Vs. Time for Run 28: Core A and Core B, 1% SD1000 125°C Dual Core Experiments

5.5 Mathematical Model of Foam Flow in a Porous Medium

Statement of the Problem and Assumption

Simulation of ~~a~~ foam in a porous medium is somewhat problematic, because it must be based upon one of the several hypothesis regarding the mechanism of foam flow, discussed in the previous section. In the present work, a two phase isothermal foam flow model was developed which is considered to be a novel approach.

Before proceeding with a discussion of the model equations, it is instructive to outline the foam flow mechanisms and the previous modelling effort. Based upon experimental work, the following mechanisms have been postulated:

1. A large portion of gas is trapped in the porous medium and a small fraction flows as free gas, following Darcy's law.

2. The foam structure moves as an entity; the rate of gas flow is the same as the rate of liquid flow

3. Gas flows as a discontinuous phase by breaking and re-forming films. Liquid flows as a free phase.

4. Foam flows as a combination of liquid and gas in a foam body and the liquid flow in a porous medium follows fixed channels,

whether or not foam is present; these channels depend solely on the liquid saturation.

5. Foam flows in a porous medium with constantly changing quality and, in certain regions, there may be four different phases.

Recently, Marfoe et al.[55] reported a one-dimensional foam flow model. Even though this model accounts for some of the features described above, it does not take into account the changes due to reservoir heterogeneities and gas velocity. The present model considers two-phase flow of a three-component system, viz. water, gas and surfactant. It is assumed that surfactant does not partition into the gas phase and that its adsorption can be described by a Langmuir type isotherm. The reduction of gas mobility due to the presence of surfactant is described by a modification of the equation due to Marfoe et al.[55], as follows:

$$\mu_{fm} = \frac{\mu_g \left[1 + D f_c (C_{ws}) (S_w - S_{wr}) f_k (k) + f_p (\Delta p) \right]}{(1 + E S_o^2)} \qquad (1)$$

with $S_o = 0$.

The constant D and the functions f_c, f_k, f_p allow a large variation in foam viscosity. Also, this formulation allows the dependence of foam viscosity on absolute permeability of the porous medium, as well as surfactant concentration, pressure drop, and oil saturation.

The implication of the above relationship is that the foam viscosity will increase with increasing absolute permeability of the porous medium until an optimum permeability is reached. Raza[20] and Best et al.[34] observed that the blocking action with foam improves as the absolute permeability increases. Khatib, Hirasaki and Falls[56] observed that there exists an optimum value (12 darcies) for which the gas mobility is the lowest. This concept has been incorporated in the above formulation. The exact nature of the function f_k is determined by obtaining a best match with experimental results. Islam et al.[57] observed that the mobility of the foam increased considerably as the Δp increased. For a given flow rate, lower absolute permeability leads to lower foam viscosity. This phenomenon will increase foam mobility. However, in the above formulation the absolute permeability is decoupled from Δp in order to allow for a different dependence on Δp. An equation similar to the following may be used:

$$f_p = p_1(\Delta p) - p_2(\Delta p)^2 \qquad (2)$$

However, due to lack of experimental data which may support the above relationship, f_p is set to zero for the present study.

Raza[20] reported that the longest delay in foam breakthrough took place at a surfactant concentration of 1%. Islam et al.[57] observed similar optimum concentration. However, this value was shifted to 4% in the presence of excess water in the bottom-water zone. Therefore, a functional form with deflection point at around 1 percent surfactant concentration was chosen. The exact nature of this function was obtained by matching experimental data at different surfactant concentrations.

Experimental data was used to obtain the following relationships for f_c and f_k:

$$f_c = \sqrt{250\,C_{ws} - 1.56 * 10^{4}\,C_{ws}^{2}} \qquad \text{for} \quad C_{ws} \leq 0.0155 \qquad (3)$$

$$f_c = 0.35 \qquad \text{for} \quad C_{ws} > 0.0155 \qquad (4)$$

$$f_k = \sqrt{0.125\,k - 3.91 * 10^{-3}\,k^{2}} \qquad \text{for} \quad k \leq 30\,\mu\text{m}^{2} \qquad (5)$$

$$f_k = 0.5 \qquad \text{for} \quad k > 30\,\mu\text{m}^{2} \qquad (6)$$

5.5.1 Mathematical Foundations

Given the above assumptions, mass balances for water, gas, and surfactant can be derived, which are as follows for a three-dimensional geometry:

Water:

$$\nabla\left(\frac{k\,k_{rw}}{\mu_w B_w}\nabla\Phi_w\right)+\overset{*}{q}_w=\frac{\partial}{\partial t}\left(\frac{\phi S_w}{B_w}\right) \tag{7}$$

Gas:

$$\nabla\left(\frac{k\,k_{rg}}{\mu_g B_g}\nabla\Phi_g+\frac{R_{sw}\,k\,k_{rw}}{\mu_w B_w}\nabla\Phi_w\right)+\overset{*}{q}_g+\overset{*}{q}_w R_{sw}=\frac{\partial}{\partial t}\left(\frac{\phi R_{sw} S_w}{B_w}+\frac{\phi S_g}{B_g}\right) \tag{8}$$

Surfactant:

$$\nabla\left(\frac{C_{ws}\,k\,k_{rw}}{\mu_w B_w}\nabla\Phi_w\right)+\overset{*}{q}_w C_{ws}=\frac{\partial}{\partial t}\left(\frac{\phi S_w C_{ws}}{B_w}\right)+\frac{\rho_r}{\rho_w}\,\frac{A}{\left(1+B\,C_{ws}\right)^2}\,\frac{\partial}{\partial t}\left[\left(1-\phi\right)C_{ws}\right] \tag{9}$$

where $A = B\,C^*_{rp}$, $B = k_1/k_2$, and A and B are specfic to a given surfactant type.

In addition to the above relationship, effective permeabilities to gas and water are considered to be unique function of each phase. That is,

$$k_{rw}=k_{rw}(S_w) \tag{10}$$

$$k_{rg}=k_{rg}(S_g) \tag{11}$$

This way, the dependence of relative permeabilities on surfactant concentration was eliminated. This simplified approach was found to be adequate.

Capillary pressure is given by:

$$P_{cgw}(S_w) = p_g - p_w. \tag{12}$$

The saturation constraint is:

$$S_w + S_g = 1 \tag{13}$$

The unknowns in the above equations are: p_w, p_g, S_w, S_g, and C_{ws}, for a total of five. The equations are: three mass balances, the capillary pressure relationship and the saturation—constraint, for a total of five. Thus the problem is properly formulated.

The boundary conditions for the one-dimensional system solved were that the flow rate at the inlet end of the porous medium (x=0) is specified, and that at the outlet (x=L), the pressure is specified. The initial condition was that the saturation and pressure distributions at t=0 are known, and that the surfactant concentration concentration at t=0 is 0.

5.5.2 Solution Technique

The above equation were solved by the well-known Implicit Pressure Explicit Saturation Method (IMPES), discussed by Peaceman[58], and others. This method is based upon the reduction of the five eqations (7), (8), (9), (12) and (13) to a single equation in p_w, through elimination of the other four variables. The resulting single equation is solved for p_w by a direct approach.

The calculated pressures are then used to solve for the remaining variables in an explicit manner. This constitutes one iteration within a time step, because the accumulation terms must be iterated until convergence is obtained.

Equations (7), (8) and (9) were first discretized by finite differences. For example, for block i, Equation (7) takes the following form:

$$\left(\frac{Akk_{rw}}{\mu_w B_w \Delta x}\right)^{n}_{i+\frac{1}{2}}\left(\Phi^{n+1}_{w_{i+1}} - \Phi^{n+1}_{w_i}\right) - \left(\frac{Akk_{rw}}{\mu_w B_w \Delta x}\right)^{n}_{i\,\frac{1}{2}}\left(\Phi^{n+1}_{w_i} - \Phi^{n+1}_{w_{i-1}}\right) + q^{*}_{w_i}$$

$$= \frac{\Phi_i V_{bi}}{\Delta t}\left[\frac{S^{n+1}_{w_i}}{B^{n+1}_{w_i}} - \frac{S^{n}_{w_i}}{B^{n}_{w_i}}\right] \qquad (14)$$

where $\Phi_w = p_w - \rho_w gZ$, Z being depth below a reference plane. Where n+1 is the new time level, and n is the old time level, and $V_{bi} = A_i$

Δx_i, being the bulk volume of block i. The accumulation term is differenced in the following manner:

$$\frac{S^{n+1}_{w_i}}{B^{n+1}_{w_i}} - \frac{S^{n}_{w_i}}{B^{n}_{w_i}} = \frac{1}{B^{n+1}_{w_i}}\left(S^{n+1}_{w_i} - S^{n}_{w_i}\right) + S^{n}_{w_i}\left(\frac{1}{B^{n}_{w_i}}\right)'\left(p^{n+1}_{w_i} - p^{n}_{w_i}\right) \tag{15}$$

where $\left(\frac{1}{B^{n}_{w_i}}\right)'$ is the chord slope, given by $\left(\frac{1}{B^{n}_{w_i}}\right)' = \dfrac{\left(\frac{1}{B^{n+1}_{w_i}} - \frac{1}{B^{n}_{w_i}}\right)}{\left(p^{n+1}_{w_i} - p^{n}_{w_i}\right)}$, where the n+1 terms refer to the previous iterates of pressure. Equations (8) and (9) were differenced in the same way.

Equation (12) was used to eliminate p_g from the above equations. Finally, the three difference equations were multiplied by suitable multipliers, and added such that the accumulation terms permitted cancelling S_w and S_g via Equation (13).
The final equation has the form:

$$D_i^{(m)}\, p_{w_{i-1}}^{\substack{(m+1)\\ n+1}} + E_i^{(m)}\, p_{w_i}^{\substack{(m+1)\\ n+1}} + F_i^{(m)}\, p_{w_{i+1}}^{\substack{(m+1)\\ n+1}} = q_i^{(m)} \tag{16}$$

where (m+1) refers to the iteration level. The procedure for advancing the solution to a new time step is as follows: given the pressures, saturations, and surfactant concentration as the current time step, all of the coefficients D_i, E_i, F_i, and q_i are calculated. This permits writing Equation (16) for the entire grid. The resulting system of algebraic equations is solved by Gaussian elimination for $p_{w_i}^{\overset{(1)}{n+1}}$, being the first iterate of pressure $p_{w_i}^{n+1}$. This is now used to solve for the other four variables. For example, Equation (14) is used to solve for $S_{w_i}^{n+1}$, written as an explicit expression for $S_{w_i}^{\overset{(m+1)}{n+1}}$, as follows:

$$S_{w_i}^{\overset{(m+1)}{n+1}} = S^{n}_{w_i} + \frac{B_{w_i}^{\overset{(m+1)}{n+1}}\Delta t}{\Phi_i V_{bi}}\left[\left(\frac{Akk_{rw}}{\mu_w B_w \Delta x}\right)^{n}_{i+\frac{1}{2}}\left(\Phi_{w_{i+1}}^{\overset{(m+1)}{n+1}} - \Phi_{w_i}^{\overset{(m+1)}{n+1}}\right) - \left(\frac{Akk_{rw}}{\mu_w B_w \Delta x}\right)^{n}_{i-\frac{1}{2}}\left(\Phi_{w_i}^{\overset{(m+1)}{n+1}} - \Phi_{w_{i-1}}^{\overset{(m+1)}{n+1}}\right) + q_{w_i}^{*(m+1)}\right] - B_{w_i}^{\overset{(m+1)}{n+1}} S^{n}_{w_i}\left(\frac{1}{B^{n}_{w_i}}\right)^{\prime(m)}\left(p_{w_i}^{\overset{(m+1)}{n+1}} - p^{n}_{w_i}\right) \tag{17}$$

The new (m+1) level iterates are used to recalulate D_i, E_i, F_i, and Equation (16) is again solved to obtain new iterates of $p_{w_i}^{n+1}$. The iteration is continued until the maximum absolute pressure difference is less than 0.01 psi.

5.6 Discussion of Numerical Simulator Results

A computer program was developed for solving the above equations. A listing of this program is given in Appendix A. Figure 5.112A shows a flow diagram for the program. The program was used to simulate selected runs, to determine how far the model could match experimental results, without adjusting the foam mobility characteristics.

The results of the numerical simulator are compared to the experimental data in Fig. 5.113 to Fig. 5.120. The inlet pressures show similar trends, but the values do not compare exactly. The following points must be considered before analysis of the simulator results:

5.6.1 Adsorption

The adsorption data were taken from Novosad et al.[45] This was done due to a lack of appropriate data obtained during this study. The type of surfactant was not the same as was used in this study, consequently, there may be a divergence in the adsorption properties. A different adsorption coefficient would lead to a different concentration, which in turn will effect foam viscosity. A more rigorous treatment would involve determining the adsorption independently.

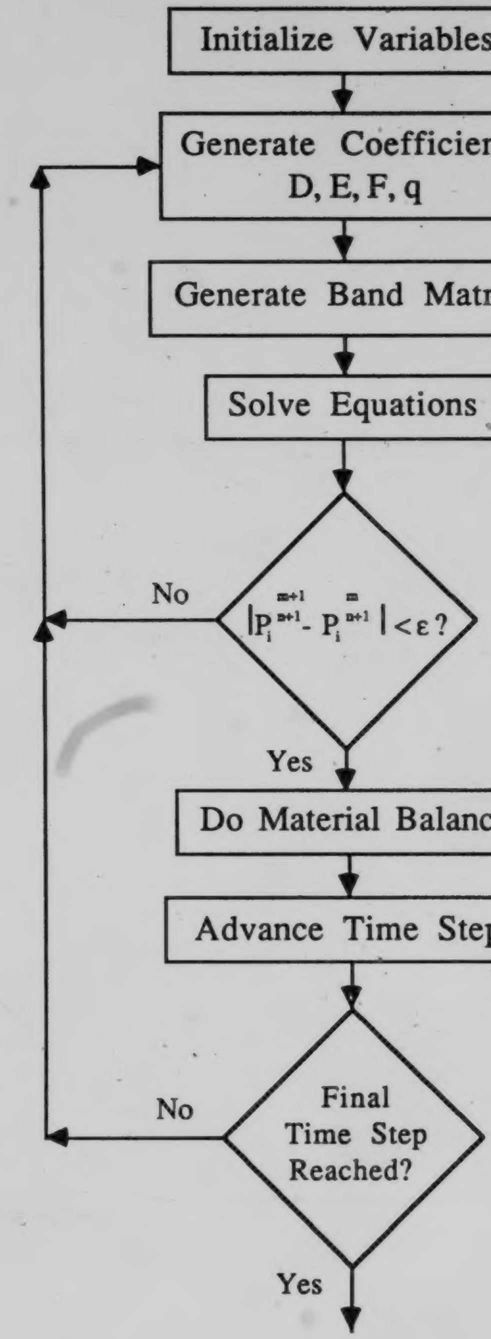
Initialize Variables
Generate Coefficients D, E, F, q
Generate Band Matrix
Solve Equations
No
$|P_i^{m+1}{}_{n+1} - P_i^{m}{}_{n+1}| < \varepsilon$?
Yes
Do Material Balance
Advance Time Step
No
Final Time Step Reached?
Yes

Figure 5.112A Flow Diagram For Numerical Simulator

5.6.2 Relative Permeability

The relative permeability data were obtained from Islam and Farouq Ali[59]. They obtained this data by history matching one of their experimental runs. Their main objective was to simulate foam flow in the presence of oil and a bottom water zone. Their relative permeability data were adapted to a three-phase system for which they assumed that the relative permeability to each phase is a unique function of its own saturation. While this set of relative permeability gave good results, the same set of relative permeability may not be appropriate for gas-water co-injection. A more rigorous treatment should include measuring gas-water relative permeability independently.

Once the set of relative permeability data is obtained in the absence of surfactant, this could be used for foam as well, since the relative permability to foam is assumed to be unaffected by surfactant. The purpose of the numerical study was a qualitative comparison, therefore, no relative permeability was independently measured.

5.6.3 Effect of Absolute Permeability

Islam and Farouq Ali[59] argued that the foam viscosity should be a function of absolute permeability, among other variables.

However, they obtained a better agreement between experimental and numerical results, by assuming a function which shows a maximum around 16 darcies. They showed therefore, that foam mobility increases if the absolute permeability were less than or greater than 16 darcies. The same function was used in the present numerical simulation study for the sake of consistency. However, the study shows no presence of optimum behaviour as a function of absolute permeability. The mobility reduction was in fact, the highest for the lowest absolute permeability. The absolute permeability function reported by Islam and Farouq Ali[59] , is therefore not applicable in the present study. In fact, the present study suggests that a function, opposite in nature to that proposed by Islam and Farouq Ali[59] be used.

5.6.4 Comparison of Experimental and Numerical Simulator Results

The comparison graph for Run 11 is located in Fig 5.113. The steady state condition for the simulation data is 6.4 psi. For the experimental run the steady state pressure differential was 5.0 psi. These curves show fair agreement between the two cases. The simulator results give higher values for the pressure differential. This run was performed on a 12.2 darcy glass bead pack; recall that the optimal permeability as specified in the simulator was 12 darcies.

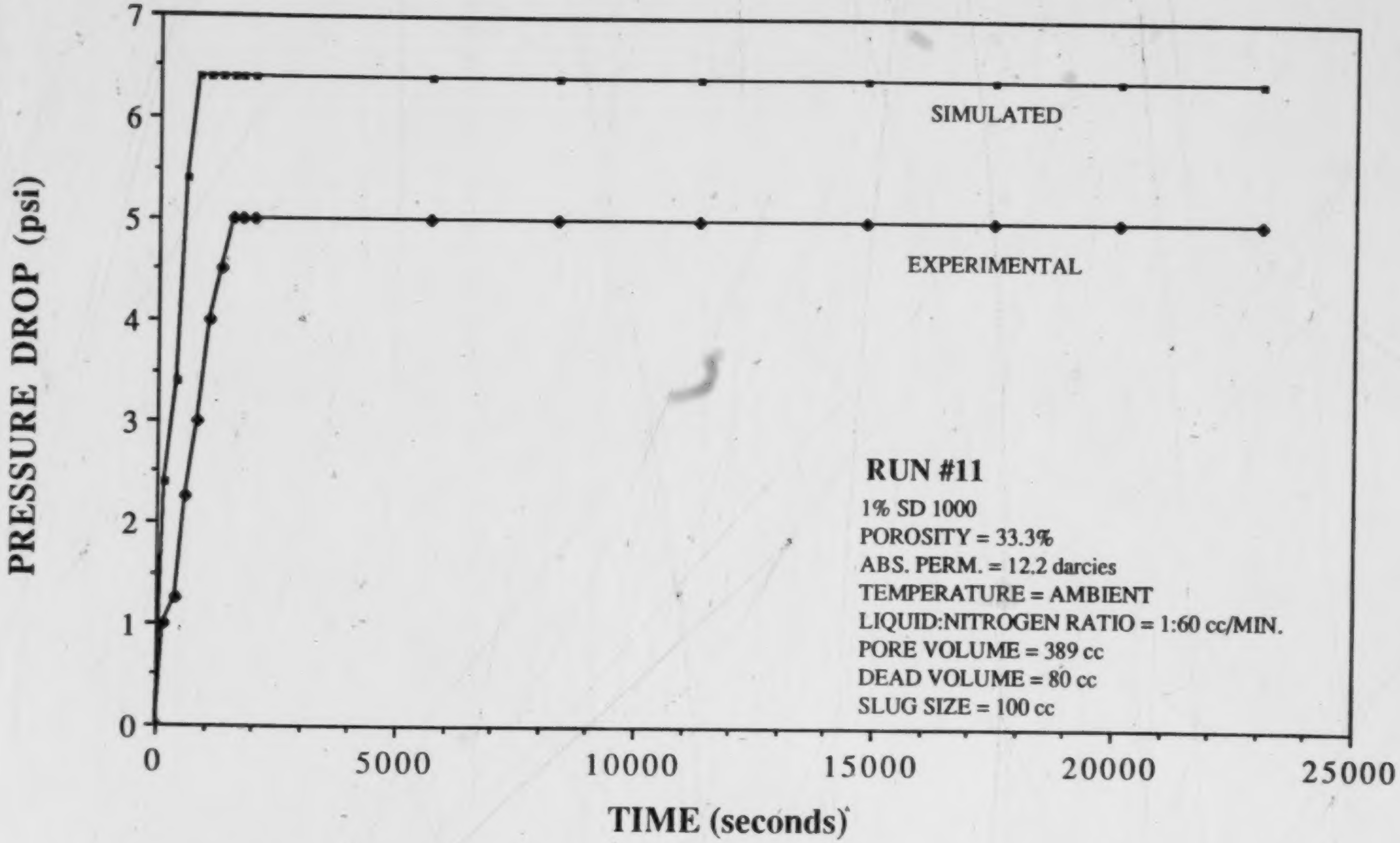

Figure 5.113 Comparison of Experimental and Simulated Results of Differential Pressure for Run 11

Run 18 was performed on a 15.2 darcy glass bead pack with a 2.5 percent solution of SD1000. The differential pressure comparison is presented in Fig 5.114. The differential pressure established in the experimental run was 7.5 psi and in the simulated results it was 8.0 psi. There is, therefore, good agreement between the simulated and experimental results.

Run 5 was performed on a 17.5 darcy glass bead pack with 5 percent SD1000. The differential pressure comparison is presented in Fig 5.115. The experimental stabilized pressure was 4.5 psi. The simulated results were 7.0 psi.

Run 14 was performed on a consolidated core with an absolute permeability of 0.651 darcies. The differential pressure comparison graph for the experimental and simulated results is presented in Fig. 5.116. This run was performed with 1 percent SD1000. The simulated results stabilize at 10.5 psi; the experimental results stabilize at 27.5. This discrepancy could have been removed by adjusting foam mobility versus permeability relationship. However, the objective of this work was to examine the simulator results without such adjustment.

Run 17 was performed on a 30 darcy glass bead pack, with 1 percent SD1000. The differential comparison graph is presented in Fig 5.117 For this case, the simulated results are much higher than the experimental results. This is the opposite of the phenomena found in Run 14, however, it is due to the same

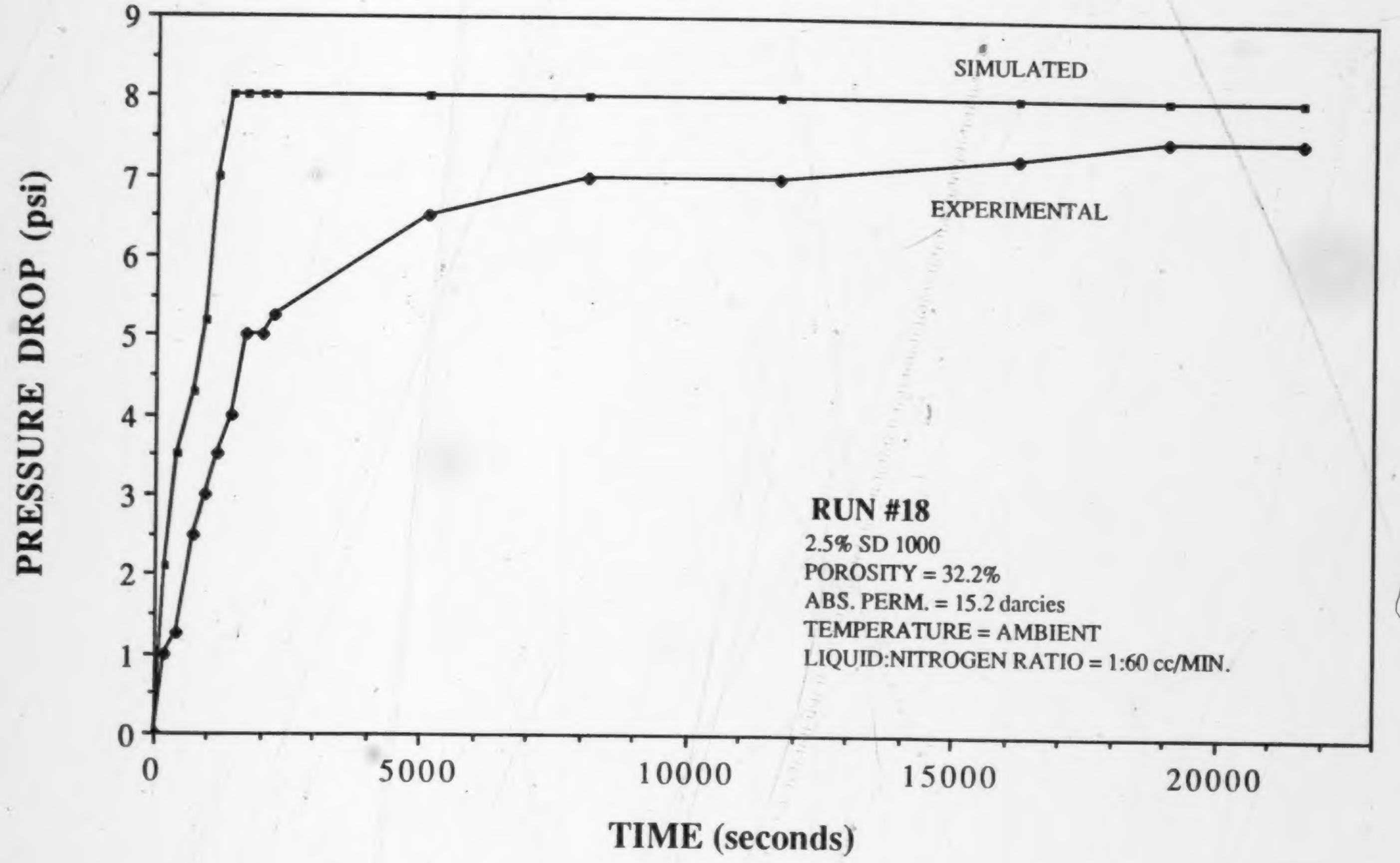

Figure 5.114 Comparison of Experimental and Simulated Results of Differential Pressure for Run 18

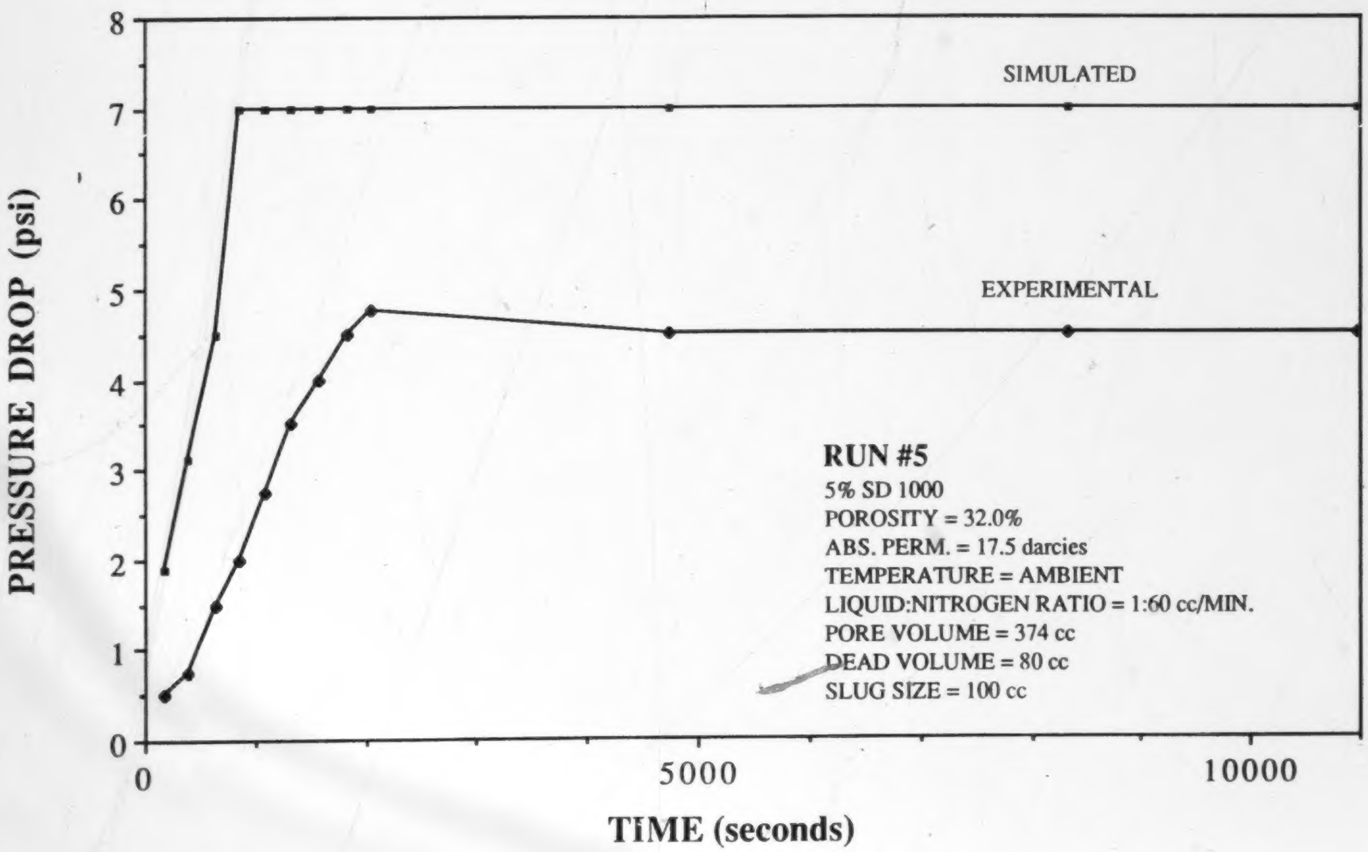

Figure 5.115 Comparison of Experimental and Simulated Results of Differential Pressure for Run 5

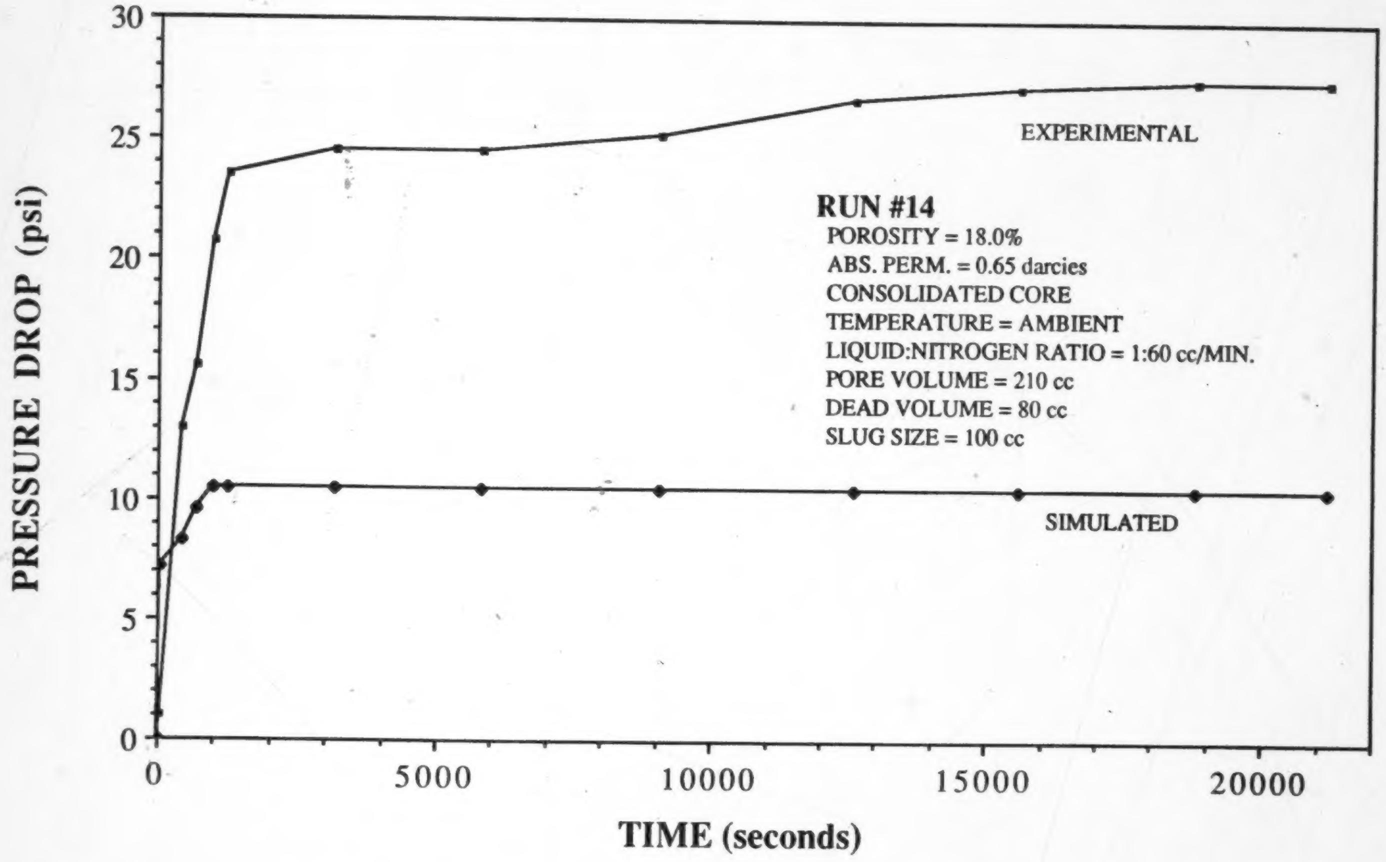

Figure 5.116 Comparison of Experimental and Simulated Results of Differential Pressure for Run 14

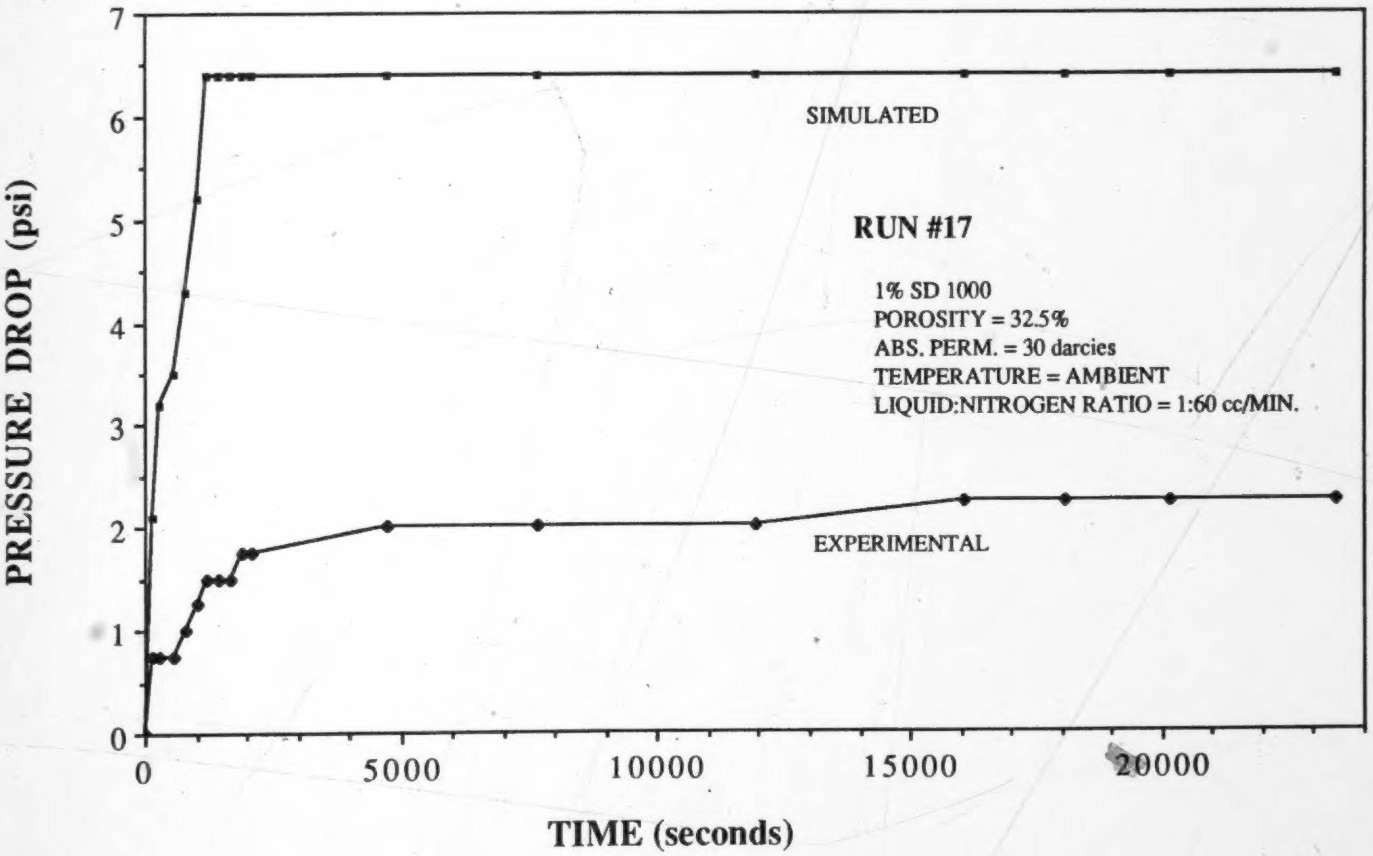

Figure 5.117 Comparison of Experimental and Simulated Results of Differential Pressure for Run 17

assumption. It was not found in the experimental portion of this research that foam mobility decreases with increasing absolute permeability. The opposite of this was suggested, that foam mobility increases with decreasing absolute permeability.

Runs 13, 16 and 15 were performed at elevated temperatures, with 1 percent SD1000. Run 13 was performed at 54° C. The differential pressure comparison graph is located in Figure 5.118. The stabilized experimental pressure drop was found to be 12.75 psi and the simulated pressure drop was 6.4 psi. The discrepancy is due to the elevated temperature. Because this is not a thermal simulator this effect could not be simulated. Run 16 was performed at 90° C. The stabilized experimental differential pressure was 18.75 psi. The simulated result was 6.6 psi. The problem of not considering elevated temperature had a more pronounced effect at the higher temperature. Run 15 was performed at 125° C. The comparison graph is Fig 5.119. No stabilized pressure was obtained for this experiment. The differential pressure rose past the pressure transducer capacity, and reached 59 psi before the run was concluded. It is evident from this graph that the divergence due to temperature, increases as the temperature increases.

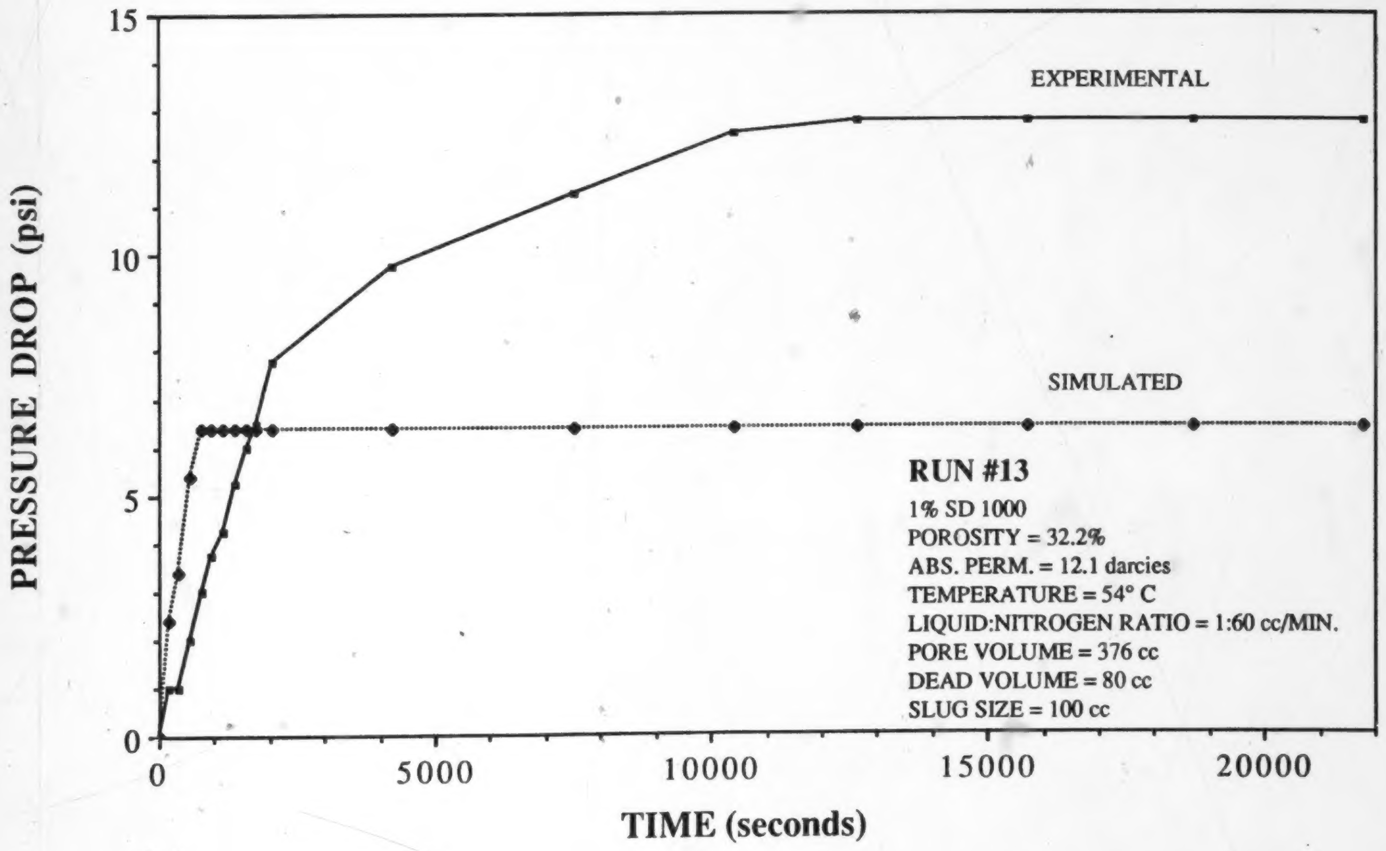

Figure 5.118 Comparison of Experimental and Simulated Results of Differential Pressure for Run 13

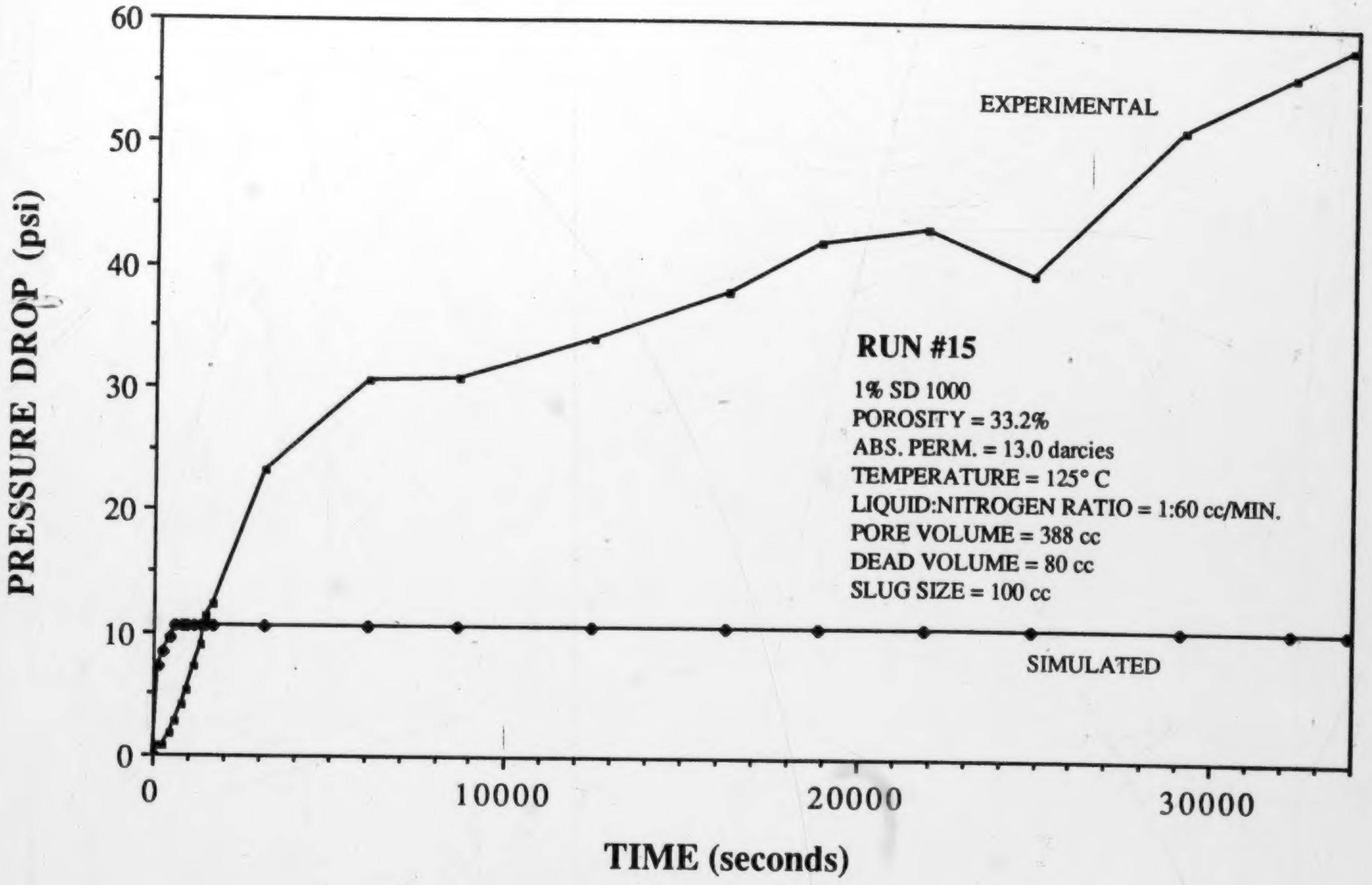

Figure 5.119 Comparison of Experimental and Simulated Results of Differential Pressure for Run 15

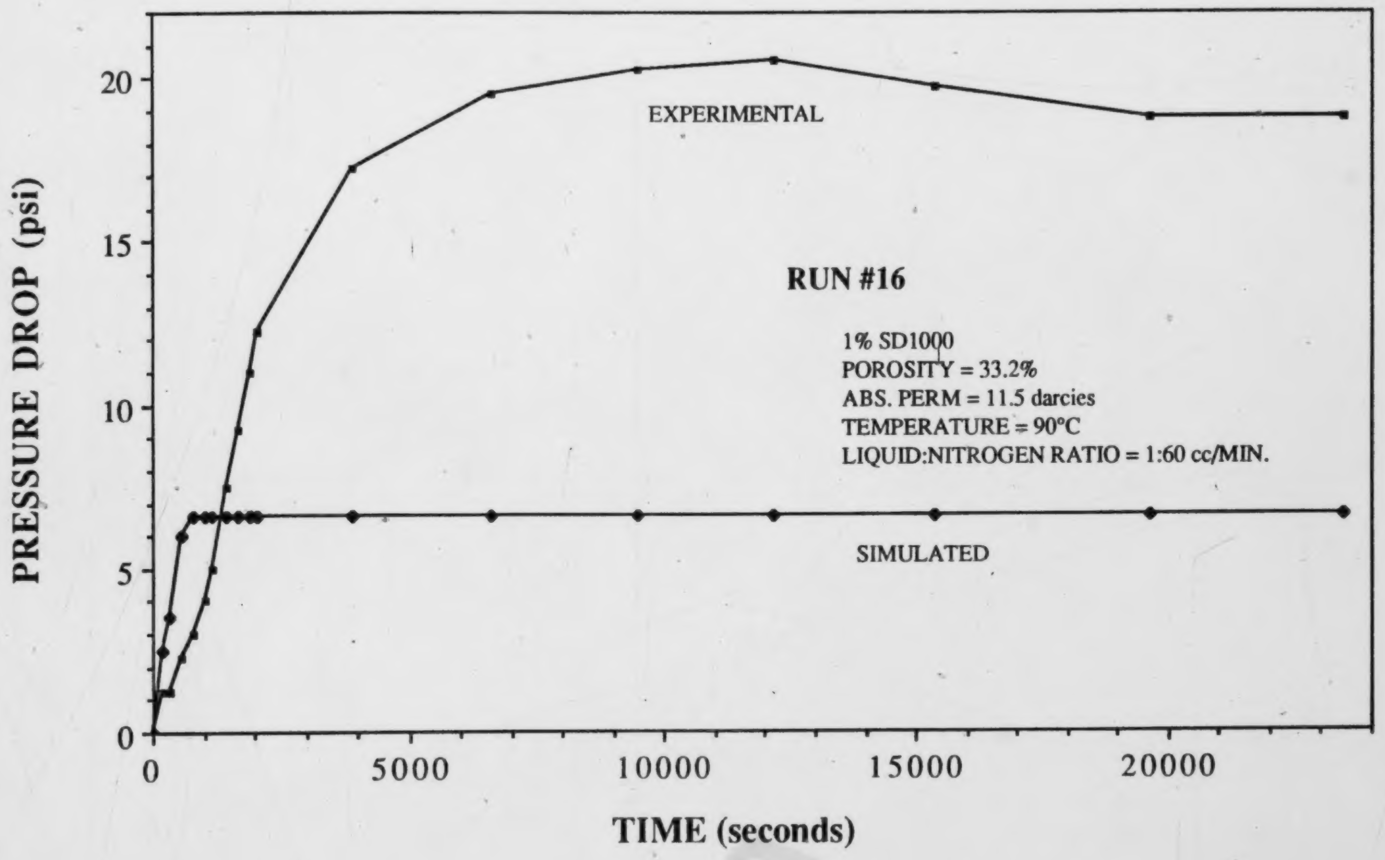

Figure 5.120 Comparison of Experimental and Simulated Results of Differential Pressure for Run 16

VI Conclusions

In this research, an experimental apparatus was designed and built for carrying out experiments of foam flooding at temperatures up to 250° C. The experimental design had several novel features related to the generation and visual observation of the foam. Based upon the experiments carried out on this apparatus, the following conclusions are drawn:

1. In two-phase water-gas displacements, addition of a surfactant to water decreases the gas phase mobility, if conditions are suitable for the formation of a foam. If a foam does form, displacement efficiency increases, resulting in increased recovery of water by gas at gas breakthrough.

2. There is an optimum surfactant concentration for reducing gas phase mobility. This optimum concentration seems to vary with absolute permeability of the porous medium.

3. A low mobility foam can be generated by injecting a slug of an appropriate surfactant, rather than continuous co-injection of surfactant and gas.

4. The total foam mobility was found to increase with increasing absolute permeability.

5. At room temperature, as well as at elevated temperatures, the Dow surfactant was the most effective gas phase mobility reduction agent tested, followed by SD1000 and XP100. At elevated temperatures, the two surfactants tested, viz. SD1000 and Dow, both showed increases in their effectiveness as gas mobility reducing, or foaming agents.

6. Presence of an oil saturation in the porous medium was found to be detrimental to foam formation. A higher surfactant concentration was needed when oil was present than when water was the only liquid present. Similarly, the presence of a residual gas saturation had a detrimental effect on gas phase mobility.

7. A computer model was developed to simulate the basic aspects of the flow of a foam in a porous media under isothermal conditions. In a few cases, the simulator was successful in modelling the essential features of the experiments, employing minimal experimentally derived information.

REFERENCES

1. Holm, L.W. : "The Mechanism of Gas and Liquid Flow Through Porous Media in the Presence of Foam", Society of Petroleum Engineers Journal, December 1968, p. 359-369.

2. Albrecht, R.A and Marsden, S.S. : "Foams as Blocking Agents in Porous Media", Society of Petroleum Engineers Journal, March 1970, p. 51-55.

3. Minssieux, L. : "Oil Displacement by Foams in Relation to Their Physical Properties in Porous Media", Journal of Petroleum Technology, January 1974, p. 100-108.

4. Lord, D.L. : "Analysis of Dynamic and Static Foam Behavior", Journal of Petroleum Technology, January 1981, p. 39-45.

5. Friedmann, F. and Jensen, J.A. : "Some Parameters Influencing the Formation and Propagation of Foams in Porous Media", SPE 15087, presented at the 56th California Regional Meeting, Oakland, April 2-4, 1986, p. 441-449.

6. Fried, A.N. : "The Foam-Drive Process for Increasing the Recovery of Oil", United States Bureau of Mines, Report of Investigations #5866, 1961.

7. Raza, S.H., and Marsden, S.S. : "The Flow of Foam: 1. Rheology and Streaming Potential", Presented at SPE Annual Fall Meeting held in Denver, Colorado, Oct. 3-6, 1965.

8. David, A. and Marsden, S.S. : "The Rheology of Foam", SPE 2544. Prepared for the 44th Annual Fall Meeting to be held in Denver, CO, September 28- October 1, 1969.

9. Marsden, S.S. and Khan, S.A. : "The Flow of Foam Through Short Porous Media and Apparent Viscosity Measurements", Society of Petroleum Engineers Journal, March 1966, p. 17-25.

10. Clark, N.O. : "The Degree of Dispersion of the Gas Phase in Foam", Transaction of the Faraday Society, 1948, Vol. 44, 1.

11. Ross, S. : "Mechanisms of Foam Stabilization and Antifoaming Action", Chemical Engineering Progress, September 1967, p. 41-47.

12. Rayleigh, Lord : "Scientific Papers", Cambridge University Press, Cambridge, England, 1902, vol. 3, p. 361,

13. Marangoni, C. : "Nuovo Cimento", 2, 1871, p. 5-6, 239; "Nuovo Cimento", 3, 1878, p. 50, 97, 192.

14. Raza, S.H. and Marsden, S.S. : "The Streaming Potential and the Rheology of Foam", Society of Petroleum Engineers Journal, December 1967, p. 359-368.

15. Dietz, D.N., Bruining, J., and Heijna, H.B. : "Foamdrive Seldom Meaningful", Journal of Petroleum Technology, May 1985, p. 921-922.

16. Bernard, G.G., Holm, L.W., and Jacobs, W.L. : "Effect of Foam on Trapped Gas Saturation and on Permeability of Porous Media to Water", Society of Petroleum Engineers Journal, December 1965, p. 295-300.

17. Kolb, G.E. : "Several Parameters Affecting the Foam-Drive Process for the Removal of Water from Consolidated Porous Media", MS Thesis, Pennsylvania State U., University Park, 1964.

18. Mast, R.F. : "Microscopic Behavior of Foam in Porous Media", SPE 3997. Prepared for the 47th Annual Fall Meeting held in San Antonio, Texas, October 8-11, 1972.

19. Owete, O.S. and Brigham, W.E. : "Flow Behavior of Foam: A Porous Micromodel Study", Society of Petroleum Engineers Reservoir Engineering, August 1987, p. 315-323.

20. Raza, S.H. : "Foam in Porous Media: Characteristics and Potential Applications", Society of Petroleum Engineers Journal, December 1970, p. 327-336.

21. Bernard, G.G. : "Effect of Foam on Recovery of Oil by Gas-Drive", Producers Monthly, January 1963, p. 18-21.

22. Owete, O.S., Al-Khafaji, A., Wang, F., Castanier, L.M., Sanyal, S.K., and Brigham, W.E. : "Screening of Foaming Agents for use in Steam Injection Processes", 1980 Annual Heavy Oil/EOR Contractor Presentations - Proceedings Presented July 22-24, 1980 in San Fransico, p. 145-159.

23. Duerksen, J.H. : "Laboratory Study of Foaming Surfactants as Steam-Diverting Additives", SPE 12785. Presented at the 1984 California Regional Meeting held in Long Beach, CA, April11-13, 1984.

24. Isaacs, E.E., McCarthy, F.C., and Maunder, J.D. : "Investigation of Foam Stability in Porous Media at Elevated Temperatures", SPE 15647. Presented at the 1986 Annual Technical Conference held in New Orleans, LA, October 5-8, 1986.

25. Bernard, G. and Holm, L. : "Effect of Foam on Permeability of Porous Media to Gas", Society of Petroleum Engineers Journal, September 1964, p. 267-274.

26. Bond, D.C. and Holbrook, O.C. : U. S. Patent 2,866,507, Gas drive oil recovery process (1958).

27. Sibree, J.O. : "The Viscosity of Froth", Trans. Farad. Soc. , Vol. 30, 1934, p. 325-331.

28. Grove, C.S., Wise, G.E., Marsh, W.C., and Gray, J.B. : "Viscosity of Fire-Fighting Foam", Industrial and Engineering Chemistry, May 1951, p. 1120-1122.

29. Mooney, M. : "Explicit Formulas for Slip and Fluidity", Jour. Rheol. (1931), Vol. 2, p. 230.

30. Patton, J.T., Holbrook, S.T., and Hsu, W. : "Rheology of Mobility Control Foams", SPE/DOE 9809. Presented at the 1981 Second Joint Symposium on Enhanced Oil Recovery held in Tulsa, OK, April 5-8, 1981.

31. Blauer, R.E., Mitchell, B.J., and Kohlhaas, C.A. : "Determination of Laminar, Turbulent, and Transitional Foam Flow Losses in

Pipes", SPE 4885. Prepared for the 44th Annual California Regional Meeting held in San Francisco, CA, April 4-5, 1974.

32. Reidenbach, V.G., Harris, P.C., Lee, Y.N., and Lord, D.L. : "Rheological Study of Foam Fracturing Fluids Using Nitrogen and Carbon Dioxide", SPE 12026. Presented at the 58th Annual Technical Conference and Exhibition held in San Francisco, CA, October 5-8, 1983.

33. Hirasaki, G.J. and Lawson, J.B. : "Mechanisms of Foam Flow in Porous Media - Apparent Viscosity in Smooth Capillaries", SPE 12129. Presented at the 58th Annual Technical Conference and Exhibition held in San Francisco, CA, October 5-8, 1983.

34. Best, D.A., Tam, E.S., and Isaacs, E. : "A Discussion on the Mechanism of Foam Flow Through Porous Media", Presented at the Third International Conference on Heavy Crude and Tar Sands held in Long Beach, California, July 21-31, 1985.

35. Maini, B.B., : "Evaluation of Mobility Control Foams at High Temperatures", Petroleum Recovery Institute Report 1985-3, November, 1985.

36. Heller, J.P., Lien, C.L., and Kuntamukkula, M.S. : "Foam-Like Dispersions for Mobility Control in CO_2 Floods", SPE 11233. Presented at the 57th Annual Fall Technical Conference and Exhibition held in New Orleans, LA, September 26-29, 1982.

37. Maini, B.B. and Ma, V. : "Relationship Between Foam Stability Measured in Static Tests and Flow Behavior of Foams in Porous Media", SPE 13073. Presented at the 59th Annual Technical Conference and Exhibition held in Houston, Tex., September 16-19, 1984.

38. Chiang, J.C., Sanyal, S.K., Castanier, L.M., Brigham, W.E., and Sufi, A. : "Foam as a Mobility Control Agent in Steam Injection Processes", SPE 8912. Presented at the 50th Annual California Regional Meeting held in Los Angeles, CA, April 9-11, 1980.

39. Huh, D.G. and Handy, L.L. : "Comparison of Steady and Unsteady-State Flow of Gas and Foaming Solution in Porous

Media", Paper SPE 15078, Presented at the 1986 California Regional Meeting, Oakland, April 2-4.

40. Huh, D.G., Cochrane, T.S., and Kovarik, F.S. : "The Effect of Microscopic Heterogeneity on CO_2/Foam Mobility: Part 1 - A Mechanistic Study", Paper SPE 17359, Presented at the SPE/DOE Enhanced Oil Recovery Symposium held in Tulsa, Oklahoma, April 17-20, 1988.

41. Lee, H.O. and Heller, J.P. : "Laboratory Measurements of CO_2-Foam Mobility", Paper SPE 17363, Presented at the SPE/DOE Enhanced Oil Recovery Symposium held in Tulsa, Oklahoma, April 17-20, 1988.

42. Wang, G.C. : "A Laboratory Study of CO_2 Foam Properties and Displacement Mechanism", SPE/DOE 12645. Presented at the Fourth Symposium on Enhanced Oil Recovery held in Tulsa, OK, April 15-18, 1984.

43. Robin, M. : "Laboratory Evaluation of Foaming Additives Used To Improve Steam Efficiency", SPE 16729. Presented at the 1987 Annual Technical Conference held in Dallas, Texas, September 27-30, 1987.

44. Elson, T.D. and Marsden Jr., S.S. : "The Effectiveness of Foaming Agents at Elevated Temperatures Over Extended Periods of Time", SPE 7116, Presented at the 1978 California Regional Meeting of the SPE, San Fransico, California, April 12-14, 1978.

45. Novosad, J., Maini, B.B, and Huang, A. : "Retention of Foam Forming Surfactants at Elevated Temperatures", Presented at the 36th Annual Technical Meeting of the Petroleum Society of CIM held jointly with the Canadian Society of Petroleum Geologists in Edmonton, Alberta, June 2-5, 1985.

46. Al-Khafaji, A.H., Wang, P.F., Castanier, L.M., and Brigham, W.E. : "Steam Surfactant Systems at Reservoir Conditions", SPE 10777. Presented at the 1982 California Regional Meeting held in San Francisco, CA, March 24-26, 1982.

47. Maini, B.B. : "Laboratory Evaluation of Foaming Agents of High Temperature Applications. II - Measurements of Thermal

Stability and Foam Mobility in Porous Media", Presented at the 36th Annual Technical Meeting of the Petroleum Society of CIM held jointly with the Canadian Society of Petroleum Geologists in Edmonton, Alberta, June 2-5, 1985.

48. Dilgren, R.E., Deemer, A.R., and Owens, K.B. : "The Laboratory Development and Field Testing of Steam/Noncondensible Gas Foams for Mobility Control in Heavy Oil Recovery", SPE 10774. Presented at the 1982 California Regional Meeting held in San Francisco, CA, March 24-26, 1982.

49. Kuhlmann, M.I. : "Visualizing the Effect of Light Oil on CO_2 Foams", Paper SPE 17356, Presented at the SPE/DOE Enhanced Oil Recovery Symposium held in Tulsa, Oklahoma, April 17-20, 1988.

50. Isaacs, E., Jian, L., Green, K., McCarthy, C., and Maunder, D. : "Use of Foam Forming Surfactants to Enhance the Recovery of Heavy Oils", Presented at the China-Canada Heavy Oil Symposium, October 26-30, 1987.

51. McPhee, C.A., Tehrani, A.D.H., and Jolly, R.P.S. : "Foam Flooding of Cores Under North Sea Reservoir Conditions", Paper SPE 17360, Presented at the SPE/DOE Enhanced Oil Recovery Symposium held in Tulsa, Oklahoma, April 17-20, 1988.

52. Kanda, M., and Schechter, R.S. : "On the Mechanism of Foam Formation in Porous Media", SPE 6200. Prepared for the 51st Annual Fall Technical Conference and Exhibition held in New Orleans, October 3-6, 1976.

53. Hanssen, J.E. : "A New Method for Testing of Gas-Blocking Foams", Paper SPE 17362, Presented at the SPE/DOE Enhanced Oil Recovery Symposium held in Tulsa, Oklahoma, April 17-20, 1988.

54. Slattery, J.C. : "Interfacial Effects in the Displacement of Residual Oil by Foam", AIChE Journal, March 1979, p. 283-289.

55. Marfoe, C.H., Kazemi, H., and Ramirez, W.F. : "Numerical Simulation of Foam Flow Through Porous Media", Paper SPE

16709, presented at the 62nd Annual Technical Conference and Exhibition of the SPE, Held in Dallas, 1987.

56. Khatib, Z.I., Hirasaki, G.J., and Falls, A.H. : "Effects of Capillary Pressure on Coalescence and Phase Mobilities in Foams Flowing Through Porous Media", SPE 15442. Presented at the 1986 Annual Technical Conference held in New Orleans, LA, October 5-8, 1986.

57. Islam, M.R., Selby, R.J., and Farouq Ali, S.M. : "Mechanics of Foam Flow in Porous Media and Applications", paper CIM 87-38-77, Presented at the 38th Meeting of the Petroleum Society of CIM, held in Calgary, AB, 1987.

58. Peaceman, D.W. : "Fundamentals of Numerical Reservoir Simulation", Elsevier Scientific Publishing Company, Amsterdam, The Netherlands, 1977.

59 Farouq Ali, S.M. and Islam, M.R.: Mobility Control-part I AOSTRA Annual Report, 1988

Appendix A

Listing of Computer Program for Simulating Foam Flow

```
      IMPLICIT REAL*8(A - H,O - Z)
      LOGICAL*1 FREE(1) /'*'/
      COMMON /ADS/ A4, B4, CN, CWSI
      COMMON /ADS1/ VB(10,10,3), GWWT1(10,10,3), WW1(11,10,3),
     1       WS1(10,11,3), WN1(10,11,3), WT1(10,10,4), WB1(10,10,4)
      COMMON /ADS2/ WE1(11,10,3), CWSN(10,10,3), CWS(10,10,3)
      COMMON /FOAM/ DCONST, ECONST
      COMMON /GASSAT/ PBO, VSLOPE, BSLOPE, RSLOPE, PMAXT, RHOSCO,
     1       RHOSCG, RHOSCW, PBOT(10,10,3)
      COMMON /NPTS/ MSAT, MPOT, MPWT, MPGT, IREPRS
      COMMON /COEF/ AW(10,10,3), AE(10,10,3), AN(10,10,3), AS(10,10,3),
     1       AB(10,10,3), AT(10,10,3), E(10,10,3), B(10,10,3)
      COMMON /PARRAY/ PN(10,10,3), SON(10,10,3), SWN(10,10,3),
     1       SGN(10,10,3), SO1(10,10,3), SW1(10,10,3), SG1(10,10,3),
     2       A1(10,10,3), A2(10,10,3), A3(10,10,3), SUM(10,10,3),
     3       GAM(10,10,3), RS(10,10,3)
      COMMON /SBAND/ BMAT(300,300), QVEC(300), PVEC(300)
      COMMON /SPARM/ PX(10,10,3), PY(10,10,3), PZ(10,10,3), EL(10,10,3),
     1       TX(11,10,3), TY(10,11,3), TZ(10,10,4)
      COMMON /SPRS/ P(10,10,3), SO(10,10,3), SW(10,10,3), SG(10,10,3)
      COMMON /SPVT/ SAT(25), PRMROT(25), PRMRWT(25), PRMRGT(25),
     1       PCOWT(25), PCGOT(25), POT(25), VSOT(25), BOT(25), BOPT(25),
     2       RSOT(25), RSOPT(25), PWT(25), VSWT(25), BWT(25), BWPT(25),
     3       RSWT(25), RSWPT(25), PGT(25), VSGT(25), BGT(25), BGPT(25),
     4       CRT(25)
      COMMON /SRATE/ PIN(20,3), PWF(20,3), PWFC(20,3), KIP(20),
     1       GMO(20,3), GMW(20,3), GMG(20,3), WELLID(20), LAYER(20),
     2       QVO(20), QVW(20), QVG(20), QVT(20), CUMO(20,3), CUMW(20,3),
     3       CUMG(20,3)
      COMMON /SGAS/ BO(10,10,3), BW(10,10,3), BG(10,10,3), QO(10,10,3),
     1       QW(10,10,3), QG(10,10,3), GOWT(10,10,3), GWWT(10,10,3),
     2       GGWT(10,10,3), OW(11,10,3), OE(11,10,3), WW(11,10,3),
     3       WE(11,10,3), OS(10,11,3), ON(10,11,3), WS(10,11,3),
     4       WN(10,11,3), OT(10,10,4), OB(10,10,4), WT(10,10,4),
     5       WB(10,10,4), QOWG(10,10,3), VP(10,10,3), CT(10,10,3)
      COMMON /SDELTA/ DX(10,10,3), DY(10,10,3), DZ(10,10,3), IQN1(20),
     1       IQN2(20), IQN3(20)
      COMMON /POR/ PORVOL
C
C
      READ (20,FREE) B4, CN, CWSI, RHOR, RHOW, DCONST, ECONST
      DO 10 I = 1, 11
        DO 10 J = 1, 10
          DO 10 K = 1, 3
            TX(I,J,K) = 0.D0
            OW(I,J,K) = 0.D0
            OE(I,J,K) = 0.D0
            WW(I,J,K) = 0.D0
            WE(I,J,K) = 0.D0
   10 CONTINUE
      DO 20 I = 1, 20
        DO 20 J = 1, 3
          CUMO(I,J) = 0.D0
          CUMW(I,J) = 0.D0
          CUMG(I,J) = 0.D0
   20 CONTINUE
      DO 30 I = 1, 10
        DO 30 J = 1, 11
          DO 30 K = 1, 3
            TY(I,J,K) = 0.D0
            OS(I,J,K) = 0.D0
            ON(I,J,K) = 0.D0
            WS(I,J,K) = 0.D0
            WN(I,J,K) = 0.D0
   30 CONTINUE
      DO 40 I = 1, 10
        DO 40 J = 1, 10
          DO 40 K = 1, 4
            TZ(I,J,K) = 0.D0
   40 CONTINUE
      DO 50 I = 1, 10
        DO 50 J = 1, 10
          DO 50 K = 1, 3
            AW(I,J,K) = 0.D0
            AE(I,J,K) = 0.D0
            AS(I,J,K) = 0.D0
            AN(I,J,K) = 0.D0
            AT(I,J,K) = 0.D0
            AB(I,J,K) = 0.D0
            QO(I,J,K) = 0.D0
            QW(I,J,K) = 0.D0
            QG(I,J,K) = 0.D0
            CWS(I,J,K) = 0.D0
            CWSN(I,J,K) = 0.D0
   50 CONTINUE
      DO 60 I = 1, 10
        DO 60 J = 1, 10
          DO 60 K = 1, 4
            OT(I,J,K) = 0.D0
            OB(I,J,K) = 0.D0
            WT(I,J,K) = 0.D0
            WB(I,J,K) = 0.D0
   60 CONTINUE
      IM = 10
      JM = 10
      KM = 3
      ETI = 0.D0
      FT = 0.D0
      FTMAX = 0.D0
      COP = 0.D0
      CWP = 0.D0
      CGP = 0.D0
      CWI = 0.D0
      CGI = 0.D0
      SCFW = 0.D0
      SCFG = 0.D0
      RSOPT(1) = 0.D0
      RSWPT(1) = 0.D0
      BOPT(1) = 0.D0
      BWPT(1) = 0.D0
      BGPT(1) = 0.D0
      SCFO = 0.D0
      ACFGT = 0.D0
      CALL SGRID(IM, II, JJ, KK)
      CALL PARM(II, JJ, KK, IM, JM)
      PORVOL = 0.D0
      DO 70 IKL = 1, II
        DO 70 JKL = 1, JJ
          P12 = DZ(IKL,JKL,1) * DX(IKL,JKL,1) * DY(IKL,JKL,1) * VP(IKL,
     1    JKL,1)
```

```
          PORVOL = PORVOL + P12
   70 CONTINUE
      PORVOL = PORVOL * 28316.84659D0
      OIP = 374.
      CALL TRAN1(II, JJ, KK, IM, JM)
      CALL TABLE
      DO 80 I = 1, II
        DO 80 J = 1, JJ
          DO 80 K = 1, KK
   80 PBOT(I,J,K) = PBO
      CALL INITL(KPI, II, JJ, KK, PI, IM, JM, ETO, CUMPO, BEO, CUMPW,
     1     BEW, CUMPG, BEG, SOI, SWI, SGI, WOC, GOC, PGOC, CUMIW, CUMIG)
C
C**** SOLUTION METHOD, DEBUG PRINT, AND TIME-STEP CONTROL PARAMETERS
C
      READ (20,FREE) NN, TMAX, WORMAX, GORMAX, PAMIN, PAMAX
      READ (20,FREE) TOL, TOL1, DSMAX, DPMAX
      D288 = 1.D0 / 288.D0
      NMAX = NN + 1
      DO 480 N = 1, NMAX
        NLOOP = N
        IF (FT .LT. FTMAX) GO TO 120
        READ (20,FREE,END=530) IWLONG, ICHANG, IWLREP, ISUMRY
        READ (20,FREE) DELT, DTMIN, DTMAX, FACT1, FACT2
   90   FORMAT (10I5)
  100   FORMAT (6F10.0)
        IF (IWLONG .EQ. 0) GO TO 110
        CALL WELLS(IM, JM, NWELL)
  110   CONTINUE
        FTMAX = ETI + ICHANG * DELT
  120   IF (N .EQ. 1) DELTO = DELT
        IF (N .EQ. 1) GO TO 140
  130   IF (DSMC .LT. DSMAX .AND. DPMC .LT. DPMAX) DELT = DELT * FACT1
        IF (DSMC .GT. DSMAX .OR. DPMC .GT. DPMAX) DELT = DELT * FACT2
        IF (DELT .LT. DTMIN) DELT = DTMIN
        IF (DELT .GT. DTMAX) DELT = DTMAX
        IF (ETI + DELT .GT. FTMAX) DELT = FTMAX - ETI
  140   FT = ETI + DELT
        IF (ETI + DELT*0.5D0 .GE. TMAX) GO TO 530
        ITFLAG = 0
  150   CONTINUE
        DIV1 = 1.D0 / DELT
        IF (N .GT. 1 .OR. ITFLAG .GT. 0) GO TO 180
        RESVOL = 0.D0
        BVOL = 0.D0
        SCFO = 0.D0
        SCFG = 0.D0
        SCFG1 = 0.D0
        DO 170 K = 1, KK
          DO 160 J = 1, JJ
            DO 160 I = 1, II
              PP = P(I,J,K)
              BPT = PBOT(I,J,K)
              VP(I,J,K) = VP(I,J,K) * DX(I,J,K) * DY(I,J,K) * DZ(I,J,K)
              VB(I,J,K) = DX(I,J,K) * DY(I,J,K) * DZ(I,J,K)
              RESVOL = RESVOL + VP(I,J,K)
  160     CONTINUE
          CALL INTPVT(BPT, RSLOPE, POT, RSOT, MPOT, PP, RSO)
          CALL INTERP(PWT, RSWT, MPWT, PP, RSW)
          CALL INTPVT(BPT, BSLOPE, POT, BOT, MPOT, PP, BO(I,J,K))
        CALL INTERP(PWT, BWT, MPWT, PP, BW(I,J,K))
        CALL INTERP(PGT, BGT, MPGT, PP, BG(I,J,K))
        FF1 = SO(I,J,K) / BO(I,J,K)
        FF2 = SW(I,J,K) / BW(I,J,K)
        SCFO = SCFO + VP(I,J,K) * FF1
        SCFW = SCFW + VP(I,J,K) * FF2
        SCFG = SCFG + VP(I,J,K) * SG(I,J,K) / BG(I,J,K)
        SCFG1 = SCFG1 + VP(I,J,K) * (RSO*FF1 + RSW*FF2)
        CALL INTERP(POT, BOPT, MPOT, PP, BODER)
        CALL INTERP(POT, RSOPT, MPOT, PP, RSODER)
        CALL INTERP(PWT, BWPT, MPWT, PP, BWDER)
        CALL INTERP(PWT, RSWPT, MPWT, PP, RSWDER)
        CALL INTERP(PGT, BGPT, MPGT, PP, BGDER)
        IF (PP .GT. PBOT(I,J,K)) BODER = BSLOPE
        IF (PP .GT. PBOT(I,J,K)) RSODER = RSLOPE
        CO = -(BODER - BG(I,J,K)*RSODER) / BO(I,J,K)
        CW = -(BWDER - BG(I,J,K)*RSWDER) / BW(I,J,K)
        CG = -BGDER / BG(I,J,K)
        CALL INTERP(PGT, CRT, MPGT, PP, CR)
        CT(I,J,K) = CR + CO * SO(I,J,K) + CW * SW(I,J,K) + CG * SG(I,
     1  J,K)
170   CONTINUE
      STBO = SCFO
      STBW = SCFW
      ACFG = SCFG
      ACFG1 = SCFG1
      STBOI = STBO
      STBWI = STBW
      ACFGI = ACFG + ACFG1
      IF (ACFGI .LE. 1.D-7 .AND. ACFGT .LE. 1.D-7) BEG = 0.D0
180   IF (N .EQ. 1 .AND. ITFLAG .LE. 0) CALL SUMM(NLOOP, KPI, II, JJ,
     1     KK, IM, JM, PAVGO, PAVG, STBOI, STBWI, ACFGI, COP, CWP,
     2     CWI, CGP, CGI, BEO, BEW, BEG, OPR, WP, WPR, GP, GPR, WI,
     3     WIR, GI, GIR, STBO, STBW, ACFG, ACFG1, WOR, GOR, DELTO, OP,
     4     ACFGT, ETI)
190   CONTINUE
      IF (N .EQ. NMAX) GO TO 530
      IF (NWELL .EQ. 0) GO TO 200
      CALL RATES(NWELL)
200   CONTINUE
      CALL SOLMAT(II, JJ, KK, IM, JM, DIV1, D288, NLOOP, NN)
      IF (NWELL .EQ. 0) GO TO 210
      CALL PRATEI(NWELL)
210   CONTINUE
      CALL BANDIN(II, JJ, KK)
      IF (NWELL .EQ. 0) GO TO 220
      CALL RATEO(NWELL)
220   CONTINUE
      SCFO = 0.D0
      SCFW = 0.D0
      SCFG = 0.D0
      SCFG1 = 0.D0
      RESVOL = 0.D0
      DO 260 K = 1, KK
        DO 260 J = 1, JJ
          DO 260 I = 1, II
            PPN = PN(I,J,K)
            PP = P(I,J,K)
            BPT = PBOT(I,J,K)
            CALL INTPVT(BPT, RSLOPE, POT, RSOT, MPOT, PP, RSO)
          CALL INTERP(PWT, RSWT, MPWT, PP, RSW)
          CALL INTERP(PGT, CRT, MPGT, PPN, CR)
          BPT = PBOT(I,J,K)
          CALL INTPVT(BPT, BSLOPE, POT, BOT, MPOT, PP, BBO)
          CALL INTERP(PWT, BWT, MPWT, PP, BBW)
          CALL INTERP(PGT, BGT, MPGT, PP, BBG)
          VPP = VP(I,J,K) * (1.D0+CR*(P(I,J,K) - PPN))
          RESVOL = RESVOL + VPP
          DP1 = 0.D0
          DP2 = 0.D0
          DP3 = 0.D0
          DP4 = 0.D0
          DP5 = 0.D0
          DP6 = 0.D0
          IF ((I - 1) .GT. 0) DP1 = P(I - 1,J,K) - PP
          IF ((I + 1) .LE. II) DP2 = P(I + 1,J,K) - PP
          IF ((J - 1) .GT. 0) DP3 = P(I,J - 1,K) - PP
          IF ((J + 1) .LE. JJ) DP4 = P(I,J + 1,K) - PP
          IF ((K - 1) .GT. 0) DP5 = P(I,J,K - 1) - PP
          IF ((K + 1) .LE. KK) DP6 = P(I,J,K + 1) - PP
          DAODP = OW(I,J,K) * DP1 + OE(I,J,K) * DP2 + OS(I,J,K) *
     1    DP3 + ON(I,J,K) * DP4 + OT(I,J,K) * DP5 + OB(I,J,K) * DP6
          DAWDP = WW(I,J,K) * DP1 + WE(I,J,K) * DP2 + WS(I,J,K) *
     1    DP3 + WN(I,J,K) * DP4 + WT(I,J,K) * DP5 + WB(I,J,K) * DP6
          DAWDP1 = WW1(I,J,K) * DP1 + WE1(I,J,K) * DP2 + WS1(I,J,K)
     1    * DP3 + WN1(I,J,K) * DP4 + WT1(I,J,K) * DP5 + WB1(I,J,K) *
     2     DP6
          SW(I,J,K) = ((DAWDP + GWWT(I,J,K) - QW(I,J,K))*DELT + VP(
     1    I,J,K)*SWN(I,J,K)/BW(I,J,K)) * BBW / VPP
          DENOM1 = (1 + B4*CWSN(I,J,K)) * (1 + B4*CWSN(I,J,K))
          CWSNN = (DAWDP1 + GWWT1(I,J,K) - QW(I,J,K)*CWSI) * DELT +
     1    VP(I,J,K) * SWN(I,J,K) * CWSN(I,J,K) / BW(I,J,K) + CWSN(I,
     2    J,K) * (VB(I,J,K) - VP(I,J,K)) * RHOR / RHOW * B4 * CN /
     3    DENOM1
          CWSN(I,J,K) = CWSNN / (VPP*SWN(I,J,K)/BBW + (VB(I,J,K) -
     1    VPP)*RHOR*B4*CN/RHOW/(1 + B4*CWSN(I,J,K))**2)
          CWSN(1,1,1) = CWSI
          IF (CWSN(I,J,K) .LT. 0.D0) CWSN(I,J,K) = 0.D0
          SO(I,J,K) = ((DAODP + GOWT(I,J,K) - QO(I,J,K))*DELT + VP(
     1    I,J,K)*SON(I,J,K)/BO(I,J,K)) * BBO / VPP
          SG(I,J,K) = 1.D0-DABS(SO(I,J,K)) - DABS(SW(I,J,K))
          IF (SG(I,J,K) .GT. 0.D0) GO TO 240
  230     SG(I,J,K) = 0.D0
          SO(I,J,K) = 1.D0-SW(I,J,K)
  240     CONTINUE
  250     VP(I,J,K) = VPP
          BO(I,J,K) = BBO
          BW(I,J,K) = BBW
          BG(I,J,K) = BBG
          FF1 = SO(I,J,K) / BO(I,J,K)
          FF2 = SW(I,J,K) / BW(I,J,K)
          SCFO = SCFO + VP(I,J,K) * FF1
          SCFW = SCFW + VP(I,J,K) * FF2
          SCFG = SCFG + VP(I,J,K) * SG(I,J,K) / BG(I,J,K)
          SCFG1 = SCFG1 + VP(I,J,K) * (RSO*FF1 + RSW*FF2)
          CALL INTERP(POT, BOPT, MPOT, PP, BODER)
          CALL INTERP(POT, RSOPT, MPOT, PP, RSODER)
          CALL INTERP(PWT, BWPT, MPWT, PP, BWDER)
          CALL INTERP(PWT, RSWPT, MPWT, PP, RSWDER)
          CALL INTERP(PGT, BGPT, MPGT, PP, BGDER)
```

```
            IF (PP .GT. PBOT(I,J,K)) BODER = BSLOPE
            IF (PP .GT. PBOT(I,J,K)) RSODER = RSLOPE
            CO = -(BODER - BG(I,J,K)*RSODER) / BO(I,J,K)
            CW = -(BWDER - BG(I,J,K)*RSWDER) / BW(I,J,K)
            CG = -BGDER / BG(I,J,K)
            CALL INTERP(PGT, CRT, MPGT, PP, CR)
            CT(I,J,K) = CR + CO * SO(I,J,K) + CW * SW(I,J,K) + CG *
   1       SG(I,J,K)
260   CONTINUE
      PPM = 0.D0
      SOM = 0.D0
      SWM = 0.D0
      SGM = 0.D0
      DO 300 K = 1, KK
        DO 300 J = 1, JJ
          DO 300 I = 1, II
            DPO = P(I,J,K) - PN(I,J,K)
            DSO = SO(I,J,K) - SON(I,J,K)
            DSW = SW(I,J,K) - SWN(I,J,K)
            DSG = SG(I,J,K) - SGN(I,J,K)
            IF (DABS(DPO) .LE. DABS(PPM)) GO TO 270
            PPM = DPO
270         IF (DABS(DSO) .LE. DABS(SOM)) GO TO 280
            SOM = DSO
280         IF (DABS(DSW) .LE. DABS(SWM)) GO TO 290
            SWM = DSW
290         IF (DABS(DSG) .LE. DABS(SGM)) GO TO 300
            SGM = DSG
300   CONTINUE
      DPMC = DABS(PPM)
      DSMC = DABS(SOM)
      IF (DSMC .LT. DABS(SGM)) DSMC = DABS(SGM)
      IF (DSMC .LT. DABS(SWM)) DSMC = DABS(SWM)
      IF (DSMC .LT. DSMAX .AND. DPMC .LT. DPMAX) GO TO 320
      IF (DELT .LE. DTMIN .OR. FACT2 .GE. 1.D0) GO TO 320
      ITFLAG = ITFLAG + 1
      DELT = DELT * FACT2
      IF (DELT .LT. DTMIN) DELT = DTMIN
      FT = ETI + DELT
      IF (FT .GT. FTMAX) DELT = FTMAX - ETI
      DO 310 I = 1, II
        DO 310 J = 1, JJ
          DO 310 K = 1, KK
            P(I,J,K) = PN(I,J,K)
            SO(I,J,K) = SON(I,J,K)
            SW(I,J,K) = SWN(I,J,K)
            SG(I,J,K) = SGN(I,J,K)
            CWS(I,J,K) = CWSN(I,J,K)
310   CONTINUE
      GO TO 150
320   CONTINUE
      DO 390 I = 1, II
        DO 390 J = 1, JJ
          DO 390 K = 1, KK
            IF (P(I,J,K) .GT. PN(I,J,K)) GO TO 390
            IF (P(I,J,K) .LT. PBOT(I,J,K)) GO TO 390
            IP = I + 1
            IM = I - 1
            JP = J + 1
            JM = J - 1
            KP = K + 1
            KM = K - 1
            IF (IP .GT. II) GO TO 330
            IF (SGN(IP,J,K) .GT. 1.D-04) GO TO 390
  330       IF (IM .LT. 1) GO TO 340
            IF (SGN(IM,J,K) .GT. 1.D-04) GO TO 390
  340       IF (JP .GT. JJ) GO TO 350
            IF (SGN(I,JP,K) .GT. 1.D-04) GO TO 390
  350       IF (JM .LT. 1) GO TO 360
            IF (SGN(I,JM,K) .GT. 1.D-04) GO TO 390
  360       IF (KP .GT. KK) GO TO 370
            IF (SGN(I,J,KP) .GT. 1.D-04) GO TO 390
  370       IF (KM .LT. 1) GO TO 380
            IF (SGN(I,J,KM) .GT. 1.D-04) GO TO 390
  380       SG(I,J,K) = 0.D0
            SO(I,J,K) = 1.D0-SW(I,J,K)
  390 CONTINUE
      IF (IREPRS .EQ. 1) GO TO 410
      DO 400 I = 1, II
        DO 400 J = 1, JJ
          DO 400 K = 1, KK
            IF (SG(I,J,K) .LE. 1.D-04) GO TO 400
            PP = P(I,J,K)
            IF (P(I,J,K) .GT. PBOT(I,J,K)) PP = PBOT(I,J,K)
            CALL INTERP(POT, BOT, MPOT, PP, BBO)
            CALL INTERP(POT, RSOT, MPOT, PP, RSO)
            CALL INTERP(PGT, BGT, MPGT, PP, BBG)
  400 CONTINUE
  410 CONTINUE
      STBOI = STBO
      STBWI = STBW
      ACFGI = ACFGT
      STBO = SCFO
      STBW = SCFW
      ACFG = SCFG
      ACFG1 = SCFG1
      ACFGT = ACFG + ACFG1
  420 CONTINUE
      DO 440 J = 1, NWELL
        GOR = 0.D0
        WOR = 0.D0
        IQ1 = IQN1(J)
        IQ2 = IQN2(J)
        IQ3 = IQN3(J)
        IJ = IJ + 1
        LAY = IQ3 + (LAYER(J) - 1)
        DO 440 K = IQ3, LAY
          QOO = QO(IQ1,IQ2,K)
          QWW = QW(IQ1,IQ2,K)
          QGG = QG(IQ1,IQ2,K)
          CUMO(J,K) = CUMO(J,K) + QOO * DELT
          CUMW(J,K) = CUMW(J,K) + QWW * DELT
          CUMG(J,K) = CUMG(J,K) + QGG * DELT
          IF (IWLREP .EQ. 0) GO TO 440
          IF (QOO .EQ. 0.D0) GO TO 430
          GOR = QGG / QOO
          WOR = QWW / QOO
  430     CONTINUE
  440 CONTINUE
      DELTO = DELT
```

```
       ETI = ETI + DELT
       CALL MATBAL(II, JJ, KK, IM, JM, STBO, STBOI, STBW, STBWI, ACFG,
    1       ACFGI, BEO, BEW, BEG, DELTO, RESVOL, OP, WP, GP, WI, GI,
    2       PAVGO, PAVG, NLOOP, OPR, WPR, GPR, WIR, GIR, COP, CWP, CGP,
    3       CWI, CGI, ACFG1, ACFGT, WOR, GOR)
       IF (WOR .GT. WORMAX) GO TO 490
       IF (GOR .GT. GORMAX) GO TO 500
       IF (PAVG .LT. PAMIN) GO TO 510
       IF (PAVG .GT. PAMAX) GO TO 520
       IF (ISUMRY .EQ. 0) GO TO 460
       NLP = N + 1
       CALL SUMM(NLP, KPI, II, JJ, KK, IM, JM, PAVGO, PAVG, STBOI,
    1       STBWI, ACFGI, COP, CWP, CWI, CGP, CGI, BEO, BEW, BEG, OPR,
    2       WP, WPR, GP, GPR, WI, WIR, GI, GIR, STBO, STBW, ACFG,
    3       ACFG1, WOR, GOR, DELTO, OP, ACFGT, ETI)
 450   CONTINUE
 460   CONTINUE
       DO 470 K = 1, KK
         DO 470 J = 1, JJ
           DO 470 I = 1, II
             QO(I,J,K) = 0.D0
             QW(I,J,K) = 0.D0
             QG(I,J,K) = 0.D0
             PN(I,J,K) = P(I,J,K)
             SON(I,J,K) = SO(I,J,K)
             SWN(I,J,K) = SW(I,J,K)
             SGN(I,J,K) = SG(I,J,K)
             CWSN(I,J,K) = CWS(I,J,K)
 470   CONTINUE
 480 CONTINUE
C
 490 WRITE (1,540)
     GO TO 530
 500 WRITE (1,550)
     GO TO 530
 510 WRITE (1,560)
     GO TO 530
 520 WRITE (1,570)
 530 CONTINUE
 540 FORMAT (/T15, 'MAXIMUM WOR HAS BEEN EXCEEDED --- SIMULATION',
    1       ' IS BEING TERMINATED')
 550 FORMAT (/T15, 'MAXIMUM GOR HAS BEEN EXCEEDED --- SIMULATION',
    1       ' IS BEING TERMINATED')
 560 FORMAT (/T15, 'MINIMUM AVERAGE RESERVOIR PRESSURE WAS NOT',
    1       ' ACHIEVED --- SIMULATION IS BEING TERMINATED')
 570 FORMAT (/T15, 'MAXIMUM AVERAGE RESERVOIR PRESSURE
    1  HAS BEEN EXCEEDED --- SIMULATION IS BEING TERMINATED')
 580 FORMAT (1X, 10E13.6)
 590 FORMAT (1X, 3I3, 9E15.6)
     STOP
     END
     SUBROUTINE BANDIN(NX, NY, NZ)
     IMPLICIT REAL*8(A - H,O - Z)
     LOGICAL*1 FREE(1) /'*'/
     COMMON /COEF/ AW(10,10,3), AE(10,10,3), AN(10,10,3), AS(10,10,3),
    1       AB(10,10,3), AT(10,10,3), E(10,10,3), B(10,10,3)
     COMMON /SPRS/ P(10,10,3), SO(10,10,3), SW(10,10,3), SG(10,10,3)
     COMMON /SBAND/ BMAT(300,300), QVEC(300), PVEC(300)
     NROW = 300
     NMAX = NX * NY * NZ
```

```
      DO 10 I = 1, NMAX
        DO 10 J = 1, NMAX
   10 BMAT(I,J) = 0.D0
      IC = 0
      DO 80 I = 1, NX
        DO 80 J = 1, NY
          DO 80 K = 1, NZ
            IC = IC + 1
            ICM = IC - 1
            ICMM = IC - NZ
            ICMMM = IC - NZ * NY
            ICP = IC + 1
            ICPP = IC + NZ
            ICPPP = IC + NY * NZ
            IF (ICMMM .LT. 1) GO TO 20
            BMAT(IC,ICMMM) = AW(I,J,K)
   20       IF (ICMM .LT. 1 .OR. NY .EQ. 1) GO TO 30
            BMAT(IC,ICMM) = AS(I,J,K)
   30       IF (ICM .LT. 1 .OR. NZ .EQ. 1) GO TO 40
            BMAT(IC,ICM) = AT(I,J,K)
   40       BMAT(IC,IC) = E(I,J,K)
            IF (ICP .GT. NMAX .OR. NZ .EQ. 1) GO TO 50
            BMAT(IC,ICP) = AB(I,J,K)
   50       IF (ICPP .GT. NMAX .OR. NY .EQ. 1) GO TO 60
            BMAT(IC,ICPP) = AN(I,J,K)
   60       IF (ICPPP .GT. NMAX) GO TO 70
            BMAT(IC,ICPPP) = AE(I,J,K)
   70       QVEC(IC) = B(I,J,K)
   80 CONTINUE
      NBAND = 2 * NY * NZ + 1
      CALL BAND(NROW, NMAX, NBAND, BMAT, QVEC, PVEC)
      IC = 0
      DO 100 I = 1, NX
        DO 100 J = 1, NY
          DO 100 K = 1, NZ
            IC = IC + 1
   90       FORMAT ('STRANG', D11.4)
  100 P(I,J,K) = PVEC(IC)
      RETURN
      END
      SUBROUTINE BAND(NROW, NMAX, NBAND, BMAT, QVEC, PVEC)
      IMPLICIT REAL*8(A - H,O - Z)
      LOGICAL*1 FREE(1) /'*'/
      DIMENSION BMAT(NROW,NMAX), QVEC(NMAX), PVEC(NMAX), GVEC(300)
      NW = (NBAND - 1) / 2
      DO 60 I = 1, NMAX
        L1 = I - NW
        IF (L1 .LT. 1) L1 = 1
        DO 30 J = L1, I
          IF (J .EQ. 1) GO TO 30
          JM = J - 1
          ADD = 0.D0
          DO 10 K = L1, JM
            IF (L1 .GT. JM) GO TO 20
   10     ADD = ADD + BMAT(I,K) * BMAT(K,J)
   20     BMAT(I,J) = BMAT(I,J) - ADD
   30   CONTINUE
        IF (I .EQ. NMAX) GO TO 60
        IP = I + 1
        IM = I - 1
        L2 = I + NW
        IF (L2 .GT. NMAX) L2 = NMAX
        DO 50 J = IP, L2
          ADD = 0.D0
          IF (I .EQ. 1) GO TO 50
          L3 = J - NW
          IF (L3 .LT. 1) L3 = 1
          DO 40 K = L3, IM
            IF (L3 .GT. IM) GO TO 50
   40     ADD = ADD + BMAT(I,K) * BMAT(K,J)
   50   BMAT(I,J) = (BMAT(I,J) - ADD) / BMAT(I,I)
   60 CONTINUE
      GVEC(1) = QVEC(1) / BMAT(1,1)
      DO 80 I = 2, NMAX
        L1 = I - NW
        IF (L1 .LT. 1) L1 = 1
        IM = I - 1
        ADD = 0.D0
        DO 70 K = L1, IM
   70   ADD = ADD + BMAT(I,K) * GVEC(K)
   80 GVEC(I) = (QVEC(I) - ADD) / BMAT(I,I)
      PVEC(NMAX) = GVEC(NMAX)
      DO 100 I = 2, NMAX
        INVI = (NMAX + 1) - I
        INVIP = INVI + 1
        L2 = INVI + NW
        IF (L2 .GT. NMAX) L2 = NMAX
        ADD = 0.D0
        DO 90 K = INVIP, L2
   90   ADD = ADD + BMAT(INVI,K) * PVEC(K)
  100 PVEC(INVI) = GVEC(INVI) - ADD
      RETURN
      END
      SUBROUTINE SGRID(IM, II, JJ, KK)
      IMPLICIT REAL*8(A - H,O - Z)
      LOGICAL*1 FREE(1) /'*'/
      COMMON /SPARM/ PX(10,10,3), PY(10,10,3), PZ(10,10,3), EL(10,10,3),
     1       TX(11,10,3), TY(10,11,3), TZ(10,10,4)
      COMMON /SDELTA/ DX(10,10,3), DY(10,10,3), DZ(10,10,3), IQN1(20),
     1       IQN2(20), IQN3(20)
      DIMENSION SUM(10,10), VAREL(10,10), RDXL(10), RDYL(10), RDZL(3)
      READ (20,FREE) II, JJ, KK
   10 FORMAT (3I5)
      READ (20,FREE) KDX, KDY, KDZ
      IF (KDX .GT. 0) GO TO 30
      READ (20,FREE) DXC
      DO 20 K = 1, KK
        DO 20 J = 1, JJ
          DO 20 I = 1, II
   20 DX(I,J,K) = DXC
      WRITE (1,410) DXC
      GO TO 110
   30 IF (KDX .GT. 0) GO TO 60
      READ (20,FREE) (RDXL(I),I=1,II)
      DO 40 K = 1, KK
        DO 40 J = 1, JJ
          DO 40 I = 1, II
   40 DX(I,J,K) = RDXL(I)
      DO 50 I = 1, II
   50 WRITE (1,510) I, RDXL(I)
```

```
      GO TO 110
   60 WRITE (1,480)
      K = 1
      WRITE (1,460) K
      DO 70 J = 1, JJ
        READ (20,FREE) (DX(I,J,K),I=1,II)
   70 WRITE (1,400) (DX(I,J,K),I=1,II)
   80 CONTINUE
      DO 100 K = 2, KK
        WRITE (1,460) K
        DO 100 J = 1, JJ
          DO 100 I = 1, II
   90       DX(I,J,K) = DX(I,J,1)
  100 WRITE (1,400) DX(I,J,K)
  110 CONTINUE
      IF (KDY .GE. 0) GO TO 130
      READ (20,FREE) DYC
      DO 120 K = 1, KK
        DO 120 J = 1, JJ
          DO 120 I = 1, II
  120 DY(I,J,K) = DYC
      WRITE (1,430) DYC
      GO TO 210
  130 IF (KDY .GT. 0) GO TO 160
      READ (20,FREE) (RDYL(J),J=1,JJ)
      DO 140 K = 1, KK
        DO 140 J = 1, JJ
          DO 140 I = 1, II
  140 DY(I,J,K) = RDYL(J)
      DO 150 J = 1, JJ
  150 WRITE (1,520) J, RDYL(J)
      GO TO 210
  160 WRITE (1,490)
      K = 1
      WRITE (1,460) K
      DO 170 I = 1, II
        READ (20,FREE) (DY(I,J,K),J=1,JJ)
  170 WRITE (1,400) (DY(I,J,K),J=1,JJ)
      DO 190 K = 2, KK
        WRITE (1,460) K
        DO 190 J = 1, JJ
          DO 180 I = 1, II
  180       DY(I,J,K) = DY(I,J,1)
  190 WRITE (1,400) (DY(I,J,K),II=1,II)
  200 CONTINUE
  210 CONTINUE
      IF (KDZ .GE. 0) GO TO 230
      READ (20,FREE) DZC
      DO 220 K = 1, KK
        DO 220 J = 1, JJ
          DO 220 I = 1, II
  220 DZ(I,J,K) = DZC
      WRITE (1,440) DZC
      GO TO 290
  230 IF (KDZ .GT. 0) GO TO 260
      READ (20,FREE) (RDZL(K),K=1,KK)
      DO 240 K = 1, KK
        DO 240 J = 1, JJ
          DO 240 I = 1, II
  240 DZ(I,J,K) = RDZL(K)
```

```
      DO 250 K = 1, KK
  250 WRITE (1,530) K, RDZL(K)
      GO TO 290
  260 WRITE (1,500)
      DO 280 K = 1, KK
        WRITE (1,460) K
        DO 270 J = 1, JJ
          READ (20,FREE) (DZ(I,J,K),I=1,II)
  270   WRITE (1,400) (DZ(I,J,K),I=1,II)
  280 CONTINUE
  290 CONTINUE
      READ (20,FREE) KEL
      IF (KEL .EQ. 1) GO TO 320
      READ (20,FREE) ELEV
  300 FORMAT (8F10.0)
      DO 310 J = 1, JJ
        DO 310 I = 1, II
  310 VAREL(I,J) = ELEV
  320 IF (KEL .NE. 1) GO TO 340
      DO 330 J = 1, JJ
        READ (20,FREE) (VAREL(I,J),I=1,II)
  330 CONTINUE
  340 CONTINUE
      DO 350 I = 1, II
        DO 350 J = 1, JJ
  350 SUM(I,J) = 0.D0
      DO 360 K = 1, KK
        DO 360 J = 1, JJ
          DO 360 I = 1, II
            DEL = SUM(I,J) + DZ(I,J,K) * 0.5D0
            EL(I,J,K) = VAREL(I,J) + DEL
  360 SUM(I,J) = DZ(I,J,K) + SUM(I,J)
      WRITE (1,470)
      DO 370 K = 1, KK
        WRITE (1,460) K
        DO 370 J = 1, JJ
          WRITE (1,400) (EL(I,J,K),I=1,II)
  370 CONTINUE
  380 CONTINUE
  390 FORMAT (3I5, F10.0)
  400 FORMAT (1X, 20F6.0)
  410 FORMAT (T15, 'GRID BLOCK LENGTH (DX) IS ', ' SET AT', F10.4,
     1        ' FOR ALL BLOCKS'//)
  420 FORMAT (15X, 3I5, 5X, F14.4)
  430 FORMAT (T15, 'GRID BLOCK WIDTH  (DY) IS ', ' SET AT', F10.4,
     1        ' FOR ALL BLOCKS'//)
  440 FORMAT (T15, 'GRID BLOCK DEPTH  (DZ) IS ', ' SET AT', F10.4,
     1        ' FOR ALL BLOCKS'//)
  450 FORMAT (I5)
  460 FORMAT (/1X, 'K -', I2/)
  470 FORMAT (//T15, '********** NODE MIDPOINT ELEVATIONS **********'/)
  480 FORMAT (//T15, '********GRID BLOCK LENGTH (DX) DISTRIBUTION*******
     1*'/)
  490 FORMAT (//T15, '********GRID BLOCK WIDTH  (DY) DISTRIBUTION*******
     1*'/)
  500 FORMAT (//T15, '********GRID BLOCK DEPTH  (DZ) DISTRIBUTION*******
     1*'/)
  510 FORMAT (T15, 'GRID SIZE (DX) IN COLUMN', I5, ' IS ', F8.2,
     1        ' FOR ALL BLOCKS', /)
  520 FORMAT (T15, 'GRID SIZE (DY) IN ROW   ', I5, ' IS ', F8.2,
     1         ' FOR ALL BLOCKS', /)
  530 FORMAT (T15, 'GRID SIZE (DZ) IN LAYER ', I5, ' IS INITIALLT SET AT
     1', F8.2, ' FOR ALL BLOCKS', /)
      RETURN
      END
      SUBROUTINE INTERP(X, Y, N, XO, YO)
      IMPLICIT REAL*8(A - H,O - Z)
      LOGICAL*1 FREE(1) /'*'/
      DIMENSION X(25), Y(25)
      IF (XO .GE. X(N)) YO = Y(N)
      IF (XO .GE. X(N)) RETURN
      DO 10 I = 2, N
        IF (XO .GE. X(I)) GO TO 10
        YO = Y(I - 1) + (XO - X(I - 1)) * (Y(I) - Y(I - 1)) / (X(I) - X(
     1  I - 1))
        RETURN
   10 CONTINUE
      END
      SUBROUTINE INTPVT(BPT, RM, X, Y, N, XO, YO)
      IMPLICIT REAL*8(A - H,O - Z)
      LOGICAL*1 FREE(1) /'*'/
      DIMENSION X(25), Y(25)
      IF (XO .GT. BPT) GO TO 20
      IF (XO .GE. X(N)) YO = Y(N)
      IF (XO .GE. X(N)) RETURN
      DO 10 I = 2, N
        IF (XO .GE. X(I)) GO TO 10
        YO = Y(I - 1) + (XO - X(I - 1)) * (Y(I) - Y(I - 1)) / (X(I) - X(
     1  I - 1))
        RETURN
   10 CONTINUE
   20 CONTINUE
      DO 30 I = 2, N
        IF (BPT .GE. X(I)) GO TO 30
        YOBP = Y(I - 1) + (BPT - X(I - 1)) * (Y(I) - Y(I - 1)) / (X(I) -
     1   X(I - 1))
        YO = YOBP + RM * (XO - BPT)
        RETURN
   30 CONTINUE
      END
      SUBROUTINE MATBAL(II, JJ, KK, IM, JM, STBO, STBOI, STBW, STBWI,
     1           ACFG, ACFGI, BEO, BEW, BEG, DELTO, RESVOL, OP, WP, GP,
     2           WI, GI, PAVGO, PAVG, N, OPR, WPR, GPR, WIR, GIR, COP,
     3           CWP, CGP, CWI, CGI, ACFG1, ACFGT, WOR, GOR)
      IMPLICIT REAL*8(A - H,O - Z)
      LOGICAL*1 FREE(1) /'*'/
      COMMON /PARRAY/ PN(10,10,3), SON(10,10,3), SWN(10,10,3),
     1        SGN(10,10,3), SO1(10,10,3), SW1(10,10,3), SG1(10,10,3),
     2        A1(10,10,3), A2(10,10,3), A3(10,10,3), SUM(10,10,3),
     3        GAM(10,10,3), QS(10,10,3)
      COMMON /SPRS/ P(10,10,3), SO(10,10,3), SW(10,10,3), SG(10,10,3)
      COMMON /SGAS/ BO(10,10,3), BW(10,10,3), BG(10,10,3), QO(10,10,3),
     1        QW(10,10,3), QG(10,10,3), GOWT(10,10,3), GWWT(10,10,3),
     2        GGWT(10,10,3), OW(11,10,3), OE(11,10,3), WW(11,10,3),
     3        WE(11,10,3), OS(10,11,3), ON(10,11,3), WS(10,11,3),
     4        WN(10,11,3), OT(10,10,4), OB(10,10,4), WT(10,10,4),
     5        WB(10,10,4), QOWG(10,10,3), VP(10,10,3), CT(10,10,3)
      FACT = DELTO
      PAVGO = 0.D0
      PAVG = 0.D0
      OP = 0.D0
      WP = 0.D0
      GP = 0.D0
      WI = 0.D0
      GI = 0.D0
      DO 10 K = 1, KK
        DO 10 J = 1, JJ
          DO 10 I = 1, II
            PAVGO = PAVGO + PN(I,J,K) * VP(I,J,K)
            PAVG = PAVG + P(I,J,K) * VP(I,J,K)
            OP = OP + QO(I,J,K) * FACT
            IF (QW(I,J,K) .GT. 0.D0) WP = WP + QW(I,J,K) * FACT
            IF (QW(I,J,K) .LT. 0.D0) WI = WI + QW(I,J,K) * FACT
            IF (QG(I,J,K) .GT. 0.D0) GP = GP + QG(I,J,K) * DELTO
            IF (QG(I,J,K) .LT. 0.D0) GI = GI + QG(I,J,K) * DELTO
   10 CONTINUE
      COP = COP + OP
      CWP = CWP + WP
      CGP = CGP + GP
      CWI = CWI + WI
      CGI = CGI + GI
      DIV = 1.D0 / DELTO
      OPR = OP * DIV
      WPR = WP * DIV
      GPR = GP * DIV
      WIR = WI * DIV
      GIR = GI * DIV
      PAVG = PAVG / RESVOL
      PAVGO = PAVGO / RESVOL
      DENOM1 = STBOI - OP
      IF (DENOM1 .LT. 1.D-07) GO TO 20
      BEO = (STBO/(STBOI - OP) - 1.D0) * 100.D0
   20 CONTINUE
      DENOM2 = STBWI - WP - WI
      IF (DENOM2 .LT. 1.D-07) GO TO 30
      BEW = (STBW/(STBWI - WP - WI) - 1.D0) * 100.D0
   30 CONTINUE
      DENOM3 = ACFGI - GP - GI
      IF (DENOM3 .LT. 1.D-07) GO TO 40
      BEG = (ACFGT/(ACFGI - GP - GI) - 1.D0) * 100.D0
   40 CONTINUE
      IF (OP .EQ. 0.D0) GOR = 0.D0
      IF (OP .EQ. 0.D0) WOR = 0.D0
      IF (OP .EQ. 0.D0) GO TO 50
      WOR = WP / OP
   50 CONTINUE
   60 CONTINUE
      RETURN
      END
      SUBROUTINE WELLS(IM, JM, NWELL)
      IMPLICIT REAL*8(A - H,O - Z)
      LOGICAL*1 FREE(1) /'*'/
      COMMON /PARRAY/ PN(10,10,3), SON(10,10,3), SWN(10,10,3),
     1       SGN(10,10,3), SO1(10,10,3), SW1(10,10,3), SG1(10,10,3),
     2       A1(10,10,3), A2(10,10,3), A3(10,10,3), SUM(10,10,3),
     3       GAM(10,10,3), QS(10,10,3)
      COMMON /SPRS/ P(10,10,3), SO(10,10,3), SW(10,10,3), SG(10,10,3)
      COMMON /SRATE/ PIN(20,3), PWF(20,3), PWFC(20,3), KIP(20),
     1       GMO(20,3), GMW(20,3), GMG(20,3), WELLID(20), LAYER(20),
     2       QVO(20), QVW(20), QVG(20), QVT(20), CUMO(20,3), CUMW(20,3),
     3          CUMG(20,3)
      COMMON /SDELTA/ DX(10,10,3), DY(10,10,3), DZ(10,10,3), IQN1(20),
     1         IQN2(20), IQN3(20)
      READ (20,FREE) NWELL
      IF (NWELL .EQ. 0) RETURN
      WRITE (1,80)
      WRITE (1,90)
      DO 40 J = 1, NWELL
        READ (20,10) WELLID(J)
        READ (20,FREE) IQN1(J), IQN2(J), IQN3(J), LAYER(J), KIP(J),
     1       QVO(J), QVW(J), QVG(J), QVT(J), CWSI
   10   FORMAT (A5, 5I5, 4F10.0)
        IQ3 = IQN3(J)
        LAY = IQ3 + (LAYER(J) - 1)
        DO 30 K = IQ3, LAY
          READ (20,FREE) PIN(J,K), PWF(J,K)
   20     FORMAT (2F10.0)
          WRITE (1,100) IQN1(J), IQN2(J), K, QVO(J), QVW(J), QVG(J),
     1    QVT(J), PWF(J,K), PIN(J,K)
   30   CONTINUE
   40 CONTINUE
      DO 50 J = 1, NWELL
        IQ3 = IQN3(J)
        LAY = IQ3 + (LAYER(J) - 1)
        DO 50 K = IQ3, LAY
          IF (KIP(J) .EQ. 1) WRITE (1,120) IQN1(J), IQN2(J), K
          IF (KIP(J) .EQ. 2) WRITE (1,130) IQN1(J), IQN2(J), K
          IF (KIP(J) .EQ. 3) WRITE (1,140) IQN1(J), IQN2(J), K
          IF (KIP(J) .EQ. - 1) WRITE (1,150) IQN1(J), IQN2(J), K
          IF (KIP(J) .EQ. - 2) WRITE (1,160) IQN1(J), IQN2(J), K
          IF (KIP(J) .EQ. - 3) WRITE (1,170) IQN1(J), IQN2(J), K
          IF (KIP(J) .EQ. - 11) WRITE (1,180) IQN1(J), IQN2(J), K
          IF (KIP(J) .EQ. - 12) WRITE (1,190) IQN1(J), IQN2(J), K
          IF (KIP(J) .EQ. - 13) WRITE (1,200) IQN1(J), IQN2(J), K
   50 CONTINUE
   60 FORMAT (3I5, 6F10.0, I5)
   70 FORMAT (4F10.0)
   80 FORMAT (//T15, 'RESERVOIR CONTAINS THE FOLLOWING RATE BLOCKS'/)
   90 FORMAT (T2, '   BLOCK   ', 3X, '  OIL(SCFD)', 3X, 'WATER(SCFD)',
     1       3X, 'GAS(SCFD)', 3X, 'TOTAL(CFT)', 3X, 'BHFP(PSIA)', 3X,
     2       'PID')
  100 FORMAT (1X, 3I3, 3X, F11.2, 4F13.2, F10.6)
  110 FORMAT (9X, 3I4, F10.2, 3F5.1, 10X, F10.2, 3F5.1, F12.3)
  120 FORMAT (T15, 'BLOCK ', 3I3, ' CONTAINS A RATE SPECIFIED PRODUCING
     1WELL')
  130 FORMAT (T15, 'BLOCK ', 3I3, ' CONTAINS A RATE SPECIFIED WATER INJE
     1CTION WELL')
  140 FORMAT (T15, 'BLOCK ', 3I3, ' CONTAINS A RATE SPECIFIED GAS INJECT
     1ION WELL')
  150 FORMAT (T15, 'BLOCK ', 3I3, ' CONTAINS AN  ',
     1       'EXPLICIT PRESSURE SPECIFIED PRODUCING WELL')
  160 FORMAT (T15, 'BLOCK ', 3I3, ' CONTAINS AN ', 'EXPLICIT PRESSURE SP
     1ECIFIED WATER INJECTION WELL')
  170 FORMAT (15X, 'BLOCK ', 3I3, ' CONTAINS AN ', 'EXPLICIT PRESSURE SP
     1ECIFIED GAS INJECTION WELL')
  180 FORMAT (T15, 'BLOCK ', 3I3, ' CONTAINS AN ', 'IMPLICIT PRESSURE SP
     1ECIFIED PRODUCING WELL')
  190 FORMAT (T15, 'BLOCK ', 3I3, ' CONTAINS AN ', 'IMPLICIT PRESSURE SP
     1ECIFIED  WATER INJECTION WELL')
  200 FORMAT (T15, 'BLOCK ', 3I3, ' CONTAINS AN ', 'IMPLICIT PRESSURE SP
     1ECIFIED GAS INJECTION WELL')
      RETURN
      END
      SUBROUTINE PARM(II, JJ, KK, IM, JM)
      IMPLICIT REAL*8(A - H,O - Z)
      LOGICAL*1 FREE(1) /'*'/
      DIMENSION RPHL(3), RPXL(3), RPYL(3), RPZL(3)
      COMMON /SGAS/ BO(10,10,3), BW(10,10,3), BG(10,10,3), QO(10,10,3),
     1       QW(10,10,3), QG(10,10,3), GOWT(10,10,3), GWWT(10,10,3),
     2       GGWT(10,10,3), OW(11,10,3), OE(11,10,3), WW(11,10,3),
     3       WE(11,10,3), OS(10,11,3), ON(10,11,3), WS(10,11,3),
     4       WN(10,11,3), OT(10,10,4), OB(10,10,4), WT(10,10,4),
     5       WB(10,10,4), QOWG(10,10,3), VP(10,10,3), CT(10,10,3)
      COMMON /SPARM/ PX(10,10,3), PY(10,10,3), PZ(10,10,3), EL(10,10,3),
     1       TX(11,10,3), TY(10,11,3), TZ(10,10,4)
      READ (20,FREE) KPH, KPX, KPY, KPZ
      IF (KPH .GE. 0) GO TO 20
      READ (20,FREE) PHIC
      DO 10 K = 1, KK
        DO 10 J = 1, JJ
          DO 10 I = 1, II
   10 VP(I,J,K) = PHIC
      WRITE (1,350) PHIC
      GO TO 80
   20 IF (KPH .GT. 0) GO TO 50
      READ (20,FREE) (RPHL(K),K=1,KK)
      DO 30 K = 1, KK
        DO 30 J = 1, JJ
          DO 30 I = 1, II
   30 VP(I,J,K) = RPHL(K)
      DO 40 K = 1, KK
   40 WRITE (1,450) K, RPHL(K)
      GO TO 80
   50 WRITE (1,400)
      DO 70 K = 1, KK
        WRITE (1,390) K
        DO 60 J = 1, JJ
          READ (20,FREE) (VP(I,J,K),I=1,II)
   60   WRITE (1,340) (VP(I,J,K),I=1,II)
   70 CONTINUE
   80 CONTINUE
      IF (KPX .GE. 0) GO TO 100
      READ (20,FREE) PERMXC
      DO 90 K = 1, KK
        DO 90 J = 1, JJ
          DO 90 I = 1, II
   90 PX(I,J,K) = PERMXC
      WRITE (1,360) PERMXC
      GO TO 160
  100 IF (KPX .GT. 0) GO TO 130
      READ (20,FREE) (RPXL(K),K=1,KK)
      DO 110 K = 1, KK
        DO 110 J = 1, JJ
          DO 110 I = 1, II
  110 PX(I,J,K) = RPXL(K)
      DO 120 K = 1, KK
  120 WRITE (1,460) K, RPXL(K)
      GO TO 160
  130 WRITE (1,420)
      DO 150 K = 1, KK
```

```
        WRITE (1,390) K
        DO 140 J = 1, JJ
          READ (20,FREE) (PX(I,J,K),I=1,II)
  140   WRITE (1,330) (PX(I,J,K),I=1,II)
  150 CONTINUE
  160 CONTINUE
      IF (KPY .GE. 0) GO TO 180
      READ (20,FREE) PERMYC
      DO 170 K = 1, KK
        DO 170 J = 1, JJ
          DO 170 I = 1, II
  170 PY(I,J,K) = PERMYC
      WRITE (1,370) PERMYC
      GO TO 240
  180 IF (KPY .GT. 0) GO TO 210
      READ (20,FREE) (RPYL(K),K=1,KK)
      DO 190 K = 1, KK
        DO 190 J = 1, JJ
          DO 190 I = 1, II
  190 PY(I,J,K) = RPYL(K)
      DO 200 K = 1, KK
  200 WRITE (1,470) K, RPYL(K)
      GO TO 240
  210 WRITE (1,430)
      DO 230 K = 1, KK
        WRITE (1,390) K
        DO 220 J = 1, JJ
          READ (20,FREE) (PY(I,J,K),I=1,II)
  220   WRITE (1,330) (PY(I,J,K),I=1,II)
  230 CONTINUE
  240 CONTINUE
      IF (KPZ .GE. 0) GO TO 260
      READ (20,FREE) PERMZC
      DO 250 K = 1, KK
        DO 250 J = 1, JJ
          DO 250 I = 1, II
  250 PZ(I,J,K) = PERMZC
      WRITE (1,380) PERMZC
      GO TO 320
  260 IF (KPZ .GT. 0) GO TO 290
      READ (20,FREE) (RPZL(K),K=1,KK)
      DO 270 K = 1, KK
        DO 270 J = 1, JJ
          DO 270 I = 1, II
  270 PZ(I,J,K) = RPZL(K)
      DO 280 K = 1, KK
  280 WRITE (1,480) K, RPZL(K)
      GO TO 320
  290 WRITE (1,440)
      DO 310 K = 1, KK
        WRITE (1,390) K
        DO 300 J = 1, JJ
          READ (20,FREE) (PZ(I,J,K),I=1,II)
  300   WRITE (1,330) (PZ(I,J,K),I=1,II)
  310 CONTINUE
  320 CONTINUE
  330 FORMAT (1X, 20F6.2)
  340 FORMAT (1X, 20F6.4)
  350 FORMAT (T15, 'POROSITY (PHI) IS ', F8.4, ' FOR ALL', ' BLOCKS'//)
  360 FORMAT (T15, 'PERMEABILITY (PX) IS ', ' SET AT', F10.4,
   1       ' FOR ALL BLOCKS'//)
370 FORMAT (T15, 'PERMEABILITY (PY) IS ', ' SET AT', F10.4,
   1       ' FOR ALL BLOCKS'//)
380 FORMAT (T15, 'PERMEABILITY (PZ) IS ', ' SET AT', F10.4,
   1       ' FOR ALL BLOCKS'//)
390 FORMAT (/1X, 'K =', I2/)
400 FORMAT (//T15, '**********POROSITY DISTRIBUTION FOLLOWS**********'
   1       /)
410 FORMAT (//T15, '********** NODE MIDPOINT ELEVATIONS **********'/)
420 FORMAT (//T15, '**********PERMEABILITY (PX) DISTRIBUTION**********
   1'/)
430 FORMAT (//T15, '**********PERMEABILITY (PY) DISTRIBUTION**********
   1'/)
440 FORMAT (//T15, '**********PERMEABILITY (PZ) DISTRIBUTION**********
   1'/)
450 FORMAT (//T15, 'POROSITY IN LAYER', I5, ' IS ', F8.5,
   1       ' FOR ALL BLOCKS', /)
460 FORMAT (T15, 'PERMEABILITY (PX) IN LAYER', I5, ' IS ', F8.2,
   1       ' FOR ALL BLOCKS', /)
470 FORMAT (T15, 'PERMEABILITY (PY) IN LAYER', I5, ' IS ', F8.2,
   1       ' FOR ALL BLOCKS', /)
480 FORMAT (T15, 'PERMEABILITY (PZ) IN LAYER', I5, ' IS ', F8.2,
   1       ' FOR ALL BLOCKS', /)
    RETURN
    END
    SUBROUTINE SUMM(NLOOP, KPI, II, JJ, KK, IM, JM, PAVGO, PAVG,
   1           STBOI, STBWI, ACFGI, COP, CWP, CWI, CGP, CGI, BEO, BEW,
   2           BEG, OPR, WP, WPR, GP, GPR, WI, WIR, GI, GIR, STBO,
   3           STBW, ACFG, ACFG1, WOR, GOR, DELTO, OP, ACFGT, ETI)
    IMPLICIT REAL*8(A - H,O - Z)
    LOGICAL*1 FREE(1) /'*'/
    COMMON /ADS/ A4, B4, CN, CWSI
    COMMON /ADS1/ VB(10,10,3), GWWT1(10,10,3), WW1(11,10,3),
   1       WS1(10,11,3), WN1(10,11,3), WT1(10,10,4), WB1(10,10,4)
    COMMON /ADS2/ WE1(11,10,3), CWSN(10,10,3), CWS(10,10,3)
    COMMON /GASSAT/ PBO, VSLOPE, BSLOPE, RSLOPE, PMAXT, RHOSCO,
   1       RHOSCG, RHOSCW, PBOT(10,10,3)
    COMMON /NPTS/ MSAT, MPOT, MPWT, MPGT, IREPRS
    COMMON /PARRAY/ PN(10,10,3), SON(10,10,3), SWN(10,10,3),
   1       SGN(10,10,3), SO1(10,10,3), SW1(10,10,3), SG1(10,10,3),
   2       A1(10,10,3), A2(10,10,3), A3(10,10,3), SUM(10,10,3),
   3       GAM(10,10,3), QS(10,10,3)
    COMMON /SPRS/ P(10,10,3), SO(10,10,3), SW(10,10,3), SG(10,10,3)
    COMMON /POR/ PORVOL
    PPM = 0.D0
    SOM = 0.D0
    SWM = 0.D0
    SGM = 0.D0
    IF (NLOOP .EQ. 1) GO TO 70
    DO 40 K = 1, KK
      DO 40 J = 1, JJ
        DO 40 I = 1, II
          CWS(I,J,K) = CWSN(I,J,K)
          DPO = P(I,J,K) - PN(I,J,K)
          DSO = SO(I,J,K) - SON(I,J,K)
          DSW = SW(I,J,K) - SWN(I,J,K)
          DSG = SG(I,J,K) - SGN(I,J,K)
          IF (DABS(DPO) .LE. DABS(PPM)) GO TO 10
          PPM = DPO
          IPM = I
```

```
                JPM = J
                KPM = K
   10           IF (DABS(DSO) .LE. DABS(SOM)) GO TO 20
                SOM = DSO
                IOM = I
                JOM = J
                KOM = K
   20           IF (DABS(DSW) .LE. DABS(SWM)) GO TO 30
                SWM = DSW
                IWM = I
                JWM = J
                KWM = K
   30           IF (DABS(DSG) .LE. DABS(SGM)) GO TO 40
                SGM = DSG
                IGM = I
                JGM = J
                KGM = K
   40 CONTINUE
        NLM = NLOOP - 1
        COPNW = COP * 28317.D0
        CWPNW = CWP * 28317.D0
        CGPNW = CGP * 28317.D0
        OPRNW = OPR * 28317.D0 / 24.D0
        GPRNW = GPR * 28317.D0 / 24.D0
        WPRNW = WPR * 28317.D0 / 24.D0
        GIRNW = GIR * 28317.D0 / 24.D0
        WIRNW = WIR * 28317.D0 / 24.D0
        GORNW = GOR
        PVPROD = (COPNW + CWPNW)
        IF (WPRNW .GT. 0.D0) GLR = GPRNW / (GPRNW + WPRNW) * 100.D0
        PNEW = P(1,1,1) - P(II,1,1)
        WRITE (1,60) PVPROD, PNEW, GLR, SG(II,1,1)
   50 CONTINUE
   60 FORMAT ('VOL=', D10.4, ' DEL P=', D8.2, ' GLR=', D8.2, ' Sg=',
     1        D8.2)
   70 CONTINUE
      RETURN
      END
C..................................................................RATES
      SUBROUTINE RATES(NWELL)
      IMPLICIT REAL*8(A - H,O - Z)
      LOGICAL*1 FREE(1) /'*'/
      COMMON /ADS/ A4, B4, CN, CWSI
      COMMON /ADS1/ VB(10,10,3), GWWT1(10,10,3), WW1(11,10,3),
     1       WS1(10,11,3), WN1(10,11,3), WT1(10,10,4), WB1(10,10,4)
      COMMON /ADS2/ WE1(11,10,3), CWSN(10,10,3), CWS(10,10,3)
      COMMON /GASSAT/ PBO, VSLOPE, BSLOPE, RSLOPE, PMAXT, RHOSCO,
     1       RHOSCG, RHOSCW, PBOT(10,10,3)
      COMMON /NPTS/ MSAT, MPOT, MPWT, MPGT, IREPRS
      COMMON /COEF/ AW(10,10,3), AE(10,10,3), AN(10,10,3), AS(10,10,3),
     1       AB(10,10,3), AT(10,10,3), E(10,10,3), B(10,10,3)
      COMMON /PARRAY/ PN(10,10,3), SON(10,10,3), SWN(10,10,3),
     1       SGN(10,10,3), SO1(10,10,3), SW1(10,10,3), SG1(10,10,3),
     2       A1(10,10,3), A2(10,10,3), A3(10,10,3), SUM(10,10,3),
     3       GAM(10,10,3), QS(10,10,3)
      COMMON /SPARM/ PX(10,10,3), PY(10,10,3), PZ(10,10,3), EL(10,10,3),
     1       TX(11,10,3), TY(10,11,3), TZ(10,10,4)
      COMMON /SPRS/ P(10,10,3), SO(10,10,3), SW(10,10,3), SG(10,10,3)
      COMMON /SPVT/ SAT(25), PRMROT(25), PRMRWT(25), PRMRGT(25),
     1       PCOWT(25), PCGOT(25), POT(25), VSOT(25), BOT(25), BOPT(25),
     2      RSOT(25), RSOPT(25), PWT(25), VSWT(25), BWT(25), BWPT(25),
     3      RSWT(25), RSWPT(25), PGT(25), VSGT(25), BGT(25), BGPT(25),
     4      CRT(25)
      COMMON /SRATE/ PIN(20,3), PWF(20,3), PWFC(20,3), KIP(20),
     1      GMO(20,3), GMW(20,3), GMG(20,3), WELLID(20), LAYER(20),
     2      QVO(20), QVW(20), QVG(20), QVT(20), CUMO(20,3), CUMW(20,3),
     3      CUMG(20,3)
      COMMON /SGAS/ BO(10,10,3), BW(10,10,3), BG(10,10,3), QO(10,10,3),
     1      QW(10,10,3), QG(10,10,3), GOWT(10,10,3), GWWT(10,10,3),
     2      GGWT(10,10,3), OW(11,10,3), OE(11,10,3), WW(11,10,3),
     3      WE(11,10,3), OS(10,11,3), ON(10,11,3), WS(10,11,3),
     4      WN(10,11,3), OT(10,10,4), OB(10,10,4), WT(10,10,4),
     5      WB(10,10,4), QOWG(10,10,3), VP(10,10,3), CT(10,10,3)
      COMMON /SDELTA/ DX(10,10,3), DY(10,10,3), DZ(10,10,3), IQN1(20),
     1      IQN2(20), IQN3(20)
C
      DO 130 J = 1, NWELL
        IQ1 = IQN1(J)
        IQ2 = IQN2(J)
        IQ3 = IQN3(J)
        LAY = IQ3 + (LAYER(J) - 1)
        DO 10 K = IQ3, LAY
          PWFC(J,K) = -1.D0
          PP = P(IQ1,IQ2,K)
          BPT = PBOT(IQ1,IQ2,K)
          CALL INTPVT(BPT, VSLOPE, POT, VSOT, MPOT, PP, VSO)
          CALL INTERP(PWT, VSWT, MPWT, PP, VSW)
          SSO = SO(IQ1,IQ2,K)
          SSW = SW(IQ1,IQ2,K)
          SSG = SG(IQ1,IQ2,K)
          CALL AMUG(PGT, VSGT, MPGT, PP, VSG, CWSI, PX(IQ1,IQ2,K), SSW,
     1        SSO)
          CALL INTERP(SAT, PRMRWT, MSAT, SSW, PRMRW)
          CALL INTERP(SAT, PRMROT, MSAT, SSO, PRMRO)
          CALL INTERP(SAT, PRMRGT, MSAT, SSG, PRMRG)
          GMW(J,K) = PRMRW / VSW
          GMO(J,K) = PRMRO / VSO
          GMG(J,K) = PRMRG / VSG
   10   CONTINUE
        IF (KIP(J) .LT. 0) GO TO 130
        IF (KIP(J) .NE. 1) GO TO 70
        ITERQ = 0
        QDENOM = 0.D0
        ALPHAO = 0.D0
        ALPHAW = 0.D0
        ALPHAG = 0.D0
        LAY = IQ3 + (LAYER(J) - 1)
   20   ITERQ = ITERQ + 1
        DO 60 K = IQ3, LAY
          PP = P(IQ1,IQ2,K)
          BPT = PBOT(IQ1,IQ2,K)
          CALL INTPVT(BPT, BSLOPE, POT, BOT, MPOT, PP, BBO)
          CALL INTERP(PWT, BWT, MPWT, PP, BBW)
          CALL INTERP(PGT, BGT, MPGT, PP, BBG)
          CALL INTPVT(BPT, RSLOPE, POT, RSOT, MPOT, PP, RSO)
          CALL INTERP(PWT, RSWT, MPWT, PP, RSW)
          IF (ITERQ .NE. 1) GO TO 30
          QDENOM = QDENOM + PIN(J,K) * GMO(J,K) / BBO
          GMT = GMO(J,K) + GMW(J,K) + GMG(J,K)
          ALPHAO = GMO(J,K) / GMT + ALPHAO
          ALPHAW = GMW(J,K) / GMT + ALPHAW
          ALPHAG = GMG(J,K) / GMT + ALPHAG
          GO TO 60
   30     IF (QVT(J) .EQ. 0.D0) GO TO 40
          QW(IQ1,IQ2,K) = QVT(J) * ALPHAW / (ALPHAO + ALPHAW + ALPHAG)
          QG(IQ1,IQ2,K) = QVT(J) * ALPHAG / (ALPHAO + ALPHAG + ALPHAW)
          QO(IQ1,IQ2,K) = QVT(J) * ALPHAO / (ALPHAW + ALPHAO + ALPHAG)
          GO TO 50
   40     TOTOR = QVO(J)
   50     CONTINUE
   60   CONTINUE
        IF (ITERQ .EQ. 1) GO TO 20
        GO TO 130
   70   CONTINUE
        LAY = IQ3 + (LAYER(J) - 1)
        ITERQ = 0
        QDENOM = 0.D0
   80   ITERQ = ITERQ + 1
        DO 120 K = IQ3, LAY
          IF (ITERQ .NE. 1) GO TO 90
          QDENOM = QDENOM + PIN(J,K) * (GMO(J,K) + GMW(J,K) + GMG(J,K))
          GO TO 120
   90     IF (KIP(J) .NE. 2) GO TO 100
          QW(IQ1,IQ2,K) = QVW(J) * PIN(J,K) * (GMO(J,K) + GMW(J,K) +
     1    GMG(J,K)) / QDENOM
          GO TO 120
  100     CONTINUE
          IF (KIP(J) .NE. 3) GO TO 110
          QW(IQ1,IQ2,K) = QVW(J) * PIN(J,K) * (GMO(J,K) + GMW(J,K) +
     1    GMG(J,K)) / QDENOM
  110     CONTINUE
          QG(IQ1,IQ2,K) = QVG(J) * PIN(J,K) * (GMO(J,K) + GMW(J,K) +
     1    GMG(J,K)) / QDENOM
  120   CONTINUE
        IF (ITERQ .EQ. 1) GO TO 80
  130 CONTINUE
      DO 150 J = 1, NWELL
        IQ1 = IQN1(J)
        IQ2 = IQN2(J)
        IQ3 = IQN3(J)
        IF (KIP(J) .LT. 0) GO TO 150
        LAY = IQ3 + (LAYER(J) - 1)
        DO 140 K = IQ3, LAY
          PWFC(J,K) = 0.D0
          IF (PIN(J,K) .LE. 1.D-04) GO TO 140
          PP = P(IQ1,IQ2,K)
          BPT = PBOT(IQ1,IQ2,K)
          CALL INTPVT(BPT, BSLOPE, POT, BOT, MPOT, PP, BBO)
          CALL INTERP(PWT, BWT, MPWT, PP, BBW)
          CALL INTERP(PGT, BGT, MPGT, PP, BBG)
          CALL INTPVT(BPT, RSLOPE, POT, RSOT, MPOT, PP, RSO)
          CALL INTERP(PWT, RSWT, MPWT, PP, RSW)
          FAC = PIN(J,K)
          GMTB = GMO(J,K) / BBO + GMW(J,K) / BBW + GMG(J,K) / BBG
          SOLN = RSO * QO(IQ1,IQ2,K) + RSW * QW(IQ1,IQ2,K)
          QT = QO(IQ1,IQ2,K) + QW(IQ1,IQ2,K) + QG(IQ1,IQ2,K)
          PWFC(J,K) = PP - (QT - SOLN) / (FAC*GMTB)
  140   CONTINUE
  150 CONTINUE
      DO 190 J = 1, NWELL
```

```
        IF (KIP(J) .GE. 0) GO TO 200
        IQ1 = IQN1(J)
        IQ2 = IQN2(J)
        IQ3 = IQN3(J)
        LAY = IQ3 + (LAYER(J) - 1)
        DO 190 K = IQ3, LAY
          PPN = PN(IQ1,IQ2,K)
          BPT = PBOT(IQ1,IQ2,K)
          CALL INTPVT(BPT, BSLOPE, POT, BOT, MPOT, PPN, BBO)
          CALL INTERP(PWT, BWT, MPWT, PPN, BBW)
          CALL INTERP(PGT, BGT, MPGT, PPN, BBG)
          CALL INTPVT(BPT, RSLOPE, POT, RSOT, MPOT, PPN, RSO)
          CALL INTERP(PWT, RSWT, MPWT, PPN, RSW)
          IF (KIP(J) .NE. - 1) GO TO 160
          QO(IQ1,IQ2,K) = PIN(J,K) * GMO(J,K) * (PPN - PWF(J,K)) / BBO
          IF (PPN .LE. PWF(J,K)) QO(IQ1,IQ2,K) = 0.D0
          QW(IQ1,IQ2,K) = PIN(J,K) * GMW(J,K) * (PPN - PWF(J,K)) / BBW
          QG(IQ1,IQ2,K) = PIN(J,K) * GMG(J,K) * (PPN - PWF(J,K)) / BBG
          GO TO 190
  160     IF (KIP(J) .NE. - 2) GO TO 170
          QW(IQ1,IQ2,K) = PIN(J,K) * (GMO(J,K) + GMW(J,K) + GMG(J,K)) *
     1    (PPN - PWF(J,K)) / BBW
          IF (PPN .GE. PWF(J,K)) QW(IQ1,IQ2,K) = 0.D0
          GO TO 190
  170     IF (KIP(J) .NE. - 3) GO TO 180
          QG(IQ1,IQ2,K) = PIN(J,K) * (GMO(J,K) + GMW(J,K) + GMG(J,K)) *
     1    (PPN - PWF(J,K)) / BBG
          IF (PPN .GE. PWF(J,K)) QG(IQ1,IQ2,K) = 0.D0
  180     CONTINUE
  190 CONTINUE
  200 CONTINUE
      RETURN
      ENTRY PRATEI(NWELL)
      DO 220 J = 1, NWELL
        IF (KIP(J) .GE. - 10) GO TO 220
        IQ1 = IQN1(J)
        IQ2 = IQN2(J)
        IQ3 = IQN3(J)
        LAY = IQ3 + (LAYER(J) - 1)
        DO 210 K = IQ3, LAY
          P56 = PIN(J,K)
          PPN = PN(IQ1,IQ2,K)
          BPT = PBOT(IQ1,IQ2,K)
          CALL INTPVT(BPT, BSLOPE, POT, BOT, MPOT, PPN, BBO)
          CALL INTPVT(BPT, RSLOPE, POT, RSOT, MPOT, PPN, RSO)
          CALL INTERP(PWT, BWT, MPWT, PPN, BBW)
          CALL INTERP(PGT, BGT, MPGT, PPN, BBG)
          CALL INTERP(PWT, RSWT, MPWT, PPN, RSW)
          CPIO = GMO(J,K) * P56 * (BBO - BBG*RSO) / BBO
          CPIW = GMW(J,K) * P56 * (BBW - BBG*RSW) / BBW
          CPIG = GMG(J,K) * P56
          CPI = CPIO + CPIW + CPIG
          B(IQ1,IQ2,K) = B(IQ1,IQ2,K) - CPI * PWF(J,K)
          E(IQ1,IQ2,K) = E(IQ1,IQ2,K) - CPI
  210   CONTINUE
  220 CONTINUE
      RETURN
      ENTRY RATEO(NWELL)
      DO 250 J = 1, NWELL
        IF (KIP(J) .GE. - 10) GO TO 250
```

```
         IQ1 = IQN1(J)
         IQ2 = IQN2(J)
         IQ3 = IQN3(J)
         LAY = IQ3 + (LAYER(J) - 1)
         DO 240 K = IQ3, LAY
           PP = P(IQ1,IQ2,K)
           PPN = PN(IQ1,IQ2,K)
           BPT = PBOT(IQ1,IQ2,K)
           CALL INTPVT(BPT, RSLOPE, POT, RSOT, MPOT, PPN, RSON)
           CALL INTPVT(BPT, RSLOPE, POT, RSOT, MPOT, PP, RSO)
           CALL INTERP(PWT, RSWT, MPWT, PPN, RSWN)
           CALL INTERP(PWT, RSWT, MPWT, PP, RSW)
           RSOAV = 0.5D0 * (RSO + RSON)
           RSWAV = 0.5D0 * (RSW + RSWN)
           FACTOR = PIN(J,K) * (PP - PWF(J,K))
           IF (KIP(J) .EQ. - 13) GO TO 230
           QW(IQ1,IQ2,K) = GMW(J,K) / BW(IQ1,IQ2,K) * FACTOR
           IF (KIP(J) .EQ. - 12) QW(IQ1,IQ2,K) = (GMO(J,K) + GMW(J,K) +
     1     GMG(J,K)) / BW(IQ1,IQ2,K) * FACTOR
           IF (KIP(J) .EQ. - 12) GO TO 240
           QO(IQ1,IQ2,K) = 0.D0
           QG(IQ1,IQ2,K) = GMG(J,K) / BG(IQ1,IQ2,K) * FACTOR + RSOAV *
     1     QO(IQ1,IQ2,K) + RSWAV * QW(IQ1,IQ2,K)
           GO TO 240
  230      QG(IQ1,IQ2,K) = (GMO(J,K) + GMW(J,K) + GMG(J,K)) / BG(IQ1,IQ2,
     1     K) * FACTOR
  240    CONTINUE
  250 CONTINUE
      RETURN
      END
      SUBROUTINE SOLMAT(II, JJ, KK, IM, JM, DIV1, D288, N, NN)
      IMPLICIT REAL*8(A - H,O - Z)
      LOGICAL*1 FREE(1) /'*'/
      COMMON /ADS/ A4, B4, CN, CWSI
      COMMON /ADS1/ VB(10,10,3), GWWT1(10,10,3), WW1(11,10,3),
     1       WS1(10,11,3), WN1(10,11,3), WT1(10,10,4), WB1(10,10,4)
      COMMON /ADS2/ WE1(11,10,3), CWSN(10,10,3), CWS(10,10,3)
      COMMON /FOAM/ DCONST, ECONST
      COMMON /GASSAT/ PBO, VSLOPE, BSLOPE, RSLOPE, PMAXT, RHOSCO,
     1       RHOSCG, RHOSCW, PBOT(10,10,3)
      COMMON /NPTS/ MSAT, MPOT, MPWT, MPGT, IREPRS
      COMMON /COEF/ AW(10,10,3), AE(10,10,3), AN(10,10,3), AS(10,10,3),
     1       AB(10,10,3), AT(10,10,3), E(10,10,3), B(10,10,3)
      COMMON /PARRAY/ PN(10,10,3), SON(10,10,3), SWN(10,10,3),
     1       SGN(10,10,3), SO1(10,10,3), SW1(10,10,3), SG1(10,10,3),
     2       A1(10,10,3), A2(10,10,3), A3(10,10,3), SUM(10,10,3),
     3       GAM(10,10,3), QS(10,10,3)
      COMMON /SPARM/ PX(10,10,3), FY(10,10,3), PZ(10,10,3), EL(10,10,3),
     1       TX(11,10,3), TY(10,11,3), TZ(10,10,4)
      COMMON /SPRS/ P(10,10,3), SO(10,10,3), SW(10,10,3), SG(10,10,3)
      COMMON /SPVT/ SAT(25), PRMROT(25), PRMRWT(25), PRMRGT(25),
     1       PCOWT(25), PCGOT(25), POT(25), VSOT(25), BOT(25), BOPT(25),
     2       RSOT(25), RSOPT(25), PWT(25), VSWT(25), BWT(25), BWPT(25),
     3       RSWT(25), RSWPT(25), PGT(25), VSGT(25), BGT(25), BGPT(25),
     4       CRT(25)
      COMMON /SGAS/ BO(10,10,3), BW(10,10,3), BG(10,10,3), QO(10,10,3),
     1       QW(10,10,3), QG(10,10,3), GOWT(10,10,3), GWWT(10,10,3),
     2       GGWT(10,10,3), OW(11,10,3), OE(11,10,3), WW(11,10,3),
     3       WE(11,10,3), OS(10,11,3), ON(10,11,3), WS(10,11,3),
     4       WN(10,11,3), OT(10,10,4), OB(10,10,4), WT(10,10,4),
     5       WB(10,10,4), QOWG(10,10,3), VP(10,10,3), CT(10,10,3)
      DATA RSO1, RSO2, RSO3, RSO4, RSO5, RSO6 /6*0.D0/
      DATA RSW1, RSW2, RSW3, RSW4, RSW5, RSW6 /6*0.D0/
      CTEMP1 = 0.D0
      CTEMP2 = 0.D0
      CTEMP3 = 0.D0
      CTEMP4 = 0.D0
      CTEMP5 = 0.D0
      CTEMP6 = 0.D0
      GGW1 = 0.D0
      GGW2 = 0.D0
      GGW3 = 0.D0
      GGW4 = 0.D0
      GGW5 = 0.D0
      GGW6 = 0.D0
      VISO1 = 0.D0
      VISW1 = 0.D0
      VISG1 = 0.D0
      VISO3 = 0.D0
      VISW3 = 0.D0
      VISG3 = 0.D0
      VISO4 = 0.D0
      VISW4 = 0.D0
      VISG4 = 0.D0
      VISO5 = 0.D0
      VISW5 = 0.D0
      VISG5 = 0.D0
      VISO6 = 0.D0
      VISW6 = 0.D0
      VISG6 = 0.D0
      GOW1 = 0.D0
      GOW2 = 0.D0
      GOW3 = 0.D0
      GOW4 = 0.D0
      GOW5 = 0.D0
      GOW6 = 0.D0
      GWW1 = 0.D0
      GWW2 = 0.D0
      GWW3 = 0.D0
      GWW4 = 0.D0
      GWW5 = 0.D0
      GWW6 = 0.D0
      DO 70 K = 1, KK
        DO 70 J = 1, JJ
          DO 70 I = 1, II
            PP = P(I,J,K)
            BPT = PBOT(I,J,K)
            CALL INTPVT(BPT, RSLOPE, POT, RSOT, MPOT, PP, RSO)
            CALL INTPVT(BPT, VSLOPE, POT, VSOT, MPOT, PP, VSO)
            CALL INTERP(PWT, RSWT, MPWT, PP, RSW)
            CALL INTERP(PWT, VSWT, MPWT, PP, VSW)
            SSO = SO(I,J,K)
            SSW = SW(I,J,K)
            SSG = SG(I,J,K)
            CALL AMUG(PGT, VSGT, MPGT, PP, VSG, CWSN(I,J,K), PX(I,J,K),
     1           SSW, SSO)
            CALL INTERP(SAT, PCOWT, MSAT, SSW, PCOW)
            CALL INTERP(SAT, PCGOT, MSAT, SSG, PCGO)
            RO = (RHOSCO + RSO*RHOSCG) / BO(I,J,K)
            RW = (RHOSCW + RSW*RHOSCG) / BW(I,J,K)
      RG = RHOSCG / BG(I,J,K)
      IF (I .EQ. 1) GO TO 10
      P1 = P(I - 1,J,K)
      BPT = PBOT(I - 1,J,K)
      CALL INTPVT(BPT, RSLOPE, POT, RSOT, MPOT, P1, RSO1)
      CALL INTPVT(BPT, VSLOPE, POT, VSOT, MPOT, P1, VSO1)
      CALL INTERP(PWT, RSWT, MPWT, P1, RSW1)
      CALL INTERP(PWT, VSWT, MPWT, P1, VSW1)
      SO1S = SO(I - 1,J,K)
      SW1S = SW(I - 1,J,K)
      SG1S = SG(I - 1,J,K)
      CALL AMUG(PGT, VSGT, MPGT, P1, VSG1, CWSN(I - 1,J,K), PX(I -
     1    1,J,K), SW1S, SO1S)
      CALL INTERP(SAT, PCOWT, MSAT, SW1S, PCOW1)
      CALL INTERP(SAT, PCGOT, MSAT, SG1S, PCGO1)
      RO1 = (RHOSCO + RSO1*RHOSCG) / BO(I - 1,J,K)
      RW1 = (RHOSCW + RSW1*RHOSCG) / BW(I - 1,J,K)
      RG1 = RHOSCG / BG(I - 1,J,K)
C
      FACT = -D288 * (EL(I - 1,J,K) - EL(I,J,K))
      GOW1 = (RO1 + RO) * FACT
      GWW1 = (RW1 + RW) * FACT + PCOW - PCOW1
      GGW1 = (RG1 + RG) * FACT + PCGO1 - PCGO
      P11 = P1 - PP
      HO1 = P11 + GOW1
      HW1 = P11 + GWW1
      HG1 = P11 + GGW1
      IF (HO1 .GE. 0.D0) CALL INTERP(SAT, PRMROT, MSAT, SO1S,
     1    PRMRO1)
      IF (HO1 .LT. 0.D0) CALL INTERP(SAT, PRMROT, MSAT, SSO,
     1    PRMRO1)
      IF (HW1 .GE. 0.D0) CALL INTERP(SAT, PRMRWT, MSAT, SW1S,
     1    PRMRW1)
      IF (HW1 .LT. 0.D0) CALL INTERP(SAT, PRMRWT, MSAT, SSW,
     1    PRMRW1)
      IF (HG1 .GE. 0.D0) CALL INTERP(SAT, PRMRGT, MSAT, SG1S,
     1    PRMRG1)
      IF (HG1 .LT. 0.D0) CALL INTERP(SAT, PRMRGT, MSAT, SSG,
     1    PRMRG1)
      VISO1 = 4.D0 * PRMRO1 / ((BO(I - 1,J,K) + BO(I,J,K))*(VSO1 +
     1 VSO))
      VISW1 = 4.D0 * PRMRW1 / ((BW(I - 1,J,K) + BW(I,J,K))*(VSW1 +
     1 VSW))
      VISG1 = 4.D0 * PRMRG1 / ((BG(I - 1,J,K) + BG(I,J,K))*(VSG1 +
     1 VSG))
      CTEMP1 = 0.5D0 * (CWS(I,J,K) + CWS(I - 1,J,K))
   10 AOW = TX(I,J,K) * VISO1
      AWW = TX(I,J,K) * VISW1
      AWW1 = AWW * CTEMP1
      AGW = TX(I,J,K) * VISG1
C
      IF (I .EQ. II) GO TO 20
      P2 = P(I + 1,J,K)
      BPT = PBOT(I + 1,J,K)
      CALL INTPVT(BPT, RSLOPE, POT, RSOT, MPOT, P2, RSO2)
      CALL INTPVT(BPT, VSLOPE, POT, VSOT, MPOT, P2, VSO2)
      CALL INTERP(PWT, RSWT, MPWT, P2, RSW2)
      CALL INTERP(PWT, VSWT, MPWT, P2, VSW2)
      SO2 = SO(I + 1,J,K)
      SW2 = SW(I + 1,J,K)
      SG2 = SG(I + 1,J,K)
      CALL AMUG(PGT, VSGT, MPGT, P2, VSG2, CWSN(I + 1,J,K), PX(I +
     1    1,J,K), SW2, SO2)
      CALL INTERP(SAT, PCOWT, MSAT, SW2, PCOW2)
      CALL INTERP(SAT, PCGOT, MSAT, SG2, PCGO2)
      RO2 = (RHOSCO + RSO2*RHOSCG) / BO(I + 1,J,K)
      RW2 = (RHOSCW + RSW2*RHOSCG) / BW(I + 1,J,K)
      RG2 = RHOSCG / BG(I + 1,J,K)
C
      FACT = -D288 * (EL(I + 1,J,K) - EL(I,J,K))
      GOW2 = (RO2 + RO) * FACT
      GWW2 = (RW2 + RW) * FACT + PCOW - PCOW2
      GGW2 = (RG2 + RG) * FACT + PCGO2 - PCGO
      P22 = P2 - PP
      HO2 = P22 + GOW2
      HW2 = P22 + GWW2
      HG2 = P22 + GGW2
      IF (HO2 .GE. 0.D0) CALL INTERP(SAT, PRMROT, MSAT, SO2,
     1      PRMRO2)
      IF (HO2 .LT. 0.D0) CALL INTERP(SAT, PRMROT, MSAT, SSO,
     1      PRMRO2)
      IF (HW2 .GE. 0.D0) CALL INTERP(SAT, PRMRWT, MSAT, SW2,
     1      PRMRW2)
      IF (HW2 .LT. 0.D0) CALL INTERP(SAT, PRMRWT, MSAT, SSW,
     1      PRMRW2)
      IF (HG2 .GE. 0.D0) CALL INTERP(SAT, PRMRGT, MSAT, SG2,
     1      PRMRG2)
      IF (HG2 .LT. 0.D0) CALL INTERP(SAT, PRMRGT, MSAT, SSG,
     1      PRMRG2)
      VISO2 = 4.D0 * PRMRO2 / ((BO(I + 1,J,K) + BO(I,J,K))*(VSO2 +
     1 VSO))
      VISW2 = 4.D0 * PRMRW2 / ((BW(I + 1,J,K) + BW(I,J,K))*(VSW2 +
     1 VSW))
      VISG2 = 4.D0 * PRMRG2 / ((BG(I + 1,J,K) + BG(I,J,K))*(VSG2 +
     1 VSG))
      CTEMP2 = 0.5D0 * (CWS(I + 1,J,K) + CWS(I,J,K))
   20 AOE = TX(I + 1,J,K) * VISO2
      AWE = TX(I + 1,J,K) * VISW2
      AWE1 = AWE * CTEMP2
      AGE = TX(I + 1,J,K) * VISG2
      IF (J .EQ. 1) GO TO 30
      P3 = P(I,J - 1,K)
      BPT = PBOT(I,J - 1,K)
      CALL INTPVT(BPT, RSLOPE, POT, RSOT, MPOT, P3, RSO3)
      CALL INTPVT(BPT, VSLOPE, POT, VSOT, MPOT, P3, VSO3)
      CALL INTERP(PWT, RSWT, MPWT, P3, RSW3)
      CALL INTERP(PWT, VSWT, MPWT, P3, VSW3)
      SO3 = SO(I,J - 1,K)
      SW3 = SW(I,J - 1,K)
      SG3 = SG(I,J - 1,K)
      CALL AMUG(PGT, VSGT, MPGT, P3, VSG3, CWSN(I,J - 1,K),
     1      PX(I,J - 1,K), SW3, SO3)
      CALL INTERP(SAT, PCOWT, MSAT, SW3, PCOW3)
      CALL INTERP(SAT, PCGOT, MSAT, SG3, PCGO3)
      RO3 = (RHOSCO + RSO3*RHOSCG) / BO(I,J - 1,K)
      RW3 = (RHOSCW + RSW3*RHOSCG) / BW(I,J - 1,K)
      RG3 = RHOSCG / BG(I,J - 1,K)
C
      FACT = -D288 * (EL(I,J - 1,K) - EL(I,J,K))
      GOW3 = (RO3 + RO) * FACT
      GWW3 = (RW3 + RW) * FACT + PCOW - PCOW3
      GGW3 = (RG3 + RG) * FACT + PCGO3 - PCGO
      P33 = P3 - PP
      HO3 = P33 + GOW3
      HW3 = P33 + GWW3
      HG3 = P33 + GGW3
      IF (HO3 .GE. 0.D0) CALL INTERP(SAT, PRMROT, MSAT, SO3,
     1     PRMRO3)
      IF (HO3 .LT. 0.D0) CALL INTERP(SAT, PRMROT, MSAT, SSO,
     1     PRMRO3)
      IF (HW3 .GE. 0.D0) CALL INTERP(SAT, PRMRWT, MSAT, SW3,
     1     PRMRW3)
      IF (HW3 .LT. 0.D0) CALL INTERP(SAT, PRMRWT, MSAT, SSW,
     1     PRMRW3)
      IF (HG3 .GE. 0.D0) CALL INTERP(SAT, PRMRGT, MSAT, SG3,
     1     PRMRG3)
      IF (HG3 .LT. 0.D0) CALL INTERP(SAT, PRMRGT, MSAT, SSG,
     1     PRMRG3)
      VISO3 = 4.D0 * PRMRO3 / ((BO(I,J - 1,K) + BO(I,J,K))*(VSO3 +
     1 VSO))
      VISW3 = 4.D0 * PRMRW3 / ((BW(I,J - 1,K) + BW(I,J,K))*(VSW3 +
     1 VSW))
      VISG3 = 4.D0 * PRMRG3 / ((BG(I,J - 1,K) + BG(I,J,K))*(VSG3 +
     1 VSG))
      CTEMP3 = 0.5D0 * (CWS(I,J - 1,K) + CWS(I,J,K))
   30 AOS = TY(I,J,K) * VISO3
      AWS = TY(I,J,K) * VISW3
      AWS1 = AWS * CTEMP3
      AGS = TY(I,J,K) * VISG3
C
      IF (J .EQ. JJ) GO TO 40
      P4 = P(I,J + 1,K)
      BPT = PBOT(I,J + 1,K)
      CALL INTPVT(BPT, RSLOPE, POT, RSOT, MPOT, P4, RSO4)
      CALL INTPVT(BPT, VSLOPE, POT, VSOT, MPOT, P4, VSO4)
      CALL INTERP(PWT, RSWT, MPWT, P4, RSW4)
      CALL INTERP(PWT, VSWT, MPWT, P4, VSW4)
      SO4 = SO(I,J + 1,K)
      SW4 = SW(I,J + 1,K)
      SG4 = SG(I,J + 1,K)
      CALL AMUG(PGT, VSGT, MPGT, P4, VSG4, CWSN(I,J + 1,K),
     1     PX(I,J + 1,K), SW4, SO4)
      CALL INTERP(SAT, PCOWT, MSAT, SW4, PCOW4)
      CALL INTERP(SAT, PCGOT, MSAT, SG4, PCGO4)
      RO4 = (RHOSCO + RSO4*RSOSCG) / BO(I,J + 1,K)
      RW4 = (RHOSCW + RSW4*RHOSCG) / BW(I,J + 1,K)
      RG4 = RHOSCG / BG(I,J + 1,K)
C
      FACT = -D288 * (EL(I,J + 1,K) - EL(I,J,K))
      GOW4 = (RO4 + RO) * FACT
      GWW4 = (RW4 + RW) * FACT + PCOW - PCOW4
      GGW4 = (RG4 + RG) * FACT + PCGO4 - PCGO
C
      P44 = P4 - PP
      HO4 = P44 + GOW4
      HW4 = P44 + GWW4
      HG4 = P44 + GGW4
      IF (HO4 .GE. 0.D0) CALL INTERP(SAT, PRMROT, MSAT, SO4,
     1     PRMRO4)
      IF (HO4 .LT. 0.D0) CALL INTERP(SAT, PRMROT, MSAT, SSO,
     1          PRMRO4)
           IF (HW4 .GE. 0.D0) CALL INTERP(SAT, PRMRWT, MSAT, SW4,
     1          PRMRW4)
           IF (HW4 .LT. 0.D0) CALL INTERP(SAT, PRMRWT, MSAT, SSW,
     1          PRMRW4)
           IF (HG4 .GE. 0.D0) CALL INTERP(SAT, PRMRGT, MSAT, SG4,
     1          PRMRG4)
           IF (HG4 .LT. 0.D0) CALL INTERP(SAT, PRMRGT, MSAT, SSG,
     1          PRMRG4)
           VISO4 = 4.D0 * PRMRO4 / ((BO(I,J + 1,K) + BO(I,J,K))*(VSO4 +
     1      VSO))
           VISW4 = 4.D0 * PRMRW4 / ((BW(I,J + 1,K) + BW(I,J,K))*(VSW4 +
     1      VSW))
           VISG4 = 4.D0 * PRMRG4 / ((BG(I,J + 1,K) + BG(I,J,K))*(VSG4 +
     1      VSG))
           CTEMP4 = 0.5D0 * (CWS(I,J + 1,K) + CWS(I,J,K))
C
  40       AON = TY(I,J + 1,K) * VISO4
           AWN = TY(I,J + 1,K) * VISW4
           AWN1 = AWN * CTEMP4
           AGN = TY(I,J + 1,K) * VISG4
C
C
           IF (K .EQ. 1) GO TO 50
           P5 = P(I,J,K - 1)
           BPT = PBOT(I,J,K - 1)
           CALL INTPVT(BPT, RSLOPE, POT, RSOT, MPOT, P5, RSO5)
           CALL INTPVT(BPT, VSLOPE, POT, VSOT, MPOT, P5, VSO5)
           CALL INTERP(PWT, RSWT, MPWT, P5, RSW5)
           CALL INTERP(PWT, VSWT, MPWT, P5, VSW5)
           SO5 = SO(I,J,K - 1)
           SW5 = SW(I,J,K - 1)
           SG5 = SG(I,J,K - 1)
           CALL AMUG(PGT, VSGT, MPGT, P5, VSG5, CWSN(I,J,K - 1),
     1          PX(I,J,K - 1), SW5, SO5)
           CALL INTERP(SAT, PCOWT, MSAT, SW5, PCOW5)
           CALL INTERP(SAT, PCGOT, MSAT, SG5, PCGO5)
           RO5 = (RHOSCO + RSO5*RHOSCG) / BO(I,J,K - 1)
           RW5 = (RHOSCW + RSW5*RHOSCG) / BW(I,J,K - 1)
           RG5 = RHOSCG / BG(I,J,K - 1)
C
           FACT = -D288 * (EL(I,J,K - 1) - EL(I,J,K))
           GOW5 = (RO5 + RO) * FACT
           GWW5 = (RW5 + RW) * FACT + PCOW - PCOW5
           GGW5 = (RG5 + RG) * FACT + PCGO5 - PCGO
           P55 = P5 - PP
           HO5 = P55 + GOW5
           HW5 = P55 + GWW5
           HG5 = P55 + GGW5
           IF (HO5 .GE. 0.D0) CALL INTERP(SAT, PRMROT, MSAT, SO5,
     1          PRMRO5)
           IF (HO5 .LT. 0.D0) CALL INTERP(SAT, PRMROT, MSAT, SSO,
     1          PRMRO5)
           IF (HW5 .GE. 0.D0) CALL INTERP(SAT, PRMRWT, MSAT, SW5,
     1          PRMRW5)
           IF (HW5 .LT. 0.D0) CALL INTERP(SAT, PRMRWT, MSAT, SSW,
     1          PRMRW5)
           IF (HG5 .GE. 0.D0) CALL INTERP(SAT, PRMRGT, MSAT, SG5,
     1          PRMRG5)
           IF (HG5 .LT. 0.D0) CALL INTERP(SAT, PRMRGT, MSAT, SSG,
   1           PRMRG5)
      VISO5 = 4.D0 * PRMRO5 / ((BO(I,J,K - 1) + BO(I,J,K))*(VSO5 +
   1   VSO))
      VISW5 = 4.D0 * PRMRW5 / ((BW(I,J,K - 1) + BW(I,J,K))*(VSW5 +
   1   VSW))
      VISG5 = 4.D0 * PRMRG5 / ((BG(I,J,K - 1) + BG(I,J,K))*(VSG5 +
   1   VSG))
      CTEMP5 = 0.5D0 * (CWS(I,J,K - 1) + CWS(I,J,K))
C
C
 50   AOT = TZ(I,J,K) * VISO5
      AWT = TZ(I,J,K) * VISW5
      AWT1 = AWT * CTEMP5
      AGT = TZ(I,J,K) * VISG5
C
      IF (K .EQ. KK) GO TO 60
      P6 = P(I,J,K + 1)
      BPT = PBOT(I,J,K + 1)
      CALL INTPVT(BPT, RSLOPE, POT, RSOT, MPOT, P6, RSO6)
      CALL INTPVT(BPT, VSLOPE, POT, VSOT, MPOT, P6, VSO6)
      CALL INTERP(PWT, RSWT, MPWT, P6, RSW6)
      CALL INTERP(PWT, VSWT, MPWT, P6, VSW6)
      SO6 = SO(I,J,K + 1)
      SW6 = SW(I,J,K + 1)
      SG6 = SG(I,J,K + 1)
      CALL AMUG(PGT, VSGT, MPGT, P6, VSG6, CWSN(I,J,K + 1),
   1     PX(I,J,K + 1), SW6, SO6)
C
      CALL INTERP(SAT, PCOWT, MSAT, SW6, PCOW6)
      CALL INTERP(SAT, PCGOT, MSAT, SG6, PCGO6)
      RO6 = (RHOSCO + RSO6*RHOSCG) / BO(I,J,K + 1)
      RW6 = (RHOSCW + RSW6*RHOSCG) / BW(I,J,K + 1)
      RG6 = RHOSCG / BG(I,J,K + 1)
C
      FACT = -D288 * (EL(I,J,K + 1) - EL(I,J,K))
      GOW6 = (RO6 + RO) * FACT
      GWW6 = (RW6 + RW) * FACT + PCOW - PCOW6
      GGW6 = (RG6 + RG) * FACT + PCGO6 - PCGO
C
      P66 = P6 - PP
      HO6 = P66 + GOW6
      HW6 = P66 + GWW6
      HG6 = P66 + GGW6
      IF (HO6 .GE. 0.D0) CALL INTERP(SAT, PRMROT, MSAT, SO6,
   1     PRMRO6)
      IF (HO6 .LT. 0.D0) CALL INTERP(SAT, PRMROT, MSAT, SSO,
   1     PRMRO6)
      IF (HW6 .GE. 0.D0) CALL INTERP(SAT, PRMRWT, MSAT, SW6,
   1     PRMRW6)
      IF (HW6 .LT. 0.D0) CALL INTERP(SAT, PRMRWT, MSAT, SSW,
   1     PRMRW6)
      IF (HG6 .GE. 0.D0) CALL INTERP(SAT, PRMRGT, MSAT, SG6,
   1     PRMRG6)
      IF (HG6 .LT. 0.D0) CALL INTERP(SAT, PRMRGT, MSAT, SSG,
   1     PRMRG6)
      VISO6 = 4.0D0 * PRMRO6 / ((BO(I,J,K + 1) + BO(I,J,K))*(VSO6
   1  + VSO))
      VISW6 = 4.0D0 * PRMRW6 / ((BW(I,J,K + 1) + BW(I,J,K))*(VSW6
   1  + VSW))
      VISG6 = 4.0D0 * PRMRG6 / ((BG(I,J,K + 1) + BG(I,J,K))*(VSG6
     1        + VSG))
              CTEMP6 = 0.5D0 * (CWS(I,J,K + 1) + CWS(I,J,K))
C
   60         AOB = TZ(I,J,K + 1) * VISO6
              AWB = TZ(I,J,K + 1) * VISW6
              AWB1 = AWB * CTEMP6
              AGB = TZ(I,J,K + 1) * VISG6
C
C
              RSO1A = 0.5D0 * (RSO1 + RSO)
              RSO2A = 0.5D0 * (RSO2 + RSO)
              RSO3A = 0.5D0 * (RSO3 + RSO)
              RSO4A = 0.5D0 * (RSO4 + RSO)
              RSO5A = 0.5D0 * (RSO5 + RSO)
              RSO6A = 0.5D0 * (RSO6 + RSO)
              RSW1A = 0.5D0 * (RSW1 + RSW)
              RSW2A = 0.5D0 * (RSW2 + RSW)
              RSW3A = 0.5D0 * (RSW3 + RSW)
              RSW4A = 0.5D0 * (RSW4 + RSW)
              RSW5A = 0.5D0 * (RSW5 + RSW)
              RSW6A = 0.5D0 * (RSW6 + RSW)
              AO1 = AOW * GOW1
              AO2 = AOE * GOW2
              AO3 = AOS * GOW3
              AO4 = AON * GOW4
              AO5 = AOT * GOW5
              AO6 = AOB * GOW6
              AW1 = AWW * GWW1
              AW2 = AWE * GWW2
              AW3 = AWS * GWW3
              AW4 = AWN * GWW4
              AW5 = AWT * GWW5
              AW6 = AWB * GWW6
              AW1A = AWW1 * GWW1
              AW2A = AWE1 * GWW2
              AW3A = AWS1 * GWW3
              AW4A = AWN1 * GWW4
              AW5A = AWT1 * GWW5
              AW6A = AWB1 * GWW6
C
              GOWT(I,J,K) = AO1 + AO2 + AO3 + AO4 + AO5 + AO6
              GWWT(I,J,K) = AW1 + AW2 + AW3 + AW4 + AW5 + AW6
              GWWT1(I,J,K) = AW1A + AW2A + AW3A + AW4A + AW5A + AW6A
              GGWT(I,J,K) = AGW * GGW1 + AGE * GGW2 + AGS * GGW3 + AGN *
     1        GGW4 + AGT * GGW5 + AGB * GGW6 + RSO1A * AO1 + RSO2A * AO2 +
     2         RSO3A * AO3 + RSO4A * AO4 + RSO5A * AO5 + RSO6A * AO6 +
     3        RSW1A * AW1 + RSW2A * AW2 + RSW3A * AW3 + RSW4A * AW4 +
     4        RSW5A * AW5 + RSW6A * AW6
C
              QOWG(I,J,K) = (BO(I,J,K) - BG(I,J,K)*RSO) * (-GOWT(I,J,K) +
     1        QO(I,J,K)) + (BW(I,J,K) - BG(I,J,K)*RSW) * (-GWWT(I,J,K) +
     2        QW(I,J,K)) + BG(I,J,K) * (-GGWT(I,J,K) + QG(I,J,K))
C
              AW(I,J,K) = (BO(I,J,K) + 0.5D0*BG(I,J,K)*(RSO1 - RSO)) *
     1        AOW + (BW(I,J,K) + 0.5D0*BG(I,J,K)*(RSW1 - RSW)) * AWW + BG(
     2        I,J,K) * AGW
              AE(I,J,K) = (BO(I,J,K) + 0.5D0*BG(I,J,K)*(RSO2 - RSO)) *
     1        AOE + (BW(I,J,K) + 0.5D0*BG(I,J,K)*(RSW2 - RSW)) * AWE + BG(
     2        I,J,K) * AGE
              AS(I,J,K) = (BO(I,J,K) + 0.5D0*BG(I,J,K)*(RSO3 - RSO)) *
     1         AOS + (BW(I,J,K) + 0.5D0*BG(I,J,K)*(RSW3 - RSW)) * AWS + BG(
     2         I,J,K) * AGS
               AN(I,J,K) = (BO(I,J,K) + 0.5D0*BG(I,J,K)*(RSO4 - RSO)) *
     1         AON + (BW(I,J,K) + 0.5D0*BG(I,J,K)*(RSW4 - RSW)) * AWN + BG(
     2         I,J,K) * AGN
               AT(I,J,K) = (BO(I,J,K) + 0.5D0*BG(I,J,K)*(RSO5 - RSO)) *
     1         AOT + (BW(I,J,K) + 0.5D0*BG(I,J,K)*(RSW5 - RSW)) * AWT + BG(
     2         I,J,K) * AGT
               AB(I,J,K) = (BO(I,J,K) + 0.5D0*BG(I,J,K)*(RSO6 - RSO)) *
     1         AOB + (BW(I,J,K) + 0.5D0*BG(I,J,K)*(RSW6 - RSW)) * AWB + BG(
     2         I,J,K) * AGB
               OW(I,J,K) = AOW
               OE(I,J,K) = AOE
               OS(I,J,K) = AOS
               ON(I,J,K) = AON
               OT(I,J,K) = AOT
               OB(I,J,K) = AOB
               WW(I,J,K) = AWW
               WE(I,J,K) = AWE
               WS(I,J,K) = AWS
               WN(I,J,K) = AWN
               WT(I,J,K) = AWT
               WB(I,J,K) = AWB
               WW1(I,J,K) = AWW1
               WE1(I,J,K) = AWE1
               WS1(I,J,K) = AWS1
               WN1(I,J,K) = AWN1
               WT1(I,J,K) = AWT1
               WB1(I,J,K) = AWB1
   70 CONTINUE
      DO 80 K = 1, KK
        DO 80 J = 1, JJ
          DO 80 I = 1, II
            SUM(I,J,K) = AW(I,J,K) + AE(I,J,K) + AS(I,J,K) + AN(I,J,K) +
     1       AT(I,J,K) + AB(I,J,K)
            GAM(I,J,K) = VP(I,J,K) * CT(I,J,K) * DIV1
            E(I,J,K) = -SUM(I,J,K) - GAM(I,J,K)
            B(I,J,K) = QOWG(I,J,K) - GAM(I,J,K) * P(I,J,K)
   80 CONTINUE
      RETURN
      RETURN
      END
      SUBROUTINE TABLE
      IMPLICIT REAL*8(A - H,O - Z)
      LOGICAL*1 FREE(1) /'*'/
      COMMON /GASSAT/ PBO, VSLOPE, BSLOPE, RSLOPE, PMAXT, RHOSCO,
     1        RHOSCG, RHOSCW, PBOT(10,10,3)
      COMMON /NPTS/ MSAT, MPOT, MPWT, MPGT, IREPRS
      COMMON /SPVT/ SAT(25), PRMROT(25), PRMRWT(25), PRMRGT(25),
     1        PCOWT(25), PCGOT(25), POT(25), VSOT(25), BOT(25), BOPT(25),
     2        RSOT(25), RSOPT(25), PWT(25), VSWT(25), BWT(25), BWPT(25),
     3        RSWT(25), RSWPT(25), PGT(25), VSGT(25), BGT(25), BGPT(25),
     4        CRT(25)
C
C
C
C****  RELATIVE PERMEABILITY & CAPILLARY PRESSURE TABLE
C
      READ (20,FREE) IPERM
      IF (IPERM .EQ. 1) GO TO 20
      DO 10 I = 1, 25
        READ (20,FREE) SAT(I), PRMROT(I), PRMRWT(I), PRMRGT(I),
     1        PCOWT(I), PCGOT(I)
        WRITE (1,150) SAT(I), PRMROT(I), PRMRWT(I), PRMRGT(I), PCOWT(I),
     1  PCGOT(I)
        IF (SAT(I) .GE. 1.1D0) GO TO 40
   10 CONTINUE
        GO TO 30
   20 CONTINUE
   30 CONTINUE
C
C****  BUBBLE POINT & MAXIMUM PRESSURES
C
   40 MSAT = I
      READ (20,FREE) PBO, VSLOPE, BSLOPE, RSLOPE, PMAXT, IREPRS
      WRITE (1,180) PBO, VSLOPE, BSLOPE, RSLOPE, PMAXT, IREPRS
      DO 50 I = 1, 25
        READ (20,FREE) POT(I), VSOT(I), BOT(I), RSOT(I)
        WRITE (1,160) POT(I), VSOT(I), BOT(I), RSOT(I)
        RSOT(I) = 0.17809D0 * RSOT(I)
        IF (POT(I) .GE. PMAXT) GO TO 60
   50 CONTINUE
   60 MPOT = I
      DO 70 I = 1, 25
        READ (20,FREE) PWT(I), VSWT(I), BWT(I), RSWT(I)
        WRITE (1,160) PWT(I), VSWT(I), BWT(I), RSWT(I)
        RSWT(I) = 0.17809D0 * RSWT(I)
        IF (PWT(I) .GE. PMAXT) GO TO 80
   70 CONTINUE
   80 MPWT = I
      DO 90 I = 1, 999
        READ (20,FREE) PGT(I), VSGT(I), BGT(I), CRT(I)
        WRITE (1,170) PGT(I), VSGT(I), BGT(I), CRT(I)
        IF (PGT(I) .GE. PMAXT) GO TO 100
   90 CONTINUE
  100 MPGT = I
      CONTINUE
      READ (20,FREE) RHOSCO, RHOSCW, RHOSCG
      WRITE (1,140) RHOSCO, RHOSCW, RHOSCG
      DO 110 I = 2, MPOT
        DIV = 1.0D0 / (POT(I) - POT(I - 1))
        BOPT(I) = (BOT(I) - BOT(I - 1)) * DIV
        RSOPT(I) = (RSOT(I) - RSOT(I - 1)) * DIV
  110 CONTINUE
      WRITE (1,190)
      DO 120 I = 2, MPWT
        DIV = 1.0D0 / (PWT(I) - PWT(I - 1))
        BWPT(I) = (BWT(I) - BWT(I - 1)) * DIV
        RSWPT(I) = (RSWT(I) - RSWT(I - 1)) * DIV
  120 CONTINUE
      DO 130 I = 2, MPGT
        BGPT(I) = (BGT(I) - BGT(I - 1)) / (PGT(I) - PGT(I - 1))
  130 CONTINUE
  140 FORMAT (2X, 8F10.4)
  150 FORMAT (1X, 4F10.4, 2F10.2)
  160 FORMAT (3X, F10.1, 1X, F8.4, 2X, F8.4, 2X, F8.2)
  170 FORMAT (3X, F10.1, 1X, F8.4, D10.4, D10.3)
  180 FORMAT (F10.2, D10.3, 1X, D10.3, 2F10.2, 15)
  190 FORMAT ('P', T25, 'BW', T33, 'DBW/DP', T47, 'RSW', T55, 'DRSW/DP'/
     1       )
```

```
      RETURN
      END
C.....................................................................TRAN1
      SUBROUTINE TRAN1(II, JJ, KK, IM, JM)
      IMPLICIT REAL*8(A - H,O - Z)
      LOGICAL*1 FREE(1) /'*'/
C
      COMMON /PARRAY/ PN(10,10,3), SON(10,10,3), SWN(10,10,3),
     1       SGN(10,10,3), SO1(10,10,3), SW1(10,10,3), SG1(10,10,3),
     2       A1(10,10,3), A2(10,10,3), A3(10,10,3), SUM(10,10,3),
     3       GAM(10,10,3), QS(10,10,3)
      COMMON /SPARM/ PX(10,10,3), PY(10,10,3), PZ(10,10,3), EL(10,10,3),
     1       TX(11,10,3), TY(10,11,3), TZ(10,10,4)
      COMMON /SDELTA/ DX(10,10,3), DY(10,10,3), DZ(10,10,3), IQN1(20),
     1       IQN2(20), IQN3(20)
      DO 10 K = 1, KK
        DO 10 J = 1, JJ
          DO 10 I = 1, II
            FACX = 1.0D0
            FACY = 1.0D0
            FACZ = 1.0D0
            IF (I .GT. 1 .AND. I .LT. II) FACX = 4.D0 * DX(I,J,K) / (2.*
     1      DX(I,J,K) + DX(I + 1,J,K) + DX(I - 1,J,K))
            IF (J .GT. 1 .AND. J .LT. JJ) FACY = 4.D0 * DY(I,J,K) / (2.*
     1      DY(I,J,K) + DY(I,J + 1,K) + DY(I,J - 1,K))
            IF (K .GT. 1 .AND. K .LT. KK) FACZ = 4.D0 * DZ(I,J,K) / (2.*
     1      DZ(I,J,K) + DZ(I,J,K + 1) + DZ(I,J,K - 1))
            A1(I,J,K) = FACX * PX(I,J,K) * DY(I,J,K) * DZ(I,J,K)
            A2(I,J,K) = FACY * PY(I,J,K) * DX(I,J,K) * DZ(I,J,K)
            A3(I,J,K) = FACZ * PZ(I,J,K) * DX(I,J,K) * DY(I,J,K)
   10 CONTINUE
      IF (II .EQ. 1) GO TO 30
      DO 20 K = 1, KK
        DO 20 J = 1, JJ
          DO 20 I = 2, II
            IF (PX(I - 1,J,K) .LE. 1.D-04 .AND. PX(I,J,K) .LE. 1.D-04)
     1         GO TO 20
            TX(I,J,K) = 1.2656D-2 * A1(I - 1,J,K) * A1(I,J,K) / (DX(I -
     1      1,J,K)*A1(I,J,K) + DX(I,J,K)*A1(I - 1,J,K))
   20 CONTINUE
   30 CONTINUE
      IF (JJ .EQ. 1) GO TO 50
      DO 40 K = 1, KK
        DO 40 J = 2, JJ
          DO 40 I = 1, II
            IF (PY(I,J - 1,K) .LE. 1.D-04 .AND. PY(I,J,K) .LE. 1.D-04)
     1         GO TO 40
            TY(I,J,K) = 1.2656D-2 * A2(I,J - 1,K) * A2(I,J,K) / (DY(I,J
     1      - 1,K)*A2(I,J,K) + DY(I,J,K)*A2(I,J - 1,K))
   40 CONTINUE
   50 CONTINUE
      IF (KK .EQ. 1) GO TO 70
      DO 60 K = 2, KK
        DO 60 J = 1, JJ
          DO 60 I = 1, II
            IF (PZ(I,J,K - 1) .LE. 1.D-04 .AND. PZ(I,J,K) .LE. 1.D-04)
     1         GO TO 60
            TZ(I,J,K) = 1.2656D-2 * A3(I,J,K - 1) * A3(I,J,K) / (DZ(I,J,
     1      K - 1)*A3(I,J,K) + DZ(I,J,K)*A3(I,J,K - 1))
   60 CONTINUE
   70 CONTINUE
   80 RETURN
      END
      SUBROUTINE INITL(KPI, II, JJ, KK, PI, IM, JM, ETO, CUMPO, BEO,
     1           CUMPW, BEW, CUMPG, BEG, SOI, SWI, SGI, WOC, GOC, PGOC,
     2           CUMIW, CUMIG)
      IMPLICIT REAL*8(A - H,O - Z)
      LOGICAL*1 FREE(1) /'*'/
      COMMON /GASSAT/ PBO, VSLOPE, BSLOPE, RSLOPE, PMAXT, RHOSCO,
     1       RHOSCG, RHOSCW, PBOT(10,10,3)
      COMMON /NPTS/ MSAT, MPOT, MPWT, MPGT, IREPRS
      COMMON /PARRAY/ PN(10,10,3), SON(10,10,3), SWN(10,10,3),
     1       SGN(10,10,3), SO1(10,10,3), SW1(10,10,3), SG1(10,10,3),
     2       A1(10,10,3), A2(10,10,3), A3(10,10,3), SUM(10,10,3),
     3       GAM(10,10,3), QS(10,10,3)
      COMMON /SPARM/ PX(10,10,3), PY(10,10,3), PZ(10,10,3), EL(10,10,3),
     1       TX(11,10,3), TY(10,11,3), TZ(10,10,4)
      COMMON /SPRS/ P(10,10,3), SO(10,10,3), SW(10,10,3), SG(10,10,3)
      COMMON /SPVT/ SAT(25), PRMROT(25), PRMRWT(25), PRMRGT(25),
     1       PCOWT(25), PCGOT(25), POT(25), VSOT(25), BOT(25), BOPT(25),
     2       RSOT(25), RSOPT(25), PWT(25), VSWT(25), BWT(25), BWPT(25),
     3       RSWT(25), RSWPT(25), PGT(25), VSGT(25), BGT(25), BGPT(25),
     4       CRT(25)
      ETO = 0.D0
      CUMPO = 0.D0
      CUMPW = 0.D0
      CUMPG = 0.D0
      CUMIW = 0.D0
      CUMIG = 0.D0
      BEO = 0.D0
      BEW = 0.D0
      BEG = 0.D0
      READ (20,FREE) KPI, KSI
      IF (KPI .NE. 0) GO TO 40
      READ (20,FREE) PI, PGOC, WOC, GOC
      DO 30 K = 1, KK
        DO 30 J = 1, JJ
          DO 30 I = 1, II
            IF (EL(I,J,K) .LT. GOC) GO TO 20
            IF (EL(I,J,K) .GT. WOC) GO TO 10
            BPT = PBOT(I,J,K)
            CALL INTPVT(BPT, RSLOPE, POT, BOT, MPOT, PI, BBO)
            CALL INTPVT(BPT, RSLOPE, POT, RSOT, MPOT, PI, RSO)
            RHOO = (RHOSCO + RSO*RHOSCG) / BBO
            PN(I,J,K) = PI + RHOO * (EL(I,J,K) - WOC) / 144.D0
            GO TO 30
   10       CALL INTERP(PWT, BWT, MPWT, PI, BBW)
            CALL INTERP(PWT, RSWT, MPWT, PI, RSW)
            RHOW = (RHOSCW + RSW*RHOSCG) / BBW
            PN(I,J,K) = PI + RHOW * (EL(I,J,K) - WOC) / 144.D0
            GO TO 30
   20       CALL INTERP(PGT, BGT, MPGT, PGOC, BBG)
            RHOG = RHOSCG / BBG
            PN(I,J,K) = PGOC + RHOG * (EL(I,J,K) - GOC) / 144.D0
   30 CONTINUE
      GO TO 70
   40 DO 60 K = 1, KK
        DO 50 J = 1, JJ
   50   READ (20,FREE) (PN(I,J,K),I=1,II)
   60 CONTINUE
   70 CONTINUE
      DO 80 I = 1, II
        DO 80 J = 1, JJ
          DO 80 K = 1, KK
   80 P(I,J,K) = PN(I,J,K)
      IF (KSI .NE. 0) GO TO 110
      READ (20,FREE) SOI, SWI, SGI
      DO 90 K = 1, KK
        DO 90 J = 1, JJ
          DO 90 I = 1, II
            SON(I,J,K) = SOI
            SWN(I,J,K) = SWI
            SGI = 1.D0-SOI - SWI
            SGN(I,J,K) = SGI
            SO(I,J,K) = SOI
            SW(I,J,K) = SWI
            SG(I,J,K) = SGI
            IF (SG(I,J,K) .LT. 0.D0) SG(I,J,K) = 0.D0
   90 CONTINUE
  100 RETURN
  110 DO 130 K = 1, KK
        DO 120 J = 1, JJ
  120   READ (20,FREE) (SO(I,J,K),I=1,II)
  130 CONTINUE
      DO 150 K = 1, KK
        DO 140 J = 1, JJ
  140   READ (20,FREE) (SW(I,J,K),I=1,II)
  150 CONTINUE
      DO 160 K = 1, KK
        DO 160 J = 1, JJ
          DO 160 I = 1, II
            SG(I,J,K) = 1.D0-SO(I,J,K) - SW(I,J,K)
            IF (SG(I,J,K) .LT. 0.D0) SG(I,J,K) = 0.D0
            SON(I,J,K) = SO(I,J,K)
            SWN(I,J,K) = SW(I,J,K)
            SGN(I,J,K) = SG(I,J,K)
  160 CONTINUE
      RETURN
      END
      SUBROUTINE AMUG(X, Y, N, XO, YO, CCS, PPX, SW, SO)
      IMPLICIT REAL*8(A - H,O - Z)
      COMMON /FOAM/ DCONST, ECONST
      LOGICAL*1 FREE(1) /'*'/
      DIMENSION X(25), Y(25)
      PX = PPX / 1000.D0
      CS = CCS
      IF (XO .GE. X(N)) YO = Y(N)
      IF (XO .GE. X(N)) GO TO 30
      DO 20 I = 2, N
        IF (XO .GE. X(I)) GO TO 20
   10   FORMAT (4E12.4)
        YO = Y(I - 1) + (XO - X(I - 1)) * (Y(I) - Y(I - 1)) / (X(I) - X(
     1  I - 1))
        GO TO 30
   20 CONTINUE
   30 CONTINUE
      IF (CS .LE. 0.D0) RETURN
      IF (CS .LE. 0.0155D0) FC = DSQRT(250.D0*CS - 1.56D04*CS*CS)
      IF (CS .GT. 0.0155D0) FC = 0.35D0
      IF (PX .GT. 3.D01) FK = 0.5D0
```

```
IF (PX .LE. 3.D01) FK = DSQRT(0.125D0*PX - 3.91D-03*PX*PX)
YO = YO * (1.D0+DCONST*FC*(SW - .1D0)*FK) / (1.D0+ECONST*SO*SO)
RETURN
END
```